2021

Photoredox-Mediated Dual Catalysis, 1,2-Difunctionalizations, And Reaction Development For Dna-Encoded Library Technology

Shorouk Badir
University of Pennsylvania

Photoredox-Mediated Dual Catalysis, 1,2-Difunctionalizations, And Reaction Development For Dna-Encoded Library Technology

Abstract

Reactions for the controlled, catalytic formation of carbon-carbon bonds are crucial for modern organic synthesis. In an idealized sense, they enable a rapid, convergent assembly of molecular complexity. Among such transformations, the formation of C–C bonds at Csp3-hybridized centers is a particularly desirable construct because of its potential to provide access to 3D-rich architectures and, akin to the Suzuki sp2-sp2 coupling, impact the way that novel chemical space is accessed.

Toward this goal, metallaphotoredox catalysis has been enlisted as a valuable advance to forge Csp3–Csp2 linkages through single-electron-transfer (SET) under mild reaction conditions. Recent research efforts have broadened the scope of radical progenitors from feedstock chemicals including aliphatic carboxylic acids, aldehydes, bromides, and organosilanes. In subsequent studies, a photochemical/Ni-mediated decarboxylative strategy is accomplished through electron donor-acceptor (EDA) complex activation bypassing the need for stoichiometric metal reductants or exogenous photocatalysts. To facilitate sequential bond formation, net-neutral radical/polar crossover is utilized to achieve the 1,2-dicarbofunctionalization of olefins with organotrifluoroborate nucleophiles.

Among the applications in which the ability to accommodate diverse reaction modalities and molecular complexity becomes critical is DNA-Encoded Library (DEL) synthesis. Recently, DEL technology has emerged as an innovative screening modality for the discovery of therapeutic candidates in the pharmaceutical industry. The platform enables a cost-effective, time-efficient, and large-scale assembly and interrogation of billions of small organic ligands against a biological target in a single experiment. To increase chemical diversity, the implementation of photoredox catalysis in DELs, including Ni-catalyzed manifolds and radical/polar crossover, has enabled the construction of novel structural scaffolds. To expand chemical space, a decarboxylative-based hydroalkylation of DNA-conjugated trifluoromethyl-substituted alkenes driven by SET and subsequent hydrogen atom termination through EDA complex activation is detailed. In a further protocol, the coupling of electronically unbiased olefins is achieved through the intermediacy of (hetero)aryl radical species with full retention of the DNA tag integrity.

In summary, photoredox catalysis offers new avenues for unique synthetic disconnections toward bioactive molecules. The diverse nature of amenable radical precursors, combined with the mild and modular character of photochemical paradigms, facilitate the generation of chemotypes that possess a high density of pendant functional groups.

Degree Type

Dissertation

Degree Name

Doctor of Philosophy (PhD)

Graduate Group

Chemistry

First Advisor

Gary A. Molander

PHOTOREDOX-MEDIATED DUAL CATALYSIS, 1,2-DIFUNCTIONALIZATIONS, AND REACTION DEVELOPMENT FOR DNA-ENCODED LIBRARY TECHNOLOGY

Shorouk O. Badir

A DISSERTATION

in

Chemistry

Presented to the Faculties of the University of Pennsylvania

in

Partial Fulfillment of the Requirements for the

Degree of Doctor of Philosophy

2021

Supervisor of Dissertation

_____

Gary A. Molander

Professor of Chemistry

Graduate Group Chairperson

_____

Daniel J. Mindiola

Brush Family Professor of Chemistry

Dissertation Committee:

Megan L. Matthews, Assistant Professor of Chemistry

Donna M. Huryn, Adjunct Professor of Chemistry

David M. Chenoweth, Associate Professor of Chemistry

PHOTOREDOX-MEDIATED DUAL CATALYSIS, 1,2-DIFUNCTIONALIZATIONS, AND REACTION DEVELOPMENT FOR DNA-ENCODED LIBRARY TECHNOLOGY

لأمي وأبي

For my fellow resilient Palestinian people

In memory of Nawal El Saadawi and Mahmoud Darwish

ACKNOWLEDGMENTS

First and foremost, I would like to express my sincere gratitude to Professor Gary Molander for his unwavering support and guidance throughout my educational journey. Indeed, he has been my biggest advocate. I first met Professor Molander when I was an undergraduate student at Bryn Mawr College. Professor Molander was very generous to offer me an internship in his group that was instrumental in shaping my understanding of scientific research leading to my decision to pursue graduate studies in chemistry. He has always been an exemplary mentor, educator, and a role model. I would like to thank him for teaching me how to communicate my research effectively and write scientifically. Under his guidance, I have been very fortunate to work on review articles and grant proposals that helped me acquire knowledge in various fields of organometallic chemistry. I would like to thank him for allowing me the intellectual freedom to conceive and direct research projects. This has been an integral part of my professional development and for that I am forever grateful.

Furthermore, many thanks are owed to my committee members at the University of Pennsylvania. First, I would like to thank Professor Megan Matthews, Professor Donna Huryn, Professor David Chenoweth, and Professor Patrick Walsh for their constructive feedback and encouragement throughout my studies here. I have learned a great deal of chemistry from all of them, and they have inspired me to creatively address my research challenges. I especially would like to thank Professor Huryn for giving me the opportunity to volunteer for the EWOC (Empowering Women in Organic Chemistry) conference, where I have had the pleasure of connecting with amazing mentors and scientists. In addition, I would like to thank Dr. Charles Ross III and Judith Currano for their guidance and mentorship.

Over my time in the Molander group, I had the pleasure of collaborating with wonderful postdocs, visiting scholars, graduate students, and undergraduate researchers. In particular, I would like to thank Dr. Steven Wisniewski, Dr. Javad Amani, and Dr. Audrey Dumoulin for teaching me the ropes as I began my research journey. Special thanks to Dr. Jaehoon Sim for his guidance with respect to reaction development for DNA-encoded libraries. In addition, Dr. Jun Yi has been a constructive critic and a great mentor. During the latter part of my graduate career, Dr. Eugénie Romero, Dr. Loïc Pantaine, Dr. Álvaro Gutiérrez Bonet, and Anasheh Sookezian have been outstanding coworkers. I would like to thank Dr. María Ribagorda for being a great role model and a voice of reason. Moreover, I have been exceptionally lucky to work alongside Dr. María Jesús Cabrera Afonso, Dr. Alexander Lipp, Dr. Lisa Kammer, and Dr. Matthias Krumb, who are not only brilliant scientists, but also wonderful friends. You have always been a solid support system, and I will forever treasure our friendship.

A sincere thank you goes to my friends in the chemistry department at the University of Pennsylvania. In particular, Dr. Andy Glass has been a wonderful running partner. Russell Shelp has been a great friend from the start, and I have thoroughly enjoyed all our conversations from exploring chemistry topics to deliberating world affairs to discussing the challenges that face women in the workspace. Outside the department, Holly Borg has been as an amazing friend and support system since the day we've met at Bryn Mawr College.

I must acknowledge all my mentors at Bryn Mawr College who have played an essential role in my growth as a scientist. Professor William Malachowski served as an outstanding advisor and provided me with the intellectual freedom that has shaped my curiosity and enthusiasm for research. Special thanks to Dr. Krynn Lukacs, Dr. Michelle Frnacl, and Dr. Yan Kung for taking interest in my professional and personal development. I would like to take a moment and

remember Professor Maryellen Nerz-Stormes, a thoughtful and wonderful role model who was my biggest advocate during my time at Bryn Mawr College. Not only did she help me develop a solid foundation in organic chemistry through her rigorous coursework, Dr. Nerz-Stormes also provided me the opportunity to work alongside her as a teaching assistant where I have acquired confidence and a passion for teaching. My education at Bryn Mawr College is one of the greatest gifts, and I am forever grateful to this community.

I am beyond thankful for the support of my family (Mom, Dad, Shireen, Bisan, Sarah, Sulaf, and Mohamed). When I embarked on my educational journey, I was not aware I would not be able to see them or my home country for +9 years. Although I have since learned that home to me is the world, my family has always been a phone call away to lend their unwavering support, understanding, encouragement, and hopefulness. Growing up in a conservative society under military control, I am especially grateful to my parents for taking special interest in my education and dedicating endless resources to help me realize my goals. I'd like to thank my grandmother Sadaa' for teaching me her feminism: the value of solidarity between women.

Finally, I am very proud of my Palestinian heritage. I attribute my passion for education, relentless dedication to my work, and understanding of others to my upbringing in Palestine. In the words of the Palestinian poet Mahmoud Darwish, we Palestinians "suffer from an incurable malady: hope".

ABSTRACT

PHOTOREDOX-MEDIATED DUAL CATALYSIS, 1,2-DIFUNCTIONALIZATIONS, AND REACTION DEVELOPMENT FOR DNA-ENCODED LIBRARY TECHNOLOGY

Shorouk O. Badir

Gary A. Molander

Reactions for the controlled, catalytic formation of carbon-carbon bonds are crucial for modern organic synthesis. In an idealized sense, they enable a rapid, convergent assembly of molecular complexity. Among such transformations, the formation of C–C bonds at Csp^3-hybridized centers is a particularly desirable construct because of its potential to provide access to 3D-rich architectures and, akin to the Suzuki sp^2-sp^2 coupling, impact the way that novel chemical space is accessed.

Toward this goal, metallaphotoredox catalysis has been enlisted as a valuable advance to forge Csp^3–Csp^2 linkages through single-electron-transfer (SET) under mild reaction conditions. Recent research efforts have broadened the scope of radical progenitors from feedstock chemicals including aliphatic carboxylic acids, aldehydes, bromides, and organosilanes. In subsequent studies, a photochemical/Ni-mediated decarboxylative strategy is accomplished through electron donor-acceptor (EDA) complex activation bypassing the need for stoichiometric metal reductants or exogenous photocatalysts. To facilitate sequential bond formation, net-neutral radical/polar crossover is utilized to achieve the 1,2-dicarbofunctionalization of olefins with organotrifluoroborate nucleophiles.

Among the applications in which the ability to accommodate diverse reaction modalities and molecular complexity becomes critical is DNA-Encoded Library (DEL) synthesis. Recently, DEL technology has emerged as an innovative screening modality for the discovery of therapeutic candidates in the pharmaceutical industry. The platform enables a cost-effective, time-efficient, and large-scale assembly and interrogation of billions of small organic ligands against a biological target in a single experiment. To increase chemical diversity, the implementation of photoredox catalysis in DELs, including Ni-catalyzed manifolds and radical/polar crossover, has enabled the construction of novel structural scaffolds. To expand chemical space, a decarboxylative-based hydroalkylation of DNA-conjugated trifluoromethyl-substituted alkenes driven by SET and subsequent hydrogen atom termination through EDA complex activation is detailed. In a further protocol, the coupling of electronically unbiased olefins is achieved through the intermediacy of (hetero)aryl radical species with full retention of the DNA tag integrity.

In summary, photoredox catalysis offers new avenues for unique synthetic disconnections toward bioactive molecules. The diverse nature of amenable radical precursors, combined with the mild and modular character of photochemical paradigms, facilitate the generation of chemotypes that possess a high density of pendant functional groups.

TABLE OF CONTENTS

DEDICATION ..... **III**

ACKNOWLEDGMENTS ..... **IV**

ABSTRACT ..... **VII**

TABLE OF CONTENTS ..... **IX**

LIST OF ABBREVIATIONS ..... **XII**

CHAPTER 1. INTRODUCTION: PHOTOREDOX CATALYSIS **1**

1.1 Carbon–Carbon Bond Formation by Nickel/Photoredox Dual Catalysis 1

1.2 Multicomponent Reactions: Radical/Polar and Radical/HAT Crossover Strategies 22

1.3 Photoredox-Mediated Alkylation for DNA-Encoded Libraries 26

1.4 References 42

CHAPTER 2. SYNTHESIS OF REVERSED *C*-ACYL GLYCOSIDES THROUGH NICKEL/PHOTOREDOX DUAL CATALYSIS **54**

2.1 Introduction 54

2.2 Results and Discussion 57

2.3 Conclusion 61

2.4 Experimental 62

2.5 References 89

CHAPTER 3. DEAMINATIVE REDUCTIVE ARYLATION ENABLED BY NICKEL/PHOTOREDOX DUAL CATALYSIS **93**

3.1 Introduction 93

3.2 Results and Discussion 95

3.3 Conclusion 102

3.4 Experimental 103

3.5 References 131

CHAPTER 4. DECARBOXYLATIVE REDUCTIVE ARYLATION ENABLED BY ELECTRON DONOR-ACCEPTOR COMPLEX PHOTOACTIVATION 135

4.1 Introduction 135

4.2 Results and Discussion 138

4.3 Conclusion 147

4.4 Experimental 148

4.5 References 178

CHAPTER 5. PHOTOINDUCED 1,2-DICARBOFUNCTIONALIZATION OF ALKENES WITH ORGANOTRIFLUOROBORATE NUCLEOPHILES VIA RADICAL/POLAR CROSSOVER 184

5.1 Introduction 184

5.2 Results and Discussion 186

5.3 Conclusion 194

5.4 Experimental 195

5.5 References 235

CHAPTER 6. PHOTOREDOX-CATALYZED MULTICOMPONENT ALKYL PETASIS REACTION WITH ORGANOTRIFLUOROBORATES 242

6.1 Introduction 242

6.2 Results and Discussion 245

6.3 Conclusion 249

6.4 Experimental 250

6.5 References 286

CHAPTER 7. MULTIFUNCTIONAL BUILDING BLOCKS COMPATIBLE WITH PHOTOREDOX-MEDIATED ALKYLATION FOR DNA-ENCODED LIBRARY SYNTHESIS 290

7.1 Introduction 290
7.2 Results and Discussion 293
7.3 Conclusion 300
7.4 Experimental 300
7.5 References 320

CHAPTER 8. PHOTOREDOX-MEDIATED HYDROALKYLATION AND HYDROARYLATION OF FUNCTIONALIZED OLEFINS FOR DNA-ENCODED LIBRARY SYNTHESIS 325

8.1 Introduction 325
8.2 Results and Discussion 329
8.3 Conclusion 341
8.4 Experimental 342
8.5 References 361

ABOUT THE AUTHOR 369

LIST OF ABBREVIATIONS

A	acceptor
acac	acetylacetonate
Ac	acyl
Alk	alkyl
CAN	ammonium cerium (IV) nitrate
Ar	aryl
BET	back-electron transfer
Bz	benzoyl
Bn	benzyl
bpy	bipyridine
TBAF	tetrabutylammonium fluoride
Boc	*tert*-butyloxycarbonyl
dtbpy	4,4′-di-*tert*-butyl-2,2′-dipyridyl
4CzIPN	2,4,5,6-tetra(9*H*-carbazol-9-yl)isophthalonitrile
Cbz	carboxybenzyl
CFL	compact fluorescent light
Cy	cyclohexyl
COD	1,5-cyclooctadiene
CPME	cyclopentyl methyl ether
DFT	density functional theory
dr	diastereomeric ratio
DCF	dicarbofunctionalization
DEL	DNA-encoded library
D	donor
EDA	electron donor-acceptor
ET	electron transfer
EWG	electron withdrawing group
EI	electrophile
ee	enantiomeric ratio
equiv	equivalent
dme	ethylene glycol dimethyl ether
[PC]*	excited state photocatalyst
Fmoc	fluorenylmethoxycarbonyl
dF(CF_3)ppy	2-(2,4-difluorophenyl)-5-(trifluoromethyl)pyridine
dF(F)ppy	2-(2,4-difluorophenyl)-5-fluoropyridine
dFppy	2-(2,4-difluorophenyl)pyridine

HFIP	1,1,1,3,3,3-hexafluoro-2-propanol
HE	Hantzsch ester
Het	heteroaryl
THF	tetrahydrofuran
HAT	hydrogen atom transfer
THP	tetrahydropyran
1,4-DHP	1,4-dihydropyridine
NHPI	*N*-hydroxyphthalimide
IR	infrared
Cl-4CzIPN	2,4,5,6-tetrakis(3,6-dichloro-9*H*-carbazol-9-yl)isophthalonitrile
LG	leaving group
LA	lewis acid
L	ligand
LED	light emitting diode
Mes-Acr	mesityl acridinium
MLCT	metal-to-ligand charge transfer
dMeObpy	4-4′-dimethoxy-2-2′-bipyridine
DMA	*N,N*-dimethylacetamide
pin	2,3-dimethylbutane-2,3-diol
DMDC	dimethyl dicarbonate
DMF	*N,N*-dimethylformamide
TMG	1,1,3,3-tetramethylguanidine
TMHD	2,2,6,6-tetramethyl-3,5-heptanedionate
DMI	1,3-dimethyl-2-imidazolidinone
TMS	trimethylsilyl
DMSO	dimethyl sulfoxide
MOPS	3-(*N*-morpholino)propanesulfonic acid
Nu	nucleophile
phen	1,10-phenanthroline
PTH	*N*-phenylphenothiazine
ppy	2-phenylpyridine
[PC]	photocatalyst
RP	radical precursor
RPC	radical/polar crossover
RAE	redox-active ester
RT	room temperature
SCE	saturated calomel electrode
SET	single-electron transfer

Chapter 1. Introduction: Photoredox Catalysis

1.1 Carbon–Carbon Bond Formation by Nickel/Photoredox Dual Catalysis[†]

1.1.1 Introduction

Reactions for the controlled, catalytic formation of carbon-carbon bonds are crucial for modern organic synthesis. In an idealized sense, they enable a rapid, convergent assembly of molecular complexity.[1] Toward this goal, numerous elegant and robust methods for C–C coupling, such as Pd-catalyzed cross couplings,[2] Ru-mediated olefin-metathesis,[3] and C–H functionalization,[4] have been developed. Among such transformations, the formation of C–C bonds at sp^3-hybridized centers is a particularly desirable construct because of its potential to provide rapid access to 3D-rich architectures and, akin to the Suzuki sp^2-sp^2 coupling, impact the way that novel chemical space is accessed.[5] A significant limitation of many state-of-the-art cross-coupling methods is the inability to access sp^3-hybridized carbon centers, particularly in complex molecular environments.[6] Although some success has been achieved,[7] the use of forcing conditions and/or the pre-formation of more reactive coupling partners are needed for productive reactivity, thereby limiting functional group compatibility when attempting to forge this type of bond.[8] The challenges encountered when attempting sp^2–sp^3 cross-coupling prompted the exploration of alternate mechanistic paradigms.

In 2014, alkyl radicals were first shown to be viable partners in Ni-catalyzed cross-coupling, funneling into a cycle to assemble new C(sp^3)–C(sp^2) bonds.[9] The development of this paradigm was the culmination of several concepts. First, the intermediacy of carbon-centered

---

[†] Reproduced in part with permission from a) J. A. Milligan, J. P. Phelan, S. O. Badir, G. A. Molander, *Angew. Chem. Int. Ed.* **2019**, *58*, 6152–6163. Copyright 2019, Wiley; b) A. Lipp, S. O. Badir, G. A. Molander, *Angew. Chem. Int. Ed.* **2021**, *60*, 1714–1726. Copyright 2021, Wiley.

C(sp^3)-hybridized radicals in Ni-catalyzed coupling processes such as reductive cross-electrophile couplings had been well-documented.[10] Second, the pioneering reports on palladium- and copper photoredox dual catalysis suggested transition-metals could readily be accommodated in photocatalytic cycles.[11] Finally, the rich chemistry of Ni-catalyzed cross-couplings[12] implied that an array of ligands and electrophiles would be compatible with such a dual catalytic reaction.

Since this disclosure, metallaphotoredox catalysis has emerged as a valuable advance for the rapid assembly of challenging C–C linkages under mild reaction conditions. Upon excitation with visible light, a transition-metal-based photocatalyst or a highly conjugated organic molecule such as 1,2,3,5-tetrakis(carbazol-9-yl)-4,6-dicyanobenzene (4CzIPN)[13] engages in sequential single-electron-transfer (SET) events through reductive or oxidative quenching cycles (Figure 1.1 A and B), generating reactive radical intermediates that can be tamed and utilized for targeted transformations.

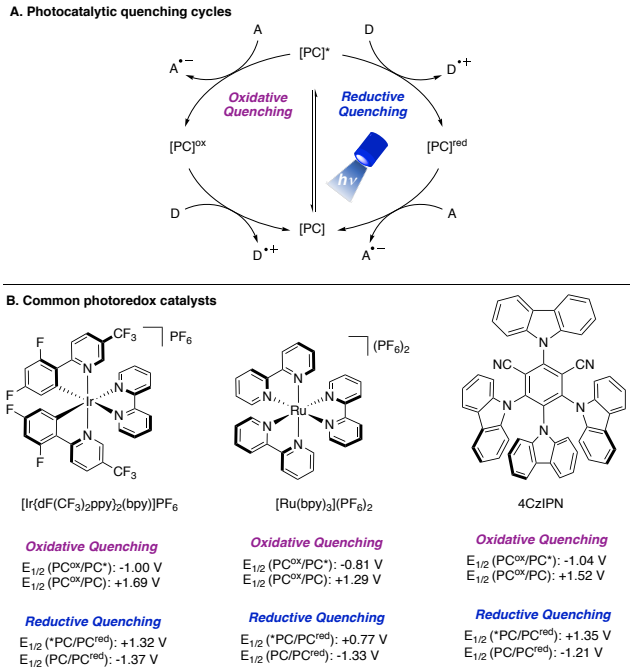

Figure 1.1 Photocatalytic quenching cycles (A) and common photoredox catalysts (B).

Owing to the strong correlation between the fraction of C(sp^3)-hybridized centers in drug candidates and their ultimate probability of clinical success,[5] metallaphotoredox catalysis has gained considerable traction in medicinal chemistry discovery efforts. This new coupling paradigm offered a solution to the challenge of conducting two-electron alkyl cross-couplings by subdividing the process into multiple, lower barrier single-electron steps (Figure 1.2 A). These steps can be partitioned into two distinct, yet interconnected, catalytic cycles – a photoredox cycle and a cross-coupling cycle. In the cross-coupling cycle, capture of a photoredox-generated radical species by ligated Ni^0 (**D**) to generate a Ni^I intermediate (**E**) and subsequent oxidative addition of an aryl halide onto this species provides a Ni^{III} intermediate (**F**) (Figure 1.2 A).[14] This Ni^{III} intermediate (**F**) could also be accessed through the reverse order of events (oxidative addition followed by radical capture), depending on the nature of the electrophile. In any event, reductive elimination of the carbon fragments provides the desired product along with a Ni^I halide species (**G**), which is reduced back to Ni^0 (**D**) by the reduced photocatalyst in the photoredox cycle.

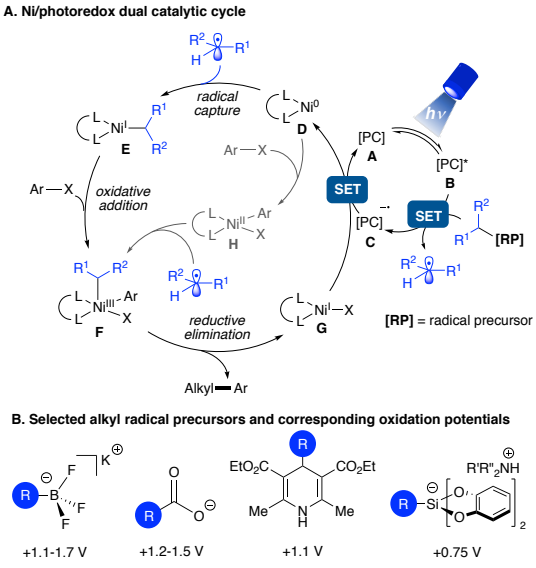

Figure 1.2. Net-neutral Ni/photoredox dual catalytic cycle (A) and common radical precursors (B).

The inherently mild nature of this reaction has permitted unprecedented retrosynthetic disconnections to be established. Even more impressive than its mild conditions, this dual catalytic system is extraordinarily modular. An array of radical precursors originating from feedstock chemicals such as organoboron reagents, carboxylic acids, aldehydes, and organosilanes has been employed in these transformations (Figure 1.2 B). Since the initial disclosures in this area, the general pathway depicted in Figure 1.2 has been adapted for the arylation, vinylation, acylation, and alkylation of these alkyl radical precursors. Because of the relative "blindness" of the reaction pathway to the origin of the radical, even alkyl radicals arising from hydrogen atom transfer (HAT) processes can be employed in these cross-couplings.

Owing to the sheer number of Ni-catalyzed transformations that proceed through photochemical paradigms,[9,15] the following discussion conveys an overview of seminal developments in photoredox reactions that use C(sp^3) radicals to forge carbon-carbon bonds through Ni-catalyzed arylation and acylation manifolds. Photoredox reactions that accomplish carbon-heteroatom coupling or that employ other metals are therefore excluded. Processes that form carbon-carbon bonds through Ni-catalyzed vinylation,[15] Ni-catalyzed C(sp^3)–C(sp^3) alkylation,[15] as well as non-metal catalyzed photoredox mechanisms such as the Giese addition,[16] proton-coupled electron transfer (PCET),[17] radical/polar crossover processes,[18] the Minisci reaction,[19] or cycloadditions,[20] although useful in their own right, are also not discussed in this subchapter.

1.1.2 Alkyl-aryl cross-couplings

A longstanding challenge for transition-metal cross-coupling has been the construction of alkyl-aryl linkages under mild conditions and with broad functional group tolerance. The seminal work in the field of Ni/photoredox dual catalysis reported methods for the cross-coupling of alkyl

radical precursors with aryl halides.[10] Subsequently, multiple strategies for C(sp^3) radical generation have been developed. Some approaches rely on redox-active groups, such as alkyltrifluoroborates, carboxylates, bis(catecholato)silicates, and alkyl 1,4-dihydropyridines (1,4-DHPs), to achieve programmed reactivity (Figure 1.2 B), and others utilize the innate reactivity of substrates (via hydrogen or halogen atom transfer) to generate alkyl radicals. Radicals originating from the oxidation of sulfinate salts,[21] xanthates,[22] and α-silylamines[23] have also been employed in this cross-coupling strategy, although they are not discussed in this subchapter.

- **Couplings with alkyltrifluoroborates**

Alkyltrifluoroborates are a class of readily prepared, bench-stable reagents that have gained prominence over the past two decades.[24] The enhanced polarity of the carbon-boron bond in these salts allows the controlled, *in situ* hydrolytic generation of boronic acid derivatives that would be difficult or impossible to isolate. Despite the advantages of these reagents, the palladium-mediated cross-coupling of alkyltrifluoroborates is beset by the characteristic limitations of C(sp^3) cross-coupling; namely, the forcing conditions required (elevated temperatures, stoichiometric base) and the susceptibility of these species to undergo β-hydride elimination.

In 2014, our group demonstrated the first photoredox/Ni dual catalytic system to construct C(sp^2)–C(sp^3) linkages under remarkably mild reaction conditions with high functional group tolerance (Figure 1.3, entry 1).[10a] In this seminal report, we established that benzyltrifluoroborates (E_{red} = +1.10 V vs SCE, on average) undergo oxidative fragmentation to deliver alkyl radicals that function as suitable partners in Ni-catalyzed arylation. To probe the mechanistic intricacies of this unprecedented paradigm, density functional theory (DFT) calculations were conducted to deduce the order of radical addition to the Ni center with respect

to oxidative addition.[14] Although both mechanistic scenarios outlined in Figure 1.2 A give rise to an identical high-valent Ni(III) intermediate (**F**), the formation of alkylNi(I) species **E** through an initial radical capture event proceeds via a lower energy barrier. Subsequent reductive elimination and SET from the reduced state of the photocatalyst to a Ni(I) complex regenerates both catalytic cycles. Most notably, these calculations suggest that the stereodetermining step in this manifold is reductive elimination. As such, radical combination is governed by Curtin-Hammett conditions whereby one of two equilibrating diastereomeric Ni(III) intermediates proceeds to yield the desired C–C bond more rapidly. Utilizing a chiral bis(oxazoline) (BOX) ligand, modest enantioselectivity was observed (50% ee) when subjecting a racemic α-methylbenzyltrifluoroborate mixture to the reaction conditions.[10a] This observed stereoconvergence validated for the first time the merger of photoredox catalysis with asymmetric transition-metal-catalyzed cross-couplings.[10a] A general solution, however, to accomplish enantioselective cross-couplings remains challenging to date.

A wide array of alkyltrifluoroborates can be cross-coupled with aryl- and heteroaryl bromides using the dual catalytic manifold, including secondary alkyltrifluoroborates, which exhibit relatively high reduction potentials (E_{red} = +1.50 V vs SCE).[25] Based on this outcome, a unified approach toward the arylation of secondary alkyl β-trifluoroborato carbonyl substrates was designed as a complementary approach to existing synthetic routes (Figure 1.3, entry 3).[26]

A major feature of this Ni/photoredox dual catalytic cross-coupling method is the orthogonality of the single-electron oxidation of alkyltrifluoroborates to the palladium-mediated activation of arylboron reagents.[27] This was leveraged in an iterative cross-coupling approach, wherein rapid diversification of borylated arenes such as **17** was realized (Figure 1.3, entry 5).[28]

In an effort to target pharmaceutically relevant structural motifs, conditions for coupling α-alkoxy-,[29] α-amino-,[30] α-hydroxyalkyl-,[31] and α-trifluoromethyltrifluoroborates[32] were developed (Figure 1.3, Entries 4-8). In the latter case, the reaction represents the first general route toward unsymmetrical 1,1-diaryl-2,2,2-trifluoroethanes such as **26**. The intrinsically low nucleophilicity of α-CF_3 organoboron reagents and the propensity for β-fluoride elimination rendered conventional Pd-catalyzed cross-coupling protocols unfeasible.[33] Other organoboron derivatives can be employed in these couplings, as illustrated by a protocol for the cross-coupling of benzylboronic pinacol esters in continuous flow by Ley and coworkers.[34]

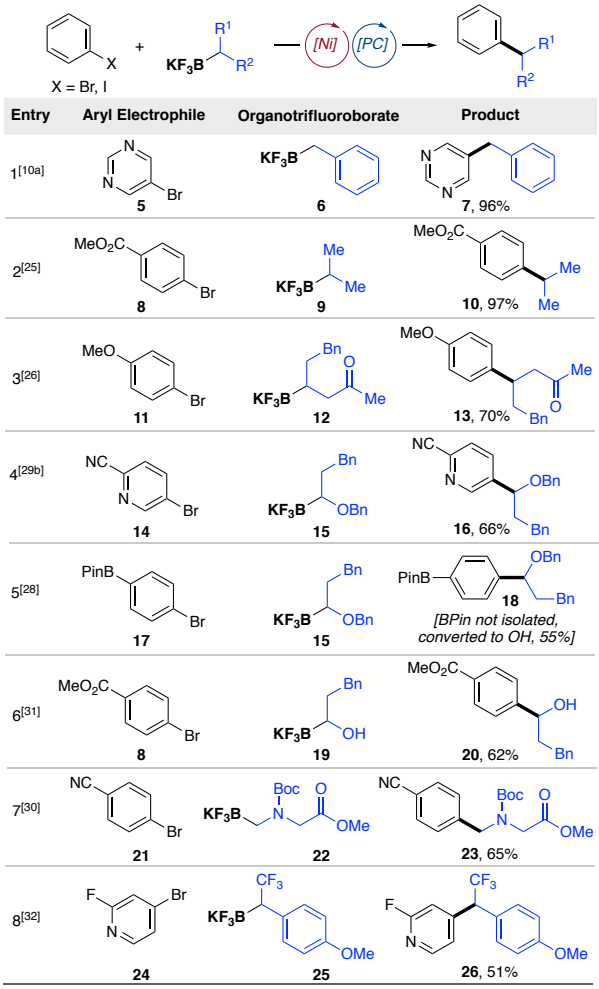

Figure 1.3. Alkyl-aryl dual cross-couplings using alkyltrifluoroborates.

More recently, a strategy was reported for the installation of challenging arylated quaternary carbon centers using tertiary alkyltrifluoroborates (Figure 1.4).[35] High-throughput screening[36] was critical for identifying a unique ligand, 2,2,6,6-tetramethylheptanedione (TMHD), that enabled the cross-coupling of these sterically-hindered radical species. Although the aryl halide scope was limited to electron-withdrawing and electron-neutral arenes (likely because of poor oxidative addition rates), the types of 3° alkyl fragments that could be installed were diverse. Further, this shortcoming is not surprising given relevant precedents on the coupling of tertiary pinacol boronates with electron-rich arenes.[37]

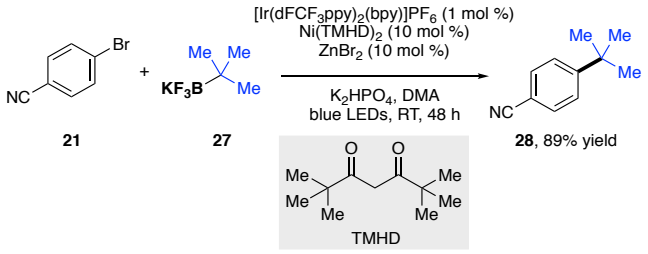

Figure 1.4. Cross-coupling of tertiary alkyl fragments.

■ Couplings with carboxylic acid radical precursors

Concurrent with our efforts to activate alkyltrifluoroborates using Ni/photoredox dual catalysis, carboxylic acids were demonstrated to undergo single-electron oxidative decarboxylation to generate C(sp^3)-centered radicals under a parallel mechanistic manifold.[10b] Carboxylic acids are highly attractive as radical precursors because of their synthetic accessibility and widespread commercial availability. Although transition-metal-catalyzed decarboxylative cross-couplings using aryl carboxylic acids are well-documented,[38] engaging aliphatic carboxylic acids in these two-electron pathways can be challenging. To overcome this limitation, a single-electron approach was undertaken by using $NiCl_2$(dme)/dtbbpy in combination with the

photocatalyst [Ir(dF(CF$_3$)ppy)$_2$(dtbbpy)](PF$_6$) to forge the desired C(sp^2)-C(sp^3) bond.[10b] This protocol is effective with secondary-, benzylic-, α-amino-, and α-oxy carboxylic acids with aryl iodides, -bromides, and -chlorides (Figure 1.5 A). An enantioselective arylation of α-amino acids was subsequently reported.[39] By employing ligand **37** (Figure 1.5 B), the stereoconvergent synthesis of benzylamine **36** was accomplished.

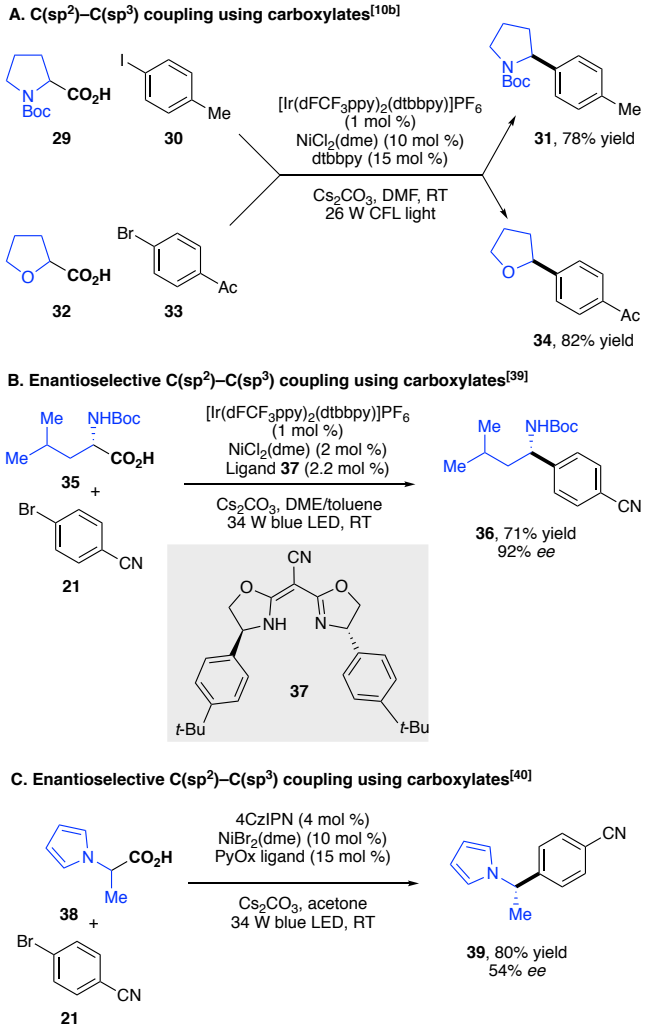

Figure 1.5. Alkyl-aryl cross-coupling using carboxylic acids.

Under a similar paradigm, Davidson and co-workers developed an enantioselective synthesis of *N*-benzylic heterocycles from stabilized carboxylic acids using an organic photocatalyst and a chiral pyridine-oxazoline (PyOx) ligand (Figure 1.5 C).[40] Limitations in the electronic profile of the electrophile persist, with trace product observed in the case of electron-rich aryl bromides.

Alcohols, activated *in situ* with oxalyl chloride, have also been used in alkyl-aryl cross-coupling (Figure 1.6).[41] The oxalic acid redox handle functions analogously to carboxylic acids. After deprotonation and single-electron oxidation, two successive decarboxylation events occur to form an alkyl radical that is engaged in cross-coupling. More recently, innovative approaches to engage alkyl carboxylic acids in Ni/photoredox cross-coupling have been developed, including those that use flow chemistry.[42]

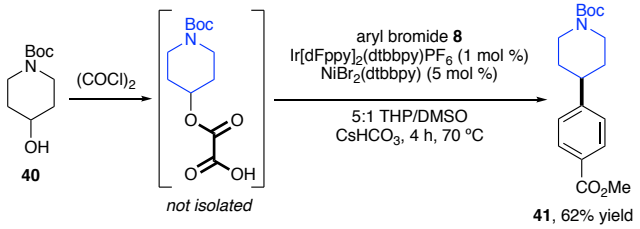

Figure 1.6. Alkyl-aryl cross-coupling using activated alcohols.

■ Couplings with alkyl bis(catecholato)silicates

Alkyltrifluoroborates and carboxylic acids that result in primary, non-stabilized radicals are challenging to oxidize, and consequently, their use in Ni/photoredox cross-coupling is sometimes challenging.[9a] New classes of radical precursors with lower oxidation potentials were therefore sought. Specifically, molecules were designed in which a redox-active group would provide an "antenna" for SET processes to occur, facilitating a homolytic scission of a Si–C bond. One class of precursor that was readily identified were alkyl bis(catecholato)silicates.

Although encumbered by suboptimal atom-economy, these reagents are bench-stable, crystalline solids or powders that possess low oxidation potentials (E_{red} = +0.75 V vs SCE), allowing the use of less oxidizing (and inexpensive) photocatalysts.[43]

In 2015, a Ni/photoredox-catalyzed C(sp^2)-C(sp^3) cross-coupling between 4-bromobenzonitrile and a series of alkyl bis(catecholato)silicates possessing potassium 18-crown-6 counterions was reported.[44] These silicate coupling partners incorporated a variety of functional groups, including esters, nitriles, oxiranes, and halides (Figure 1.7 A).[45] Concurrent with these studies, cross-coupling protocols with bis(catecholato)silicates bearing more practical and less expensive (albeit more acidic) alkylammonium counterions (analogous to the previously reported aryl variants,[46] Figure 1.7 B) was developed.[47] Couplings with these reagents display exquisite chemoselectivity when dihalogenated arenes were used as coupling partners (Figure 1.7 C).[48] This class of radical precursors has also been cross-coupled with borylated aryl bromides[49] as well as aryl triflates, -tosylates, and -mesylates.[50]

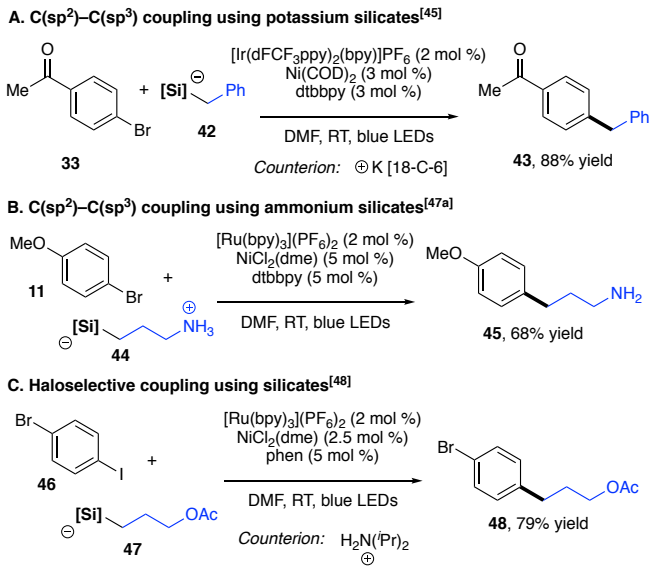

Figure 1.7. Alkyl-aryl cross-coupling using potassium- and ammonium silicates.

■ Couplings with 1,4-DHP radical precursors

Another class of radical precursors that has been investigated is 1,4-DHPs. DHPs are typically bench-stable solids that can be prepared in a single step from the corresponding aliphatic aldehyde, the widespread commercial availability of which make DHPs highly accessible radical feedstocks.[51] These heterocyclic species can be thought of as residing at a thermodynamic local minimum, primed to become fully aromatic pyridines through a facile photoredox-catalyzed oxidation (E_{ox} = +1.05 V vs SCE, on average).[52,53] Indeed, many long-utilized methods for the synthesis of substituted pyridines pass through DHP intermediates and require stoichiometric oxidants to achieve aromaticity. It therefore comes as no surprise that photocatalytic SET oxidation occurs with ease.[52c] DHPs bearing 4-alkyl substituents readily undergo oxidative fragmentation to extrude alkyl radicals,[53] and these radicals have been shown to participate in transformations such as aromatic substitution.[54]

Two groups,[55,56] have reported the cross-coupling of aryl halides and alkyl DHPs. One employed a basic additive to deprotonate the DHP and form a more easily oxidized anionic species (Figure 1.8 A). The second was able to omit the basic additive by employing the more oxidizing 4CzIPN photocatalyst (Figure 1.1 B). Both sets of conditions allow the cross-coupling of various alkyl radicals with either aryl bromides or -iodides. Saccharide-derived DHPs can also be used in the Ni/photoredox cross-coupling cycle to afford reversed *C*-aryl glycosides such as **53** (Figure 1.8 B).[57] The latter substrate would be prone to β-elimination using traditional cross-coupling methods. A recent report indicated the possibility of direct photoexcitation of DHPs to trigger the formation of alkyl radicals in the absence of a photocatalyst (Figure 1.8 C).[58]

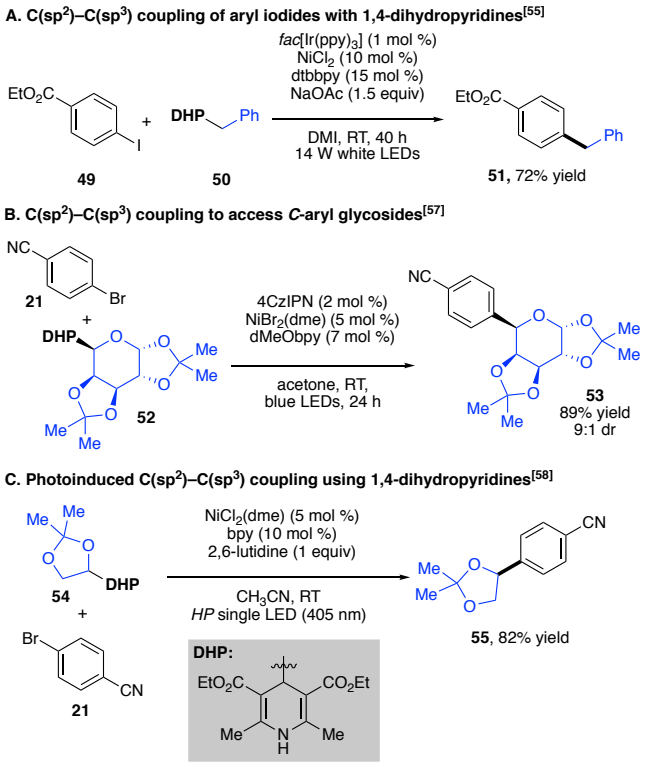

Figure 1.8. Alkyl-aryl cross-coupling using 1,4-DHPs.

■ Hydrogen atom transfer in the dual catalytic manifold

A key feature of Ni/photoredox dual catalysis is the relative "blindness" of the Ni cross-coupling cycle to the origin of the alkyl radical coupling partner. This allows compatibility with unique methods for alkyl radical generation, such as hydrogen atom transfer (HAT).[17b,59] HAT processes exploit the innate reactivity of saturated heterocycles possessing homolytically labile C–H bonds adjacent to heteroatoms. Regioselective hydrogen atom abstraction provides a heteroatom-stabilized radical that gets funneled into a Ni cross-coupling cycle. The major significance of this approach is that radical generation *via* HAT obviates the need for a pre-functionalized alkyl radical precursor, thus enabling highly atom economical cross-coupling processes.

In 2016, two groups reported that Ni/photoredox cross-couplings can be initiated by hydrogen atom abstraction of ethers (Figure 1.9, entries 1-2).[60,61] Experimental evidence suggests that the couplings proceed through stable and isolable Ni^{II} aryl halide oxidative addition complexes (**I**, Figure 1.10 A). Photoexcitation of these complexes in the presence of ethers or amines, typically as the solvent, promotes C–H cleavage to form the coupled product. Dioxolane **59** is also amenable to HAT/cross-coupling, which provides a mild and redox-neutral method to access masked aldehydes (Figure 1.9, entry 3).[62]

Entry	Substrate	Aryl Halide	HAT agent	Product
1[61]	**56**, (solvent)	**21**	Br•	**57**, 89%
2[60]	**56**, (solvent)	**58**	Cl•	**57**, 83%
3[62]	**59**, (solvent)	**60**	Cl•	**61**, 76%
4[66]	**62**	**63**	TBADT **64**	**65**, 66%
5[63]	**66**	**33**	**67**	**40**, 84%
6[65]	**68**	**69**	**70**	**71**, 75%

Figure 1.9. Alkyl-aryl dual cross-couplings mediated by hydrogen atom transfer.

An alternative approach to accomplish HAT-initiated dual catalytic cross-coupling is the use of an amine reagent to conduct targeted H-atom abstraction (Figure 1.10 B). Thus,

quinuclidine derivatives were used to accomplish C-H arylation of pyrrolidine derivatives (Figure 1.9, entry 5).[63,64] This strategy has been extended to the C-H arylation of free alcohols. The latter transformation required the use of $ZnCl_2$ as a Lewis acid activator to achieve efficient hydrogen atom transfer (Figure 1.9, entry 6).[65] Alternative HAT agents, such as photoexcitable polyoxometalates, have been recently described.[66]

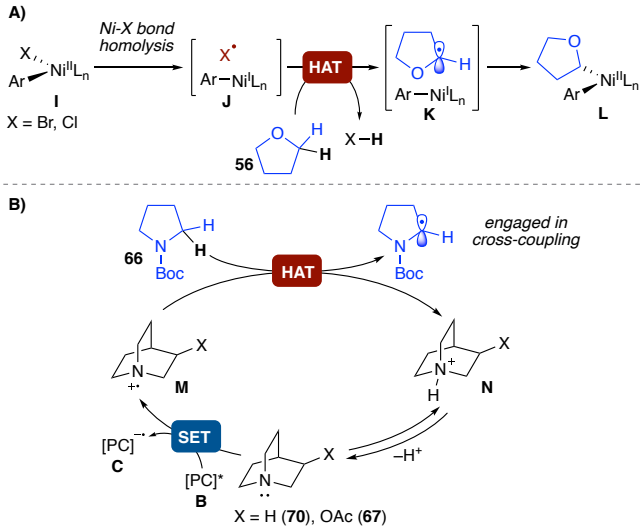

Figure 1.10. Pathways for hydrogen atom transfer.

■ Net-reductive alkyl-aryl couplings

Although most Ni/photoredox dual catalytic reactions occur through a redox neutral pathway, net-reductive transformations have recently gained considerable attention. These transformations are conceptually similar to Ni-catalyzed reductive cross-electrophile couplings.[11] By using a photoredox catalyst as an electron shuttle, the stoichiometric manganese and zinc reductants that are typically used to turn over the active Ni catalyst can be replaced by homogeneous, organic reductants including amines, Hantzsch esters, or silanes. The process proceeds through a similar series of mechanistic steps as the redox-neutral variants (Figure 1.11).

The major distinction is that the photocatalyst cycle is turned over by a terminal reductant and that the radical precursor is reduced by a Ni^0 intermediate and/or the excited state photocatalyst to generate the alkyl radical for metalation.

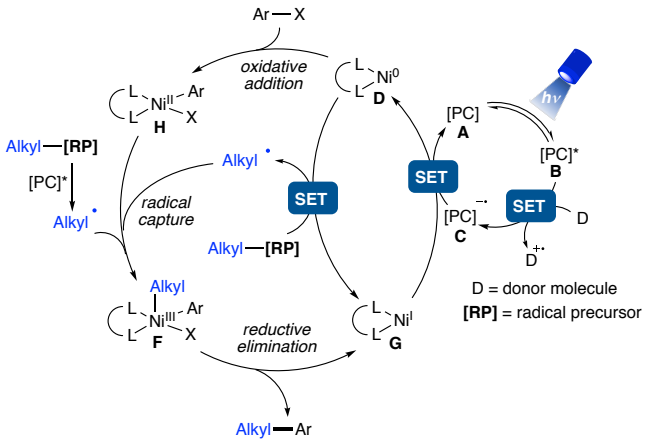

Figure 1.11. Net-reductive Ni/photoredox cross-coupling cycle.

To accomplish the photocatalytic, net-reductive cross-electrophile coupling of alkyl bromides and aryl halides, silanes and amines have been used as terminal reductants (Figure 1.12). In the first entry, oxidation of tris(trimethylsilyl)silane was employed as an electron source to enable the reductive generation of radicals from alkyl bromides. The reaction could proceed by either direct reduction of the alkyl halide or, more likely, halogen atom abstraction. Overall, both pathways result in a net reductive catalytic cycle. This method was used to couple heteroaryl bromides with various functionalized 1º, 2º, and even 3º alkyl bromides.[67] Other reductive systems employ amines as terminal reductants to achieve couplings similar to those of alkyl bromides.[68] Notably, the use of bathocuproine **76** (entry 4) as a Ni ligand promotes sequential β-hydride elimination and migratory insertion events to form a more stabilized benzylic Ni^{II} complex that generates diarylmethine **75** upon reductive elimination.[69]

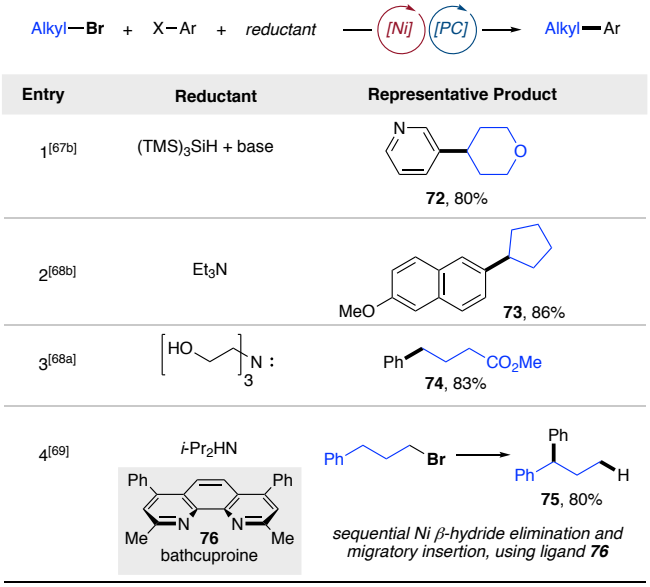

Figure 1.12. Net-reductive Ni/photoredox cross-couplings of alkyl bromides and aryl halides.

In addition to the use of alkyl bromides as radical precursors, we have recently reported a photocatalytic, net-reductive cross-electrophile coupling of (het)aryl bromides and Katritzky salts, prepared *via* condensation of the corresponding amines with a commercially-available pyrylium salt.[70] Under this catalytic manifold, the photocoupling of C(sp^3)-hybridized centers, stemming from amine feedstocks, with diverse aryl halides can be accomplished using the organic dye 4CzIPN and triethylamine as the terminal reductant.

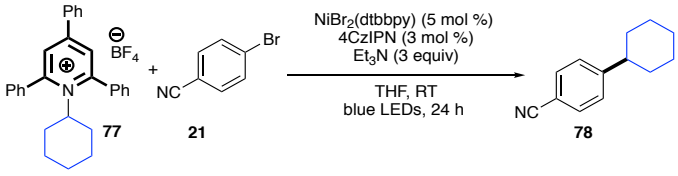

Figure 1.13. Net-reductive Ni/photoredox cross-couplings of Katritzky salts and aryl halides.

An alternative approach to accomplish Ni-catalyzed reductive cross-couplings is the use of photoactive electron donor-acceptor (EDA) complexes.[71] Upon light excitation, an organic

electron donor serves as a potent photoreductant to deliver radical species from electron-deficient acceptor molecules. As part of its dual role, the organic donor modulates the oxidation state of the nickel catalyst to regenerate the active low-valent metal species, thus bypassing the need for exogenous photoredox catalysts. Taking advantage of this catalytic mode, our group recently reported a cross-electrophile decarboxylative strategy for the assembly of $C(sp^3)$–$C(sp^2)$ linkages from alkyl-*N*-hydroxyphthalimide esters (redox active esters, RAEs, readily prepared from the corresponding carboxylic acids). Under the developed conditions, the coupling of primary-, secondary-, stabilized α-oxy-, α-amino-, and benzylic radicals was accomplished using Hantzsch ester as the electron donor (Figure 1.14).[72]

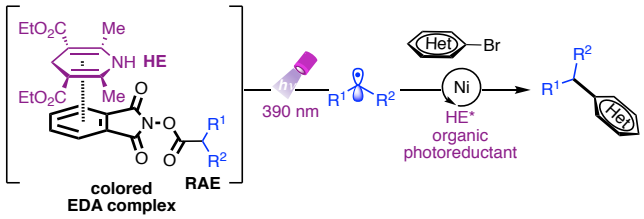

Figure 1.14. Net-reductive Ni-catalyzed cross-couplings with EDA complexes.

1.1.3 Alkyl-acyl cross-couplings

Ketones are a versatile functional group, capable of accessing myriad chemical motifs. One convergent strategy for ketone synthesis is through direct acylation of alkyl fragments. Typically, such disconnections employ reactive, nucleophilic organometallic reagents (as in the Weinreb ketone synthesis), inherently limiting both the scope and functional group compatibility of the transformation. Conversely, a catalytic method for the acylation of otherwise unreactive acyl- and alkyl fragments would provide rapid access to complex molecules and mark a clear improvement over the traditional nucleophilic acyl substitution chemistry.

The ability of organonickel intermediates to engage acyl electrophiles in oxidative addition has been reported.[73] Building on this work, Ni/photoredox dual catalysis was employed to couple numerous acyl electrophiles with alkyl radical precursors. As a testament to the modularity of the catalytic system, multiple classes of both acyl electrophiles (acyl chlorides,[74] acyl imides,[75] anhydrides,[76] isocyanates,[77] and thioesters[76d]) and radical precursors have been engaged within the reaction manifold. Achieving selective acyl transfer when using mixed anhydrides can prove challenging because of the presence of two C(sp^2)–O bonds that must be differentiated by the Ni-catalyst. One strategy relies on the *in situ* formation of carbonic anhydrides (Figure 1.15, entries 4 and 5).

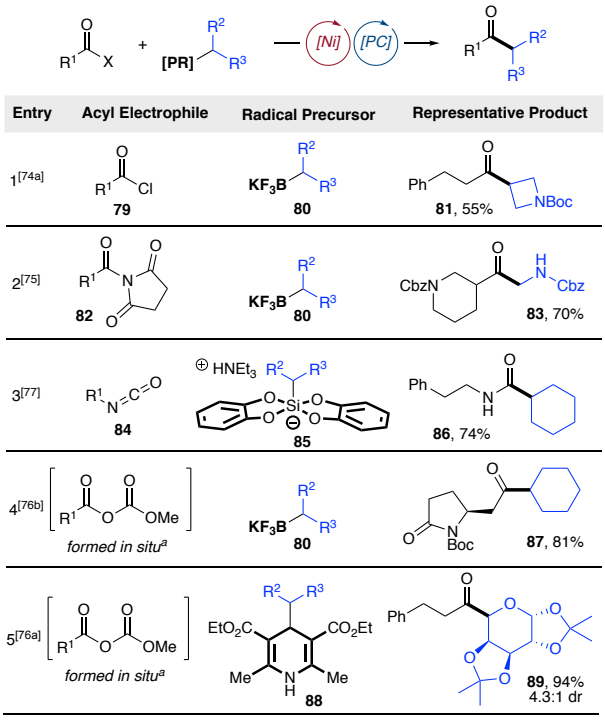

Figure 1.15. Acyl-alkyl cross-couplings. [a]Formed through the reaction of the corresponding acid with dimethyl dicarbonate.

In another approach, reactivity reminiscent of Tsuji-Trost chemistry is exploited to effect CO_2 extrusion from a pre-formed mixed anhydride.[76e] HAT strategies for acylation have also

been reported, including the coupling of aldehydes with alkyl bromides[78] and the synthesis of alkyl thioesters.[79] A Ni/photoredox-catalyzed cross-coupling of *meso*-anhydrides was reported to access phenylacetone derivatives such as **91** (Figure 1.16).[78c] The key stereodetermining step is the oxidative addition of the chiral Ni species onto the *meso*-anhydride. Although the transformation was limited to aliphatic anhydrides and benzylic trifluoroborates as radical precursors, it is notable as one of the few enantioselective Ni/photoredox dual catalytic transformations.

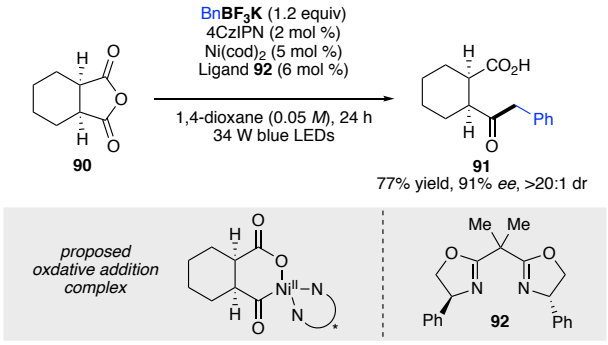

Figure 1.16. Desymmetrization of *meso*-anhydrides to effect acyl-alkyl cross-coupling.

1.1.4 Conclusion

In a very short period of time, Ni/photoredox dual catalysis has become a workhorse for the construction of an array of carbon-carbon bonds. Many of the bond disconnections achievable by this method could not be plausibly accomplished using traditional cross-coupling approaches. This, combined with the mild and modular nature of these reactions, enables the rapid generation of diverse chemotypes that possess a range of unprotected functional groups. In this manner, Ni/photoredox dual catalysis is a major contribution to the modern vision of "ideal" organic synthesis,[80] wherein highly functionalized molecules can be prepared with minimal protection/deprotection or redox fluctuation steps. The active and near immediate uptake of

Ni/photoredox cross-coupling in the industrial sector serves as a testament to both the utility and potential of this reaction paradigm.[41,81] Herein, efforts to expand the scope of electrophiles and radical precursors in Ni/photoredox dual cross-couplings are outlined. Additional fruitful results in the development of multicomponent reactions and radical-mediated synthesis for DNA-encoded libraries (DELs) are described.

1.2 Multicomponent Reactions: Radical/Polar and Radical/HAT Crossover Strategies[†]

The pursuit of efficient synthetic tools to assemble complex molecular architectures is of longstanding interest in organic synthesis. The disclosure of metallaphotoredox catalysis has offered new avenues for unique C–C bond disconnections, especially in the context of biologically relevant targets.[15,82] Through SET, the installation of C(sp^3)-hybridized centers under mild reaction conditions (weak bases, room temperature, near-neutral pH, and visible light) can be accomplished with excellent functional group tolerance.[15,82] Owing to the enhanced solubility and specificity in clinical candidates bearing C(sp^3) centers, Ni/photoredox dual catalysis has found extensive application in the medicinal chemistry community.[5] As outlined in Chapter 1.1, although progress has been made, the vast majority of these dual catalytic processes forge exclusively one C–C or C–heteroatom bond.[82] In this vein, the development of multicomponent transformations from commodity chemicals has the potential to yield greater atom economy, dramatically increase molecular complexity, eliminate sequential independent transformations, and enhance reaction simplicity.[83]

An attractive subset of multicomponent reactions are vicinal difunctionalizations, enabling the installation of two carbon- and/or heteroatom-based entities across unsaturated systems in one synthetic step (Figure 1.17).[84,85,86,87] Despite recent advances in this arena, conventional two-electron 1,2-difunctionalizations rely on the use of organometallic reagents, elevated temperatures, and expensive metal catalysts.[84,85,86,87] Seminal research from the groups of Baran,[88] Zhang,[89] Nevado,[90,91] Giri,[92] Chu,[93] and Wang,[94] among others,[95] has demonstrated the potential of conjunctive radical- and transition-metal-based cross-couplings as enabling tools to

---

[†] Reproduced in part with permission from S. O. Badir, G. A. Molander, *Chem* **2020**, *6*, 1327–1339. Copyright 2020, Elsevier.

address the aforementioned challenges. However, these transformations in large part operate using stoichiometric metal reductants, with associated characteristics that would benefit from complementary reactivity modes. More recently, the development of 1,2-difunctionalizations with the aid of a photocatalyst[96] has expanded the scope of disubstituted products. A formidable challenge, however, associated with transition-metal-based sequential reactions is β-hydride elimination from alkylmetal intermediates, particularly for unactivated alkenes, limiting the use of C(sp^3)-hybridized reagents.[84,87] Additional deleterious pathways such as homocoupling of radical species, isomerization, or proto-demetalation further complicate these processes.[84,87]

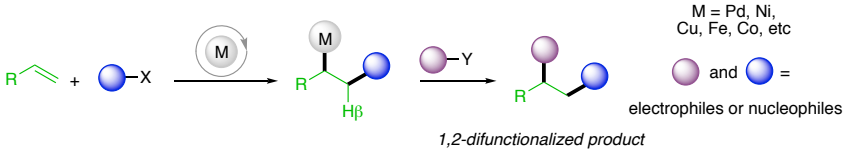

Figure 1.17. Transition-metal-catalyzed 1,2-difunctionalization of olefins.

Among the numerous unique features of photoredox catalysis is the inherent ability to access both radical and polar reaction intermediates within the same overall mechanistic paradigm.[18d] To advance the field of synthesis, radical/polar crossover (RPC) has recently been enlisted to facilitate the assembly of structural motifs with a high density of pendant functional groups through sequential bond-forming processes under mild reaction conditions (Figure 1.18).[18d] Governed by RPC pathways, high-energy radical species are generated through SET events and subsequently engage in odd-electron transformations.[18d] Through single-electron oxidation or reduction steps, the newly formed radical intermediates enter the two-electron reaction domain for further functionalization. In particular, RPC protocols can be categorized as net-neutral, net-oxidative, or net-reductive reactions.[18d]

Of pertinence to the research described herein, net-neutral RPC proceeds through single-electron oxidation and reductions steps occurring between the photoredox catalyst and reaction components, thus bypassing the need for exogenous oxidants or reductants and providing a low barrier for practical implementation.[18d] In general, net-neutral RPC can operate through two distinct mechanistic scenarios: reductive or oxidative quenching modes (Figure 1.18). In the reductive quenching pathway, the excited state photocatalyst initially undergoes single-electron reduction by a suitable electron donor. Oxidative-based homolytic cleavage of this precursor then generates reactive radical species that engage in further transformations. At this juncture, another SET event between the radical intermediate and the reduced state photocatalyst produces an anionic intermediate that can be quenched with diverse electrophiles. As a complementary reactivity mode, oxidative quenching[18d] is characterized by an initial reduction of the radical precursor. Upon radical-based diversification, the radical intermediate is oxidized to a cationic species that can be trapped by a suitable nucleophile through intermolecular or intramolecular reactions.

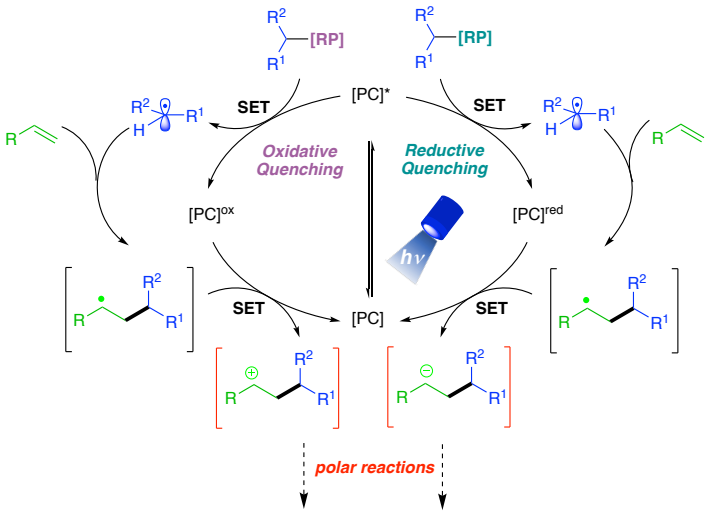

Figure 1.18. Net-neutral radical/polar crossover: reductive and oxidative quenching modes.

In a slight departure, radical/HAT crossover can be envisioned in which radicals generated through SET events can participate in further alkylation with olefinic substrates, prior to undergoing hydrogen atom termination (HAT, Figure 1.19 A).[59b] As a result, selective hydroalkylation and hydroarylation can be accomplished. This mechanistic paradigm is particularly advantageous to achieve the hydrocarbofunctionalization of trifluoromethyl-substituted alkenes, whereby the formation of anionic intermediates through radical/polar crossover or the presence of alkylmetal complexes can lead to competitive β–F elimination (Figure 1.19 B). Depending on the nature of the radical precursor and the overall mechanistic pathway, the alkylation of these electrophilic alkenes can generate one of two medicinally relevant scaffolds: *gem*-difluoroalkenes[98] or benzylic trifluoromethyl subunits.[99,100]

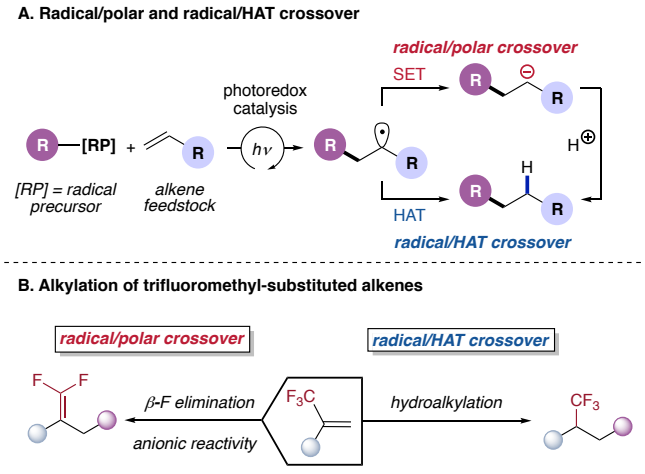

Figure 1.19. Radical/polar and radical/HAT crossover strategies toward the alkylation of trifluoromethyl-substituted alkenes.

In conclusion, photoinduced net-neutral radical/polar and radical/HAT crossover have revolutionized the way chemists think about constructing small organic molecules.[18d] Our research group has been at the forefront of these enabling techniques,[18d] and parts of the research

presented herein harness photochemically generated radical and ionic intermediates to accomplish the synthesis of medicinally relevant scaffolds with high content of $C(sp^3)$ carbons.

1.3 Photoredox-Mediated Alkylation for DNA-Encoded Libraries[†]

1.3.1 Introduction

Bridging the gaps between biology and chemistry, small organic compounds remain at the core of discovery research in the pharmaceutical and agrochemical industries.[101] The global pharmaceutical industry invests an estimated $150 billion annually toward the advancement of safe, effective, and affordable therapeutics to combat human diseases (https://www.ifpma.org/wp-content/uploads/2017/02/IFPMA-Facts-And-Figures-2017.pdf). Traditionally, high-throughput screening (HTS)[102] and phage display[103] have played prominent roles in hit identification. These efforts, however, are flawed by their sheer cost and time-intensive labor.[102,103] In recent years, DNA-encoded library (DEL) technology has emerged as an enabling tool in the drug discovery field, featuring an incredibly convenient and rapid way to assess the potential efficacy of billions of chemical compounds (Figure 1.20).[104-108] Thus, extremely large libraries can be assembled and screened against a biological target in a single experiment, bypassing the need for special infrastructure. Additionally, DEL platforms afford a time-saving and cost-effective screening format. Compared to the roughly $2 billion spent on HTS campaigns of millions of compounds contained in extant pharmaceutical libraries, the general cost associated with the assembly and screening of a DEL library of 800 million compounds is about $150,000 ($0.0002 per library member).[109]

[†] Reproduced in part with permission from S. Patel, S. O. Badir, G. A. Molander, *Trends Chem.* **2021**, *3*, 161–175. Copyright 2020, Elsevier.

The overall goal in DEL technology is to sample as much chemical space as possible in an effort to increase the probability of hit identification.[110-121] Initially, "split and pool" synthesis attaches building blocks to unique DNA barcodes, after which further diversification can be carried out. Separate reactions are pooled together and then re-arrayed for further building block addition. Multiple cycles of reactions can be performed consecutively to introduce additional units. Following DEL synthesis, the assembled compounds are incubated with the biomolecular target affixed to a solid support (polymer or resin). Low affinity ligands are washed away, after which the DNA barcode of the remaining high affinity ligands can be PCR-amplified for hit identification by sequencing the DNA "barcode" associated with each small molecule building block. To grow DEL platforms, library members should ideally possess functional handles for derivatization. The presence of DNA, however, imposes restrictions on the types of chemical transformations that are amenable to DEL environments. These constraints include the necessity of mild, aqueous, and dilute conditions. Therefore, robust reaction optimization is crucial to the development of DEL-compatible methods.

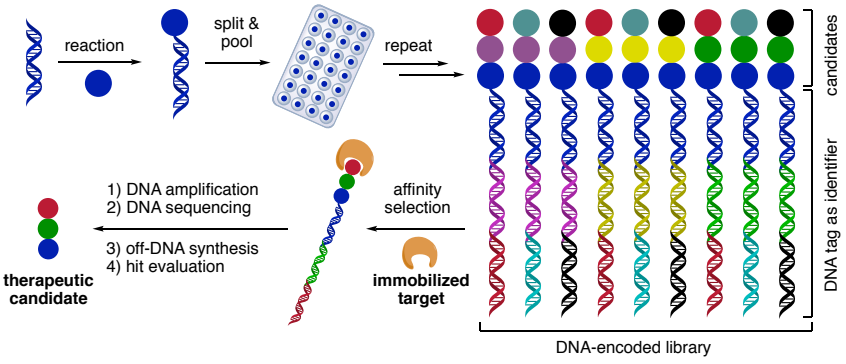

Figure 1.20. Overview of DNA-encoded library (DEL) technology.

To address these limitations, photoredox catalysis has been enlisted to enable a variety of mild on-DNA modifications using photoexcitable catalysts that harness visible light to assemble

challenging structural motifs.[122] Traditionally, palladium-catalyzed two-electron cross couplings with alkyl partners involve harsh reaction conditions and elevated temperatures.[123] Photocatalytic strategies have the potential to revolutionize DEL chemistry, as they are inherently mild, occur mostly at room temperature and without pyrophoric reagents, and the open shell intermediates are able to react productively in aqueous media. The following discussion seeks to highlight recent milestones in photoinduced alkylation processes in DEL platforms.

1.3.2 Emerging DEL successes

Although DEL technology has been adapted only recently in pharmaceutical settings, it has already given rise to novel drug candidates. In 2016, GSK employed their 7.7 billion-member DEL platform to identify a potent inhibitor of receptor interacting protein 1 (RIP1) kinase, which plays a prominent role in regulating cell death and inflammation. As a result of this screening, a benzoxazepinone inhibitor (GSK 481) was selected as the lead compound.[108] Another DEL success was reported in 2017 when AstraZeneca, Heptares Therapeutics, and X–Chem recognized the role of protease-activated receptor 2 (PAR2) in the treatment of many cancers and inflammatory diseases, and they sought to employ DEL technology to identify a high-affinity inhibitor.[124,125] This led to the identification of AZ3451, a potent and selective allosteric antagonist of PAR2. Additional emerging success stories from academic groups have also been reported recently.[126-129]

1.3.3 Ni/photoredox dual catalysis

Recently, the adaptation of Ni/photoredox dual manifolds in DEL synthesis has enabled the incorporation of a diverse pool of alkyl feedstocks, including aliphatic carboxylic acids,[130-132] α-silylamines,[133] alkyl 1,4-DHPs,[130] and aliphatic bromides.[133,134] The success of this integration is owed in large part to the mild nature of photoinduced alkylation pathways, whereby odd-

electron intermediates, generated in a regulated fashion, are able to operate under high dilutions (~ 1 mM) and in the presence of air and water (~20% by volume).[14,135] Excess reagents are leveraged to induce selectivity in DEL reactions typically carried out on minute scales (~25 nmol). In this section, milestones in Ni/photoredox dual cross-couplings in DEL platforms are highlighted.

- **Carboxylic acids**

Carboxylic acids are an important class of radical precursors because of their versatile and abundant nature. In particular, these multifunctional building blocks allow an overabundance of diversifications in DEL settings. In collaboration with scientists at GlaxoSmithKline, our group devised a cross-coupling protocol of amino acid derivatives with a wide array of DNA-conjugated (het)aryl bromides and -iodides to derive α-heterosubstituted products (Figure 1.21 A).[130] Remarkably, the reaction can be performed under blue light irradiation within 10 minutes and without the need for inert atmosphere. A large excess of base in the presence of a buffer system (TMG and MOPS pH 8, respectively) led to enhanced reactivity under aqueous conditions. Control experiments (no light, no Ni, no PC) demonstrated that all components were necessary for the reaction to proceed.

With respect to the cross-coupling scope, aryl iodides engaged effectively with complex *N*-Boc-protected derivatives under the developed conditions. Specifically, aryl systems encompassing tertiary amines and free aniline motifs were tolerated. Unfortunately, diminished reactivity was observed with electron-neutral and electron-rich aryl bromides. The use of more activated heteroaryl bromides proved successful in obtaining pyrrolidine- and indole-containing substrates.

Independently, Flanagan and colleagues at Pfizer demonstrated the merger of photoredox with nickel catalysis in aqueous media in the presence of a nickel precatalyst, employing a pyridyl carboxamidine ligand.[131] Under a similar mechanistic paradigm, cyclic and acyclic α-heterosubstituted products were obtained in excellent yields (Figure 1.21 B). Notably, the use of tertiary *N*-Boc-protected α-amino acids resulted in decreased yield, presumably because of steric congestion at the Ni center. Other scaffolds encompassing acidic carbamate protons displayed sluggish reactivity under the developed conditions. As a further extension of this water-compatible Ni-catalyzed manifold, the developed reaction conditions were applied to the cross-coupling of an aliphatic bromide, a secondary alkyltrifluoroborate, and an alkyl sulfinate salt. As highlighted, the scope of methods employing carboxylic acid precursors on DNA is largely limited to stabilized radical species (e.g., α-heterosubstituted amino acids). Another inherent limitation is the need for protecting groups for amine functional groups.

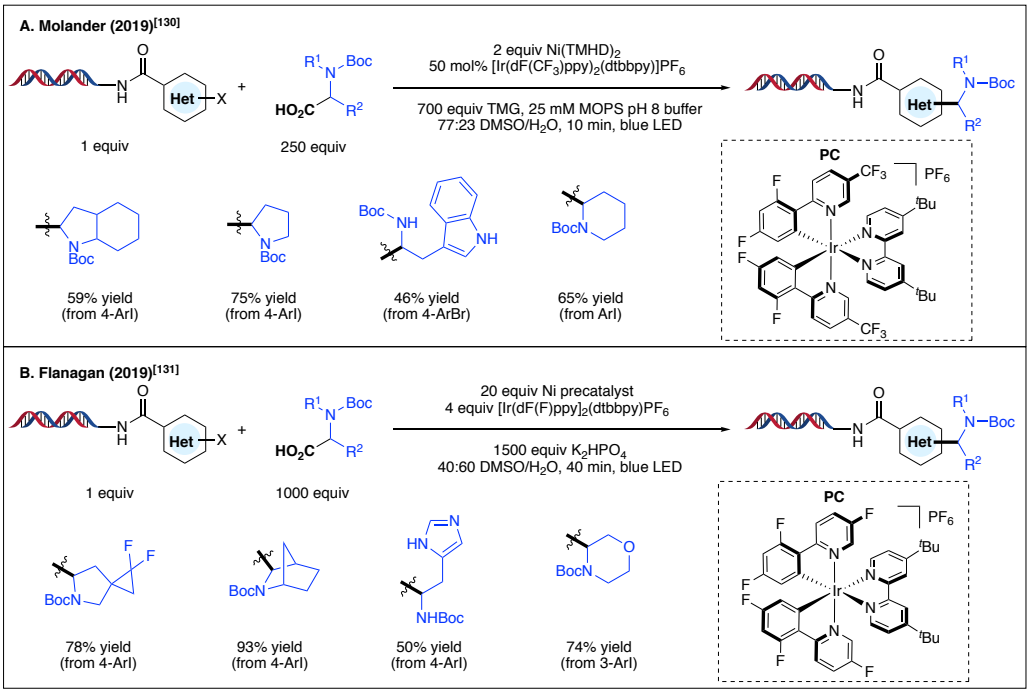

Figure 1.21. On-DNA Ni/photoredox decarboxylative arylation.

Critical to the success of DELs as a platform for ligand discovery in pharmaceutical settings is the integrity of the DNA tag. To probe the potential for radical-based DNA damage, Flanagan and colleagues conducted DNA ligation experiments followed by qPCR analysis.[131] It was determined that the DNA tag was not significantly damaged as a result of radical species or blue light irradiation in the absence of oxygen. Importantly, the amount of amplifiable DNA was comparable to a control sample that was not subjected to the metallaphotoredox-catalyzed cross coupling.

In another report, Novartis researchers reported a catch-and-release strategy using a cationic, amphiphilic PEG-based polymer to perform Ni/photoredox dual-catalyzed decarboxylative cross-couplings of DNA aryl halides.[132] This scope of this method was extended to non-stabilized primary and secondary radical architectures. However, diminished reactivity was observed with tertiary aliphatic carboxylic acids. With respect to the integrity of the DNA tag under the developed conditions, the authors determined that 48% of amplifiable DNA is recovered after release from the resin that was subjected to the photochemical decarboxylative arylation. The corresponding DNA substrate was competent in subsequent elongations.

- **Organosilanes**

To access free amine functional handles that allow direct derivatization in DEL platforms, the use of organosilanes as radical precursors was investigated because of their favorable redox potentials [E_{red} = ~ +0.4 – 0.8 V vs SCE].[23a,133] This class of reagents allows the introduction of aminomethyl subunits, a structural motif functioning as a pivotal linker embedded in pharmacologically active molecules.[23a] Importantly, silylamines can be readily synthesized by alkylation of diverse, commercially available amines with chloromethyltrimethylsilane. They can

also be accessed via reductive amination from commercially available aminomethyltrimethylsilane with assorted ketone and aldehyde feedstocks.[133]

Using an Ir-based PC under blue light irradiation, effective single-electron oxidation of electron-rich alkyl(trimethyl)silanes can be accomplished to yield silylaminomethyl radical cations (Figure 1.22).[133] Under aqueous conditions, rapid desilylation occurs to yield neutral α-aminomethyl radicals that intercept low-valent Ni species to furnish the desired product. Taking advantage of the low oxidation potentials of this class of reagents, scope elaboration using unprotected aminomethyl derivatives proved successful. Additionally, an organosilane stemming from proline served as a competent substrate with diverse (het)aryl halides, including systems encompassing *N*-Boc-protected amines, free anilines, and tertiary amines prone to SET oxidation under photoredox conditions.[70]

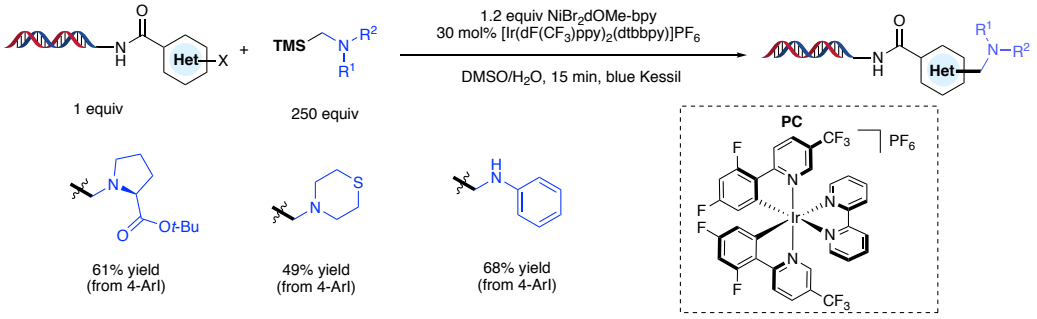

Figure 1.22. On-DNA Ni/photoredox aminomethylation of (het)aryl halides.

■ 1,4-DHPs

The introduction of 4-alkyl 1,4-DHPs in photoredox-mediated on-DNA alkylation efforts has expanded the structural feedstock amenable to DEL libraries to include aliphatic aldehydes, an abundant class of reagents. In 2019, our group demonstrated that 1,4-DHPs can be utilized as radical precursors for on-DNA Ni/photoredox cross couplings with diverse aryl bromides and -

iodides (Figure 1.23).[130] The use of the organic dye 4CzIPN as PC and $Ni(TMHD)_2$ as a user-friendly cross-coupling precatalyst resulted in the formation of the desired $C(sp^2)$–$C(sp^3)$ linkage under blue light irradiation. Typically, the major byproduct observed in this reaction stems from a protodehalogenation event of the corresponding aryl halides under aqueous conditions. The use of buffer to modify the pK_a of the reaction environment proved unsuccessful. With respect to the versatility of this method, DHPs bearing tertiary, secondary, and stabilized primary substituents showed excellent yields. Unfortunately, unactivated primary alkyl fragments or cyclopropyl motifs on the DHPs did not yield the cross-coupled product because of the high oxidation potentials associated with the instability of the corresponding radical. Of note, reversed *C*-aryl glycosides were synthesized from saccharide-derived aldehydes. As for the scope of the organic electrophile, electron-neutral aryl bromides showed diminished conversion, while aryl iodides bearing electron-donating functional groups showed high conversion.

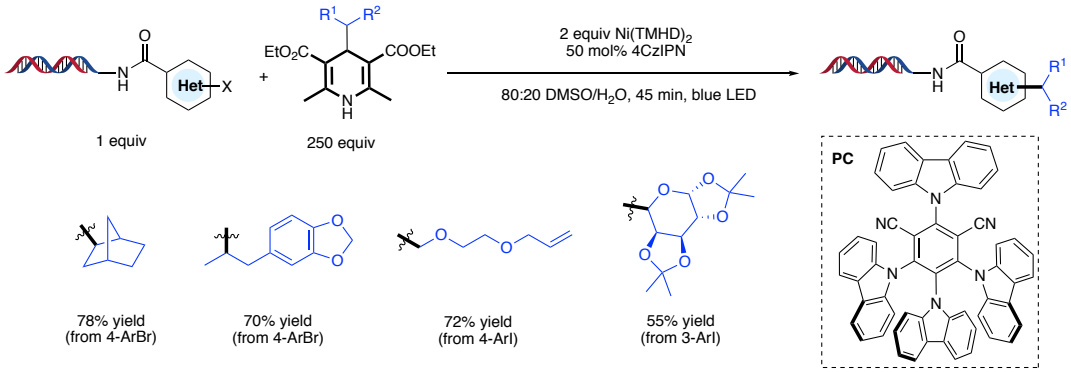

Figure 1.23. On-DNA Ni/photoredox alkylation using 1,4-dihydropyridines.

- **Alkyl bromides**

To access unactivated primary radical species, the use of alkyl bromides as commercially abundant feedstocks was examined.[133] These substrates undergo oxidative quenching, thereby necessitating the use of a terminal reductant.[68b,136] Traditional cross-electrophile couplings

employ a stoichiometric amount of zinc or manganese metal reductants.[137] Inspired by Lei and colleagues,[68b] a cross coupling of aliphatic bromides was developed with on-DNA conjugated aryl halides to furnish the desired $C(sp^2)$–$C(sp^3)$ bonds using triethylamine as a mild and benign reductant (Figure 1.24 A). To enhance selectivity in substrates displaying similar reactivity profiles, a large excess of the radical precursor was leveraged (250 equiv equating to only ~6 μmol of reactants). Of note, enhanced stabilization of the DNA phosphate backbone was achieved using bidentate Mg^{2+} ions, preventing undesired interactions with iridium. Under these conditions, a wide array of abundant and structurally diverse alkyl bromides was accommodated, with electronically distinct organic electrophiles. Significantly, alkyl bromides featuring bifunctional handles, such as nitriles and free alcohols, were incorporated, allowing further direct derivatization in DEL platforms. Finally, in collaboration with scientists at GlaxoSmithKline, our group evaluated the ability of the arylated products to undergo PCR amplification and sequencing.[133] In contrast to a no-light control reaction, the samples subjected to the photochemical conditions imposed no significant difficulty with respect to ligation, PCR amplification, quantification, or sequencing. These studies highlight the compatibility of photoredox-mediated alkylation with DEL synthesis.

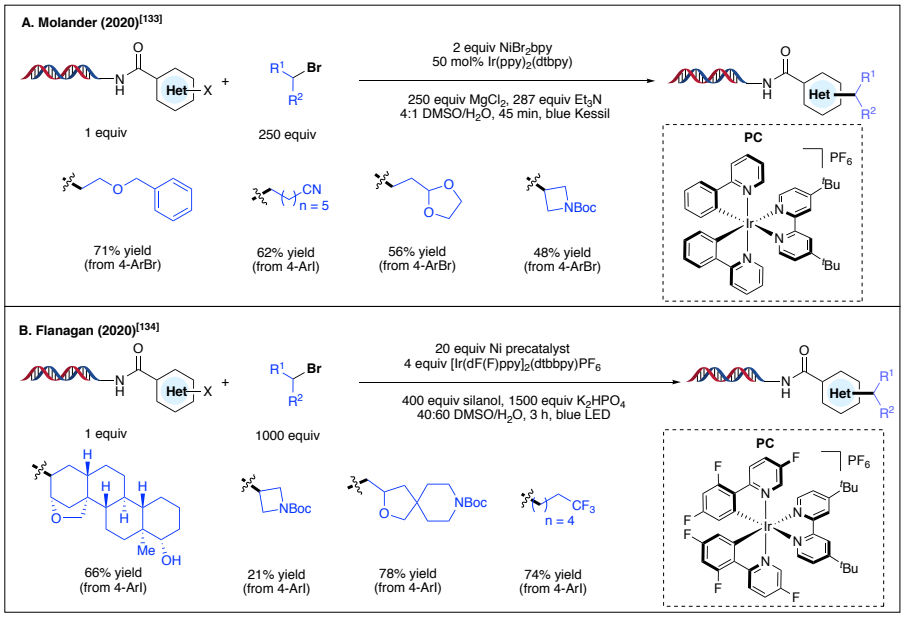

Figure 1.24. On-DNA Ni/photoredox alkylation using alkyl bromides.

Shortly after, Flanagan and colleagues independently devised a net-reductive on-DNA alkylation that proceeds through the intermediacy of a silyl radical intermediate (Figure 1.24 B).[134] In this transformation, excess inorganic base and silanol reductant[67b] were employed in conjunction with an Ir-based PC under blue light irradiation. This enabled the installation of spirocyclic amine substrates with high conversion to the alkylated product. Of note, natural product and biologically active scaffolds (a steroid and a pesticide, respectively) were successfully embedded into the cross-coupled product. With respect to DNA-tagged aryl halides, electron-rich and electron-deficient groups were amenable. Notably, sulfonamide and aliphatic cyclopropyl-substituted aryl electrophiles yielded considerable product. To probe DNA compatibility, using an elongated double-stranded DNA substrate (39 base pairs), the authors observed 96% ligation efficiency and 67% PCR amplifiability of the DNA tag upon elimination of residual nickel.

1.3.4 Photoinduced radical/polar crossover reactions

As depicted in Chapter 1.2, synthesis pathways empowered by photoredox catalysis have allowed rapid access to bioactive subunits.[18d] In particular, radical/polar crossover manifolds are attractive for achieving *gem*-difluoroethylene motifs.[97,138,139] These scaffolds function as synthetic carbonyl mimics, preserving the electronic and geometric nature of the C=O bond with inherent metabolic stability.[98a] In particular, fluorinated motifs are omnipresent in drug candidates as they lead to enhanced binding affinity, cell membrane transport, and cellular specificity.[140]

With several commercially available radical precursors and diverse trifluoromethyl-substituted alkenes, unexplored partners can be united in a regulated radical defluorinative alkylation to yield medicinally relevant *gem*-difluoroalkenes. Carboxylic acids,[130] silylamines,[133] alkylbis(catecholato)silicates,[130] and 1,4-DHPs[130] were studied as radical progenitors. Mechanistically, radicals are generated through oxidative fragmentation by the excited state (Figure 1.25 A). A subsequent radical addition occurs with the electron-deficient trifluoromethyl-substituted alkene, yielding an α-CF_3 radical. At this juncture, SET reduction of this latter species by the reduced state PC yields a carbanion, which undergoes E1cB-type fluoride elimination to form the desired *gem*-difluoroalkene. Alternatively, with electron-deficient alkenes, protonation of the α-carbanion occurs to furnish Giese-type adducts.[141]

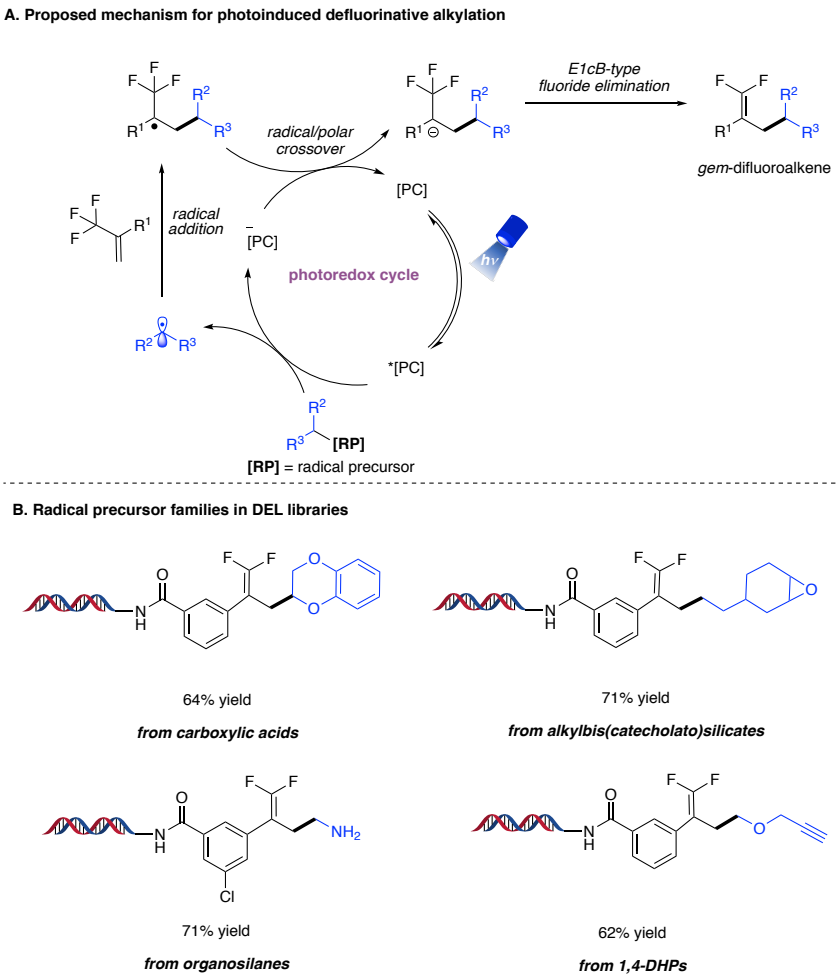

Figure 1.25. On-DNA defluorinative alkylation. (A) Proposed mechanism for photoredox-mediated defluorinative alkylation. (B) Selected examples of radical precursor families.

In the following section, photoredox-mediated radical/polar crossover methods are highlighted using various radical precursor feedstocks in conjunction with on-DNA tethered olefins (Figure 1.25 B).

■ Carboxylic acids

To harness the power of photoredox catalysis for DEL synthesis in other ways, our group demonstrated the use of carboxylic acids as radical precursors to access *gem*-difluoroalkenes from

on-DNA tethered trifluoromethyl-substituted olefins (Figure 1.25 B).[130] Given the importance of amino acids as bifunctional handles, their incorporation allows subsequent derivatization in DEL platforms. In the presence of an oxidizing Ir-based photocatalyst under blue light irradiation, diverse feedstocks including primary, secondary, and tertiary carboxylic acid derivatives were incorporated. In addition, heterocyclic α-amino acids, including pyridyl, imidazolyl, and benzothienyl groups afforded the desired product in good yields. Of note, Fmoc-protected acids and tertiary derivatives encompassing free alcohol functional groups were accommodated. With respect to the trifluoromethyl-substituted alkene scope, diverse substrates including chloroaryl- and pyridinyl-substituted alkenes reacted efficiently.

During the course of reaction optimization, we observed the formation of benzylic trifluoromethylated moieties, resulting from a protonation of the corresponding α-CF_3 carbanion under aqueous conditions.[130] Importantly, only trace amounts of this alkane were observed, even in the presence of acidic functional groups. In addition, high loadings of radical precursors resulted in a double addition to the corresponding *gem*-difluoroalkenes. Therefore, fewer equivalents of radical precursor (5-50 equivalents) were utilized to obtain the desired product selectively.

Independently, Flanagan and colleagues at Pfizer demonstrated a decarboxylative alkylation of α-amino acids in conjunction with DNA-tagged alkenes.[141] Using an inorganic base, effective decarboxylation of the corresponding acid using [Ir{dF(CF_3)ppy}$_2$(bpy)] was accomplished in under 6 hours of blue light irradiation. The scope was extended to thioethers and other heterocyclic α-amino acids. With respect to the DNA-tagged radical acceptor scope, α-substituted acrylamides, cyclic α,β-unsaturated ketones, and diverse styrene derivatives were all employed. Subsequently, the Liu group demonstrated a similar photochemical strategy using

Fmoc- and Boc-protected α-amino acids in conjunction with α,β-unsaturated ketones.[142] The scope was extended to stabilize α-oxy- and benzylic radical architectures. In a subsequent report, Mendoza and colleagues developed a decarboxylative alkyl coupling using NADH and BuNAH as potent organic photoreductants.[143] Employing electron-poor olefins in conjunction with secondary or tertiary *N*-hydroxyphthalimide-esters (prepared from carboxylic acid feedstocks), the alkylation protocol can be carried out under air- and water-compatible conditions. Finally, the decarboxylative coupling of α-amino acids and DNA-conjugated carbonyls has also been explored to generate 1,2-amino alcohols.[144] Under the developed conditions, no DNA damage was detected based on qPCR analysis and next-generation sequencing.

- **Organosilanes**

In 2020, our group demonstrated that α-silylamines can be subjected to radical/polar crossover defluorinative alkylation to induce *gem*-difluoroalkenes in DEL platforms (Figure 1.25 B).[133] Of note, the introduction of primary amine functional handles can be incorporated through the use of commercially available aminomethyltrimethylsilane as a radical precursor. Using 10 equivalents of the corresponding organosilanes, effective aminomethylation of the trifluoromethyl-substituted alkene is observed in less than 5 minutes of blue light irradiation. Structurally, a wide array of silylamines was efficiently integrated. Amino-acid-based organosilanes also provided excellent yields. Substrates with diverse functional groups, such as glycosides, oxetanes, pyridines, and amides show competent conversion to products.

- **Alkylbis(catecholato)silicates**

To expand the toolbox of alkyl feedstocks available to DEL chemists, our group demonstrated further the use of alkylbis(catecholato)silicates as radical precursors to access *gem*-difluoroalkenes under mild reaction conditions (additive-free and near-neutral pH, Figure 1.25

B).[130] In particular, this class of reagent allows the introduction of unactivated primary alkyl feedstocks as a result of favorable redox potentials.[47a] Similarly, upon radical generation using an organic photocatalyst variant, primary- and secondary alkylbis(catecholato)silicates showed high conversion. Some noteworthy examples included the incorporation of free urea, epoxide, and *N*-Boc amine scaffolds. Significantly, under higher loadings of the radical precursor, unactivated alkenes remained intact without subsequent addition, providing access to orthogonal reactivity in DEL settings.

- **1,4-DHPs**

Finally, the pool of radical precursors was further extended to include 1,4-DHPs (Figure 1.25 B).[130] Lower loading of the 1,4-DHPs (12.5 equivalents) compared to alkylbis(catecholato)silicates resulted in full consumption of the corresponding trifluoromethyl-substituted olefin. To demonstrate the versatility of this defluorinative alkylation process, glycosidic moieties and ether functional groups were incorporated. Of note, α-alkoxy motifs demonstrated that stabilized radicals are also compatible. Employing chloroaryl- and pyridinyl-substituted olefins provided good conversions to the desired product.

- **DNA compatibility**

As highlighted above, retaining integrity of the DNA tag during library synthesis enables accurate identification of building blocks and determination of their corresponding binding affinity. In collaboration with scientists at GlaxoSmithKline, our group evaluated the compatibility of the developed photochemical radical/polar crossover reactions in DEL settings.[130] Using three families of radical precursors, a 4-cycle tag elongated DNA headpiece was subjected to the defluorinative alkylation conditions. The corresponding samples imposed no significant challenges with respect to PCR amplification and quantitation. Remarkably, there was

no disparity with respect to the frequency of misreads between the alkylated products and the control samples (no light and no photocatalyst). These findings highlight the power of photoredox manifolds as enabling tools to further grow structural complexity in DELs.

1.3.5 Conclusion

The journey toward innovative drug discovery has overcome a significant challenge with the adaptation of DEL technology in pharmaceutical settings. Immense, uncharted chemical space can now be sampled using a single Eppendorf tube in one experiment, providing a time- and cost-effective format for hit identification. Small-scale, one-pot chemical transformations enable the rapid assembly of DELs with low barriers of implementation. In this vein, high affinity compounds can be pinpointed via PCR amplification and sequencing of the binder's DNA barcode. After identification, the compound can be synthesized off DNA and subsequently studied for biological activity, promoting further ligand design. Drugs that tackle humanity's most complicated diseases can be revealed in a drastically shorter time with the wide implementation of DEL technology.

Sampling as many unique chemical motifs as possible increases the probability of hit identification, enabling accelerated drug development. More recently, photoredox catalysis has provided exciting opportunities for unique synthetic disconnections toward biologically relevant molecules. In particular, Ni/photoredox cross-couplings have filled a void in DELs by increasing the fraction of $C(sp^3)$ fragments, which are known to enhance advantageous pharmacological characteristics. In addition, metal-free photoinduced radical/polar crossover pathways, as well as Giese-type additions, have facilitated the synthesis of underexplored motifs, including *gem*-difluoroalkenes, from on-DNA tagged trifluoromethyl-substituted olefins. Because of the diverse nature of amenable radical precursor families in DELs, photoredox-mediated alkylation enables

the introduction of multifunctional subunits that allow rapid derivatization in library settings. Herein, efforts in the development of photochemical carbofunctionalizations for DEL synthesis are described. In addition to work accomplished in the areas of radical/polar crossover and dual catalysis, the integration of photoactive electron donor-acceptor complexes as an enabling technology to increase molecular complexity in DELs is outlined.

1.4 References

(1) C. C. C. J. Seechurn, M. O. Kitching, T. J. Colacot, V. Snieckus. *Angew. Chem. Int. Ed.* **2012**, *51*, 5062–5085.

(2) (a) X.-F. Wu, P. Anbarasan, H. Neumann, M. Beller, *Angew. Chem. Int. Ed.* **2010**, *49*, 9047–9050; (b) Nobel Prizes 2010: Richard F. Heck / Ei-ichi Negishi / Akira Suzuki. *Angew. Chem. Int. Ed.* **2010**, *49*, 8300–8300.

(3) C. P. Casey, *J. Chem. Educ.* **2006**, *83*, 192–195.

(4) H. M. L. Davies, D. Morton, *J. Org. Chem.* **2016**, *81*, 343–350.

(5) (a) D. G. Brown, J. Boström, *J. Med. Chem.* **2016**, *59*, 4443–4458; (b) F. Lovering, *Med. Chem. Commun.* **2013**, *4*, 515–519; (c) S. D. Roughley, A. M. Jordan, *J. Med. Chem.* **2011**, *54*, 3451–3479.

(6) (a) J. Choi, G. C. Fu, *Science* **2017**, *356*, 152–160; (b) A. Rudolph, M. Lautens, *Angew. Chem. Int. Ed.* **2009**, *48*, 2656–2670.

(7) (a) D. Leonori, V. K. Aggarwal, *Angew. Chem. Int. Ed.* **2015**, *54*, 1082–1096; (b) L. Li, S. Zhao, A. Joshi-Pangu, M. Diane, M. R. Briscoe, *J. Am. Chem. Soc.* **2014**, *136*, 14027–14030; (c) A. He, J. R. Falck, *J. Am. Chem. Soc.* **2010**, *132*, 2524–2525.

(8) R. Jana, T. P. Pathak, M. S. Sigman, *Chem. Rev.* **2011**, *111*, 1417–1492.

(9) (a) J. C. Tellis, D. N. Primer, G. A. Molander, *Science* **2014**, *345*, 433–436; (b) Z. Zuo, D. T. Ahneman, L. Chu, J. A. Terrett, A. G. Doyle, D. W. C. MacMillan, *Science* **2014**, *345*, 437–440.

(10) (a) D. J. Weix, *Acc. Chem. Res.* **2015**, *48*, 1767–1775; (b) S. Biswas, D. J. Weix, *J. Am. Chem. Soc.* **2013**, *135*, 16192–16197.

(11) For Palladium examples, see: (a) S. R. Neufeldt, M. S. Sanford, *Adv. Synth. Catal.* **2012**, *354,* 3517–3522; (b) D. Kalyani, K. B. McMurtrey, M. S. Sanford. *J. Am. Chem. Soc.* **2011**, *133,* 18566–18569; For copper example, see: (c) Y. Yingda, M. S. Sanford, *J. Am. Chem. Soc.* **2012**, *134*, 9034–9037.

(12) (a) V. P. Ananikov, *ACS Catal.* **2015**, *5*, 1964–1971; (b) S. Z. Tasker, E. A. Standley, T. F. Jamison, *Nature* **2014**, *509*, 299–309.

(13) (a) J. Luo, J. Zhang, *ACS Catal.* **2016**, *6*, 873-877; (b) N. A. Romero, D. A. Nicewicz, *Chem. Rev.* **2016**, *116*, 10075–10166; (c) M. H. Shaw, J. Twilton, D. W. C. MacMillan, *J. Org. Chem.* **2016**, *81*, 6898–6926; (d) C. K. Prier, D. A. Rankic, D. W. C. MacMillan, *Chem. Rev.* **2013**, *113*, 5322–5363.

(14) O. Gutierrez, J. C. Tellis, D. N. Primer, G. A. Molander, M. C. Kozlowski, *J. Am. Chem. Soc.* **2015**, *137,* 4896–4899.

(15) (a) J. Twilton, C. Le, P. Zhang, M. H. Shaw, R. W. Evans, D. W. C. MacMillan, *Nat. Rev. Chem.* **2017**, 0052; (b) J. K. Matsui, S. B. Lang, D. R. Heitz, G. A. Molander, *ACS Catal.* **2017**, *7*, 2563–2575; (c) J. C. Tellis, C. B. Kelly, D. N. Primer, M. Jouffroy, N. R. Patel, G. A. Molander, *Acc. Chem. Res.* **2016**, *49*, 1429–1439; (d) K. L. Skubi, T. R. Blum, T. P. Yoon, *Chem. Rev.* **2016**, *116*, 10035–10074; (e) S. O. Badir, G. A. Molander, *Chem* **2020**, *6*, 1327–1339; (f) C. Zhu, H. Yue, J. Jia, M. Rueping, *Angew. Chem. Int. Ed.* **2021**, *60*, 2–24.

(16) For a recent example, see: J. Ma, J. Lin, L. Zhao, K. Harms, M. Marsch, X. Xie, E. Meggers, *Angew. Chem. Int. Ed.* **2018**, *57*, 11193–11197.

(17) For recent reviews, see: (a) N. Hoffmann, *Eur. J. Org. Chem.* **2017**, 1982–1992; (b) E. C. Gentry, R. R. Knowles, *Acc. Chem. Res.* **2016**, *49*, 1546–1556.

(18) For select recent examples, see: (a) J. P. Phelan, S. B. Lang, J. S. Compton, C. B. Kelly, R. Dykstra, O. Gutierrez, G. A. Molander, *J. Am. Chem. Soc.* **2018**, *140*, 8037–8047; (b) C. L. Cavanaugh, D. A. Nicewicz, *Org. Lett.* **2015**, *17*, 6082–6085; (c) K. A. Hollister, E. S. Conner, M. L. Spell, K. Deveaux, L. Maneval, M. W. Beal, J. R. Ragains, *Angew. Chem. Int. Ed.* **2015**, *54*, 7837–7841; (d) R. J. Wiles, G. A. Molander, *Isr. J. Chem*. **2020**, *60*, 281-293.

(19) For a recent review, see: C.-S. Wang, P. H. Dixneuf, J.-F. Soulé, *Chem. Rev.* **2018**, *118*, 7532–7585.

(20) For a review, see: T. P. Yoon, *ACS Catal.* **2013**, *3*, 895–902.

(21) T. Knauber, R. Chandrasekaran, J. W. Tucker, J. M. Chen, M. Reese, D. A. Rankic, N. Sach, C. Helal, *Org. Lett.* **2017**, *19*, 6566-6569.

(22) B. A. Vara, N. R. Patel, G. A. Molander, *ACS Catal.* **2017**, *7*, 3955-3959.

(23) (a) C. Remeur, C. B. Kelly, N. R. Patel, G. A. Molander, *ACS Catal.* **2017**, *7*, 6065-6069; (b) W. Dong, S. O. Badir, X. Zhang, G. A. Molander, *Org. Lett.* **2021**, 10.1021/acs.orglett.1c01207.

(24) G. A. Molander, *J. Org. Chem.* **2015**, *80*, 7837–7848.

(25) D. N. Primer, I. Karakaya, J. C. Tellis, G. A. Molander, *J. Am. Chem. Soc.* **2015**, *137*, 2195–2198.

(26) J. C. Tellis, J. Amani, G. A. Molander, *Org. Lett.* **2016**, *18*, 2994–2997.

(27) For Palladium examples, see: (a) C. R. Sun, B. Potter, J. P. Morken, *J. Am. Chem. Soc.* **2014**, *136*, 6534–6537; (b) S. N. Mlynarski, C. H. Schuster, J. P. Morken, *Nature* **2014**, *505*, 386–390.

(28) Y. Yamashita, J. C. Tellis, G. A. Molander, *Proc. Natl. Acad. Sci. U. S. A.* **2015**, *112*, 12026–12029.

(29) (a) J. K. Matsui, G. A. Molander, *Org. Lett.* **2017**, *19*, 436–439; (b) R. Karimi-Nami, J. C. Tellis, G. A. Molander, *Org. Lett.* **2016**, *18*, 2572–2575; (c) I. Karakaya, D. N. Primer, G. A. Molander, *Org. Lett.* **2015**, *17*, 3294–3297.

(30) M. El Khatib, R. A. M. Serafim, G. A. Molander, *Angew. Chem. Int. Ed.* **2016**, *55*, 254–258.

(31) R. Alam, G. A. Molander, *J. Org. Chem.* **2017**, *82*, 13728–13734.

(32) D. Ryu, D. N. Primer, J. C. Tellis, G. A. Molander, *Chem. Eur. J.* **2016**, *22*, 120–123.

(33) T. Furuya, A. S. Kamlet, T. Ritter, *Nature* **2011**, *473*, 470–477.

(34) F. Lima, M. A. Kabeshow, D. N. Tran, C. Battilocchio, J. Sedelmeier, G. Sedelmeier, B. Schenkel, S. V. Ley, *Angew. Chem. Int. Ed.* **2016**, *55*, 14085–14089.

(35) D. N. Primer, G. A. Molander, *J. Am. Chem. Soc.* **2017**, *139*, 9847–9850.

(36) J. R. Schmink, A. Bellomo, S. Berritt, *Aldrichimica Acta* **2013**, *46*, 71–80.

(37) C. Sandford, V. K. Aggarwal, *Chem. Commun.* **2017**, *53*, 5481–5494

(38) N. Rodriguez, L. J. Goossen, *Chem. Soc. Rev.* **2011**, *40*, 5030–5048.

(39) Z. Zuo, H. Cong, W. Li, J. Choi, G. C. Fu, D. W. C. MacMillan, *J. Am. Chem. Soc.* **2016**, *138*, 1832–1835.

(40) C. Pezzetta, D. Bonifazi, R. W. M. Davidson, *Org. Lett.* **2019**, *21*, 8957–8961.

(41) X. Zhang, D. W. C. MacMillan, *J. Am. Chem. Soc.* **2016**, *138*, 13862–13865.

(42) H-W. Hsieh, C. W. Coley, L. M. Baumgartner, K. F. Jensen, R. I. Robinson, *Org. Process Res. Dev.* **2018**, *22*, 542–550.

(43) (a) D. Matsuoka, Y. Nishigaichi, *Chem. Lett.* **2015**, *44*, 163−165; (b) D. Matsuoka, Y. Nishigaichi, *Chem. Lett.* **2014**, *43*, 559−561; (c) Y. Nishigaichi, A. Suzuki, A. Takuwa, *Tetrahedron Lett.* **2007**, *48*, 211–214.

(44) V. Corce, L. M. Chamoreau, E. Derat, J. P. Goddard, C. Ollivier, L. Fensterbank, *Angew. Chem. Int. Ed.* **2015**, *54*, 11414–11418.

(45) C. Lévêque, L. Chenneberg, V. Corcé, J.-P. Goddard, C. Ollivier, L. Fensterbank, *Org. Chem. Front*. **2016**, *3*, 462−465.

(46) W. M. Seganish, P. DeShong, *J. Org. Chem.* **2004**, *69*, 1137–1143.

(47) (a) M. Jouffroy, D. N. Primer, G. A. Molander, *J. Am. Chem. Soc.* **2016**, *138*, 475–478; For preparation of ammonium silicates, see: (b) K. Lin, C. B. Kelly, M. Jouffroy, G. A. Molander, *Org. Synth.* **2017**, *94*, 16–33.

(48) K. Lin, R. J. Wiles, C. B. Kelly, G. H. M. Davies, G. A. Molander, *ACS Catal.* **2017**, *7*, 5129–5133.

(49) B. A. Vara, M. Jouffroy, G. A. Molander, *Chem. Sci.* **2017**, *8*, 530–535.

(50) N. R. Patel, G. A. Molander, *J. Org. Chem.* **2016**, *81*, 7271–7275.

(51) For examples, see: (a) A. Heydari, S. Khaksar, M. Tajbakhsh, H. R. Bijanzadeh, *J. Fluorine Chem.* **2009**, *130*, 609−614; (b) H. Adibi, H. A. Samimi, M. Beygzadeh, *Catal. Commun.* **2007**, *8*, 2119−2124; (c) N. Tewari, N. Dwivedi, R. Tripathi, *Tetrahedron Lett.* **2004**, *45*, 9011−9014.

(52) (a) X. Wei, L. Wang, W. Jia, S. Du, L. Wu, Q. Liu, *Chin. J. Chem.* **2014**, *32*, 1245−1250; (b) Wang, Q. Liu, B. Chen, L. Zhang, C. Tung, L. Wu, *Chin. Sci. Bull.* **2010**, *55*, 2855−2858; (c) D. Zhang, L.-Z. Wu, L. Zhou, X. Han, Q.-Z. Yang, L.-P. Zhang, C.-H. Tung, *J. Am. Chem. Soc.* **2004**, *126*, 3440−3441; (d) S. Fukuzumi, T. Suenobu, M. Patz, T. Hirasaka, S. Itoh, M. Fujitsuka, O. Ito, *J. Am. Chem. Soc.* **1998**, *120*, 8060−8068.

(53) J. P. Cheng, Y. Lu, X. Q. Zhu, Y. Sun, F. Bi, J. He, *J. Org. Chem.* **2000**, *65*, 3853–3857.

(54) K. Nakajima, S. Nojima, K. Sakata, Y. Nishibayashi, *ChemCatChem* **2016**, *8*, 1028−1032.

(55) K. Nakajima, S. Nojima, Y. Nishibayashi, *Angew. Chem. Int. Ed.* **2016**, *55*, 14106–14110.

(56) A. Gutierrez-Bonet, J. C. Tellis, J. K. Matsui, B. A. Vara, G. A. Molander, *ACS Catal.* **2016**, *6*, 8004–8008.

(57) A. Dumoulin, J. K. Matsui, A. Gutierrez-Bonet, G. A. Molander, *Angew. Chem. Int. Ed.* **2018**, *57*, 6614-6618.

(58) L. Buzzetti, A. Prieto, S. R. Roy, P. Melchiorre, *Angew. Chem. Int. Ed.* **2017**, *56*, 15039–15043.

(59) For a review on PCET, see: (a) J. J. Warren, T. A. Tronic, J. M. Mayer, *Chem. Rev.* **2010**, *110*, 6961–7001; For a review on photocatalyzed HAT reactions, see: (b) L. Capaldo, D. Ravelli *Eur. J. Org. Chem.* **2017**, 2056–2071.

(60) B. J. Shields, A. G. Doyle, *J. Am. Chem. Soc.* **2016**, *138*, 12719–12722.

(61) D. R. Heitz, J. C. Tellis, G. A. Molander, *J. Am. Chem. Soc.* **2016**, *138*, 12715–12718.

(62) M. K. Nielsen, B. J. Shields, J. Liu, M. J. Williams, M. J. Zacuto, A. G. Doyle, *Angew. Chem. Int. Ed.* **2017**, *56*, 7191–7194.

(63) M. H. Shaw, V. W. Shurtleff, J. A. Terrett, J. D. Cuthbertson, D. W. MacMillan, *Science* **2016**, *352*, 1304–1308.

(64) For a reaction that provides similar products via a non-HAT mechanism, see: D. T. Ahneman, A. G. Doyle. *Chem. Sci*. **2016**, *7*, 7002-7006.

(65) J. Twilton, M. Christensen, D. A. DiRocco, R. T. Ruck, I. W. Davies, D. W. C. MacMillan, *Angew. Chem. Int. Ed.* **2018**, *57*, 5369–5373.

(66) I. B. Perry, T. F. Brewer, P. J. Sarver, D. M. Schultz, D. A. DiRocco, D. W. C. MacMillan, *Nature* **2018**, *560*, 70–75.

(67) (a) V. Bacauanu, S. Cardinal, M. Yamauchi, M. Kondo, F. Fernández, R. Remu, D. W. C. MacMillan, *Angew. Chem. Int. Ed.* **2018**, *57*, 12543–12548; (b) P. Zhang, C. C. Le, D. W. MacMillan, *J. Am. Chem. Soc.* **2016**, *138*, 8084–8087.

(68) (a) A. Paul, M. D. Smith, A. K. Vannucci, *J. Org. Chem.* **2017**, *82*, 1996–2003; (b) Z. Duan, W. Li, A. Lei, *Org. Lett.* **2016**, *18*, 4012–4015.

(69) L. Peng, Z. Li, G. Yin, *Org. Lett.* **2018**, *20*, 1880–1883.

(70) J. Yi, S. O. Badir, L. M. Kammer, M. Ribagorda, G. A. Molander, *Org. Lett.* **2019**, *21*, 3346–3351.

(71) G. E. Crisenza, D. Mazzarella, P. Melchiorre, *J. Am. Chem. Soc.* **2020**, *142*, 5461–5476.

(72) L. M. Kammer, S. O. Badir, R.-M. Hu, G. A. Molander, *Chem. Sci.* **2021**, *12*, 5450–5457.

(73) L. Guo, M. Rueping, *Chem. Eur. J.* **2018**, *24*, 7794–7809.

(74) (a) J. Amani, G. A. Molander, *J. Org. Chem.* **2017**, *82*, 1856–1863; (b) J. Amani, E. Sodagar, G. A. Molander, *Org. Lett.* **2016**, *18*, 732–735.

(75) J. Amani, R. Alam, S. Badir, G. A. Molander, *Org. Lett.* **2017**, *19*, 2426-2429.

(76) (a) S. O. Badir, A. Dumoulin, J. K. Matsui, G. A. Molander, *Angew. Chem. Int. Ed.* **2018**, *57*, 6610–6613; (b) J. Amani, G. A. Molander, *Org. Lett.* **2017**, *19*, 3612–3615; (c) E. E. Stache, T. Rovis, A. G. Doyle, *Angew. Chem. Int. Ed.* **2017**, *56*, 3679–3683; (d) C. L. Joe, A. G. Doyle, *Angew. Chem. Int. Ed.* **2016**, *55*, 4040-4043; (e) C. C. Le, D. W. MacMillan, *J. Am. Chem. Soc.* **2015**, *137*, 11938–11941.

(77) S. Zheng, D. N. Primer, G. A. Molander, *ACS Catal.* **2017**, *7*, 7957–7961.

(78) X. Zhang, D. W. C. MacMillan, *J. Am. Chem. Soc.* **2017**, *139*, 11353–11356.

(79) B. Kang, S. H. Hong, *Chem. Sci.* **2017**, *8*, 6613–6618.

(80) T. Gaich, P. S. Baran, *J. Org. Chem.* **2010**, *75*, 4657–4673.

(81) For reports on Ni/photoredox chemistry from companies, see: (a) R. Zhang, G. Li, M. Wismer, P. Vachal, S. L. Colletti, Z.-C. Shi, *ACS Med. Chem. Lett.* **2018**, *9*, 773–777; (b) C. C. Le, M. K. Wismer, Z. C. Shi, R. Zhang, D. V. Conway, G. Li, P. Vachal, I. W. Davies, D. W. C. MacMillan, *ACS Cent. Sci.* **2017**, *3*, 647–653; (c) T. J. DeLano, U. K. Bandarage, N. Palaychuk, J. Green, M. J. Boyd, *J. Org. Chem.* **2016**, *81*, 12525–12531; (d) N. Palaychuk, T. J. DeLano, M. J. Boyde, J. Green, U. K. Bandarage, *Org. Lett.* **2016**, *18*, 6180–6183; (e) K. D. Raynor, G. D. May, U. K. Bandarage, M. J. Boyd, *J. Org. Chem.* **2018**, *83*, 1551–1557.

(82) J. A. Milligan, J. P. Phelan, S. O. Badir, G. A. Molander, *Angew. Chem. Int. Ed.* **2019**, *58*, 6152–6163.

(83) A. Dömling, W. Wang, K. Wang, *Chem. Rev.* **2012**, *112*, 3083–3135.

(84) J. Derosa, O. Apolinar, T. Kang, V. T. Tran, K. M. Engle, *Chem. Sci.* **2020**, *11*, 4287–4296.

(85) H. Y. Tu, S. Zhu, F. L. Qing, L. Chu, *Synth.* **2020**, *52*, 1346–1356.

(86) For a selected review on asymmetric 1,2-difunctionalizations using copper catalysis, see: Z. L. Li, G. C. Fang, Q. S. Gu, X. Y. Liu, *Chem. Soc. Rev.* **2020**, *49*, 32–48.

(87) For a selected review on 1,2-difunctionalizations using palladium catalysis, see: G. Yin, X. Mu, G. Liu, *Acc. Chem. Res.* **2016**, *49*, 2413–2423.

(88) T. Qin, J. Cornella, C. Li, L. R. Malins, J. T. Edwards, S. Kawamura, B. D. Maxwell, M. D. Eastgate, P. S. Baran, *Science* **2016**, *352*, 801–805.

(89) J. W. Gu, Q. Q. Min, L. C. Yu, X. Zhang, *Angew. Chem. Int. Ed.* **2016**, *55*, 12270–12274.

(90) A. García-Domínguez, Z. Li, C. Nevado, *J. Am. Chem. Soc.* **2017**, *139*, 6835–6838.

(91) W. Shu, A. García-Domínguez, M. T. Quirós, R. Mondal, D. J. Cárdenas, C. Nevado, *J. Am. Chem. Soc.* **2019**, *141*, 13812–13821.

(92) S. Kc, R. K. Dhungana, B. Shrestha, S. Thapa, N. Khanal, P. Basnet, R. W. Lebrun, R. Giri, *J. Am. Chem. Soc.* **2018**, *140*, 9801–9805.

(93) X. Zhao, H. Y. Tu, L. Guo, S. Zhu, F. L. Qing, L. Chu, *Nat. Commun.* **2018**, *9*, 1–7.

(94) K. F. Zhang, K. J. Bian, C. Li, J. Sheng, Y. Li, X. S. Wang, *Angew. Chem. Int. Ed.* **2019**, *58*, 5069–5074.

(95) D. Anthony, Q. Lin, J. Baudet, T. Diao, *Angew. Chem. Int. Ed.* **2019**, *58*, 3198–3202.

(96) C. Zhu, H. Yue, L. Chu, M. Rueping, *Chem. Sci.* **2020**, *11*, 4051–4064.

(97) For a selected example on the alkylation of trifluoromethyl-substituted alkenes through radical/polar crossover, see: S. B. Lang, R. J. Wiles, C. B. Kelly, G. A. Molander, *Angew. Chem., Int. Ed.* **2017**, *56*, 15073–15077. In this case, the intermediacy of carbanion species results in β-F elimination. No hydroalkylation is detected in this protocol.

(98) (a) G. Magueur, B. Crousse, M. Ourévitch, D. Bonnet-Delpon, J.-P. Bégué, *J. Fluorine Chem.* **2006**, *127*, 637–642; (b) C. Leriche, X. He, C.-w. T. Chang, H.-w. Liu, *J. Am. Chem. Soc.* **2003**, *125*, 6348–6349.

(99) (a) S. Purser, P. R. Moore, S. Swallow, V. Gouverneur, *Chem. Soc. Rev.* **2008**, *37*, 320–330; (b) D. B. Harper, D. O'Hagan, *Nat. Prod. Rep.* **1994**, *11*, 123–133; (c) J. Wang, M. Sánchez-Roselló, J. L. Aceña, C. del Pozo, A. E. Sorochinsky, S. Fustero, V. A. Soloshonok, H. Liu, *Chem. Rev.* **2014**, *114*, 2432–2506.

(100) For a review on bioisosterism, see: G. A. Patani, E. J. LaVoie, *Chem. Rev.* **1996**, *96*, 3147–3176.

(101) B. R. Stockwell, *Nature* **2004**, *432*, 846–854.

(102) A. A. Shelat, R. K. Guy, *Nat. Chem. Biol.* **2007**, *3*, 442–446.

(103) G. P. Smith, V. A. Petrenko, *Chem. Rev.* **1997**, *97*, 391–410.

(104) L. Mannocci, Y. X. Zhang, J. Scheuermann, M. Leimbacher, G. De Bellis, E. Rizzi, C. Dumelin, S. Melkko, D. Neri, *Proc. Natl. Acad. Sci. U.S.A.* **2008**, *105*, 17670–17675.

(105) F. Buller, L. Mannocci, Y. X. Zhang, C. E. Dumelin, J. Scheuermann, D. Neri, *Bioorg. Med. Chem. Lett.* **2008**, *18*, 5926–5931.

(106) M. A. Clark, R. A. Acharya, C. C. Arico-Muendel, S. L. Belyanskaya, D. R. Benjamin, N. R. Carlson, P. A. Centrella, C. H. Chiu, S. P. Creaser, J. W. Cuozzo, C. P. Davie, Y. Ding, G. J. Franklin, K. D. Franzen, M. L. Gefter, S. P. Hale, N. J. V. Hansen, D. I. Israel, J. W. Jiang, M. J. Kavarana, M. S. Kelley, C. S. Kollmann, F. Li, K. Lind, S. Mataruse, P. F. Medeiros, J. A. Messer, P. Myers, H. O'Keefe, M. C. Oliff, C. E. Rise, A. L. Satz, S. R. Skinner, J. L. Svendsen, L. J. Tang, K. van Vloten, R. W. Wagner, G. Yao, B. G. Zhao, B. A. Morgan, *Nat. Chem. Biol.* **2009**, *5*, 647–654.

(107) A. Litovchick, C. E. Dumelin, S. Habeshian, D. Gikunju, M. A. Guie, P. Centrella, Y. Zhang, E. A. Sigel, J. W. Cuozzo, A. D. Keefe, M. A. Clark, *Sci. Rep.* **2015**, *5*, 10916.

(108) P. A. Harris, B. W. King, D. Bandyopadhyay, S. B. Berger, N. Campobasso, C. A. Capriotti, J. A. Cox, L. Dare, X. Y. Dong, J. N. Finger, L. C. Grady, S. J. Hoffmann, J. U. Jeong, J. Kang, V. Kasparcova, A. S. Lakdawala, R. Lehr, D. E. McNulty, R. Nagilla, M. T. Ouellette, C. S. Pao, A. R. Rendina, M. C. Schaeffer, J. D. Summerfield, B. A. Swift, R. D. Totoritis, P. Ward, A. M. Zhang, D. H. Zhang, R. W. Marquis, J. Bertin, P. J. Gough, *J. Med. Chem.* **2016**, *59*, 2163–2178.

(109) R. A. Goodnow, C. E. Dumelin, A. D. Keefe, *Nat. Rev. Drug. Discov.* **2017**, *16*, 131–147.

(110) S. Brenner, R. A. Lerner, *Proc. Natl. Acad. Sci. U.S.A.* **1992**, *89*, 5381–5383.

(111) D. Neri, R. A. Lerner, *Annu. Rev. Biochem.* **2018**, *87*, 479–502.

(112) D. L. Usanov, A. I. Chan, J. P. Maianti, D. R. Liu, *Nat. Chem.* **2019**, *11*, 704–714.

(113) A. Gironda-Martinez, D. Neri, F. Samain, E. J. Donckele, *Org. Lett.* **2019**, *21*, 9555–9558.

(114) J. Ottl, L. Leder, J. V. Schaefer, C. E. Dumelin, *Molecules* **2019**, *24*, 1629.

(115) D. T. Flood, C. Kingston, J. C. Vantourout, P. E. Dawson, P. S. Baran, *Isr. J. Chem.* **2020**, *60*, 268–280.

(116) K. Gotte, S. Chines, A. Brunschweiger, *Tetrahedron Lett.* **2020**, *61*, 151889.

(117) M. Catalano, M. Moroglu, P. Balbi, F. Mazzieri, J. Clayton, K. H. Andrews, M. Bigatti, J. Scheuermann, S. J. Conway, D. Neri, *Chemmedchem* **2020**, *15*, 1752–1756.

(118) M. Song, G. T. Hwang, *J. Med. Chem.* **2020**, *63*, 6578–6599.

(119) M. V. Westphal, L. Hudson, J. W. Mason, J. A. Pradeilles, F. J. Zecri, K. Briner, S. L. Schreiber, *J. Am. Chem. Soc.* **2020**, *142*, 7776–7782.

(120) D. Madsen, C. Azevedo, I. Micco, L. K. Petersen, N. J. Vest Hansen, *Prog. Med. Chem.* **2020**, *59*, 181–249.

(121) C. J. Gerry, S. L. Schreiber, *Curr. Opin. Chem. Biol.* **2020**, 56, 1–9.

(122) P. J. Li, J. A. Terrett, J. R. Zbieg, *ACS Med. Chem. Lett.* **2020**, *11*, 2120–2130.

(123) H. Doucet, *Eur. J. Org. Chem.* **2008**, *2008*, 2013–2030.

(124) R. K. Y. Cheng, C. Fiez-Vandal, O. Schlenker, K. Edman, B. Aggeler, D. G. Brown, G. A. Brown, R. M. Cooke, C. E. Dumelin, A. S. Dore, S. Geschwindner, C. Grebner, N. O. Hermansson, A. Jazayeri, P. Johansson, L. Leong, R. Prihandoko, M. Rappas, H. Soutter, A. Snijder, L. Sundstrom, B. Tehan, P. Thornton, D. Troast, G. Wiggin, A. Zhukov, F. H. Marshall, N. Dekker, *Nature* **2017**, *545*, 112–115.

(125) X. J. Huang, B. W. Ni, Y. Xi, X. Y. Chu, R. Zhang, H. B. You, *Aging (Albany. NY).* **2019**, *11*, 12532–12545.

(126) J. P. Maianti, A. McFedries, Z. H. Foda, R. E. Kleiner, X. Q. Du, M. A. Leissring, W. J. Tang, M. J. Charron, M. A. Seeliger, A. Saghatelian, D. R. Liu, *Nature* **2014**, *511*, 94–98.

(127) F. Buller, M. Steiner, K. Frey, D. Mircsof, J. Scheuermann, M. Kalisch, P. Buhlmann, C. T. Supuran, D. Neri, *ACS Chem. Biol.* **2011**, *6*, 336–344.

(128) F. Samain, T. Ekblad, G. Mikutis, N. Zhong, M. Zimmermann, A. Nauer, D. Bajic, W. Decurtins, J. Scheuermann, P. J. Brown, J. Hall, S. Graslund, H. Schuler, D. Neri, R. M. Franzinit, *J. Med. Chem.* **2015**, *58*, 5143–5149.

(129) M. Leimbacher, Y. X. Zhang, L. Mannocci, M. Stravs, T. Geppert, J. Scheuermann, G. Schneider, D. Neri, *Chem. Eur. J.* **2012**, *18*, 7729–7737.

(130) J. P. Phelan, S. B. Lang, J. Sim, S. Berritt, A. J. Peat, K. Billings, L. J. Fan, G. A. Molander, *J. Am. Chem. Soc.* **2019**, *141*, 3723–3732.

(131) D. K. Kölmel, J. Meng, M.-H. Tsai, J. Que, R. P. Loach, T. Knauber, J. Wan, M. E. Flanagan, *ACS Comb. Sci.* **2019**, *21*, 8, 588–597.

(132) Y. Ruff, R. Martinez, X. Pelle, P. Nimsgern, P. Fille, M. Ratnikov, F. Berst, *ACS Comb. Sci.* **2020**, *22*, 120–128.

(133) S. O. Badir, J. Sim, K. Billings, A. Csakai, X. Zhang, W. Dong, G. A. Molander, *Org. Lett.* **2020**, *22*, 1046–1051.

(134) D. K. Kolmel, A. S. Ratnayake, M. E. Flanagan, *Biochem. Bioph. Res. Commun.* **2020**, *533*, 201–208.

(135) For a selected example on radical-mediated alkylation processes under aqueous conditions, see: J. K. Matsui, D. N. Primer, G. A. Molander, *Chem. Sci.* **2017**, *8*, 3512–3522.

(136) W. J. Yu, L. Chen, J. S. Tao, T. Wang, J. K. Fu, *Chem. Commun.* **2019**, *55*, 5918–5921.

(137) D. A. Everson, D. J. Weix, *J. Org. Chem.* **2014**, *79*, 4793–4798.

(138) T. B. Xiao, L. Y. Li, L. Zhou, *J. Org. Chem.* **2016**, *81*, 7908–7916.

(139) R. J. Wiles, J. P. Phelan, G. A. Molander, *Chem. Commun.* **2019**, *55*, 7599–7602.

(140) N. A. Meanwell, *J. Med. Chem.* **2011**, *54*, 2529–2591.

(141) For a selected example, see: D. K. Kolmel, R. P. Loach, T. Knauber, M. E. Flanagan, *Chemmedchem* **2018**, *13*, 2159–2165.

(142) R. F. Wu, S. Gao, T. Du, K. L. Cai, X. M. Cheng, J. Fan, J. Feng, A. Shaginian, J. Li, J. Q. Wan, G. S. Liu, *Chem. Asian. J.* **2020**, *15*, 4033–4037.

(143) R. Chowdhury, Z. Yu, M. L. Tong, S. V. Kohlhepp, X. Yin, A. Mendoza, *J. Am. Chem. Soc.* **2020**, *142*, 20143–20151.

(144) H. Wen, R. Ge, Y. Qu, J. Sun, X. Shi, W. Cui, H. Yan, Q. Zhang, Y. An, W. Su, H. Yang, L. Kuai, A. L. Satz, X. Peng, *Org. Lett.* **2020**, *22*, 9484–9489.

Chapter 2. Synthesis of Reversed *C*-Acyl Glycosides through Nickel/Photoredox Dual Catalysis[‡]

2.1 Introduction

Glycodiversification of drug scaffolds is a powerful tool invoked by medicinal chemists to enhance pharmacokinetic and/or pharmacodynamic properties of therapeutic targets.[1,2] Glycosidic attachment in natural products renders enhanced solubility, membrane transport, and specificity in cellular tissues.[3] As important representatives, *C*-glycosides are a privileged class of saccharides containing a C–C linkage joining a carbohydrate unit to an aglycone or another sugar moiety.[1c,4] These compounds are ubiquitous in nature and serve as key structural motifs in numerous antitumor, antibiotic, and type II antidiabetic agents.[1c] Given their *in vivo* resistance toward basic, acidic, and enzymatic hydrolysis, *C*-glycosides function as successful mimetic forms of the more labile *O*-glycosides.[4] In particular, *C*-acyl glycosides exhibit important biological activities such as inhibition against reactive oxygen species, playing a major role in cell signaling (oxidative stress), and glutamate-induced cell death.[5] Notably, *C*-acyl-glycosylation has proven efficient in providing unique synthetic disconnections toward complex, bioactive molecules.[6] A prominent example is the synthesis of zaragozic acid C, a potent squalene synthase inhibitor, based on a photochemical C(sp^3)–H acylation strategy of a glycosidic moiety.[6a]

Consequently, various strategies have been devised to introduce acyl groups at the anomeric carbon in glycosides. Conventional methods include: i) nucleophilic additions of organometallic reagents to *C*-glycosyl aldehydes followed by an oxidation step to furnish the

---

[‡] Reproduced in part with permission from S. O. Badir, A. Dumoulin, J. K. Matsui, G. A. Molander, *Angew. Chem. Int. Ed.* **2018**, *57*, 6610–6613. Copyright 2018, Wiley.

desired ketones,[7] ii) addition of aldehydes[8] or electrophilic acylating agents[9] to glycosyl-based lithium, tin, or samarium reagents (Figure 2.1 A), and iii) addition of Grignard reagents to glyconitriles[10] or masked aldehydes such as glycosyl benzothiazoles.[11] These acylation strategies rely on harsh conditions and pyrophoric organometallic reagents, thus limiting their functional group tolerance and widespread applicability in pharmaceutical settings.

More recently, Gong *et al.* described a nickel-catalyzed reductive coupling of aliphatic carboxylic acids with glycosyl bromides with complete α-selectivity in the mannose series (Figure 2.1 B).[12] Employing two electrophiles, this report documents the most straightforward route toward anomeric *C*-acyl glycosides to date. Traditional transition metal-catalyzed cross-couplings remain in large part inapplicable in the context of *C*-acyl-glycosylation because of the C(sp^3)-hybridized nature of the anomeric position. As a result, the development of efficient and catalytic transformations toward *C*-acyl glycosides is highly desired. Specifically, non-anomeric acylation strategies that preserve the anomeric carbon for further functionalization remain scarce and challenging.

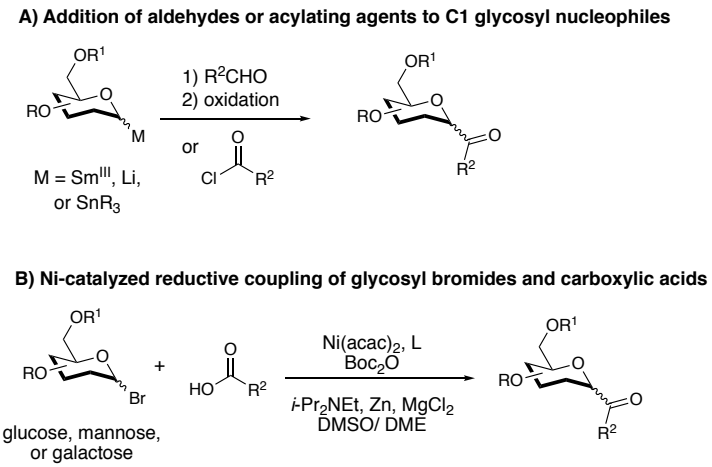

Figure 2.1. Strategies toward the synthesis of anomeric *C*-acyl glycosides.

Routes based on Wacker oxidation of terminal olefins have been reported for the synthesis of non-anomeric *C*-acyl glycosides (Figure 2.2 A).[13] However, such protocols are limited to methyl ketones and require elevated temperatures. Other strategies to assemble complex sugar units take advantage of the addition of sugar aldehydes to stabilized sugar phosphonates to furnish unsaturated ketones (Figure 2.2 B).[14] Conversion of glycosyl carboxylic acids to more reactive acyl chlorides has been utilized in the synthesis of α-diazocarbonyl saccharides.[15] Finally, the addition of organomagnesium or organolithium reagents to sugar aldehydes at C5 has been described (Figure 2.2 C).[16] These transformations, however, are generally not applicable to substrates containing reactive functional groups.

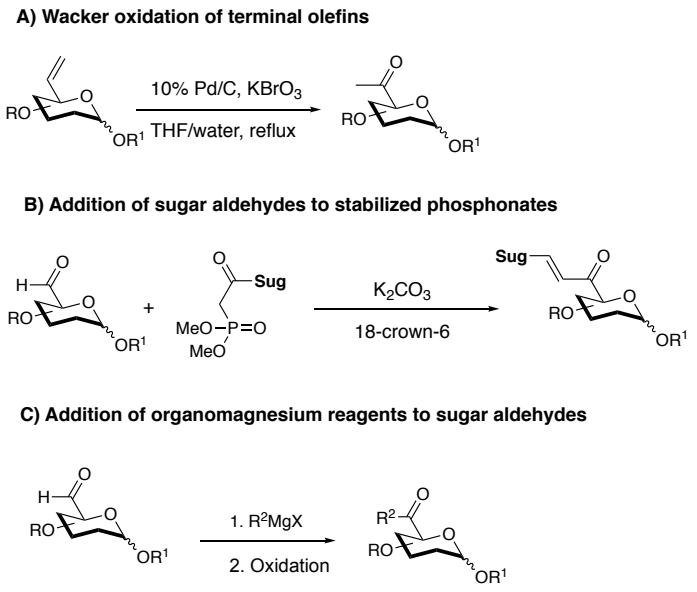

Figure 2.2. Traditional routes toward non-anomeric, reversed *C*-acyl glycosides.

Recent efforts have demonstrated that Ni/photoredox cross-coupling reactions are valuable tools for the construction of new C–C bonds.[17] These processes are governed by a single-electron transmetalation pathway, with an inherent low activation energy barrier favoring C_{sp3}-hybridized nucleophiles.[18] In this context, we explored 1,4-dihydropyridines (1,4-DHPs)[19] as

glycosyl-based radical precursors. These coupling partners are bench stable and can be prepared from inexpensive starting materials.[19c] Although 1,4-DHPs stem from the corresponding *C*-formyl glycosides, they are of immense synthetic value as they have low oxidation potentials and thus are amenable for fragmentation using inexpensive organic photocatalysts in lieu of stoichiometric oxidants.[19c] They also bypass the inherent challenge associated with the generation of alkyl radicals directly from aldehydes; namely undesired acylated byproducts.[19c] To address the challenges associated with the synthesis of non-anomeric *C*-acyl glycosides, we investigated the feasibility of a Ni-catalyzed cross-coupling reaction of *in situ* activated carboxylic acids[20] with glycosyl based DHPs, in an attempt to access such challenging structural motifs from aldehyde precursors (Figure 2.3).

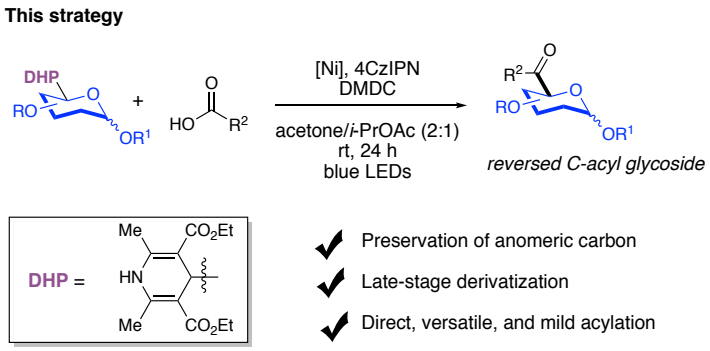

Figure 2.3. Envisioned transformation toward the synthesis of reversed *C*-acyl glycosides.

2.2 Results and Discussion

Studies were initiated by evaluating suitable activators of hydrocinnamic acid using high-throughput experimentation techniques[20] (see the Experimental Section). Dimethyl dicarbonate (DMDC),[21] a beverage preservative, served as an ideal activator. This species is atom-economical and has benign by-products: carbon dioxide and methanol. Next, a more robust screening of photocatalysts was carried out using **1a** and hydrocinnamic acid as a model system. It became

apparent that 4CzIPN, an inexpensive organic dye, performed more efficiently than Ir- and Ru-based photocatalysts. Screening studies of other reaction parameters (e.g., solvents, ligands, and loadings of starting materials) afforded the desired final conditions of this cross-coupling reaction. As anticipated, control experiments proved that all components were necessary for the reaction to proceed.[21]

Subsequently, the generality of this transformation with respect to the DHP coupling partner was examined (Figure 2.4. Various functionalized glycosidic scaffolds are well-tolerated under the reaction conditions, affording the desired *C*-acyl glycosides in high yields.

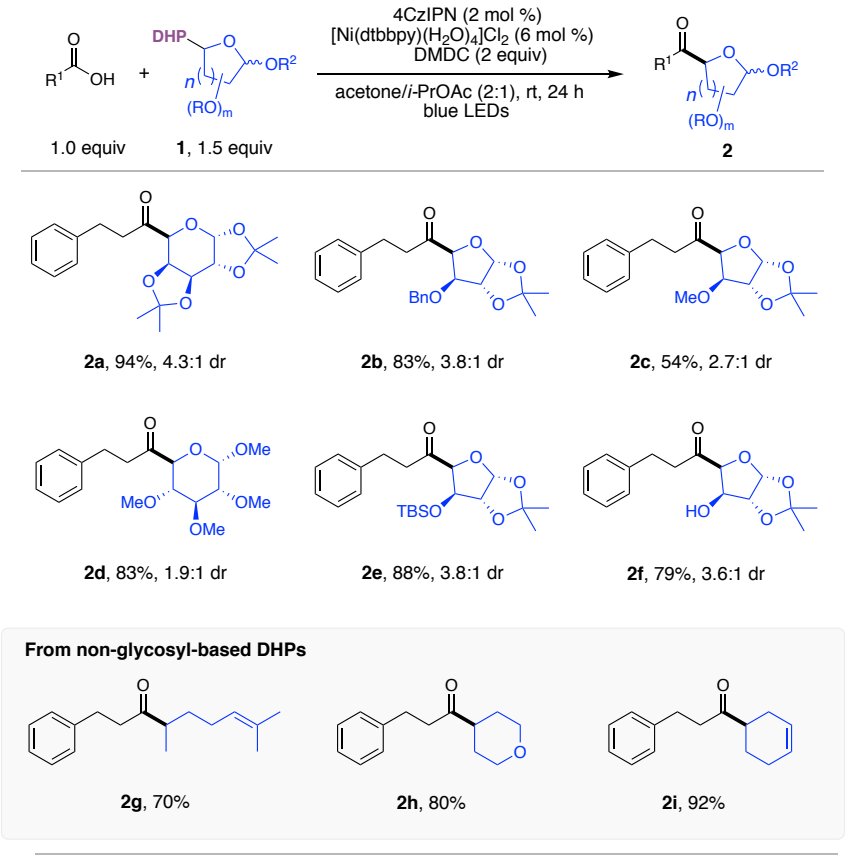

Figure 2.4. Scope with respect to 1,4-DHPs in the cross-coupling with carboxylic acids. All values correspond to isolated yields after purification.

Sterically hindered pyranose and furanose moieties (**2a**, **2b**, and **2e**) performed equally well when compared to those with less steric constraints (**2c** and **2d**). Notably, synthetically challenging *C*-acyl glycoside **2f**, exhibiting a free hydroxyl group, can be obtained in good yield in one-step starting from the corresponding DHP **1e**. Finally, to demonstrate the broad applicability of this cross-coupling reaction, we also attempted the reaction with non-glycosyl based DHPs and obtained the desired aliphatic ketones (**2g**, **2h**, and **2i**) in high yields.

Next, we focused our attention on the compatibility of abundant carboxylic acids as cross-coupling partners (Figure 2.5). We were pleased to discover that this mild acylation protocol is widely applicable to a vast array of substrates. Carboxylic acids containing nitriles (**2j** and **2v**) and esters (**2k** and **2r**) were well tolerated under the reaction conditions. A carboxylic acid bearing a free hydroxyl group were amenable in this transformation, despite the potential reactivity of the nucleophilic free hydroxyl groups with DMDC (**2l**). Reversed *C*-acyl glycosides bearing small, strained rings were incorporated without compromising yields (**2m**, **2o**, **2p**, **2r**, and **2s**). Moreover, *N*-Boc-protected amino acid and Fmoc-protected amine, respectively, afforded the desired ketones in high yields and excellent diasteroselectivities (**2k** and **2n**, respectively). Glycosides **2w**, **3b**, and **3c** derived from indomethacin and naproxen (NSAIDs), were successfully obtained. Less nucleophilic carboxylic acids were compatible structural motifs in this transformation, providing ketones **2s** and **2t**. Remarkably, substitution at the α-position of the carboxylic acids did not hinder the cross-coupling reaction. Moreover, reversed *C*-acyl glycosides containing steroidal moieties, abundant motifs in synthetic drugs and natural products, are accommodated in this cross-coupling reaction (**2x**). We examined the feasibility of coupling carboxylic acids with non-glycosyl based DHPs to exploit this acylation strategy further. Indeed, such radical precursors can be harnessed under the reaction conditions as demonstrated by the synthesis of dialkyl ketones **3b**-**3f**.

Most notably, employing glycosyl-based carboxylic acids effectively generated the desired disaccharide alkyl ketones (**2z** and **3a**, Figure 2.5) despite the challenging steric demands of both cross-coupling partners. This structural motif appears to be underexplored in the literature. Therefore, this acylation strategy provides a straightforward route to access new chemical space in carbohydrate chemistry. Furthermore, complete retention of the configuration of the saccharide moiety stemming from the carboxylic acid is observed.

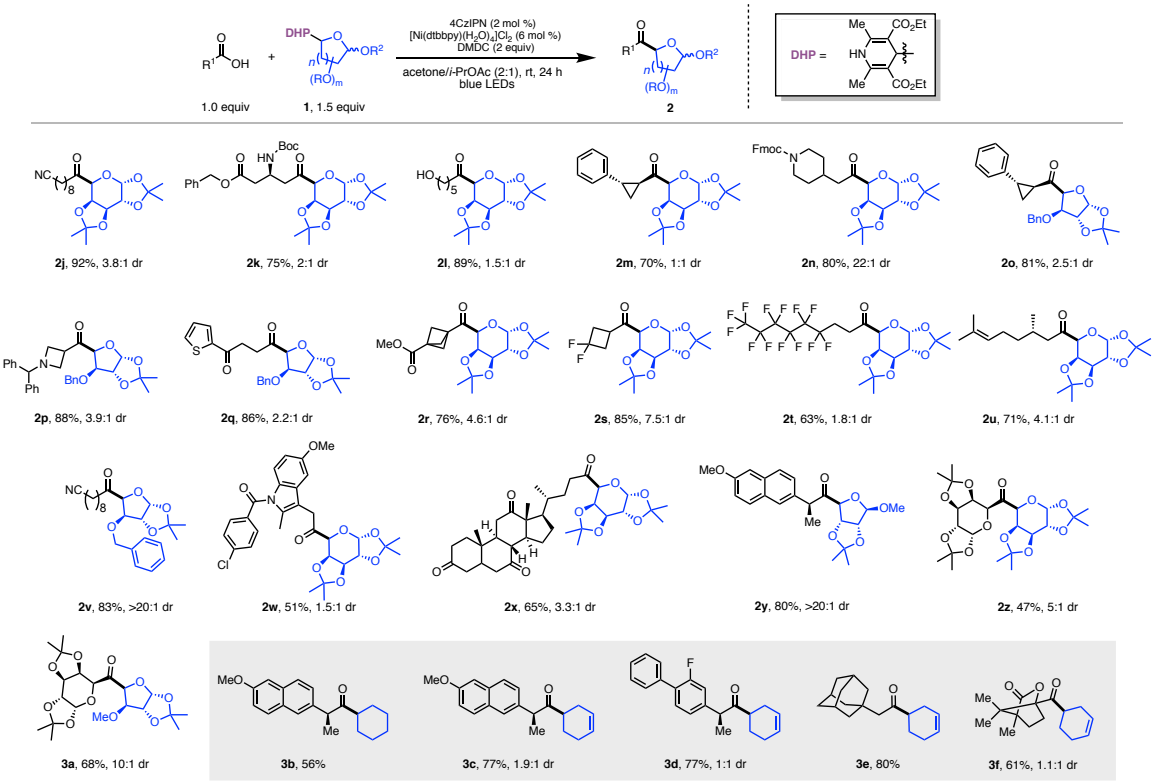

Figure 2.5. Scope with respect to 1,4-DHPs in the cross-coupling with carboxylic acids. All values correspond to isolated yields after purification.

To assess the scalability of this protocol, we conducted the reaction to access **2x** on 2.5 mmol scale (Figure 2.6). Because of its economical profile [~$5/mmol], 4CzIPN is an attractive photocatalyst for large-scale applications when compared to those based on Ir or Ru. The

resulting yield was comparable to the reaction on 0.3 mmol scale. This highlights the tolerability of this cross-coupling reaction toward complex structures, and demonstrates the usefulness of glycosyl-based DHPs in the synthesis of *C*-acyl glycosides, especially within the context of rapid, late-stage functionalization of desired targets bearing a carboxylic acid handle.

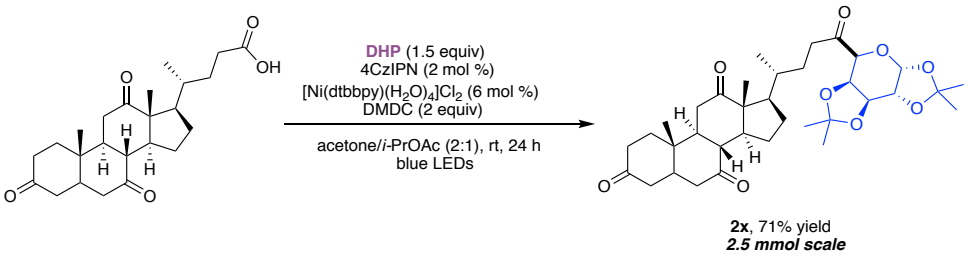

Figure 2.6. Scale-up of the photochemical *C*-acyl-glycosylation.

2.3 Conclusion

In conclusion, this study details a practical and versatile route toward the construction of highly functionalized, reversed *C*-acyl glycosides in high yields and acceptable diastereoselectivities. Utilizing a dual-catalytic Ni/photoredox system, a broad palette of glycosyl-based radicals is generated from abundant aldehyde feedstocks for subsequent metal-catalyzed functionalization, facilitating the synthesis of diverse carbohydrate units with retention of the anomeric carbon; a useful handle for structural elaboration. This mild acylation protocol can be utilized in industrial settings to access medicinally relevant *C*-acyl glycosides with high functional group tolerance, as well as provide unique and alternative disconnections in the synthetic design of complex, bioactive molecules.

2.4 Experimental

General Consideration

General: All chemical transformations requiring inert atmospheric conditions were carried out using Schlenk line techniques with a 4- or 5-port dual-bank manifold. LED irradiation was accomplished as described in precedent reports.[22] NMR spectra (^{1}H, ^{13}C, ^{19}F) were obtained at 298 ºK. ^{1}H NMR spectra were referenced to residual, $CHCl_3$ (δ 7.26) in $CDCl_3$. ^{13}C NMR spectra were referenced to $CDCl_3$ (δ 77.30). In the case of diastereomeric mixtures, crude NMR was recorded to determine the ratio. Reactions were monitored by LC/MS, GC/MS, ^{1}H NMR, and/or TLC on silica gel plates (60 Å porosity, 250 μm thickness). TLC analysis was performed using hexanes/EtOAc as the eluent and visualized using ninhydrin, *p*-anisaldehyde stain, and/or UV light. Flash chromatography was accomplished using an automated system (CombiFlash®, UV detector, λ = 254 nm and 280 nm) with RediSep® R_f silica gel disposable flash columns (60 Å porosity, 40–60 μm) or RediSep R_f Gold® silica gel disposable flash columns (60 Å porosity, 20–40 μm). Accurate mass measurement analyses were conducted using electron ionization (EI) or electrospray ionization (ESI). The signals were mass measured against an internal lock mass reference of perfluorotributylamine (PFTBA) for EI-GC/MS and leucine enkephalin for ESI-LC/MS. The utilized software calibrates the instruments and reports measurements by use of neutral atomic masses. The mass of the electron is not included. IR spectra were recorded on an FT-IR using either neat oil or solid products. Solvents were purified with drying cartridges through a solvent delivery system. Melting points (°C) are uncorrected.

Chemicals: Deuterated NMR solvents were purchased and stored over 4Å molecular sieves. EtOAc, hexanes, MeOH, Et_2O, and toluene were obtained from commercial suppliers and used as purchased. CH_2Cl_2 and THF were purchased and dried *via* a solvent delivery system. Anhydrous

acetone and anhydrous *i*-PrOAc were purchased and stored over 4Å molecular sieves. Ethylene glycol, carboxylic acids, aldehydes, dimethyl dicarbonate, 3-aminocrotonate, and ethyl acetoacetate were purchased from commercial suppliers and used without further purification. The quality of DMDC is crucial to the cross-coupling reactions. Residual water causes hydrolysis and renders the activator (DMDC) ineffective. The organic photocatalyst 2,4,5,6-tetra(9H-carbazol-9-yl)isophthalonitrile (4CzIPN) and the nickel complex $[Ni(dtbbpy)(H_2O)_4]Cl_2$ were prepared in-house by the procedures outlined in precedent reports.[19c,23] All new 1,4 DHPs were prepared from their corresponding aldehydes according to the representative procedure outlined below. Information (preparation protocols, characterization, etc.) for all other 1,4 DHP derivatives can be found in previous reports.[19c,24] All other reagents were purchased commercially and used as received. Photoredox-catalyzed reactions were performed using 8 mL Chemglass vials (2-dram, 17 x 60 mm, 15-425 Green Open Top Cap, TFE Septa).

General Procedures

Preparation of 1,4-DHPs (GP1): DHP derivatives were prepared following a modified literature protocol.[24] A round-bottom flask was charged with ethyl 3-aminocrotonate (1.0 equiv) in ethylene glycol (2.5 M). To this mixture was added ethyl acetoacetate (1.0 equiv) followed by the corresponding aldehyde (1.0 equiv). In some cases, the aldehyde was added as a stock soln in CH_2Cl_2. Finally, Bu_4NHSO_4 (12 mol %) was added in one portion. The reaction vessel was heated at 80 ºC for 3-4 h. Upon complete consumption of the aldehyde starting material, the reaction was cooled to rt and diluted with EtOAc. The reaction mixture was extracted three times with EtOAc using a separatory funnel containing brine. The organic layers were then combined, dried ($MgSO_4$), filtered, and taken to dryness. The crude reaction mixture was purified using an

automated system (visualizing at 254 nm, monitoring at 280 nm) with silica cartridges (60 Å porosity, 20-40 μm) using hexanes/EtOAc (0 to 60%) as eluent.

Cross-coupling of 1,4-DHPs (GP2): To an 8 mL reaction vial with a stir bar were added 4CzIPN (4.7 mg, 0.006 mmol, 2 mol %), $[Ni(dtbbpy)(H_2O)_4]Cl_2$ (8.4 mg, 0.018 mmol, 6 mol %), 1,4-DHP (0.45 mmol, 1.5 equiv), and carboxylic acid (0.3 mmol, 1.0 equiv), if a solid. The vial was sealed with a cap containing a TFE-lined silicone septa and placed under an argon atmosphere *via* an inlet needle. The vial was evacuated three times *via* an inlet needle then purged with argon. A dry and degassed mixture of acetone/*i*-PrOAc (2 :1) was then added (3.0 mL, 0.1 M). If the carboxylic acid was an oil, it was added at this point directly *via* microsyringe. DMDC (64 μL, 0.6 mmol, 2 equiv) was then added to the reaction *via* a microsyringe. The reaction was placed under blue LED irradiation and stirred for 24 h. The reaction was maintained at approximately 24 °C *via* a fan. Upon completion, the reaction mixture was taken to dryness and then a crude NMR was obtained. The reaction mixture was then purified on an automated liquid chromatographic system to obtain the pure product.

Reaction Optimization using High Throughput Experimentation (HTE)

HTE screens were performed at the University of Pennsylvania/Merck Catalysis Center. The screens were conducted on 0.01 mmol scale (relative to the carboxylic acid starting material) and analyzed *via* ultra performance liquid chromatography (UPLC) with addition of 4,4′-di-*tert*-butylbiphenyl as internal standard (IS). To assess reactions, ratios corresponding to the areas of product to internal standard (P/IS) were calculated. Each screen was conducted independently, and the ratios from one screen should not be quantitatively compared to those from a different screen.

The reactions were carried out in 96-well plate reactor blocks containing 1 mL glass vials equipped with a Teflon-coated magnetic stir bar. The plate was placed in a glovebox, and stock solns of the appropriate reagents (1,4-DHP, carboxylic acid, ligands, Ni complexes, and photocatalysts) were added using micropipettes. A centrifugal evaporator was used to remove excess solvents. To these vials was then added 100 μL of the appropriate solvent. The vials were sealed and stirred under blue LED irradiation at rt (~24 °C). After 24 hr, the reactions were exposed to air and diluted with 500 µL of a 0.002 µM soln of internal standard in MeCN. The vials were stirred for 5 min to ensure adequate mixing. Aliquots (25 µL) were transferred into a 96-well UPLC block, diluted with MeCN (700 µL) and then analyzed by UPLC.

Screen 1. Variation of activators, Ni sources, ligands, and solvents.

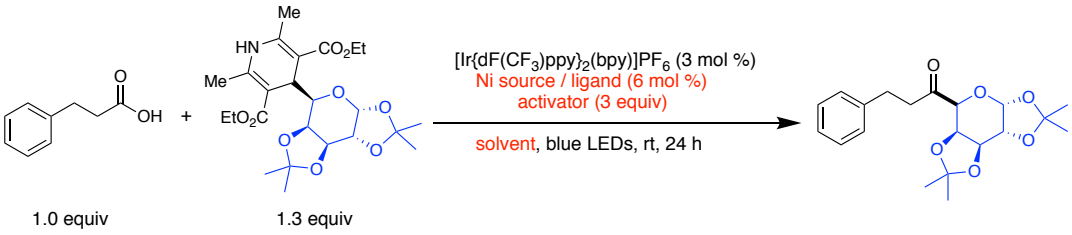

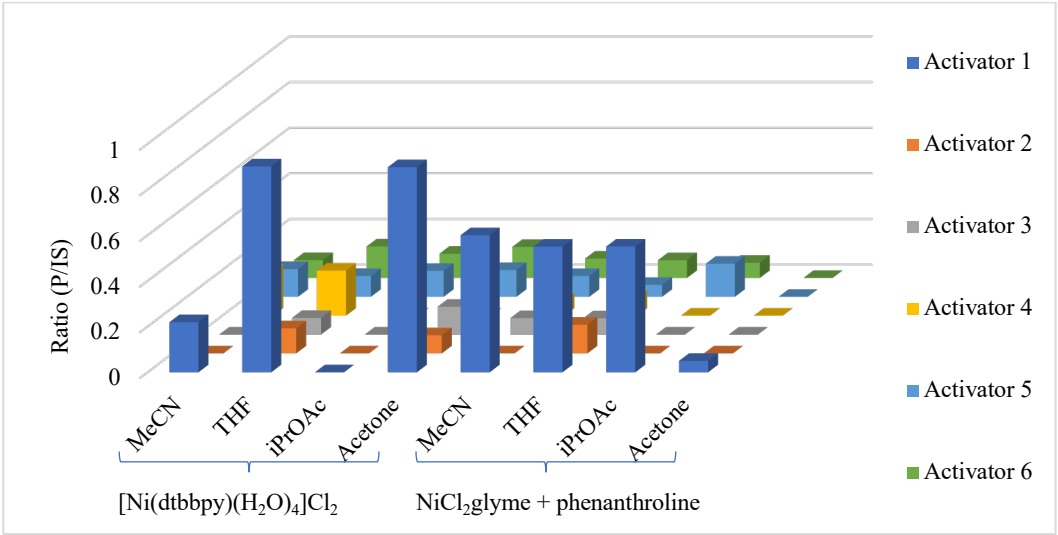

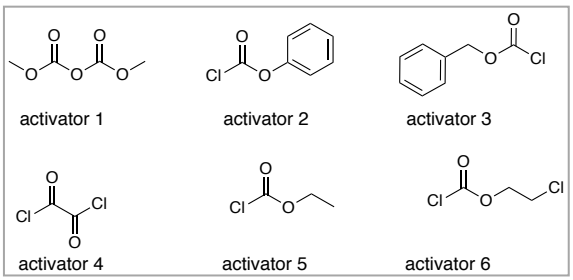

Screen 2. Variation of photocatalysts and solvents with different loadings of starting materials.

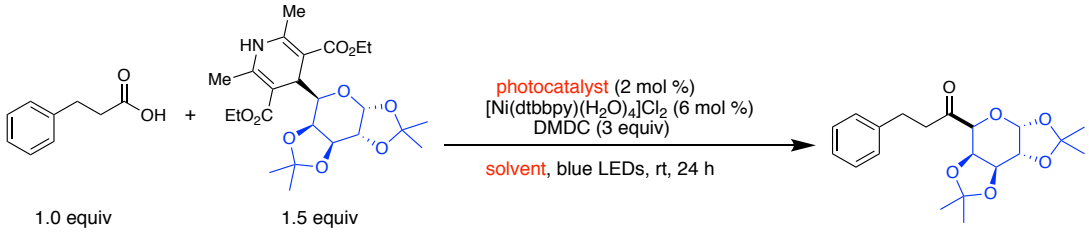

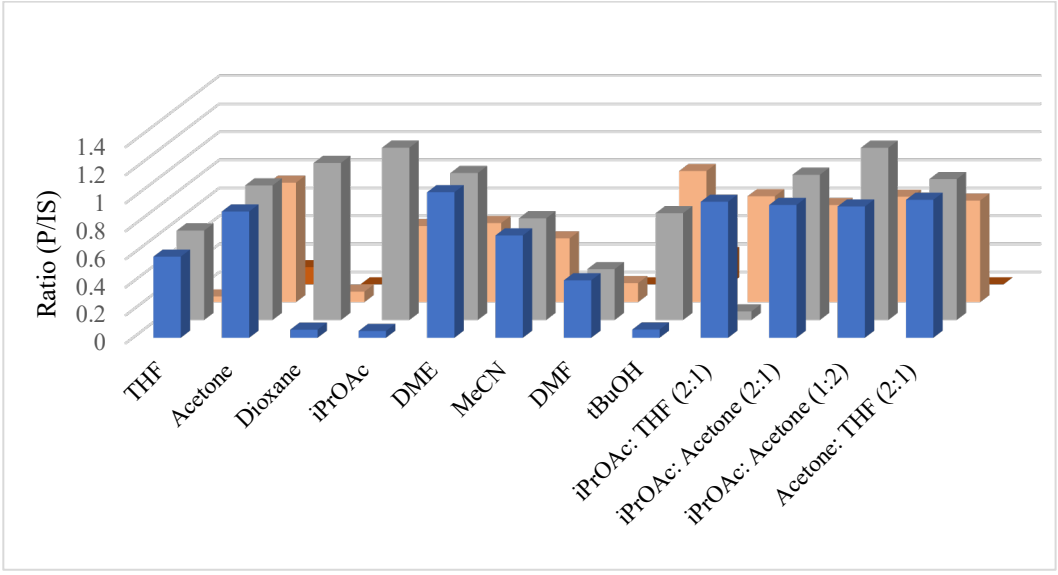

[Ir{dF(CF3)ppy}2(bpy)]PF6 4CzIPN Rhodamine 6G [Ru(bpy)3](PF6)2

Characterization Data

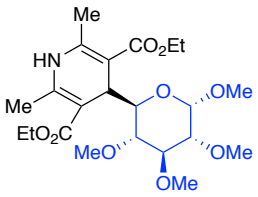

Diethyl 2,6-Dimethyl-4-((2*R*,3*R*,4*S*,5*R*,6*S*)-3,4,5,6-tetramethoxytetrahydro-2H-pyran-2-yl)-1,4-dihydropyridine-3,5-dicarboxylate, **1d** (4.2 mmol scale, 0.54 g, 28%) was prepared following *GP1*. The product was isolated as a slightly yellow foam. **^{1}H NMR** (500 MHz, $CDCl_3$) δ 6.40 (s, 1H), 4.63 (d, *J* = 3.1 Hz, 1H), 4.46 (d, *J* = 4.2 Hz, 1H), 4.28 – 4.08 (m, 4H), 3.57 (s, 3H), 3.49 (s, 3H), 3.47 (s, 3H), 3.31 (dd, *J* = 9.8, 4.3 Hz, 1H), 3.25 (s, 3H), 3.13 – 3.05 (m, 2H), 2.29 (s, 6H), 1.30 (t, *J* = 7.0 Hz, 7H). **^{13}C NMR** (126 MHz, $CDCl_3$) δ 168.7, 167.9, 145.1, 145.0, 99.7, 98.8, 96.3, 84.0, 81.8, 79.7, 72.8, 60.2, 59.6, 59.5, 58.7, 58.6, 54.1, 35.5, 19.3, 19.0, 14.3, 14.3. **FT-IR** (cm^{-1}, neat, ATR): 3342, 2979, 2933, 1677, 1487, 1304, 1209, 1154, 1092, 1047. **HRMS** (EI) calcd for $C_{22}H_{35}NO_9$ $[M]^+$: 458.2390, found: 458.2379.

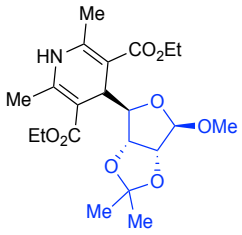

Diethyl 4-((3a*R*,4*R*,6*R*,6a*R*)-6-Methoxy-2,2-dimethyltetrahydrofuro[3,4-*d*][1,3]dioxol-4-yl)-2,6-dimethyl-1,4-dihydropyridine-3,5-dicarboxylate, **1y** (8.3 mmol scale, 1.4 g, 41%) was prepared following *GP1*. The product was isolated as a yellow solid. **mp** = 112-116 ºC. **^{1}H NMR** (500 MHz, $CDCl_3$) δ 5.83 (s, 1H), 4.87 (s, 1H), 4.71 (dd, *J* = 6.0, 1.5 Hz, 1H), 4.45 (d, *J* = 6.0 Hz, 1H), 4.33 – 4.07 (m, 5H), 3.94 (dd, *J* = 7.8, 1.4 Hz, 1H), 3.31 (s, 3H), 2.36 (s, 3H), 2.32 (s, 3H),

1.42 (s, 3H), 1.33 – 1.28 (m, 6H), 1.27 (s, 3H). **^{13}C NMR** (126 MHz, $CDCl_3$) δ 168.2, 167.5, 147.0, 144.6, 112.1, 110.9, 101.4, 99.0, 89.5, 85.4, 81.6, 60.0, 60.0, 56.3, 37.3, 27.1, 25.5, 19.9, 19.5, 14.6, 14.5. **FT-IR** (cm^{-1}, neat, ATR): 3335, 2978, 1687, 1661, 1483, 1210, 1093, 1050. HRMS (EI) calcd for $C_{21}H_{31}NO_8$ $[M]^+$: 425.2050, found: 425.2025.

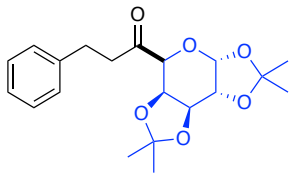

3-Phenyl-1-((3a*R*,5a*R*,8a*S*,8b*R*)-2,2,7,7-tetramethyltetrahydro-5H-bis([1,3]dioxolo)[4,5-b:4',5'-d]pyran-5-yl)propan-1-one, **2a** (102.5 mg, 94%) was prepared following *GP2*. The product was isolated as a colorless oil. dr = 4.3:1 based on ^{1}H NMR of the crude reaction mixture. **^{1}H NMR** (500 MHz, $CDCl_3$, major diastereomer) δ 7.33 – 7.14 (m, 5H), 5.62 (d, *J* = 4.6 Hz, 1H), 4.63 (d, *J* = 7.4 Hz, 1H), 4.58 (d, *J* = 8.9 Hz, 1H), 4.38 – 4.31 (m, 1H), 4.21 (s, 1H), 2.97 – 2.84 (m, 4H), 1.50 (s, 3H), 1.42 (s, 3H), 1.33 (s, 3H), 1.31 (s, 3H). **^{1}H NMR** (500 MHz, $CDCl_3$, minor diastereomer) δ 7.33 – 7.14 (m, 5H), 5.30 (s, 1H), 4.63 (d, *J* = 7.4 Hz, 1H), 4.58 (d, *J* = 8.9 Hz, 1H), 4.24 (s, 1H), 3.71 (d, *J* = 8.7 Hz, 1H), 3.10 – 2.98 (m, 4H), 1.57 (s, 3H), 1.48 (s, 3H), 1.38 (s, 3H), 1.36 (s, 3H). **^{13}C NMR** (126 MHz, $CDCl_3$, major diastereomer) δ 208.6, 141.4, 128.5 (4C), 126.0, 109.7, 109.0, 96.5, 73.8, 72.6, 70.7, 70.5, 41.7, 28.7, 26.1, 25.9, 24.9, 24.3. **^{13}C NMR** (126 MHz, $CDCl_3$, minor diastereomer) δ 205.6, 141.1, 128.6 (4C), 126.2, 111.1, 109.5, 97.1, 77.5, 75.2, 74.2, 69.7, 41.1, 29.3, 27.9, 27.7, 25.8, 25.6. **FT-IR** (cm^{-1}, neat, ATR): 2988, 2935, 1719, 1382, 1372, 1255, 1211, 1166, 1066. **HRMS** (ESI) calcd for $C_{20}H_{26}O_6Na$ $[M+Na]^+$: 385.1627, found: 385.1646.

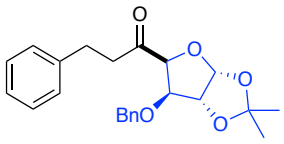

1-((3a*R*,6*R*,6a*R*)-6-(Benzyloxy)-2,2-dimethyltetrahydrofuro[2,3-d][1,3]dioxol-5-yl)-3-phenylpropan-1-one, **2b** (95.2 mg, 83%) was prepared following *GP2*. The product was isolated as a colorless oil. dr = 3.8:1 based on ^{1}H NMR of the crude reaction mixture. **^{1}H NMR** (500 MHz, $CDCl_3$, major diastereomer) δ 7.37 – 7.15 (m, 10H), 5.99 (d, *J* = 3.9 Hz, 1H), 4.61 (d, *J* = 3.9 Hz, 1H), 4.59 – 4.56 (m, 1H), 4.46 (s, 1H), 4.45 (s, 1H), 4.03 (d, *J* = 1.8 Hz, 1H), 3.21 – 2.80 (m, 4H), 1.32 (s, 3H), 1.26 (s, 3H). **^{1}H NMR** (500 MHz, $CDCl_3$, minor diastereomer) δ 7.37 – 7.15 (m, 10H), 5.96 (d, *J* = 3.7 Hz, 1H), 4.61 (d, *J* = 3.9 Hz, 1H), 4.59 – 4.56 (m, 1H), 4.46 (s, 1H), 4.45 (s, 1H), 4.02 (d, *J* = 1.6 Hz, 1H), 3.21 – 2.80 (m, 4H), 1.61 (s, 3H), 1.47 (s, 3H). **^{13}C NMR** (126 MHz, $CDCl_3$, major diastereomer) δ 208.3, 141.0, 137.1, 128.7 (2C), 128.6 (2C), 128.5 (2C), 128.2, 128.0 (2C), 126.2, 112.2, 106.5, 89.7, 83.8 (2C), 72.0, 40.7, 29.2, 26.0, 25.8. **^{13}C NMR** (126 MHz, $CDCl_3$, minor diastereomer) δ 208.3, 141.3, 137.5, 128.6 (2C), 128.5 (2C), 128.0 (2C), 127.9, 127.8 (2C), 126.1, 111.7, 105.7, 83.1, 82.0, 71.3, 70.5, 42.3, 28.8, 26.9, 26.8. **FT-IR** (cm^{-1}, neat, ATR): 2986, 1715, 1454, 1374, 1260, 1211, 1163, 1070, 1011. **HRMS** (ESI) calcd for $C_{23}H_{26}O_5Na$ $[M+Na]^+$: 405.1678, found: 405.1664.

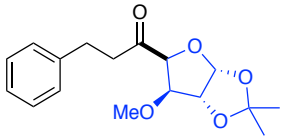

1-((3a*R*,6*R*,6a*R*)-6-Methoxy-2,2-dimethyltetrahydrofuro[2,3-d][1,3]dioxol-5-yl)-3-phenylpropan-1-one, **2c** (49.8 mg, 54%) was prepared following *GP2*. The product was isolated as a colorless oil. dr = 2.7:1 based on ^{1}H NMR of the crude reaction mixture. **^{1}H NMR** (500 MHz, $CDCl_3$, major diastereomer) δ 7.33 – 7.11 (m, 5H), 5.96 (d, *J* = 3.9 Hz, 1H), 4.55 (t, *J* = 4.4

Hz, 1H), 4.37 (s, 1H), 4.23 (s, 1H), 3.40 (s, 3H), 3.23 – 2.84 (m, 4H), 1.33 (s, 3H), 1.27 (s, 3H). **^{1}H NMR** (500 MHz, $CDCl_3$, minor diastereomer) δ 7.33 – 7.11 (m, 5H), 6.02 (d, *J* = 3.5 Hz, 1H), 4.62 (d, *J* = 3.6 Hz, 1H), 4.56 (d, *J* = 4.7 Hz, 1H), 4.02 (d, *J* = 3.6 Hz, 1H), 3.26 (s, 3H), 3.23 – 2.84 (m, 4H), 1.47 (s, 3H), 1.33 (s, 3H). **^{13}C NMR** (126 MHz, $CDCl_3$, major diastereomer) δ 208.4, 141.1, 128.6 (2C), 128.5 (2C), 126.2, 112.2, 106.4, 89.4, 85.7, 83.3, 57.5, 40.8, 29.3, 26.0, 25.8. **^{13}C NMR** (126 MHz, $CDCl_3$, minor diastereomer) δ 207.5, 141.3, 128.6 (2C), 128.5 (2C), 126.1, 112.4, 106.0, 86.1, 85.5, 81.3, 58.3, 42.0, 28.7, 27.0, 26.4. **FT-IR** (cm^{-1}, neat, ATR): 2988, 2936, 1715, 1375, 1212, 1049, 1079, 1016, 962. **HRMS** (ESI) calcd for $C_{17}H_{22}O_5Na$ $[M+Na]^+$: 329.1365, found: 329.1365.

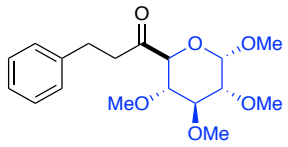

3-Phenyl-1-((3*S*,4*S*,5*R*,6*S*)-3,4,5,6-tetramethoxytetrahydro-2H-pyran-2-yl)propan-1-one, **2d** (70.5 mg, 83%) was prepared following *GP2*. The product was isolated as a colorless oil. dr = 1.9:1 based on ^{1}H NMR of the crude reaction mixture. **^{1}H NMR** (500 MHz, $CDCl_3$) δ 7.33 – 7.24 (m, 2H), 7.24 – 7.14 (m, 3H), 4.84 (d, *J* = 3.5 Hz, 1H), 4.01 (d, *J* = 9.9 Hz, 1H), 3.61 (s, 3H), 3.57 – 3.52 (m, 1H), 3.51 (s, 3H), 3.41 (s, 3H), 3.40 (s, 3H), 3.27 – 3.17 (m, 2H), 3.03 – 2.84 (m, 4H). **^{13}C NMR** (126 MHz, $CDCl_3$) δ 205.9, 141.0, 128.6 (2C), 128.5 (2C), 126.2, 98.1, 83.5, 81.4, 80.8, 73.6, 61.1, 60.5, 59.3, 55.7, 42.8, 29.2. (*Only the signals corresponding to the major stereoisomer are reported*). **FT-IR** (cm^{-1}, neat, ATR): 2931, 2834, 1727, 1453, 1361, 1187, 1094, 1064, 1046. **HRMS** (ESI) calcd for $C_{18}H_{26}O_6Na$ $[M+Na]^+$: 361.1627, found: 361.1626.

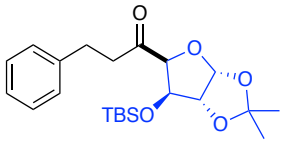

1-((3a*R*,6*R*,6a*R*)-6-((*tert*-Butyldimethylsilyl)oxy)-2,2-dimethyltetrahydrofuro[2,3-d][1,3]dioxol-5-yl)-3-phenylpropan-1-one, **2e** (89.8 mg, 88%) was prepared following *GP2*. The product was isolated as a colorless oil. dr = 3.8:1 based on ^{1}H NMR of the crude reaction mixture. **^{1}H NMR** (500 MHz, $CDCl_3$) δ 7.28 – 7.24 (m, 2H), 7.21 – 7.15 (m, 3H), 6.00 (d, *J* = 3.7 Hz, 1H), 4.72 (s, 1H), 4.40 (d, *J* = 3.7 Hz, 1H), 4.23 (s, 1H), 3.29 – 3.10 (m, 1H), 2.99 – 2.78 (m, 3H), 1.31 (s, 3H), 1.26 (s, 3H), 0.89 (s, 9H), 0.13 (s, 3H), 0.11 (s, 3H). **^{13}C NMR** (126 MHz, $CDCl_3$) δ 208.5, 141.1, 128.6 (2C), 128.5 (2C), 126.2, 111.9, 106.5, 92.7, 86.3, 77.6, 40.8, 29.2, 25.9, 25.8 (3C), 25.7, 18.1, -4.8, -4.7. (*Only the signals corresponding to the major stereoisomer are reported*). **FT-IR** (cm^{-1}, neat, ATR): 2980, 2976, 1703, 1403, 1402, 1187, 1163, 1076, 1003. **HRMS** (ESI) calcd for $C_{22}H_{34}O_5SiNa$, $[M+Na]^+$: 429.2073, found: 429.2086.

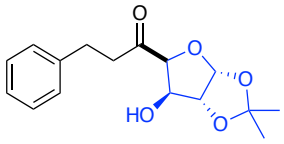

1-((3a*R*,6*R*,6a*R*)-6-Hydroxy-2,2-dimethyltetrahydrofuro[2,3-d][1,3]dioxol-5-yl)-3-phenylpropan-1-one, **2f** (58.1 mg, 79%) was prepared following *GP2*. After 24 h, a soln of TBAF (1.25 mL, 1.0 M in THF, 6.0 equiv) was added dropwise at 0 °C. The reaction was allowed to stir for 2 h at rt, then quenched by addition of saturated aqueous soln of $NaHCO_3$. The aqueous layer was extracted with EtOAc, and the combined organic layers were dried ($MgSO_4$) and concentrated under reduced pressure. The product was isolated as a crystalline solid. **mp** = 124-126 °C. dr = 3.6:1 based on ^{1}H NMR of the crude reaction mixture. **^{1}H NMR** (500 MHz, $CDCl_3$, major diastereomer) δ 7.30 – 7.25 (m, 2H), 7.21 – 7.16 (m, 3H), 6.00 (d, *J* = 3.8 Hz, 1H),

4.72 (d, J = 3.2 Hz, 1H), 4.53 (d, J = 3.8 Hz, 1H), 4.33 (s, 1H), 3.24 – 3.14 (m, 1H), 3.03 – 2.81 (m, 4H), 1.33 (s, 3H), 1.27 (s, 3H). **^{1}H NMR** (500 MHz, $CDCl_3$, minor diastereomer) δ 7.29 – 7.24 (m, 2H), 7.22 – 7.16 (m, 3H), 5.96 (d, J = 3.6 Hz, 1H), 4.51 (d, J = 3.6 Hz, 1H), 4.28 (s, 1H), 4.10 (dd, J = 10.2, 2.7 Hz, 1H), 3.88 (dd, J = 10.2, 0.9 Hz, 1H), 3.24 – 3.14 (m, 1H), 3.03 – 2.81 (m, 2H), 1.90 (s, 1H), 1.49 (s, 3H), 1.32 (s, 3H). **^{13}C NMR** (126 MHz, $CDCl_3$, major diastereomer) δ 208.7, 140.9, 128.6 (2C), 128.5 (2C), 126.2, 112.3, 106.3, 91.7, 85.8, 76.7, 40.8, 29.2, 25.9, 25.7. **^{13}C NMR** (126 MHz, $CDCl_3$, minor diastereomer) δ 208.5, 141.0, 128.6 (2C), 128.5 (2C), 126.3, 111.9, 105.3, 85.1, 75.5, 73.0, 40.8, 29.2, 25.9, 25.8. **FT-IR** (cm^{-1}, neat, ATR): 3417, 2979, 1724, 1374, 1219, 1061, 1009, 974. **HRMS** (ESI) calcd for $C_{16}H_{20}O_5Na$ $[M+Na]^+$: 315.1208, found: 315.1218.

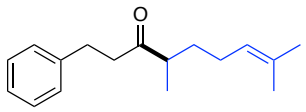

4,8-Dimethyl-1-phenylnon-7-en-3-one, **2g** (51.3 mg, 70%) was prepared following *GP2*. The product was isolated as a colorless oil. **^{1}H NMR** (500 MHz, $CDCl_3$) δ 7.30 – 7.26 (m, 2H), 7.18 (ddt, J = 7.3, 3.2, 1.4 Hz, 3H), 5.04 (ddq, J = 8.6, 5.8, 1.5 Hz, 1H), 2.89 (t, J = 7.6 Hz, 2H), 2.81 – 2.64 (m, 2H), 2.50 (q, J = 6.9 Hz, 1H), 2.00 – 1.76 (m, 2H), 1.75 – 1.61 (m, 1H), 1.68 (d, J = 1.3 Hz, 3H), 1.57 (d, J = 1.3 Hz, 3H), 1.33 (ddt, J = 13.5, 8.3, 6.8 Hz, 1H), 1.04 (d, J = 6.9 Hz, 3H).**^{13}C NMR** (126 MHz, $CDCl_3$) δ 213.9, 141.7, 132.5, 128.7 (2C), 128.6 (2C), 126.3, 124.0, 46.2, 43.0, 33.2, 30.1, 26.0, 25.9, 18.0, 16.5. **FT-IR** (cm^{-1}, neat, ATR): 2967, 2928, 1711, 1454, 1377, 905, 729, 700, 650 ppm. **HRMS** (EI) calcd for $C_{17}H_{24}O$ $[M]^+$: 244.1827, found: 244.1843.

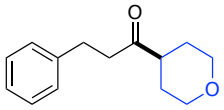

3-Phenyl-1-(tetrahydro-2*H*-pyran-4-yl)propan-1-one, **2h** (52.4 mg, 80%) was prepared following *GP2*. The product was isolated as a colorless oil. **^{1}H NMR** (500 MHz, $CDCl_3$) δ 7.37 – 7.26 (m, 2H), 7.23 – 7.03 (m, 3H), 3.97 (ddd, *J* = 11.4, 4.1, 2.6 Hz, 2H), 3.39 (td, *J* = 11.3, 2.9 Hz, 2H), 2.90 (t, *J* = 7.5 Hz, 2H), 2.77 (dd, *J* = 8.0, 6.9 Hz, 2H), 2.50 (m, 1H), 1.83 – 1.60 (m, 4H). **^{13}C NMR** (126 MHz, $CDCl_3$) δ 211.2, 141.4, 128.8 (2C), 128.6 (2C), 126.4, 67.5 (2C), 48.0, 42.2, 30.0, 28.3 (2C). **FT-IR** (cm^{-1}, neat, ATR): 2952, 2847, 1707, 1445, 1387, 1276, 1240, 1113, 1092, 1016. **HRMS** (EI) calcd for $C_{14}H_{18}O_2$ $[M]^+$: 218.1307, found: 218.1315.

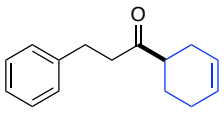

1-(Cyclohex-3-en-1-yl)-3-phenylpropan-1-one, 2i (98.5 mg, 92%) was prepared following *GP2*. The product was isolated as a colorless oil. **^{1}H NMR** (500 MHz, $CDCl_3$) δ 7.30 – 7.26 (m, 2H), 7.19 (m, 3H), 5.68 (m, 2H), 2.91 (m, 2H), 2.85 – 2.76 (m, 2H), 2.58 (m, 1H), 2.15 (dd, *J* = 14.4, 4.6 Hz, 2H), 2.08 (qt, *J* = 9.7, 3.7 Hz, 2H), 1.91 (dq, *J* = 12.6, 4.1 Hz, 1H), 1.59 – 1.52 (m, 1H). **^{13}C NMR** (126 MHz, $CDCl_3$) δ 212.7, 141.5, 128.6 (2C), 128.5 (2C), 126.8, 126.2, 125.5, 46.9, 42.5, 29.9, 26.9, 24.9, 24.7. **FT-IR** (cm^{-1}, neat, ATR): 3026, 2924, 2839, 1707, 1604, 1496, 1453, 1374, 1104.

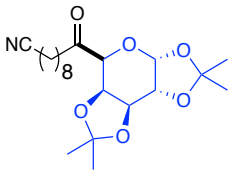

10-Oxo-10-((3a*R*,5*S*,5a*R*,8a*S*,8b*R*)-2,2,7,7-tetramethyltetrahydro-5*H*-bis([1,3]dioxolo)[4,5-*b*:4',5'-*d*]pyran-5-yl)decanenitrile, **2j** (109.0 mg, 92%) was prepared following *GP2*. The product was isolated as a colorless oil. dr = 3.8:1 based on ^{1}H NMR of the crude reaction mixture. **^{1}H NMR** (500 MHz, $CDCl_3$) δ 5.63 (d, *J* = 4.9 Hz, 1H), 4.68 – 4.59 (m, 1H), 4.55 (dd, *J* = 7.7, 1.9 Hz, 1H), 4.34 (dd, *J* = 4.8, 2.3 Hz, 1H), 4.16 (d, *J* = 1.7 Hz, 1H), 2.76 – 2.46 (m, 2H), 2.31 (t, *J* = 7.1 Hz, 2H), 1.69 – 1.20 (m, 24H). **^{13}C NMR** (126 MHz, $CDCl_3$) δ 209.5, 119.9, 109.6, 109.0, 96.6, 73.8, 72.6, 70.7, 70.5, 39.9, 29.2, 29.0, 28.7, 28.7, 26.1, 26.0, 25.5, 24.9, 24.4, 22.5, 17.2. (*Only the signals corresponding to the major stereoisomer are reported*). **FT-IR** (cm^{-1}, neat, ATR): 2988, 2933, 2857, 1718, 1382, 1372, 1255, 1211, 1166, 1065. **HRMS** (ESI) calcd for $C_{21}H_{33}NO_6Na$ $[M+Na]^+$: 418.2206, found: 418.2203.

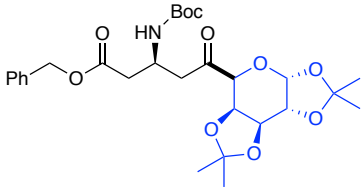

Benzyl (3*S*)-3-((*tert*-Butoxycarbonyl)amino)-5-oxo-5-((3a*R*,5a*R*,8a*S*,8b*R*)-2,2,7,7-tetramethyltetrahydro-5*H*-bis([1,3]dioxolo)[4,5-*b*:4',5'-*d*]pyran-5-yl)pentanoate, **2k** (124 mg, 75%) was prepared following *GP2*. The product was isolated as a pale-yellow oil. dr = 2:1 based on ^{1}H NMR of the crude reaction mixture. **^{1}H NMR** (500 MHz, $CDCl_3$) δ 7.50 – 7.29 (m, 5H), 5.61 (d, *J* = 4.7 Hz, 1H), 5.37 – 5.18 (m, 1H), 5.11 (s, 2H), 4.62 (dd, *J* = 7.9, 2.6 Hz, 1H), 4.53 (dd, *J* = 7.8, 2.3 Hz, 1H), 4.34 (dd, *J* = 5.0, 2.5 Hz, 1H), 4.18 (d, *J* = 2.3 Hz, 1H), 3.13 – 2.85 (m, 2H), 2.79 (dd, *J* = 16.1, 5.6 Hz, 1H), 2.66 (dd, *J* = 16.4, 6.4 Hz, 1H), 1.51 (s, 3H), 1.42 (s, 12H),

1.34 (s, 3H), 1.29 (s, 3H). (*Only the signals corresponding to the major stereoisomer are reported*). **FT-IR** (cm^{-1}, neat, ATR): 3425, 2981, 2936, 1715, 1498, 1456, 1383, 1369, 1306, 1254, 1211, 1165, 1108, 1067, 1006. **HRMS** (ESI) calcd for $C_{28}H_{40}NO_{10}$ $[M+H]^+$: 550.2652, found: 550.2651.

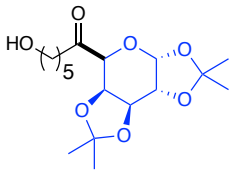

6-Hydroxy-1-((3a*R*,5a*R*,8a*S*,8b*R*)-2,2,7,7-tetramethyltetrahydro-5*H*-bis([1,3]dioxolo)[4,5-*b*:4',5'-*d*]pyran-5-yl)hexan-1-one, **2l** (91.9 mg, 89%) was prepared following *GP2*. The product was isolated as a colorless oil. dr = 1.5:1 based on ^1H NMR of the crude reaction mixture. **^1H NMR** (500 MHz, $CDCl_3$) δ 5.63 (d, *J* = 5.0 Hz, 1H), 4.62 (dd, *J* = 7.8, 2.4 Hz, 1H), 4.56 (dd, *J* = 7.8, 2.2 Hz, 1H), 4.34 (dd, *J* = 5.0, 2.4 Hz, 1H), 4.17 (d, *J* = 2.1 Hz, 1H), 3.64 (t, *J* = 6.6 Hz, 2H), 2.80 – 2.39 (m, 3H), 1.70 – 1.52 (m, 6H), 1.49 (s, 3H), 1.43 (s, 3H), 1.33 (s, 3H), 1.30 (s, 3H). **^{13}C NMR** (126 MHz, $CDCl_3$) δ 209.7, 109.8, 109.2, 96.7, 74.0, 72.8, 70.9, 70.7, 63.0, 40.0, 32.8, 26.2, 26.1, 25.4, 25.1, 24.5, 22.4. **FT-IR** (cm^{-1}, neat, ATR): 3426, 2988, 2936, 1717, 1383, 1373, 1255, 1211, 1166, 1140, 1109, 1064, 1005. **HRMS** (ESI) calcd for $C_{17}H_{28}O_7Na$ $[M+Na]^+$: 367.1733, found: 367.1737

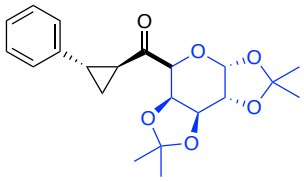

((1*S*,2*S*)-2-Phenylcyclopropyl)((3a*R*,5a*R*,8a*S*,8b*R*)-2,2,7,7-tetramethyltetrahydro-5*H*-bis([1,3]dioxolo)[4,5-*b*:4',5'-*d*]pyran-5-yl)methanone, **2m** (78.6 mg, 70%) was prepared

following *GP2*. The product was isolated as a colorless oil. dr = 1:1 based on ^{1}H NMR of the crude reaction mixture. **^{1}H NMR** (500 MHz, $CDCl_3$) δ 7.34 – 7.24 (m, 2H), 7.24 – 7.16 (m, 1H), 7.17 – 6.90 (m, 2H), 5.67 (d, *J* = 5.0 Hz, 1H), 4.65 (dd, *J* = 7.8, 2.6 Hz, 1H), 4.59 (dd, *J* = 7.8, 2.3 Hz, 1H), 4.38 (dd, *J* = 5.0, 2.6 Hz, 1H), 4.33 (d, *J* = 2.3 Hz, 1H), 2.73 (ddd, *J* = 8.3, 5.3, 4.1 Hz, 1H), 2.62 (ddd, *J* = 8.9, 6.7, 4.1 Hz, 1H), 1.73 (ddd, *J* = 9.2, 5.3, 4.0 Hz, 1H), 1.50 (s, 3H), 1.48 (s, 3H), 1.45 – 1.36 (m, 1H), 1.33 (d, *J* = 1.8 Hz, 6H). **^{13}C NMR** (126 MHz, $CDCl_3$) δ 206.6, 140.6, 128.6 (2C), 126.74, 126.72 (2C), 110.0, 109.2, 96.8, 74.3, 72.5, 71.0, 70.6, 30.1, 29.2, 26.2, 26.2, 25.1, 24.7, 20.0. **FT-IR** (cm^{-1}, neat, ATR): 2988, 2935, 1698, 1382, 1341, 1255, 1212, 1166, 1103, 1068, 1005. **HRMS** (EI) calcd for $C_{21}H_{26}O_6$ $[M]^+$: 374.1726, found: 374.1733.

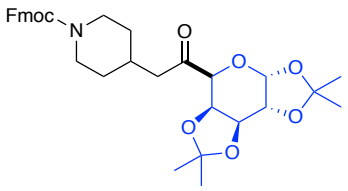

(9*H*-Fluoren-9-yl)methyl 4-(2-Oxo-2-((3a*R*,5a*R*,8a*S*,8b*R*)-2,2,7,7-tetramethyltetrahydro-5*H*-bis([1,3]dioxolo)[4,5-*b*:4',5'-*d*]pyran-5-yl)ethyl)piperidine-1-carboxylate, **2n** (138.5 mg, 80%) was prepared following *GP2*. The product was isolated as a pale-yellow oil. dr = 22:1 based on ^{1}H NMR of the crude reaction mixture. **^{1}H NMR** (500 MHz, $CDCl_3$) δ 7.76 (m, 2H), 7.58 (m, 2H), 7.40 (t, *J* = 7.4 Hz, 2H), 7.31 (td, *J* = 7.5, 1.1 Hz, 2H), 5.65 (d, *J* = 4.9 Hz, 1H), 4.63 (dd, *J* = 7.8, 2.5 Hz, 1H), 4.57 (dd, *J* = 7.8, 2.2 Hz, 1H), 4.47 – 4.38 (m, 2H), 4.36 (dd, *J* = 5.0, 2.5 Hz, 1H), 4.24 (t, *J* = 6.9 Hz, 1H), 4.16 (d, *J* = 2.2 Hz, 1H), 4.07 – 3.98 (m, 2H), 3.01 – 2.74 (m, 2H), 2.57 (dd, *J* = 6.7, 3.6 Hz, 2H), 2.09 (qd, *J* = 6.8, 6.1, 4.0 Hz, 1H), 1.71 (t, *J* = 12.4 Hz, 2H), 1.51 (s, 3H), 1.44 (s, 3H), 1.35 (s, 3H), 1.31 (s, 3H), 1.28 – 1.16 (m, 2H). (*Only the signals corresponding to the major stereoisomer are reported*). **FT-IR** (cm^{-1}, neat, ATR): 2988, 2934,

1698, 1450, 1382, 1254, 1237, 1211, 1066, 1006. **HRMS** (ESI) calcd for $C_{33}H_{40}NO_8$ $[M+H]^+$: 578.2754, found: 578.2764.

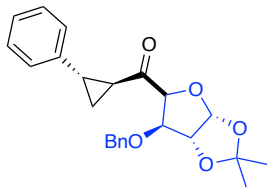

((3a*R*,6*R*,6a*R*)-6-(Benzyloxy)-2,2-dimethyltetrahydrofuro[2,3-d][1,3]dioxol-5-yl)((1S,2S)-2-phenylcyclopropyl)methanone, **2o** (95.9 mg, 81%) was prepared following *GP2*. The product was isolated as a colorless oil. dr = 2.5:1 based on ^{1}H NMR of the crude reaction mixture. **^{1}H NMR** (500 MHz, $CDCl_3$, major diastereomer) δ 7.44 – 7.05 (m, 10H), 6.03 (d, *J* = 3.6 Hz, 1H), 4.67 – 4.47 (m, 4H), 4.03 (d, *J* = 8.4 Hz, 1H), 2.86 – 2.79 (m, 1H), 2.67 (t, *J* = 9.7 Hz, 1H), 1.58 (dd, *J* = 9.2, 4.3 Hz, 1H), 1.41 (td, *J* = 8.2, 4.0 Hz, 1H), 1.22 (s, 3H), 1.14 (s, 3H). **^{1}H NMR** (500 MHz, $CDCl_3$, minor diastereomer) δ 7.44 – 7.05 (m, 10H), 5.97 (d, *J* = 3.5 Hz, 1H), 4.67 – 4.47 (m, 4H), 4.03 (d, *J* = 8.4 Hz, 1H), 2.86 – 2.79 (m, 1H), 2.67 (t, *J* = 9.7 Hz, 1H), 1.58 (dd, *J* = 9.2, 4.3 Hz, 1H), 1.47 (s, 3H), 1.41 (td, *J* = 8.2, 4.0 Hz, 1H), 1.31 (s, 3H). **^{13}C NMR** (126 MHz, $CDCl_3$, major diastereomer) δ 207.0, 140.1, 137.1, 128.7 (2C), 128.5 (2C), 128.1 (2C), 127.8, 126.6, 126.4 (2C), 112.6, 106.6, 89.8, 84.0, 83.8, 72.0, 29.1, 28.1, 26.0, 25.9, 22.1. **^{13}C NMR** (126 MHz, $CDCl_3$, minor diastereomer) δ 207.0, 140.0, 137.5, 128.7 (2C), 128.2 (2C), 128.1 (2C), 127.8, 126.6, 126.4 (2C), 111.7, 105.7, 83.1, 82.0, 71.4, 70.5, 29.8, 26.9, 26.4, 25.9, 22.1. **FT-IR** (cm^{-1}, neat, ATR): 2927, 1694, 1398, 1374, 1212, 1075, 1013. **HRMS** (EI) calcd for $C_{24}H_{26}O_5$ $[M]^+$: 394.1780, found: 394.1767.

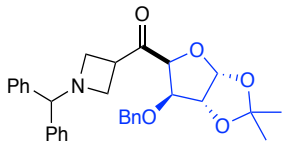

(1-Benzhydrylazetidin-3-yl)((3a*R*,6*R*,6a*R*)-6-(benzyloxy)-2,2-dimethyltetrahydrofuro[2,3-d][1,3]dioxol-5-yl)methanone, **2o** (132.0 mg, 88%) was prepared following *GP2*. The product was isolated as a white foam. dr = 3.9:1 based on ^{1}H NMR of the crude reaction mixture. **^{1}H NMR** (500 MHz, $CDCl_3$, major diastereomer) δ 7.45 – 7.10 (m, 15H), 5.94 (d, *J* = 3.8 Hz, 1H), 4.61 – 4.56 (m, 3H), 4.52 (s, 1H), 4.42 (s, 1H), 4.33 (s, 1H), 4.04 – 3.96 (m, 1H), 3.55 (t, *J* = 7.9 Hz, 1H), 3.37 (t, *J* = 7.5 Hz, 1H), 3.27 (t, *J* = 7.4 Hz, 1H), 3.03 (t, *J* = 7.4 Hz, 1H), 1.29 (s, 3H), 1.24 (s, 3H). **^{1}H NMR** (500 MHz, $CDCl_3$, minor diastereomer) δ 7.36 – 7.27 (m, 7H), 7.26 – 7.14 (m, 8H), 5.97 (d, *J* = 3.6 Hz, 1H), 4.69 (d, *J* = 3.7 Hz, 1H), 4.57 – 4.53 (m, 2H), 4.43 (d, *J* = 11.4 Hz, 1H), 4.27 (d, *J* = 3.7 Hz, 1H), 4.20 (s, 1H), 3.73 (t, *J* = 8.2 Hz, 1H), 3.39 (t, *J* = 7.9 Hz, 1H), 3.30 (t, *J* = 7.8 Hz, 1H), 3.22 (t, *J* = 7.8 Hz, 1H), 3.16 (t, *J* = 7.9 Hz, 1H), 1.44 (s, 3H), 1.30 (s, 3H). **^{13}C NMR** (126 MHz, $CDCl_3$, major diastereomer) δ 207.9, 141.9, 141.8, 137.0, 128.7 (2C), 128.6 (2C), 128.2 (2C), 128.0 (2C), 127.8, 127.6 (2C), 127.5 (2C), 127.3 (2C), 112.2, 106.4, 88.4, 83.8, 83.7, 77.8, 72.0, 56.8, 54.1, 37.0, 26.0, 25.8. **^{13}C NMR** (126 MHz, $CDCl_3$, minor diastereomer) δ 207.4, 142.0, 142.0, 136.9, 128.6 (2C), 128.5 (2C), 128.5 (2C), 128.3, 128.0 (2C), 127.7 (2C), 127.6 (2C), 127.2, 127.2, 112.5, 106.1, 85.6, 84.1, 81.9, 77.8, 72.9, 55.2, 54.8, 38.8, 27.1, 26.4. **FT-IR** (cm^{-1}, neat, ATR): 2939, 2848, 1712, 1453, 1374, 1211, 1163, 1074, 1011. **HRMS** (ESI) calcd for $C_{31}H_{34}NO_5$ $[M+H]^+$: 500.2437, found: 500.2456.

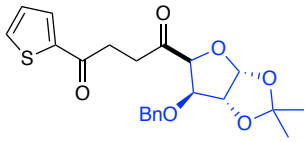

1-((3a*R*,6*R*,6a*R*)-6-(Benzyloxy)-2,2-dimethyltetrahydrofuro[2,3-d][1,3]dioxol-5-yl)-4-(thiophen-2-yl)butane-1,4-dione, **2q** (108.5 mg, 86%) was prepared following *GP2*. The product was isolated as a colorless oil. dr = 2.2:1 based on ^{1}H NMR of the crude reaction mixture. **^{1}H NMR** (500 MHz, $CDCl_3$, major diastereomer) δ 7.76 (dd, *J* = 3.8, 1.1 Hz, 1H), 7.62 (dd, *J* = 4.9, 1.0 Hz, 1H), 7.37 – 7.25 (m, 5H), 7.13 (dd, *J* = 4.9, 3.8 Hz, 1H), 6.03 (d, *J* = 3.9 Hz, 1H), 4.65 – 4.63 (m, 2H), 4.62 (d, *J* = 3.2 Hz, 2H), 4.51 (d, *J* = 1.2 Hz, 1H), 3.36 – 3.28 (m, 1H), 3.19 – 3.00 (m, 3H), 1.41 (s, 3H), 1.29 (s, 3H). **^{1}H NMR** (500 MHz, $CDCl_3$, minor diastereomer) δ 7.69 (dd, *J* = 3.8, 1.0 Hz, 1H), 7.61 (d, *J* = 1.0 Hz, 1H), 7.37 – 7.25 (m, 5H), 7.10 (dd, *J* = 5.0, 3.8 Hz, 1H), 6.09 (d, *J* = 3.6 Hz, 1H), 4.74 (d, *J* = 3.7 Hz, 1H), 4.63 – 4.57 (m, 3H), 4.30 (d, *J* = 3.7 Hz, 1H), 3.37 – 3.25 (m, 1H), 3.18 – 3.00 (m, 3H), 1.48 (s, 3H), 1.33 (s, 3H). **^{13}C NMR** (126 MHz, $CDCl_3$, major diastereomer) δ 207.7, 191.3, 143.8, 137.2, 133.6, 132.0, 128.7 (2C), 128.2, 128.1, 128.0 (2C), 112.3, 106.5, 89.6, 84.1, 83.8, 72.1, 33.3, 32.8, 26.1, 25.9. **^{13}C NMR** (126 MHz, $CDCl_3$, minor diastereomer) δ 207.1, 191.4, 144.0, 137.1, 133.5, 132.0, 128.6 (2C), 128.2, 128.1, 127.9 (2C), 112.5, 106.1, 85.6, 83.8, 82.0, 72.6, 34.9, 32.5, 27.1, 26.5. **FT-IR** (cm^{-1}, neat, ATR): 2987, 1717, 1662, 1415, 1374, 1236, 1212, 1075, 1012. **HRMS** (ESI) calcd for $C_{22}H_{24}O_{56}SNa$ $[M+Na]^+$: 439.1191, found: 439.1193.

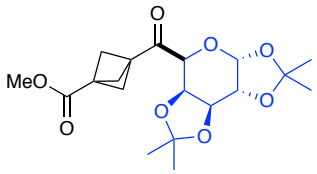

Methyl 3-((3a*R*,5a*R*,8a*S*,8b*R*)-2,2,7,7-Tetramethyltetrahydro-5H-bis([1,3]dioxolo)[4,5-b:4',5'-d]pyran-5-carbonyl)bicyclo[1.1.1]pentane-1-carboxylate, **2r** (42.5 mg, 76%) was prepared following *GP2*. The product was isolated as a crystalline white solid. dr = 4.6:1 based on ^{1}H NMR of the crude reaction mixture. **mp** = 58-60 °C. **^{1}H NMR** (500 MHz, $CDCl_3$) δ 5.61 (d, *J* = 5.0 Hz, 1H), 4.60 (dd, *J* = 7.8, 1.9 Hz, 1H), 4.51 (dd, *J* = 7.8, 1.5 Hz, 1H), 4.32 (s, 2H), 3.66 (s, 3H), 2.37 (s, 6H), 1.48 (s, 3H), 1.42 (s, 3H), 1.32 (s, 3H), 1.28 (s, 3H). **^{13}C NMR** (126 MHz, $CDCl_3$) δ 204.3, 170.3, 109.7, 108.9, 96.4, 74.6, 72.3, 70.6, 70.3, 53.7 (2C), 53.5, 51.9, 43.6, 38.3, 26.1, 25.9, 24.9, 24.1. (*Only the signals corresponding to the major stereoisomer are reported*). **FT-IR** (cm^{-1}, neat, ATR): 2989, 2928, 1732, 1704, 1256, 1205, 1165, 1109, 1064, 999. **HRMS** (ESI) calcd for $C_{19}H_{26}O_6Na$, $[M+Na]^+$: 405.1549, found: 405.1535.

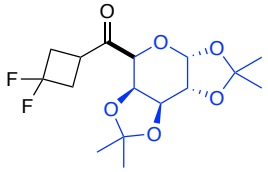

(3,3-Difluorocyclobutyl)((3a*R*,5a*R*,8a*S*,8b*R*)-2,2,7,7-tetramethyltetrahydro-5H-bis([1,3]dioxolo) [4,5-b:4',5'-d]Pyran-5-yl)methanone, **2s** (88.7 mg, 85%) was prepared following *GP2*. The product was isolated as a colorless oil. dr = 7.5:1 based on ^{1}H NMR of the crude reaction mixture. **^{1}H NMR** (500 MHz, $CDCl_3$) δ 5.60 (d, *J* = 4.9 Hz, 1H), 4.62 (dd, *J* = 7.8, 2.1 Hz, 1H), 4.57 (dd, *J* = 7.8, 1.7 Hz, 1H), 4.33 (dd, *J* = 4.8, 2.2 Hz, 1H), 4.27 (d, *J* = 1.5 Hz, 1H), 3.68 – 3.52 (m, 1H), 2.91 – 2.77 (m, 2H), 2.72 – 2.59 (m, 2H), 1.48 (s, 3H), 1.41 (s, 3H), 1.33 (s, 3H), 1.30 (s, 3H). **^{13}C NMR** (126 MHz, $CDCl_3$) δ 207.6, 119.1 (dd, $^{1}J_{C\text{-}F}$ = 285.1, 269.6

Hz), 109.7, 109.1, 96.6, 73.6, 72.2, 70.6, 70.5, 37.74 (t, $^{2}J_{C\text{-}F}$ = 24.3 Hz), 36.91 (t, $^{2}J_{C\text{-}F}$ = 24.3 Hz), 30.76 (dd, $^{3}J_{C\text{-}F}$ = 14.2, 5.0 Hz), 26.1, 25.9, 24.9, 24.1. **^{19}F NMR** (471 MHz, $CDCl_3$) δ -82.9 (d, $^{1}J_{F\text{-}F}$ = 191.9 Hz), -97.0 (d, $^{1}J_{F\text{-}F}$ = 192.0 Hz). (*Only the signals corresponding to the major stereoisomer are reported*). **FT-IR** (cm^{-1}, neat, ATR): 2987, 2939, 1718, 1294, 1210, 1162, 1063, 1006, 897. **HRMS** (ESI) calcd for $C_{16}H_{22}F_2O_6Na$ $[M+Na]^+$: 371.1282, found: 371.1284.

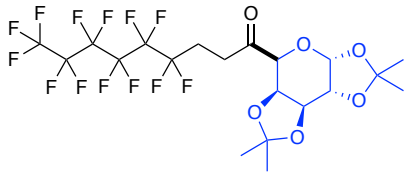

4,4,5,5,6,6,7,7,8,8,9,9,9-Tridecafluoro-1-((3a*R*,5a*R*,8a*S*,8b*R*)-2,2,7,7-tetramethyltetrahydro-5*H*-bis([1,3]dioxolo)[4,5-*b*:4',5'-*d*]pyran-5-yl)nonan-1-one, **2t** (114 mg, 63%) was prepared following *GP2*. The product was isolated as a colorless oil. dr = 1.8:1 based on ^{1}H NMR of the crude reaction mixture. **^{1}H NMR** (500 MHz, $CDCl_3$) δ 5.65 (d, *J* = 4.9 Hz, 1H), 4.64 (dd, *J* = 7.8, 2.5 Hz, 1H), 4.53 (dd, *J* = 7.8, 2.2 Hz, 1H), 4.37 (dd, *J* = 5.0, 2.5 Hz, 1H), 4.24 (d, *J* = 2.2 Hz, 1H), 3.01 (ddd, *J* = 19.2, 9.9, 5.7 Hz, 1H), 2.90 (dq, *J* = 15.5, 5.3, 4.8 Hz, 1H), 2.50 – 2.18 (m, 2H), 1.50 (s, 3H), 1.44 (s, 3H), 1.34 (s, 3H), 1.30 (s, 3H). **^{13}C NMR** (126 MHz, $CDCl_3$) δ 207.0, 120.6, 118.8, 118.6, 116.3, 111.3, 110.8, 110.0, 109.4, 96.6, 74.0, 72.8, 70.8, 70.6, 31.7, 30.0, 26.2, 26.0, 25.1, 24.4. **^{19}F NMR** (471 MHz, $CDCl_3$) δ -80.8 (t, *J* = 10.0 Hz, 3F), -107.6 – -118.7 (m, 2F), -121.9 (q, *J* = 13.6, 13.0 Hz, 2F), -122.4 – -123.1 (m, 2F), -123.5 (t, *J* = 15.1 Hz, 2F), -126.1 (td, *J* = 14.9, 6.4 Hz, 2F). (*Only the signals corresponding to the minor stereoisomer are reported*). **FT-IR** (cm^{-1}, neat, ATR): 2986, 2935, 1724, 1381, 1372, 1250, 1210, 1166, 1145, 1114, 1077, 1052. **HRMS** (ESI) calcd for $C_{20}H_{22}F_{13}O_6$ $[M+H]^+$: 605.1209, found: 605.1219.

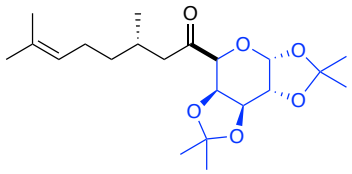

(3*S*)-3,7-Dimethyl-1-((3a*R*,5a*R*,8a*S*,8b*R*)-2,2,7,7-tetramethyltetrahydro-5*H*bis([1,3]dioxolo)[4,5-*b*:4',5'-*d*]pyran-5-yl)oct-6-en-1-one, **2u** (81.5 mg, 71%) was prepared following *GP2*. The product was isolated as a colorless oil. dr = 4.1:1 based on ^{1}H NMR of the crude reaction mixture. **^{1}H NMR** (500 MHz, $CDCl_3$) δ 5.64 (d, *J* = 5.0 Hz, 1H), 5.09 (tdt, *J* = 5.7, 2.8, 1.4 Hz, 1H), 4.62 (dd, *J* = 7.8, 2.4 Hz, 1H), 4.58 (dd, *J* = 7.8, 2.1 Hz, 1H), 4.34 (dd, *J* = 5.0, 2.4 Hz, 1H), 4.14 (d, *J* = 2.1 Hz, 1H), 2.64 (dd, *J* = 17.8, 5.1 Hz, 1H), 2.41 (dd, *J* = 17.7, 8.2 Hz, 1H), 2.13 – 2.04 (m, 1H), 1.97 (m, 2H), 1.67 (d, *J* = 1.4 Hz, 3H), 1.59 (d, *J* = 1.3 Hz, 3H), 1.50 (s, 3H), 1.43 (s, 3H), 1.34 (s, 3H), 1.30 (s, 3H), 1.19 (m, 2H), 0.89 (d, *J* = 6.6 Hz, 3H). **^{13}C NMR** (126 MHz, $CDCl_3$) δ 209.3, 131.5, 124.9, 109.8, 109.1, 96.8, 74.0, 72.8, 70.9, 70.7, 47.3, 37.4, 27.9, 26.2, 26.2, 26.0, 25.8, 25.1, 24.6, 20.1, 17.9. (*Only the signals corresponding to the major stereoisomer are reported*). **FT-IR** (cm^{-1}, neat, ATR): 2982, 2928, 1719, 1382, 1255, 1212, 1067, 1006. **HRMS** (EI) calcd for $C_{21}H_{34}O_6$ $[M]^+$: 382.2355, found: 382.2360.

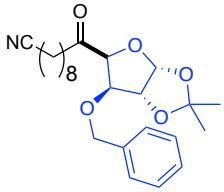

10-((3a*R*,5*S*,6*R*,6a*R*)-6-(Benzyloxy)-2,2-dimethyltetrahydrofuro[2,3-*d*][1,3]dioxol-5-yl)-10-oxodecanenitrile, **2v** (83.2 mg, 83%) was prepared following *GP2*. The product was isolated as a colorless oil. dr > 20:1 based on ^{1}H NMR of the crude reaction mixture. **^{1}H NMR** (500 MHz, $CDCl_3$) δ 7.36 – 7.30 (m, 5H), 6.01 (s, 1H), 4.62 (s, 3H), 4.47 (s, 2H), 2.83 – 2.70 (m, 1H), 2.67 (t, *J* = 7.7 Hz, 1H), 2.33 (t, *J* = 7.4 Hz, 2H), 1.67 – 1.62 (m, 2H), 1.55 – 1.42 (m, 4H), 1.37 (s,

3H), 1.32 – 1.28 (m, 9H). **^{13}C NMR** (126 MHz, CDCl3) δ 209.4, 137.1, 128.7, 128.6, 128.6, 128.2, 128.0, 127.8, 127.8, 112.2, 106.5, 89.7, 83.80, 72.0, 39.1, 29.2, 29.1, 28.7, 28.7, 26.0, 25.8, 25.5, 23.1, 17.2. **FT-IR** (cm^{-1}, neat, ATR): 2933, 2858, 1715, 1456, 1375, 1213, 1164. **HRMS** (ESI) calcd for $C_{24}H_{34}NO_5$ $[M+H]^+$: 416.2437, found: 416.2420.

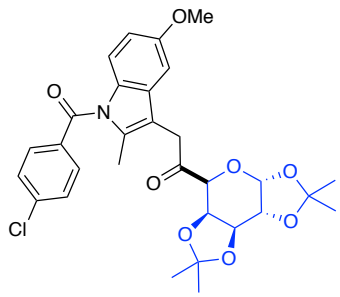

2-(1-(4-Chlorobenzoyl)-5-methoxy-2-methyl-1*H*-indol-3-yl)-1-((3a*R*,5a*R*,8a*S*,8b*R*)-2,2,7,7-tetramethyltetrahydro-5*H*-bis([1,3]dioxolo)[4,5-*b*:4',5'-*d*]pyran-5-yl)ethan-1-one, **2w** (82.6 mg, 51%) was prepared following *GP2*. The product was isolated as a yellow oil. dr = 1.5:1 based on ^{1}H NMR of the crude reaction mixture. **^{1}H NMR** (500 MHz, $CDCl_3$) δ 7.80 – 7.55 (m, 2H), 7.53 – 7.36 (m, 2H), 7.00 – 6.79 (m, 2H), 6.67 (dd, *J* = 9.0, 2.5 Hz, 1H), 5.41 – 5.07 (m, 1H), 4.58 (dd, *J* = 5.8, 1.3 Hz, 1H), 4.47 (dd, *J* = 8.2, 5.7 Hz, 1H), 4.25 (dd, *J* = 3.0, 1.3 Hz, 1H), 4.11 (d, *J* = 16.3 Hz, 1H), 3.91 – 3.09 (m, 5H), 2.34 (s, 3H), 1.51 (s, 3H), 1.39 (s, 3H), 1.35 (d, *J* = 4.4 Hz, 6H). **^{13}C NMR** (126 MHz, $CDCl_3$) δ 203.2, 168.5, 156.4, 139.6, 136.6, 134.2, 131.5 (2C), 131.1, 130.9 (2C), 129.4, 115.3, 112.4, 112.3, 111.2, 109.6, 101.3, 97.4, 76.1, 75.1, 74.0, 69.5, 55.9, 35.9, 27.9, 27.6, 25.9, 25.7, 13.8. (*Only the signals corresponding to the major stereoisomer are reported*). **FT-IR** (cm^{-1}, neat, ATR): 2989, 2936, 1728, 1682, 1479, 1371, 1322, 1257, 1214, 1088, 1067, 1006. **HRMS** (ESI) calcd for $C_{30}H_{33}ClNO_8$ $[M+H]^+$: 570.1895, found: 570.1870.

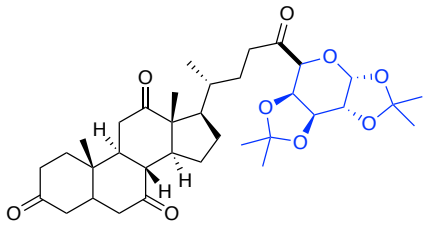

(8*R*,9*S*,10*S*,13*R*,14*S*,17*R*)-10,13-Dimethyl-17-((2*R*)-5-oxo-5-((3a*R*,5a*R*,8a*S*,8b*R*)-2,2,7,7-tetramethyltetrahydro-5*H*-bis([1,3]dioxolo)[4,5-*b*:4',5'-*d*]pyran-5-yl)pentan-2-yl)dodecahydro-3*H*-cyclopenta[*a*]phenanthrene-3,7,12(2*H*,4*H*)-trione, **2x** (119.8 mg, 65%) was prepared following *GP2*. The product was isolated as a white solid. **mp** = 200-204 °C. dr = 3.3:1 based on ^{1}H NMR of the crude reaction mixture. **^{1}H NMR** (500 MHz, $CDCl_3$) δ 5.64 (d, *J* = 5.0 Hz, 1H), 4.75 – 4.59 (m, 1H), 4.60 – 4.41 (m, 1H), 4.34 (ddd, *J* = 5.2, 2.4, 0.9 Hz, 1H), 4.17 (d, *J* = 2.0 Hz, 1H), 2.96 – 2.77 (m, 3H), 2.79 – 2.63 (m, 1H), 2.55 (ddd, *J* = 18.2, 8.5, 6.3 Hz, 1H), 2.28 (dddd, *J* = 42.4, 20.8, 14.3, 5.1 Hz, 6H), 2.17 – 2.06 (m, 2H), 2.09 – 1.88 (m, 4H), 1.90 – 1.75 (m, 2H), 1.67 – 1.53 (m, 1H), 1.50 (d, *J* = 3.0 Hz, 3H), 1.43 (s, 3H), 1.39 (s, 3H), 1.33 (s, 3H), 1.30 (s, 3H), 1.47 – 1.15 (m, 4H), 1.06 (s, 3H), 0.83 (d, *J* = 6.0 Hz, 3H). **^{13}C NMR** (126 MHz, $CDCl_3$) δ 212.2, 210.0, 209.4, 209.0, 109.8, 109.1, 96.7, 74.0, 72.8, 70.9, 70.7, 57.2, 52.0, 49.3, 47.1, 46.0, 45.8, 45.3, 43.1, 38.9, 37.1, 36.8, 36.3, 35.6, 35.5, 28.2, 27.8, 26.2, 26.2, 25.5, 25.1, 24.5, 22.2, 19.1, 12.2. (*Only the signals corresponding to the major stereoisomer are reported*). **FT-IR** (cm^{-1}, neat, ATR): 2984, 1718, 1372, 1252, 1212, 1067, 1002. **HRMS** (ESI) calcd for $C_{35}H_{50}O_9Na$ $[M+Na]^+$: 637.3353, found: 637.3343.

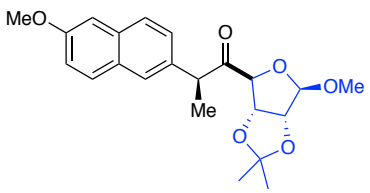

(*S*)-1-((3a*S*,4*S*,6*R*,6a*R*)-6-Methoxy-2,2-dimethyltetrahydrofuro[3,4-*d*][1,3]dioxol-4-yl)-2-(6-methoxynaphthalen-2-yl)propan-1-one, **2y** (77.2 mg, 80%) was prepared following *GP2*. The product was isolated as a colorless oil. dr > 20:1 based on ^{1}H NMR of the crude reaction mixture. **^{1}H NMR** (500 MHz, $CDCl_3$) δ 7.74 – 7.66 (m, 2H), 7.64 (s, 1H), 7.35 (d, *J* = 8.4 Hz, 1H), 7.18 – 7.05 (m, 2H), 5.10 (d, *J* = 5.8 Hz, 1H), 5.02 (s, 1H), 4.74 (s, 1H), 4.50 (d, *J* = 5.9 Hz, 1H), 4.35 (d, *J* = 7.1 Hz, 1H), 3.91 (s, 3H), 3.34 (s, 3H), 1.56 (d, *J* = 7.1 Hz, 3H), 1.47 (s, 3H), 1.33 (s, 3H). **^{13}C NMR** (126 MHz, $CDCl_3$) δ 208.1, 157.8, 135.0, 133.9, 129.4, 129.2, 127.4, 126.9, 126.7, 119.1, 113.1, 109.8, 105.7, 89.4, 84.8, 81.1, 56.1, 55.5, 47.9, 26.8, 25.3, 18.6. **FT-IR** (cm^{-1}, neat, ATR): 2987, 2937, 1720, 1633, 1606, 1506, 1485, 1267, 1094 ppm. **HRMS** (EI) calcd for $C_{22}H_{26}O_6$ $[M]^+$: 386.1729, found: 386.1738.

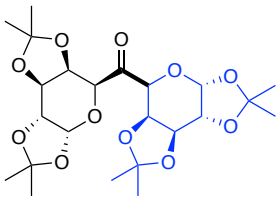

bis((3a*R*,5a*R*,8a*S*,8b*R*)-2,2,7,7-Tetraethyltetrahydro-5*H*-bis([1,3]dioxolo)[4,5-*b*:4',5'-*d*]pyran-5-yl)methanone, **2z** (68 mg, 47%) was prepared following *GP2*. The product was isolated as a foam. dr = 5:1 based on ^{1}H NMR of the crude reaction mixture. **^{1}H NMR** (500 MHz, $CDCl_3$) δ 5.65 (d, *J* = 4.9 Hz, 2H), 4.80 – 4.66 (m, 4H), 4.63 (dd, *J* = 7.8, 2.4 Hz, 2H), 4.34 (dd, *J* = 5.0, 2.4 Hz, 2H), 1.52 (s, 6H), 1.44 (s, 6H), 1.33 (s, 6H), 1.29 (s, 6H). **^{13}C NMR** (126 MHz, $CDCl_3$) δ 200.5, 110.0 (2C), 109.2 (2C), 96.9 (2C), 72.5 (2C), 71.3 (2C), 71.0 (4C), 26.3 (2C),

26.1 (2C), 25.2 (2C), 24.5 (2C). (*Only the signals corresponding to the major stereoisomer are reported*). **FT-IR** (cm^{-1}, neat, ATR): 1744, 1373, 1253, 1211, 1167, 1139, 1103, 1066, 1019, 999, 976, 920, 889. **HRMS** (ESI) calcd for $C_{23}H_{35}O_{11}$ $[M+H]^+$: 487.2179, found 487.2200.

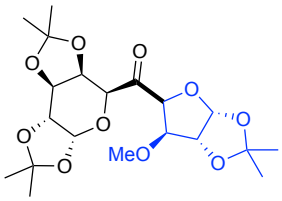

((3a*R*,5*S*,6*R*,6a*R*)-6-Methoxy-2,2-dimethyltetrahydrofuro[2,3-*d*][1,3]dioxol-5-yl)((3a*R*,5*S*,5a*R*,8a*S*,8b*R*)-2,2,7,7-tetramethyltetrahydro-5*H*-bis([1,3]dioxolo)[4,5-*b*:4',5'-*d*]pyran-5-yl)methanone, **3a** (87.2 mg, 68%) was prepared following *GP2*. The product was isolated as a clear oil. dr = 10:1 based on ^{1}H NMR of the crude reaction mixture. **^{1}H NMR** (500 MHz, $CDCl_3$) δ 6.05 (d, *J* = 3.7 Hz, 1H), 5.65 (d, *J* = 4.8 Hz, 1H), 5.09 (d, *J* = 3.5 Hz, 1H), 4.73 (d, *J* = 8.2 Hz, 1H), 4.61 (d, *J* = 8.1 Hz, 1H), 4.58 (d, *J* = 3.8 Hz, 1H), 4.50 (s, 1H), 4.33 – 4.31 (m, 1H), 4.21 (d, *J* = 3.5 Hz, 1H), 3.34 (s, 3H), 1.51 (s, 6H), 1.43 (s, 3H), 1.34 (s, 6H), 1.32 (s, 3H). **^{13}C NMR** (126 MHz, CDCl3) δ 199.9, 112.3, 109.7, 108.9, 105.3, 96.8, 85.2, 83.6, 82.0, 73.0, 71.3, 71.0, 70.8, 58.2, 27.1, 26.5, 26.3, 26.2, 23.0, 24.2. (*Only the signals corresponding to the major stereoisomer are reported*). **FT-IR** (cm^{-1}, neat, ATR): 2987, 2938, 1740, 1457, 1375, 1257, 1212, 1070, 1009, 732. **HRMS** (ESI) calcd for $C_{23}H_{34}O_{11}Na$ $[M+Na]^+$: 453.1750, found: 453.1737.

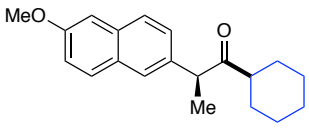

(*S*)-1-Cyclohexyl-2-(6-methoxynaphthalen-2-yl)propan-1-one, 3b (83.4 mg, 56%) was prepared following *GP2*. The product was isolated as a colorless oil. **^{1}H NMR** (500 MHz, $CDCl_3$)

δ 7.71 (d, *J* = 3.9 Hz, 1H), 7.69 (d, *J* = 3.5 Hz, 1H), 7.60 (s, 1H), 7.29 (d, *J* = 8.4 Hz, 1H), 7.15 (dd, *J* = 9.0, 2.6 Hz, 1H), 7.12 (d, *J* = 2.5 Hz, 1H), 4.04 (q, *J* = 6.9 Hz, 1H), 3.92 (s, 3H), 2.45 (tt, *J* = 11.3, 3.6 Hz, 1H), 1.87 (d, *J* = 12.1 Hz, 1H), 1.77 – 1.71 (m, 1H), 1.64 – 1.57 (m, 2H), 1.43 (d, *J* = 6.8 Hz, 3H), 1.40 – 1.00 (m, 6H). **^{13}C NMR** (126 MHz, $CDCl_3$) δ 214.2, 157.8, 136.0, 133.7, 129.3 (2C), 127.5, 126.7 (2C), 119.2, 105.7, 55.5, 51.2, 49.6, 29.7, 28.4, 26.1, 25.9, 25.4, 18.4. **FT-IR** (cm^{-1}, neat, ATR): 2930, 2854, 1707, 1633, 1606, 1505, 1484, 1266, 853. **HRMS** (EI) calcd for $C_{20}H_{24}O_2$ $[M]^+$: 296.1776, found: 296.1776.

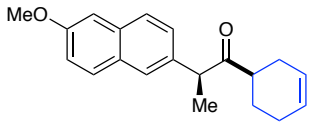

(*S*)-1-(Cyclohex-3-en-1-yl)-2-(6-methoxynaphthalen-2-yl)propan-1-one, **3c** (113.3 mg, 77%) was prepared following *GP2*. The product was isolated as a colorless oil. dr = 1.9:1 based on ^{1}H NMR of the crude reaction mixture. **^{1}H NMR** (500 MHz, $CDCl_3$) δ 7.70 (d, *J* = 8.6 Hz, 2H), 7.61 (d, *J* = 8.6 Hz, 1H), 7.30 (t, *J* = 9.5 Hz, 1H), 7.16 (dd, *J* = 8.9, 2.5 Hz, 1H), 7.12 (s, 1H), 5.71 – 5.51 (m, 2H), 4.13 – 4.00 (m, 1H), 3.92 (s, 3H), 2.77 – 2.66 (m, 1H), 2.25 – 2.16 (m, 1H), 2.15 – 1.78 (m, 3H), 1.74 – 1.54 (m, 2H), 1.46 (d, *J* = 6.9 Hz, 3H). **^{13}C NMR** (126 MHz, $CDCl_3$) δ 213.4, 213.7, 157.8, 157.7, 135.8, 135.7, 133.8, 129.3, 129.3, 129.2, 129.1, 127.6, 127.5, 127.1, 126.7, 126.6, 126.1, 125.9, 125.3, 119.3, 119.2, 105.7, 55.5, 51.5, 51.4, 45.4, 45.3, 28.2, 27.2, 25.8, 25.0, 24.7, 24.6, 18.29, 18.6 (mixture of diastereomers, 5 overlapping peaks). **FT-IR** (cm^{-1}, neat, ATR): 1705, 1632, 1605, 1505, 1484, 1452, 1437, 1391, 1372, 1266, 1228, 1216. **HRMS** (EI) calcd for $C_{20}H_{22}O_2$ $[M]^+$: 294.1620, found: 294.1600.

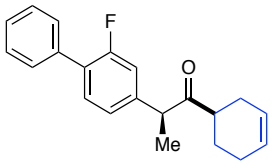

(*S*)-1-(Cyclohex-3-en-1-yl)-2-(2-fluoro-[1,1'-biphenyl]-4-yl)propan-1-one, 3b (113.3 mg, 77%) was prepared following *GP2*. The product was isolated as a colorless oil. dr = 1:1 based on ^{1}H NMR of the crude reaction mixture. **^{1}H NMR** (500 MHz, $CDCl_3$) δ 7.59 – 7.51 (m, 2H), 7.51 – 7.33 (m, 4H), 7.15 – 6.99 (m, 2H), 5.67 (d, *J* = 18.1 Hz, 2H), 4.00 (dq, *J* = 13.8, 6.9 Hz, 1H), 2.73 (ddt, *J* = 14.0, 8.0, 2.8 Hz, 1H), 2.31 – 2.19 (m, 1H), 2.18 – 2.03 (m, 2H), 1.96 (dt, *J* = 13.6, 4.4 Hz, 1H), 1.88 – 1.56 (m, 2H), 1.44 (dd, *J* = 7.0, 1.9 Hz, 3H).**^{13}C NMR** (126 MHz, $CDCl_3$, mixture of two diastereomers) δ 213.4, 213.1, 161.0, 159.0, 142.1, 142.1, 135.6, 135.6, 131.3, 131.3, 131.3, 131.2, 129.2, 129.1, 128.7, 128.0, 128.0, 128.0, 127.9, 127.2, 126.3, 125.9, 125.3, 124.2, 124.2, 124.2, 116.0, 115.9, 115.8, 115.7, 50.9, 50.8, 45.7, 45.6, 30.0, 28.1, 27.2, 25.7, 25.1, 24.7, 18.4, 18.4. **FT-IR** (cm^{-1}, neat, ATR): 3027, 2929, 1709, 1484, 1451, 1436, 1417, 1374, 1268, 1132, 1030.

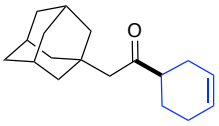

2-(Adamantan-1-yl)-1-(cyclohex-3-en-1-yl)ethan-1-one, **3e** (103.4, 80%) was prepared following *GP2*. The product was isolated as a colorless oil. **^{1}H NMR** (500 MHz, $CDCl_3$) δ 5.71 – 5.66 (m, 2H), 2.63 – 2.50 (m, 1H), 2.27 – 2.19 (m, 2H), 2.15 – 2.06 (m, 4H), 1.95 (s, 4H), 1.69 (d, *J* = 12.3 Hz, 4H), 1.64 (d, *J* = 7.3 Hz, 8H), 1.53 – 1.44 (m, 1H). **^{13}C NMR** (126 MHz, $CDCl_3$) δ 213.8, 126.7, 125.7, 54.3, 48.7, 42.7 (3C), 37.0 (3C), 33.8, 28.8 (3C), 26.7, 25.1, 24.6. **FT-IR** (cm^{-1}, neat, ATR): 1705, 1632, 1605, 1505, 1484, 1452, 1437, 1391, 1372, 1266, 1228, 1216. **HRMS** (EI) calcd for $C_{18}H_{26}O$ $[M]^+$: 258.1984, found: 258.1992.

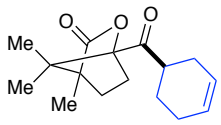

1-(Cyclohex-3-ene-1-carbonyl)-4,7,7-trimethyl-2-oxabicyclo[2.2.1]heptan-3-one, **3f (**80.7 mg, 61%) was prepared following *GP2*. The product was isolated as a colorless oil. dr = 1.1:1 based on ^{1}H NMR of the crude reaction mixture. **^{1}H NMR** (500 MHz, $CDCl_3$) δ 5.70 (m, 2H), 3.23 – 3.10 (m, 1H), 2.45 – 2.28 (m, 2H), 2.20 – 1.97 (m, 4H), 1.97 – 1.87 (m, 2H), 1.74 – 1.64 (m, 1H), 1.53 – 1.21 (m, 1H), 1.11 (s, 3H), 1.05 (s, 3H; 1:1 mixture of diastereomers), 0.92 (s, 3H; 1:1 mixture of diastereomers). **^{13}C NMR** (126 MHz, $CDCl_3$, mixture of two diastereomers) δ 211.2, 210.6, 179.1, 179.0, 126.8, 126.5, 125.3, 125.0, 96.7, 96.7, 60.5, 55.4, 55.3, 55.1, 43.7, 43.5, 31.8, 31.8, 29.4, 29.4, 27.5, 25.2, 25.1, 24.9, 24.5, 23.0, 16.9, 16.8, 16.8, 14.3, 9.7, 9.6. **FT-IR** (cm^{-1}, neat, ATR): 3025, 1787, 1704, 1449, 1438, 1395, 1376, 1162. **HRMS** (EI) calcd for $C_{16}H_{22}O_3$ $[M]^+$: 262.1569, found: 262.1563.

2.5 References

(1) For selected examples, see: a) T. Bililign, B. R. Griffith, J. S. Thorson, *Nat. Prod. Rep.* **2005**, *22*, 742-760; b) P. G. Hultin, *Curr. Top. Med. Chem.* **2005**, *5*, 1299-1331; c) Y. Yang, B. Yu, *Chem. Rev.* **2017**, *117*, 12281-12356; d) J. Stambasky, M. Hocek, P. Kocovsky, *Chem. Rev.* **2009**, *109*, 6729-6764.

(2) A. Holemann, P. H. Seeberger, *Curr. Opin. Biotechnol.* **2004**, *15*, 615-622.

(3) R. W. Gantt, P. Peltier-Pain, J. S. Thorson, *Nat. Prod. Rep.* **2011**, *28*, 1811-1853.

(4) D. C. Koester, A. Holkenbrink, D. B. Werz, *Synthesis* **2010**, *19*, 3217-3242.

(5) Reports on the biological activities of *C*-acyl glycosides: a) Q. Wu, J.-G. Cho, D.-S. Lee, D.-Y. Lee, N.-Y. Song, Y.-C. Kim, K.-T. Lee, H.-G. Chung, M.-S. Choi, T.-S. Jeong, E.-M. Ahn, G.-S. Kim, N.-I. Baek, *Carbohydr. Res.* **2013**, *372*, 9-14; b) W. Disadee, C. Mahidol, P.

Sahakitpichan, S. Sitthimonchai, S. Ruchirawat, T. Kanchanapoom, *Phytochemistry* **2012**, *74*, 115-122.

(6) For selected examples, see: a) T. Kawamata, M. Nagatomo, M. Inoue, *J. Am. Chem. Soc.* **2017**, *139*, 1814-1817; b) S. Inuki, T. Aiba, S. Kawakami, T. Akiyama, J.-I. Inoue, Y. Fujimoto, *Org. Lett.* **2017**, *19*, 3079-3082; c) S. Dhar, J. J. La Clair, B. Leon, J. C. Hammons, Z. Yu, M. K. Kashyap, J. E. Castro, M. D. Burkart, *J. Am. Chem. Soc.* **2016**, *138*, 5063-5068.

(7) For examples highlighting nucleophilic additions to *C*-glycosyl aldehydes, see: (a) J. Picard, N. Lubin-Germain, J. Uziel, J. Augé, *Synthesis* **2006**, *6*, 979-982; (b) M. Kolympadi, M. Fontanella, C. Venturi, S. André, H.-J. Gabius, J. Jiménez-Barbero, P. Vogel, *Chem. Eur. J.* **2009**, *15*, 2861-2873; c) Y. Geng, A. Kumar, H. M. Faidallah, H. A. Albar, I. A. Mhkalid, R. R. Schmidt, *Bioorg. Med. Chem.* **2013**, *21*, 4793-4802.

(8) For examples highlighting glycosyl-based nucleophiles, see: a) P. Lesimple, J.-M. Beau, *Bioorg. Med. Chem.* **1994**, *2*, 1319-1330; b) D. Mazéas, T. Skrydstrup; J.-M. Beau, *Angew. Chem. Int. Ed.* **1995**, *34*, 909-912.

(9) Y. Y. Belosludtev, R. K. Bhatt, J. R. Falck, *Tetrahedron Lett.* **1995**, *36*, 5881-5882.

(10) N. E. S. Guisot, I. Ella Obame, P. Ireddy, A. Nourry, C. Saluzzo, G. Dujardin, D. Dubreuil, M. Pipelier, S. Guillarme, *J. Org. Chem.* **2016**, *81*, 2364-2371.

(11) A. Dondoni, N. Catozzi, A. Marra, *J. Org. Chem.* **2005**, *70*, 9257-9268.

(12) C. Zhao, X. Jia, X. Wang, H. Gong, *J. Am. Chem. Soc.* **2014**, *136*, 17645-17651.

(13) M. G. Kulkarni, Y. B. Shaikh, A. S. Borhade, S. W. Chavhan, A. P. Dhondge, D. D. Gaikwad, M. P. Desai, D. R. Birhade, N. R. Dhatrak, *Tetrahedron Lett.* **2013**, *54*, 2293-2295.

(14) M. A. Potopnyk, P. Cmoch, M. Cieplak, A. Gajewska, S. Jarosz, *Tetrahedron: Asymmetry* **2011**, *22*, 780-786.

(15) Z. Guan, L. H. Zhang, P. Sinay, Y. Zhang, *J. Org. Chem.* **2012**, *77*, 8888-8895.

(16) M. Kolympadi, M. Fontanella, C. Venturi, S. Andre, H. J. Gabius, J. Jimenez-Barbero, P. Vogel, *Chem. Eur. J.* **2009**, *15*, 2861-2873.

(17) For reviews on Ni/photoredox dual catalysis, see: a) J. C. Tellis, C. B. Kelly, D. N. Primer, M. Jouffroy, N. R. Patel, G. A. Molander, *Acc. Chem. Res.* **2016**, *49*, 1429-1439; b) C. K. Prier, D. A. Rankic, D. W. C. MacMillan, *Chem. Rev.* **2013**, *49*, 1429-1439; c) J. K. Matsui, S. B. Lang, D. R. Heitz, G. A. Molander, *ACS. Catal.* **2017**, *7*, 2563-2575; d) L. N. Cavalcanti, G. A. Molander, *Top. Curr. Chem.* **2016**, *374*, 39.

(18) a) J. C. Tellis, D. N. Primer, G. A. Molander, *Science* **2014**, *345*, 433-436; b) D. N. Primer, I. Karakaya, J. C. Tellis, G. A. Molander, *J. Am. Chem. Soc.* **2015**, *137*, 2195-2198.

(19) For selected examples, see: a) W. Chen, Z. Liu, J. Tian, J. Li, J. Ma, X. Cheng, G. Li, *J. Am. Chem. Soc.* **2016**, *138*, 12312-12315; b) Á. Gutiérrez-Bonet, C. Remeur, J. K. Matsui, G. A. Molander, *J. Am. Chem. Soc.* **2017***, 139,* 12251-12258; c) Á. Gutiérrez-Bonet, J. C. Tellis, J. K. Matsui, B. A. Vara, G. A. Molander, *ACS Catal.* **2016***, 6,* 8004-8008; d) L. Buzzetti, A. Prieto, S. R. Roy, P. Melchiorre, *Angew. Chem. Int. Ed.* **2017**, *56*, 15039-15043.

(20) J. R. Schmink, A. Bellomo, S. Berritt, *Aldrichimica Acta.* **2013**, *46*, 71-80.

(21) J. Amani, G. A. Molander, *Org. Lett.* **2017**, *19*, 3612-3615.

(22) For information on the construction of LED reactors, see the Supporting Information of: N. R. Patel, C. B. Kelly, M. Jouffroy, G. A. Molander, *Org. Lett.* **2016**, *18*, 764-767.

(23) N. R. Patel, C. B. Kelly, A. P. Siegenfeld, G. A. Molander, *ACS Catal.* **2017**, *7*, 1766-1770.

(24) N. Tewari, N. Dwivedi, R. Tripathi, *Tetrahedron Lett*. **2004**, *45*, 9011-9014.

Author Contributions: Shorouk O. Badir conceived the topic, performed the reaction optimization, and prepared some of the compounds used in this study. All authors contributed to

the experimental work and discussion of results. Shorouk O. Badir wrote the manuscript with input from Gary A. Molander.

Chapter 3. Deaminative Reductive Arylation Enabled by Nickel/Photoredox Dual Catalysis[§]

3.1 Introduction

The introduction of 1,4-dihydropyridines in Ni/photoredox dual cross-coupling manifolds provided access to diverse glycosyl-based radicals from aldehyde feedstocks, facilitating the synthesis of complex *C*-acyl glycosides. Moving forward, we focused our efforts on the development of a cross-electrophilic strategy to forge C(sp^3)-hybridized centers from aliphatic amines. In particular, aliphatic primary amines are a privileged class of compounds prevalent in natural products, valued synthetic intermediates, and pharmaceutical drugs such as Tamiflu, Linagliptin, Amlodipine, and Sitagliptin.[1] Although considerable achievements have been made in the area of C–N bond activation, direct cross-coupling protocols remain elusive. Recent studies from the Watson group demonstrated the use of Katritzky salts, formed *via* a simple condensation of the corresponding amines with a bench-stable, commercially-available pyrylium salt, as alkyl radical precursors in cross-coupling with arylboronic acids.[2,3] Subsequently, Glorius, Aggarwal, Shi, Gryko, and Liu further demonstrated the utility of these redox-active amines in C–H arylation,[4] borylation,[5] alkynylation,[6] allylation,[7] and dicarbofunctionalization, respectively.[8] More recently, Watson and co-workers disclosed a deaminative alkyl-alkyl Negishi cross-coupling with alkylzinc halides.[9] The growing interest in this area highlights the challenges associated with C–N bond activation and presents new opportunities to address these limitations,

---

[§] Reproduced in part with permission from J. Yi, S. O. Badir, L. M. Kammer, M. Ribagorda, G. A. Molander, *Org. Lett.* **2019**, *21*, 3346–3351. Copyright 2019, American Chemical Society.

in particular with regard to the development of cross-electrophilic strategies to install C(sp^3)-hybridized centers under mild reaction conditions.

Ni/photoredox dual catalysis has been enlisted as a powerful tool to construct C–C bonds *via* a single-electron transmetalation pathway.[10] In this context, the unique characteristics of this reaction manifold favors the formation of tetrahedral carbon centers without the need for harsh nucleophilic organometallic reagents or elevated temperature.[11] As part of a program centered on the development of Ni-catalyzed alkylation protocols,[12,13] we envisioned the application of Katritzky salts as a new species of alkyl radical precursors in a reductive, cross-electrophilic coupling with (hetero)aryl bromides (Figure 3.1) – *representing one of the few synthetic methods employing a net reductive photoredox/Ni dual catalytic transformation.*[14]

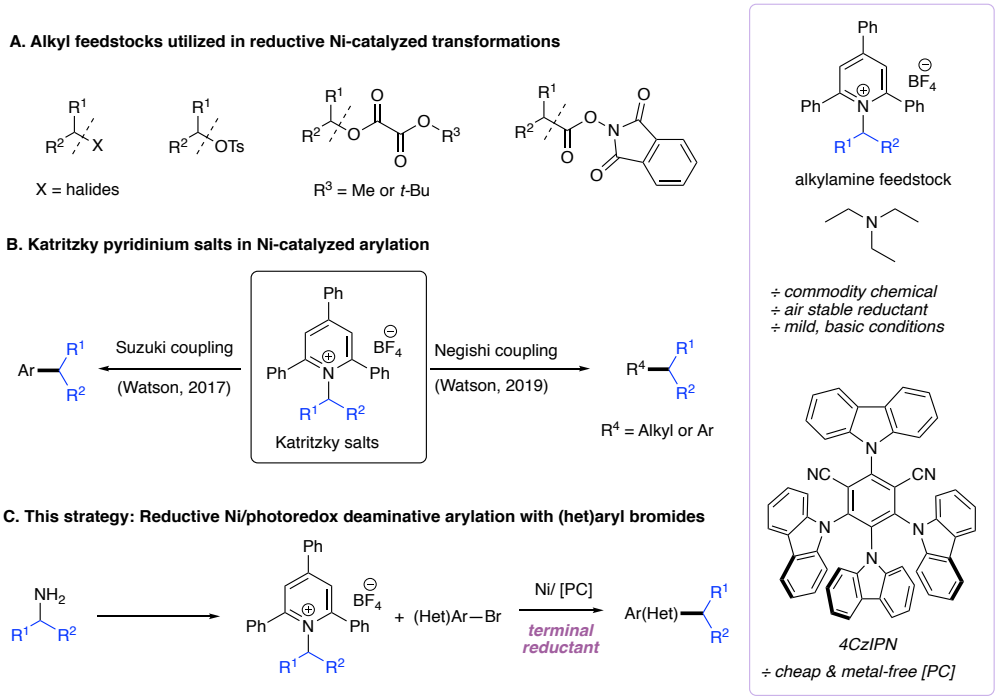

Figure 3.1. Strategies toward net-reductive Ni-catalyzed cross-couplings and envisioned transformation.

3.2 Results and Discussion

Given the accessible redox potential of Katritzky salts ($E_{1/2}$ = −0.93 V vs SCE),[7] the organic dye 4CzIPN (reduced photocatalyst $E_{1/2}$ = -1.21 V vs. SCE) was examined and proved effective at delivering the desired coupled product (Figure 3.2).

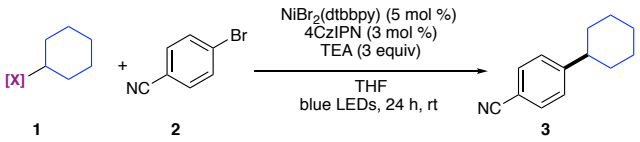

1 2 3

Entry	Deviation from standard conditions	3 %[a]
1	**None**	**93 (86)[b]**
2	$[Ir\{dF(CF_3)_2ppy\}(dtbbpy)]PF_6$	87
3	$[Ir(dtbbpy)(ppy)_2]PF_6$	99
4	3.0 equiv Hantzsch ester	33
5	CH_3CN	73
6	DMA	92
7	No light (dark)	0
8	No photocatalyst	0
9	No Ni catalyst	0
10	No amine	0

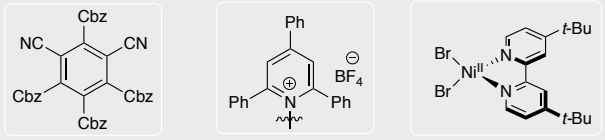

4CzIPN [X] $NiBr_2(dtbbpy)$

Figure 3.2. Optimization studies. Reactions were performed using **1** (0.45 mmol), **2** (0.3 mmol), 4CzIPN (3 mol %), $NiBr_2(dtbbpy)$ (5 mol %) in dry, degassed solvent (3.0 mL, 0.1 M) under blue LED irradiation for 24 h. [a]GC/MS yield using 1,3,5-trimethoxybenzene as internal standard. [b]Isolated yield of **3.**

Other photocatalysts were also tested (entries 2 and 3, Figure 3.2). Not surprisingly, $[Ir(dtbbpy)(ppy)_2]PF_6$ provided quantitative conversion to the desired product, likely because of

its strongly reductive nature ($E_{1/2}$ = −1.51 V vs SCE).[4,10b] Considering the low cost, ease of preparation, and excellent reactivity of 4CzIPN,[15] it was chosen as the photocatalyst of choice. Although DMA provided equally good results in this cross-coupling (entry 6, Figure 3.2), THF was chosen because of its low boiling point. However, it should be noted that the use of DMA for electron-rich substrates proved effective at times (see the Experimental Section). As anticipated, control experiments proved that all components of the reaction were necessary for the dual catalytic system to proceed (entries 7-10, Figure 3.2). Finally, in an attempt to provide a user-friendly reaction set-up, the optimization was carried out using the precomplex $NiBr_2$•dtbbpy.

With suitable reaction conditions in hand, the scope of this deaminative cross-coupling was examined (Figure 3.3). To this end, a wide array of aryl bromides bearing electron-withdrawing substituents at the *para*-position exhibited excellent reactivity (**3**-**10**, **16**). Electron-rich aryl bromides were also compatible substrates (**11** and **12**). Importantly, aryl bromides bearing an additional handle for further elaboration in Chan-Lam and Suzuki couplings, such as pinacol boronic ester (**17**) and aryl chlorides (**6** and **13**), reacted to afford the corresponding products in good yields. Given the mildly basic conditions of this protocol, a variety of sensitive functional groups, including lactone **15** and sulfonamide **16**, were compatible structural motifs. Substitution at the *meta*-position (**13**, **15**, **17**, and **18**) and *ortho*-position (**14** and **18**) was explored; whereby efficient cross-coupling events took place. Moreover, electron deficient difluoroaryl bromide **18** and several heteroaryl systems (**19**-**22**) were successfully employed. Because of their notoriously unstable nature as the corresponding boronic acids (owing to protodeboronation under strongly basic conditions),[16] the analogous substructural partners had provided sluggish reactivity in previous reports.[2]

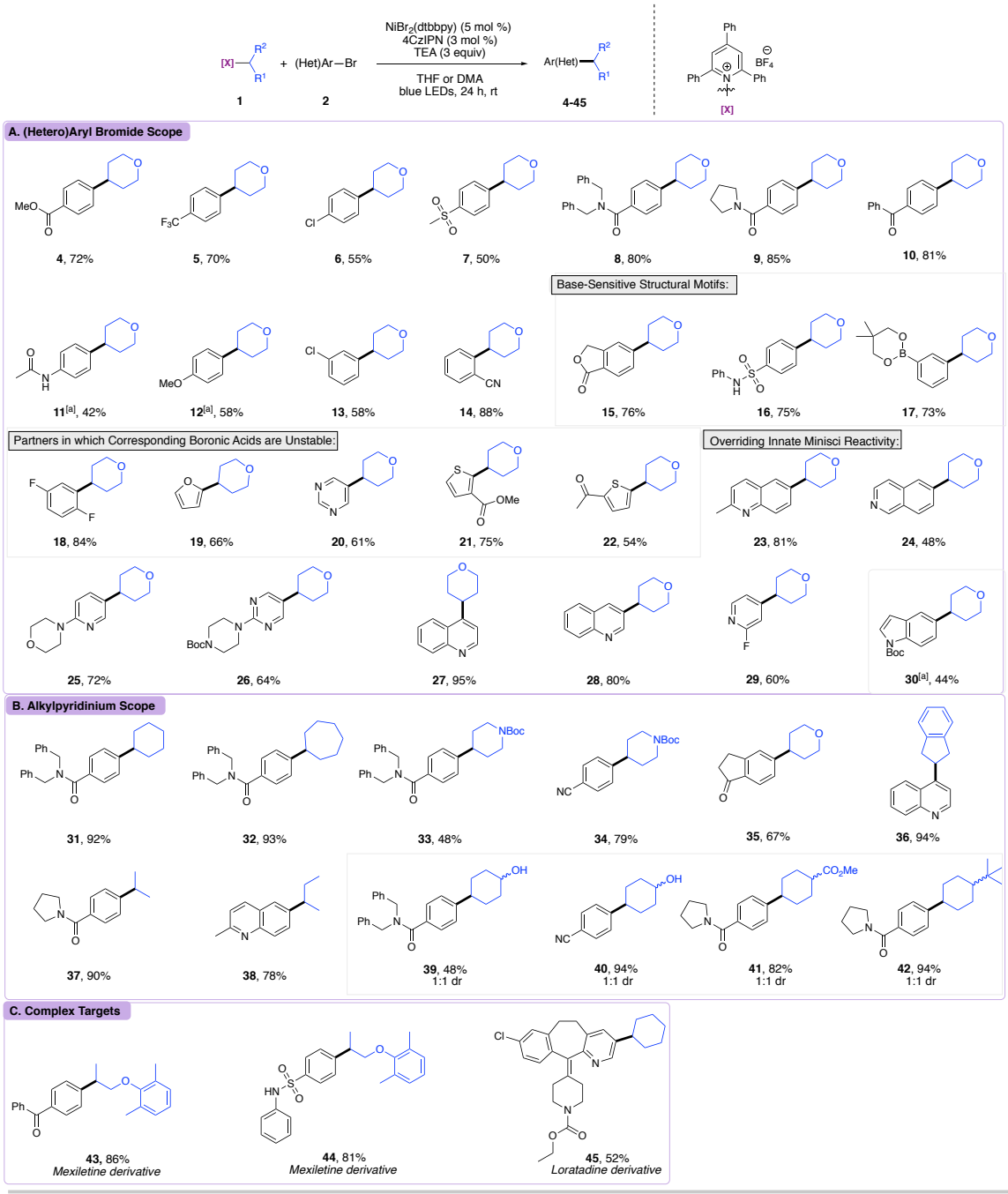

Figure 3.3. Scope of the developed $C(sp^3)$-$C(sp^2)$ cross-coupling. All values correspond to isolated yields after purification. Reaction conditions as depicted in Figure 3.2, entry 1 (0.5 mmol scale). [a]Using DMA as a solvent, 48 h.

Given their importance in pharmaceutical settings,[17] a variety of nitrogen-containing heteroaryl bromides, including pyrimidine (**20** and **26**), quinoline (**23**, **27** and **28**), isoquinoline **24**, pyridine (**25** and **29**), and indole (**30**) electrophiles were effectively incorporated under this reaction manifold (Figure 3.3). It is worth highlighting that heteroaromatics (**23** and **24**), previously well-behaved under photoinduced deamination C–H arylation conditions,[3] reacted in a chemoselective manner. This highlights the complementary advantages of this protocol to existing Minisci transformations.[4,18]

Next, attention was turned to the scope of the alkylpyridinium salts, where a wide array of functional groups was tolerated (Figure 3.3). Katritzky salts bearing a free hydroxyl group (**39** and **40)** did not inhibit the reaction, presenting orthogonal reactivity to C–O bond activation previously reported by MacMillan.[19] Other pyridinium salts bearing an ester handle (**41**) and nitrogen heterocyclic structural motifs (**33** and **34**) afforded the desired products in excellent yields. Notably, both cyclic (**31**-**36**, **39**-**42**) and acyclic (**37**, **38**, **43**, and **44**) alkylpyridinium salts reacted efficiently under the reaction conditions. Finally, to demonstrate the applicability of this protocol to the synthesis of bioactive molecules, we prepared the corresponding alkylpyridinium salt from Mexiletine, a voltage-gated sodium channel blocker used as an antiarrhythmic.[20] Utilizing two different aryl bromides, success was achieved at delivering the cross-coupled products **43** and **44** in excellent yields. Finally, a complex aryl bromide derived from Loratadine,[21] used in the treatment of allergies, was accommodated under the reaction conditions (**45**).

To highlight the benefits of employing 4CzIPN as an inexpensive organic photocatalyst [~\$5 $mmol^{-1}$], a transformation was successfully performed on gram-scale, whereby the desired heteroaryl coupled product **27** was obtained in 90% yield (Figure 3.4). Taking further advantage

of the inherent chemoselectivity of this cross-coupling as described earlier, the quinoline scaffold of **27** was further elaborated at the C2 position to obtain **46** and **47** in good yields, utilizing Minisci-type photoinduced deaminative and decarboxylative strategies previously reported by Glorius and Dhar, respectively.[4,18c] The ease with which a wide array of aryl- and heteroaryl systems can be fashioned showcases the significant potential of deaminative-based C–C bond construction in industrial settings.

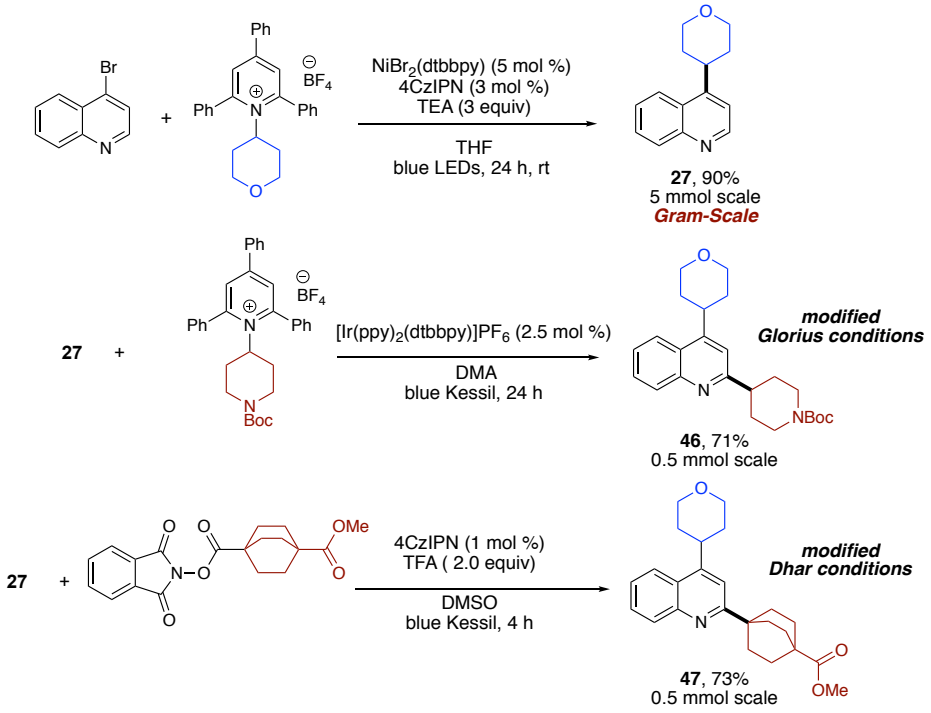

Figure 3.4. Sequential gram-scale deaminative cross-Coupling and Minisci C-H Arylation.

To probe the reaction pathway, we conducted a series of mechanistic experiments. In the presence of the radical scavenger TEMPO [(2,2,6,6-tetramethylpiperidin-1-yl)oxyl], the arylation was completely inhibited, with full recovery of the aryl bromide (Figure 3.5 A). This is suggestive of the involvement of radical species under this metallaphotoredox manifold. This hypothesis was further corroborated by isolation of **48**, a byproduct likely formed via a radical-

radical coupling of the persistent dihydropyridine radical intermediate **A** with a transient secondary alkyl radical during the course of the reaction[6] (Figure 3.5 B).

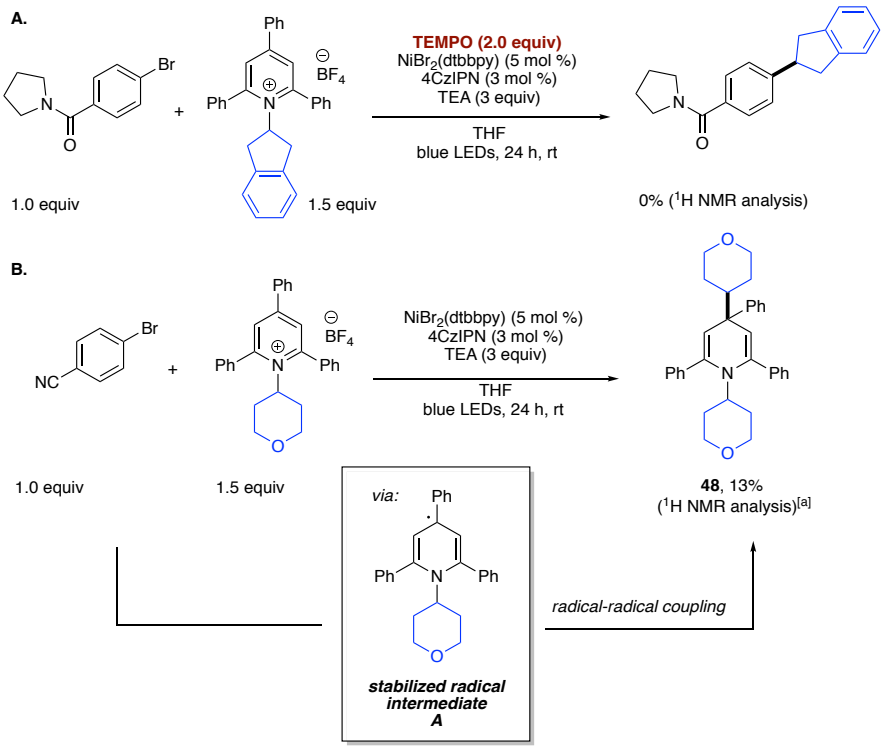

Figure 3.5. Support for involvement of radical intermediates. [a]^{1}H NMR yield was calculated based on the loading of the alkylpyridinium reagent.

To gain further understanding of the role of the photocatalyst, fluorescence quenching studies were performed (Figure 3.6). As anticipated, the Stern-Volmer relationship confirmed that both triethylamine and the Katritzky salt were effectively quenched by the photoexcited state of 4CzIPN. Although these results could support an operative single-electron-transfer (SET) reduction of the alkylpyridinium salt by the photocatalyst, we cannot rule out the possibility of a direct SET event from a low-valent nickel intermediate as proposed by Watson and Lei.[2,14a]

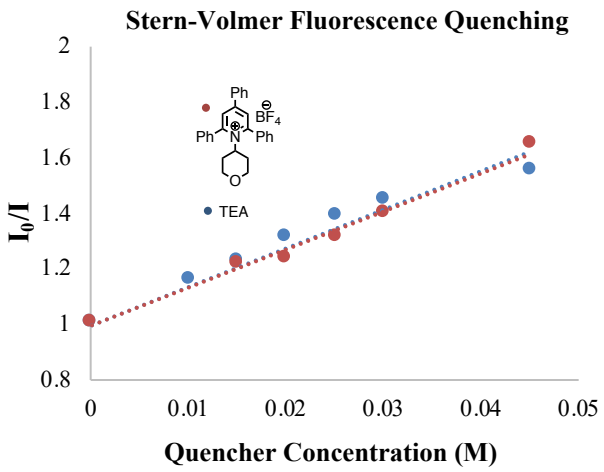

Figure 3.6. Stern-Volmer fluorescence quenching studies of 4CzIPN in THF.

Based on these results and precedented literature reports detailing the reductive cleavage of Katritzky salts,[2-8] a plausible mechanism is depicted in Figure 3.7. First, visible-light irradiation of 4CzIPN generates a potent excited-state oxidant ($E_{1/2}$ = +1.35 V vs SCE),[22] which is sufficiently quenched by triethylamine **D** ($E_{1/2}$ = +1.0 V vs SCE),[10b] thus forming the reduced state of the photocatalyst. Upon generation of alkyl radical **IV** from the Katritzky salt ($E_{1/2}$ = −0.93 V vs. SCE)[7] via SET from the photoexcited 4CzIPN or a low-valent nickel intermediate, the radical is intercepted by a ligated Ni(0) complex **V** to afford a Ni(I) intermediate. Subsequently, **VI** undergoes oxidative addition with the (hetero)aryl bromide to afford the corresponding high-valent Ni(III) complex **VII**. Reductive elimination would then occur to yield the desired coupled product **3** and Ni—Br species **VIII**. Reduction of **VIII** by the ground state of the reduced photocatalyst **III** ($E_{1/2}$ = -1.21 V vs SCE) concurrently completes both catalytic cycles.

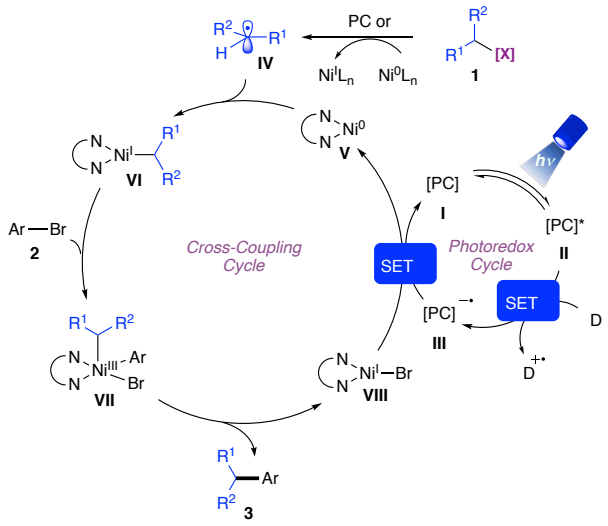

Figure 3.7. Proposed mechanism.

The developed arylation protocol does exhibit a limitation owing to the inherent stability of the dihydropyridine radical intermediate **A** generated (Figure 3.5 B). Thus, primary alkylpyridinium salts preferentially undergo reoxidation to deliver the corresponding pyridine byproduct.[6] Considering the sheer number of existing, complementary cross-coupling approaches for primary alkyl radicals developed by our group and others,[22] we foresee the current work as an important, complementary approach to the challenges associated with the activation of inert C–N bonds in recently described systems that appear restricted to aryl iodides and use excess metal reductants at elevated temperatures.[23]

3.3 Conclusion

In summary, a cross-electrophilic, deaminative strategy to achieve net-reductive protocol under photoredox conditions has been developed, using triethylamine as the terminal reductant. Eliminating the need for stoichiometric metal reductants, elevated temperatures, and/or strong bases, an exceptional array of functional groups and complex structural scaffolds can be

incorporated, including those from bioactive molecules. This arylation protocol is scalable, operationally simple, and utilizes alkylamines as abundant feedstocks.

3.4 Experimental

General Consideration

General: All chemical transformations requiring inert atmospheric conditions were carried out using Schlenk line techniques with a 4- or 5-port dual-bank manifold. LED irradiation was accomplished as described in our previous reports.[24] NMR spectra (^{1}H, ^{13}C, ^{19}F) were obtained at 298 ºK. ^{1}H NMR spectra were referenced to residual, $CHCl_3$ (δ 7.26) in $CDCl_3$. ^{13}C NMR spectra were referenced to $CDCl_3$ (δ 77.3). Reactions were monitored by LC/MS, GC/MS, ^{1}H NMR, and/or TLC on silica gel plates (60 Å porosity, 250 μm thickness). TLC analysis was performed using hexanes/EtOAc as the eluent and visualized using ninhydrin, *p*-anisaldehyde stain, and/or UV light. Flash chromatography was accomplished using an automated system (CombiFlash®, UV detector, λ = 254 nm and 280 nm) with RediSep® R_f silica gel disposable flash columns (60 Å porosity, 40–60 μm) or RediSep R_f Gold® silica gel disposable flash columns (60 Å porosity, 20–40 μm). Accurate mass measurement analyses were conducted using electron ionization (EI) or electrospray ionization (ESI). The signals were mass measured against an internal lock mass reference of perfluorotributylamine (PFTBA) for EI-GC/MS and leucine enkephalin for ESI-LC/MS. The utilized software calibrates the instruments and reports measurements by use of neutral atomic masses. The mass of the electron is not included. IR spectra were recorded on an FT-IR using either neat oil or solid products. Solvents were purified with drying cartridges through a solvent delivery system. Melting points (°C) are uncorrected.

Chemicals: Deuterated NMR solvents were purchased and stored over 4Å molecular sieves. CH_2Cl_2, EtOAc, hexanes, MeOH, Et_2O, and toluene were obtained from commercial suppliers

and used as purchased. THF was purchased and dried *via* a solvent delivery system. Triphenylpyrylium tetrafluoroborate and aliphatic amines were purchased from commercial suppliers and used without further purification. Et_3N was purchased from commercial suppliers and used without further distillation. The organic photocatalyst 2,4,5,6-tetra(9H-carbazol-9-yl)isophthalonitrile (4CzIPN) was prepared in-house by the procedure outlined in our previous publication.[25] New alkylpyridinium salts were prepared according to the representative procedure outlined below from their corresponding amines. Information (preparation, characterization, etc.) for all other alkylpyridinium salts can be found in previous literature reports.[2,4,9,26] All other reagents were purchased commercially and used as received. Photoredox-catalyzed reactions were performed using 8 mL Chemglass vials (2-dram, 17 x 60 mm, 15-425 Green Open Top Cap, TFE Septa).

General Procedures

Preparation of alkylpyridinium salts (GP1): To a Schlenk tube equipped with a stir bar was added 2,4,6-triphenylpyrylium tetrafluoroborate (1.0 equiv) and amine (1.2 equiv) in EtOH (1.0 M). The tube was sealed and stirred at 90 ºC for 4 h. Upon completion, the reaction mixture was cooled to rt. If precipitation occurred, the solid was filtered, washed with EtOH and then Et_2O. If no precipitation occurred, Et_2O was added and the reaction was stirred at rt for 1 h. The solid was then collected and washed with Et_2O. Upon drying under reduced pressure, the alkylpyridinium salts were used without further purification. In the case of amine hydrochlorides, Et_3N (1.3 equiv) was added to a soln of the amine (1.2 equiv) in EtOH (1.0 M). The reaction was stirred at rt for 30 min. After this time, triphenylpyrylium tetrafluoroborate (1.0 equiv) was added, and the reaction was stirred at 90 ºC for 4 h. Upon precipitation of the product with Et_2O, the solid was collected and washed with H_2O before washing with EtOH and Et_2O.

Cross-coupling of alkylpyridinium salts (GP2): To an 8 mL reaction vial equipped with a stir bar were added 4CzIPN (11.8 mg, 0.015 mmol, 3 mol %), $NiBr_2$(dtbbpy) (12.2 mg, 0.025 mmol, 5 mol %), alkylpyridinium salt (0.75 mmol, 1.5 equiv), and aryl bromide (0.50 mmol, 1.0 equiv), if a solid. The vial was sealed with a cap containing a TFE-lined silicone septa and placed under an argon atmosphere *via* an inlet needle. The vial was evacuated three times *via* an inlet needle then purged with argon. The vial was then charged with a dry and degassed soln of THF or DMA (5.0 mL, 0.1 M). If the aryl bromide was an oil, it was added at this point directly *via* a microsyringe. Et_3N (0.21 mL, 1.5 mmol, 3 equiv) was then added to the reaction *via* a syringe. The reaction was placed under blue LED irradiation (approximately 2 cm from a ring of blue LED light strips) and stirred for 24 h. The temperature of the reaction was maintained at approximately 24 °C *via* a fan. After completion, the reaction mixture was taken to dryness and purified on an automated liquid chromatographic system to obtain the pure product.

Characterization Data

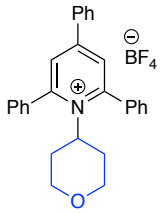

2,4,6-Triphenyl-1-(tetrahydro-2*H*-pyran-4-yl)pyridin-1-ium, **3a** (20.0 mmol scale, 6.2 g, 65%) was prepared following *GP1*. The desired product was isolated as a white foam. **^{1}H NMR** ($CDCl_3$, 500 MHz) δ 7.81 (s, 2H), 7.75 (dd, *J* = 13.5, 7.4 Hz, 6H), 7.67 – 7.37 (m, 9H), 4.89 (t, *J* = 12.6 Hz, 1H), 4.11 – 3.30 (m, 2H), 2.81 (t, *J* = 11.6 Hz, 2H), 2.24 – 1.66 (m, 4H). **^{13}C NMR** ($CDCl_3$, 125 MHz) δ 157.5, 155.6, 134.2, 134.0, 132.2, 131.3, 129.8, 129.6, 129.3, 128.5, 128.5,

69.3, 68.1, 34.0. **FT-IR** (cm^{-1}, neat, ATR): 1708, 1619, 1564, 1494, 1413, 1357, 1290, 1241, 1148, 983. **HRMS** (EI) calcd for $C_{28}H_{26}NO$ $[M]^+$: 392.2014, found: 392.1992.

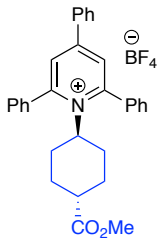

1-*trans*-4-(Methoxycarbonyl)cyclohexyl)-2,4,6-triphenylpyridin-1-ium, **3b** (2.0 mmol scale, 0.5 g, 50%) was prepared following *GP1*. The desired product was isolated as a white foam. **^{1}H NMR** ($CDCl_3$, 500 MHz) δ 7.84 (s, 2H), 7.75 (t, *J* = 6.9 Hz, 6H), 7.55 (ddt, *J* = 49.4, 15.0, 7.2 Hz, 9H), 4.65 (dd, *J* = 13.8, 10.8 Hz, 1H), 3.54 (s, 3H), 2.24 (d, *J* = 12.4 Hz, 2H), 1.85 (d, *J* = 13.3 Hz, 2H), 1.79 – 1.64 (m, 1H), 1.67 – 1.44 (m, 2H), 1.14 – 0.55 (m, 2H). **^{13}C NMR** ($CDCl_3$, 125 MHz) δ 174.7, 157.3, 155.5, 134.3, 134.1, 132.2, 131.3, 129.8, 129.6 (2C), 129.2, 128.6, 70.8, 52,0, 41.8, 32.3, 29.0. **FT-IR** (cm^{-1}, neat, ATR): 1728, 1619, 1599, 1563, 1456, 1436, 1414, 1356, 1198, 892. **HRMS** (EI) calcd for $C_{31}H_{30}NO_2$ $[M]^+$: 448.2277, found: 448.2267.

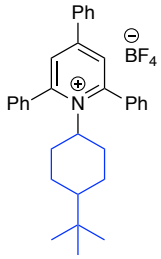

1-*trans*-4-Hydroxycyclohexyl)-2,4,6-triphenylpyridin-1-ium, **3c** (5.0 mmol scale, 1.35 g, 55%) was prepared following *GP1*. The desired product was isolated as a white foam. **^{1}H NMR** (500 MHz, acetone-d_6) δ 8.32 (s, 2H), 8.16 (d, *J* = 7.6 Hz, 2H), 7.85 (d, *J* = 7.2 Hz, 4H), 7.72 (m, 6H), 7.63 (dt, *J* = 15.0, 7.3 Hz, 3H), 4.75 (tt, *J* = 12.3, 3.1 Hz, 1H), 3.62 (s, 1H), 2.99 (pseudeo d, *J* =

11.1 Hz, 1H), 2.25 (d, J = 12.4 Hz, 2H), 1.79 - 1.65 (m, 4H), 0.78 (qd, J = 12.8, 3.2 Hz, 2H).**^{13}C NMR** (acetone-d_6, 125 MHz) δ 158.6, 155.3, 135.2, 134.5, 133.2, 131.9, 130.6, 130.3, 129.7, 129.4, 128.5, 72.0, 68.8, 35.9, 31.8. **FT-IR** (cm^{-1}, neat, ATR): 2960, 1621, 1055, 760, 705. **HRMS** (EI) calcd for $C_{29}H_{28}NO$ $[M]^+$: 406.2171, found: 406.2156.

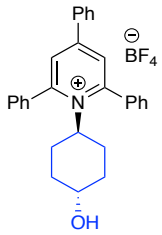

1-(4-(*tert*-Butyl)cyclohexyl)-2,4,6-triphenylpyridin-1-ium, **3d** (2.0 mmol scale, 0.53 g, 50%) was prepared following *GP1*. The desired product was isolated as a white foam. **^{1}H NMR** ($CDCl_3$, 500 MHz) δ 7.84 (s, 2H), 7.76 (ddd, J = 14.9, 7.9, 1.6 Hz, 6H), 7.70 – 7.38 (m, 9H), 4.87 – 4.38 (m, 1H), 2.17 (d, J = 12.0 Hz, 2H), 1.63 (d, J = 12.8 Hz, 2H), 1.50 (tt, J = 13.3, 7.2 Hz, 2H), 1.24 (t, J = 7.0 Hz, 1H), 0.63 (s, 9H), 0.56 – 0.37 (m, 2H). **^{13}C NMR** ($CDCl_3$, 125 MHz) δ 157.4, 155.2, 134.33, 134.3, 132.1, 131.1, 129.8, 129.6, 129.1, 128.5, 128.4, 72.5, 46.8, 33.6, 32.2, 27.7, 27.5. **FT-IR** (cm^{-1}, neat, ATR): 2986, 1737, 1421, 1360, 1092, 938, 847, 785. **HRMS** (EI) calcd for $C_{33}H_{36}N$ $[M]^+$: 446.2848, found: 446.2842.

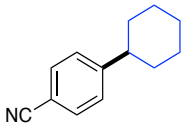

4-(Tetrahydro-2*H*-pyran-4-yl)benzonitrile, **3** (80 mg, 86%) was prepared following *GP2*. The desired product was isolated as an oil (24 g column, 100:0→95:5 hexanes/EtOAc). **^{1}H NMR** ($CDCl_3$, 500 MHz) δ 7.82 – 7.52 (m, 2H), 7.33 (d, J = 8.0 Hz, 2H), 4.09 (ddd, J = 11.5, 4.5, 1.9 Hz, 2H), 3.53 (td, J = 11.4, 2.9 Hz, 2H), 2.82 (tt, J = 11.3, 4.6 Hz, 1H), 2.13 – 1.59 (m, 4H). **^{13}C**

NMR ($CDCl_3$, 125 MHz) δ 151.4, 132.7, 127.9, 119.2, 110.5, 68.3, 42.0, 33.7. **FT-IR** (cm^{-1}, neat, ATR): 2941, 2842, 2225, 1607, 1505, 1443, 1387, 1238, 1178, 1123. **HRMS** (EI) calcd for $C_{12}H_{13}NO$ $[M]^+$: 187.0997, found: 187.1002.

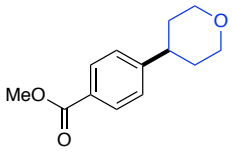

Methyl 4-(Tetrahydro-2*H*-pyran-4-yl)benzoate, **4** (79 mg, 72%) was prepared following *GP2*. The desired product was isolated as an oil (24 g column, 100:0→95:5 hexanes/EtOAc). **^{1}H NMR** ($CDCl_3$, 500 MHz) δ 7.99 (d, *J* = 8.0 Hz, 2H), 7.29 (d, *J* = 8.0 Hz, 2H), 4.43 – 4.00 (m, 2H), 3.91 (s, 3H), 3.54 (td, *J* = 11.6, 2.5 Hz, 2H), 2.82 (tt, *J* = 11.7, 4.2 Hz, 1H), 2.00 – 1.66 (m, 4H). **^{13}C NMR** ($CDCl_3$, 125 MHz) δ 167.3, 151.3, 130.2, 128.6, 127.1, 68.5, 52.3, 41.9, 33.9. **FT-IR** (cm^{-1}, neat, ATR): 1718, 1611, 1436, 1310, 1238, 1182, 1111, 1097, 1084. **HRMS** (EI) calcd for $C_{13}H_{16}O_3$ $[M]^+$: 220.1099, found: 220.1099.

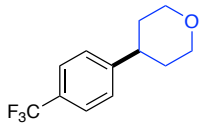

4-(4-(Trifluoromethyl)phenyl)tetrahydro-2*H*-pyran, **5** (81 mg, 70%) was prepared following *GP2*. The desired product was isolated as an oil (24 g column, 100:0→98:2 hexanes/EtOAc). **^{1}H NMR** ($CDCl_3$, 500 MHz) δ 7.57 (d, *J* = 7.9 Hz, 2H), 7.34 (d, *J* = 7.9 Hz, 2H), 4.10 (dd, *J* = 11.7, 4.1 Hz, 2H), 3.54 (td, *J* = 11.6, 2.4 Hz, 2H), 2.83 (tt, *J* = 11.4, 4.4 Hz, 1H), 1.82 (ddt, *J* = 20.1, 15.4, 7.6 Hz, 4H). **^{13}C NMR** ($CDCl_3$, 125 MHz) δ 149.9, 128.8 (q, *J* = 32.4 Hz), 127.2, 125.6, 125.59, 68.3, 41.6, 33.8. **^{19}F NMR** (471 MHz, $CDCl_3$) δ -62.37. **FT-IR** (cm^{-1}, neat, ATR): 2938,

2845, 1619, 1420, 1323, 1258, 1238, 1189, 1161, 1116. **HRMS** (EI) calcd for $C_{12}H_{13}OF_3$ $[M]^+$: 230.0918, found: 230.0926.

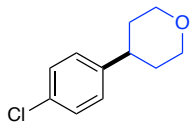

4-(4-Chlorophenyl)tetrahydro-2*H*-pyran, **6** (54 mg, 55%) was prepared following *GP2*. The desired product was isolated as an oil (24 g column, 100:0→98:2 hexanes/EtOAc). **^{1}H NMR** ($CDCl_3$, 500 MHz) δ 7.28 (d, *J* = 8.1 Hz, 2H), 7.15 (d, *J* = 8.0 Hz, 2H), 4.08 (dd, *J* = 10.5, 4.1 Hz, 2H), 3.52 (td, *J* = 11.3, 3.2 Hz, 2H), 2.73 (tt, *J* = 11.1, 4.8 Hz, 1H), 1.97 – 1.39 (m, 4H). **^{13}C NMR** ($CDCl_3$, 125 MHz) δ 144.6, 132.2, 128.9, 128.4, 68.6, 41.3, 34.2. **FT-IR** (cm^{-1}, neat, ATR): 2937, 2841, 1493, 1466, 1442, 1410, 1386, 1262, 1167, 1139. **HRMS** (EI) calcd for $C_{11}H_{13}ClO$ $[M]^+$: 196.0655, found: 196.0654.

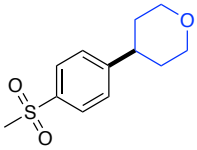

4-(4-(Methylsulfonyl)phenyl)tetrahydro-2*H*-pyran, **7** (60 mg, 50%) was prepared following *GP2*. The desired product was isolated as an oil (24 g column, 80:20→60:40 hexanes/EtOAc). **^{1}H NMR** ($CDCl_3$, 500 MHz) δ 7.88 (d, *J* = 8.1 Hz, 2H), 7.41 (d, *J* = 8.1 Hz, 2H), 4.09 (dt, *J* = 11.0, 3.3 Hz, 2H), 3.53 (td, *J* = 11.5, 2.7 Hz, 2H), 3.04 (s, 3H), 2.86 (tt, *J* = 11.5, 4.5 Hz, 1H), 1.88 – 1.68 (m, 4H).**^{13}C NMR** ($CDCl_3$, 125 MHz) δ 152.4, 138.8, 128.0, 128.0, 68.3, 44.8, 41.9, 33.8. **FT-IR** (cm^{-1}, neat, ATR): 2945, 2844, 1507, 1383, 1305, 1296, 1237, 1142. **HRMS** (EI) calcd for $C_{12}H_{16}O_3S$ $[M]^+$: 240.0820, found: 240.0829.

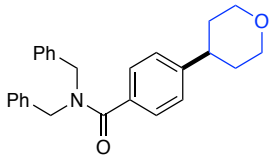

***N*,*N*-Dibenzyl-4-(tetrahydro-2*H*-pyran-4-yl)benzamide**, **8** (154 mg, 80%) was prepared following *GP2*. The desired product was isolated as an oil (24 g column, 80:20→50:50 hexanes/EtOAc). **^{1}H NMR** ($CDCl_3$, 500 MHz) δ 7.71 – 6.43 (m, 14H), 4.94 – 4.60 (m, 2H), 4.43 (s, 2H), 4.07 (ddd, *J* = 11.6, 4.5, 1.7 Hz, 2H), 3.51 (td, *J* = 11.6, 2.5 Hz, 2H), 2.76 (tt, *J* = 11.6, 4.2 Hz, 1H), 2.09 – 1.65 (m, 4H). **^{13}C NMR** ($CDCl_3$, 125 MHz) δ 172.5, 147.8, 137.2, 136.8, 134.4, 129.1, 129.0, 128.7, 127.9, 127.8, 127.3, 127.3, 127.2, 68.5, 51.9, 47.1, 41.7, 34.0. **FT-IR** (cm^{-1}, neat, ATR): 1631, 1450, 1418, 1386, 1363, 1370, 1237, 1120, 1100. **HRMS** (EI) calcd for $C_{26}H_{27}NO_2$ $[M]^+$: 385.2042, found: 385.2023.

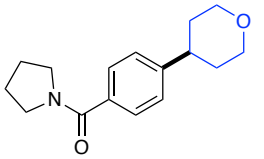

Pyrrolidin-1-yl(4-(tetrahydro-2*H*-pyran-4-yl)phenyl)methanone, **9** (110 mg, 85%) was prepared following *GP2*. The desired product was isolated as an oil (24 g column, 80:20→50:50 hexanes/EtOAc). **^{1}H NMR** ($CDCl_3$, 500 MHz) δ 7.47 (d, *J* = 8.3 Hz, 2H), 7.34 – 7.02 (m, 2H), 4.26 – 3.87 (m, 2H), 3.64 (t, *J* = 7.0 Hz, 2H), 3.52 (td, *J* = 11.6, 2.6 Hz, 2H), 3.45 (t, *J* = 6.6 Hz, 2H), 2.77 (tt, *J* = 11.7, 4.3 Hz, 1H), 2.00 – 1.52 (m, 8H). **^{13}C NMR** ($CDCl_3$, 125 MHz) δ 169.8, 147.8, 135.5, 127.6, 126.8, 68.5, 49.8, 46.4, 41.7, 34.0, 26.6, 24.7. **FT-IR** (cm^{-1}, neat, ATR): 2948, 2872, 2842, 1618, 1564, 1406, 1339, 1236, 1187, 1127. **HRMS** (EI) calcd for $C_{16}H_{21}NO_2$ $[M]^+$: 259.1572, found: 259.1577.

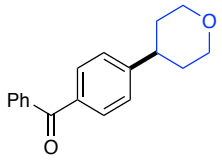

Phenyl(4-(tetrahydro-2*H*-pyran-4-yl)phenyl), **10** (108 mg, 80%) was prepared following *GP2*. The desired product was isolated as an oil (24 g column, 100:0→80:20 hexanes/EtOAc). **^{1}H NMR** ($CDCl_3$, 500 MHz) δ 7.79 (t, *J* = 8.3 Hz, 5H), 7.58 (t, *J* = 7.4 Hz, 1H), 7.49 (d, *J* = 7.6 Hz, 2H), 7.34 (d, *J* = 7.9 Hz, 2H), 4.11 (dd, *J* = 11.4, 4.1 Hz, 2H), 3.55 (td, *J* = 11.6, 2.5 Hz, 2H), 2.86 (tt, *J* = 11.7, 4.3 Hz, 1H), 2.08 – 1.52 (m, 4H). **^{13}C NMR** ($CDCl_3$, 125 MHz) δ 196.3, 150.7, 137.8, 135.8, 132.3, 130.6, 130.0, 128.3, 126.7, 68.2, 41.7, 33.6. **FT-IR** (cm^{-1}, neat, ATR): 3248, 2938, 2851, 1613, 1513, 1443, 1311, 1249, 1156, 1132, 1029, 833, 752, 514. **HRMS** (EI) calcd for $C_{18}H_{18}O_2$ $[M]^+$: 266.1307, found: 266.1309.

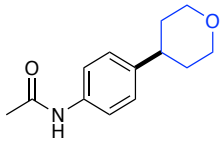

***N*-(4-(Tetrahydro-2H-pyran-4-yl)phenyl)acetamide**, **11** (46 mg, 42%) was prepared following *GP2* (in DMA as a solvent, 48 h). The desired product was isolated as a white solid (24 g column, 100:0→80:20 hexanes/EtOAc). **mp** = 181-182 ºC. **^{1}H NMR** ($CDCl_3$, 500 MHz) δ 7.44 (d, *J* = 8.2 Hz, 2H), 7.24 – 7.02 (m, 3H), 4.20 – 3.98 (m, 2H), 3.53 (td, *J* = 11.4, 2.9 Hz, 2H), 2.73 (tt, *J* = 11.3, 4.6 Hz, 1H), 2.18 (s, 3H), 1.86 – 1.68 (m, 4H). **^{13}C NMR** ($CDCl_3$, 125 MHz) δ 168.3, 141.9, 136.0, 127.1, 120.2, 68.3, 40.9, 33.9, 24.4. **FT-IR** (cm^{-1}, neat, ATR): 3301, 2931, 2845, 1665, 1538, 1515, 1316, 826, 541. **HRMS** (EI) calcd for $C_{13}H_{17}NO_2$ $[M]^+$: 219.1259, found: 219.1263.

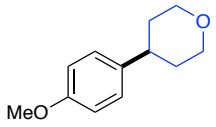

4-(4-Methoxyphenyl)tetrahydro-2H-pyran, **12** (56 mg, 58%) was prepared following *GP2* (in DMA as a solvent, 48 h). The desired product was isolated as an oil (24 g column, 100:0→98:2 hexanes/EtOAc). **^{1}H NMR** ($CDCl_3$, 500 MHz) δ 7.15 (d, *J* = 8.6 Hz, 2H), 6.87 (d, *J* = 8.7 Hz, 2H), 4.12 – 4.01 (m, 2H), 3.80 (s, 3H), 3.52 (td, *J* = 11.4, 3.1 Hz, 2H), 2.70 (tt, *J* = 11.2, 4.7 Hz, 1H), 1.84 – 1.69 (m, 4H). **^{13}C NMR** ($CDCl_3$, 125 MHz) δ 158.2, 138.3, 127.7, 114.0, 68.6, 55.4, 40.9, 34.4. **FT-IR** (cm^{-1}, neat, ATR): 2934, 2836, 1610, 1512, 1243, 1035, 1020, 842, 827, 541. **HRMS** (EI) calcd for $C_{12}H_{16}O_2$ $[M]^+$: 192.1150, found: 192.1146.

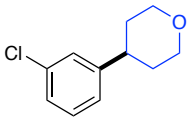

4-(3-Chlorophenyl)tetrahydro-2*H*-pyran, **13** (57 mg, 58%) was prepared following *GP2*. The desired product was isolated as an oil (24 g column, 100:0→98:2 hexanes/EtOAc). **^{1}H NMR** ($CDCl_3$, 500 MHz) δ 7.58 – 7.15 (m, 3H), 7.10 (d, *J* = 7.6 Hz, 1H), 4.48 – 3.80 (m, 2H), 3.52 (td, *J* = 11.3, 3.2 Hz, 2H), 2.74 (tt, *J* = 10.9, 4.9 Hz, 1H), 2.17 – 1.63 (m, 4H). **^{13}C NMR** ($CDCl_3$, 125 MHz) δ 148.1, 134.6, 130.0, 127.3, 126.7, 125.2, 68.5, 41.6, 34.0. **FT-IR** (cm^{-1}, neat, ATR): 2937, 2841, 1596, 1573, 1479, 1386, 1236, 1129, 1116. **HRMS** (EI) calcd for $C_{11}H_{13}ClO$ $[M]^+$: 196.0655, found: 196.0649.

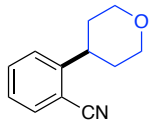

2-(Tetrahydro-2H-pyran-4-yl)benzonitrile, **14** (82 mg, 88%) was prepared following *GP2*. The desired product was isolated as an oil (24 g column, 100:0→95:5 hexanes/EtOAc). **^{1}H NMR** ($CDCl_3$, 500 MHz) δ 7.63 (dd, *J* = 7.7, 1.5 Hz, 1H), 7.57 (td, *J* = 7.8, 1.4 Hz, 1H), 7.38 (d, *J* = 8.0 Hz, 1H), 7.31 (td, *J* = 7.6, 1.2 Hz, 1H), 4.17 – 4.00 (m, 2H), 3.59 (td, *J* = 11.4, 3.2 Hz, 2H), 3.34 – 3.18 (m, 1H), 1.90 – 1.74 (m, 4H). **^{13}C NMR** ($CDCl_3$, 125 MHz) δ 149.3, 133.3, 133.2, 127.0, 126.7, 118.1, 112.0, 68.2, 40.0, 33.2. **FT-IR** (cm^{-1}, neat, ATR): 2944, 2847, 2223, 1266, 1129, 761, 732, 518**. HRMS** (EI) calcd for $C_{12}H_{13}NO$ $[M]^+$: 187.0997, found: 187.1003.

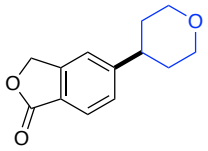

5-(Tetrahydro-2*H*-pyran-4-yl)isobenzofuran-1(3*H*)-one, **15** (82.7 mg, 76%) was prepared following *GP2*. The desired product was isolated as a colorless solid (24 g column, 100:0→80:20 hexanes/EtOAc). **mp** = 142-144 °C. **^{1}H NMR** ($CDCl_3$, 500 MHz) δ 7.78 (t, *J* = 8.5 Hz, 1H), 7.42 – 7.22 (m, 2H), 5.24 (d, *J* = 8.1 Hz, 2H), 4.04 (dt, *J* = 11.4, 5.5 Hz, 2H), 3.49 (q, *J* = 10.3 Hz, 2H), 2.86 (dt, *J* = 11.3, 5.4 Hz, 1H), 1.94 – 1.65 (m, 4H). **^{13}C NMR** ($CDCl_3$, 125 MHz) δ 170.9, 152.9, 147.3, 128.2, 125.8, 124.0, 120.2, 69.6, 68.1, 42.0, 33.7. **FT-IR** (cm^{-1}, neat, ATR): 3400, 2928, 1606, 1503, 1415, 1255, 1119, 999. **HRMS** (EI) calcd for $C_{13}H_{14}O_2$ $[M]^+$: 218,0943 found: 218.0945.

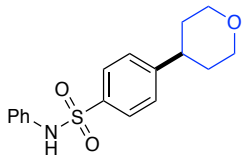

***N*-Phenyl-4-(tetrahydro-2*H*-pyran-4-yl)benzenesulfonamide**, **16** (113 mg, 75%) was prepared following *GP2*. The desired product was isolated as an oil (24 g column, 80:20→50:50 hexanes/EtOAc). **^{1}H NMR** ($CDCl_3$, 500 MHz) δ 7.72 (d, *J* = 8.3 Hz, 2H), 7.52 – 7.17 (m, 4H), 7.17 – 6.94 (m, 3H), 6.60 (s, 1H), 4.38 – 3.84 (m, 2H), 3.51 (td, *J* = 11.5, 2.9 Hz, 2H), 2.79 (td, *J* = 11.3, 5.2 Hz, 1H), 2.09 – 1.61 (m, 4H).**^{13}C NMR** ($CDCl_3$, 125 MHz) δ 151.5, 137.4, 136.8, 129.6, 127.8, 127.7, 125.5, 121.7, 68.3, 41.8, 33.7. **FT-IR** (cm^{-1}, neat, ATR): 3300, 2950, 2484, 1598, 1495, 1415, 1344, 1300, 1238, 1222. **HRMS** (EI) calcd for $C_{17}H_{19}NO_3S$ $[M]^+$: 318.1164, found: 318.1172.

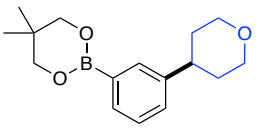

5,5-Dimethyl-2-(3-(tetrahydro-2H-pyran-4-yl)phenyl)-1,3,2-dioxaborinane, **17** (100 mg, 73%) was prepared following *GP2*. The desired product was isolated as an oil (24 g column, 100:0→95:5 hexanes/EtOAc). **^{1}H NMR** ($CDCl_3$, 500 MHz) δ 7.73 – 7.62 (m, 2H), 7.36 – 7.28 (m, 2H), 4.08 (dd, *J* = 11.4, 4.3 Hz, 2H), 3.77 (s, 4H), 3.52 (td, *J* = 11.7, 2.2 Hz, 2H), 2.77 (tt, *J* = 12.0, 4.0 Hz, 1H), 1.92 – 1.73 (m, 4H), 1.03 (s, 6H). **^{13}C NMR** ($CDCl_3$, 125 MHz) δ 145.0, 132.4, 132.0, 129.2, 127.9, 72.4, 68.6, 41.7, 34.1, 32.0, 22.0. **FT-IR** (cm^{-1}, neat, ATR): 2955, 2933, 2840, 1476, 1305, 1247, 1129, 708. **HRMS** (EI) calcd for $C_{16}H_{23}BO_3$ $[M]^+$: 274.1740, found: 274.1729.

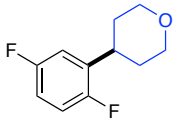

4-(2,5-Difluorophenyl)tetrahydro-2H-pyran, **18** (83 mg, 84%) was prepared following *GP2*. The desired product was isolated as an oil (24 g column, 100:0→98:2 hexanes/EtOAc). **^{1}H NMR** ($CDCl_3$, 500 MHz) δ 7.03 – 6.90 (m, 2H), 6.90 – 6.80 (m, 1H), 4.09 (d, *J* = 10.6 Hz, 2H), 3.55 (d, *J* = 11.4 Hz, 2H), 3.11 (m, 1H), 1.86 – 1.72 (m, 4H). **^{13}C NMR** ($CDCl_3$, 125 MHz) δ 158.9 (dd, *J* = 241.6, 2.2 Hz), 156.4 (dd, *J* = 240.5, 2.5 Hz), 134.1 (dd, *J* = 17.1, 7.1 Hz), 116.2 (dd, *J* = 25.9, 8.7 Hz), 114.0 (dd, *J* = 24.3, 5.3 Hz), 113.7 (dd, *J* = 24.1, 8.8 Hz), 68.1, 34.4, 32.3. **^{19}F NMR** (471 MHz, $CDCl_3$) δ -118.7 – -118.8 (m), -125.4 – -125.6 (m). **FT-IR** (cm^{-1}, neat, ATR): 2952, 2844, 1491, 1233, 1180, 1130, 1091, 878, 813, 734. **HRMS** (EI) calcd for $C_{11}H_{12}F_2O$ $[M]^+$: 198.0856, found: 198.0858.

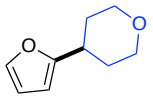

4-(Furan-2-yl)tetrahydro-2H-pyran, **19** (50 mg, 66%) was prepared following *GP2*. The desired product was isolated as an oil (24 g column, 100:0→95:5 hexanes/EtOAc). **^{1}H NMR** ($CDCl_3$, 500 MHz) δ 7.32 (s, 1H), 6.29 (s, 1H), 5.99 (s, 1H), 4.02 (dt, *J* = 11.5, 2H), 3.54 – 3.43 (m, 2H), 2.94 – 2.82 (m, 1H), 1.92 (d, *J* = 13.3 Hz, 2H), 1.82 – 1.70 (m, 2H). **^{13}C NMR** (126 MHz, $CDCl_3$) δ 159.1, 141.0, 110.0, 103.3, 67.6, 34.5, 31.3. **FT-IR** (cm^{-1}, neat, ATR): 2944, 2844, 1506, 1128, 1089, 1008, 875, 728. **HRMS** (EI) calcd for $C_9H_{12}O_2$ $[M]^+$: 152.0837, found: 152.0848.

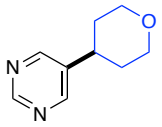

5-(Tetrahydro-2*H*-pyran-4-yl)-pyrimidine, **20** (50.3 mg, 61%) was prepared following *GP2*. The desired product was isolated as a yellow foam (24 g column, 80:20→30:70 hexanes/EtOAc).**^{1}H NMR** ($CDCl_3$, 500 MHz) δ 9.09 (s, 1H), 8.61 (s, 2H), 4.32 – 4.00 (m, 2H), 3.53 (td, *J* = 11.5, 2.9 Hz, 2H), 2.80 (tt, *J* = 11.5, 4.6 Hz, 1H), 1.90 – 1.67 (m, 4H). **^{13}C NMR** ($CDCl_3$, 125 MHz) δ 157.4, 155.7, 138.3, 68.0, 37.2, 33.2. **FT-IR** (cm^{-1}, neat, ATR): 2939, 2844, 1561, 1443, 1276, 1164, 1086, 896. **HRMS** (EI) calcd for $C_9H_{12}ON_2$ $[M]^+$: 164.0950, found:164.0964.

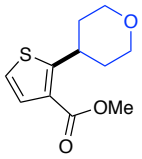

Methyl 3-(Tetrahydro-2H-pyran-4-yl)thiophene-2-carboxylate, **21** (85 mg, 75%) was prepared following *GP2*. The desired product was isolated as a white solid (24 g column, 100:0→80:20 hexanes/EtOAc). **mp** = 110 – 112 ºC. **^{1}H NMR** ($CDCl_3$, 500 MHz) δ 7.45 (d, *J* = 5.2 Hz, 1H), 7.09 (d, *J* = 5.2 Hz, 1H), 4.05 (dt, *J* = 11.3, 3.2 Hz, 2H), 3.95 – 3.82 (m, 4H), 3.64 – 3.52 (m, 2H), 1.84 – 1.73 (m, 4H). **^{13}C NMR** ($CDCl_3$, 125 MHz) δ 162.7, 154.5, 130.7, 127.4, 125.6, 68.1, 51.6, 35.1, 33.2. **FT-IR** (cm^{-1}, neat, ATR): 3103, 2952, 2845, 1706, 1437, 1228, 1125, 1071, 783. **HRMS** (EI) calcd for $C_{11}H_{14}O_3S$ $[M]^+$: 226.0664, found: 226.0659.

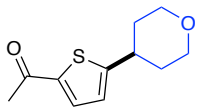

1-(5-(Tetrahydro-2H-pyran-4-yl)thiophen-2-yl)ethan-1-one, **22** (57 mg, 54%) was prepared following *GP2*. The desired product was isolated as an oil (24 g column, 100:0→80:20 hexanes/EtOAc). **^{1}H NMR** ($CDCl_3$, 500 MHz) δ 7.56 (d, *J* = 3.8 Hz, 1H), 6.87 (d, *J* = 3.9 Hz, 1H), 4.06 (dd, *J* = 11.3, 3.5 Hz, 2H), 3.52 (td, *J* = 11.8, 2.1 Hz, 2H), 3.07 (tt, *J* = 11.6, 4.0 Hz, 1H), 2.52 (s, 3H), 1.99 – 1.90 (m, 2H), 1.90 – 1.75 (m, 2H). **^{13}C NMR** ($CDCl_3$, 125 MHz) δ 190.7, 159.7, 142.1, 132.8, 123.9, 67.8, 37.4, 34.6, 26.6. **FT-IR** (cm^{-1}, neat, ATR): 2923, 2852, 1655, 1604, 1449, 1123, 866, 812, 602. **HRMS** (EI) calcd for $C_{11}H_{14}O_2S$ $[M]^+$: 210.0715, found: 210.0723.

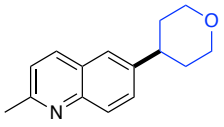

2-Methyl-6-(tetrahydro-2H-pyran-4-yl)quinolone, **23** (92 mg, 81%) was prepared following *GP2*. The desired product was isolated as a white solid (24 g column, 100:00→80:20 hexanes/EtOAc). **mp** = 104-106 ºC. **^{1}H NMR** ($CDCl_3$, 500 MHz) δ 8.07 – 7.85 (m, 2H), 7.56 (d, *J* = 8.0 Hz, 2H), 7.24 (s, 1H), 4.24 – 3.90 (m, 2H), 3.57 (td, *J* = 11.6, 2.6 Hz, 2H), 2.91 (tt, *J* = 11.6, 4.3 Hz, 1H), 2.72 (s, 3H), 1.98 – 1.80 (m, 4H). **^{13}C NMR** ($CDCl_3$, 125 MHz) δ 158.6, 147.1, 143.3, 136.1, 129.4, 128.9, 126.7, 124.3, 122.2, 68.5, 41.5, 34.0, 25.4. **FT-IR** (cm^{-1}, neat, ATR): 2934, 2840, 1600, 1125, 1084, 834. **HRMS** (EI) calcd for $C_{15}H_{17}NO$ $[M]^+$: 227.1310, found: 227.1312.

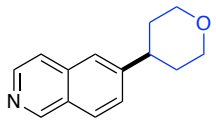

6-(Tetrahydro-2H-pyran-4-yl)isoquinoline, **24** (51 mg, 48%) was prepared following *GP2*. The desired product was isolated as a white solid (24 g column, 80:20→60:40 hexanes/EtOAc). **mp** = 57-59 °C. **^{1}H NMR** ($CDCl_3$, 500 MHz) δ 9.21 (s, 1H), 8.50 (d, *J* = 5.8 Hz, 1H), 7.92 (d, *J* = 8.4 Hz, 1H), 7.69 – 7.56 (m, 2H), 7.50 (dd, *J* = 8.5, 1.7 Hz, 1H), 4.23 – 3.99 (m, 2H), 3.58 (td, *J* = 11.7, 2.4 Hz, 2H), 2.96 (tt, *J* = 11.8, 4.1 Hz, 1H), 1.99 – 1.79 (m, 4H). **^{13}C NMR** ($CDCl_3$, 125 MHz) δ 152.3, 148.4, 143.3, 136.3, 128.0, 127.8, 127.4, 123.4, 120.5, 68.4, 42.1, 33.7. **FT-IR** (cm^{-1}, neat, ATR): 2936, 2840, 1630, 1238, 1124, 1084, 830, 732. **HRMS** (EI) calcd for $C_{14}H_{15}NO$ $[M]^+$: 213.1154, found: 213.1155.

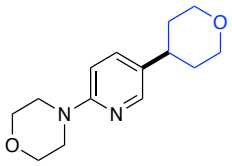

4-(5-(Tetrahydro-2H-pyran-4-yl)pyridin-2-yl)morpholine, **25** (89 mg, 72%) was prepared following *GP2*. The desired product was isolated as an oil (24 g column, 80:20→40:60 hexanes/EtOAc). **^{1}H NMR** ($CDCl_3$, 500 MHz) δ 8.10 (d, *J* = 2.4 Hz, 1H), 7.44 – 7.33 (m, 1H), 6.64 (d, *J* = 8.8 Hz, 1H), 4.08 (dd, *J* = 11.4, 3.8 Hz, 2H), 3.87 – 3.72 (m, 4H), 3.58 – 3.38 (m, 6H), 2.68 (td, *J* = 11.4, 5.7 Hz, 1H), 1.86 – 1.66 (m, 4H). **^{13}C NMR** ($CDCl_3$, 125 MHz) δ 158.7, 146.4, 136.1, 131.1, 107.1, 68.4, 66.9, 46.1, 38.3, 34.0. **FT-IR** (cm^{-1}, neat, ATR): 2954, 2844, 1605, 1495, 1239, 945, 764, 750. **HRMS** (ESI) calcd for $C_{14}H_{21}N_2O_2$ $[M+H]^+$: 249.1603, found: 249.1595.

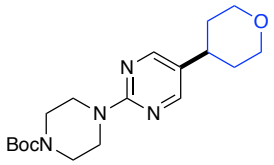

***tert*-Butyl 4-(5-(Tetrahydro-2H-pyran-4-yl)pyrimidin-2-yl)piperazine-1-carboxylate**, **26** (112 mg, 64%) was prepared following *GP2*. The desired product was isolated as a white solid (24 g column, 80:20→40:60 hexanes/EtOAc). **mp** = 158-160 ºC. **^{1}H NMR** ($CDCl_3$, 500 MHz) δ 8.21 (s, 2H), 4.11 – 4.02 (m, 2H), 3.77 (t, *J* = 5.2 Hz, 4H), 3.56 – 3.43 (m, 6H), 2.68 – 2.57 (m, 1H), 1.81 – 1.67 (m, 4H), 1.48 (s, 9H). **^{13}C NMR** ($CDCl_3$, 125 MHz) δ 161.1, 156.5, 155.0, 126.8, 80.1, 68.3, 43.9, 43.2, 36.3, 33.7, 28.6. **FT-IR** (cm^{-1}, neat, ATR): 2850,1688, 1497, 1418, 1264, 1243, 1168, 732, 702. **HRMS** (ESI) calcd for $C_{18}H_{29}N_4O_3$ $[M+H]^+$: 349.2240, found: 349.2256.

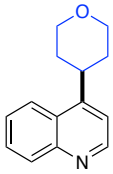

4-(Tetrahydro-2*H*-pyran-4-yl)quinoline, **27** (102 mg, 95%) was prepared following *GP2*. The desired product was isolated as an oil (24 g column, 80:20→60:40 hexanes/EtOAc). **^{1}H NMR** ($CDCl_3$, 500 MHz) δ 8.88 (d, *J* = 4.6 Hz, 1H), 8.12 (dd, *J* = 22.8, 8.4 Hz, 2H), 7.71 (t, *J* = 7.6 Hz, 1H), 7.58 (t, *J* = 7.7 Hz, 1H), 7.43 – 6.88 (m, 1H), 4.61 – 3.91 (m, 2H), 3.69 (td, *J* = 11.5, 2.6 Hz, 2H), 3.61 (ddd, *J* = 11.4, 7.1, 4.2 Hz, 1H), 2.26 – 1.66 (m, 4H). **^{13}C NMR** ($CDCl_3$, 125 MHz) δ 151.2, 150.6, 148.6, 130.8, 129.1, 126.7, 126.6, 122.7, 117.7, 68.4, 36.4, 33.2. **FT-IR** (cm^{-1}, neat, ATR): 2947, 2919, 2843, 1590, 1569, 1508, 1386, 1238, 1126, 1112. **HRMS** (ESI) calcd for $C_{14}H_{16}NO$ $[M+H]^+$: 214.1232, found: 214.1218.

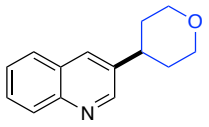

3-(Tetrahydro-2*H*-pyran-4-yl)quinoline, **28** (80 mg, 80%) was prepared following *GP2*. The desired product was isolated as an oil (24 g column, 60:40→20:80 hexanes/EtOAc). **^{1}H NMR** ($CDCl_3$, 500 MHz) δ 8.84 (d, *J* = 2.3 Hz, 1H), 8.09 (d, *J* = 8.4 Hz, 1H), 7.94 (d, *J* = 2.2 Hz, 1H), 7.79 (dd, *J* = 8.2, 1.4 Hz, 1H), 7.67 (ddd, *J* = 8.4, 6.8, 1.5 Hz, 1H), 7.54 (td, *J* = 7.4, 6.8, 1.2 Hz, 1H), 4.14 (ddd, *J* = 11.6, 4.3, 1.8 Hz, 2H), 3.60 (td, *J* = 11.5, 2.7 Hz, 2H), 2.99 (tt, *J* = 11.6, 4.3 Hz, 1H), 2.19 – 1.52 (m, 4H). **^{13}C NMR** ($CDCl_3$, 125 MHz) δ 151.0, 147.2, 138.4, 132.7, 129.3, 129.0, 128.3, 127.7, 126.9, 68.3, 39.3, 33.7. **FT-IR** (cm^{-1}, neat, ATR): 2850,1688, 1497, 1418, 1264, 1243, 1168, 732, 702. **HRMS** (EI) calcd for $C_{14}H_{15}NO$ $[M]^+$: 213.1154, found: 213.1155.

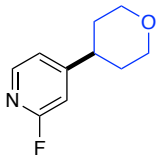

2-Fluoro-4-(tetrahydro-2*H*-pyran-4-yl)pyridine, **29** (54 mg, 60%) was prepared following *GP2*. The desired product was isolated as an oil (24 g column, 80:20→40:60 hexanes/EtOAc). **^{1}H NMR** ($CDCl_3$, 500 MHz) δ 8.11 (d, *J* = 5.2 Hz, 1H), 7.02 (d, *J* = 5.1 Hz, 1H), 6.75 (s, 1H), 4.07 (d, *J* = 11.7 Hz, 2H), 3.80 – 3.36 (m, 1H), 2.79 (m, *J* = 7.9 Hz, 2H), 1.77 (d, *J* = 7.3 Hz, 4H). **^{13}C NMR** ($CDCl_3$, 125 MHz) δ 165.1, 163.2, 160.3 (d, *J* = 7.5 Hz), 147.6 (d, *J* = 15.4 Hz), 119.9 (d, *J* = 3.9 Hz), 107.4 (d, *J* = 37.1 Hz), 67.7, 40.7 (d, *J* = 2.9 Hz), 32.7. **^{19}F NMR** (471 MHz**,** $CDCl_3$**)** δ -68.41. **FT-IR** (cm^{-1}, neat, ATR): 1680, 1565, 1555, 1411, 1387, 1239, 1153, 1126. **HRMS** (EI) calcd for $C_{10}H_{12}FNO$ $[M]^+$: 181.0903, found: 181.0908.

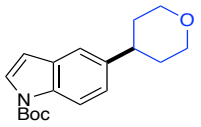

***tert*-Butyl 5-(Tetrahydro-2H-pyran-4-yl)-1H-indole-1-carboxylate**, **30** (66 mg, 44%) was prepared following *GP2*. The desired product was isolated as an oil (24 g column, 100:0→80:20 hexanes/EtOAc). **^{1}H NMR** ($CDCl_3$, 500 MHz) δ 8.06 (d, *J* = 8.6 Hz, 1H), 7.58 (d, *J* = 3.7 Hz, 1H), 7.40 (d, *J* = 1.8 Hz, 1H), 7.19 (dd, *J* = 8.6, 1.8 Hz, 1H), 6.53 (d, *J* = 3.7 Hz, 1H), 4.16 – 4.05 (m, 2H), 3.56 (td, *J* = 11.7, 2.3 Hz, 2H), 2.85 (tt, *J* = 11.9, 4.1 Hz, 1H), 1.94 – 1.77 (m, 4H), 1.67 (s, 9H). **^{13}C NMR** ($CDCl_3$, 125 MHz) δ 149.9, 140.6, 134.0, 131.0, 126.3, 123.5, 118.7, 115.3, 107.4, 83.7, 68.7, 41.7, 34.6, 28.4. **FT-IR** (cm^{-1}, neat, ATR): 2978, 2838, 1728, 1470, 1362, 1325, 1272, 1260, 1247, 1161, 1128, 1082, 1022, 764, 749. **HRMS** (EI): calcd for $C_{18}H_{23}NO_3$ $[M]^+$: 301.1678, found: 301. 1683.

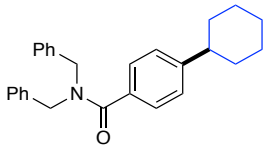

***N*,*N*-Dibenzyl-4-cyclohexylbenzamide**, **31** (177.1 mg, 92%) was prepared following *GP2*. The desired product was isolated as a colorless solid (24 g column, 80:20→50:50 hexanes/EtOAc). **mp** = 165-166 ºC. **^{1}H NMR** ($CDCl_3$, 500 MHz) δ 7.46 – 7.44 (m, 2H), 7.38 – 7.36 (m, 4H), 7.32 - 7.29 (m, 4H), 7.22 (d, *J* = 8.1 Hz, 2H), 7.17 - 7.16 (m, 1H), 4.71 (s, 2H), 4.45 (s, 2H), 2.51 (dq, *J* = 5.4, 4.0 Hz, 1H), 1.86 - 1.83 (m, 4H), 1.76 - 1.73 (m, 1H), 1.42 -1.38 (m, 4H), 1.29 -1.23 (m, 2H). **^{13}C NMR** ($CDCl_3$, 125 MHz) δ 172.6, 150.0, 133.6, 131.9, 128.9, 128.8, 128.6, 128.5, 127.7, 127.6, 127.2, 127.0, 51.8, 47.0, 44.6, 34.4, 29.8, 26.9, 26.2. **FT-IR** (cm^{-1}, neat, ATR): 2923, 2850, 1633, 1494, 1307, 1185, 1028, 836. **HRMS** (EI) calcd for $C_{27}H_{29}NO$ $[M]^+$: 383.2249, found: 383.2245.

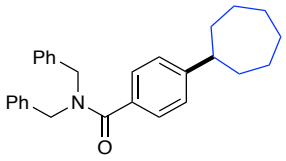

***N*,*N*-Dibenzyl-4-cycloheptylbenzamide**, **32** (184.3 mg, 93%) was prepared following *GP2*. The desired product was isolated as a pale-yellow oil (24 g column, 80:20→50:50 hexanes/EtOAc). **^{1}H NMR** ($CDCl_3$, 500 MHz) δ 7.47 (d, *J* = 7.9 Hz, 2H), 7.39 – 7.36 (m, 4H), 7.32 (d, *J* = 7.2 Hz, 4H), 7.22 (d, *J* = 7.9 Hz, 2H), 7.19 (s, 2H), 4.74 (s, 2H), 4.47 (s, 2H), 2.70 – 2.67 (m, 1H), 1.93 - 1.88 (m, 2H), 1.84 - 1.78 (m, 2H), 1.73 - 1.68 (m, 2H), 1.64 - 1.53 (m, 6H). **^{13}C NMR** ($CDCl_3$, 125 MHz) δ 172.4, 151.7, 137.1, 136.7, 133.3, 131.7, 128.8, 127.6, 127.5, 126.9, 126.8, 51.4, 46.9, 36.6, 27.9, 27.2. **FT-IR** (cm^{-1}, neat, ATR): 2924, 1494, 1363, 1308, 1141, 992, 826, 647. **HRMS** (EI) calcd for $C_{28}H_{31}NO$ $[M]^+$: 397.2406, found: 397.2400.

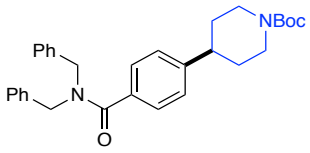

***tert*-Butyl 4-(4-(Dibenzylcarbamoyl)phenyl)piperidine-1-carboxylate**, **33** (115.4 mg, 48%) was prepared following *GP2*. The desired product was isolated as a pale-yellow foam (24 g column, 80:20→40:60 hexanes/EtOAc). **^{1}H NMR** ($CDCl_3$, 500 MHz) δ 7.45 (d, *J* = 7.9 Hz, 2H), 7.36 (t, *J* = 7.4 Hz, 4H), 7.33 - 7.28 (m, 4H), 7.20 (d, *J* = 8.0 Hz, 2H), 7.15 (s, 2H), 4.69 (s, 2H), 4.42 (s, 2H), 4.23 (s, 1H), 2.78 (s, 2H), 2.69 - 2.58 (m, 1H), 1.79 (d, *J* = 13.0 Hz, 2H), 1.60 (t, *J* = 12.8 Hz, 2H), 1.47 (s, 9H). **^{13}C NMR** ($CDCl_3$, 125 MHz) δ 172.4, 155.0, 147.7, 137.1, 136.7, 134.3, 129.0, 128.9, 128.6, 127.8, 127.6, 127.2, 79.7, 51.7, 47.0, 44.5, 42.8, 33.2, 28.6. **FT-IR** (cm^{-1}, neat, ATR): 1449, 1364, 1287, 1125, 1012, 989, 842, 698. **HRMS** (ESI) calcd for $C_{31}H_{36}N_2O_3$ $[M+H]^+$: 485.2804, found: 485.2824.

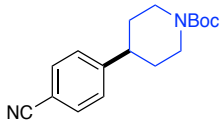

***tert*-Butyl 4-(4-Cyanophenyl)piperidine-1-carboxylate**, **34** (112.5 mg, 79%) was prepared following *GP2*. The desired product was isolated as a colorless oil (24 g column, 100:0→80:20 hexanes/EtOAc). **^{1}H NMR** ($CDCl_3$, 500 MHz) δ 7.57 (d, *J* = 7.9 Hz, 2H), 7.29 (d, *J* = 7.9 Hz, 2H), 4.24 (s, 2H), 2.80 (brs, 2H), 2.69 (tt, *J* = 12.7, 2.6 Hz, 1H), 1.79 (d, *J* = 13.0 Hz, 2H), 1.58 (qd, *J* = 12.7, 4.2 Hz, 2H), 1.46 (s, 9H). **^{13}C NMR** ($CDCl_3$, 125 MHz) δ 154.7, 151.2, 132.4, 127.7, 118.9, 110.3, 79.6, 44.2, 42.9, 32.7, 28.4. **FT-IR** (cm^{-1}, neat, ATR): 1476, 1465, 1392, 1125, 1107, 986, 884, 860. **HRMS** (ESI) calcd for $C_{17}H_{23}N_2O_2$ $[M+H]^+$: 287.1760, found: 287.1747.

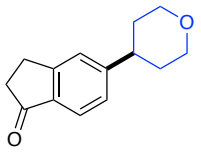

5-(Tetrahydro-2*H*-pyran-4-yl)-2,3-dihydro-1*H*-inden-1-one, **35** (72.5 mg, 67%) was prepared following *GP2*. The desired product was isolated as a colorless solid (24 g column, 100:0→90:10 hexanes/EtOAc). **mp** = 74–75 °C. **^{1}H NMR** ($CDCl_3$, 500 MHz) δ 7.62 (s, 1H), 7.53 – 7.40 (m, 2H), 4.08 (dd, *J* = 11.4, 3.9 Hz, 2H), 3.53 (td, *J* = 11.4, 2.7 Hz, 2H), 3.20 – 3.05 (m, 2H), 2.83 (ddt, *J* = 11.4, 8.9, 3.9 Hz, 1H), 2.75 – 2.64 (m, 2H), 1.87 – 1.73 (m, 4H). **^{13}C NMR** ($CDCl_3$, 125 MHz) δ 207.2, 153.6, 145.5, 137.6, 133.9, 126.9, 121.6, 68.4, 41.4, 36.7, 34.0, 25.6. **FT-IR** (cm^{-1}, neat, ATR): 2932, 2841, 1709, 1615, 1444, 1284, 1128, 1086. **HRMS** (EI) calcd for $C_{14}H_{16}O_2$ $[M]^+$: 216.1150, found: 216.1140.

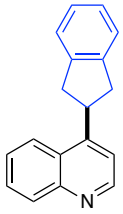

4-(2,3-Dihydro-1*H*-Inden-2-yl)quinoline, **36** (115.0 mg, 94%) was prepared following *GP2*. The desired product was isolated as a yellow oil (24 g column, 80:20→40:60 hexanes/EtOAc).**^{1}H NMR** ($CDCl_3$, 500 MHz) δ 8.79 (d, *J* = 4.6 Hz, 1H), 8.16 (ddd, *J* = 8.4, 4.3, 1.4 Hz, 2H), 7.74 (ddd, *J* = 8.4, 6.9, 1.4 Hz, 1H), 7.60 (ddd, *J* = 8.4, 6.9, 1.4 Hz, 1H), 7.29 (dd, *J* = 5.5, 3.8 Hz, 3H), 7.24 – 7.22 (m, 2H), 4.68 – 4.28 (m, 1H), 3.54 (dd, *J* = 15.8, 8.3 Hz, 2H), 3.23 (dd, *J* = 15.8, 6.8 Hz, 2H). **^{13}C NMR** ($CDCl_3$, 125 MHz) δ 150.4, 142.2, 131.5, 130.4, 129.2, 127.4, 126.9, 126. 6, 124.6, 123.5, 117.9, 40.0, 39.9. **FT-IR** (cm^{-1}, neat, ATR): 3066, 2940, 2844, 1568, 1483, 1446, 1336, 869. **HRMS** (ESI) calcd for $C_{18}H_{16}N$ $[M+H]^+$: 246.1283, found: 246.1261.

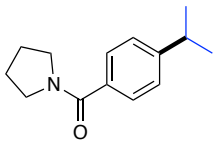

(4-Isopropylphenyl)(pyrrolidin-1-yl)methanone, **37** (98 mg, 90%) was prepared following *GP2*. The desired product was isolated as an oil (24 g column, 80:20→50:50 hexanes/EtOAc). **^{1}H NMR** ($CDCl_3$, 500 MHz) δ 7.46 (d, *J* = 7.7 Hz, 2H), 7.24 (d, *J* = 7.8 Hz, 2H), 3.65 (t, *J* = 6.8 Hz, 2H), 3.46 (t, *J* = 6.5 Hz, 2H), 2.93 (m, *J* = 7.0 Hz, 1H), 1.91 (m, 4H), 1.25 (d, *J* = 6.9 Hz, 6H). **^{13}C NMR** ($CDCl_3$, 125 MHz) δ 169.7, 150.6, 134.6, 127.2, 127.1, 126.1, 49.5, 46.0, 33.9, 30.8, 26.3, 24.4, 23.7. **FT-IR** (cm^{-1}, neat, ATR): 2959, 2872, 1621, 1417, 1403, 1260, 842, 765, 750. **HRMS** (EI) calcd for $C_{14}H_{19}NO$ $[M]^+$: 217.1467, found: 217.1484.

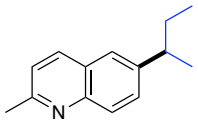

6-(*sec*-Butyl)-2-methylquinoline, **38** (78 mg, 78%) was prepared following *GP2*. The desired product was isolated as an oil (24 g column, 100:0→80:20 hexanes/EtOAc). **^{1}H NMR** ($CDCl_3$, 500 MHz) δ 7.95 (dd, *J* = 8.5, 3.2 Hz, 2H), 7.59 – 7.43 (m, 2H), 7.21 (d, *J* = 8.4 Hz, 1H), 2.80 – 2.66 (m, 4H), 1.72 – 1.60 (m, 2H), 1.30 (d, *J* = 6.9 Hz, 3H), 0.82 (t, *J* = 7.3 Hz, 3H). **^{13}C NMR** ($CDCl_3$, 125 MHz) δ 158.2, 147.0, 145.1, 136.0, 129.5, 128.6, 126.6, 124.8, 122.0, 41.7, 31.2, 25.4, 22.0, 12.4. **FT-IR** (cm^{-1}, neat, ATR): 2959, 2922, 2872, 1600, 1496, 1375, 885, 835. **HRMS** (EI) calcd for $C_{14}H_{17}N$ $[M]^+$: 199.1361, found: 199.1387.

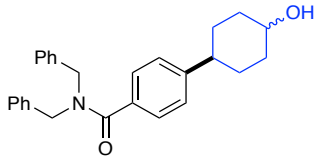

***N,N*-Dibenzyl-4-(4-hydroxycyclohexyl)benzamide**, **39** (115.4 mg, 48%, dr 1:1) was prepared following *GP2*. The desired product was isolated as a pale-yellow foam (24 g column, 70:30→20:80 hexanes/EtOAc). **^{1}H NMR** ($CDCl_3$, 500 MHz) δ 7.52 – 7.18 (m, 12H), 7.14 (s, 2H), 4.67 (s, 2H), 4.42 (s, 2H), 4.10 (d, *J* = 5.8 Hz, 1H), 2.63 – 2.38 (m, 1H), 2.11 – 1.78 (m, 4H), 1.64 (d, *J* = 15.5 Hz, 4H), 1.52 – 1.19 (m, 1H). **^{13}C NMR** ($CDCl_3$, 125 MHz) 172.6, 149.3, 133.8, 129.0, 128.8, 128.5, 128.2, 128.2, 128.1, 128.0, 127.8, 127.6, 127.2, 127.0, 65.6, 43.9, 33.1, 29.8. **FT-IR** (cm^{-1}, neat, ATR): 1449, 1364, 1287, 1125, 1012, 989, 842, 698. **HRMS** (ESI) calcd for $C_{27}H_{29}NO_2$ $[M+H]^+$: 400.2277, found: 400.2286.

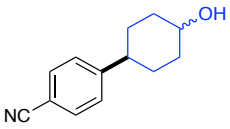

4-(4-Hydroxycyclohexyl)benzonitrile, **40** (94.7 mg, 94%, dr 1:1) was prepared following *GP2*. The desired product was isolated as a pale-yellow solid (24 g column, 70:30→40:60 hexanes/EtOAc). **mp** = 29-30 °C. **^{1}H NMR** ($CDCl_3$, 500 MHz) δ 7.57 (d, *J* = 8.0 Hz, 2H), 7.33 (d, *J* = 8.0 Hz, 2H), 4.15 (q, *J* = 3.1 Hz, 1H), 2.59 (tt, *J* = 11.4, 3.4 Hz, 1H), 1.91 – 1.86 (m, 4H), 1.73 – 1.61 (m, 4H), 1.49 (s, 1H). **^{13}C NMR** ($CDCl_3$, 125 MHz) δ 153.0, 132.3, 127.8, 119.2, 109.8, 65.2, 44.1, 32.9, 27.4. **FT-IR** (cm^{-1}, neat, ATR): 3400, 2928, 1606, 1503, 1415, 1255, 1119, 999. **HRMS** (EI) calcd for $C_{13}H_{15}NO$ $[M]^+$: 201.1154, found: 201.1167.

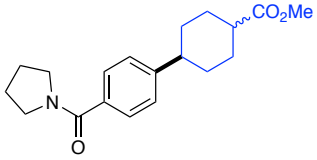

Methyl 4-(4-(Pyrrolidine-1-carbonyl)phenyl)cyclohexane-1-carboxylate, **41** (129.8 mg, 82%, dr 1:1) was prepared following *GP2*. The desired product was isolated as a colorless foam (24 g column, 80:20→50:50 hexanes/EtOAc). **^{1}H NMR** ($CDCl_3$, 500 MHz) δ 7.44 (dd, *J* = 8.1, 6.5 Hz, 2H), 7.20 (dd, *J* = 8.1, 6.5 Hz, 2H), 3.70 (s, 3H), 3.63 (t, *J* = 7.1 Hz, 2H), 3.43 (t, *J* = 6.7 Hz, 2H), 2.71 (t, *J* = 3.5 Hz, 0.5 H), 2.54 (ddd, *J* = 15.4, 9.6, 6.1 Hz, 1H), 2.35 (tt, *J* = 12.2, 3.5 Hz, 0.5 H), 2.24 (t, *J* = 6.4 Hz, 1 H), 2.15 – 2.07 (m, 1H), 1.95 (dt, *J* = 13.4, 5.4 Hz, 3H), 1.86 (q, *J* = 6.7 Hz, 2H), 1.75 (q, *J* = 4.2 Hz, 1H), 1.69 – 1.54 (m, 3H), 1.47 (qd, *J* = 12.9, 3.2 Hz, 1H). **^{13}C NMR** ($CDCl_3$, 125 MHz) δ 176.4, 175.6, 169.9, 169.8, 149.0, 148.8, 135.2, 135.0, 127.4, 127.4, 126.8, 126.7 51.7, 49.8, 46.3, 43.6, 43.5, 43.0, 38.9, 33.2, 30.4, 29.3, 27.6, 26.5, 24.6. **FT-IR** (cm^{-1}, neat, ATR): 2933, 1728, 1564, 1376, 1255, 1144, 1018, 836. **HRMS** (EI) calcd for $C_{19}H_{25}NO_3$ $[M]^+$: 315.1837, found: 315.1836.

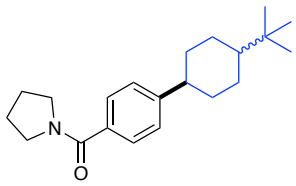

(4-(4-(*tert*-Butyl)Cyclohexyl)phenyl)(pyrrolidin-1-yl)methanone, **42** (82.6 mg, 88%, dr 1:1) was prepared following *GP2*. The desired product was isolated as a pale-yellow solid (24 g column, 80:20→50:50 hexanes/EtOAc). **mp** = 37-39 °C. **^{1}H NMR** ($CDCl_3$, 500 MHz, signals reported from the diastereomeric mixture) δ 7.47 – 7.41 (m, 4H), 7.36 (d, *J* = 8.0 Hz, 2H), 7.23 – 7.18 (m, 2H), 3.63 (td, *J* = 6.8, 4.5 Hz, 4H), 3.45 (q, *J* = 6.8 Hz, 4H), 3.02 (dd, *J* = 5.7, 3.0 Hz, 1H), 2.45 (tt, *J* = 12.2, 3.4 Hz, 1H), 2.31 – 2.18 (m, 2H), 1.94 – 1.84 (m, 13H), 1.76 (td, *J* = 12.2, 4.7 Hz, 2H), 1.61 – 1.50 (m, 2H), 1.42 (tt, *J* = 13.6, 6.9 Hz, 2H), 1.18 – 1.06 (m, 6H), 0.87 (s, 9H), 0.78 (s, 9H). **^{13}C NMR** ($CDCl_3$, 125 MHz, signals reported from the diastereomeric mixture) δ 170.0, 169.9, 149.8, 147.3, 134.8, 134.1, 127.6, 127.3, 127.1, 126.7, 49.7, 48.3, 47.8, 46.3, 46.2, 44.6, 36.4, 34.7, 32.7, 32.6, 30.7, 27.7, 27.7, 27.6, 26.5, 24.6, 22.8. **FT-IR** (cm^{-1}, neat, ATR): 2937, 2866, 1563, 1419, 1365, 1229, 1186, 1113. **HRMS** (EI) calcd for $C_{21}H_{31}NO$ $[M]^+$: 313.2406, found: 313.2411.

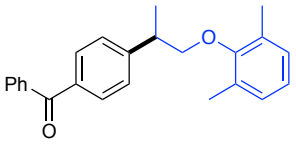

(4-(1-(2,6-Dimethylphenoxy)propan)-2-yl)phenyl)(phenyl)methanone, **43** (147.9 mg, 86%) was prepared following *GP2*. The desired product was isolated as a colorless oil (24 g column, 100:0→70:30 hexanes/EtOAc). **^{1}H NMR** ($CDCl_3$, 500 MHz) δ 7.89 – 7.78 (m, 4H), 7.66 – 7.55 (m, 1H), 7.54 – 7.42 (m, 4H), 6.98 (d, *J* = 7.4 Hz, 2H), 6.90 (dd, *J* = 8.2, 6.7 Hz, 1H), 3.93 – 3.84 (m, 2H), 3.36 (q, *J* = 6.8 Hz, 1H), 2.17 (s, 6H), 1.51 (d, *J* = 6.8 Hz, 3H). **^{13}C NMR** ($CDCl_3$, 125

MHz) 196.6, 155.7, 149.3, 138.0, 136.1, 132.4, 131.0, 130.5, 130.1, 129.0, 128.4, 127.7, 124.0, 41.0, 18.1, 16.3. **FT-IR** (cm^{-1}, neat, ATR): 2890, 1606, 1447, 1382, 1178, 1091, 1008, 938. **HRMS** (EI) calcd for $C_{24}H_{24}O_2$ $[M]^+$: 344.1776, found: 344.1786.

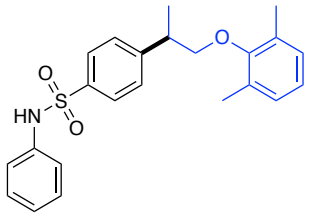

4-(1-(2,6-Dimethylphenoxy)propan)-2-yl)phenylbenzenesulfonamide, **44** (159.8 mg, 81%) was prepared following *GP2*. The desired product was isolated as a colorless foam (24 g column, 80:20→50:50 hexanes/EtOAc).**^{1}H NMR** ($CDCl_3$, 500 MHz) 7.75 (d, *J* = 8.1 Hz, 2H), 7.41 (d, *J* = 8.1 Hz, 2H), 7.24 (dd, *J* = 13.9, 6.3 Hz, 2H), 7.17 – 7.04 (m, 3H), 6.94 (d, *J* = 7.4 Hz, 2H), 6.88 (dd, *J* = 8.3, 6.4 Hz, 1H), 6.75 (s, 1H), 3.81 – 3.75 (m, 2H), 3.31 – 3.24 (m, 1H), 2.03 (s, 6H), 1.43 (d, *J* = 7.0 Hz, 3H). **^{13}C NMR** ($CDCl_3$, 125 MHz) δ 155.4, 150.1, 137.3, 136.6, 130.9, 129.5, 129.0, 128.5, 127.5, 125.5, 124.1, 121.7, 76.5, 40.8, 17.7, 16.2. **FT-IR** (cm^{-1}, neat, ATR): 3250, 1495, 1412, 1277, 1069, 1011, 822, 578. **HRMS** (ESI) calcd for $C_{23}H_{24}NO_3S$ $[M-H]^-$: 394.1477, found: 394.1483.

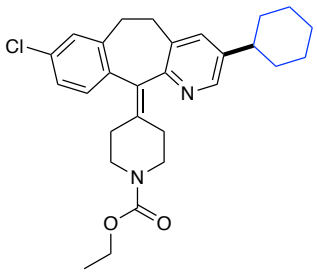

Ethyl 4-(2-Chloro-8-(tetrahydro-2*H*-pyran-4-yl)-10,11-dihydro-5*H*-dibenzo[*a*,*d*][7]annulen-5-ylidene)cyclohexane-1-carboxylate, **45** (120 mg, 81%) was prepared following *GP2*. The

desired product was isolated as a white foam (24 g column, 70:30→20:80 hexanes/EtOAc).**^{1}H NMR** ($CDCl_3$, 500 MHz) δ 8.24 (d, *J* = 2.1 Hz, 1H), 7.24 (d, *J* = 2.2 Hz, 1H), 7.20 – 7.05 (m, 3H), 4.13 (q, *J* = 7.1 Hz, 2H), 3.81 (s, 2H), 3.56 – 3.19 (m, 2H), 3.11 (tt, *J* = 13.1, 3.5 Hz, 2H), 2.92 – 2.69 (m, 2H), 2.48 (ddt, *J* = 18.5, 13.3, 6.5 Hz, 2H), 2.34 (dq, *J* = 14.4, 4.8 Hz, 3H), 1.82 (d, *J* = 7.5 Hz, 4H), 1.74 (d, *J* = 13.0 Hz, 1H), 1.38 (ddq, *J* = 11.6, 8.9, 4.4, 3.7 Hz, 4H), 1.24 (t, *J* = 7.0 Hz, 4H). **^{13}C NMR** ($CDCl_3$, 125 MHz) δ 155.6, 154.4, 145.8, 141.7, 139.9, 138.3, 137.4, 136.0, 134.3, 133.0, 132.8, 130.5, 129.0, 126.3, 61.4, 44.97, 44.95, 41.7, 34.3, 34.2, 31.9, 31.8, 30.9, 30.7, 26.8, 26.1, 14.8. **FT-IR** (cm^{-1}, neat, ATR): 3250, 1495, 1412, 1277, 1069, 1011, 822, 578. **HRMS** (ESI) calcd for $C_{28}H_{34}ClN_2O_2$ $[M+H]^+$: 465.2309, found: 465.2329.

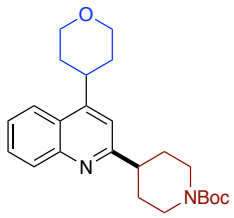

***tert*-Butyl 4-(4-Tetrahydro-2*H*-pyran-4-yl)quinolin-2-yl)piperidine-1-carboxylate**, **46** (141.2 mg, 71%) was prepared according to a modified procedure of Glorius et al.[3c] The desired product was isolated as a yellow oil (24 g column, 80:20→50:50 hexanes/EtOAc).**^{1}H NMR** ($CDCl_3$, 500 MHz) δ 8.09 – 8.00 (m, 2H), 7.67 (ddd, *J* = 8.2, 6.8, 1.3 Hz, 1H), 7.51 (ddd, *J* = 8.2, 6.8, 1.3 Hz, 1H), 7.18 (s, 1H), 4.29 (s, 2H), 4.15 (ddd, *J* = 11.5, 4.2, 1.8 Hz, 2H), 3.68 (td, *J* = 11.5, 2.7 Hz, 2H), 3.57 (tt, *J* = 11.2, 4.2 Hz, 1H), 3.03 (ddt, *J* = 12.0, 7.4, 3.7 Hz, 1H), 2.89 (s, 2H), 2.01 – 1.73 (m, 8H), 1.49 (s, 9H). **^{13}C NMR** ($CDCl_3$, 125 MHz) δ 164.6, 154.9, 151.6, 148.3, 130.3, 129.1, 125.9, 125.5, 122.5, 115.9, 79.5, 68.4, 45.8, 36.5, 33.3, 31.7, 28.6. **FT-IR** (cm^{-1}, neat, ATR): 2891, 1599, 1465, 1446, 1389, 1275, 1013, 961. **HRMS** (ESI) calcd for $C_{24}H_{33}N_2O_3$ $[M+H]^+$: 397.2497, found: 397.2498.

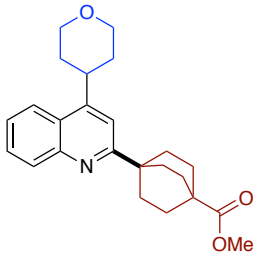

Methyl 4-(4-(Tetrahydro-2*H*-pyran-4-yl)quinolin-2-yl)bicyclo[2.2.2.]octane-1-carboxylate, **47** (138.4 mg, 73%) was prepared according to a modified procedure of Dhar et al.[18c] The desired product was isolated as a pale-yellow foam (24 g column, 80:20→50:50 hexanes/EtOAc).**^{1}H NMR** ($CDCl_3$, 500 MHz) δ 8.04 (dd, *J* = 9.8, 8.4 Hz, 2H), 7.72 – 7.62 (m, 1H), 7.49 (t, *J* = 7.8 Hz, 1H), 7.30 (s, 1H), 4.16 (dd, *J* = 11.5, 4.6 Hz, 1H), 3.74 – 3.67 (m, 5H), 3.58 – 3.54 (m, 1H), 2.37 (dd, *J* = 10.1, 5.7 Hz, 1H), 2.14 – 1.83 (m, 16H). **^{13}C NMR** ($CDCl_3$, 125 MHz) δ 178.6, 171.2, 167.5, 150.8, 148.0, 130.6, 128.8, 125.7, 125.1, 122.4, 114.6, 68.5, 60.5, 51.8, 39.5, 38.5, 36.5, 33.3, 30.7, 28.8. **FT-IR** (cm^{-1}, neat, ATR): 2947, 2866, 1598, 1455, 1434, 1239, 1113, 1004. **HRMS** (EI) calcd for $C_{24}H_{29}NO_3$ $[M]^+$: 379.2147, found: 379.2166.

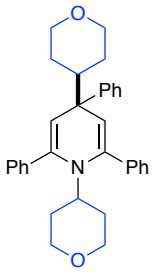

Methyl 4-(4-(Tetrahydro-2*H*-pyran-4-yl)quinolin-2-yl)bicyclo[2.2.2.]octane-1-carboxylate, **48** was isolated following *GP2*. The byproduct was isolated as a white foam (24 g column, 100:0→80:20 hexanes/EtOAc).**^{1}H NMR** ($CDCl_3$, 500 MHz) δ 7.63 (d, *J* = 7.2 Hz, 4H), 7.53 – 7.30 (m, 10H), 7.18 (t, *J* = 7.3 Hz, 1H), 5.41 (s, 2H), 3.90 (dd, *J* = 11.5, 4.2 Hz, 2H), 3.50 (dd, *J* = 11.4, 3.2 Hz, 2H), 3.24 (t, *J* = 11.7 Hz, 2H), 3.12 – 2.97 (m, 1H), 2.79 (td, *J* = 11.1, 5.4 Hz, 2H),

1.81 (td, *J* = 12.1, 6.0 Hz, 1H), 1.40 (qd, *J* = 12.5, 4.4 Hz, 2H), 1.42 – 1.14 (m, 2H), 1.12 (dd, *J* = 8.1, 3.4 Hz, 4H).**^{13}C NMR** ($CDCl_3$, 125 MHz) δ 149.9, 145.4, 140.0, 128.1, 127.9, 127.95, 127.7, 126.7, 125.4, 115.9, 68.3, 67.9, 59.6, 47.3, 46.2, 33.2, 28.5. **HRMS** (EI) calcd for $C_{33}H_{135}NO_2$ $[M]^+$: 477.2668, found: 477.2672.

3.5 References

(1) (a) N. A. McGrath, M. Brichacek, J. T. Njardarson, *J. Chem. Educ.* **2010**, *87*, 1348-1349; (b) P. Ruiz-Castillo, S. L. Buchwald, *Chem. Rev.* **2016**, *116*, 12564-12649; (c) Y. Liu, H. Ge, *Nat. Chem.* **2017**, *9*, 26-32.

(2) C. H. Basch, J. Liao, J. Xu, J. J. Piane, M. P. Watson, *J. Am. Chem. Soc.* **2017**, *139*, 5313-5316.

(3) D. Moser, Y. Duan, F. Wang, Y. Ma, M. J. O'Neill, J. Cornella, *Angew. Chem. Int. Ed.* **2018**, *57*, 11035-11039.

(4) F. J. R. Klauck, M. J. James, F. Glorius, *Angew. Chem. Int. Ed.* **2017**, *56*, 12336-12339.

(5) (a) J. Wu, L. He, A. Noble, V. K. Aggarwal, *J. Am. Chem. Soc.* **2018**, *140*, 10700-10704; (b) F. Sandfort, F. Strieth-Kalthoff, F. J. R. Klauck, M. J. James, F. Glorius, *Chem. Eur. J.* **2018**, *24*, 17210-17214; (c) J. Hu, G. Wang, S. Li, Z. Shi, *Angew. Chem. Int. Ed.* **2018**, *57*, 15227-15231.

(6) M. Ociepa, J. Turkowska, D. Gryko, *ACS Catal.* **2018**, *8*, 11362-11367.

(7) M.-M. Zhang, F. Liu, *Org. Chem. Front.* **2018**, *5*, 3443-3446.

(8) (a) F. J. R. Klauck, H. Yoon, M. J. James, M. Lautens, F. Glorius, *ACS Catal.* **2019**, *9*, 236-241; (b) X. Jiang, M. M. Zhang, W. Xiong, L. Q.; Lu, W. J. Xiao, *Angew. Chem. Int. Ed.* **2019**, *58*, 2402-2406; (c) J. Wu, P. S. Grant, X. Li, A. Noble, V. K. Aggarwal, *Angew. Chem. Int. Ed.* **2019***, 58,* 5697-5701.

(9) S. Plunkett, C. H. Bash, S. O. Santana, M. P. Watson, *J. Am. Chem. Soc.* **2019**, *141*, 2257-2262.

(10) For reviews on Ni/photoredox dual catalysis: (a) J. C. Tellis, C. B. Kelly, D. N. Primer, M. Jouffroy, N. R. Patel, G. A. Molander, *Acc. Chem. Res.* **2016**, *49*, 1429-1439; (b) C. K. Prier, D. A. Rankic, D. W. C. MacMillan, *Chem. Rev.* **2013**, *113*, 5322-5363; (c) J. K. Matsui, S. B. Lang, D. R. Heitz, G. A. Molander, *ACS Catal.* **2017**, *7*, 2563-2575.

(11) (a) J. C. Tellis, D. N. Primer, G. A. Molander, *Science* **2014**, *345*, 433-436; (b) I. B. Perry, T. F. Brewer, P. J. Sarver, D. M. Schultz, D. A. DiRocco, D. W. C. MacMillan, *Nature* **2018**, *560*, 70-75; (c) C. Le, Y. Liang, R. W. Evans, X. Li, D. W. C. MacMillan, *Nature* **2017**, *547*, 79-83; (d) C. P. Johnston, R. T. Smith, S. Allmendinger, D. W. C. MacMillan, *Nature* **2016**, *536*, 322-325; (e) M. H. Shaw, V. W. Shurtleff, J. A. Terrett, J. D. Cuthbertson, D. W. C. MacMillan, *Science* **2016**, *352*, 1304-1308; (f) Z. Zuo, D. T. Ahneman, L. Chu, J. A. Terrett, A. G. Doyle, D. W. C. MacMillan, *Science* **2014**, *345*, 437-440.

(12) (a) G. A. Molander, K. M. Traister, B. T. O'Neill, *J. Org. Chem.* **2015**, *80*, 2907–2911; (b) G. A. Molander, K. M. Traister, B. T. O'Neill, *J. Org. Chem.* **2014**, *79*, 5771–5780; (c) G. A. Molander, S. R. Wisniewski, K. M. Traister, *Org. Lett.* **2014**, *16*, 3692–3695; (d) K. J. Garcia, M. M. Gilbert, D. J. Weix, *J. Am. Chem. Soc.* **2019,** *141*, 1823-1827; (e) A. M. Olivares, D. J. Weix, *J. Am. Chem. Soc.* **2018,** *140*, 2446-2449; (f) L. Huang, A. M. Olivares, D. J. Weix, *Angew. Chem. Int. Ed.* **2017**, *56*, 11901-11905; (g) L. K. G. Ackerman, M. M. Lovell, D. J. Weix, *Nature* **2015,** *524*, 454-457; (h) C. Heinz, J. P. Lutz, E. M. Simmons, M. M. Miller, W. R. Ewing, A. G. Doyle, *J. Am. Chem. Soc.* **2018**, *140*, 2292-2300; (i) J. L. Hofstra, A. H. Cherney, C. M. Ordner, S. E. Reisman, *J. Am. Chem. Soc.* **2018***, 140*, 139-142; (j) K. E. Poremba, N. T. Kadunce, N. Suzuki, A. H. Cherney, S. E. Reisman, *J. Am. Chem. Soc*. **2017**, *139*, 5684-5687; (k) Y. Ye, H. Chen, J. L. Sessler, H. Gong, *J. Am. Chem. Soc.* **2019**, *141*, 820–824; (l) X. Wang, S. Wang,

W. Xue, H. Gong, *J. Am. Chem. Soc.* **2015**, *137*, 11562-11565; (m) C. Zhao, X. Jia, X. Wang, H. Gong, *J. Am. Chem. Soc.* **2014**, *136*, 17645-17651; (n) A. García-Domínguez, Z. Li, C. Nevado, *J. Am. Chem. Soc.* **2017**, *139*, 6835-6838.

(13) O. Gutierrez, J. C. Tellis, D. N. Primer, G. A. Molander, *J. Am. Chem. Soc.* **2015**, *137*, 4896-4899.

(14) (a) Z. Duan, W. Li, A. Lei, *Org. Lett.* **2016**, *18*, 4012-4015; (b) L. Peng, Z. Li, G. Yin, *Org. Lett.* **2018**, *20*, 1880–1883; (c) A. Paul, M. D. Smith, A. K. Vannucci, *J. Org. Chem.* **2017**, *82*,1996-2003.

(15) J. Luo, J. Zhang, *ACS Catal.* **2016**, *6*, 873-877.

(16) L. Chen, D. R. Sanchez, B. Zhang, B. P. Carrow, *J. Am. Chem. Soc.* **2017**, *139*, 12418-12421.

(17) M. E. Welsch, S. A. Snyder, B. R. Stockwell, *Curr. Opin. Chem. Biol.* **2010**, *14*, 347-361.

(18) For selected examples, see: (a) L. M. Kammer, A. Rahman, T. Opatz, *Molecules* **2018**, *23*, 764; (b) J. K. Matsui, D. N. Primer, G. A. Molander, *Chem. Sci.* **2017**, *8*, 3512-3522; (c) T. C. Sherwoord, N. Li, A. N. Yazdani, T. G. Murali Dhar, *J. Org. Chem.* **2018**, *83*, 3000-3012; (d) W.-M. Cheng, R. Shang, Y. Fu, *ACS Catal.* **2017**, *7*, 907-911.

(19) J. A. Terrett, J. D. Cuthbertson, V. W. Shurleff, D. W. C. MacMillan, *Nature* **2015**, *524*, 330-334.

(20) D. Koszelewski, D. Pressnitz, D. Clay, W. Kroutil, *Org. Lett.* **2009**, *11*, 4810-4812.

(21) R. S. Geha, E. O. Meltzer, *J. Allergy Clin. Immunol.* **2001**, *107*, 751-762.

(22) (a) M. Jouffroy, D. N. Primer, G. A. Molander, *J. Am. Chem. Soc.* **2016**, *138*, 475-478; (b) R. Jana, T. P. Pathak, M. S. Sigman, *Chem. Rev.* **2011**, *111*, 1417-1492.

(23) S. Ni, C. X. Li, Y. Mao, J. Han, Y. Wang, H. Yan, Y. Pan, *Sci. Adv.* **2019**, *5*, 9516-9544.

(24) For information on the construction of LED reactors, see the Supporting Information of: (a) N. R. Patel, C. B. Kelly, M. Jouffroy, G. A. Molander, *Org. Lett.* **2016**, *18*, 764-767; (b) M. Jouffroy, C. B. Kelly, G. A. Molander, *Org. Lett.* **2016**, *18*, 876-879.

(25) N. R. Patel, C. B. Kelly, A. P. Siegenfeld, G. A. Molander, *ACS Catal.* **2017**, *7*, 1766-1770.

(26) X. Jiang, M.-M. Zhang, W. Xiong, L.-Q. Lu, W.-J. Xiao, *Angew. Chem. Int. Ed.* **2019**, *58*, 2402-2406.

Author Contributions: Shorouk O. Badir and Jun Yi contributed to the design of the project, performed the reaction optimization, and prepared some of the compounds used in this study. All authors contributed to the experimental work and discussion of results. Shorouk O. Badir wrote the original draft of the manuscript with input from Gary A. Molander.

Chapter 4. Decarboxylative Reductive Arylation Enabled by Electron Donor-Acceptor Complex Photoactivation**

4.1 Introduction

The disclosure of Ni/photoredox dual catalysis using triethylamine as a terminal reductant enabled a cross-electrophilic strategy to forge C(sp^3)-hybridized centers from aliphatic amines. Moving forward, we sought to develop a general net-reductive arylation platform using carboxylic acids as abundant and commercially available feedstocks. In the last decades, transition-metal-catalyzed cross-couplings have become indispensable tools for the rapid assembly of C(sp^3)-C(sp^2) linkages in medicinal settings.[1] Among these platforms, net-reductive cross-electrophile couplings are particularly advantageous because they facilitate the direct integration of alkyl electrophiles,[1f,1j,2] bypassing the necessity for preformed, reactive carbon nucleophiles.[3]

However, the vast majority of reductive cross-coupling reactions require (super)stoichiometric loadings of metal powders, including manganese and zinc as chemical reductants, to restore the active metal catalyst.[1f,1j,2] In addition to safety concerns with respect to metal waste disposal, the industry's dependence on these reaction paradigms highlights the necessity for inexpensive and scalable strategies for the incorporation of abundant feedstocks in cross-coupling manifolds.[1d,4] Recently, several seminal studies have demonstrated the use of organic reducing agents in cross-electrophile processes. Pioneering work from Tanaka and colleagues showcased the use of tetrakis(dimethylamino)ethylene (TDAE) as a homogeneous

---

** Reproduced in part with permission from L. M. Kammer, S. O. Badir, R.-M. Hu, G. A. Molander, *Chem. Sci.* **2021**, *12*, 5450–5457. This article is licensed under a Creative Commons Attribution NonCommercial 3.0 Unported License.

organic reductant to achieve the homo-coupling of aryl halides.[5] Subsequently, the Weix group utilized this reductant to activate C(sp^3)-hybridized electrophiles.[2a,6] In 2017, Reisman demonstrated that TDAE, in place of manganese or zinc, functions as a terminal organic reductant in the enantioselective cross-coupling of alkyl-*N*-hydroxyphthalimide esters (redox-active esters, RAEs) with alkenyl bromides (Figure 4.1).[7] These protocols, however, are complicated by the air-sensitive nature of the organic super-electron-donor.[8] Strategies utilizing amines and tris(trimethylsilyl)silane as non-metallic reducing agents have also been disclosed.[9]

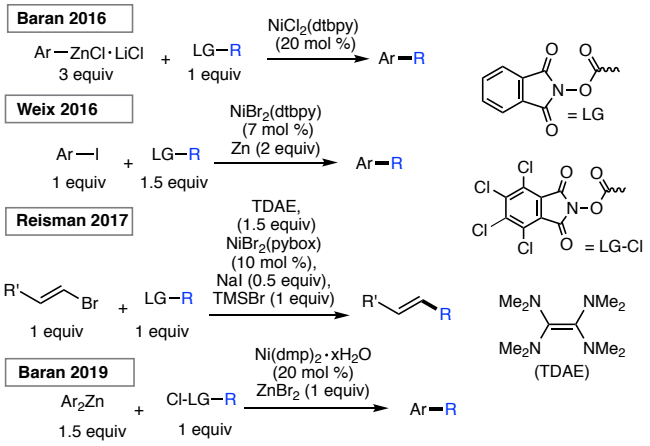

Figure 4.1. Exemplary decarboxylative net-reductive cross-couplings.

In recent years, photochemical methods have been enlisted to assemble challenging structural motifs using excitable catalysts under visible-light conditions. Such systems are inherently mild, efficient at room temperature, and evade the need for reactive additives (pyrophoric reagents, strong bases, harsh oxidants and reductants).[10] In these dual manifolds, the reduced state of the photocatalyst has been proposed to restore the catalytically active Ni^0 species through single-electron transfer (SET) events.[11] However, the majority of these redox-active auxiliaries are based on precious metals including ruthenium and iridium, presenting limitations with respect to scalability and sustainability.[12] These processes are further complicated by the

oxidation/reduction steps of the photocatalyst. To establish a complementary reactivity mode, the Melchiorre group elegantly reported the direct photoexcitation of 4-alkyl-1,4-dihydropyridines (DHPs) to trigger the generation of C(sp^3)-centered radicals in the absence of external catalysts.[13,14] Although this advancement presented a milestone in its own right, the scope of the radical precursor in the reported Ni-catalyzed C(sp^3)-C(sp^2) cross-coupling was limited to secondary and stabilized primary systems[13a] owing to competitive C-H bond scission inherent to DHP feedstocks.[15] In this context, the generation of heteroatom- and unactivated carbon-based radicals through direct visible-light excitation in Ni-catalyzed cross-couplings remains underdeveloped.

Recently, synthetic methods driven by the photoactivity of electron donor–acceptor (EDA) complexes (Figure 4.2) have gained considerable momentum, including borylation, thioetherification, and sulfonylation.[16] Inspired by this advance, the feasibility of EDA complex photoactivation was examined as an enabling technology in Ni-mediated C(sp^3)–C(sp^2) cross-couplings (Figure 4.2). Under light irradiation at 390 nm, a commercially available and inexpensive electron donor, Hantzsch ester (HE, diethyl 1,4-dihydro-2,6-dimethyl-3,5-pyridinedicarboxylate), serves as a potent organic photoreductant to deliver diverse radical architectures from carboxylic acid feedstocks[17] for further functionalization in Ni-catalyzed cross-couplings. As part of its dual role, the photoexcited HE modulates the oxidation state of the metal, delivering catalytically active Ni(0) species, thus bypassing the need for exogenous, expensive photocatalysts.

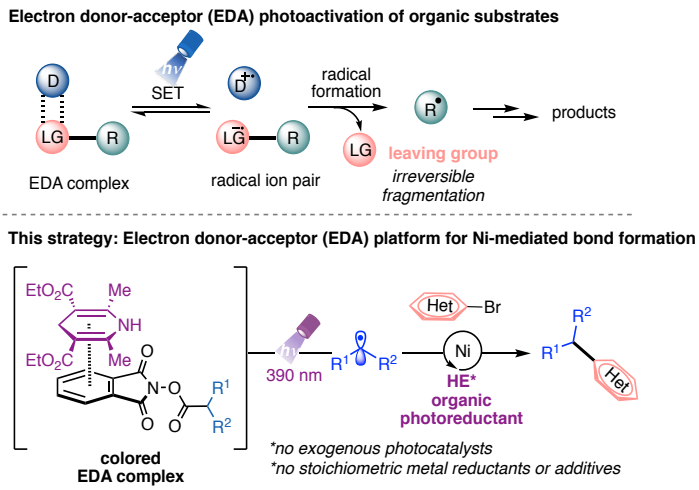

Figure 4.2. Envisioned transformation using EDA photoactivation.

4.2 Results and Discussion

Encouraged by the potential synthetic applications of harnessing photoactive EDA complexes toward Ni-mediated bond formation, the feasibility of the proposed net-reductive cross-electrophile coupling was investigated using 5-bromo-2-cyanopyridine **1** and cyclohexyl-*N*-hydroxyphthalimide-ester **2** as model substrates (Figure 4.3). From the outset of our investigation, it was evident that the solvent plays a key role in this process (entries 1-4), as it heavily affects the molecular assembly and formation of EDA complexes. Once exciplex-based charge transfer occurs, the resulting radical ion pair is stabilized by interaction with solvent dipoles.[18] In this vein, dimethylacetamide (DMA) proved crucial to the success of this photochemical method.

We then studied the influence of the dihydropyridine (DHP) backbone on the efficacy of the cross-coupling (Figure 4.3, entries 5-7). To this end, we subjected four different DHP derivatives to the reaction conditions to gain a deeper understanding of their dual role in EDA complex photoactivation as well as the reduction of Ni species through SET paradigms. It was demonstrated that HE and cyano substitution at C3 and C5 of the DHP (HE **A**, entry 5) promoted

the reaction most efficiently. For experimental simplicity, commercially available and inexpensive HE was adopted as the standard photoreductant.

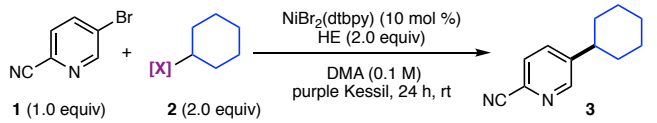

Entry	Deviation from std. conditions	3/IS ratio[a]	Entry	Deviation from std. conditions	3/IS ratio[a]
1	None	1.42 (79%)[b]	9	under air	0.93
2	DMSO	traces	10	$NiBr_2$(dMe-phen)	traces
3	THF	traces	11	$NiBr_2$(bpy)	1.32
4	ACN	0.32	12	$NiBr_2$(dMeObpy)	1.37
5	HE **A**	1.40	13	$NiBr_2 \cdot 3H_2O$	0.92
6	HE **B**	0.36	14	no light	0
7	HE **C**	0	15	no Ni	0
8	blue Kessil	1.34	16	no HE	traces

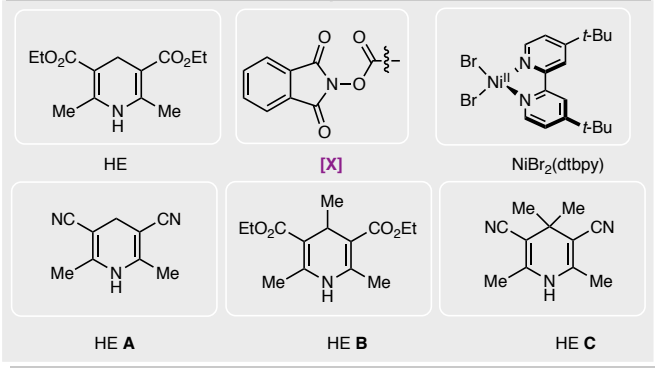

Figure 4.3. Optimization studies. Reactions were performed using **1** (0.1 mmol), **2** (0.2 mmol), HE (0.2 mmol), and $NiBr_2$(dtbpy) (10 mol %) in dry, degassed solvent (1.0 mL, 0.1 M) under purple Kessil irradiation for 24 h at rt. [a]Product to internal standard ratio (P/IS) was calculated using 1,3,5-trimethoxybenzene as internal standard using LC-MS analysis of the crude reaction mixture. [b]Isolated yield of **3** on 0.5 mmol scale.

The C-4-substituted DHP (HE **B**, entry 6) resulted in diminished reactivity. Not surprisingly, 4,4'-dimethyl HE **C** (entry 7) led to no product formation. This result can be rationalized by the lack of photooxidative aromatization as an intrinsic driving force to suppress a

competitive back electron transfer (BET) event from the radical ion pair, restoring the ground-state EDA complex.[16a,19] Finally, a ligand screen was performed (Figure 4.3, entries 10-12), demonstrating that 4,4'-di-*tert*-butyl-2,2'-bipyridine (dtbpy), 2,2'-bipyridine (bpy), and electron-rich 4,4'-dimethoxy-2,2'-bipyridine (dMeObpy) function as viable ligand frameworks. Of note, modest conversion to **3** was observed using ligand-free nickel(II) bromide trihydrate.

Notably, the developed net-reductive photochemical conditions are user-friendly, employing an air-stable nickel precatalyst and a mild, homogeneous reductant (HE). Deviations from the standard reaction setup are tolerated. For example, modest product formation was observed when the reaction was carried out under air (Figure 4.3, entry 9). Similarly, although superior reactivity was accomplished using purple Kessil irradiation (λ_{max} = 390 nm), affording a potent photoreductant [E_{red} (HE*/HE^{-+}) = –2.28 V vs SCE],[20] comparable results were achieved under blue light (entry 8, λ_{max} = 456 nm). Control experiments demonstrated that all reaction parameters are key to the formation of C(sp^3)-C(sp^2) linkages (Figure 4.3, entries 14-16).

With suitable conditions established, we examined the scope of the decarboxylative arylation employing a broad palette of (hetero)aryl bromides (Figure 4.4). In general, organic halides substituted with electron-withdrawing groups exhibited excellent reactivity, although electron-neutral and electron-donating groups also afforded the desired products in modest yields. More sterically-encumbered *ortho*-substituted aryl bromides (**5**, **9**) did not hinder the cross-coupling efficacy. Furthermore, substitution at the meta position (**4**, **6**) is tolerated. Several sensitive functional groups, including secondary sulfonamides (**8**, **19**, **20**, **31**), ketones (**4**, **11**, **18**), trimethylsilylalkyne (**9**), and terminal alkene (**22**) remained intact under the developed photoredox conditions. To this end, substrates **6**, **9** and **22** can be further diversified via Kumada-, sila-Sonogashira-couplings, as well as Giese-type additions, respectively.[21]

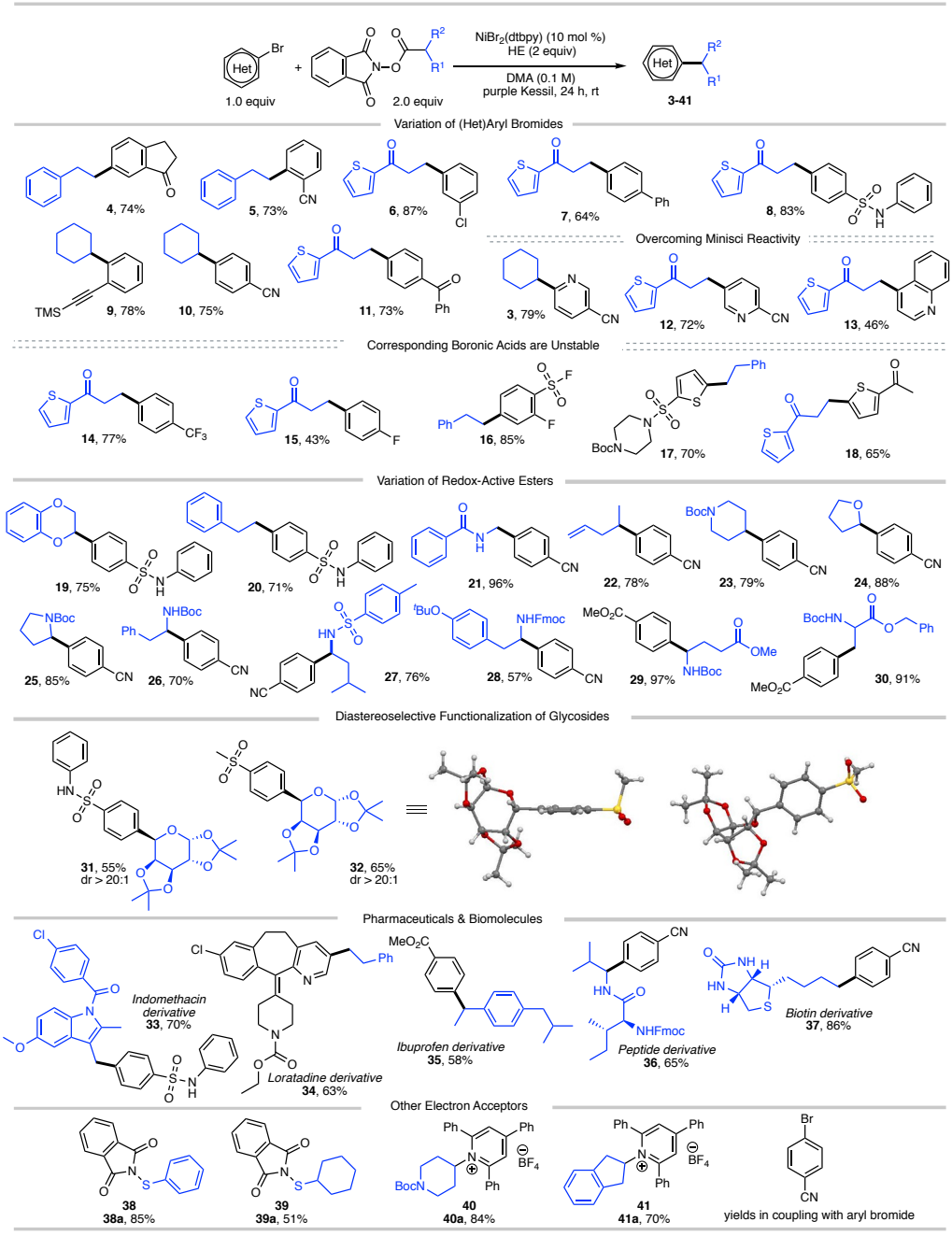

Figure 4.4. Scope of the developed C(sp^3)-C(sp^2) cross-coupling. All values correspond to isolated yields after purification. Reaction conditions as depicted in Figure 4.3, entry 1 (0.5 mmol scale).

Notably, several heteroarenes (electron-deficient: **3**, **12**, **13**, **34** and electron-rich: **17**, **18**) were compatible structural motifs. In particular, nitrogen-containing heteroaryl bromides, including quinoline (**13**) and pyridine (**3**, **12**, **34**) scaffolds, reacted in a chemoselective fashion to yield $C(sp^3)$-$C(sp^2)$ linkages, despite their propensity to undergo visible light-mediated Minisci C-H alkylation with alkyl-*N*-hydroxyphthalimide-esters.[22] This demonstrates a complementary reactivity mode to existing Minisci protocols, delivering linchpins that drive molecular complexity.[23]

Next, the aliphatic photocoupling was evaluated with respect to redox-active carboxylate derivatives (Figure 4.4). The reaction proceeded smoothly using a diverse array of proteinogenic and non-proteinogenic amino acids (**21**, **23**, **25**-**30**). Bifunctional reagents, including Boc- (**17**, **23**, **25**-**26**, **29**-**30**) and Fmoc-protected (**28**) amines, afforded the arylated products without compromising yields.

The scope was further extended to secondary, benzylic (**35**), and stabilized α-oxy (**19**, **24**, **31**, **32**) radical architectures. Remarkably, primary alkyl systems that lack any radical stabilizing groups displayed exceptional reactivity (**4**-**8**, **11**-**18**), providing a clear advantage in terms of scope over previously reported protocols.[13a] Of note, medicinally relevant structures including thiophene (**6**-**8**), piperidine (**23**), and pyrrolidine (**25**) motifs were efficiently incorporated.

To demonstrate the amenability of this cross-coupling for late-stage functionalization, including glycodiversification of drug scaffolds, photoredox-generated glycosyl radicals were successfully harnessed in this dual-catalytic manifold (Figure 4.4). The desired *C*-aryl carbohydrates (**31** and **32**) were obtained in good yields and excellent diastereoselectivity (dr > 20:1). The relative configuration of the major diastereomer **32** was elucidated based on X-ray crystallography with the aryl group *cis* with respect to the dimethyl acetal protecting group

(Figure 4.4). Efficient decarboxylative arylation was observed with pharmaceutically relevant cores, displaying a high density of pendant functional groups, including Indomethacin[24] and Loratadine[25] precursors (**33**, **34**). To evaluate the amenability toward bioactive molecules further, carboxylic acid derivatives stemming from dipeptide (**36**) and *D*-biotin (**37**) were subjected to the reaction conditions. The corresponding cross-coupled products were obtained in moderate to high yields (65–86%). Finally, to demonstrate the versatility of EDA paradigms toward Ni-catalyzed bond-forming processes, the cross-coupling was further extended to other electron acceptors including redox-active thiols (**38a**-**39a**)[16c,26] and pyridinium-activated amines (**40a**-**41a**)[9b,16d,27] in the absence of external catalysts.

To gain insight into the mechanism of this photochemical net-reductive cross-coupling, we analyzed the reaction components by UV/vis absorption spectroscopy (Figure 4.5). In line with seminal reports,[16] although cyclohexyl-*N*-hydroxyphthalimide-ester shows absorption in the visible light region, mixtures of the RAE and HE in DMA at 0.2 M display a significant bathochromic shift (Figure 4.5 B, brick red and blue lines). The absorption band (brick red line) stems from the formation of a new molecular aggregation, a colored EDA complex (Figure 4.5 B), exhibiting a wavelength band tailing to 500 nm. Preliminary studies revealed an association constant of 2.04 M^{-1} of HE with **2**, indicating a plausible EDA complex association event prior to homolytic fragmentation (Figure 4.5 C). Analysis of this complex using Job's method[29] revealed a 1:1 stoichiometry of the most absorbing species (Figure 4.5 D). Notably, concentration is a crucial parameter for effective cross-coupling. A dilute reaction mixture (10^{-4} M) exhibits a blue-shifted absorption band, indicating the inhibition of EDA complex formation (see the Experimental Section). Furthermore, a DMA soln of HE was found to absorb visible light (λ >400 nm), indicating selective photoexcitation of this species at 390 nm to generate a potent reducing agent (Figure 4.5 B, purple line).

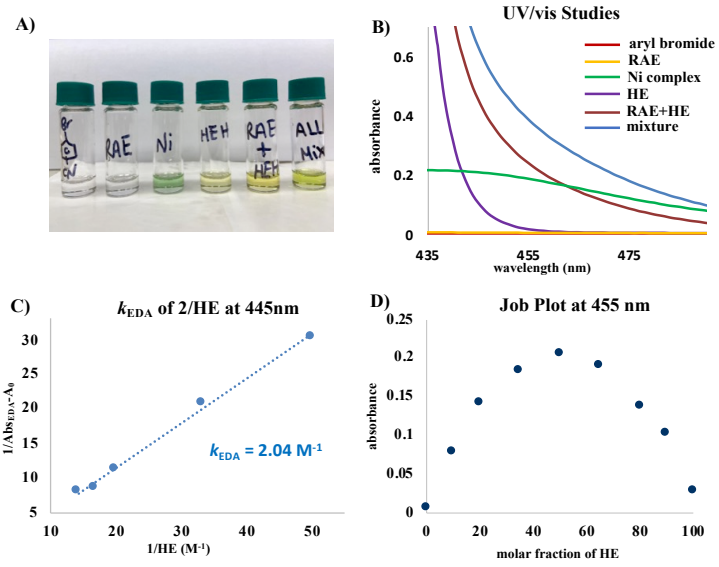

Figure 4.5. (A) Visual appearance of reaction components and mixtures thereof. (B) UV/vis absorption spectra measured in DMA (0.1 M) unless otherwise noted. Ni complex = $NiBr_2$(dtbpy), aryl bromide = 4-bromobenzonitrile, and RAE = cyclohexyl-*N*-hydroxyphthalimide ester. Mixture refers to a DMA soln of all reaction components. (C) Benesi–Hildebrand plot.[28] (D) Job plot[29] for a mixture of *N*-(cyclohexyl)-hydroxyphthalimide ester (**2**) and **HE** in DMA (0. 2 M).

Under the optimized reaction conditions, near full recovery of pyridine was observed (relative to 2.0 equiv of HE), demonstrating the role of excited HE as an organic single-electron donor in this system (Figure 4.6 A). To probe the formation of alkyl radical intermediates, TEMPO trapping experiments were performed. The corresponding TEMPO-adduct was isolated in 63% yield and confirmed via HRMS analysis (Figure 4.6 B, bottom right). Stoichiometric experiments with Ni complex **46**, synthesized through oxidative addition of 4-bromobenzotrifluoride to $Ni(cod)_2$/dtbpy, revealed that C(sp^3) alkyl transfer does not occur in the

absence of HE, thus highlighting the likelihood of EDA complex activation for effective cross-coupling (Figure 4.6 B, bottom left).

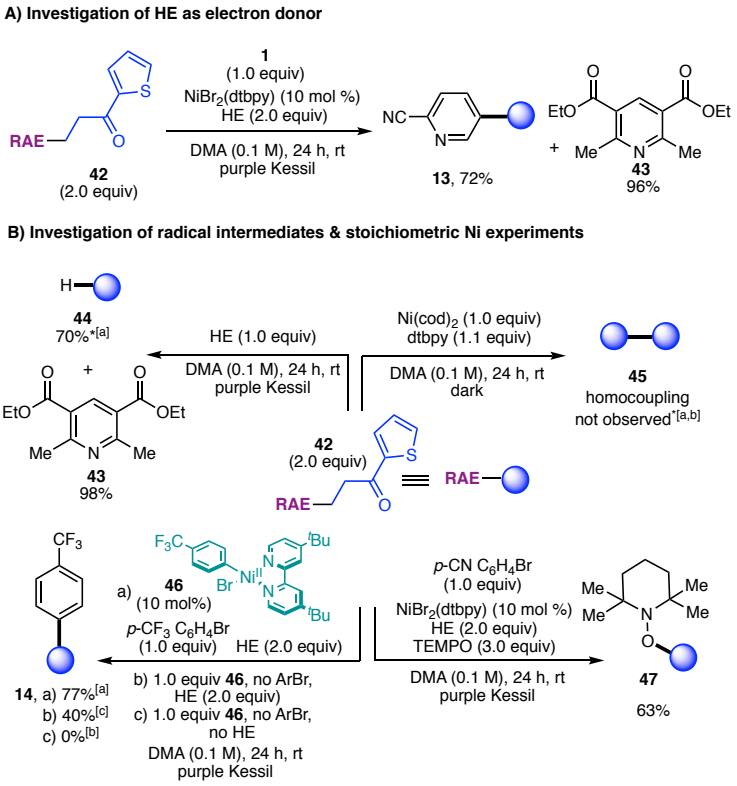

Figure 4.6. Mechanistic studies. (A) Investigation of HE as electron donor. (B) Mechanistic experiments. [a]Isolated yield on 0.3 mmol scale, [b]analyzed via GC/MS analysis, [c]NMR yield, *1.0 equiv of 42.

As anticipated, Ni complex **46** is catalytically active in the reaction, delivering the desired arylated product in 77% yield (Figure 4.6 B, bottom left). Furthermore, negligible conversion of **42** was observed in the presence of stoichiometric amounts of $Ni(COD)_2$/dtbpy; traces of homocoupling or alkene-side products, if any, were detected in the crude mixture, ruling out the role of Ni as a catalytic reductant toward RAEs (Figure 4.6 B, top right). Finally, it is worth noting that reduction of RAEs with photoredox catalysts is reported in the presence of HE

as a hydrogen atom transfer (HAT) donor.[30] A model reaction in the absence of Ni/dtbpy and aryl halide afforded the hydroalkylated product in 70% yield with full recovery of pyridine (Figure 4.6 B, top left). These findings demonstrate that the rate of alkyl radical addition to aryl-Ni(II) species **VII** must be faster than hydrogen atom abstraction from HE.

Based on these experiments, we propose a mechanistic scenario involving the intermediacy of an EDA complex between the electron-deficient, aliphatic RAEs and the electron-rich HE (Figure 4.7). Photoirradiation at 390 nm triggers an intra-complex SET event, generating a dihydropyridine radical cation and a phthalimide radical anion. The latter species undergoes decarboxylative fragmentation to yield an alkyl radical $\mathbf{I}^{\cdot}$. Although the absorptivity of the EDA complex is significantly greater than that of the HE itself, and although the entropic advantage inherent in intra-complex charge transfer provides an enormous rate enhancement over intermolecular SET, we cannot rule out the intervention of some direct electron transfer from the photoexcited HE to initiate radical formation from the RAE. This high-energy, C(sp^3)-hybridized intermediate can suffer two potential fates. Based on previous computational studies,[11] one plausible mechanistic pathway involves initial radical combination with a Ni^0 species, generating a Ni^I intermediate that engages in oxidative addition with the aryl halides to produce high valent Ni^{III} species **II**. Subsequent reductive elimination from this complex yields the desired cross-coupled product and the corresponding L_nNi^I species **IV**. At this juncture, a key SET event from the excited state HE [E_{red} (HE*/$HE^{\cdot+}$) = –2.28 V vs SCE[20]] to Ni [E_{red} (Ni^I/Ni^0) = −1.17 V vs. SCE in THF[10d]] regenerates the active Ni^0 catalyst. However, a process that involves initial oxidative addition of the aryl halides to Ni^0 species **V**, affording aryl-Ni^{II} complex **VII**, cannot be ruled out based on stoichiometric experiments with Ni complex **46** (Figure 4.6 B). In this scenario, **VII** would engage the radical to generate Ni^{III} complex **II**, which would then be carried on through the catalytic cycle.

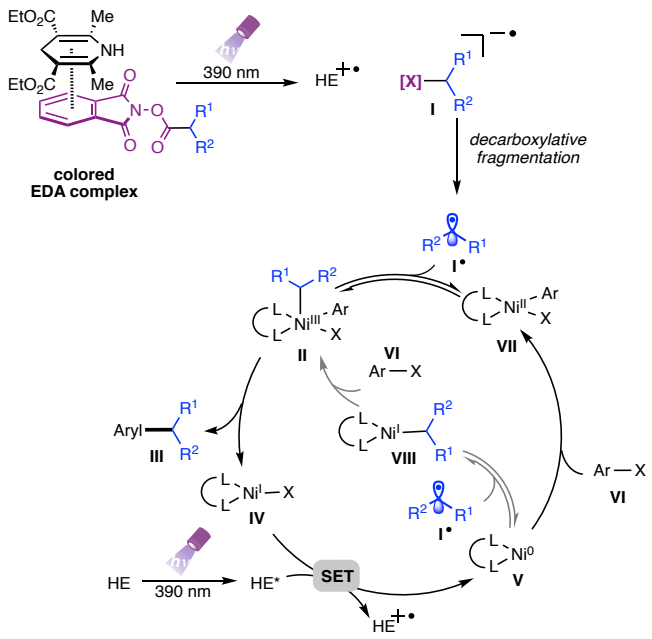

Figure 4.7. Proposed mechanism.

4.3 Conclusion

In summary, we have demonstrated the implementation of an electron donor-acceptor (EDA) complex platform toward Ni-catalyzed C(sp^3)-C(sp^2) bond formation, circumventing the need for exogenous photocatalysts, additives, and stoichiometric metal reductants. Under the developed conditions, the generation of heteroatom- and unactivated carbon-based radicals through direct visible-light excitation of diverse electron acceptors is feasible, providing a clear advantage in terms of scope over previously reported photochemical systems.[13] Upon light irradiation at 390 nm, excited HE functions as a potent organic photoreductant exhibiting a dual role: generation of reactive C(sp^3)-hybridized radicals through EDA complex activation as well as restoration of the desired catalytically active Ni(0) species through SET paradigms. This decarboxylative cross-electrophile arylation is amenable to the synthesis of peptidomimetics, drug-like molecules, and the diastereoselective functionalization of carbohydrates. The

commercial availability of carboxylic acids and related electron acceptor species facilitates the rapid incorporation of diverse carbon- and heteroatom-based radical architectures with high functional group tolerance. Key mechanistic and spectroscopic studies highlight the necessity for EDA photoactivation for efficient alkyl transfer and help inform the design of improved EDA-based paradigms in Ni-catalyzed cross-couplings.

4.4 Experimental

General Consideration

General: All chemical transformations requiring inert atmospheric conditions were carried out using Schlenk line techniques with a 4- or 5-port dual-bank manifold. For purple and blue light irradiation, two Kessil PR160-purple LED lamps (30 W High Luminous DEX 2100 LED, λ_{max} = 390 nm) or two Kessil A160WE Tuna Blue LED lamps (40 W, λ_{max} = 456 nm) were placed 1.5 inches away from the reaction vials. NMR spectra (^{1}H, ^{13}C, ^{19}F) were obtained at 298 ºK using 300, 400 and 500 MHz spectrometers. ^{1}H NMR spectra were referenced to residual, $CHCl_3$ (δ 7.26) in $CDCl_3$ or DMSO-d_6 (δ 2.50). ^{13}C NMR spectra were referenced to $CDCl_3$ (δ 77.3) or DMSO-d_6 (δ 39.5). Reactions were monitored by LC/MS, GC/MS, ^{1}H NMR, and/or TLC on silica gel plates (60 Å porosity, 250 μm thickness). TLC analysis was performed using hexanes/EtOAc as the eluent and visualized using ninhydrin, *p*-anisaldehyde stain, and/or UV light. Flash chromatography was accomplished using an automated system (CombiFlash®, UV detector, λ = 254 nm and 280 nm) with RediSep® R_f silica gel disposable flash columns (60 Å porosity, 40–60 μm) or RediSep R_f Gold® silica gel disposable flash columns (60 Å porosity, 20–40 μm). Accurate mass measurement analyses were conducted using electron ionization (EI) or electrospray ionization (ESI). The signals were mass measured against an internal lock mass reference of perfluorotributylamine (PFTBA) for EI-GC/MS and leucine enkephalin for ESI-

LC/MS. The utilized software calibrates the instruments and reports measurements by use of neutral atomic masses. The mass of the electron is not included. IR spectra were recorded on an FT-IR using either neat oil or solid products. Solvents were purified with drying cartridges through a solvent delivery system. Melting points (°C) are uncorrected.

Chemicals: Deuterated NMR solvents were purchased and stored over 4Å molecular sieves. CH_2Cl_2, EtOAc, hexanes, MeOH, Et_2O, and toluene were obtained from commercial suppliers and used as purchased. DMAP and DCC were purchased from commercial suppliers and used without further purification. THF and CH_2Cl_2 were purchased and dried *via* a solvent delivery system. RAEs were prepared according to the literature.[3d,30] Synthesis of all new RAEs is outlined here. HE was obtained commercially or prepared according to the literature.[32] Aryl bromides were purchased from commercial suppliers. The Ni complex **46** was synthesized according to Martin et al.[9e] All other reagents were purchased commercially and used as received. Photoredox-catalyzed reactions were performed using 8 mL Chemglass vials (2-dram, 17 x 60 mm, 15-425 Green Open Top Cap, TFE Septa). DMA 99.5% extra pure over molecular sieves was purchased from Acros Organics and used as received.

General Procedures

Preparation of RAEs (GP1): To a round-bottom flask equipped with a stir bar was added the corresponding carboxylic acid (if solid) (1.0 equiv), *N*-hydroxyphthalimide (1.0 equiv), and DMAP (0.1 equiv). The flask was then charged with CH_2Cl_2 or THF (0.2 M). At this point, carboxylic acid (1.0 equiv) was added via syringe (if liquid). DCC (1.1 equiv) was added, and the reaction was allowed to stir at rt until full consumption of the starting material. The mixture was then filtered over Celite and rinsed with additional CH_2Cl_2. The solvent was removed under reduced pressure, and the crude material was purified via flash chromatography.

Cross-coupling of RAEs (GP2): To an 8 mL vial equipped with a magnetic stir bar and a rubber septum was added $NiBr_2$(dtbpy) (10 mol %), HE (2.0 equiv, 1.0 mmol), RAE (2.0 equiv, 1.0 mmol), and aryl bromide (1.0 equiv, 0.50 mmol, if solid). The vial was evacuated three times via an inlet needle then purged with argon. The vial was then charged with dry, degassed DMA (0.1 M, 5 mL) via syringe. At this point, aryl bromide (1.0 equiv, 0.50 mmol) was added via syringe (if liquid). The reaction mixture was irradiated for 24 h with two Kessil PR160-purple LED lamps (30 W High Luminous DEX 2100 LED, λ_{max} = 390 nm) as described in the "Reaction Workflow" section. The temperature of the reaction was maintained at approximately 24 °C via a fan. Upon completion, the reaction mixture was poured into a separatory funnel containing an aq 5% LiCl soln (15 mL) and extracted with Et_2O or MTBE (methyl-*tert*-butyl ether, 3 x 15 mL). The combined organic layers were dried ($MgSO_4$), and all volatiles were removed under reduced pressure. The crude mixture was purified using automatic flash column chromatography.

Reaction workflow: All photoredox reactions were performed with two Kessil PR160-purple LED lamps (30 W High Luminous DEX 2100 LED, 390 nm). The lamps were placed 1.5 inches away from the reaction vials within a ventilated fume hood. A typical reaction setup is shown below.

Mechanistic Investigation

UV/vis studies:

UV/vis absorption spectra were measured in a 1 cm quartz cuvette using a Genesys 150 UV/vis spectrophotometer from Thermo Scientific. Absorption spectra of individual reaction components and mixtures thereof were recorded. A bathochromic shift was observed for a mixture of alkyl RAE and HE in DMA (0.2 M), which was visibly yellow in color (Figure 4.8). This indicates the formation of an electron donor-acceptor (EDA) complex (Figure 4.9 A and B, orange band). Notably, concentration is a crucial parameter for effective cross-coupling. A dilute reaction mixture (10^{-4} M) exhibits a blue-shifted absorption band, indicating the inhibition of EDA complex formation (Figure 4.9 C and D, black band).

To underline the formation of EDA complexes between RAEs with HE, we further recorded the corresponding UV/vis absorption spectra using the more electron deficient tetrachloro *N*-hydroxyphthalimide ester derivative (Figure 4.9 E and F). As expected, this species functions as a potent electron acceptor, and a more significant bathochromic shift was detected in this case (Figure 4.9 E and F).

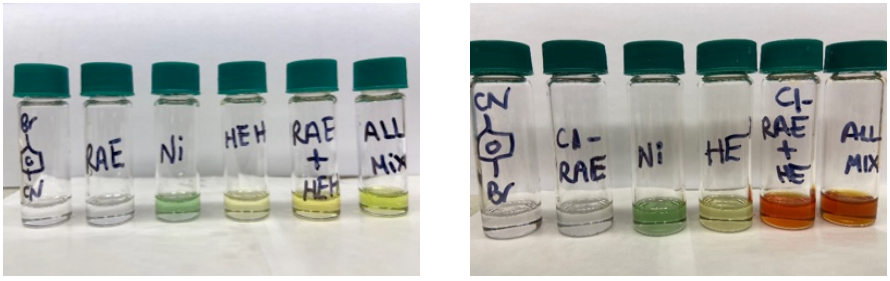

Figure 4.8. Visual appearance of reaction components and mixtures thereof.

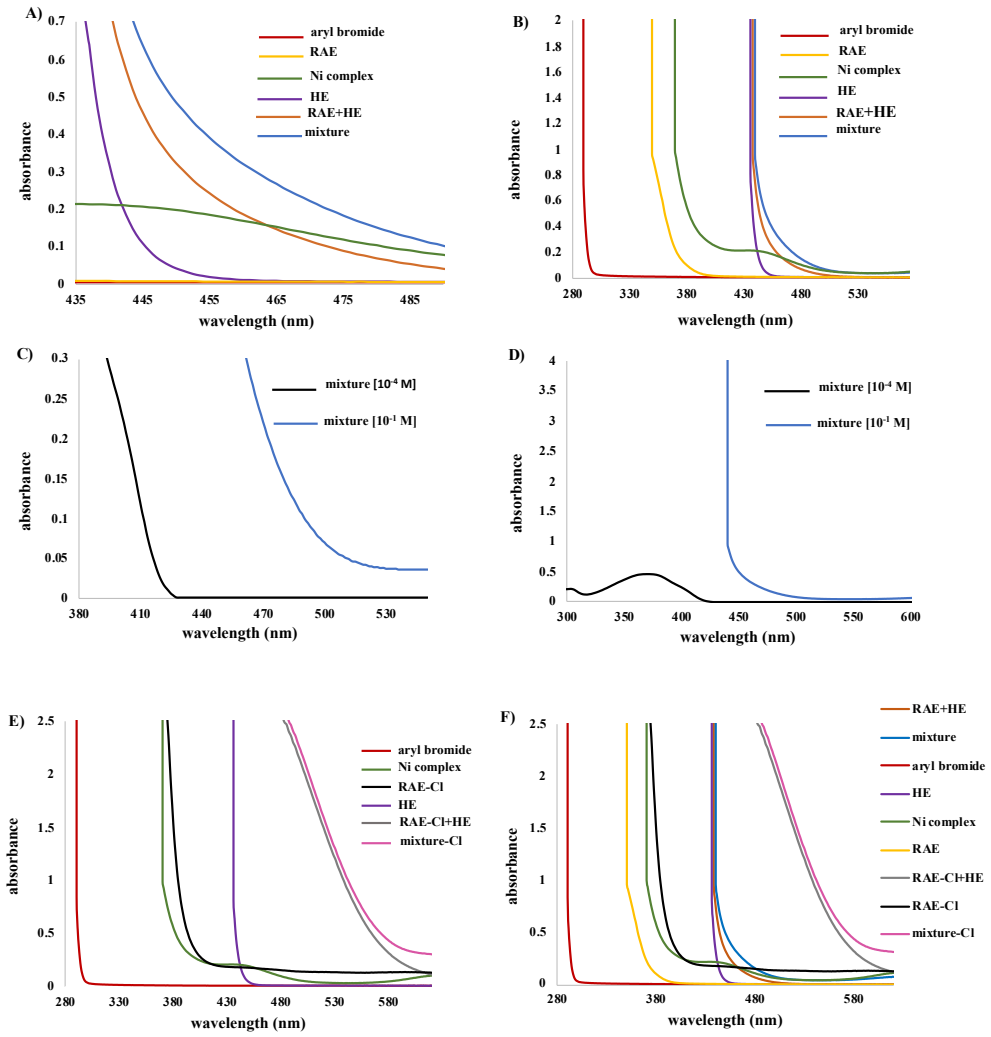

Figure 4.9. UV/vis absorption spectra of individual reaction components and a combination thereof (A–F). All spectra were measured in DMA and with a concentration of: 0.1 M aryl bromide, 0.2 M RAE/RAE-Cl, 0.2 M HE and 0.01 M Ni complex. The stoichiometry and concentration of sample "mixture" reflects the reaction conditions. The stoichiometry and concentration of sample "mixture-Cl" reflects the reaction conditions, and instead of RAE, RAE-Cl was used. Ni complex = $NiBr_2$(dtbpy), aryl bromide = 4-bromobenzonitrile, and RAE = cyclohexyl-*N*-hydroxyphthalimide-ester, RAE-Cl = cyclohexyl-*N*-hydroxy-3,4,5,6-tetra-chlorophthalimide-ester.

Job's method experiment:

The stoichiometry of the EDA complex was determined using Job's method with varying ratios of redox-active ester **2** and HE in DMA (0.2 M) at 455 nm. The absorbance was plotted against the molar fraction of HE. Maximum absorbance was detected at 50% molar fraction of HE, indicating a 1:1 stoichiometry of the EDA complex.

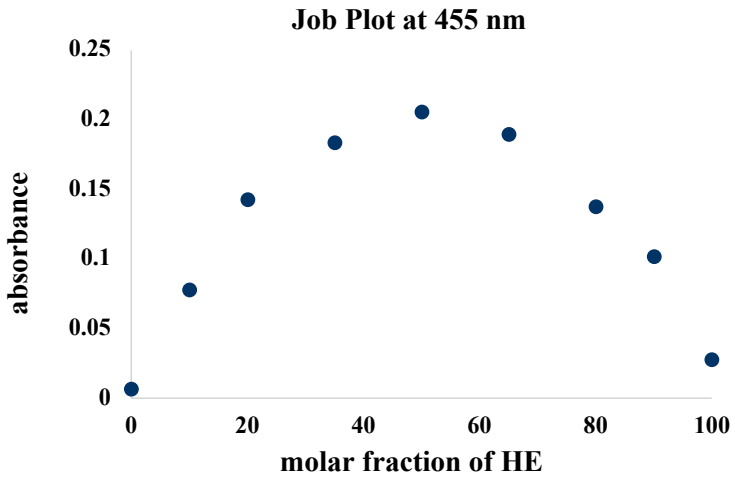

Figure 4.10. Job plot of the EDA complex (0.2 M total concentration in DMA) between HE and RAE **2** recorded at 455 nm.

Determination of association constant (k_{EDA}):

The association constant for the EDA complex formed between RAE **2** and HE was determined by UV/vis measurements in DMA employing the Benesi-Hildebrand method. The absorbance of a constant concentration of **2** (0.02 M) and an increasing concentration of HE (0.02-0.07 M) was recorded at 445 nm. The absorption spectra shown in Figure 4.11 were recorded in 1 cm path quartz cuvette. To determine the k_{EDA}, the reciprocal concentration of HE

was plotted against the reciprocal absorbance (A) of the EDA complex at 445 nm. A straight line was obtained, and by dividing the intercept through the slope: k_{EDA} = 2.04 M^{-1} for **2**/HE.

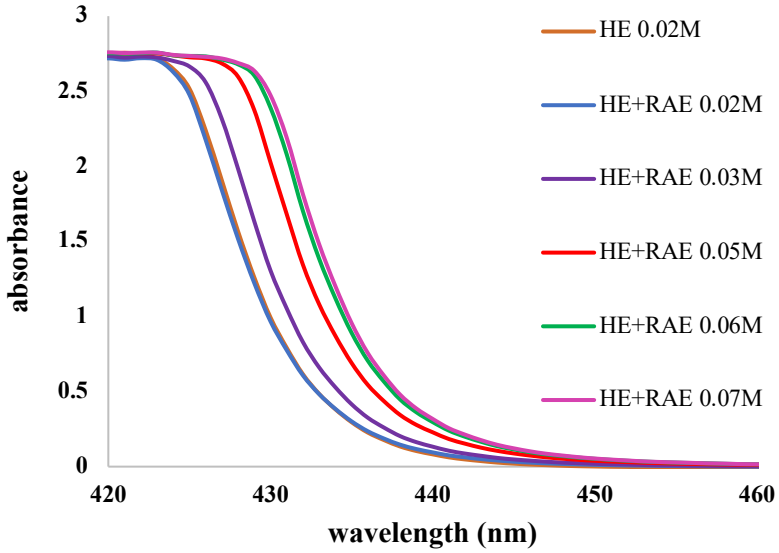

Figure 4.11. UV/vis absorption spectra of RAE (**2**, 0.02 M in DMA) in combination with increasing concentrations of HE (0.02 M up to 0.07 M in DMA).

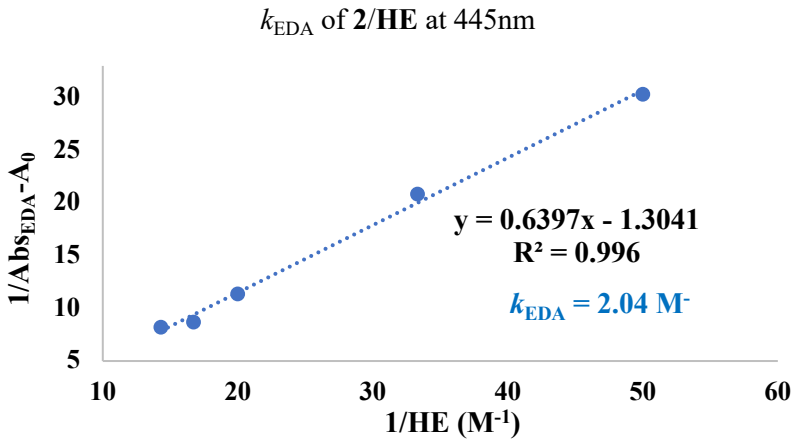

Figure 4.12. Benesi-Hildebrand plot for the EDA complex generated in DMA upon association of RAE **2** with HE.

TEMPO trapping experiment:

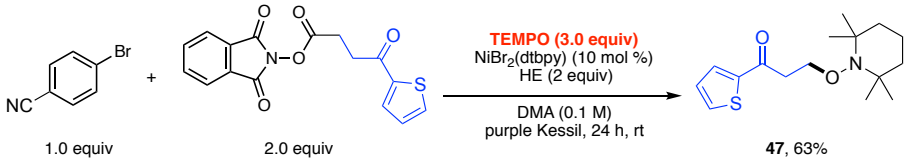

To probe the intermediacy of radical species, a trapping experiment was performed using TEMPO [(2,2,6,6-tetramethylpiperidin-1-yl)oxyl] as a radical scavenger. The reaction was performed according to *GP2* (0.3 mmol scale) in the presence of TEMPO (0.9 mmol, 3.0 equiv). The corresponding TEMPO adduct **47** was isolated in 63% yield via flash column chromatography. The product was obtained as a colorless oil. **^{1}H NMR** (500 MHz, $CDCl_3$) δ 7.77 (d, *J* = 3.8 Hz, 1H), 7.64 (d, *J* = 4.6 Hz, 1H), 7.13 (t, *J* = 4.4 Hz, 1H), 3.30 (t, *J* = 7.0 Hz, 2H), 2.81 (t, *J* = 7.0 Hz, 2H), 1.77 – 1.47 (m, 6H), 1.14 (s, 6H), 1.06 (s, 6H). **^{13}C NMR** (126 MHz, $CDCl_3$) δ 191.0, 143.8, 133.7, 132.1, 128.2, 60.2, 39.1 (2C), 34.1, 32.0 (2C), 26.8 (2C), 20.6 (2C), 17.1. **FT-IR** (cm^{-1}, neat, ATR): 2977, 2937, 1756, 1666, 1380, 1245, 1131, 1083, 904, 854. **HRMS** (EI) calc for $C_{16}H_{25}NO_2S$ $[M]^+$: 295.1606, found: 295.1557.

Investigation of HE backbone:

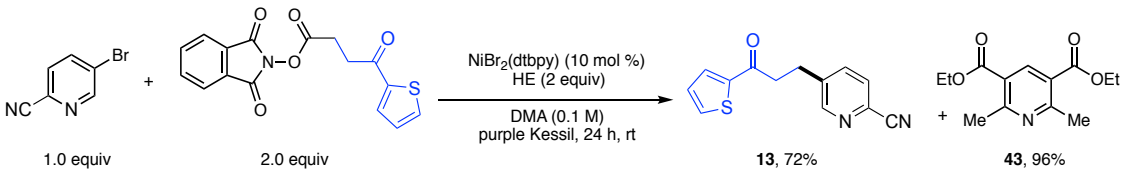

The reaction was performed according to *GP2* (0.3 mmol scale), and the corresponding (by-)products **13** and **43** were isolated via flash column chromatography. For characterization of compound **13**, see the characterization data section**.** The byproduct **43** was obtained as a white solid. **mp** = 72-74 °C. **^{1}H NMR** (500 MHz, $CDCl_3$) δ 8.66 (s, 1H), 4.39 (q, *J* = 7.1 Hz, 4H), 2.84

(s, 6H), 1.41 (t, J = 7.1 Hz, 6H). **^{13}C NMR** (126 MHz, $CDCl_3$) δ 166.1 (2C), 162.4, 141.0 (2C), 123.2 (2C), 61.5 (2C), 25.1 (2C), 14.4 (2C). **FT-IR** (cm^{-1}, neat, ATR): 2977, 2931, 1716, 1590, 1474, 1442, 1378, 1293, 1222, 1045. **HRMS** (ESI) calc for $C_{13}H_{18}NO_4$ $[M+H]^+$: 252.1236, found: 252.1234.

Investigation of radical intermediates and stoichiometric Ni experiments:

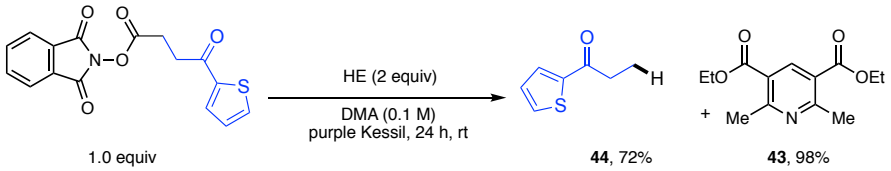

The reaction was performed according to *GP2* using **42** (1.0 equiv, 0.3 mmol), HE (1.0 equiv, 0.3 mmol) in DMA (0.1 M, 3 mL). The corresponding products (**43** and **44**) were isolated via automated flash column chromatography. Product **44** was obtained as a colorless oil. **^{1}H NMR** (500 MHz, $CDCl_3$) δ 7.71 (d, J = 3.7 Hz, 1H), 7.61 (d, J = 4.9 Hz, 1H), 7.12 (t, J = 4.4 Hz, 1H), 2.94 (q, J = 7.4 Hz, 2H), 1.24 (t, J = 7.4 Hz, 3H).**^{13}C NMR** (126 MHz, $CDCl_3$) δ 194.0, 144.3, 133.3, 131.7, 128.1, 32.7, 8.7. **FT-IR** (cm^{-1}, neat, ATR): 2978, 2937, 1660, 1518, 1459, 1376, 1277, 1225, 1085, 799.

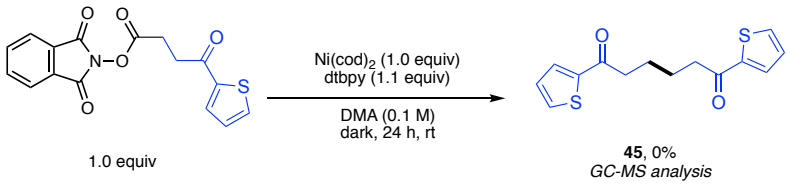

The reaction was performed according to *GP2* using **42** (1.0 equiv, 0.3 mmol), $Ni(COD)_2$ (1.0 equiv, 0.3 mmol), and 4,4'-di-*tert*-butyl-2,2'-dipyridine (dtbpy, 1.1 equiv, 0.33 mmol) in DMA (0.1 M, 3 mL). The crude reaction mixture was analyzed using GC/MS analysis whereby

no homocoupling or alkene product formation was observed, ruling out a plausible SET event from Ni(0) to the RAE.

*Stoichiometric experiments with Ni-complex **46**:*

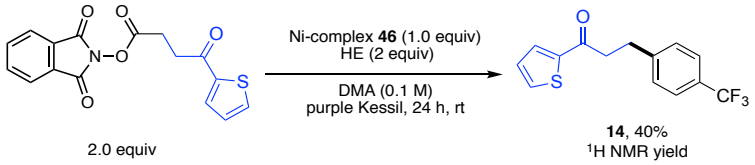

The reaction was performed in a nitrogen-filled glove box according to *GP2* using **42** (2.0 equiv, 0.6 mmol), Ni-complex **46** (1.0 equiv, 0.3 mmol), and HE (2.0 equiv, 0.6 mmol) in DMA (0.1 M). The reaction vial was removed from the glove box and irradiated for 24 h. After the work-up, the desired product was obtained in 40% yield as determined by ^{1}H-NMR spectroscopy using 1,3,5-trimethoxybenzene (0.3 mmol) as an internal standard. For characterization of compound **14**, see the characterization data section.

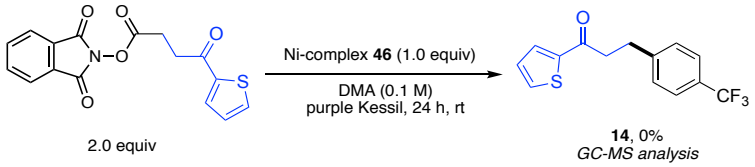

The reaction was performed in a nitrogen-filled glove box according to *GP2* using **42** (2.0 equiv, 0.6 mmol) and Ni-complex **46** (1.0 equiv, 0.3 mmol) in DMA (0.1 M). No aryl bromide or HE were added to the reaction mixture. The tube was removed from the glove box and irradiated for 24 h. The crude reaction mixture was analyzed by GC/MS. The C(sp^3)–C(sp^2) product was not observed, highlighting the necessity for EDA complexation for effective coupling.

*Catalytic competence of Ni-complex **46**:*

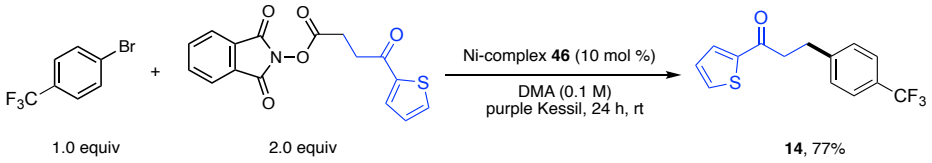

The reaction was set up in a nitrogen-filled glove box and performed according to *GP2* using **42** (2.0 equiv, 0.6 mmol) and Ni-complex **46** (10 mol %, 0.03 mmol). The reaction vial was removed from the glove box, and the reaction mixture was irradiated for 24 h. After automated flash column chromatography, the desired product (**14**) was isolated in 77% yield. For characterization of compound **14**, see the characterization data section.

Characterization Data

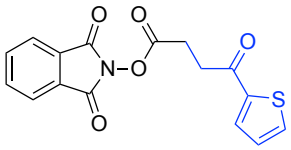

1,3-Dioxoisoindolin-2-yl 4-Oxo-4-(thiophen-2-yl)butanoate, **42** (20 mmol scale, 6.5 g, 70%) was prepared following *GP1*. The product was obtained as a brown solid. **mp** = 115 – 117 ºC. **^{1}H NMR** (400 MHz, $CDCl_3$) δ 7.90 – 7.81 (m, 2H), 7.81 – 7.73 (m, 3H), 7.64 (d, *J* = 4.9 Hz, 1H), 7.12 (t, *J* = 4.4 Hz, 1H), 3.39 (t, *J* = 7.0 Hz, 2H), 3.12 (t, *J* = 7.0 Hz, 2H). **^{13}C NMR** (101 MHz, $CDCl_3$) δ 189.4, 169.2, 161.8 (2C), 143.1, 134.9 (2C), 134.2, 132.4, 128.9 (2C), 128.3, 124.0 (2C), 33.6, 25.4. **FT-IR** (cm^{-1}, neat, ATR): 1816, 1787, 1741, 1666, 1518, 1467, 1415, 1356, 1250, 1219, 1186. **HRMS** (ESI) calc for $C_{16}H_{12}NO_5S$ $[M+H]^+$: 330.0436, found: 330.0452.

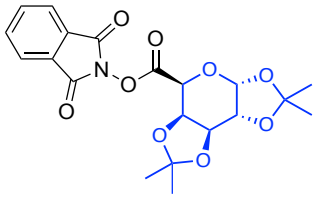

1,3-Dioxoisoindolin-2-yl

(3a*R*,5a*R*,8a*S*,8b*R*) 2,2,7,7 tetramethyltetrahydro 5*H*-bis([1,3]dioxolo)[4,5-b:4',5'-*d*]pyran-5-carboxylate, **31a** (20 mmol scale, 6.0 g, 72%) was prepared following *GP1*. The product was obtained as a white solid. **mp** = 176 – 178 ºC. **^{1}H NMR** (500 MHz, $CDCl_3$) δ 7.92 – 7.87 (m, 2H), 7.82 – 7.76 (m, 2H), 5.70 (d, *J* = 5.0 Hz, 1H), 4.83 (d, *J* = 2.3 Hz, 1H), 4.73 (qd, *J* = 7.5, 2.5 Hz, 2H), 4.45 (dd, *J* = 5.1, 2.7 Hz, 1H), 1.54 (s, 3H), 1.40 (s, 3H), 1.37 (s, 3H), 1.27 (s, 3H). **^{13}C NMR** (101 MHz, $CDCl_3$) δ 164.9 (2C), 161.4, 134.9 (2C), 129.0, 128.9, 124.1 (2C), 111.0, 109.6, 96.6, 72.0, 70.9, 70.3, 68.4, 26.2, 26.0, 25.1, 24.9. **FT-IR** (cm^{-1}, neat, ATR): 2989, 2933, 1833, 1792, 1624, 1374, 1256, 1213, 1186, 1071. **HRMS** (ESI) calcd for $C_{20}H_{21}NO_9Na$ $[M+Na]^+$: 442.1114, found: 442.1118.

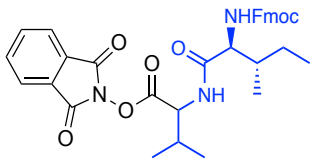

1,3-Dioxoisoindolin-2-yl (((9*H*-Fluoren-9-yl)methoxy)carbonyl)-*L*-isoleucylvalinate, **48** (1.73 mmol scale, 383 mg, 37%) was prepared following *GP1*. The product was obtained as a colorless oil. **^{1}H NMR** (300 MHz, $CDCl_3$) δ 7.91 – 7.82 (m, 2H), 7.81 – 7.70 (m, 4H), 7.59 – 7.56 (m, 2H), 7.44 – 7.27 (m, 4H), 6.50 – 6.43 (m, 1H), 5.43 – 5.33 (m, 1H), 4.96 (dd, *J* = 8.8, 5.0 Hz, 1H), 4.39 (q, *J* = 10.6, 8.1 Hz, 2H), 4.27 – 4.01 (m, 2H), 2.38 (dd, *J* = 12.9, 6.6 Hz, 1H), 2.04 – 1.84 (m, 1H), 1.62 (brs, 2H), 1.09 (dd, *J* = 6.9, 2.7 Hz, 6H), 0.93 (d, *J* = 10.3 Hz, 6H).**^{13}C NMR** (75 MHz, $CDCl_3$) δ 183.0, 172.8, 168.4, 161.6, 141.5 (2C), 135.0 (3C), 129.0 (2C), 127.9 (2C), 127.2

(4C), 125.2 (2C), 124.2 (2C), 120.1 (2C), 67.3, 55.7, 47.3, 37.5, 31.6, 18.9, 17.7, 15.8, 15.5, 11.6, 11.4. **FT-IR** (cm^{-1}, neat, ATR): 3298, 2966, 1789, 1746, 1661, 1537, 1467, 758, 696. **HRMS** (ESI) calc for $C_{34}H_{35}N_3NaO_7$ $[M+Na]^+$: 620.2367, found: 620.2370.

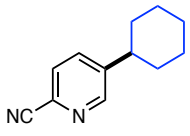

5-Cyclohexylpicolinonitrile, **3** (74 mg, 79%) was prepared following *GP2*. The product was obtained as a yellow oil. **^{1}H NMR** (300 MHz, $CDCl_3$) δ 8.55 (pseudo t, *J* = 1.6 Hz, 1H), 7.62 (pseudo t, *J* = 1.6 Hz, 2H), 2.60 (tt, *J* = 9.0, 2.5 Hz, 1H), 1.93 – 1.69 (m, 5H), 1.49 – 1.17 (m, 5H). **^{13}C NMR** (75 MHz, $CDCl_3$): δ 150.7, 147.2, 135.0, 131.3, 128.4, 117.6, 42.2, 33.8 (2C), 26.5 (2C), 25.8. **FT-IR** (cm^{-1}, neat, ATR): 2927, 2853, 2234, 1720, 1566, 1470, 1397, 1024, 999. **HRMS** (ESI) calc for $C_{12}H_{15}N_2$ $[M+H]^+$: 187.1230, found 187.1226.

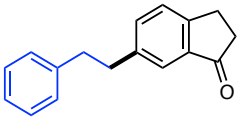

6-Phenethyl-2,3-dihydro-1*H*-inden-1-one, **4** (87.4 mg, 74%) was prepared following *GP2*. The product was obtained as a colorless solid. **mp** = 87-88 °C. **^{1}H NMR** (500 MHz, $CDCl_3$) δ 7.82 (d, *J* = 7.9 Hz, 1H), 7.31 – 7.29 (m, 4H), 7.19 (t, *J* = 6.9 Hz, 3H), 5.27 (br s, 2H), 2.78 (t, *J* = 7.8 Hz, 2H), 2.68 (t, *J* = 7.7 Hz, 2H), 2.01 (q, *J* = 7.8 Hz, 2H).**^{13}C NMR** (126 MHz, $CDCl_3$) δ 171.2, 149.7, 147.2, 141.7, 129.8 (2C), 128.5 (2C), 126.1, 125.7 (2C), 123.7, 121.9, 69.6, 35.9, 35.4, 32.9. **FT-IR** (cm^{-1}, neat, ATR): 3025, 2930, 1757, 1619, 1601, 1495, 1357, 1282, 1209, 1118. **HRMS** (EI) calc for $C_{17}H_{16}O_7$ $[M]^+$: 236.1201, found: 236.1203.

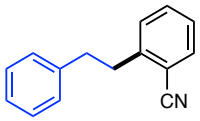

2-Phenethylbenzonitrile, **5** (75.7 mg, 73%) was prepared following *GP2*. The product was obtained as a pale-yellow oil. **^{1}H NMR** (500 MHz, $CDCl_3$) δ 7.63 (d, *J* = 7.7 Hz, 1H), 7.49 (t, *J* = 7.6 Hz, 1H), 7.33 – 7.18 (m, 7H), 3.16 (dd, *J* = 9.6, 6.6 Hz, 2H), 2.99 (dd, *J* = 9.5, 6.5 Hz, 2H). **^{13}C NMR** (126 MHz, $CDCl_3$) δ 145.6, 140.6, 132.9, 132.8 (2C), 129.8 (2C), 128.6 (2C), 126.7, 126.4, 118.1, 112.5, 37.3, 36.9. **FT-IR** (cm^{-1}, neat, ATR): 3062, 2929, 2862, 2223, 1600, 1494, 1485, 1452, 1311, 1163, 1072. **HRMS** (EI) calc for $C_{15}H_{13}N$ $[M]^+$: 207.1048, found: 207.1050.

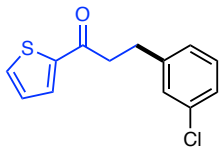

3-(3-Chlorophenyl)-1-(thiophen-2-yl)propan-1-one, **6** (109.1 mg, 87%) was prepared following *GP2*. The product was obtained as a pale-yellow oil. **^{1}H NMR** (500 MHz, $CDCl_3$) δ 7.68 – 7.64 (m, 2H), 7.30 – 7.05 (m, 5H), 3.22 (t, *J* = 7.7 Hz, 2H), 3.05 (t, *J* = 7.7 Hz, 2H). **^{13}C NMR** (126 MHz, $CDCl_3$) δ 191.7, 144.1, 143.1, 134.4, 133.8, 132.0, 129.9, 128.7, 128.2, 126.8, 126.5, 40.8, 30.0. **FT-IR** (cm^{-1}, neat, ATR): 1659, 1597, 1518, 1477, 1414, 1355, 1289, 1237, 1207, 1079. **HRMS** (EI) calc for $C_{13}H_{11}OSCl$ $[M]^+$: 250.0219, found: 250.0218.

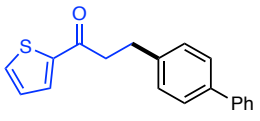

3-([1,1'-Biphenyl]-4-yl)-1-(thiophen-2-yl)propan-1-one, **7** (93.6 mg, 64%) was prepared following *GP2*. The product was obtained as a colorless oil. **^{1}H NMR** (500 MHz, $CDCl_3$) δ 7.72 (dd, *J* = 3.8, 1.2 Hz, 1H), 7.67 – 7.50 (m, 5H), 7.44 (t, *J* = 7.7 Hz, 2H), 7.34 (dd, *J* = 7.7, 6.1 Hz,

3H), 7.13 (dd, J = 5.0, 3.7 Hz, 1H), 3.28 (dd, J = 8.5, 6.8 Hz, 2H), 3.13 (t, J = 7.7 Hz, 2H). **^{13}C NMR** (126 MHz, $CDCl_3$) δ 192.2, 144.3, 141.1, 140.3, 139.4, 133.7, 132.0, 129.0 (2C), 128.9, 128.3 (2C), 127.4 (2C), 127.3 (2C), 127.2, 41.2, 30.1. **FT-IR** (cm^{-1}, neat, ATR): 2980, 1662, 1518, 1486, 1415, 1238, 1205, 1063, 933, 827. **HRMS** (EI) calc for $C_{19}H_{16}OS$ $[M]^+$: 292.0922, found: 292.0912.

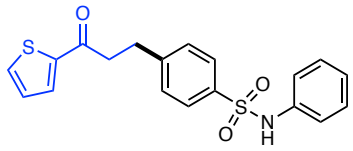

4-(3-Oxo-3-(thiophen-2-yl)propyl)-*N*-phenylbenzenesulfonamide, **8** (154.2 mg, 83%) was prepared following *GP2*. The product was obtained as a pale-yellow oil. **^{1}H NMR** (500 MHz, $CDCl_3$) δ 7.83 – 7.57 (m, 4H), 7.36 – 7.20 (m, 4H), 7.18 – 7.01 (m, 4H), 6.71 (d, J = 6.8 Hz, 1H), 3.21 (t, J = 7.4 Hz, 2H), 3.09 (t, J = 7.4 Hz, 2H). **^{13}C NMR** (126 MHz, $CDCl_3$) δ 191.5, 146.9, 143.9, 137.1, 136.6, 134.0, 132.1 (2C), 129.4, 129.3 (2C), 128.3 (2C), 127.6 (2C), 125.4, 121.6, 40.3, 30.1. **FT-IR** (cm^{-1}, neat, ATR): 3253, 1657, 1598, 1518, 1495, 1415, 1300, 1219, 1092, 920. **HRMS** (ESI) calc for $C_{19}H_{17}NNaO_3S_2$ $[M+Na]^+$: 394.0548, found: 394.0558.

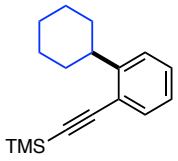

((2-Cyclohexylphenyl)ethynyl)trimethylsilane, **9** (100 mg, 78%) was prepared following *GP2*. The product was obtained as a colorless oil. **^{1}H NMR** (300 MHz, $CDCl_3$): δ 7.44 (ddd, J = 7.6, 1.5, 0.6 Hz, 1H), 7.32 – 7.19 (m, 2H), 7.11 (ddd, J = 7.6, 7.0, 1.7 Hz, 1H), 3.08 – 3.04 (m, 1H), 2.15 – 1.68 (m, 5H), 1.54 – 1.19 (m, 5H), 0.28 (s, 9H). **^{13}C NMR** (75 MHz, $CDCl_3$): δ 150.3, 132.5, 128.9 (2C), 125.5 (2C), 122.2, 104.2, 98.0, 42.2, 33.0 (2C), 27.2 (3C), 26.4, 0.2. **FT-IR**

(cm^{-1}, neat, ATR): 2925, 2851, 2155, 1447, 1248, 861, 841, 756. **HRMS** (EI), calc for $C_{17}H_{24}Si$ $[M]^+$: 256.1647, found :256.1645.

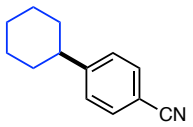

4-Cyclohexylbenzonitrile, **10** (64.5 mg, 70%) was prepared following *GP2*. The product was obtained as a colorless oil. **^{1}H NMR** (300 MHz, $CDCl_3$): δ 7.61 – 7.46 (m, 2H), 7.35 – 7.21 (m, 2H), 2.58 – 2.51 (m, 1H), 1.96 – 1.71 (m, 5H), 1.49 – 1.16 (m, 5H). **^{13}C NMR** (75 MHz, $CDCl_3$): δ 153.6, 132.3 (2C), 127.8 (2C), 119.3, 109.6, 44.8, 34.1 (2C), 26.7 (2C), 26.0. **FT-IR** (cm^{-1}, neat, ATR): 2924, 2851, 2226, 1606, 1504, 1448, 1415, 1175, 999, 827. **HRMS** (ESI) calc for $C_{13}H_{16}N$ $[M+H]^+$: 186.1277, found 186.1271.

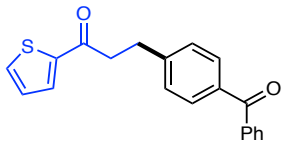

3-(4-Benzoylphenyl)-1-(thiophen-2-yl)propan-1one, **11** (116.9 mg, 73%) was prepared following *GP2*. The product was obtained as a colorless solid. **mp** = 119-120 °C. **^{1}H NMR** (500 MHz, $CDCl_3$) δ 7.83 – 7.68 (m, 5H), 7.64 (d, J = 5.0 Hz, 1H), 7.58 (t, J = 7.5 Hz, 1H), 7.47 (t, J = 7.7 Hz, 2H), 7.36 (d, J = 7.7 Hz, 2H), 7.12 (t, J = 4.4 Hz, 1H), 3.28 (t, J = 7.5 Hz, 2H), 3.16 (t, J = 7.5 Hz, 2H). **^{13}C NMR** (126 MHz, $CDCl_3$) δ 196.5, 191.7, 146.2, 144.1, 137.9, 135.8, 133.9, 132.4, 132.0, 130.6 (2C), 130.1 (2C), 128.6 (2C), 128.4 (2C), 128.3, 40.6, 30.4. **FT-IR** (cm^{-1}, neat, ATR): 2970, 1655, 1518, 1446, 1415, 1355, 1316, 1278, 1177, 1063. **HRMS** (EI) calc for $C_{20}H_{16}O_2S$ $[M]^+$: 320.0871, found: 320.0883.

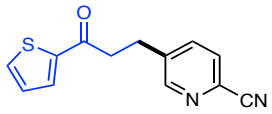

5-(4-Oxo-4-(thiophen-2-yl)butyl)picolinonitrile, **12** (0.30 mmol scale, 52 mg, 72%) was prepared following *GP2*. The product was obtained as a pale-yellow oil. **^{1}H NMR** (500 MHz, $CDCl_3$) δ 8.63 (s, 1H), 7.83 – 7.50 (m, 4H), 7.13 (t, *J* = 4.4 Hz, 1H), 3.30 (t, *J* = 7.1 Hz, 2H), 3.16 (t, *J* = 7.1 Hz, 2H). **^{13}C NMR** (126 MHz, $CDCl_3$) δ 190.6, 151.7, 143.6, 140.9, 137.2, 134.3, 132.2, 131.9, 128.4, 128.3, 117.4, 39.7, 27.3. **FT-IR** (cm^{-1}, neat, ATR): 2835, 2473, 1651, 1414, 1250, 1089, 722.

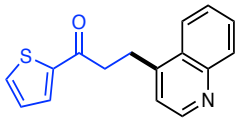

3-(Quinoline-4-yl)-1-(thiophen-2-yl)propan-1-one, **13** (61.5 mg, 46%) was prepared following *GP2*. The product was obtained as a yellow solid. **mp** = 104-105 °C. **^{1}H NMR** (500 MHz, $CDCl_3$) δ 7.93 – 7.72 (m, 7H), 7.66 (d, *J* = 4.9 Hz, 1H), 7.14 (t, *J* = 4.4 Hz, 1H), 3.41 (t, *J* = 7.0 Hz, 2H), 3.15 (t, *J* = 7.0 Hz, 2H). **^{13}C NMR** (126 MHz, $CDCl_3$) δ 189.5, 169.3, 168.0, 161.9, 143.2, 134.9, 134.5, 134.2, 132.8, 132.4, 129.0, 128.3, 124.1, 123.7, 33.8, 25.5. **FT-IR** (cm^{-1}, neat, ATR): 1816, 1787, 1774, 1739, 1665, 1415, 1373, 1303, 1250, 1219, 1185.

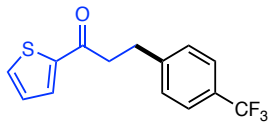

1-(Thiophen-2-yl)-3-(4-(trifluoromethyl)phenyl)propan-1-one, **14** (0.30 mmol scale, 65.9 mg, 77%) was prepared following *GP2*. The product was obtained as a pale-yellow oil. **^{1}H NMR** (500 MHz, $CDCl_3$) δ 7.68 – 7.63 (m, 2H), 7.54 (d, *J* = 7.9 Hz, 2H), 7.37 (d, *J* = 7.9 Hz, 2H), 7.12 (t, *J*

= 4.4 Hz, 1H), 3.26 (t, *J* = 7.5 Hz, 2H), 3.13 (t, *J* = 7.5 Hz, 2H). **^{13}C NMR** (126 MHz, $CDCl_3$) δ 191.5, 145.3, 144.0, 133.8, 132.0, 128.6 (d, *J* = 32.3 Hz), 128.9 (2C), 128.3, 125.5 (q, *J* = 3.8 Hz, 2C), 124.4 (q, *J* = 271.9 Hz), 40.5, 30.0. **^{19}F NMR** (471 MHz, C_6D_6) δ -62.3. **FT-IR** (cm^{-1}, neat, ATR): 1662, 1618, 1518, 1415, 1354, 1322, 1240, 1209, 1161, 1118, 1107. **HRMS** (EI) calc for $C_{14}H_{11}OSF_3$ $[M]^+$: 284.0483, found: 284.0502.

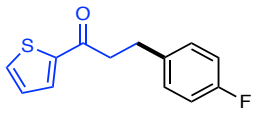

1-(Thiophen-2-yl)-3-(4-fluoro)phenyl)propan-1-one, **15** (50.4 mg, 43%) was prepared following *GP2*. The product was obtained as a colorless oil. **^{1}H NMR** (500 MHz, $CDCl_3$) δ 7.68 (dd, *J* = 3.8, 1.1 Hz, 1H), 7.63 (dd, *J* = 4.9, 1.1 Hz, 1H), 7.23 – 7.17 (m, 2H), 7.11 (dd, *J* = 4.9, 3.8 Hz, 1H), 7.02 – 6.94 (m, 2H), 3.21 (t, *J* = 7.6 Hz, 2H), 3.04 (t, *J* = 7.6 Hz, 2H). **^{13}C NMR** (126 MHz, $CDCl_3$) δ 192.1, 161.6 (d, *J* = 243.9 Hz), 144.2, 136.73, 136.71, 133.8, 132.0, 130.01, 130.0, 128.2, 115.4 (d, *J* = 21.3 Hz), 41.3, 29.7. **^{19}F NMR** (471 MHz, C_6D_6) δ -117.11. **FT-IR** (cm^{-1}, neat, ATR): 2925, 2854, 1661, 1601, 1509, 1415, 1355, 1296, 1219, 1157. **HRMS** (EI) calc for $C_{13}H_{11}OSF$ $[M]^+$: 234.0515, found: 234.0520.

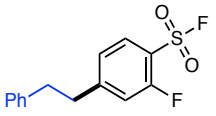

2-Fluoro-4-phenethylbenzenesulfonyl Fluoride, **16** (120 mg, 85%) was prepared following *GP2*. The product was obtained as a colorless oil. **^{1}H NMR** (500 MHz, $CDCl_3$) δ 7.84 (t, *J* = 7.5 Hz, 1H), 7.36 – 7.00 (m, 7H), 3.04 – 2.99 (m, 4H). **^{13}C NMR** (126 MHz, $CDCl_3$) δ 159.6 (d, *J* = 261.8 Hz), 154.0 (d, *J* = 8.1 Hz), 140.0, 130.8, 128.8 (2C), 128.5 (2C), 126.7, 125.16 (d, *J* = 3.6 Hz), 117.8, 117.7, 37.8, 36.8. **^{19}F NMR** (471 MHz, $CDCl_3$) δ -107.04, -107.07. **FT-IR** (cm^{-1},

neat, ATR): 1607, 1574, 1496, 1453, 1260, 1245, 1212, 1154, 1074, 779. **HRMS** (EI) calc for $C_{14}H_{12}O_2F_2S$ $[M]^+$: 282.0526, found: 282.0510.

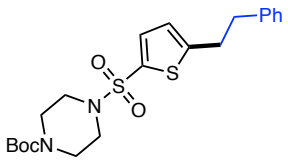

***tert*-Butyl 4-((5-Phenethylthiophen-2-yl)sulfonyl)piperazine-1-carboxylate**, **17** (152.8 mg, 70%) was prepared following *GP2*. The product was obtained as a colorless solid. **mp** = 87-88 °C. **^{1}H NMR** (500 MHz, $CDCl_3$) δ 7.40 – 7.06 (m, 6H), 6.77 (d, *J* = 3.8 Hz, 1H), 3.51 (pseudo t, *J* = 5.1 Hz, 4H), 3.14 (t, *J* = 7.7 Hz, 2H), 2.99 – 2.94 (m, 6H), 1.43 (s, 9H). **^{13}C NMR** (126 MHz, $CDCl_3$) δ 154.3, 152.7, 140.0, 133.0, 132.5 (2C), 128.6 (2C), 128.5 (2C), 126.6, 125.5, 80.5, 46.0 (2C), 42.8, 37.5, 32.1, 28.4 (3C). **FT-IR** (cm^{-1}, neat, ATR): 2979, 1736, 1694, 1454, 1421, 1355, 1310, 1249, 1221, 1162. **HRMS** (ESI) calc for $C_{21}H_{29}N_2O_4S_2$ $[M+H]^+$: 437.1569, found: 437.1578.

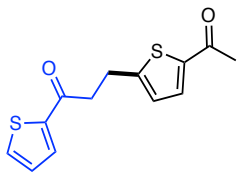

4-(5-Acetylthiophen-2-yl)-1-(thiophen-2-yl)butan-1-one, **18** (86 mg, 65%) was prepared following *GP2*. The product was obtained as a colorless solid. **mp** = 89-90 °C. **^{1}H NMR** (500 MHz, $CDCl_3$) δ 7.72 (d, *J* = 3.9 Hz, 1H), 7.65 (d, *J* = 4.6 Hz, 1H), 7.52 (d, *J* = 3.9 Hz, 1H), 7.14 (d, *J* = 4.6 Hz, 1H), 6.90 (d, *J* = 3.9 Hz, 1H), 3.31 (s, 4H), 2.51 (s, 3H). **^{13}C NMR** (126 MHz, $CDCl_3$) δ 190.9, 190.6, 153.6, 143.8, 142.8, 134.1, 133.0, 132.2 (2C), 126.6, 40.6, 26.7, 25.1. **FT-IR** (cm^{-1}, neat, ATR): 3088, 2980, 1742, 1654, 1518, 1415, 1358, 1252, 1233, 852. **HRMS** (ESI) calc for $C_{13}H_{13}O_2S_2$ $[M+H]^+$: 265.0338, found: 265.0337.

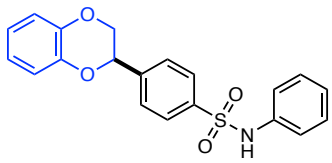

4-(2,3.Dihydrobenzo[*b*][1,4]dioxin-2-yl)-*N*-phenylbenzenesulfonamide, **19** (137.8 mg, 75%) was prepared following *GP2*. The product was obtained as a colorless solid. **mp** = 171-172 °C. **^{1}H NMR** (500 MHz, $CDCl_3$) δ 7.83 (d, *J* = 8.0 Hz, 2H), 7.52 (d, *J* = 8.0 Hz, 2H), 7.34 – 7.21 (m, 2H), 7.14 – 7.09 (m, 3H), 7.00 – 6.80 (m, 4H), 6.73 (s, 1H), 5.17 (dd, *J* = 8.6, 2.4 Hz, 1H), 4.34 (dd, *J* = 11.6, 2.4 Hz, 1H), 3.95 (dd, *J* = 11.6, 8.6 Hz, 1H). **^{13}C NMR** (126 MHz, $CDCl_3$) δ 143.4, 143.0, 141.9, 139.6, 136.3, 129.6 (2C), 127.8 (2C), 127.2 (2C), 125.8, 122.1 (2C), 122.0, 121.9, 117.6, 117.4, 74.4, 69.0. **FT-IR** (cm^{-1}, neat, ATR): 2980, 1493, 1382, 1263, 1159, 1078, 954, 751. **HRMS** (ESI) calc for $C_{20}H_{18}NO_4S$ $[M+H]^+$: 368.0965, found: 368.0957.

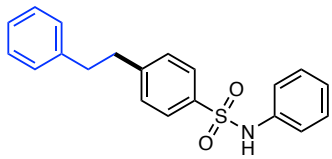

4-Phenethyl-*N*-phenylbenzenesulfonamide, **20** (133.9 mg, 71%) was prepared following *GP2*. The product was obtained as a colorless solid. **mp** = 128-129 °C. **^{1}H NMR** (500 MHz, $CDCl_3$) δ 7.71 (d, *J* = 7.9 Hz, 2H), 7.40 – 6.88 (m, 12H), 5.45 (s, 1H), 3.16 – 2.64 (m, 4H). **^{13}C NMR** (126 MHz, $CDCl_3$) δ 147.5, 140.8, 136.6, 129.4 (2C), 129.3 (2C), 128.5 (4C), 127.5 (2C), 126.3 (2C), 125.5, 121.8 (2C), 37.8, 37.4. **FT-IR** (cm^{-1}, neat, ATR): 3257, 2980, 1598, 1410, 1221, 1092, 1030, 920, 820, 752. **HRMS** (ESI) calc for $C_{20}H_{20}NO_2S$ $[M+H]^+$: 338.1214, found: 338.1215.

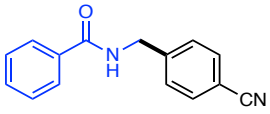

***N*-(4-Cyanobenzyl)benzamide**, **21** (114 mg, 96%) was prepared following *GP2*. The product was obtained as a colorless oil. **^{1}H NMR** (300 MHz, $CDCl_3$): δ 7.88 – 7.71 (m, 2H), 7.63 – 7.47 (m, 3H), 7.47 – 7.34 (m, 4H), 6.96 (t, *J* = 6.3 Hz, 1H), 4.66 (d, *J* = 6.3 Hz, 2H). **^{13}C NMR** (75 MHz, $CDCl_3$): δ 167.8, 144.1, 133.9, 132.6 (2C), 132.0, 128.8 (2C), 128.3 (2C), 127.1 (2C), 118.8, 111.3, 43.6. **FT-IR** (cm^{-1}, neat, ATR): 3319, 2930, 2228, 1725, 1641, 1577, 1415, 1077, 880. **HRMS** (ESI) calc for $C_{15}H_{13}N_2O$ $[M+H]^+$: 237.1022, found 237.1017.

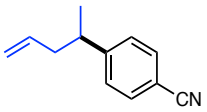

4-(Pent-4-en-2-yl)benzonitrile, **22** (67 mg, 78%) was prepared following *GP2*. The product was obtained as a colorless oil. **^{1}H NMR** (300 MHz, $CDCl_3$): δ 7.67 – 7.55 (m, 2H), 7.36 – 7.28 (m, 2H), 5.68 (ddt, *J* = 17.7, 9.6, 7.1 Hz, 1H), 5.15 – 4.76 (m, 2H), 2.92 – 2.88 (m, 1H), 2.38 – 2.33 (m, 2H), 1.29 (d, *J* = 6.9 Hz, 3H). **^{13}C NMR** (75 MHz, $CDCl_3$): δ 152.6, 136.2, 132.3 (2C), 128.0 (2C), 119.2, 116.9, 109.9, 42.3, 40.1, 21.2. **FT-IR** (cm^{-1}, neat, ATR): 2964, 2927, 2227, 1640, 1607, 1504, 1416, 1178, 993, 834. **HRMS** (ESI) calc for $C_{12}H_{14}N$ $[M+H]^+$: 172.1121, found 172.1114.

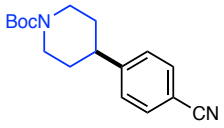

***tert*-Butyl 4-(4-Cyanophenyl)piperidine-1-carboxylate**, **23** (111 mg, 79%) was prepared following *GP2*. The product was obtained as a colorless oil. **^{1}H NMR** (300 MHz, $CDCl_3$): δ 7.55 (pseudo dt, *J* = 8.2, 1.9 Hz, 2H), 7.27 (pseudo dt, *J* = 8.4, 1.5 Hz, 2H), 4.22 (br d, *J* = 12.8 Hz,

2H), 2.87 – 2.54 (m, 3H), 1.83 – 1.69 (m, 2H), 1.66 – 1.51 (m, 2H), 1.47 – 1.41 (m, 9H). **^{13}C NMR** (75 MHz, $CDCl_3$): δ 154.8, 154.7, 151.2, 132.4, 127.7 (2C), 127.6, 118.9, 110.2, 79.6, 42.8, 41.0, 32.7, 28.4 (3C), 26.9. **FT-IR** (cm^{-1}, neat, ATR): 2939, 2225, 2167, 2029, 1691, 1422, 1365, 1279, 1170, 1014. **HRMS** (ESI) calc for $C_{17}H_{23}N_2O_2$ $[M+H]^+$: 287.1754, found 287.1766.

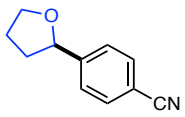

4-(Tetrahydrofuran-2-yl)benzonitrile, **24** (76 mg, 88%) was prepared following *GP2*. The product was obtained as a colorless oil. **^{1}H NMR** (300 MHz, $CDCl_3$): δ 7.70 – 7.53 (m, 2H), 7.48 – 7.36 (m, 2H), 4.93 (t, *J* = 7.2 Hz, 1H), 4.11 – 4.00 (m, 2H), 2.50 – 2.28 (m, 1H), 2.12 – 1.91 (m, 2H), 1.75 – 1.72 (m, 1H). **^{13}C NMR** (75 MHz, $CDCl_3$): δ 149.4, 132.3 (2C), 126.3 (2C), 119.1, 111.0, 80.0, 69.1, 34.9, 26.1. **FT-IR** (cm^{-1}, neat, ATR): 2953, 2923, 2852, 1726, 1609, 1459, 1261, 1066, 836. **HRMS** (ESI) calc for $C_{11}H_{12}NO$ $[M+H]^+$: 174.0913, found: 174.0907.

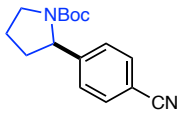

***tert*-Butyl 2-(4-Cyanophenyl)pyrrolidine-1-carboxylate**, **25** (115 mg, 85%) was prepared following *GP2*. The product was obtained as a colorless oil. **^{1}H NMR** (300 MHz, $CDCl_3$): δ 7.55 (d, *J* = 8.1 Hz, 2H), 7.25 (d, *J* = 8.1 Hz, 2H), 4.89 – 4.75 (m, 1H), 3.59 – 3.32 (m, 2H), 2.41 – 2.22 (m, 1H), 1.91 – 1.67 (m, 3H), 1.40 (s, 4H), 1.13 (s, 5H). **^{13}C NMR** (75 MHz, $CDCl_3$): δ 155.3, 132.2, 126.3 (2C), 124.9, 119.7, 110.4, 79.7, 61.2, 47.2, 35.9, 28.4, 28.1 (3C), 23.3. **FT-IR** (cm^{-1}, neat, ATR): 2975, 2227, 1693, 1608, 1477, 1454, 1365, 1249, 1111. **HRMS** (ESI) calc for $C_{16}H_{21}N_2O_2$ $[M+H]^+$: 273.1598, found: 273.1592.

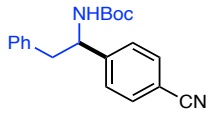

***tert*-Butyl (1-(4-Cyanophenyl)-2-phenylethyl)carbamate**, **26** (113 mg, 70%) was prepared following *GP2*. The product was obtained as a colorless oil. **^{1}H NMR** (300 MHz, DMSO-d_6): δ 7.78 (d, J = 8.0 Hz, 2H), 7.55 – 7.45 (m, 2H), 7.30 – 7.12 (m, 5H), 4.79 (q, J = 8.1 Hz, 1H), 2.89 (d, J = 8.6 Hz, 1H), 1.39 (s, 2H), 1.27 (s, 9H). **^{13}C NMR** (75 MHz, DMSO-d_6): δ 160.2, 143.5, 137.4 (2C), 134.4, 133.3 (2C), 132.7 (2C), 131.4 (2C), 124.1, 114.7, 83.2, 61.0, 47.1, 33.4 (2C), 31.6 (2C). **FT-IR** (cm^{-1}, neat, ATR): 2976, 2926, 2229, 1698, 1505, 1455, 1366, 1168, 1018, 700. **HRMS** (ESI) calc for $C_{20}H_{22}NaN_2O_2$ [M+Na]$^{+}$: 345.1573, found: 345.1566.

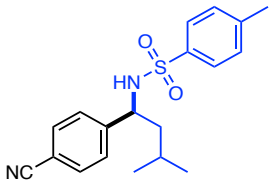

***N*-(1-(4-Cyanophenyl)-3-methylbutyl)-4-methylbenzenesulfonamide**, **27** (130 mg, 76%) was prepared following *GP2*. The product was obtained as a yellow oil. **^{1}H NMR** (300 MHz, $CDCl_3$): 7.53 – 7.46 (m, 2H), 7.45 – 7.39 (m, 2H), 7.16 – 7.10 (m, 4H), 5.25 (d, J = 7.1 Hz, 1H), 4.38 (dt, J = 8.1, 6.6 Hz,1H), 2.37 (s, 3H), 1.70 – 1.35 (m, 3H), 0.82 (dd, J = 18.4, 6.1 Hz, 6H). **^{13}C NMR** (75 MHz, $CDCl_3$): δ 147.0, 143.7, 137.4, 134.5, 132.3, 129.9, 129.5, 127.5, 127.1, 126.6, 123.8, 118.7, 111.1, 56.2, 46.9, 24.7, 22.6, 22.0, 21.6. **FT-IR** (cm^{-1}, neat, ATR): 3200, 2957, 2228, 1773, 1605, 1468, 1386, 1160, 815, 714. **HRMS** (ESI) calc for $C_{19}H_{23}N_2O_2S$ [M+H]$^{+}$: 343.1475, found: 343.1475.

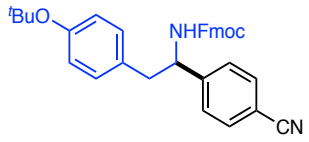

(9*H*-Fluoren-9-yl)methyl (2-(4-(*tert*-butoxy)phenyl)-1-(4-cyanophenyl)ethyl)carbamate, **28** (145 mg, 56%) was prepared following *GP2*. The product was obtained as a colorless oil. **^{1}H NMR** (300 MHz, $CDCl_3$): δ 7.88 – 7.70 (m, 2H), 7.67 – 7.49 (m, 2H), 7.40 – 7.30 (m, 5H), 7.17 (d, *J* = 8.4 Hz, 4H), 6.91 (d, *J* = 8.4 Hz, 3H), 6.70 (d, *J* = 10.9 Hz, 1H), 5.94 (d, *J* = 14.6 Hz, 1H), 4.53 (d, *J* = 6.7 Hz, 2H), 4.48 – 4.36 (m, 1H), 4.25 (t, *J* = 6.7 Hz, 1H), 1.34 (s, 9H). **^{13}C NMR** (75 MHz, $CDCl_3$): δ 154.1, 153.7, 143.7 (2C), 141.5 (2C), 131.5 (2C), 128.0 (2C), 127.3 (4C), 125.9 (2C), 125.0 (4C), 124.6 (4C), 123.1, 120.2 (2C), 110.8, 78.7, 67.3, 47.2, 29.0 (3C). **FT-IR** (cm^{-1}, neat, ATR): 2978, 1721, 1661, 1596, 1542, 1447, 1284, 1105, 951. **HRMS** (ESI) calc for $C_{34}H_{33}N_2O_3$ $[M+H]^+$: 517.2486, found: 517.2478.

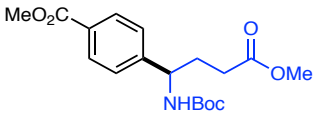

Methyl 4-(1-((*tert*-Butoxycarbonyl)amino)-4-methoxy-4-oxobutyl)benzoate, 29 (170 mg, 97%) was prepared following *GP2*. The product was obtained as a colorless foam. **^{1}H NMR** (300 MHz, $CDCl_3$): δ 8.12 – 7.85 (m, 2H), 7.32 (d, *J* = 8.1 Hz, 2H), 5.27 – 5.15 (m, 1H), 4.67 (br s, 1H), 3.87 (s, 3H), 3.63 (s, 3H), 2.34 (td, *J* = 7.4, 4.1 Hz, 2H), 2.03 (d, *J* = 7.4 Hz, 2H), 1.44 – 1.29 (m, 9H). **^{13}C NMR** (75 MHz, $CDCl_3$): δ 173.6, 166.9, 155.3, 147.7, 134.2, 130.0, 129.2, 126.3, 123.5, 79.8, 54.3, 52.1, 51.8, 51.7, 31.5, 30.9, 30.8, 28.4. **FT-IR** (cm^{-1}, neat, ATR): 2977, 1717, 1611, 1513, 1437, 1366, 1278, 1164, 1113, 859. **HRMS** (ESI) calc for $C_{18}H_{25}NaNO_6$ $[M+Na]^+$: 374.1574, found 374.1569.

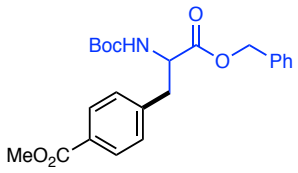

Methyl 4-(3-(Benzyloxy)-2-((tert-butoxycarbonyl)amino)-3-oxopropyl)benzoate, **30** (188 mg, 91%) was prepared following *GP2*. The product was obtained as a colorless oil. **^{1}H NMR** (300 MHz, $CDCl_3$): δ 7.88 (d, *J* = 8.0 Hz, 2H), 7.38 – 7.31 (m, 3H), 7.31 – 7.22 (m, 2H), 7.09 (d, *J* = 7.9 Hz, 2H), 5.26 – 4.93 (m, 3H), 4.71 – 4.56 (m, 1H), 3.90 (s, 3H), 3.18 – 3.10 (m, 2H), 1.41 (s, 9H). **^{13}C NMR** (75 MHz, $CDCl_3$): δ 171.5, 167.0, 155.1, 141.5, 135.1, 129.9, 129.5 (2C), 129.0 (2C), 128.8 (2C), 128.7 (2C), 80.2, 67.4, 54.3, 52.2, 38.4, 28.4 (3C). **FT-IR** (cm^{-1}, neat, ATR): 2977, 1715, 1611, 1498, 1366, 1277, 1161, 1105, 1055, 1020. **HRMS** (ESI) calc for $C_{22}H_{27}NaNO_6$ $[M+Na]^+$: 436.1731, found 436.1741.

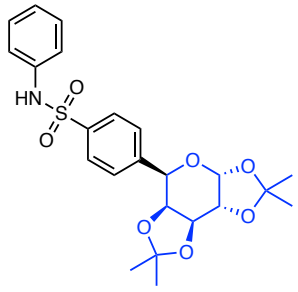

***N*-Phenyl-4-((3a*R*,5*R*,5a*S*,8a*S*,8b*R*)-2,2,7,7-tetramethyltetrahydro-5*H*-bis([1,3]dioxolo)[4,5-*b*:4',5'-*d*]pyran-5-yl)benzenesulfonamide**, **31** (127 mg, 55%, dr >20:1) was prepared following *GP2*. The product was obtained as a yellow solid. **mp** = 85-86 °C. **^{1}H NMR** (500 MHz, $CDCl_3$) δ 7.73 (d, *J* = 8.0 Hz, 2H), 7.45 (d, *J* = 8.0 Hz, 2H), 7.26 – 7.23 (m, 2H), 7.11 – 7.07 (m, 3H), 6.76 (d, *J* = 8.9 Hz, 1H), 5.69 (d, *J* = 5.0 Hz, 1H), 4.88 (s, 1H), 4.71 (d, *J* = 7.8 Hz, 1H), 4.39 (d, *J* = 8.9 Hz, 2H), 1.54 (s, 3H), 1.40 (s, 3H), 1.37 (s, 3H), 1.27 (s, 3H). **^{13}C NMR** (126 MHz, $CDCl_3$) δ 143.4, 138.1, 136.5 129.5 (2C), 127.7 (2C), 127.1 (2C), 125.6 (2C), 121.9, 109.6, 109.0, 96.9,

73.5, 71.1, 70.7, 69.2, 26.3, 26.0, 25.0, 24.4. **FT-IR** (cm^{-1}, neat, ATR): 2980, 1495, 1382, 1300, 1254, 1211, 1161, 1092, 1000, 961. **HRMS** (ESI) calc for $C_{23}H_{28}NO_7S$ $[M+H]^+$: 462.1586, found: 462.1593.

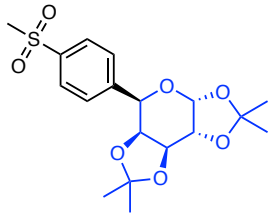

4-((3a*R*,5*R*,5a*S*,8a*S*,8b*R*)-2,2,7,7-Tetramethyltetrahydro-5*H*-bis([1,3]dioxolo)[4,5-*b*:4',5'-*d*]pyran-5-yl)methylsulfonamide, **32** (125 mg, 65%, dr. >20:1) was prepared following *GP2*. The product was obtained as a yellow solid. **mp** = 108-110 °C. **^{1}H NMR** (500 MHz, $CDCl_3$) δ 7.91 (d, *J* = 8.0 Hz, 2H), 7.59 (d, *J* = 8.0 Hz, 2H), 5.71 (d, *J* = 4.9 Hz, 1H), 4.95 (s, 1H), 4.74 (dd, *J* = 7.7, 2.5 Hz, 1H), 4.54 – 4.33 (m, 2H), 3.04 (s, 3H), 1.56 (s, 3H), 1.43 (s, 3H), 1.38 (s, 3H), 1.29 (s, 3H). **^{13}C NMR** (126 MHz, $CDCl_3$) δ 144.3, 139.5, 127.9 (2C), 127.3, 109.7, 109.0, 97.0, 73.5, 71.2, 70.7, 69.2, 44.7, 26.3, 26.0, 25.0, 24.4. **FT-IR** (cm^{-1}, neat, ATR): 2981, 1730, 1382, 1255, 1210, 1149, 1068, 1001, 957, 867.

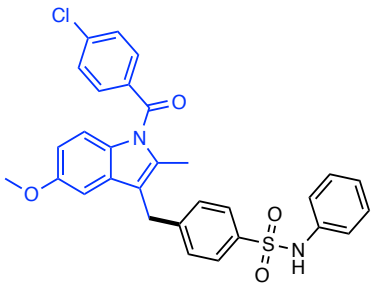

4-((1-(4-Chlorobenzoyl)5-methoxy-2-methyl-1*H*-indol-3yl)methyl-*N* phenylbenzenesulfonamide, **33** (190.1 mg, 70%) was prepared following *GP2*. The product was obtained as a yellow foam. **^{1}H NMR** (500 MHz, $CDCl_3$) δ 7.63 (dd, *J* = 14.9, 8.2 Hz, 4H), 7.43

(d, J = 8.5 Hz, 2H), 7.24 – 7.19 (m, 2H), 7.16 (t, J = 7.8 Hz, 2H), 7.09 – 7.00 (m, 3H), 6.83 (d, J = 8.5 Hz, 1H), 6.61 (d, J = 8.7 Hz, 2H), 4.32 (s, 1H), 3.99 (s, 2H), 3.66 (s, 3H), 2.29 (s, 3H). **^{13}C NMR** (126 MHz, $CDCl_3$) δ 168.5, 156.1, 145.7, 139.4, 137.1, 136.6, 135.6, 134.0, 131.3 (2C), 131.2 (2C), 130.9 (2C), 129.4 (2C), 129.3 (2C), 128.9 (2C), 127.7, 125.5, 121.7, 116.9, 115.2, 111.4, 101.7, 55.8, 30.0, 13.5. **FT-IR** (cm^{-1}, neat, ATR): 3253, 2927, 1678, 1596, 1401, 1352, 1224, 1090, 1066, 832. **HRMS** (ESI) calc for $C_{30}H_{26}ClN_2O_4S$ $[M+H]^+$: 545.1302, found 545.1293.

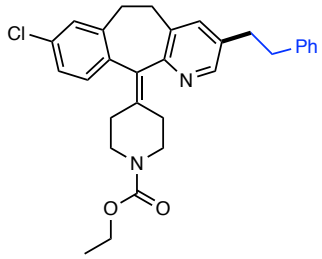

Ethyl 4-(8-Chloro-3-phenethyl-5,6-dihydro-11*H*-benzo[5,6]cyclohepta[1,2-*b*]pyridine-11-ylidene)piperidine-1-carboxylate, **34** (153.4 mg, 63%) was prepared following *GP2*. The product was obtained as a yellow oil. **^{1}H NMR** (500 MHz, $CDCl_3$) δ 8.23 (s, 1H), 7.33 – 7.06 (m, 9H), 4.14 (q, J = 7.2 Hz, 2H), 3.81 – 3.78 (m, 2H), 3.39 – 3.30 (m, 2H), 3.17 – 3.01 (m, 2H), 2.94 – 2.68 (m, 5H), 2.57 – 2.40 (m, 1H), 2.31 – 2.29 (m, 3H), 1.25 (t, J = 7.0 Hz, 4H). **^{13}C NMR** (126 MHz, $CDCl_3$) δ 155.6, 154.5, 146.6, 141.0, 139.7, 138.0, 135.7, 133.0, 130.6 (2C), 129.0 (2C), 128.6 (2C), 128.5 (4C), 126.3 (2C), 61.4, 44.9 (2C), 37.5, 34.6, 31.7, 31.6, 30.9, 30.7, 14.8. **FT-IR** (cm^{-1}, neat, ATR): 2923, 2856, 1693, 1470, 1385, 1277, 1227, 1172, 1115, 1029, 997. **HRMS** (ESI) calc for $C_{30}H_{32}ClN_2O_2$ $[M+H]^+$: 487.2152, found 487.2148.

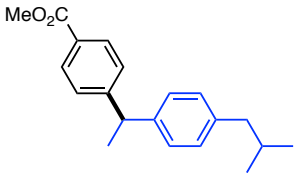

Methyl 4-(1-(4-Isobutylphenyl)ethyl)benzoate, **35** (0.29 mmol, 86 mg, 58%) was prepared following *GP2*. The product was obtained as a colorless foam. **^{1}H NMR** (300 MHz, $CDCl_3$): δ 8.03 – 7.83 (m, 2H), 7.32 – 7.26 (m, 2H), 7.14 – 7.01 (m, 4H), 4.17 (q, *J* = 7.3 Hz, 1H), 3.89 (s, 3H), 2.43 (d, *J* = 7.2 Hz, 2H), 1.88 – 1.81 (m, 1H), 1.64 (d, *J* = 7.2 Hz, 3H), 0.89 (d, *J* = 6.6 Hz, 6H). **^{13}C NMR** (75 MHz, $CDCl_3$): δ 167.2, 152.2, 142.8, 139.8, 129.9 (2C), 129.3 (2C), 128.0 (2C), 127.8 (2C), 127.4 (2C), 52.1, 45.1, 44.6, 30.3, 22.5, 21.8. **FT-IR** (cm^{-1}, neat, ATR): 2953, 1724, 1608, 1434, 1278, 1179, 1112, 1014, 848. **HRMS** (ESI) calc for $C_{20}H_{25}O_2$ $[M+H]^+$: 297.1849, found 297.1853.

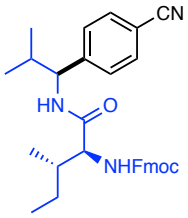

(9*H*-Fluoren-9-yl)methyl (1-((1-(4-cyanophenyl)-2-methylpropyl)amino)-4-methyl-1-oxopentan-2-yl)carbamate, **36** (168 mg, 65%, dr: 1.1:1) was prepared following *GP2*. The product was obtained as a colorless oil. **^{1}H NMR** (300 MHz, DMSO-d_6): δ 7.95 – 7.84 (m, 3H), 7.80 – 7.65 (m, 4H), 7.54 – 7.20 (m, 5H), 4.60 (q, *J* = 8.6 Hz, 1H), 4.36 – 4.10 (m, 3H), 3.99 – 3.90 (m, 1H), 2.02 – 1.87 (m, 1H), 1.70 – 1.65 m, 1H), 1.51 – 1.00 (m, 3H), 0.93 – 0.53 (m, 13H). **^{13}C NMR** (75 MHz, DMSO-d_6): δ 171.1, 156.0, 148.6, 143.9, 143.8, 140.7, 132.0, 128.9 128.2, 128.1, 127.6, 127.3, 127.0, 125.4, 120.1, 118.9, 109.5, 65.6 59.0, 58.5, 46.7, 46.0, 36.0, 32.6, 32.5, 20.1, 19.6, 19.6, 18.9, 18.5, 15.5, 15.2. **FT-IR** (cm^{-1}, neat, ATR): 3296, 3064, 2963, 1770,

1723, 1655, 1533, 1129, 1008. **HRMS** (ESI) calc for $C_{32}H_{35}NaN_3O_3$ $[M+H]^+$: 532.2570, found 532.2566.

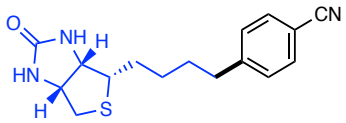

4-(4-((3a*S*,4*S*,6a*R*)-2-Oxohexahydro-1*H*-thieno[3,4-*d*]imidazole-4-yl)butyl)benzonitrile (Biotin Derivative), **37** (130 mg, 86%) was prepared following *GP2*. The product was obtained as a pale-yellow oil. **^{1}H NMR** (600 MHz, $CDCl_3$): δ 7.42 – 7.37 (m, 2H), 7.15 – 7.09 (m, 2H), 5.88 (s, 1H), 5.56 (s, 1H), 4.33 (dd, *J* = 8.0, 4.9 Hz, 1H), 4.11 (ddd, *J* =8.0, 4.7, 1.7 Hz, 1H), 2.72 (dd, *J* = 12.7, 5.0 Hz, 1H), 2.62 (d, *J* = 12.7 Hz, 1H), 2.51 (t, *J* = 7.7 Hz, 3H), 1.55 – 1.46 (m, 3H), 1.33 – 1.21 (m, 3H). **^{13}C NMR** (151 MHz, $CDCl_3$): δ 163.3, 147.9, 131.9 (2C), 129.0 (2C), 118.9, 109.3, 61.8, 60.0, 55.4, 40.3, 35.6, 30.6, 28.4, 28.3. **FT-IR** (cm^{-1}, neat, ATR): 2961, 2864, 1703, 1449, 1346, 1204, 1125, 1077, 1009, 576. **HRMS** (ESI) calc for $C_{16}H_{20}N_3OS$ $[M+H]^+$: 302.1322, found 302.1318.

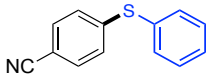

4-(Phenylthio)benzonitrile, **38** (90 mg, 85%) was prepared following *GP2*. The product was obtained as a colorless oil. **^{1}H NMR** (500 MHz, $CDCl_3$) δ 7.54 – 7.37 (m, 7H), 7.16 (d, *J* = 8.2 Hz, 2H). **^{13}C NMR** (126 MHz, $CDCl_3$) δ 145.8, 134.6 (2C), 132.5 (2C), 130.9, 130.0, 129.5 (2C), 127.4 (2C), 118.9, 108.8. **FT-IR** (cm^{-1}, neat, ATR): 2226, 1592, 1484, 1440, 1401, 1080, 1016, 822, 749, 691, 543. **HRMS** (EI) calc for $C_{13}H_9NS$ $[M]^+$: 211.0456, found: 211.0450.

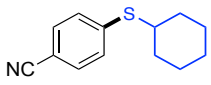

4-(Cyclohexylthio)benzonitrile, **39** (56 mg, 51%) was prepared following *GP2*. The product was obtained as a colorless oil. **^{1}H NMR** (400 MHz, $CDCl_3$) δ 7.54 – 7.49 (m, 2H), 7.36 – 7.31 (m, 2H), 3.29 (tt, *J* = 10.3, 3.7 Hz, 1H), 2.12 – 1.95 (m, 2H), 1.83 – 1.79 (m, 2H), 1.72 – 1.60 (m, 1H), 1.51 – 1.19 (m, 5H). **^{13}C NMR** (101 MHz, $CDCl_3$) δ 144.1, 132.3 (2C), 128.7 (2C), 119.1, 108.5, 45.0, 33.1 (2C), 26.0 (2C), 25.7. **FT-IR** (cm^{-1}, neat, ATR): 2931, 2854, 2225, 1592, 1485, 1449, 1088, 820, 544. **HRMS** (EI) calc for $C_{13}H_{15}NS$ $[M]^+$: 217.0925, found: 217.0923.

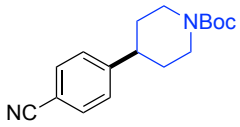

***tert*-Butyl 4-(4-Cyanophenyl)piperidine-1-carboxylate**, **40** (121 mg, 84%) was prepared following *GP2*. The product was obtained as a colorless oil. **^{1}H NMR** (400 MHz, $CDCl_3$) δ 7.72 – 7.51 (m, 2H), 7.32 – 7.27 (m, 2H), 4.26 (s, 2H), 2.92 – 2.63 (m, 3H), 1.87 – 1.74 (m, 2H), 1.60 (qd, *J* = 12.7, 4.4 Hz, 2H), 1.47 (s, 9H). **^{13}C NMR** (101 MHz, $CDCl_3$) δ 154.9, 151.3, 132.5 (2C), 128.8, 127.8 (2C), 119.1, 110.4, 79.8, 43.0 (2C), 32.9, 29.8, 28.6 (3C). **FT-IR** (cm^{-1}, neat, ATR): 1476, 1465, 1392, 1125, 1107, 986, 884, 860. **HRMS** (ESI) calcd for $C_{17}H_{23}N_2O_2$ $[M+H]^+$: 287.1760, found: 287.1747.

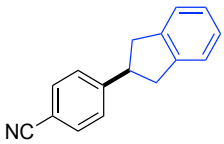

4-(2,3-Dihydro-1*H*-inden-2-yl)benzonitrile, **41** (77 mg, 70%) was prepared following *GP2*. The product was obtained as a colorless oil. **^{1}H NMR** (500 MHz, $CDCl_3$) δ 7.70 – 7.50 (m, 2H), 7.40 – 7.35 (m, 2H), 7.28 – 7.17 (m, 4H), 3.75 – 3.72 (m, 1H), 3.39 (dd, *J* = 15.6, 8.2 Hz, 2H), 3.06

(dd, J = 15.6, 8.2 Hz, 2H). **^{13}C NMR** (126 MHz, $CDCl_3$) δ 151.4, 142.2 (2C), 132.5 (2C), 128.0 (2C), 126.9 (2C), 124.5 (2C), 119.2, 110.2, 45.4, 40.8 (2C). **FT-IR** (cm^{-1}, neat, ATR): 2945, 2905, 2840, 2222, 1607, 1475, 1457, 1178, 1006, 852, 829, 754. **HRMS** (EI) calc for $C_{16}H_{13}NS$ $[M]^+$: 219.1048, found: 219.1044.

4.5 References

(1) For selected examples, see: (a) R. Jana, T. P. Pathak, M. S. Sigman, *Chem. Rev.* **2011**, *111*, 1417-1492; (b) P. G. Gildner, T. J. Colacot, *Organometallics* **2015**, *34*, 5497-5508; (c) C. C. C. Johansson Seechurn, M. O. Kitching, T. J. Colacot, V. Snieckus, *Angew. Chem. Int. Ed.* **2012**, *51*, 5062-5085; (d) L.-C. Campeau, N. Hazari, *Organometallics* **2019**, *38*, 3-35; (e) J. Choi, G. C. Fu, *Science* **2017**, *356*, 7230; (f) J. Gu, X. Wang, W. Xue, H. Gong, *Org. Chem. Front.* **2015**, *2*, 1411-1421; (g) X. Hu, *Chem. Sci.* **2011**, *2*, 1867-1886; (h) A. Kaga, S. Chiba, *ACS Catal.* **2017**, *7*, 4697-4706; (i) X. Ma, B. Murray, M. R. Biscoe, *Nat. Rev. Chem.* **2020**, *4*, 584-599; (j) D. J. Weix, *Acc. Chem. Res.* **2015**, *48*, 1767-1775.

(2) For selected examples, see: (a) D. A. Everson, R. Shrestha, D. J. Weix, *J. Am. Chem. Soc.* **2010**, *132*, 920-921; (b) D. A. Everson, D. J. Weix, *J. Org. Chem.* **2014**, *79*, 4793-4798; (c) J. Gu, C. Qiu, W. Lu, Q. Qian, K. Lin, H. Gong, *Synthesis* **2017**, *49*, 1867-1873; (d) X. Yu, T. Yang, S. Wang, H. Xu, H. Gong, *Org. Lett.* **2011**, *13*, 2138-2141; (e) B. P. Woods, M. Orlandi, C.-Y. Huang, M. S. Sigman, A. G. Doyle, *J. Am. Chem. Soc.* **2017**, *139*, 5688-5691; (f) Y. Jin, H. Yang, C. Wang, *Org. Lett.* **2019**, *21*, 7602-7608; (g) N. T. Kadunce, S. E. Reisman, *J. Am. Chem. Soc.* **2015**, *137*, 10480-10483; (h) C. E. I. Knappke, S. Grupe, D. Gärtner, M. Corpet, C. Gosmini, A. Jacobi von Wangelin, *Chem. Eur. J.* **2014**, *20*, 6828-6842; (i) T. Moragas, A. Correa, R. Martin, *Chem. Eur. J.* **2014**, *20*, 8242-8258; (j) Z.-X. Tian, J.-B. Qiao, G.-L. Xu, X. Pang, L. Qi, W.-Y. Ma, Z.-Z. Zhao, J. Duan, Y.-F. Du, P. Su, X.-Y. Liu, X.-Z. Shu, *J. Am. Chem. Soc.* **2019**, *141*,

7637-7643; (k) A. H. Cherney, S. E. Reisman, *J. Am. Chem. Soc.* **2014**, *136*, 14365-14368; (l) K. M. M. Huihui, J. A. Caputo, Z. Melchor, A. M. Olivares, A. M. Spiewak, K. A. Johnson, T. A. DiBenedetto, S. Kim, L. K. G. Ackerman, D. J. Weix, *J. Am. Chem. Soc.* **2016**, *138*, 5016-5019; For selected examples using electrochemical methods, see: (m) H. Li, C. P. Breen, H. Seo, T. F. Jamison, Y.-Q. Fang, M. M. Bio, *Org. Lett.* **2018**, *20*, 1338-1341; (n) T. Koyanagi, A. Herath, A. Chong, M. Ratnikov, A. Valiere, J. Chang, V. Molteni, J. Loren, *Org. Lett.* **2019**, *21*, 816-820; For cross-electrophile couplings in biological environments, see: (o) D. T. Flood, S. Asai, X. Zhang, J. Wang, L. Yoon, Z. C. Adams, B. C. Dillingham, B. B. Sanchez, J. C. Vantourout, M. E. Flanagan, D. W. Piotrowski, P. Richardson, S. A. Green, R. A. Shenvi, J. S. Chen, P. S. Baran, P. E. Dawson, *J. Am. Chem. Soc.* **2019**, *141*, 9998-10006.

(3) For selected examples on decarboxylative arylation using carbon preformed nucleophiles, see: (a) T.-G. Chen, H. Zhang, P. K. Mykhailiuk, R. R. Merchant, C. A. Smith, T. Qin, P. S. Baran, *Angew. Chem. Int. Ed.* **2019**, *58*, 2454-2458; (b) J. Cornella, J. T. Edwards, T. Qin, S. Kawamura, J. Wang, C.-M. Pan, R. Gianatassio, M. Schmidt, M. D. Eastgate, P. S. Baran, *J. Am. Chem. Soc.* **2016**, *138*, 2174-2177; (c) X.-G. Liu, C.-J. Zhou, E. Lin, X.-L. Han, S.-S. Zhang, Q. Li, H. Wang, *Angew. Chem. Int. Ed.* **2018**, *57*, 13096-13100; (d) F. Toriyama, J. Cornella, L. Wimmer, T.-G. Chen, D. D. Dixon, G. Creech, P. S. Baran, *J. Am. Chem. Soc.* **2016**, *138*, 11132-11135.

(4) M. J. Buskes, M.-J. Blanco, *Molecules* **2020**, *25*, 3493.

(5) (a) M. Kuroboshi, Y. Waki, H. Tanaka, *Synlett* **2002**, *2002*, 0637-0639; (b) M. Kuroboshi, Y. Waki, H. Tanaka, *J. Org. Chem.* **2003**, *68*, 3938-3942.

(6) (a) L. L. Anka-Lufford, K. M. M. Huihui, N. J. Gower, L. K. G. Ackerman, D. J. Weix, *Chem. Eur. J.* **2016**, *22*, 11564-11567; (b) D. A. Everson, B. A. Jones, D. J. Weix, *J. Am. Chem. Soc.* **2012**, *134*, 6146-6159; For a dual catalytic system utilizing TDAE as reductant, see: (c) D. J.

Charboneau, E. L. Barth, N. Hazari, M. R. Uehling, S. L. Zultanski, *ACS Catal.* **2020**, *10*, 12642-12656.

(7) N. Suzuki, J. L. Hofstra, K. E. Poremba, S. E. Reisman, *Org. Lett.* **2017**, *19*, 2150-2153.

(8) (a) C. Burkholder, W. R. Dolbier, M. Médebielle, *J. Org. Chem.* **1998**, *63*, 5385-5394; (b) A. Kolomeitsev, M. Médebielle, P. Kirsch, E. Lork, G.-V. Röschenthaler, *J. Chem. Soc., Perkin Trans. 1*, **2000**, 2183-2185; (c) F. Glaser, C. B. Larsen, C. Kerzig, O. S. Wenger, *Photochem. Photobiol. Sci.* **2020**, *19*, 1035-1041.

(9) For selected examples, see: (a) K. Shimomaki, K. Murata, R. Martin, N. Iwasawa, *J. Am. Chem. Soc.* **2017**, *139*, 9467-9470; (b) J. Yi, S. O. Badir, L. M. Kammer, M. Ribagorda, G. A. Molander, *Org. Lett.* **2019**, *21*, 9, 3346-3351; (c) T. Q. Chen, D. W. C. MacMillan, *Angew. Chem. Int. Ed.* **2019**, *58*, 14584-14588; (d) Q.-Y. Meng, T. E. Schirmer, K. Katou, B. König, *Angew. Chem. Int. Ed.* **2019**, *58*, 5723-5728; (e) F. Cong, X.-Y. Lv, C. S. Day, R. Martin, *J. Am. Chem. Soc.* **2020**, *142*, 20594-20599; (f) H. Guan, Q. Zhang, P. J. Walsh, J. Mao, *Angew. Chem. Int. Ed.* **2020**, *59*, 5172-5177; (g) S. Patel, S. O. Badir, G. A. Molander, *Trends Chem.* **2021**, *3*, 161-175; (h) P. Zhang, C. C. Le, D. W. C. MacMillan, *J. Am. Chem. Soc.* **2016**, *138*, 8084-8087.

(10) For selected examples, see: (a) J. C. Tellis, D. N. Primer, G. A. Molander, *Science* **2014**, *345*, 433-436; (b) Z. Zuo, D. T. Ahneman, L. Chu, J. A. Terrett, A. G. Doyle, D. W. MacMillan, *Science* **2014**, *345*, 437-440; (c) D. N. Primer, I. Karakaya, J. C. Tellis, G. A. Molander, *J. Am. Chem. Soc.* **2015**, *137*, 2195-2198; (d) B. J. Shields, A. G. Doyle, *J. Am. Chem. Soc.* **2016**, *138*, 12719-12722; (e) D. R. Heitz, K. Rizwan, G. A. Molander, *J. Org. Chem.* **2016**, *81*, 7308–7313; (f) J. C. Tellis, C. B. Kelly, D. N. Primer, M. Jouffroy, N. R. Patel, G. A. Molander, *Acc. Chem. Res.* **2016**, *49*, 1429-1439; (g) J. K. Matsui, S. B. Lang, D. R. Heitz, G. A. Molander, *ACS Catal.* **2017**, *7*, 2563–2575; (h) J. A. Milligan, J. P. Phelan, S. O. Badir, G. A. Molander, *Angew. Chem.*

Int. Ed. **2019**, *58*, 6152-6163; (i) S. O. Badir, G. A. Molander, *Chem* **2020**, *6*, 1327-1339; (j) A. Lipp, S. O. Badir, G. A. Molander, *Angew. Chem. Int. Ed.* **2021**, *60*, 1714-1726.

(11) O. Gutierrez, J. C. Tellis, D. N. Primer, G. A. Molander, M. C. Kozlowski, *J. Am. Chem. Soc.* **2015**, *137*, 4896-4899.

(12) K. Teegardin, J. I. Day, J. Chan, J. Weaver, *Org. Process Res. Dev.* **2016**, *20*, 1156-1163.

(13) For selected examples, see (a) L. Buzzetti, A. Prieto, S. R. Roy, P. Melchiorre, *Angew. Chem. Int. Ed.* **2017**, *56*, 15039-15043; (b) G. Goti, B. Bieszczad, A. Vega-Peñaloza, P. Melchiorre, *Angew. Chem. Int. Ed.* **2019**, *58*, 1213-1217; (c) T. van Leeuwen, L. Buzzetti, L. A. Perego, P. Melchiorre, *Angew. Chem. Int. Ed.* **2019**, *131*, 5007-5011; (d) E. Gandolfo, X. Tang, S. Raha Roy, P. Melchiorre, *Angew. Chem. Int. Ed.* **2019**, *58*, 16854-16858; (e) B. Bieszczad, L. A. Perego, P. Melchiorre, *Angew. Chem. Int. Ed.* **2019**, *58*, 16878-16883; (f) N. Alandini, L. Buzzetti, G. Favi, T. Schulte, L. Candish, K. D. Collins, P. Melchiorre, *Angew. Chem. Int. Ed.* **2020**, *59*, 5248-5253; (g) L. Cardinale, M. O. Konev, A. J. von Wangelin, *Chem. Eur. J.* **2020**, *26*, 8239-8243.

(14) For a selected example on the direct excitation of boracene-based alkylborates, see: Y. Sato, K. Nakamura, Y. Sumida, D. Hashizume, T. Hosoya, H. Ohmiya, *J. Am. Chem. Soc.* **2020**, *142*, 9938-9943.

(15) (a) R. S. Varma, D. Kumar, *Tetrahedron Lett.* **1999**, *40*, 21-24; (b) X. Bi, T. Tang, X. Meng, M. Gou, X. Liu, P. Zhao, *Catal. Sci. Technol.* **2020**, *10*, 360-371; (c) C. Zheng, S.-L. You, *Chem. Soc. Rev.* **2012**, *41*, 2498-2518; (d) G.-B. Shen, L. Xie, H.-Y. Yu, J. Liu, Y.-H. Fu, M. Yan, *RSC Adv.* **2020**, *10*, 31425-31434.

(16) For selected examples, see: (a) G. E. Crisenza, D. Mazzarella, P. Melchiorre, *J. Am. Chem. Soc.* **2020**, *142*, 5461-5476; (b) A. Noble, R. S. Mega, D. Pflästerer, E. L. Myers, V. K. Aggarwal, *Angew. Chem. Int. Ed.* **2018**, *57*, 2155-2159; (c) B. Liu, C.-H. Lim, G. Miyake, *J. Am.*

Chem. Soc. **2017**, *139*, 39, 13616-13619; (d) J. Wu, P. S. Grant, X. Li, A. Noble, V. K. Aggarwal, *Angew. Chem. Int. Ed.* **2019**, *58*, 5697-5701; (e) A. Fawcett, J. Pradeilles, Y. Wang, T. Mutsuga, E. L. Myers, V. K. Aggarwal, *Science* **2017**, *357*, 283-286; (f) L. Chen, J. Liang, Z.-Y. Chen, J. Chen, M. Yan, X.-j. Zhang, *Adv. Synth. Catal.* **2019**, *361*, 956-960; (g) J. Zhang, Y. Li, R. Xu, Y. Chen, *Angew. Chem. Int. Ed.* **2017**, *129*, 12793-12797; (h) D. Chen, L. Xu, T. Long, S. Zhu, J. Yang, L. Chu, *Chem. Sci.* **2018**, *9*, 9012-9017; (i) C. Zheng, G.-Z. Wang, R. Shang, *Adv. Synth. Catal.* **2019**, *361*, 4500-4505.

(17) S. Murarka, *Adv. Synth. Catal.* **2018**, *360*, 1735-1753.

(18) (a) B. Lipp, T. Opatz, *Photochemistry,* **2019**, *46*, 370-394; (b) G. J. Kavarnos, N. J. Turro, *Chem. Rev.* **1986**, *86*, 401-449; (c) N. J. Turro, in *Pure Appl. Chem.* **1981**, *53*, 259-286; (d) N. J. Turro, V. Rammamurthy, W. Cherry, W. Farneth, *Chem. Rev.* **1978**, *78*, 125-145.

(19) (a) R. Foster, *J. Phys. Chem.* **1980**, *84*, 2135-2141; (b) S. V. Rosokha, J. K. Kochi, *Acc. Chem. Res.* **2008**, *41*, 641-653.

(20) J. Jung, J. Kim, G. Park, Y. You, E. J. Cho, *Adv. Synth. Catal.* **2016**, *358*, 74-80.

(21) (a) B. Giese, *Angew. Chem. Int. Ed.* **1983**, *22*, 753-764; (b) J. Huang, S. P. Nolan, *J. Am. Chem. Soc.* **1999**, *121*, 9889-9890; (c) G. Dyker, *Angew. Chem. Int. Ed.* **1999**, *38*, 1698-1712.

(22) (a) T. C. Sherwood, N. Li, A. N. Yazdani, T. G. M. Dhar, *J. Org. Chem.* **2018**, *83*, 5, 3000-3012; (b) L. Kammer, A. Rahman, T. Opatz, *Molecules* **2018**, *23*, 764; (c) R. A. Garza-Sanchez, A. Tlahuext-Aca, G. Tavakoli, F. Glorius, *ACS Catal.* **2017**, *7*, 4057-4061; (d) M.-C. Fu, R. Shang, B. Zhao, B. Wang, Y. Fu, *Science* **2019**, *363*, 1429-1434.

(23) F. Minisci, R. Bernardi, F. Bertini, R. Galli, M. Perchinummo, *Tetrahedron* **1971**, *27*, 3575-3579.

(24) G. Alván, M. Orme, L. Bertilsson, R. Ekstrand, L. Palmér, *Clin. Pharmacol. Ther.* **1975**, *18*, 364-373.

(25) R. S. Geha, E. O. Meltzer, *J. Allergy Clin. Immunol.* **2001**, *107*, 751-762.

(26) (a) S. Graßl, C. Hamze, T. J. Koller, P. Knochel, *Chem. Eur. J.* **2019**, *25*, 3752-3755; (b) V. P. Reddy, A. V. Kumar, K. Swapna, K. R. Rao, *Org. Lett.* **2009**, *11*, 1697-1700.

(27) R. Martin-Montero, V. R. Yatham, H. Yin, J. Davies, R. Martin, *Org. Lett.* **2019**, *21*, 2947-2951.

(28) H. A. Benesi, J. Hildebrand, *J. Am. Chem. Soc.* **1949**, *71*, 2703-2707.

(29) J. S. Renny, L. L. Tomasevich, E. H. Tallmadge, D. B. Collum, *Angew. Chem. Int. Ed.* **2013**, *52*, 11998-12013.

(30) For a selected example, see: G. Pratsch, G. L. Lackner, L. E. Overman, *J. Org. Chem.* **2015**, *80*, 6025–6036.

(32) L. M. Schneider, V. M. Schmiedel, T. Pecchioli, D. Lentz, C. Merten, M. Christmann, *Org. Lett.* **2017**, *19*, 2310-2313.

Author Contributions: Shorouk O. Badir conceived the topic, carried out the reaction optimization, and performed the mechanistic investigation. All authors contributed to the experimental work and discussion of results. Shorouk O. Badir and Lisa Marie Kammer prepared the manuscript with input from Gary A. Molander.

Chapter 5. Photoinduced 1,2-Dicarbofunctionalization of Alkenes with Organotrifluoroborate Nucleophiles via Radical/Polar Crossover[††]

5.1 Introduction

The integration of diverse radical progenitors in Ni/photoredox dual manifolds has facilitated the synthesis of chemical motifs with a high content of C(sp^3) carbons in the presence of sensitive functional groups. Although transition-metal-mediated protocols, with[1] or without the aid of a photocatalyst[2,3,4,5,6] (Figure 5.1 A), have been utilized in the synthesis of 1,2-substituted products, these cross-couplings remain predominantly applicable to the construction of one C–C linkage. Typically, these processes are complicated by numerous deleterious pathways, such as β-hydride elimination, homocoupling, isomerization, or proto-demetalation.[1] To expand access to uncharted chemical space, the vicinal difunctionalization of alkenes has emerged as an enabling technology in organic synthesis to access diverse structural skeletons from readily available building blocks.[1] In particular, intermolecular 1,2-dicarbofunctionalization (DCF) reactions represent a powerful method to install two carbon subunits across an unsaturated system in one step with an accompanying increase in molecular complexity.[7] As a complementary approach to metallaphotoredox catalysis, we examined the utility of photochemical radical/polar crossover in sequential C–C bond formation without the need for alkylmetal species.

Radical/polar crossover (RPC) has recently been enlisted to assemble challenging structural motifs under mild reaction conditions (Figure 5.1 B).[8,9] Under RPC paradigms, odd-electron intermediates are generated through single-electron transfer (SET) and then engage in

---

[††] Reproduced in part from M. J. Cabrera-Afonso, A. Sookezian, S. O. Badir, M. El Khatib, G. A. Molander, *Chem. Sci.* **2021**, Advance Article. This article is licensed under a Creative Commons Attribution NonCommercial 3.0 Unported License.

further transformations. The resulting radical species can subsequently undergo single-electron oxidation or reduction to enter the two-electron reaction domain for further diversification. Although photo- and electrochemical RPC-mediated intermolecular 1,2-DCFs that proceed with in situ formed carbanions have been reported, these efforts are largely limited to carbonyl alkylation[8d,10] or carbocarboxylation.[8d,11] Complementary RPC protocols operating through carbocation intermediates via oxidative quenching pathways have been studied more extensively, but remain predominantly applicable to heteroatom-based nucleophiles such as alcohols, amines, water, carboxylic acids, amides, and halogens.[12] Methods to incorporate carbon-centered nucleophiles typically rely on strongly nucleophilic, electron-rich systems in conjunction with Lewis acids or peroxides as additives.[13] In this vein, the development of a general RPC route employing two carbon-based coupling partners for DCF remains elusive.

As part of a program centered on the development of catalytic tools for alkene functionalization, a photochemical intermolecular 1,2-dicarbofunctionalization of olefins with alkyl *N*-(acyloxy)phthalimide redox-active esters (RAEs) as radical progenitors has been developed (Figure 5.1 C). RAEs are bench-stable solids readily accessible from carboxylic acids with an established propensity to undergo decarboxylative fragmentation upon single-electron reduction.[14] We envisioned that radical addition to vinylarenes would generate key radical and carbocation intermediates that could be harnessed in sequential bond formation through RPC.

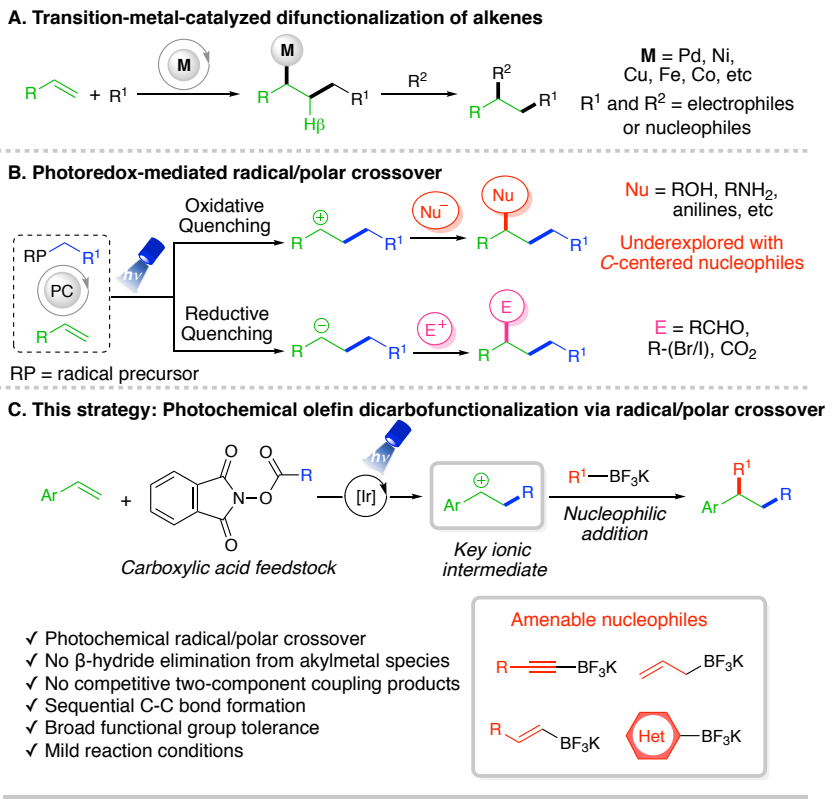

Figure 5.1. Strategies toward olefin 1,2-difunctionalization and envisioned transformation.

5.2 Results and Discussion

With these goals in mind, the interrogation of potassium organotrifluoroborates as nucleophiles to construct C–C linkages under photoredox catalysis was considered, as they have been shown to engage in nucleophilic addition reactions under Brønsted and Lewis acid catalysis.[15] Furthermore, alkynyltrifluoroborates have been enlisted as alternative nucleophilic partners in Suzuki-Miyaura cross-couplings, with the Bsp^3–Csp bond being adequately polarized to engender a direct transmetalation event.[16] From a synthetic standpoint and through the same RPC reactivity mode, the proposed strategy would facilitate carboallylation, carboalkenylation, carboalkynylation, and carboarylation from commodity chemicals with regio- and chemoselective control. Notably, this net-neutral RPC process is driven by SET events that occur predominantly

between the photocatalyst and substrates/intermediates, bypassing the requirement for stoichiometric external reductants or oxidants.

To examine the feasibility of the proposed reaction design, 4-acetoxystyrene **1a**, aliphatic RAE **2a**, and potassium (2-phenylethynyl)trifluoroborate **3a** were employed (Figure 5.2). A more detailed optimization of the equivalences of reaction components, catalyst loading, solvent, and reaction concentration is provided in the experimental section. Here, the most relevant findings are highlighted, namely the critical performance of photoredox catalysts on the DCF outcome. Notably, the crux of this net-neutral RPC approach is a series of well-orchestrated, single-electron oxidation and reduction steps. To achieve chemo- and regio-selectivity, the following criteria must be considered: (i) The aliphatic RAE should be more susceptible to reduction than the alkene or the resulting benzylic radical formed upon addition to the olefin. (ii) The alkyl radical should react with alkene **1** at a rate faster than its single-electron oxidation to a carbocation intermediate or radical dimerization. (iii) The rate of benzylic radical oxidation must be competitive with its addition to another equivalent of the styrene. (iv) The rate of single-electron oxidation of the benzylic radical must be faster than that of the radical intermediate generated from RAE reduction. (v) The rate of nucleophilic addition of the potassium organotrifluoroborate to the benzylic carbocation should take place preferentially over single-electron oxidation of the organoboron reagent under photoredox conditions. (vi) This rate must also be competitive with the nucleophilic addition of phthalimide anions generated upon decarboxylative fragmentation of the RAE. In this vein, the choice of photocatalyst significantly impacts product distributions. Given the propensity of RAEs to undergo SET ($E_{1/2}^{red}$ = -1.26 V vs SCE for 1-methylcyclohexyl-*N*-hydroxyphthalimide-ester[17]), a palette of catalysts in acetonitrile (MeCN) was surveyed (entries 1-13). Reducing iridium-based (Ir) photocatalysts in combination with 2-phenylpyridine (ppy) derived-ligands (entries 1-9) exhibited optimal reactivity, affording **4a** in excellent yield.

Importantly, in the absence of a highly oxidizing photocatalyst, the corresponding organotrifluoroborates would not undergo SET.[18] As expected, weaker reductants, **PC10** ($Ir^{IV}/*Ir^{III}$ $E_{1/2}$ = -1.00 V vs SCE[19]) and organic dye **PC11** ($PC^{\cdot+}/PC^*$ $E_{1/2}$ = -1.12 V vs SCE[19]), showed little (entry 11) to no conversion (entry 10). Notably, iron-based catalyst **PC12** ($Fe^{III}/*Fe^{II}$ $E_{1/2}$ = -1.65 V vs SCE[19]) and organic sensitizer **PC13** ($PC^{\cdot+}/PC^*$ $E_{1/2}$ = -2.1 V vs SCE[19]) resulted in full recovery of the styrene derivative (entries 12-13), presumably because they possess a short excited-state lifetime (for **PC11**, τ = ~ 0.8-2.3 ns[19]).

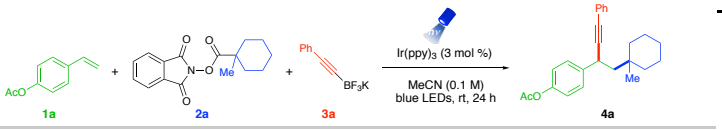

Entry	Deviation from Std Conditions	% Yield[a]	Entry	Deviation from Std Conditions	% Yield[a]
1	None	89	12	**PC12** instead of **PC1**	nr
2	**PC2** instead of **PC1**	81	13	**PC13** instead of **PC1**	nr
3	**PC3** instead of **PC1**	67	14	20 mol % $Cu(OTf)_2$	32
4	**PC4** instead of **PC1**	91	15	20 mol % $Yb(OTf)_3$	36
5	**PC5** instead of **PC1**	89	16	No PC	nr
6	**PC6** instead of **PC1**	52	17	No light	nr
7	**PC7** instead of **PC1**	58			
8	**PC8** instead of **PC1**	68			
9	**PC9** instead of **PC1**	81			
10	**PC10** instead of **PC1**	nr			
11	**PC11** instead of **PC1**	traces			

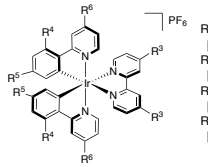

$R^3 = R^4 = R^5 = R^6 = H$; $[Ir(bpy)(ppy)_2]PF_6$ (**PC6**)
$R^3 = t$-Bu, $R^4 = R^5 = R^6 = H$; $[Ir(dtbbpy)(ppy)_2]PF_6$ (**PC7**)
$R^3 = t$-Bu, $R^4 = R^5$ = Me, $R^6 = H$; $[Ir(dtbbpy)(dMeppy)_2]PF_6$ (**PC8**)
$R^3 = R^5 = R^6 = t$-Bu, $R^4 = H$; $[Ir(dtbbpy)(dtbppy)_2]PF_6$ (**PC9**)

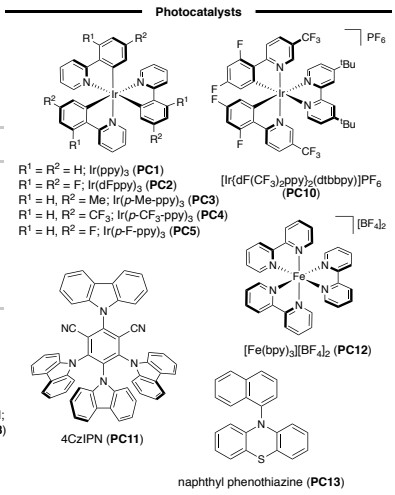

Figure 5.2. Optimization studies. Reaction conditions: styrene **1a** (0.1 or 0.2 mmol), RAE **2a** (1.5 equiv), potassium organotrifluoroborate salt **3a** (2 equiv), $Ir(ppy)_3$ (3 mol %) in MeCN (0.1 M), 24 h irradiation with blue LEDs (λ_{max} = 456 nm). [a]Yields were determined by ^1H NMR analysis using trimethoxybenzene as internal standard. Abbreviations: std, standard; nr, no reaction.

Inspired by precedents on the activation of RAEs with Lewis acids,[20] the influence of these additives on the outcome of the three-component photochemical paradigm was studied. Surprisingly, the addition of $Cu(OTf)_2$ or $Yb(OTf)_3$ led to a decrease in yield (entries 14-15).

Control experiments omitting light as well as photocatalyst validated the necessity of all reaction components to facilitate sequential bond formation (entries 16-17).

With suitable conditions established, the scope of RAEs with nucleophile **3a** was evaluated (Figure 5.3). In general, the reaction is amenable to an array of unactivated secondary and tertiary radical architectures. The method further benefits from broad substrate tolerance, facilitating the incorporation of a strained cyclobutane subunit (**4b**), a Boc-protected amine (**4d**), a bridged bicycle (**4e**), acyclic moieties, as well as biologically relevant scaffolds including lipid-lowering agent gemfibrozil (**4h**). In addition, efficient product formation occurs in the presence of an internal olefin (**4c**), showcasing the chemoselectivity of this protocol toward styrenyl-type systems. Notably, RAEs bearing reduction-labile chloride handles (**4g, 4k**, **4y**, **4ah**, **4ai**) can be introduced without compromising yields, delivering linchpins that can drive molecular complexity through subsequent transition-metal-mediated functionalization.

Next, the reactivity of various potassium organotrifluoroborates using 4-acetoxystyrene **1a** was evaluated (Figure 5.3). Carboallylation proved feasible, affording the difunctionalized product (**4j**) in good yield, while simultaneously incorporating an olefinic moiety that can engage in diverse downstream alkene transformations. Although progress has been made in conjunctive cross-couplings employing transition-metal catalysts with alkynyl-, alkenyl-, alkyl-, and aryl-electrophiles, the use of allyl counterparts remains scarce.[21,22] In addition to β-hydride elimination associated with alkylmetal species, these processes are further complicated by the generation of undesired two-component allylation products. Importantly, the allyl handle might be susceptible to additional insertion events, resulting in oligomerization.[21, 22] In this vein, the utility of the developed three-component allylation is partially driven by its ability to deliver two $C(sp^3)$–$C(sp^3)$ linkages selectively from readily available building blocks. Similarly, potassium

arylethynyltrifluoroborates bearing electron-donating (*para*-methoxy, **4k**) or electron-neutral (naphthyl, **4l**) substituents serve as effective nucleophiles.

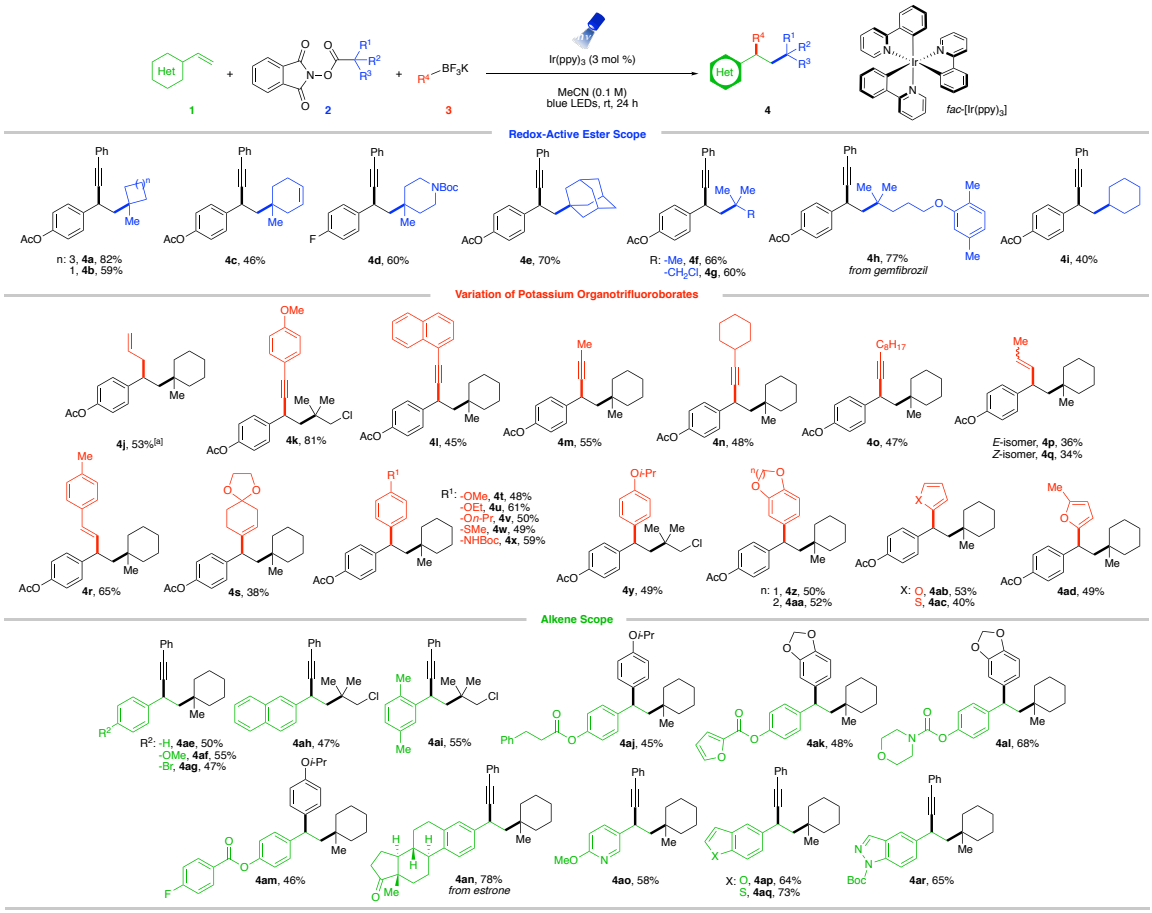

Figure 5.3. DCF scope. Reaction conditions: styrene **1** (0.3 mmol), RAE **2** (0.45 mmol, 1.5 equiv), potassium organotrifluoroborate salt **3** (0.6 mmol, 2 equiv), $Ir(ppy)_3$ (3 mol %) in MeCN (3.0 mL, 0.1 M), 24 h irradiation with blue LEDs (λ_{max} = 456 nm). [a]$[Ir(dtbbpy)(ppy)_2]PF_6$ (3 mol %) was used instead $Ir(ppy)_3$.

The phenyl moiety was successfully replaced by primary short- (**4m**) and long-chain (**4o**) alkyl groups as well as more sterically hindered carbocycles (**4n**). The scope was further extended to alkenyltrifluoroborates (**4p**-**4s**), with aryl-substituted derivatives performing slightly better

under the reaction conditions. Notably, both the (*E*)- and (*Z*)-isomers of 1-propenyltrifluoroborate resulted in product formation with retention of stereochemistry about the olefin (**4p**, **4q**).

Remarkably, aryltrifluoroborates function as competent nucleophiles, facilitating intermolecular 1,2-alkylarylation (Figure 5.3). Substitution at the *para*- and *meta*-positions of the aryl scaffolds was explored, whereby efficient photocoupling took place. Specifically, alkoxy derivatives, a methyl thioether, and a Boc-protected amine were successfully harnessed to afford difunctionalized synthetic frameworks (**4t**-**4aa**). The amenability of aryltrifluoroborates provides a facile, unique approach toward the synthesis of 1,1-diaryl compounds of significance in drug discovery efforts.[23] Furthermore, medicinally relevant heterocycles such as furan (**4ab**, **4ad**) and thiophene (**4ac**) moieties exhibited good reactivity. Notably, this photoredox-mediated RPC proceeds exceptionally well with electron-rich aryl systems that suffer from lower coupling efficiency in certain transition-metal-catalyzed cross-couplings. The mild reaction conditions (room temperature, additive-free, and near-neutral pH) serve to suppress side reactivity stemming from an otherwise competitive hydrodeboration of the trifluoroborate starting material.

Finally, the scope of olefins was investigated (Figure 5.3). In general, styrenes bearing no substitution, electron-donating, and electron-withdrawing groups at the *ortho*-, *meta*-, and *para*-positions exhibited comparable reactivity (**4ae**-**4ai**). Of note, aryl bromide **4ag** proved to be a suitable substrate with complete retention of the halide handle, providing a clear advantage in terms of scope over traditional transition-metal-catalyzed DCFs. A broad array of functional groups is tolerated, including esters, ketones, Boc-protected amines, and carbamates (**4aj**-**4ar**). Additionally, a substrate derived from estrone was examined, generating steroid derivative **4an** in excellent yield. Heterocyclic compounds including pyridine, benzofuran, benzothiophene, and indazole systems were readily incorporated under the developed conditions (**4ao**-**4ar**). In

particular, these Lewis basic moieties are traditionally challenging structures in cross-couplings because of their ability to bind and poison the catalyst.

To confirm this RPC protocol was unique to potassium organotrifluoroborates, boronic acid **3xa**, pinacol boronate **3xb**, and MIDA boronate **3xc** were tested as partner nucleophiles but proved ineffectual (Figure 5.4). These results are in accordance with the *N*-parameters reported by Mayr,[24] a solvent-dependent nucleophilicity scale, which identified potassium organotrifluoroborates as one of the most reactive nucleophilic organoboron sources.

To investigate the reaction mechanism, radical and carbocation trapping studies were performed under standard conditions (Figure 5.4). Addition of TEMPO (2,2,6,6-tetramethyl-1-piperidinyloxy) inhibited product generation. Specifically, recovery of 4-acetoxystyrene **1a** was observed, and the corresponding TEMPO adduct **5** was isolated and confirmed via NMR and HRMS analysis (Figure 5.4 B). To probe the intermediacy of carbocation species, nucleophilic trapping experiments were conducted using *O*-centered nucleophiles with slight modifications in the loading of these reagents (3.0 equiv of MeOH or 30.0 equiv of H_2O). The corresponding ether **6** and alcohol **7** were successfully isolated and characterized, providing further credence to the existence of an ionic pathway (Figure 5.4 C).

Stern-Volmer luminescence studies of individual reaction components established that the excited state photocatalyst was quenched most effectively by the aliphatic RAE with an observed constant K_{SV} of 1.4 x 10^4 M^{-1} (Figure 5.4 2D, see the Experimental Section). Furthermore, the photochemical quantum yield Φ of this reaction is 0.26, indicating that a radical chain mechanism is unlikely or inefficient (see the Experimental Section).[25]

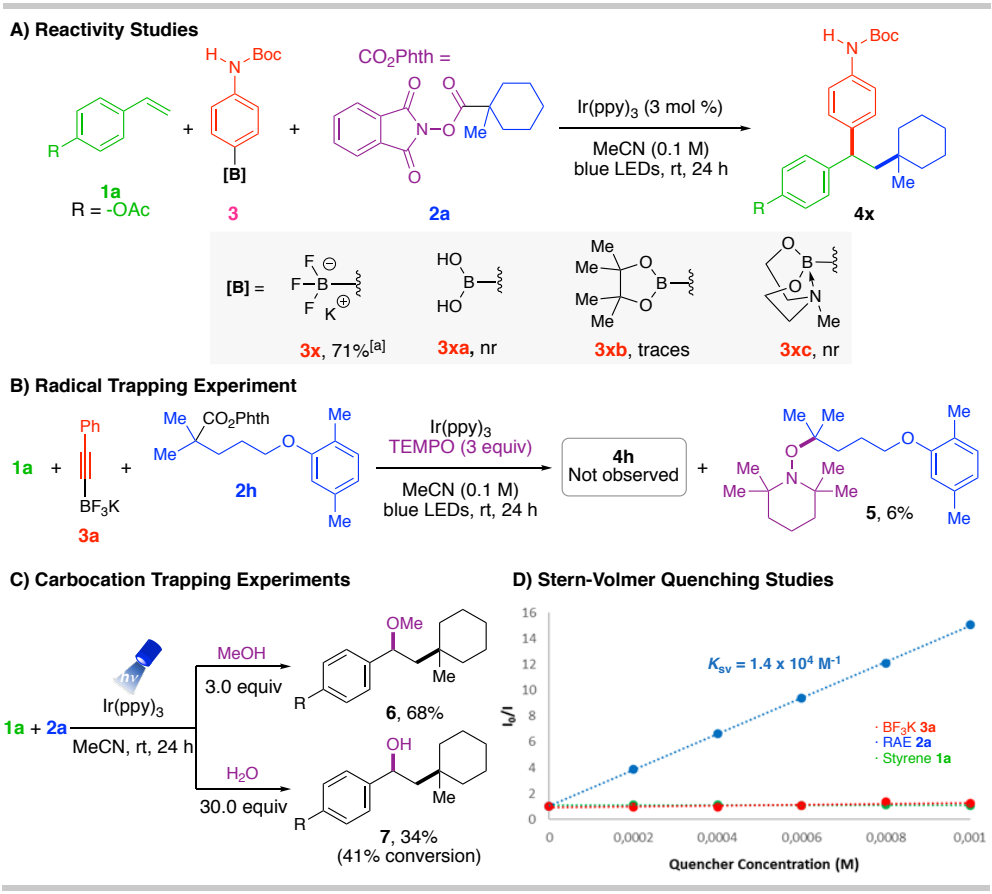

Figure 5.4. Reactivity and mechanistic studies. Reaction conditions: styrene **1** (0.2 mmol), RAE **2** (0.3 mmol, 1.5 equiv), potassium organotrifluoroborate salt **3** (0.4 mmol, 2 equiv), $Ir(ppy)_3$ (3 mol %) in MeCN (2.0 mL, 0.1 M), 24 h irradiation with blue LEDs (λ_{max} = 456 nm). [a]Yield was determined by ^1H NMR analysis using trimethoxybenzene as internal standard. Abbreviations: nr, no reaction.

Based on these findings, a mechanistic scenario is postulated (Figure 5.5) whereby excitation of $Ir(ppy)_3$ under blue light irradiation generates a potent excited state $*[Ir]^{III}$ complex ($E_{1/2}$ $[Ir^{IV}/Ir^{*III}]$ = -1.88 V vs SCE[19]). Single-electron transfer (SET) to RAE **2** ($E_{1/2}^{red}$ = -1.26 V vs SCE for 1-methylcyclohexyl-*N*-hydroxyphthalimide ester[17]) induces formation of $C(sp^3)$-hybridized radical **A** followed by extrusion of carbon dioxide. Subsequent addition of this

reactive intermediate to vinyl arene **1** furnishes a relatively stabilized 2° benzylic radical **B** ($E_{1/2}^{ox}$ = 0.37 V vs SCE[26]). Single-electron oxidation of this species by $[Ir]^{IV}$ ($E_{1/2}$ $[Ir^{IV}/Ir^{III}]$ = 0.77 V vs SCE[19]) yields the corresponding carbocation **C**, restoring the ground-state photocatalyst. At this critical juncture, ionic intermediate **C** is intercepted by the organotrifluoroborate nucleophile **3** to furnish the desired 1,2-dicarbofunctionalized product **4.**

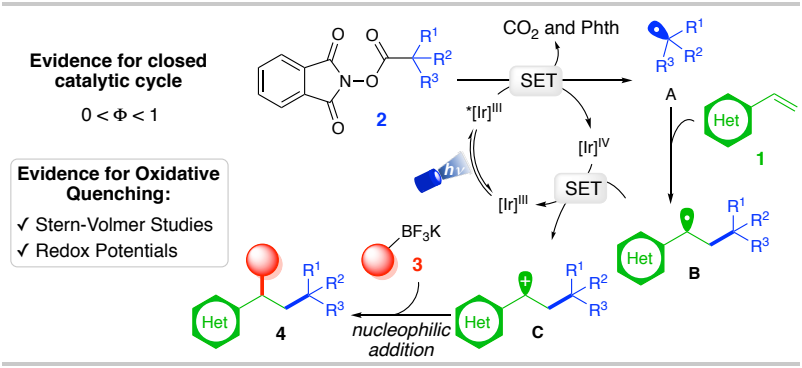

Figure 5.5. Proposed 1,2-DCF mechanism.

5.3 Conclusion

In summary, a unified protocol to achieve the carboallylation, carboalkenylation, carboalkynylation, and carboarylation of olefins with regio- and chemoselective control has been developed. Through an oxidative quenching pathway, the photoreduction of aliphatic RAEs has been enlisted to generate alkyl radical intermediates that react with alkene feedstocks in a regulated fashion. The resulting C-centered radical undergoes single-electron oxidation to afford a key carbocation intermediate that is intercepted by organotrifluoroborate nucleophiles to facilitate sequential C–C bond formation under mild reaction conditions. Mechanistic studies, including Stern-Volmer quenching studies, photochemical quantum yield measurements, and trapping experiments of radical and ionic intermediates emphasize that an RPC-mediated

mechanism is likely operational. Most importantly, this report provides a general blueprint toward 1,2-dicarbofunctionalizations in the absence of organometal species.

5.4 Experimental

General Consideration

General: All chemical transformations requiring inert atmospheric conditions were carried out using Schlenk line techniques with a 4- or 5-port dual-bank manifold. LED irradiation was accomplished as described in precedent reports.[27] NMR spectra (^{1}H, ^{13}C, ^{19}F) were obtained at 298 ºK. ^{19}F NMR spectra were referenced to hexafluorobenzene (δ –161.64 in $CDCl_3$). ^{1}H NMR spectra were referenced to residual, $CHCl_3$ (δ 7.26) in $CDCl_3$. ^{13}C NMR spectra were referenced to $CDCl_3$ (δ 77.30). In the case of diastereomeric mixtures, crude NMR was recorded to determine the ratio. Reactions were monitored by LC/MS, GC/MS, ^{1}H NMR, and/or TLC on silica gel plates (60 Å porosity, 250 μm thickness). TLC analysis was performed using hexanes/EtOAc as the eluent and visualized using ninhydrin, *p*-anisaldehyde stain, and/or UV light. Flash chromatography was accomplished using an automated system (CombiFlash®, UV detector, λ = 254 nm and 280 nm) with RediSep® R_f silica gel disposable flash columns (60 Å porosity, 40–60 μm) or RediSep R_f Gold® silica gel disposable flash columns (60 Å porosity, 20–40 μm). Accurate mass measurement analyses were conducted using electron ionization (EI) or electrospray ionization (ESI). The signals were mass measured against an internal lock mass reference of perfluorotributylamine (PFTBA) for EI-GC/MS and leucine enkephalin for ESI-LC/MS. The utilized software calibrates the instruments and reports measurements by use of neutral atomic masses. The mass of the electron is not included. IR spectra were recorded on an FT-IR using either neat oil or solid products. Solvents were purified with drying cartridges through a solvent delivery system. Melting points (°C) are uncorrected. UV/vis absorption spectra

for the quantum yield reaction were recorded on a Perkin-Elmer Lambda 365 UV/vis spectrophotometer. Quartz fluorometric cells (1 cm optical path length, Starna) were used in all optical experiments. The quantum yield reaction was conducted on a FS920 spectrofluorometer (Edinburgh Instruments, UK), equipped with R2658P red-sensitive PMT (Hamamatsu), a temperature and stir controller.

Chemicals: Deuterated NMR solvents were purchased and stored over 4Å molecular sieves. EtOAc, hexanes, MeOH, Et_2O, and toluene were obtained from commercial suppliers and used as purchased. CH_2Cl_2 and THF were purchased and dried *via* a solvent delivery system. Anhydrous MeCN was obtained from commercial sources and stored over molecular sieves. All other reagents were purchased commercially and used as received. Photoredox-catalyzed reactions were performed using 8 mL Chemglass vials (2-dram, 17 x 60 mm, 15-425 Green Open Top Cap, TFE Septa).

General Procedures

1,2-DCF protocol (GP1): To an 8 mL reaction vial (2-dram, 17 x 60 mm) equipped with a magnetic stir bar was added styrene derivative (0.3 mmol, 1.0 equiv, if solid or non-volatile liquid), redox-active ester (0.45 mmol, 1.5 equiv), potassium organotrifluoroborate salt (0.6 mmol, 2.0 equiv), and $Ir(ppy)_3$ (6 mg, 0.009 mmol, 3.0 mol %, 0.03 equiv) under air. The vial was sealed with a cap containing a TFE-lined silicone septum, evacuated, and back-filled with nitrogen. After this process was repeated 3 times, anhyd MeCN (3 mL, 0.1 M) was added followed by styrene via syringe (0.3 mmol, 1.0 equiv, if volatile liquid). The reaction was irradiated for 24 h using blue LED strips (λ_{max} = 456 nm, distance lamp–vial ~3-5 cm), whereby the temperature was maintained at approximately 25 °C via cooling with a fan. Upon completion,

the mixture was taken to dryness and then purified using column chromatography with hexanes/EtOAc as eluent.

Reaction Optimization

To an 8 mL reaction vial (2-dram, 17 x 60 mm) equipped with a magnetic stir bar was added the corresponding amounts of 1-methylcyclohexyl redox active ester, phenylethynyltrifluoroborate, and $Ir(ppy)_3$. The vial was sealed with a cap containing a TFE-lined silicone septum and then evacuated and backfilled with nitrogen three times. Corresponding amounts of MeCN and styrene were then added via syringe. The reaction was irradiated for 24 h with blue LEDs for 16 h whereby the temperature was maintained at approximately 27 °C via cooling with a fan. Upon completion, the reaction mixture was concentrated to dryness and then analyzed by crude ^{1}NMR using equimolar (0.1 mmol) trimethoxybenzene as internal standard.

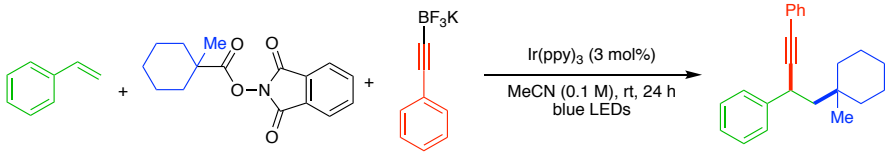

1ae 0.1 mmol | **2a** 1.5 equiv | **1a** 2.0 equiv | **4ae**

Entry	Deviation from std. conditions	Yield[a]
1	none	59%
2	3 equiv RBF_3K	55%
3	1 mol% $Ir(ppy)_3$	57%
4	10 mol% $Ir(ppy)_3$	47%
5	0.2 M MeCN	57%
6	0.05 M MeCN	36%

Figure 5.6. Supplementary optimization studies. [a]Yields were determined via ^{1}H NMR analysis using 0.1 mmol trimethoxybenzene as internal standard (IS).

Mechanistic Investigation

Reactivity studies of organoboron compounds:

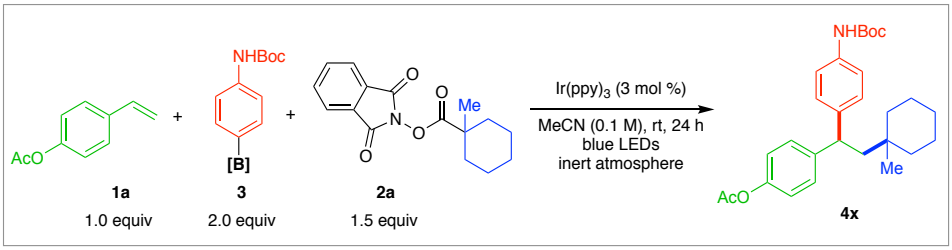

To an 8 mL reaction vial (17 x 60 mm) equipped with a magnetic stir bar was added 1,3-dioxoisoindolin-2-yl 1-methylcyclohexane-1-carboxylate (86 mg, 0.30 mmol, 1.5 equiv), boron substrate (0.20 mmol, 2.0 equiv), and $Ir(ppy)_3$ (4 mg, 0.006 mmol, 3.0 mol %, 0.03 equiv) under air. The vial was sealed with a cap containing a TFE-lined silicone septum, evacuated, and back-filled with nitrogen. After this process was repeated 3 times, MeCN (3.0 mL, 0.1 M) was added followed by 4-vinylphenyl acetate (32.4 mg, 0.2 mmol, 1.0 equiv) via syringe. The reaction was irradiated for 24 h using using blue LED strips (λ_{max} = 456 nm, distance lamp–vial ~3-5 cm), whereby the temperature was maintained at approximately 25 °C via cooling with a fan. Upon completion, the mixture was taken to dryness and then analyzed by crude ^{1}NMR using trimethoxybenzene (34 mg, 0.20 mmol, 1.0 equiv) as internal standard in MeCN-d_3 (δ 2.13).

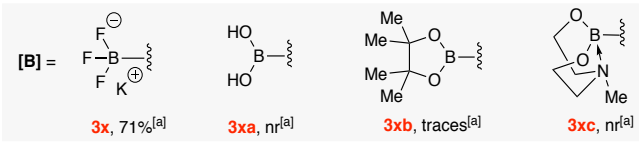

Figure 5.7. Reactivity studies with different boron compounds. [a]Yield was determined via ^{1}H NMR analysis using 0.1 mmol trimethoxybenzene as internal standard (IS). n.r. = no reaction.

Radical trapping experiment:

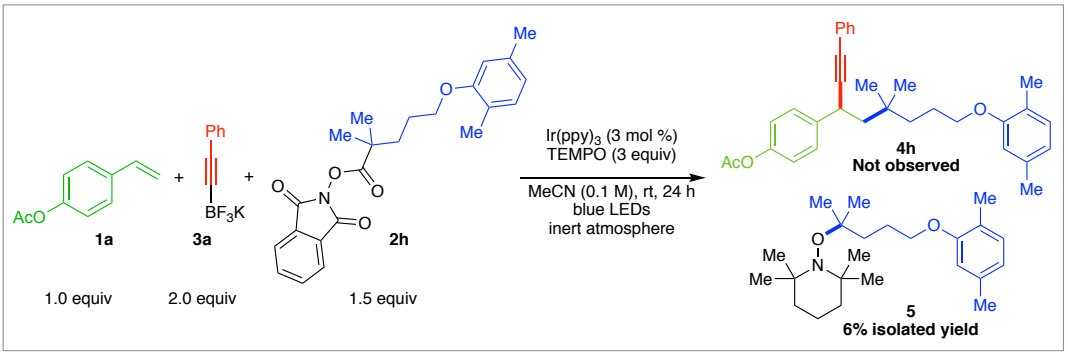

To an 8 mL reaction vial (17 x 60 mm) equipped with a magnetic stir bar was added 1,3-dioxoisoindolin-2-yl 1-methylcyclohexane-1-carboxylate (129 mg, 0.45 mmol, 1.5 equiv), TEMPO (141 mg, 0.90 mmol, 3.0 equiv), trifluoro(phenylethynyl)-λ^4-borane, potassium salt (125 mg, 0.60 mmol, 2.0 equiv), and $Ir(ppy)_3$ (6 mg, 0.009 mmol, 3.0 mol %, 0.03 equiv) under air. The vial was sealed with a cap containing a TFE-lined silicone septum, evacuated, and back-filled with nitrogen. After this process was repeated 3 times, MeCN (3.0 mL, 0.1 M) was added followed by 4-vinylphenyl acetate (48.7 mg, 0.3 mmol, 1.0 equiv) via syringe. The reaction was irradiated for 24 h using blue LED strips (λ_{max} = 456 nm, distance lamp–vial ~3-5 cm), whereby the temperature was maintained at approximately 25 °C via cooling with a fan. Upon completion, the mixture was taken to dryness and then purified using column chromatography with hexanes/EtOAc as eluent. The TEMPO derivative was isolated as a colorless oil (6 mg, 6%). **^{1}H NMR** (400 MHz, $CDCl_3$) δ 7.00 (d, *J* = 7.4 Hz, 1H), 6.68 – 6.61 (m, 2H), 3.96 (t, *J* = 6.3 Hz, 2H), 2.31 (s, 3H), 2.18 (s, 3H), 2.01 – 1.91 (m, 2H), 1.80 – 1.72 (m, 2H), 1.52 – 1.42 (m, 4H), 1.30 (s, 6H), 1.30 – 1.23 (m, 2H), 1.13 (s, 6H), 1.09 (s, 6H). **^{13}C NMR** (101 MHz, $CDCl_3$) δ 157.2, 136.4, 130.3, 123.6, 120.5, 111.9, 78.3, 68.4, 59.2 (2C), 40.9 (2C), 40.1, 34.8 (2C), 27.0 (2C), 24.4, 21.4, 20.7 (2C), 17.2, 15.9. **FT-IR** (cm^{-1}, neat, ATR): 3007, 2971, 2928, 2869, 1586,

1509, 1467, 1414, 1375, 1361, 1285, 1265, 1209, 1180, 1157, 1130, 1046. **HRMS** (ESI) calcd for $C_{23}H_{40}NO_2$ $[M+H]^+$: 361.2981, found 361.2993.

Carbocation trapping experiments:

Formation of 4-(1-Methoxy-2-(1-methylcyclohexyl)ethyl)phenyl Acetate (6)

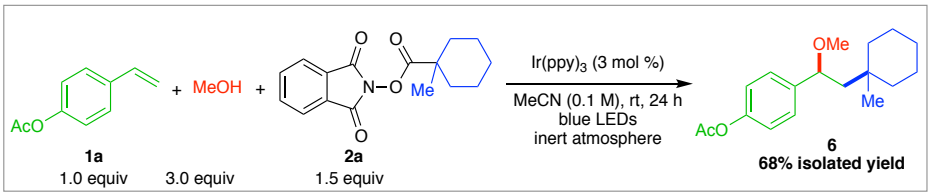

To an 8 mL reaction vial (17 x 60 mm) equipped with a magnetic stir bar was added 1,3-dioxoisoindolin-2-yl 1-methylcyclohexane-1-carboxylate (129 mg, 0.45 mmol, 1.5 equiv) and $Ir(ppy)_3$ (6 mg, 0.009 mmol, 3.0 mol %, 0.03 equiv) under air. The vial was sealed with a cap containing a TFE-lined silicone septum, evacuated, and back-filled with nitrogen. After this process was repeated 3 times, MeCN (3.0 mL, 0.1 M) and MeOH (36 µL, 0.9 mmol, 3.0 equiv) were added. This was followed by addition of 4-vinylphenyl acetate (48.7 mg, 0.3 mmol, 1.0 equiv) via syringe. The reaction was irradiated for 24 h using blue LED strips (λ_{max} = 456 nm, distance lamp–vial ~3-5 cm), whereby the temperature was maintained at approximately 25 °C via cooling with a fan. Upon completion, the mixture was taken to dryness and then purified using column chromatography with hexanes/EtOAc as eluent. The title compound was obtained as a colorless oil (59 mg, 68%). **^{1}H NMR** (400 MHz, $CDCl_3$) δ 7.28 (d, J = 8.3 Hz, 2H), 7.05 (d, J = 8.4 Hz, 2H), 4.22 (dd, J = 8.7, 2.9 Hz, 1H), 3.14 (s, 3H), 2.29 (s, 3H), 1.78 (dd, J = 14.7, 8.7 Hz, 1H), 1.51 – 1.39 (m, 6H), 1.38 – 1.23 (m, 5H), 0.97 (s, 3H). **^{13}C NMR** (101 MHz, $CDCl_3$) δ 169.6, 149.8, 141.8, 127.5 (2C), 121.5 (2C), 80.8, 56.4, 50.6, 38.7, 38.4, 33.1, 26.5, 25.8, 22.2,

22.1, 21.3. **FT-IR** (cm^{-1}, neat, ATR): 2923, 2861, 1759, 1504, 1450, 1369, 1212, 1196, 1163, 1097, 1048, 1016. **HRMS** (ESI) calcd for $C_{18}H_{26}O_3Na[M+Na]^+$: 313.1780, found 313.1782.

Formation of 4-(1-Hydroxy-2-(1-methylcyclohexyl)ethyl)phenyl Acetate (7)

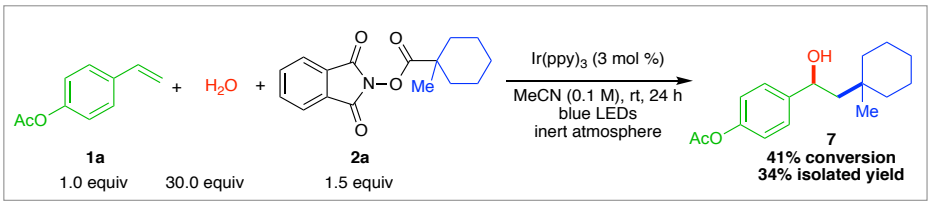

To an 8 mL reaction vial (17 x 60 mm) equipped with a magnetic stir bar was added 1,3-dioxoisoindolin-2-yl 1-methylcyclohexane-1-carboxylate (129 mg, 0.45 mmol, 1.5 equiv) and $Ir(ppy)_3$ (6 mg, 0.009 mmol, 3.0 mol %, 0.03 equiv) under air. The vial was sealed with a cap containing a TFE-lined silicone septum, evacuated, and back-filled with nitrogen. After this process was repeated 3 times, MeCN (3.0 mL, 0.1 M) and H_2O (162 µL, 9.0 mmol, 30.0 equiv) were added. This was followed by addition of 4-vinylphenyl acetate (48.7 mg, 0.3 mmol, 1.0 equiv) via syringe. The reaction was irradiated for 24 h using blue LED strips (λ_{max} = 456 nm, distance lamp–vial ~3-5 cm), whereby the temperature was maintained at approximately 25 °C via cooling with a fan. Upon completion, the mixture was taken to dryness and then purified using column chromatography with hexanes/EtOAc as eluent. The title compound was obtained as a colorless oil (30 mg, 34%). **^{1}H NMR** (400 MHz, $CDCl_3$) δ 7.35 (d, J = 8.1 Hz, 2H), 7.05 (d, J = 8.1 Hz, 2H), 4.87 (dd, J = 8.6, 3.2 Hz, 1H), 2.29 (s, 3H), 1.82 – 1.67 (m, 2H), 1.60 (dd, J = 14.8, 3.3 Hz, 1H), 1.49 – 1.26 (m, 10H), 1.01 (s, 3H). **^{13}C NMR** (101 MHz, $CDCl_3$) δ 169.7, 149.8, 144.5, 126.9 (2C), 121.7 (2C), 71.4, 51.5, 38.8, 38.4, 33.1, 26.5, 25.7, 22.1 (2C), 21.3. **FT-IR** (cm^{-1}, neat, ATR): 3431, 2923, 2859, 1758, 1606, 1505, 1451, 1369, 1196, 1165, 1061, 1016. **HRMS** (ESI) calcd for $C_{17}H_{24}O_3Na$ $[M+Na]^+$: 299.1623, found 299.1632.

Stern-Volmer quenching studies:

Fluorescence measurements were obtained using septa-capped UV-Quartz cuvettes (10 mm pathlength) obtained from Starna Cells (Cat#: 29F—Q—10). Excitation was performed at 375 nm; fluorescence spectra were obtained from 400-700 nm. In a nitrogen filled glovebox, the following stock solns were prepared:

- Photocatalyst soln (0.0002 M): To an oven dried scintillation vial equipped with a stir bar was added $Ir(ppy)_3$ (1.46 mg, $2.23x10^{-3}$ mmol). This was diluted with 10.8 mL of MeCN and stirred until completely dissolved, producing a $2.06x10^{-4}$ M soln of $Ir(ppy)_3$.

- Phthalimide ester soln (0.004 M): To an oven dried scintillation vial equipped with a stir bar, was added 1,3-dioxoisoindolin-2-yl 1-methylcyclohexane-1-carboxylate RAE **2a** (12.4 mg, $4.32x10^{-2}$ mmol). This was diluted in 10.8 mL of MeCN and stirred until completely dissolved, producing a colorless, $4.00x10^{-3}$ M soln of phthalimide ester **2a**.

- Organotrifluoroborate soln (0.004 M): To an oven dried scintillation vial equipped with a stir bar was added (trifluoro(phenylethynyl)-λ4-borane, potassium salt **3a** (8.99 mg, $4.32x10^{-2}$ mmol). This was diluted in 10.8 mL of MeCN and stirred until completely dissolved, producing a colorless, $4.00x10^{-3}$ M soln of organotrifluoroborate **3a**.

- Styrene soln (0.004 M): To an oven dried scintillation vial equipped with a stir bar, was added 10.8 mL of MeCN followed by styrene derivative **1a** (6.6 μL, $4.32x10^{-2}$ mmol). The soln was stirred until completely dissolved, producing a $4.00x10^{-3}$ M soln of styrene derivative **1a**.

Following preparation, the solns were allocated to the cuvettes and fluorescence quenching was determined with individual quenchers (phthalimide ester, styrene, and

organotrifluoroborate). The I_0/I values of each sample were calculated from the average of three scans per data point. Linear regression of I_0/I against concentration was carried out to yield the Stern-Volmer quenching rate constant (K_{SV}). The following Stern-Volmer plots for luminescence quenching of $Ir(ppy)_3$ (1.9×10^{-5} M in degassed MeCN) by quenchers were obtained. The excited catalyst is quenched most efficiently by the aliphatic phthalimide ester with a Stern-Volmer quenching rate constant of 1.4×10^4 M^{-1}.

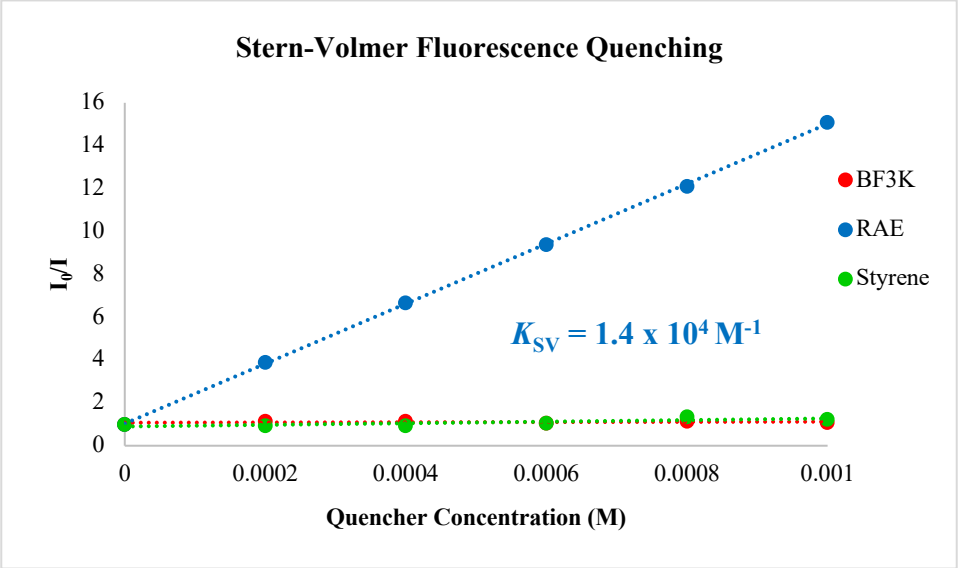

Figure 5.8. Stern-Volmer plots for luminescence quenching of $Ir(ppy)_3$ (1.9×10^{-5} M in degassed MeCN) by redox-active ester **2a** (blue), organotrifluoroborate **3a** (red), styrene **1a** (green), $\lambda_{exc.}$ = 375 nm, $\lambda_{em.}$ = 534 nm, K_{SV} = Stern-Volmer constant.

Determination of quantum yield: a closed catalytic loop (Φ ≤ 1) or radical chain process (Φ >1)?

The quantum yield of the reaction was determined using the procedure reported previously:[28,29] 4-Vinylphenyl acetate **1a**, *N*-hydroxyphthalimide ester **2a** and potassium (2-

phenylethynyl)trifluoroborate **3a** were used as a model substrates to determine the quantum yield, using trimethoxybenzene as internal standard in a proportion 1:1 with **1a**.

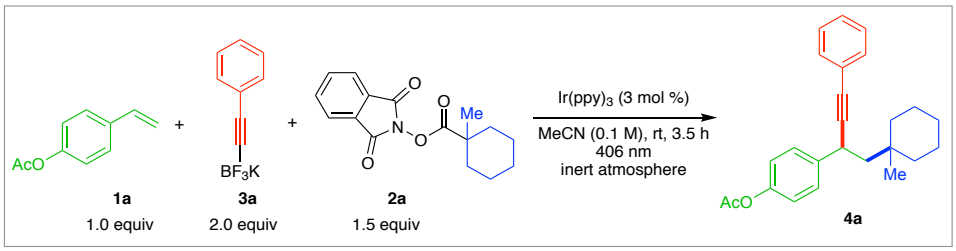

– The quantum yield of the reaction is defined as:

$$\Phi = \frac{\text{mol of product formed}}{\text{mol of photon flux} \times t \times f} \qquad (1)$$

where Φ is the quantum yield of the reaction, t is the time of the reaction (s), f is the incident light absorbed by the Ir catalyst at 406 nm and the photon flux is calculated by standard ferrioxalate actinometry[30] (section C).

A) Incident light absorbed by the Ir(ppy)$_3$ (f)

– The fraction of light, f, absorbed was determined according to equation 2:

$$f = 1 - 10^{-A} \qquad (2)$$

where A is the absorbance of the fully soluble Ir in acetonitrile at 406 nm. The wavelength of 406 nm was chosen based on two criteria: the wavelength at which the (i) absolute $\Phi(Fe^{2+})$ had been established;[30] and (ii) reaction was going to be irradiated where the Ir catalyst absorbs most. The absorbance of Ir catalyst was measured by adding Ir(ppy)$_3$ (4 mg, 0.003 mmol) in acetonitrile (2 mL) to a cuvette equipped with a Teflon-coated magnetic stir bar and stirred for 10 min. The

absorbance of the suspension was recorded. To accurately determine the fraction of light absorbed, another identical soln of Ir in acetonitrile was prepared and then filtered. The absorbance of the solvated Ir soln in acetonitrile was measured. The absorbance (A) at 406 nm was determined to be 1.94888 (Figure 5.9), and thus indicating the fraction of light absorbed is > 0.98875 according to equation 2.

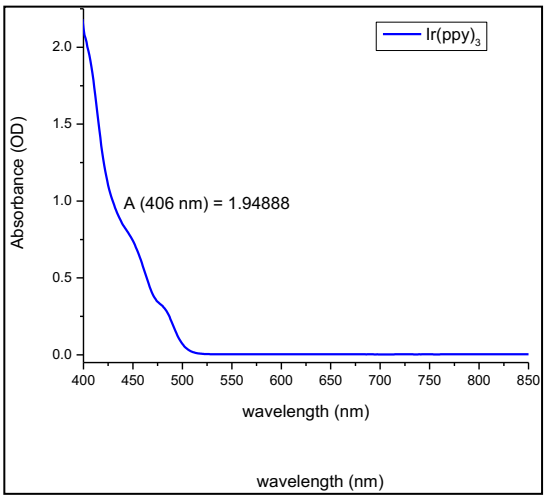

Figure 5.9. Absorption spectrum for filtered soln of $Ir(ppy)_3$ in MeCN.

B) The photoredox reaction

To the cuvette in section A containing $Ir(ppy)_3$ (4 mg, 0.003 mmol) in acetonitrile (2 mL) was added 4-vinylphenyl acetate (32.4 mg, 0.2 mmol), potassium trifluoro(phenylethynyl)borate (83.2 mg, 0.4 mmol, 2 equiv) and 1,3-dioxoisoindolin-2-yl 1-methylcyclohexane-1-carboxylate (86.2 mg, 0.3 mmol, 1.5 equiv) in a dark room (laboratory lights were shut off). The cuvette was then capped with a PTFE stopper, and Ar(g) was bubbled through for 300 s. Initial emission quenching experiments were performed on the Ir catalyst to determine the time it takes for the system to deoxygenate, and this was found to be 200 s. Under an Ar (g) atm., the sample was stirred (1200 rpm, temp maintained at 23 ºC using a temperature controller) and irradiated (λ =

406 nm, excitation slit width = 10.0 nm, step = 1.0 nm, Iris = 100) for 12600 s (3.5 h) (Figure 5.10). Note: the reaction is heterogeneous and light scattering due to solids has not been accounted for.

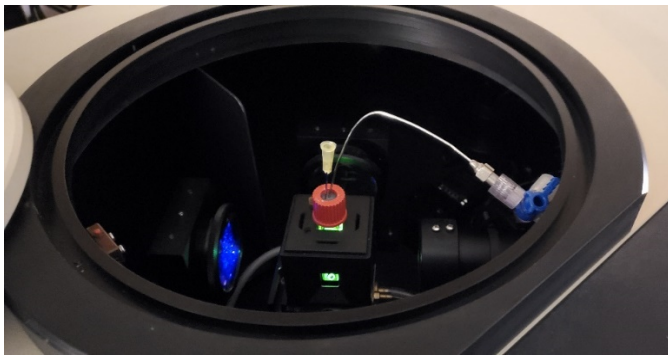

Figure 5.10. The photoredox reaction set-up. The reaction mixture was irradiated at 406 nm under an atmosphere of Ar (g) at 23 ºC.

After irradiation, the crude mixture was passed through a silica plug using EtOAc and the filtrate concentrated under reduced pressure to give a yellow residue. The reaction was repeated twice for reproducibility. The yield of product (0.01 mmol after 12,600 s) obtained after irradiating at 406 nm was determined by ^{1}H NMR based on a 1,3,5-trimethoxybenzene internal standard (internal standard added was 1:1 with **1a**, the limiting reagent).

C) Photon flux at 406 nm

Standard ferrioxalate actinometry was used to determine the photon flux of the spectrophotometer using equations 3 and 4.[28-30] For the ferrioxalate actinometer the production of iron(II) ions proceeds by the following reactions:[30]

$$[Fe(C_2O_4)_n]^{(3-2n)+} \xrightarrow{h\nu} Fe^{2+} + (n\text{-}1)(C_2O_4)^{2-} + C_2O_4^{-}$$

$$[Fe(C_2O_4)_n]^{(3-2n)+} + C_2O_4^{-} \longrightarrow Fe^{2+} + n(C_2O_4)^{2-} + 2CO_2$$

The moles of Fe^{2+} formed are determined spectrophotometrically by development with 1,10-phenanthroline (phen) to form the red $[Fe(phen)_3]^{2+}$ moiety (λ = 510 nm).[28-30] The photon flux is defined as:

$$\text{Photon flux} = \frac{\text{mol}\,(Fe^{2+})}{\Phi(Fe^{2+}) \times t \times f} \qquad (3)$$

where Φ is the quantum yield for the ferrioxalate actinometer (1.188 at λ = 406 nm),[30] t is the time (s), and f > 0.999, and the mol of Fe^{2+} are calculated according to equation 4.

$$\text{mol}\,(Fe^{2+}) = \frac{V \times \Delta A}{l \times \varepsilon} \qquad (4)$$

where V is the total volume of the soln, ΔA is the difference in absorbance between irradiated and non-irradiated solns, l is the path length (1.0 cm), ε is the molar absorptivity at 510 nm (11,110 L $mol^{-1}cm^{-1}$).[30]

D) Experimental

The following solns were prepared in the dark (flasks were wrapped in aluminum foil) and stored in the dark at room temperature:

– *Ferrioxalate soln (0.15 M):* potassium ferrioxalate hydrate (2.21 g) was added to a flask wrapped in aluminum foil containing H_2SO_4 (30 mL, 0.05 M). The flask was stirred for

complete solvation of the green solid in complete darkness. It is noteworthy that the soln should not be exposed to any incident light.

– *Developer solution:* 1,10-phenanthroline (50 mg) and NaOAc (11.25 g) was added to a flask containing H_2SO_4 (50 mL, 0.5 M) and sonicated until completely solvated.

The absorbance of the non-irradiated sample: The buffered soln of phen (0.35 mL) was added to a ferrioxalate (2.0 mL) in a vial that had been covered with aluminum foil {lights of the laboratory were switched off}. The vial was capped and allowed to rest for 1 h and then transferred to a cuvette. The absorbance of the non-irradiated was measured at 510 nm to be 0.3534 (Figure 5.11).

The absorbance of the irradiated sample: In a cuvette equipped with a stir bar was added the ferrioxalate soln (2.0 mL), and the stirred soln was irradiated for 90.0 s at λ = 406 nm with an excitation slit width = 10.0 nm (step = 1.0 nm, Iris = 100). After irradiation, the buffered phen soln (0.35 mL) was added to the cuvette and allowed to rest for 1 h in the dark to allow the ferrous ions to coordinate completely to phen. The absorbance was measured at 510 nm to be 1.93858 (Figure 5.11).

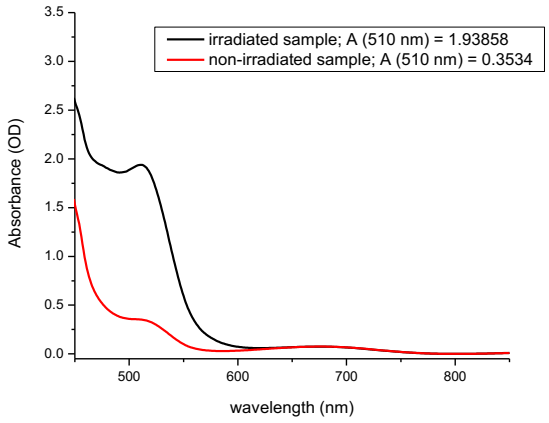

Figure 5.11. Absorption spectra for irradiated and non-irradiated samples of red $[Fe(phen)_3]^{2+}$.

– Photon flux sample calculation. Sample calculation:

$$\text{mol } (Fe^{2+}) = \frac{\text{V} \times \Delta\text{A}}{\text{l} \times \varepsilon} \qquad (4)$$

$$\text{mol } (Fe^{2+}) = \frac{0.00235\ \text{L} \times 1.58518}{1.00\ cm \times 11.110\ \text{L}mol^{-1}cm^{-1}} = 3.3530\ \times\ 10^{-7}\ mol$$

$$\text{Photon flux} = \frac{\text{mol } (Fe^{2+})}{\Phi(Fe^{2+})\ \times\ \text{t}\ \times\ \text{f}} \qquad (3)$$

$$\text{Photon flux} = \frac{3.3530\ \times\ 10^{-7}\ mol}{1.188\ \times\ 90.0\ \text{s}\ \times\ 1.00} = 3.13598 \times 10^{-9}\ \text{einstein s}^{-1}$$

E) Quantum yield of the reaction

– Therefore, the quantum yield of the reaction is determined to be:

$$\Phi = \frac{\text{mol of product formed}}{\text{mol of photon flux}\ \times\ \text{t}\ \times\ \text{f}} \qquad (1)$$

$$\Phi = \frac{0.1 \times 10^{-3}\ mol}{3.13598 \times 10^{-9}\ \text{einstein s}^{-1}\ \times\ 12600\ \text{s} \times\ 0.98875} = 0.256$$

$\Phi > 1$ would mean that the chain propagation; $\Phi \leq 1$ would mean closed photocatalytic pathway

The quantum yield studies indicate that this is not a radical-chain process as evidenced by the Φ.

Characterization Data

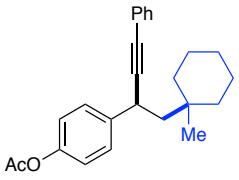

4-(1-(1-Methylcyclohexyl)-4-phenylbut-3-yn-2-yl)phenyl Acetate, **4a** (89 mg, 82%) was prepared following *GP1*. The product was obtained as a colorless oil. **^{1}H NMR** (500 MHz, $CDCl_3$) δ 7.46 – 7.39 (m, 4H), 7.33 – 7.27 (m, 3H), 7.06 (d, *J* = 8.6 Hz, 2H), 3.91 (dd, *J* = 10.2, 3.2 Hz, 1H), 2.31 (s, 3H), 2.03 (dd, *J* = 13.9, 10.1 Hz, 1H), 1.63 (dd, *J* = 14.0, 3.3 Hz, 1H), 1.62 – 1.53 (m, 2H), 1.53 – 1.32 (m, 8H), 1.12 (s, 3H). **^{13}C NMR** (101 MHz, $CDCl_3$) δ 169.7, 149.3, 142.0, 131.5 (2C), 128.5 (2C), 128.3 (2C), 127.8, 124.0, 121.7 (2C), 93.2, 83.3, 51.1, 38.5, 38.1, 33.9, 33.4, 26.5, 25.9, 22.2 (2C), 21.3. **FT-IR** (cm^{-1}, neat, ATR): 2924, 2860, 1761, 1691, 1599, 1504, 1491, 1443, 1369, 1198, 1166, 1102, 1018. **HRMS** (EI) calcd for $C_{25}H_{29}O_2$ $[M+H]^+$: 361.2168, found 361.2160.

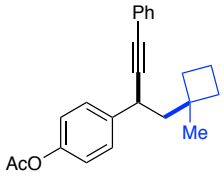

4-(1-(1-Methylcyclobutyl)-4-phenylbut-3-yn-2-yl)phenyl Acetate, **4b** (59 mg, 59%) was prepared following *GP1*. The product was obtained as a colorless oil. **^{1}H NMR** (400 MHz, $CDCl_3$) δ 7.47 – 7.39 (m, 4H), 7.33 – 7.26 (m, 3H), 7.10 – 7.03 (m, 2H), 3.87 (dd, *J* = 10.3, 4.7 Hz, 1H), 2.30 (s, 3H), 2.25 – 2.15 (m, 1H), 2.07 (dd, *J* = 13.5, 10.3 Hz, 1H), 1.97 (dddd, *J* = 15.8, 10.5, 5.0, 2.5 Hz, 1H), 1.89 – 1.75 (m, 4H), 1.73 – 1.61 (m, 1H), 1.34 (s, 3H). **^{13}C NMR** (101 MHz, $CDCl_3$) δ 169.7, 149.3, 141.0, 131.5 (2C), 128.5 (2C), 128.3 (2C), 127.8, 124.0, 121.6

(2C), 91.9, 83.6, 51.7, 38.9, 34.6, 34.6, 34.4, 25.6, 21.3, 15.8. **FT-IR** (cm^{-1}, neat, ATR): 2950, 2923, 1759, 1503, 1489, 1368, 1196, 1017, 754. **HRMS** (ESI) calcd for $C_{23}H_{25}O_2$ $[M+H]^+$: 333.1855, found 333.1852.

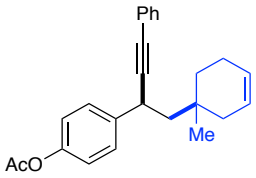

4-(1-(1-Methylcyclohex-3-en-1-yl)-4-phenylbut-3-yn-2-yl)phenyl Acetate, 4c (50 mg, 46%, isolated as an inseparable 1:1 diastereomeric mixture) was prepared following *GP1*. The product was obtained as a colorless oil. **^{1}H NMR** (400 MHz, $CDCl_3$) δ 7.41 (ddt, *J* = 6.6, 4.0, 2.1 Hz, 4H), 7.29 (dd, *J* = 5.1, 2.0 Hz, 3H), 7.07 – 7.02 (m, 2H), 5.72 – 5.55 (m, 2H), 3.96 – 3.88 (m, 1H), 2.30 (s, 3H), 2.24 – 2.12 (m, 1H), 2.10 – 1.80 (m, 4H), 1.72 – 1.64 (m, 1H), 1.64 – 1.57 (m, 1H), 1.57 – 1.45 (m, 1H), 1.13 (d, *J* = 7.4 Hz, 3H). **Diastereomer 1: ^{13}C NMR** (101 MHz, $CDCl_3$) δ 169.7, 149.3, 141.8, 131.5 (2C), 128.5 (2C), 128.4 (2C), 127.9, 125.8, 125.5, 124.0, 121.7 (2C), 93.1, 83.4, 50.5, 38.2, 33.8, 33.7, 32.4, 25.3, 22.9, 21.3. **Diastereomer 2: ^{13}C NMR** (101 MHz, $CDCl_3$) δ 169.7, 149.3, 141.8, 131.5 (2C), 128.5 (2C), 128.4 (2C), 127.9, 126.3, 125.9, 124.0, 121.7 (2C), 93.1, 83.6, 50.4, 37.9, 34.1, 33.6, 32.3, 25.3, 22.8, 21.3. **FT-IR** (cm^{-1}, neat, ATR): 2915, 1759, 1503, 1490, 1368, 1197, 1165, 1017. **HRMS** (ESI) calcd for $C_{25}H_{27}O_2$ $[M+H]^+$: 359.2011, found 359.2008.

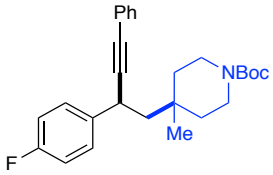

***tert*-Butyl 4-(2-(4-Fluorophenyl)-4-phenylbut-3-yn-1-yl)-4-methylpiperidine-1-carboxylate**, **4d** (75.2 mg, 60%) was prepared following *GP1*. The product was obtained as a colorless oil. **^{1}H NMR** (400 MHz, $CDCl_3$) δ 7.42 – 7.34 (m, 4H), 7.33 – 7.27 (m, 3H), 7.08 – 6.96 (m, 2H), 3.91 (dd, *J* = 10.1, 3.5 Hz, 1H), 3.62 (dd, *J* = 13.2, 6.3 Hz, 1H), 3.56 – 3.46 (m, 1H), 3.35 – 3.23 (m, 2H), 2.06 (dd, *J* = 14.0, 10.1 Hz, 1H), 1.76 – 1.67 (m, 1H), 1.61 (dd, *J* = 14.0, 3.5 Hz, 1H), 1.55 – 1.33 (m, 12H), 1.17 (s, 3H). **^{13}C NMR** (101 MHz, $CDCl_3$) δ 163.0, 160.5, 155.1, 139.5 (2C), 131.5, 128.9 (2C), 128.4, 128.1, 123.6, 115.7, 115.5, 92.5, 83.8, 79.4, 50.7, 39.9, 37.6, 37.0, 33.2, 32.5, 29.8, 28.6 (3C), 24.2. **^{19}F NMR** (377 MHz, $CDCl_3$) δ -116.34. **FT-IR** (cm^{-1}, neat, ATR): 2925, 1684, 1506, 1422, 1364, 1248, 1222, 1156, 755. **HRMS** (ESI) calcd for $C_{22}H_{25}FN$ [M-Boc+2H]$^{+}$: 322.1971, found 322.1971.

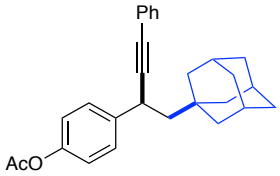

4-(1-((3r,5r,7r)-Adamantan-1-yl)-4-phenylbut-3-yn-2-yl)phenyl Acetate, **4e** (84 mg, 70%) was prepared following *GP1*. The product was obtained as a colorless oil. **^{1}H NMR** (400 MHz, $CDCl_3$) δ 7.42 (dt, *J* = 6.6, 2.3 Hz, 4H), 7.33 – 7.26 (m, 3H), 7.05 (d, *J* = 8.2 Hz, 2H), 3.93 (dd, *J* = 10.2, 3.1 Hz, 1H), 2.30 (s, 3H), 2.03 – 1.97 (m, 3H), 1.83 (dd, *J* = 14.0, 10.1 Hz, 1H), 1.78 – 1.62 (m, 12H), 1.50 (dd, *J* = 13.9, 3.1 Hz, 1H). **^{13}C NMR** (101 MHz, $CDCl_3$) δ 169.7, 149.2, 142.0, 131.5 (2C), 128.5 (2C), 128.3 (2C), 127.8, 124.1, 121.6 (2C), 93.4, 83.4, 54.2, 42.8 (3C),

37.2 (3C), 33.4, 32.5, 28.9 (3C), 21.3. **FT-IR** (cm^{-1}, neat, ATR): 2899, 2845, 1760, 1502, 1489, 1199, 1166, 755. **HRMS** (ESI) calcd for $C_{28}H_{31}O_2$ $[M+H]^+$: 399.2324, found 399.2318.

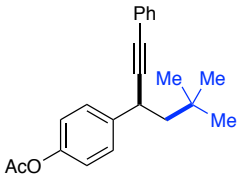

4-(5,5-Dimethyl-1-phenylhex-1-yn-3-yl)phenyl Acetate, **4f** (64 mg, 66%) was prepared following *GP1*. The product was obtained as a colorless oil. **^{1}H NMR** (400 MHz, $CDCl_3$) δ 7.46 – 7.38 (m, 4H), 7.33 – 7.26 (m, 3H), 7.06 (d, *J* = 8.5 Hz, 2H), 3.89 (dd, *J* = 10.2, 3.4 Hz, 1H), 2.30 (s, 3H), 1.93 (dd, *J* = 13.8, 10.2 Hz, 1H), 1.65 (dd, *J* = 13.8, 3.4 Hz, 1H), 1.08 (s, 9H). **^{13}C NMR** (101 MHz, $CDCl_3$) δ 169.7, 149.3, 141.8, 131.5 (2C), 128.5 (2C), 128.3 (2C), 127.8, 124.0, 121.7 (2C), 93.1, 83.6, 53.1, 34.5, 31.5, 30.0 (3C), 21.3. **FT-IR** (cm^{-1}, neat, ATR): 2954, 2866, 1762, 1692, 1599, 1504, 1490, 1476, 1367, 1199, 1166, 1103, 1018. **HRMS** (EI) calcd for $C_{22}H_{25}O_2$ $[M+H]^+$: 321.1855, found 321.1854.

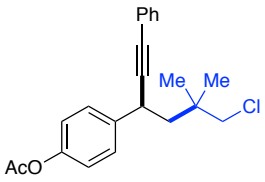

4-(6-Chloro-5,5-dimethyl-1-phenylhex-1-yn-3-yl)phenyl Acetate, **4g** (64 mg, 60%) was prepared following *GP1*. The product was obtained as a colorless oil. **^{1}H NMR** (400 MHz, $CDCl_3$) δ 7.48 – 7.41 (m, 4H), 7.35 – 7.28 (m, 3H), 7.07 (d, *J* = 8.5 Hz, 2H), 3.92 (dd, *J* = 10.8, 3.5 Hz, 1H), 3.65 – 3.53 (m, 2H), 2.31 (s, 3H), 2.02 (dd, *J* = 14.1, 10.8 Hz, 1H), 1.79 (dd, *J* = 14.1, 3.5 Hz, 1H), 1.19 (d, *J* = 1.9 Hz, 6H). **^{13}C NMR** (101 MHz, $CDCl_3$) δ 169.6, 149.5, 140.9, 131.6 (2C), 128.5 (2C), 128.4 (2C), 128.1, 123.6, 121.8 (2C), 91.9, 84.1, 55.3, 47.9, 36.2, 34.0,

26.1, 25.9, 21.3. **FT-IR** (cm^{-1}, neat, ATR): 2963, 1760, 1598, 1504, 1490, 1470, 1443, 1387, 1368, 1200, 1167, 1018. **HRMS** (EI) calcd for $C_{22}H_{24}ClO_2$ $[M+H]^+$: 354.1387, found 354.1404.

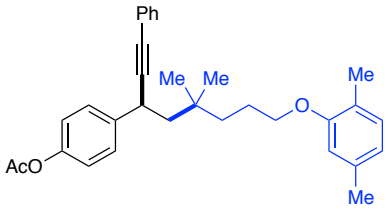

4-(8-(2,5-Dimethylphenoxy)-5,5-dimethyl-1-phenyloct-1-yn-3-yl)phenyl Acetate, **4h** (108 mg, 77%) was prepared following *GP1*. The product was obtained as a colorless oil. **^{1}H NMR** (400 MHz, $CDCl_3$) δ 7.50 – 7.40 (m, 4H), 7.28 (dd, *J* = 5.2, 2.0 Hz, 3H), 7.09 (d, *J* = 8.6 Hz, 2H), 7.04 (d, *J* = 7.4 Hz, 1H), 6.69 (d, *J* = 6.8 Hz, 1H), 6.62 (s, 1H), 4.00 – 3.88 (m, 3H), 2.33 (d, *J* = 3.7 Hz, 6H), 2.23 (s, 3H), 2.02 (dd, *J* = 13.9, 10.3 Hz, 1H), 1.96 – 1.74 (m, 2H), 1.70 (dd, *J* = 14.0, 3.3 Hz, 1H), 1.65 – 1.57 (m, 2H), 1.14 (s, 6H). **^{13}C NMR** (101 MHz, $CDCl_3$) δ 169.7, 157.2, 149.3, 141.7, 136.5, 131.5 (2C), 130.4, 128.5 (2C), 128.3 (2C), 127.9, 123.9, 123.7, 121.7 (2C), 120.7, 112.1, 92.9, 83.5, 68.6, 50.8, 38.4, 34.0, 33.7, 27.9, 27.9, 24.5, 21.5, 21.3, 16.0. **FT-IR** (cm^{-1}, neat, ATR): 2954, 2869, 1762, 1585, 1507, 1490, 1471, 1443, 1415, 1389, 1368, 1265, 1200, 1166, 1130, 1018. **HRMS** (EI) calcd for $C_{32}H_{37}O_3$ $[M+H]^+$: 496.2743, found 496.2751.

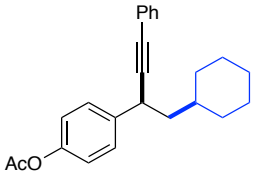

4-(1-Cyclohexyl-4-phenylbut-3-yn-2-yl)phenyl Acetate, 4i (42 mg, 40%) was prepared following *GP1*. The product was obtained as a colorless oil. **^{1}H NMR** (400 MHz, $CDCl_3$) δ 7.49 – 7.41 (m, 4H), 7.32 (dd, *J* = 5.2, 2.0 Hz, 3H), 7.11 – 7.04 (m, 2H), 3.95 (dd, *J* = 9.8, 5.2 Hz, 1H), 2.33 (s, 3H), 1.92 (d, *J* = 12.8 Hz, 1H), 1.84 – 1.57 (m, 7H), 1.37 – 1.17 (m, 3H), 1.06 – 0.91 (m,

2H). **^{13}C NMR** (101 MHz, $CDCl_3$) δ 169.7, 149.4, 140.5, 131.8 (2C), 128.5 (2C), 128.3 (2C), 127.9, 123.9, 121.6 (2C), 91.7, 83.3, 46.7, 35.7, 35.3, 33.9, 32.7, 26.8, 26.4, 26.3, 21.3. **FT-IR** (cm^{-1}, neat, ATR): 2921, 2849, 1759, 1503, 1490, 1447, 1368, 1196, 1165. **HRMS** (EI) calcd for $C_{24}H_{26}O_2$ $[M]^+$: 346.1933, found 346.1917.

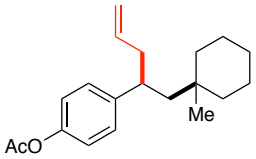

4-(1-(1-Methylcyclohexyl)pent-4-en-2-yl)phenyl Acetate, **4j** (47 mg, 53%) was prepared following *GP1*. The product was obtained as a colorless oil. **^{1}H NMR** (400 MHz, $CDCl_3$) δ 7.17 (d, *J* = 8.6 Hz, 2H), 6.99 (d, *J* = 8.5 Hz, 2H), 5.60 (ddt, *J* = 17.1, 10.1, 7.0 Hz, 1H), 4.98 – 4.87 (m, 2H), 2.74 (qd, *J* = 7.5, 3.3 Hz, 1H), 2.27 (s, 3H), 1.69 (dd, *J* = 14.2, 8.6 Hz, 1H), 1.60 (dd, *J* = 14.2, 3.4 Hz, 1H), 1.49 – 1.32 (m, 4H), 1.32 – 1.18 (m, 6H), 1.06 – 1.01 (m, 2H), 0.74 (s, 3H). **^{13}C NMR** (101 MHz, $CDCl_3$) δ 169.6, 148.7, 145.2, 137.3, 128.7 (2C), 121.2 (2C), 116.1, 48.1, 44.4, 41.2, 38.6, 38.5, 33.8, 26.5, 25.5, 22.2, 22.0, 21.3. **FT-IR** (cm^{-1}, neat, ATR): 2923, 2849, 1766, 1640, 1606, 1507, 1446, 1368, 1198, 1166, 1100, 1017. **HRMS** (EI) calcd for $C_{20}H_{28}O_2Na$ $[M+Na]^+$: 323.1982, found 323.1978.

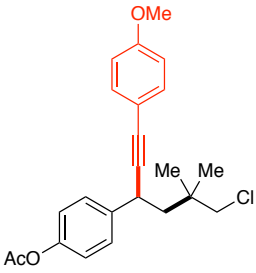

4-(6-Chloro-1-(4-methoxyphenyl)-5,5-dimethylhex-1-yn-3-yl)phenyl Acetate, **4k** (94 mg, 81%) was prepared following *GP1*. The product was obtained as a colorless oil. **^{1}H NMR** (400

MHz, $CDCl_3$) δ 7.44 (d, *J* = 8.6 Hz, 2H), 7.36 (d, *J* = 8.8 Hz, 2H), 7.06 (d, *J* = 8.6 Hz, 2H), 6.84 (d, *J* = 8.8 Hz, 2H), 3.89 (dd, *J* = 10.8, 3.5 Hz, 1H), 3.80 (s, 3H), 3.67 – 3.53 (m, 2H), 2.30 (s, 3H), 1.99 (dd, *J* = 14.1, 10.8 Hz, 1H), 1.77 (dd, *J* = 14.1, 3.5 Hz, 1H), 1.17 (d, *J* = 3.1 Hz, 6H). **^{13}C NMR** (101 MHz, $CDCl_3$) δ 169.7, 159.5, 149.4, 141.2, 132.9 (2C), 128.5 (2C), 121.7 (2C), 115.8, 114.0 (2C), 90.3, 83.9, 55.4, 55.4, 47.9, 36.2, 34.0, 26.2, 25.9, 21.3. **FT-IR** (cm^{-1}, neat, ATR): 2961, 1758, 1605, 1508, 1466, 1442, 1368, 1290, 1246, 1195, 1165, 1105, 1030, 1018. **HRMS** (EI) calcd for $C_{23}H_{26}ClO_3$ $[M+H]^+$: 385.1570, found 385.1555.

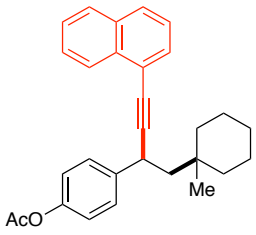

4-(1-(1-Methylcyclohexyl)-4-(naphthalen-1-yl)but-3-yn-2-yl)phenyl Acetate, **4l** (56 mg, 45%) was prepared following *GP1*. The product was obtained as a colorless oil. **^{1}H NMR** (400 MHz, $CDCl_3$) δ 8.32 (d, *J* = 8.0 Hz, 1H), 7.84 (dd, *J* = 7.9, 1.6 Hz, 1H), 7.79 (d, *J* = 8.2 Hz, 1H), 7.64 (dd, *J* = 7.2, 1.2 Hz, 1H), 7.57 – 7.48 (m, 4H), 7.41 (dd, *J* = 8.3, 7.1 Hz, 1H), 7.09 (d, *J* = 8.5 Hz, 2H), 4.07 (dd, *J* = 10.1, 3.2 Hz, 1H), 2.31 (s, 3H), 2.13 (dd, *J* = 14.0, 10.1 Hz, 1H), 1.73 (dd, *J* = 14.0, 3.2 Hz, 1H), 1.69 – 1.54 (m, 2H), 1.52 – 1.37 (m, 8H), 1.17 (s, 3H). **^{13}C NMR** (101 MHz, $CDCl_3$) δ 169.7, 149.3, 142.2, 133.6, 133.3, 130.2, 128.5 (2C), 128.3, 128.2, 126.7, 126.4, 126.4, 125.4, 121.8 (2C), 121.7, 98.2, 81.6, 51.5, 38.5, 38.3, 33.9, 33.8, 26.5, 25.8, 22.2 (2C), 21.3. **FT-IR** (cm^{-1}, neat, ATR): 2923, 2850, 1760, 1504, 1454, 1396, 1368, 1265, 1196, 1165, 1017. **HRMS** (EI) calcd for $C_{29}H_{31}O_2$ $[M+H]^+$: 411.2324, found 411.2325.

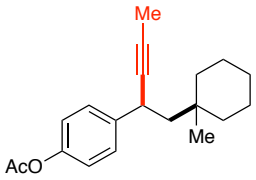

4-(1-(1-Methylcyclohexyl)pent-3-yn-2-yl)phenyl Acetate, **4m** (49.3 mg, 55%) was prepared following *GP1*. The product was obtained as a colorless oil. **^{1}H NMR** (400 MHz, $CDCl_3$) δ 7.38 – 7.29 (m, 2H), 7.05 – 6.96 (m, 2H), 3.62 (dt, *J* = 9.5, 3.0 Hz, 1H), 2.29 (s, 3H), 1.89 – 1.83 (m, 1H), 1.81 (d, *J* = 2.4 Hz, 3H), 1.56 – 1.38 (m, 7H), 1.38 – 1.22 (m, 4H), 1.01 (s, 3H). **^{13}C NMR** (101 MHz, $CDCl_3$) δ 169.7, 149.1, 142.8, 128.4 (2C), 121.5 (2C), 82.6, 78.4, 51.1, 38.4, 38.2, 33.8, 32.9, 26.6, 25.7, 22.2, 22.1, 21.3, 3.8. **FT-IR** (cm^{-1}, neat, ATR): ṽ = 2922, 2858, 1762, 1504, 1368, 1200, 1165, 1018, 911. **HRMS** (ESI) calcd for $C_{20}H_{27}O_2$ $[M+H]^+$: 299.2011, found 299.2010.

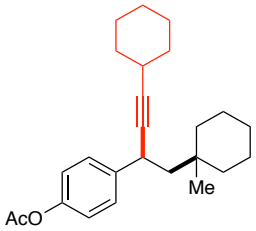

4-(4-Cyclohexyl-1-(1-methylcyclohexyl)but-3-yn-2-yl)phenyl Acetate, **4n** (52 mg, 48%) was prepared following *GP1*. The product was obtained as a colorless oil. **^{1}H NMR** (400 MHz, $CDCl_3$) δ 7.35 (d, *J* = 8.5 Hz, 2H), 7.01 (d, *J* = 8.5 Hz, 2H), 3.66 (dt, *J* = 10.2, 2.6 Hz, 1H), 2.43 – 2.32 (m, 1H), 2.29 (s, 3H), 1.89 – 1.76 (m, 3H), 1.74 – 1.66 (m, 2H), 1.59 – 1.48 (m, 3H), 1.48 – 1.27 (m, 14H), 1.05 (s, 3H). **^{13}C NMR** (101 MHz, $CDCl_3$) δ 169.7, 149.0, 143.0, 128.4 (2C), 121.4 (2C), 87.5, 83.1, 51.4, 38.5, 38.1, 33.8, 33.0 (2C), 32.8, 29.4, 26.6, 26.1, 25.9, 25.1, 22.2 (3C), 21.3. **FT-IR** (cm^{-1}, neat, ATR): 2925, 2854, 1762, 1675, 1599, 1504, 1449, 1368, 1194, 1164, 1103, 1045, 1011. **HRMS** (EI) calcd for $C_{25}H_{35}O_2$ $[M+H]^+$: 367.2637, found 367.2655.

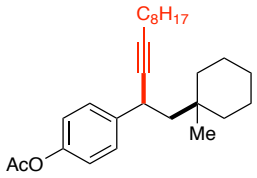

4-(1-(1-Methylcyclohexyl)dodec-3-yn-2-yl)phenyl Acetate, **4o** (56 mg, 47%) was prepared following *GP1*. The product was obtained as a colorless oil. **^{1}H NMR** (400 MHz, $CDCl_3$) δ 7.34 (d, *J* = 8.5 Hz, 2H), 7.01 (d, *J* = 8.6 Hz, 2H), 3.64 (dd, *J* = 10.1, 2.8 Hz, 1H), 2.29 (s, 3H), 2.18 (td, *J* = 7.0, 2.2 Hz, 2H), 1.85 (dd, *J* = 13.9, 10.0 Hz, 1H), 1.56 – 1.47 (m, 5H), 1.45 – 1.26 (m, 18H), 1.03 (s, 3H), 0.92 – 0.85 (m, 3H). **^{13}C NMR** (101 MHz, $CDCl_3$) δ 169.7, 149.1, 142.9, 128.4 (2C), 121.5 (2C), 83.3 (2C), 51.3, 38.4, 38.2, 33.8, 32.9, 32.0, 29.4, 29.3, 29.1, 29.0, 26.6, 25.8, 22.8, 22.2, 22.2, 21.3, 19.0, 14.3. **FT-IR** (cm^{-1}, neat, ATR): 2924, 2855, 1763, 1675, 1599, 1504, 1454, 1369, 1277, 1194, 1164, 1103, 1044, 1011. **HRMS** (EI) calcd for $C_{27}H_{41}O_2$ $[M+H]^+$: 397.3107, found 397.3094.

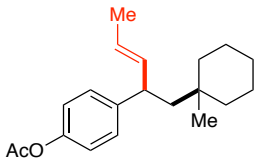

(*E*)-4-(1-(1-Methylcyclohexyl)pent-3-en-2-yl)phenyl Acetate, **4p** (33 mg, 36%) was prepared following *GP1*. The product was obtained as a colorless oil. **^{1}H NMR** (400 MHz, $CDCl_3$) δ 7.18 (d, *J* = 8.5 Hz, 2H), 6.99 (d, *J* = 8.5 Hz, 2H), 5.56 (ddd, *J* = 15.2, 8.2, 1.6 Hz, 1H), 5.41 – 5.29 (m, 1H), 3.40 (q, *J* = 6.9 Hz, 1H), 2.28 (s, 3H), 1.67 (d, *J* = 6.4 Hz, 2H), 1.62 (dd, *J* = 6.4, 1.6 Hz, 3H), 1.45 – 1.32 (m, 5H), 1.31 – 1.22 (m, 3H), 1.21 – 1.08 (m, 2H), 0.84 (s, 3H). **^{13}C NMR** (101 MHz, $CDCl_3$) δ 169.7, 148.6, 145.1, 137.5, 128.5 (2C), 123.8, 121.4 (2C), 48.6, 44.6, 38.7, 38.6, 33.9, 26.6, 25.6, 22.1 (2C), 21.3, 18.0. **FT-IR** (cm^{-1}, neat, ATR): 2922, 2853, 1766, 1605, 1505,

1451, 1368, 1197, 1166, 1100, 1044, 1017. **HRMS** (EI) calcd for $C_{20}H_{29}O_2$ $[M+H]^+$: 301.2168, found 301.2177.

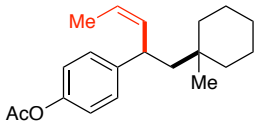

(*Z*)-4-(1-(1-Methylcyclohexyl)pent-3-en-2-yl)phenyl Acetate, 4q (31 mg, 34%) was prepared following *GP1*. The product was obtained as a colorless oil. **^{11}H NMR** (400 MHz, $CDCl_3$) δ 7.21 (d, *J* = 8.5 Hz, 2H), 6.98 (d, *J* = 8.6 Hz, 2H), 5.62 – 5.53 (m, 1H), 5.41 – 5.30 (m, 1H), 3.76 (dt, *J* = 9.7, 6.4 Hz, 1H), 2.28 (s, 3H), 1.69 – 1.64 (m, 5H), 1.45 – 1.36 (m, 5H), 1.31 – 1.19 (m, 5H), 0.89 (s, 3H). **^{13}C NMR** (101 MHz, $CDCl_3$) δ 169.7, 148.6, 145.4, 136.9, 128.2 (2C), 122.0, 121.5 (2C), 49.8, 38.7, 38.6, 38.5, 33.9, 26.6, 25.6, 22.2 (2C), 21.3, 13.2. **FT-IR** (cm^{-1}, neat, ATR): 2923, 2858, 1765, 1505, 1449, 1399, 1368, 1196, 1166, 1100, 1017. **HRMS** (EI) calcd for $C_{20}H_{29}O_2$ $[M+H]^+$: 301.2168, found 301.2174.

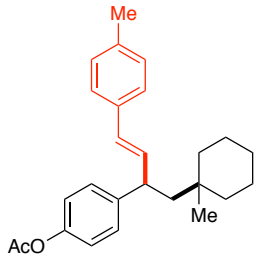

(*E*)-4-(1-(1-Methylcyclohexyl)-4-(*p*-tolyl)but-3-en-2-yl)phenyl Acetate, **4r** (73 mg, 65%) was prepared following *GP1*. The product was obtained as a colorless oil. **^{1}H NMR** (400 MHz, $CDCl_3$) δ 7.32 – 7.27 (m, 2H), 7.26 – 7.22 (m, 2H), 7.12 (d, *J* = 7.9 Hz, 2H), 7.07 – 7.02 (m, 2H), 6.37 – 6.24 (m, 2H), 3.65 (q, *J* = 6.4 Hz, 1H), 2.34 (s, 3H), 2.31 (s, 3H), 1.90 – 1.77 (m, 2H), 1.54 – 1.18 (m, 10H), 0.93 (s, 3H). **^{13}C NMR** (101 MHz, $CDCl_3$) δ 169.7, 148.8, 144.4, 136.8, 135.3, 135.0, 129.3 (2C), 128.6 (3C), 126.1 (2C), 121.5 (2C), 48.7, 44.8, 38.7, 38.6, 34.0, 26.5, 25.7,

22.2 (2C), 21.3 (2C). **FT-IR** (cm^{-1}, neat, ATR): 2922, 2853, 1765, 1504, 1452, 1367, 1199. **HRMS** (EI) calcd for $C_{26}H_{32}O_2$ $[M]^+$: 376.2402, found 376.2385.

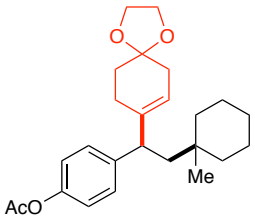

4-(2-(1-Methylcyclohexyl)-1-(1,4-dioxaspiro[4.5]dec-7-en-8-yl)ethyl)phenyl Acetate, **4s** (45 mg, 38%) was prepared following *GP1*. The product was obtained as a colorless oil. **^{1}H NMR** (400 MHz, $CDCl_3$) δ 7.20 (d, *J* = 8.4 Hz, 2H), 6.97 (d, *J* = 8.0 Hz, 2H), 5.58 (s, 1H), 3.96 – 3.83 (m, 4H), 3.35 (t, *J* = 6.4 Hz, 1H), 2.27 (s, 3H), 2.22 (s, 2H), 2.09 (q, *J* = 16.8 Hz, 2H), 1.77 (d, *J* = 6.3 Hz, 1H), 1.63 (t, *J* = 6.6 Hz, 2H), 1.42 – 1.21 (m, 10H), 1.11 (t, *J* = 5.9 Hz, 1H), 0.79 (s, 3H). **^{13}C NMR** (101 MHz, $CDCl_3$) δ 169.6, 148.8, 142.9, 139.8, 129.0 (2C), 121.1 (2C), 120.0, 108.7, 64.4 (2C), 47.6, 44.9, 38.7, 38.4, 37.0, 33.8, 30.9, 26.6, 25.0, 24.3, 22.2, 22.1, 21.3. **FT-IR** (cm^{-1}, neat, ATR): 2923, 1761, 1504, 1448, 1367, 1310, 1199, 1166, 1100, 1059, 1042, 1017. **HRMS** (EI) calcd for $C_{25}H_{35}O_4$ $[M+H]^+$: 399.2535, found 399.2551.

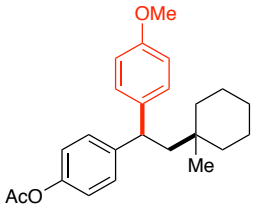

4-(1-(4-Methoxyphenyl)-2-(1-methylcyclohexyl)ethyl)phenyl Acetate, **4t** (53 mg, 48%) was prepared following *GP1*. The product was obtained as a colorless oil. **^{1}H NMR** (400 MHz, $CDCl_3$) δ 7.27 (d, *J* = 8.6 Hz, 2H), 7.20 (d, *J* = 8.7 Hz, 2H), 6.97 (d, *J* = 8.5 Hz, 2H), 6.81 (d, *J* = 8.7 Hz, 2H), 4.05 (t, *J* = 6.6 Hz, 1H), 3.77 (s, 3H), 2.26 (s, 3H), 2.07 (qd, *J* = 14.2, 6.6 Hz, 2H),

1.44 – 1.32 (m, 5H), 1.27 – 1.15 (m, 5H), 0.79 (s, 3H). **^{13}C NMR** (101 MHz, $CDCl_3$) δ 169.6, 157.9, 148.7, 145.2, 138.8, 128.8 (2C), 128.6 (2C), 121.4 (2C), 113.9 (2C), 55.3, 48.6, 46.0, 38.6 (2C), 34.0, 26.5, 25.4, 22.1, 22.1, 21.3. **FT-IR** (cm^{-1}, neat, ATR): 2923, 2848, 1761, 1609, 1504, 1462, 1368, 1301, 1247, 1198, 1166, 1110, 1037, 1017. **HRMS** (EI) calcd for $C_{24}H_{31}O_3$ $[M+H]^+$: 367.2273, found 367.2280.

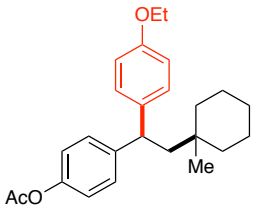

4-(1-(4-Ethoxyphenyl)-2-(1-methylcyclohexyl)ethyl)phenyl Acetate, **4u** (70 mg, 61%) was prepared following *GP1*. The product was obtained as a colorless oil. **^{1}H NMR** (400 MHz, $CDCl_3$) δ 7.26 (d, J = 8.5 Hz, 2H), 7.18 (d, J = 8.7 Hz, 2H), 6.97 (d, J = 8.6 Hz, 2H), 6.79 (d, J = 8.7 Hz, 2H), 4.04 (t, J = 6.6 Hz, 1H), 3.99 (q, J = 7.0 Hz, 2H), 2.26 (s, 3H), 2.15 – 1.97 (m, 2H), 1.45 – 1.30 (m, 8H), 1.29 – 1.16 (m, 5H), 0.78 (s, 3H). **^{13}C NMR** (101 MHz, $CDCl_3$) δ 169.6, 157.3, 148.7, 145.2, 138.7, 128.8 (2C), 128.7 (2C), 121.4 (2C), 114.5 (2C), 63.5, 48.7, 46.0, 38.7 (2C), 34.0, 26.5, 25.4, 22.2, 22.1, 21.3, 15.0. **FT-IR** (cm^{-1}, neat, ATR): 2923, 1761, 1610, 1504, 1478, 1445, 1368, 1244, 1197, 1166, 1116, 1047, 1017. **HRMS** (EI) calcd for $C_{25}H_{33}O_3$ $[M+H]^+$: 381.2430, found 381.2421.

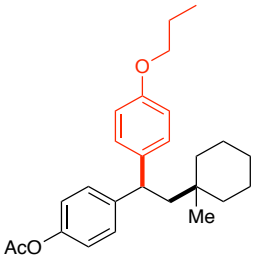

4-(2-(1-Methylcyclohexyl)-1-(4-propoxyphenyl)ethyl)phenyl Acetate, **4v** (59 mg, 50%) was prepared following *GP1*. The product was obtained as a colorless oil. **^{1}H NMR** (400 MHz, $CDCl_3$) δ 7.27 (d, *J* = 8.3 Hz, 2H), 7.19 (d, *J* = 8.3 Hz, 2H), 6.97 (d, *J* = 8.2 Hz, 2H), 6.80 (d, *J* = 8.3 Hz, 2H), 4.04 (t, *J* = 6.5 Hz, 1H), 3.88 (t, *J* = 6.5 Hz, 2H), 2.27 (s, 3H), 2.15 – 1.98 (m, 2H), 1.84 – 1.72 (m, 2H), 1.46 – 1.31 (m, 5H), 1.29 – 1.16 (m, 5H), 1.02 (t, *J* = 7.4 Hz, 3H), 0.79 (s, 3H). **^{13}C NMR** (101 MHz, $CDCl_3$) δ 169.6, 157.4, 148.6, 145.2, 138.6, 128.8 (2C), 128.6 (2C), 121.4 (2C), 114.5 (2C), 69.6, 48.7, 46.0, 38.6 (2C), 34.0, 26.5, 25.4, 22.8, 22.1 (2C), 21.3, 10.7. **FT-IR** (cm^{-1}, neat, ATR): 2924, 1761, 1504, 1455, 1368, 1243, 1197, 1166, 1112, 1068, 1048, 1017. **HRMS** (EI) calcd for $C_{26}H_{35}O_3$ $[M+H]^+$: 395.2586, found 395.2570.

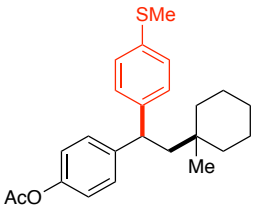

4-(2-(1-Methylcyclohexyl)-1-(4-(methylthio)phenyl)ethyl)phenyl Acetate, **4w** (56 mg, 49%) was prepared following *GP1*. The product was obtained as a colorless oil. **^{1}H NMR** (400 MHz, $CDCl_3$) δ 7.27 (d, *J* = 8.4 Hz, 2H), 7.21 (d, *J* = 8.3 Hz, 2H), 7.17 (d, *J* = 8.4 Hz, 2H), 6.97 (d, *J* = 8.5 Hz, 2H), 4.05 (t, *J* = 6.5 Hz, 1H), 2.44 (s, 3H), 2.26 (s, 3H), 2.14 – 1.99 (m, 2H), 1.45 – 1.30 (m, 5H), 1.27 – 1.16 (m, 5H), 0.79 (s, 3H). **^{13}C NMR** (101 MHz, $CDCl_3$) δ 169.6, 148.8, 144.6, 143.8, 135.6, 128.7 (2C), 128.5 (2C), 127.2 (2C), 121.5 (2C), 48.4, 46.4, 38.6 (2C), 34.0, 26.5,

25.4, 22.1 (2C), 21.3, 16.3. **FT-IR** (cm^{-1}, neat, ATR): 2921, 2847, 1757, 1504, 1492, 1441, 1406, 1367, 1195, 1166, 1094, 1015. **HRMS** (EI) calcd for $C_{24}H_{31}O_2S$ $[M+H]^+$: 383.2045, found 383.2044.

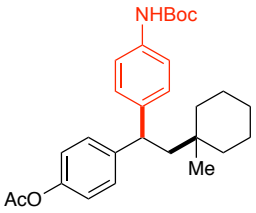

4-(1-(4-((*tert*-Butoxycarbonyl)amino)phenyl)-2-(1-methylcyclohexyl)ethyl)phenyl Acetate, **4x** (80 mg, 59%) was prepared following *GP1*. The product was obtained as a solid. **mp** = 142 – 144 ºC. **^{1}H NMR** (400 MHz, $CDCl_3$) δ 7.25 (d, *J* = 8.8 Hz, 4H), 7.20 (d, *J* = 8.7 Hz, 2H), 6.96 (d, *J* = 8.5 Hz, 2H), 6.44 (bs, 1H), 4.04 (dd, *J* = 7.3, 5.8 Hz, 1H), 2.26 (s, 3H), 2.14 – 1.98 (m, 2H), 1.50 (s, 9H), 1.44 – 1.31 (m, 5H), 1.26 – 1.13 (m, 5H), 0.78 (s, 3H). **^{13}C NMR** (101 MHz, $CDCl_3$) δ 169.6 (2C), 152.9, 148.7, 144.9, 141.3, 136.4, 128.6 (2C), 128.5 (2C), 121.4 (2C), 118.8, 80.5, 48.5, 46.2, 38.6, 38.6, 34.0, 28.5 (3C), 26.5, 25.4, 22.1, 22.1, 21.3. **FT-IR** (cm^{-1}, neat, ATR): 2925, 1756, 1725, 1594, 1521, 1504, 1454, 1412, 1392, 1367, 1314, 1218, 1199, 1157, 1052, 1016. **HRMS** (ESI) calcd for $C_{28}H_{37}NO_4Na$ $[M+Na]^+$: 474.2620, found 474.2609.

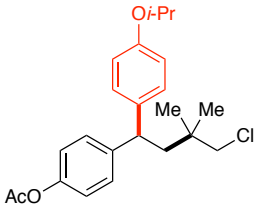

4-(4-Chloro-1-(4-isopropoxyphenyl)-3,3-dimethylbutyl)phenyl Acetate, **4y** (57 mg, 49%) was prepared following *GP1*. The product was obtained as a colorless oil. **^{1}H NMR** (400 MHz, $CDCl_3$) δ 7.28 (d, *J* = 8.5 Hz, 2H), 7.17 (d, *J* = 8.7 Hz, 2H), 6.99 (d, *J* = 8.6 Hz, 2H), 6.80 (d, *J* =

8.6 Hz, 2H), 4.53 – 4.44 (m, 1H), 4.00 (t, J = 7.0 Hz, 1H), 3.24 (d, J = 2.5 Hz, 2H), 2.27 (s, 3H), 2.17 (qd, J = 14.4, 7.0 Hz, 2H), 1.31 (d, J = 6.0 Hz, 6H), 0.91 (s, 6H). **^{13}C NMR** (101 MHz, $CDCl_3$) δ 169.6, 156.4, 148.9, 144.0, 137.3, 128.8 (2C), 128.6 (2C), 121.5 (2C), 116.0 (2C), 70.0, 56.1, 46.5, 44.9, 36.3, 26.2, 26.0, 22.2 (2C), 21.3. **FT-IR** (cm^{-1}, neat, ATR): 2975, 2933, 1759, 1609, 1505, 1468, 1384, 1369, 1297, 1243, 1198, 1167, 1118, 1017. **HRMS** (EI) calcd for $C_{23}H_{30}ClO_3$ $[M+H]^+$: 389.1883, found 389.1885.

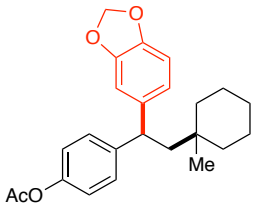

4-(1-(Benzo[*d*][1,3]dioxol-5-yl)-2-(1-methylcyclohexyl)ethyl)phenyl Acetate, **4z** (58 mg, 50%) was prepared following *GP1*. The product was obtained as a colorless oil. **^{1}H NMR** (400 MHz, $CDCl_3$) δ 7.27 (d, J = 8.0 Hz, 2H), 6.98 (d, J = 8.2 Hz, 2H), 6.83 – 6.66 (m, 3H), 5.90 (d, J = 3.6 Hz, 2H), 4.01 (t, J = 6.5 Hz, 1H), 2.27 (s, 3H), 2.11 – 1.98 (m, 2H), 1.47 – 1.29 (m, 5H), 1.29 – 1.13 (m, 5H), 0.80 (s, 3H). **^{13}C NMR** (101 MHz, $CDCl_3$) δ 169.6, 148.8, 147.7, 145.8, 144.8, 140.8, 128.6 (2C), 121.4 (2C), 120.8, 108.3, 108.2, 100.9, 48.5, 46.5, 38.6 (2C), 34.0, 26.5, 25.3, 22.1 (2C), 21.3. **FT-IR** (cm^{-1}, neat, ATR): 2923, 2859, 1761, 1503, 1487, 1440, 1368, 1244, 1197, 1166, 1120, 1097, 1038, 1017. **HRMS** (EI) calcd for $C_{24}H_{29}O_4$ $[M+H]^+$: 381.2066, found 381.2078.

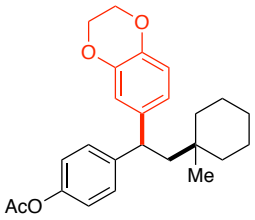

4-(1-(2,3-Dihydrobenzo[*b*][1,4]dioxin-6-yl)-2-(1-methylcyclohexyl)ethyl)phenyl Acetate, **4aa** (61 mg, 52%) was prepared following *GP1*. The product was obtained as a white solid. **mp** = 95 – 96 ºC. **^{1}H NMR** (400 MHz, $CDCl_3$) δ 7.26 (d, *J* = 8.4 Hz, 2H), 6.96 (d, *J* = 8.5 Hz, 2H), 6.79 (s, 1H), 6.74 (s, 2H), 4.21 (s, 4H), 3.97 (t, *J* = 6.5 Hz, 1H), 2.26 (s, 3H), 2.11 – 1.95 (m, 2H), 1.45 – 1.31 (m, 5H), 1.27 – 1.17 (m, 5H), 0.78 (s, 3H). **^{13}C NMR** (101 MHz, $CDCl_3$) δ 169.6, 148.7, 144.9, 143.4, 141.8, 140.2, 128.6 (2C), 121.4 (2C), 120.8, 117.2, 116.5, 64.5, 64.4, 48.5, 46.2, 38.6, 38.6, 34.0, 26.5, 25.3, 22.1 (2C), 21.3. **FT-IR** (cm^{-1}, neat, ATR): 2925, 1764, 1589, 1504, 1459, 1431, 1369, 1308, 1286, 1258, 1200, 1167, 1126, 1069, 1017. **HRMS** (EI) calcd for $C_{25}H_{31}O_4$ $[M+H]^+$: 395.2222, found 395.2231.

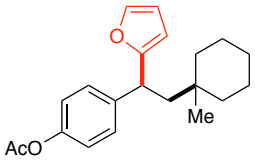

4-(1-(Furan-2-yl)-2-(1-methylcyclohexyl)ethyl)phenyl Acetate, 4ab (115 mg, 87%) was prepared following *GP1*. The product was obtained as a colorless oil. **^{1}H NMR** (400 MHz, $CDCl_3$) δ 7.31 – 7.26 (m, 3H), 7.00 (d, *J* = 8.6 Hz, 2H), 6.26 (d, *J* = 2.0 Hz, 1H), 6.02 (d, *J* = 3.2 Hz, 1H), 4.11 (dd, *J* = 7.9, 5.4 Hz, 1H), 2.28 (s, 3H), 2.20 (dd, *J* = 14.1, 7.9 Hz, 1H), 1.82 (dd, *J* = 14.1, 5.4 Hz, 1H), 1.41 – 1.36 (m, 5H), 1.25 – 1.17 (m, 5H), 0.79 (s, 3H). **^{13}C NMR** (101 MHz, $CDCl_3$) δ 169.7, 156.6, 150.6, 149.0, 143.0, 128.8 (2C), 121.4 (2C), 106.0, 105.9, 47.1, 40.6, 38.4, 38.2, 33.7, 26.5, 25.1, 22.1, 21.3, 13.7. **FT-IR** (cm^{-1}, neat, ATR): 2924, 2849, 1765, 1505,

1449, 1368, 1196, 1166, 1072, 1010. **HRMS** (EI) calcd for $C_{21}H_{27}O_3$ $[M+H]^+$: 327.1960, found 327.1959.

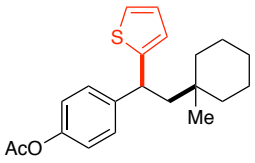

4-(2-(1-Methylcyclohexyl)-1-(thiophen-2-yl)ethyl)phenyl Acetate, **4ac** (40 mg, 39%) was prepared following *GP1*. The product was obtained as a colorless oil. **^{1}H NMR** (400 MHz, $CDCl_3$) δ 7.30 – 7.24 (m, 2H), 7.22 (dd, *J* = 5.0, 3.0 Hz, 1H), 7.03 – 6.95 (m, 4H), 4.18 (t, *J* = 6.5 Hz, 1H), 2.28 (s, 3H), 2.15 – 2.01 (m, 2H), 1.46 – 1.32 (m, 5H), 1.29 – 1.16 (m, 5H), 0.80 (s, 3H). **^{13}C NMR** (101 MHz, $CDCl_3$) δ 169.6, 148.8, 147.6, 144.3, 128.8 (2C), 127.9, 125.5, 121.4 (2C), 120.0, 49.0, 42.3, 38.6, 38.5, 33.9, 26.5, 25.3, 22.1, 22.1, 21.3. **FT-IR** (cm^{-1}, neat, ATR): 2922, 2851, 1763, 1504, 1450, 1368, 1196, 1166, 1103, 1017. **HRMS** (ESI) calcd for $C_{21}H_{27}O_2S$ $[M+H]^+$: 343.1732, found 343.1735.

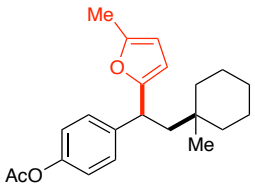

4-(2-(1-Methylcyclohexyl)-1-(5-methylfuran-2-yl)ethyl)phenyl Acetate, 4ad (50 mg, 49%) was prepared following *GP1*. The product was obtained as a colorless oil. **^{1}H NMR** (400 MHz, $CDCl_3$) δ 7.28 (d, *J* = 8.6 Hz, 2H), 6.99 (d, *J* = 8.6 Hz, 2H), 5.88 (d, *J* = 3.1 Hz, 1H), 5.82 (dd, *J* = 3.0, 1.2 Hz, 1H), 4.03 (dd, *J* = 7.8, 5.5 Hz, 1H), 2.28 (s, 3H), 2.24 (s, 3H), 2.17 (dd, *J* = 14.1, 7.8 Hz, 1H), 1.78 (dd, *J* = 14.1, 5.5 Hz, 1H), 1.42 – 1.36 (m, 5H), 1.26 – 1.17 (m, 5H), 0.80 (s, 3H). **^{13}C NMR** (101 MHz, $CDCl_3$) δ 169.7, 156.7, 150.6, 149.0, 143.0, 128.8 (2C), 121.4 (2C), 106.0, 105.9, 49.2, 40.6, 38.4, 38.2, 33.7, 26.5, 24.3, 22.1 (2C), 21.3, 13.7. **FT-IR** (cm^{-1}, neat, ATR):

2924, 2854, 1762, 1605, 1505, 1450, 1369, 1196, 1166, 1102, 1044, 1017. **HRMS** (EI) calcd for $C_{22}H_{29}O_3$ $[M+H]^+$: 341.2117, found 341.2108.

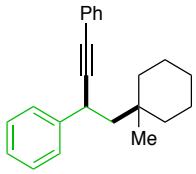

(4-(1-Methylcyclohexyl)but-1-yne-1,3-diyl)dibenzene, **4ae** (45 mg, 50%) was prepared following *GP1*. The product was obtained as a colorless oil. **^{1}H NMR** (400 MHz, $CDCl_3$) δ 7.43 (td, *J* = 7.1, 1.8 Hz, 4H), 7.34 (t, *J* = 7.6 Hz, 2H), 7.31 – 7.22 (m, 4H), 3.91 (dd, *J* = 10.1, 3.3 Hz, 1H), 2.04 (dd, *J* = 14.0, 10.1 Hz, 1H), 1.64 (dd, *J* = 14.0, 3.3 Hz, 1H), 1.63 – 1.52 (m, 2H), 1.50 – 1.33 (m, 8H), 1.12 (s, 3H). **^{13}C NMR** (101 MHz, $CDCl_3$) δ 144.5, 131.6 (2C), 128.7 (2C), 128.3 (2C), 127.7, 127.5 (2C), 126.6, 124.2, 93.6, 83.1, 51.1, 38.5, 38.2, 34.0, 33.9, 26.6, 25.9, 22.2 (2C). **FT-IR** (cm^{-1}, neat, ATR): 2923, 2849, 1692, 1673, 1598, 1490, 1450, 1377, 1350, 1318, 1262, 1177, 1071, 1025. **HRMS** (EI) calcd for $C_{23}H_{27}$ $[M+H]^+$: 303.2113, found 303.2100.

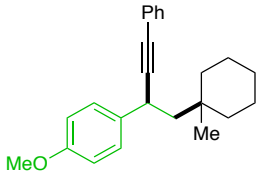

1-Methoxy-4-(1-(1-methylcyclohexyl)-4-phenylbut-3-yn-2-yl)benzene, **4af** (55 mg, 55%) was prepared following *GP1*. The product was obtained as a colorless oil. **^{1}H NMR** (400 MHz, $CDCl_3$) δ 7.42 – 7.38 (m, 2H), 7.33 (d, *J* = 8.7 Hz, 2H), 7.32 – 7.24 (m, 3H), 6.87 (d, *J* = 8.7 Hz, 2H), 3.85 (dd, *J* = 9.5, 2.9 Hz, 1H), 3.80 (s, 3H), 2.00 (dd, *J* = 13.9, 10.0 Hz, 1H), 1.61 (dd, *J* = 14.0, 3.5 Hz, 1H), 1.60 – 1.51 (m, 2H), 1.49 – 1.32 (m, 8H), 1.09 (s, 3H). **^{1}H NMR** (400 MHz, $CDCl_3$) δ 158.3, 136.7, 131.5 (2C), 128.5 (2C), 128.3 (2C), 127.7, 124.3, 114.1 (2C), 93.9, 83.0,

55.5, 44.5, 38.5, 38.2, 33.8, 33.1, 26.6, 25.9, 22.2 (2C). **FT-IR** (cm^{-1}, neat, ATR): 2925, 2860, 1749, 1726, 1610, 1510, 1490, 1462, 1301, 1250, 1211, 1175, 1118, 1037. **HRMS** (EI) calcd for $C_{24}H_{29}O$ $[M+H]^+$: 332.2140, found 332.2144.

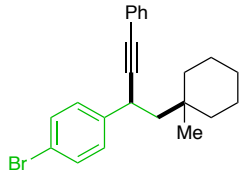

1-Bromo-4-(1-(1-methylcyclohexyl)-4-phenylbut-3-yn-2-yl)benzene, 4ag (41.4 mg, 45%) was prepared following *GP1*. The product was obtained as a colorless oil. **^{1}H NMR** (400 MHz, $CDCl_3$) δ 7.49 – 7.43 (m, 2H), 7.41 (dd, *J* = 6.6, 3.1 Hz, 2H), 7.34 – 7.27 (m, 5H), 3.87 (dd, *J* = 10.0, 3.4 Hz, 1H), 2.01 (dd, *J* = 13.9, 10.0 Hz, 1H), 1.64 – 1.30 (m, 11H), 1.10 (s, 3H). **^{13}C NMR** (101 MHz, $CDCl_3$) δ 143.5, 131.8 (2C), 131.5 (2C), 129.3 (2C), 128.4 (2C), 127.9, 123.9, 120.3, 92.8, 83.5, 51.0, 38.5, 38.2, 33.9, 33.5, 26.5, 25.8, 22.2 (2C). **FT-IR** (cm^{-1}, neat, ATR): 2923, 2848, 1597, 1486, 1071, 1011, 754. **HRMS** (EI) calcd for $C_{23}H_{25}Br$ $[M]^+$: 380.1140, found 380.1144.

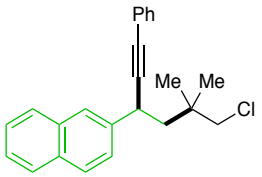

2-(6-Chloro-5,5-dimethyl-1-phenylhex-1-yn-3-yl)naphthalene, **4ah** (49 mg, 47%) was prepared following *GP1*. The product was obtained as a colorless oil. **^{1}H NMR** (400 MHz, $CDCl_3$) δ δ 7.92 – 7.80 (m, 4H), 7.57 (d, *J* = 8.5 Hz, 1H), 7.53 – 7.42 (m, 4H), 7.37 – 7.29 (m, 3H), 4.09 (dd, *J* = 10.5, 3.7 Hz, 1H), 3.62 (q, *J* = 10.8 Hz, 2H), 2.13 (dd, *J* = 14.1, 10.5 Hz, 1H), 1.91 (dd, *J* = 14.1, 3.7 Hz, 1H), 1.22 (d, *J* = 5.0 Hz, 6H). **^{13}C NMR** (101 MHz, $CDCl_3$) δ 140.7,

133.7, 132.6, 131.6 (2C), 128.6, 128.4 (2), 128.1, 127.9, 127.8, 126.3, 126.0, 125.8, 125.8, 123.8, 92.2, 84.2, 55.5, 47.7, 36.3, 34.7, 26.2, 25.9. **FT-IR** (cm^{-1}, neat, ATR): 2961, 1598, 1507, 1490, 1468, 1442, 1387, 1367, 1265. **HRMS** (EI) calcd for $C_{24}H_{24}Cl$ $[M+H]^+$: 347.1567, found 347.1557.

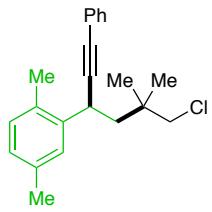

1,4-Dimethyl-2-(1-(1-methylcyclohexyl)-4-phenylbut-3-yn-2-yl)benzene, **4ai** (55 mg, 55%) was prepared following *GP1*. The product was obtained as a colorless oil. **^{1}H NMR** (400 MHz, $CDCl_3$) δ 7.46 – 7.39 (m, 3H), 7.34 – 7.26 (m, 3H), 7.06 (d, *J* = 7.6 Hz, 1H), 6.98 (dd, *J* = 7.7, 1.9 Hz, 1H), 4.10 (dd, *J* = 10.7, 2.8 Hz, 1H), 2.39 (s, 3H), 2.36 (s, 3H), 2.34 (d, *J* = 5.6 Hz, 1H), 2.04 (dd, *J* = 13.9, 10.7 Hz, 1H), 1.71 – 1.59 (m, 2H), 1.54 – 1.45 (m, 6H), 1.45 – 1.37 (m, 2H), 1.17 (s, 3H). **^{13}C NMR** (101 MHz, $CDCl_3$) δ 142.3, 136.0, 131.5 (2C), 131.2, 130.6, 128.7, 128.3 (2C), 127.6, 127.3, 124.4, 94.1, 82.4, 49.6, 38.8, 38.1, 34.0, 30.3, 26.6, 25.7, 22.3 (2C), 21.3, 19.2. **FT-IR** (cm^{-1}, neat, ATR): 2924, 2861, 1598, 1502, 1490, 1443, 1378, 1156, 1069. **HRMS** (EI) calcd for $C_{25}H_{31}$ $[M+H]^+$: 330.2348, found 330.2349.

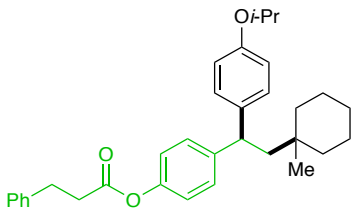

4-(1-(4-Isopropoxyphenyl)-2-(1-methylcyclohexyl)ethyl)phenyl 3-Phenylpropanoate, **4aj** (65 mg, 45%) was prepared following *GP1*. The product was obtained as a colorless oil. **^{1}H NMR** (400 MHz, $CDCl_3$) δ 7.36 – 7.30 (m, 2H), 7.31 – 7.20 (m, 5H), 7.17 (d, *J* = 8.7 Hz, 2H), 6.91 (d, *J* = 8.5 Hz, 2H), 6.79 (d, *J* = 8.7 Hz, 2H), 4.54 – 4.44 (m, 1H), 4.03 (t, *J* = 6.5 Hz, 1H), 3.07 (t, *J* = 7.7 Hz, 2H), 2.87 (t, *J* = 7.7 Hz, 2H), 2.13 – 1.99 (m, 2H), 1.47 – 1.33 (m, 5H), 1.32 (dd, *J* = 6.0, 1.3 Hz, 6H), 1.26 – 1.14 (m, 5H), 0.79 (s, 3H). **^{13}C NMR** (101 MHz, $CDCl_3$) δ 171.6, 156.2, 148.6, 145.2, 140.3, 138.7, 128.8 (2C), 128.7(4C), 128.5 (2C), 126.5, 121.3 (2C), 115.9 (2C), 70.0, 48.6, 46.0, 44.6, 38.6, 36.1, 34.0, 31.1, 29.9, 26.5, 25.4, 22.3, 22.2, 22.1. **FT-IR** (cm^{-1}, neat, ATR): 3029, 2974, 2924, 2860, 1758, 1608, 1504, 1454, 1372, 1297, 1243, 1203, 1167, 1129, 1077, 1017. **HRMS** (ESI) calcd for $C_{33}H_{40}O_3Na$ $[M+Na]^+$: 507.2875, found 507.2886.

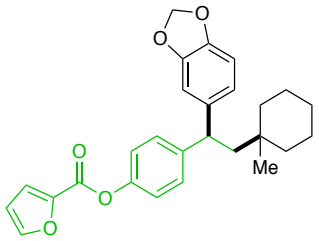

4-(1-(Benzo[*d*][1,3]dioxol-5-yl)-2-(1-methylcyclohexyl)ethyl)phenyl furan-2-carboxylate, **4ak** (63 mg, 48%) was prepared following *GP1*. The product was obtained as a white solid. **mp** = 75 – 77 ºC. **^{1}H NMR** (400 MHz, $CDCl_3$) δ 7.68 – 7.63 (m, 1H), 7.37 – 7.29 (m, 3H), 7.11 (d, *J* = 8.6 Hz, 2H), 6.82 – 6.68 (m, 3H), 6.57 (dd, *J* = 3.5, 1.8 Hz, 1H), 5.90 (d, *J* = 2.4 Hz, 2H), 4.03 (t, *J* = 6.5 Hz, 1H), 2.11 – 2.01 (m, 2H), 1.46 – 1.34 (m, 5H), 1.29 – 1.18 (m, 5H), 0.80 (s, 3H). **^{13}C**

NMR (101 MHz, $CDCl_3$) δ 157.1, 148.3, 147.8, 147.2, 145.8, 145.1, 144.2, 140.7, 128.7 (2C), 121.5 (2C), 120.8, 119.4, 112.3, 108.4, 108.3, 101.0, 48.5, 46.6, 38.6 (2C), 34.0, 26.5, 25.3, 22.1 (2C). **FT-IR** (cm^{-1}, neat, ATR): 2924, 2859, 1740, 1503, 1486, 1471, 1441, 1392, 1293, 1245, 1231, 1203, 1174, 1089, 1070, 1040, 1015. **HRMS** (ESI) calcd for $C_{27}H_{28}O_5Na$ $[M+Na]^+$: 455.1834, found 455.1835.

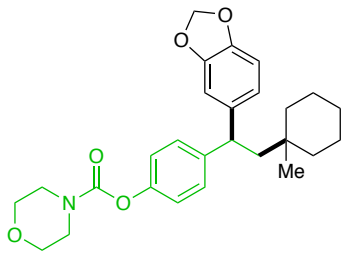

4-(1-(Benzo[*d*][1,3]dioxol-5-yl)-2-(1-methylcyclohexyl)ethyl)phenyl Morpholine-4-carboxylate, **4al** (92 mg, 68%) was prepared following *GP1*. The product was obtained as a white solid. **mp** = 103 – 105 ºC. **^{1}H NMR** (400 MHz, $CDCl_3$) δ 7.27 (d, *J* = 8.0 Hz, 2H), 7.02 (d, *J* = 8.2 Hz, 2H), 6.84 – 6.66 (m, 3H), 5.90 (d, *J* = 3.7 Hz, 2H), 4.02 (t, *J* = 6.5 Hz, 1H), 3.74 (t, *J* = 4.7 Hz, 4H), 3.61 (d, *J* = 30.7 Hz, 4H), 2.05 (d, *J* = 6.5 Hz, 2H), 1.47 – 1.33 (m, 5H), 1.30 – 1.18 (m, 5H), 0.80 (s, 3H). **^{13}C NMR** (101 MHz, $CDCl_3$) δ 153.9, 149.3, 147.7, 145.7, 144.3, 140.9, 128.5 (2C), 121.5 (2C), 120.7, 108.3, 108.2, 100.9, 66.7 (2C), 48.4, 46.5, 44.9, 44.18, 38.6 (2C), 34.0, 26.5, 25.3, 22.1 (2C). **FT-IR** (cm^{-1}, neat, ATR): 2922, 2858, 1719, 1503, 1487, 1454, 1439, 1420, 1366, 1278, 1241, 1208, 1169, 1117, 1066, 1040, 1017. **HRMS** (EI) calcd for $C_{27}H_{34}NO_5$ $[M+H]^+$: 474.2256, found 474.2259.

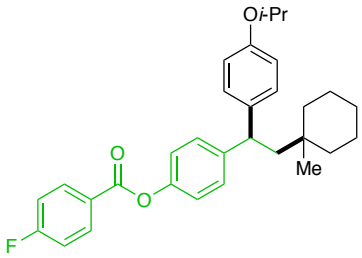

4-(1-(4-Isopropoxyphenyl)-2-(1-methylcyclohexyl)ethyl)phenyl 4-Fluorobenzoate, **4am** (65 mg, 46%) was prepared following *GP1*. The product was obtained as a white solid. **mp** = 67 – 68 ºC. **^{1}H NMR** (400 MHz, $CDCl_3$) δ 8.20 (dd, *J* = 8.7, 5.6 Hz, 2H), 7.33 (d, *J* = 8.3 Hz, 2H), 7.22 – 7.14 (m, 4H), 7.10 (d, *J* = 8.4 Hz, 2H), 6.80 (d, *J* = 8.5 Hz, 2H), 4.54 – 4.44 (m, 1H), 4.07 (t, *J* = 6.5 Hz, 1H), 2.13 – 2.05 (m, 2H), 1.44 – 1.35 (m, 5H), 1.31 (d, *J* = 6.1 Hz, 6H), 1.28 – 1.17 (m, 5H), 0.81 (s, 3H). **^{19}F NMR** (376 MHz, $CDCl_3$) *δ* -104.62. **^{13}C NMR** (101 MHz, $CDCl_3$) δ 166.1 (d, $J_{C\text{-}F}$ = 255.0 Hz), 164.3, 156.1, 148.7, 145.3, 138.6, 132.8 (d, $J_{C\text{-}F}$ = 9.4 Hz, 2C), 128.7 (4C), 126.0 (d, $J_{C\text{-}F}$ = 2.9 Hz), 121.3 (2C), 115.83 (2C), 115.76 (d, $J_{C\text{-}F}$ = 22.1 Hz, 2C), 69.9, 48.5, 46.0, 38.6 (2C), 33.9, 26.4, 25.3, 22.2, 22.1, 22.0 (2C). **FT-IR** (cm^{-1}, neat, ATR): 2975, 2924, 2860, 1739, 1604, 1507, 1452, 1297, 1262, 1242, 1202, 1168, 1154, 1120, 1071, 1015. **HRMS** (ESI) calcd for $C_{31}H_{35}FO_3Na$ $[M+Na]^+$: 492.2468, found 492.2463.

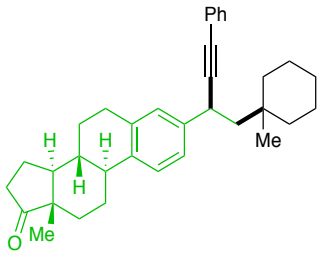

(8R,9S,13S,14S)-13-Methyl-3-(1-(1-methylcyclohexyl)-4-phenylbut-3-yn-2-yl)-6,7,8,9,11,12,13,14,15,16-decahydro-17H-cyclopenta[a]phenanthren-17-one, **4an** (112 mg, 78%, isolated as 1:1 diastereomeric mixture) was prepared following *GP1*. The product was

obtained as a colorless oil. **^{1}H NMR** (400 MHz, $CDCl_3$) δ 7.40 (ddd, *J* = 6.3, 3.1, 1.4 Hz, 2H), 7.31 – 7.25 (m, 4H), 7.20 (ddd, *J* = 8.2, 3.8, 2.1 Hz, 1H), 7.15 (d, *J* = 2.2 Hz, 1H), 3.84 (dd, *J* = 10.4, 3.0 Hz, 1H), 2.94 (dd, *J* = 9.2, 4.2 Hz, 2H), 2.51 (dd, *J* = 18.7, 8.6 Hz, 1H), 2.46 – 2.37 (m, 1H), 2.31 (td, *J* = 11.1, 4.1 Hz, 1H), 2.21 – 1.90 (m, 5H), 1.71 – 1.27 (m, 17H), 1.11 (s, 3H), 0.91 (s, 3H). **^{13}C NMR** (101 MHz, $CDCl_3$) δ 142.1, 138.1, 138.0, 136.8 (2C), 131.5, 128.3, 128.0, 127.7, 125.8, 124.9, 124.3, 93.7 (2C), 83.0 (2C), 50.7, 48.2, 44.5, 38.6, 38.3, 38.2, 36.0, 33.9, 33.5 (2C), 31.8, 29.7, 29.6, 26.7, 26.6, 25.9, 22.3, 21.8, 14.0. **FT-IR** (cm^{-1}, neat, ATR): 2923, 2856, 1739, 1489, 1453, 755. **HRMS** (ESI) calcd for $C_{35}H_{43}O$ $[M+H]^+$: 479.3314, found 479.3308.

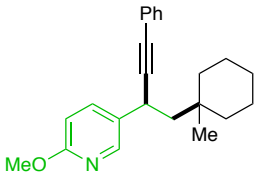

2-Methoxy-5-(1-(1-methylcyclohexyl)-4-phenylbut-3-yn-2-yl)pyridine, **4ao** (58.3 mg, 58%) was prepared following *GP1*. The product was obtained as a colorless oil. **^{1}H NMR** (400 MHz, $CDCl_3$) δ 8.18 (d, *J* = 2.6 Hz, 1H), 7.65 (dd, *J* = 8.6, 2.5 Hz, 1H), 7.41 – 7.36 (m, 2H), 7.28 (dt, *J* = 4.7, 2.8 Hz, 3H), 6.73 (d, *J* = 8.5 Hz, 1H), 3.93 (s, 3H), 3.86 (dd, *J* = 9.8, 3.6 Hz, 1H), 2.01 (dd, *J* = 14.0, 9.8 Hz, 1H), 1.63 – 1.50 (m, 3H), 1.49 – 1.31 (m, 8H), 1.09 (s, 3H). **^{13}C NMR** (101 MHz, $CDCl_3$) δ 163.1, 145.4, 138.1, 132.7, 131.5 (2C), 128.4 (2C), 127.9, 123.9, 110.9, 92.8, 83.3, 53.6, 50.9, 38.5, 38.2, 33.9, 30.7, 26.5, 25.8, 22.2 (2C). **FT-IR** (cm^{-1}, neat, ATR): 2924, 2847, 1605, 1490, 1391, 1288, 1027, 755. **HRMS** (ESI) calcd for $C_{23}H_{28}NO$ $[M+H]^+$: 334.2171, found 334.2175.

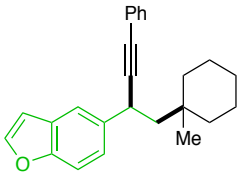

5-(1-(1-Methylcyclohexyl)-4-phenylbut-3-yn-2-yl)benzofuran, **4ap** (65.4 mg, 64%) was prepared following *GP1*. The product was obtained as a colorless oil. **^{1}H NMR** (400 MHz, $CDCl_3$) δ 7.64 (dd, *J* = 16.8, 2.0 Hz, 2H), 7.46 (d, *J* = 8.5 Hz, 1H), 7.41 (dq, *J* = 5.0, 2.9 Hz, 2H), 7.34 (dd, *J* = 8.5, 1.9 Hz, 1H), 7.31 – 7.22 (m, 3H), 6.75 (d, *J* = 2.1 Hz, 1H), 4.00 (dd, *J* = 10.0, 3.4 Hz, 1H), 2.08 (dd, *J* = 13.9, 10.0 Hz, 1H), 1.68 (dd, *J* = 14.0, 3.4 Hz, 1H), 1.63 – 1.54 (m, 2H), 1.51 – 1.30 (m, 8H), 1.12 (s, 3H). **^{13}C NMR** (101 MHz, $CDCl_3$) δ 154.0, 145.5, 139.2, 131.8, 131.6 (2C), 128.3 (2C), 127.7, 124.2, 124.1, 119.8, 111.5, 106.8, 94.0, 83.1, 51.6, 38.5, 38.2, 33.9 (2C), 26.6, 25.9, 22.3 (2C). **FT-IR** (cm^{-1}, neat, ATR): 2924, 2849, 1490, 1466, 1442, 1262, 1109, 1031, 755. **HRMS** (EI) calcd for $C_{25}H_{26}O$ $[M]^+$: 342.1984, found 342.1974.

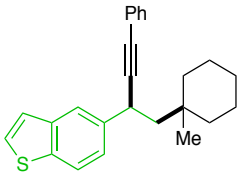

5-(1-(1-Methylcyclohexyl)-4-phenylbut-3-yn-2-yl)benzo[b]thiophene, **4aq** (78 mg, 73%) was prepared following *GP1*. The product was obtained as a colorless oil. **^{1}H NMR** (400 MHz, $CDCl_3$) δ 7.89 (d, *J* = 1.7 Hz, 1H), 7.84 (d, *J* = 8.3 Hz, 1H), 7.42 (ddd, *J* = 8.2, 7.1, 3.6 Hz, 4H), 7.35 – 7.27 (m, 4H), 4.03 (dd, *J* = 10.0, 3.3 Hz, 1H), 2.10 (dd, *J* = 13.9, 10.0 Hz, 1H), 1.70 (dd, *J* = 14.0, 3.3 Hz, 1H), 1.65 – 1.53 (m, 2H), 1.52 – 1.31 (m, 8H), 1.13 (s, 3H). **^{13}C NMR** (101 MHz, $CDCl_3$) δ 140.8, 140.1, 138.1, 131.6 (2C), 128.3 (2C), 127.8, 126.9, 124.4, 124.2, 124.0, 122.7, 122.2, 93.7, 83.2, 51.4, 38.5, 38.2, 33.9 (2C), 26.6, 25.9, 22.3 (2C). **FT-IR** (cm^{-1}, neat, ATR):

2921, 2845, 1597, 1489, 1441, 754, 690. **HRMS** (ESI) calcd for $C_{25}H_{27}S$ $[M+H]^+$: 359.1833, found 359.1826.

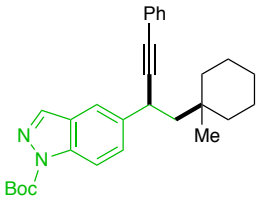

***tert*-Butyl 5-(1-(1-Methylcyclohexyl)-4-phenylbut-3-yn-2-yl)-1H-indazole-1-carboxylate**, **4ar** (86.4 mg, 65%) was prepared following *GP1*. The product was obtained as a colorless oil. **^{1}H NMR** (400 MHz, $CDCl_3$) δ 8.14 (d, *J* = 7.8 Hz, 2H), 7.80 (d, *J* = 1.7 Hz, 1H), 7.59 (dd, *J* = 8.8, 1.7 Hz, 1H), 7.42 (dd, *J* = 6.7, 2.9 Hz, 2H), 7.33 – 7.27 (m, 3H), 4.04 (dd, *J* = 9.9, 3.4 Hz, 1H), 2.08 (dd, *J* = 14.0, 9.9 Hz, 1H), 1.73 (s, 9H), 1.67 (dd, *J* = 14.0, 3.5 Hz, 1H), 1.63 – 1.53 (m, 2H), 1.51 – 1.32 (m, 8H), 1.12 (s, 3H). **^{13}C NMR** (101 MHz, $CDCl_3$) δ 149.3, 140.2, 139.7, 138.8, 131.5 (2C), 129.1, 128.4 (2C), 127.9, 126.3, 123.9, 119.2, 114.9, 93.2, 84.9, 83.5, 51.3, 38.5, 38.2, 33.9, 33.7, 28.3 (3C), 26.5, 25.9, 22.2 (2C). **FT-IR** (cm^{-1}, neat, ATR): 2923, 1758, 1734, 1384, 1369, 1350, 1290, 1249, 1162, 1149, 1029. **HRMS** (EI) calcd for $C_{24}H_{25}N_2$ [M-Boc]: 341.2018, found 341.2032.

5.5 References

(1) S. O. Badir, G. A. Molander, *Chem.* **2020**, *6*, 1327-1339.

(2) For selected reviews on DCF in the absence of a photocatalyst, see: (a) R. K. Dhungana, S. Kc, P. Basnet, R. Giri, *Chem. Rec.* **2018**, *18*, 1314-1340; (b) R. Giri, S. KC, *J. Org. Chem.* **2018**, *83*, 3013-3022; (c) J. Lin, R.-J. Song, M. Hu, J.-H. Li, *Chem. Rec.* **2019**, *19*, 440-451.

(3) For representative examples using palladium, see: (a) M. Koy, P. Bellotti, F. Katzenburg, C. G. Daniliuc, F. Glorius, *Angew. Chem. Int. Ed.* **2020**, *59*, 2375-2379; (b) M. Catellani, G. P.

Chiusoli, *Tetrahedron Lett.* **1982**, *23*, 4517-4520; (c) E. W. Werner, K. B. Urkalan, M. S. Sigman, *Org. Lett.* **2010**, *12*, 2848-2851; (d) L. Liao, R. Jana, K. B. Urkalan, M. S. Sigman, *J. Am. Chem. Soc.* **2011**, *133*, 5784-5787: (e) M. Orlandi, M. J. Hilton, E. Yamamoto, F. D. Toste, M. S. Sigman, *J. Am. Chem. Soc.* **2017**, *139*, 12688-12695.

(4) For representative examples using nickel, see: (a) X. Qi, T. Diao, *ACS Catal.* **2020**, *10*, 8542-8556; (b) J. Derosa, O. Apolinar, T. Kang, V. T. Tran, K. M. Engle, *Chem. Sci.* **2020**, *11*, 4287-4296; (c) S. KC, R. K. Dhungana, B. Shrestha, S. Thapa, N. Khanal, P. Basnet, R. W. Lebrun, R. Giri, *J. Am. Chem. Soc.* **2018**, *140*, 9801-9805; (d) Q. Lin, T. Diao, *J. Am. Chem. Soc.* **2019**, *141*, 17937-17948; (e) D. Anthony, Q. Lin, J. Baudet, T. Diao, *Angew. Chem. Int. Ed.* **2019**, *58*, 3198-3202; (f) W. Shu, A. García-Domínguez, M. T. Quirós, R. Mondal, D. J. Cárdenas, C. Nevado, *J. Am. Chem. Soc.* **2019**, *141*, 13812-13821; (g) L. Guo, H.-Y. Tu, S. Zhu, L. Chu, *Org. Lett.* **2019**, *21*, 4771-4776; (h) S.-Z. Sun, Y. Duan, R. S. Mega, R. J. Somerville, R. Martin, *Angew. Chem. Int. Ed.* **2020**, *59*, 4370-4374; (i) S. KC, R. K. Dhungana, N. Khanal, R. Giri, *Angew. Chem. Int. Ed.* **2020**, *59*, 8047-8051; (j) R. K. Dhungana, R. R. Sapkota, L. M. Wickham, D. Niroula, R. Giri, *J. Am. Chem. Soc.* **2020**, *142*, 20930-20936; (k) X. Wei, W. Shu, A. García-Domínguez, E. Merino, C. Nevado, *J. Am. Chem. Soc.* **2020**, *142*, 13515-113522; (l) D. Anthony, T. Diao, *Synlett* **2020**, *31*, 1443-1447; (m) L. Guo, M. Yuan, Y. Zhang, F. Wang, S. Zhu, O. Gutierrez, L. Chu, *J. Am. Chem. Soc.* **2020**, *142*, 20390-20399.

(5) For representative examples using copper, see: (a) Z. L. Li, G. C. Fang, Q. S. Gu, X. Y. Liu, *Chem. Soc. Rev*. **2020**, *49*, 32-48; (b) L. Wu, F. Wang, X. Wan, D. Wang, P. Chen, G. Liu, *J. Am. Chem. Soc.* **2017**, *139*, 2904-2907; (c) L. Fu, S. Zhou, X. Wan, P. Chen, G. Liu, *J. Am. Chem. Soc.* **2018**, *140*, 10965-10969; (d) W. Sha, L. Deng, S.; Ni, Mei, H.; Han J.; Pan, Y. *ACS Catal.* **2018**, *8*, 7489-7494; (e) Wu, L.; F. Wang, P. Chen, G. Liu, *J. Am. Chem. Soc.* **2019**, *141*, 1887-1892.

(6) For representative examples using other metals, see: (a) L. Liu, W. Lee, M.Y. Youshaw, M.B. Geherty, P.Y. Zavalij, O. Gutierrez, *Chem. Sci.* **2020**, *11,* 8301-8305; (b) J. Terao, K. Saito, S. Nii, N. Kambe, N. Sonoda, *J. Am. Chem. Soc.* **1998**, *120*, 11822-11823; (c) K. Mizutani, H. Shinokubo, K. Oshima, *Org. Lett.* **2003**, *5*, 3959-3961; (d) X.-H. Ouyang, R.-J. Song, M. Hu, Y. Yang, J.-H. Li, *Angew. Chem. Int. Ed.* **2016**, *55*, 3187-3191.

(7) For representative synthesis of bioactive compounds, see: (a) S. KC, P. Basnet, S. Thapa, B. Shrestha, R. Giri, *J. Org. Chem.* **2018**, *83*, 2920-2936; (b) S. KC, R. K. Dhungana, V. Aryal, R. Giri, *Org. Process Res. Dev.* **2019**, *23*, 1686-1694; (c) T. Yang, X. Chen, W. Rao, M. J. Koh, *Chem* **2020**, *6*, 738-751.

(8) For representative electrochemical DCF methods, see: (a) G. S. Sauer, S. Lin, *ACS Catal.* **2018**, *8*, 5175-5187; (b) H. Mei, Z. Yin, J. Liu, H. Sun, J. Han, *Chin. J. Chem.* **2019**, *37*, 292-301; (c) J. C. Siu, N. Fu, S. Lin, *Acc. Chem. Res.* **2020**, *53*, 547-560; (d) Zhang, W.; Lin, S. *J. Am. Chem. Soc.* **2020**, *142*, 20661-20670.

(9) For selected examples on photoredox-mediated RPC, see: (a) R. J. Wiles, G. A. Molander, *Isr. J. Chem*. **2020**, 60, 281-293; (b) L. Pitzer, J. L. Schwarz, F. Glorius, *Chem. Sci.* **2019**, *10*, 8285-8291; (c) X. Wang, Y.-F. Han, X.-H. Ouyang, R.-J. Song, J.-H. Li, *Chem. Commun.* **2019**, *55*, 14637-14640.

(10) Q.-F. Bao, Y. Xia, M. Li, Y.-Z. Wang, Y.-M. Liang, *Org. Lett.* **2020**, *22*, 7757-7761.

(11) For representative RPC-mediated carboxylation reactions, see: (a) V. R. Yatham, Y. Shen, R. Martin, *Angew. Chem. Int. Ed.* **2017**, *56*, 10915-10919; (b) J. Hou, A. Ee, H. Cao, H.-W. Ong, J.-H. Xu, J. Wu, *Angew. Chem. Int. Ed.* **2018**, *57*, 17220-17224; (c) B. Zhang, Y. Yi, Z.-Q. Wu, C. Chen, C. Xi, *Green Chem.* **2020**, *22*, 5961-5965; (d) H. Wang, Y. Gao, C. Zhou, G. Li, *J. Am. Chem. Soc.* **2020**, *142*, 8122-8129.

(12) For selected examples using heteroatom-based nucleophiles, see: (a) L. Li, H. Chen, M. Meia, L. Zhou, *Chem. Commun.* **2017**, *53*, 11544-11547; (b) X.-H. Ouyang, Y. Li, R.-J. Song, J.-H. Li, *Org. Lett.* **2018**, *20*, 6659-6662; (c) T. Patra, P. Bellotti, F. Strieth-Kalthoff, F. Glorius, *Angew. Chem. Int. Ed.* **2020**, *59*, 3172-3177; (d) E. W. Webb, J. B. Park, E. L. Cole, D. J. Donnelly, S. J. Bonacorsi, W. R. Ewing, A. G. Doyle, *J. Am. Chem. Soc.* **2020**, *142*, 9493-9500; (e) S. Shibutani, K. Nagao, H. Ohmiya, *Org. Lett.* **2021**, *23*, 1798-1803; (f) G. Fumagalli, S. Boyd, M.F. Greaney, *Org. Lett.* **2013**, *15*, 4398-4401.

(13) For selected RPC-mediated protocols using *C*-nucleophiles, see: (a) A. Carboni, G. Dagousset, E. Magnier, G. Masson, *Chem. Commun.* **2014**, *50*, 14197-14200; (b) Y. Duan, W. Li, P. Xu, M. Zhang, Y. Cheng, C. Zhu, *Org. Chem. Front.* **2016**, *3*, 1443-1446; (c) M. Lux, M. Klussmann, *Org. Lett.* **2020**, *22*, 3697-3701.

(14) S. Murarka, *Adv. Synth. Catal.* **2018,** *360*, 1735-1753.

(15) For selected examples, see: (a) S. Lee, D. W. C. MacMillan, *J. Am. Chem Soc.* **2007**, *129*, 15438-15439; (b) A. S. Vieira, P. F. Fiorante, T. L. S. Hough, F. P. Ferreira, D. S. Lüdtke, H. A. Stefani, *Org. Lett.* **2008**, *10*, 5215-5218; (c) C.-V. T. Vo, T. A. Mitchell, J. W. Bode, *J. Am. Chem. Soc.* **2011**, *133*, 14082-14089; (d) S. Roscales, A. Csákÿ, *Chem. Commun.* **2014**,*50*, 454-456; (e) H. A. Stefani, F. Manarin, A. C. S. Sousa, F. B. Souza, W. R. Ferraz, *Tetrahedron* **2014**, *70*, 3243-3248; (f) K. M. Fisher, Y. Bolshan, *J. Org. Chem.* **2015**, *80*, 12676-12685; (g) T. N. Nguyen, T. S. Nguyen, J. A. May, *Org. Lett.* **2016**, *18*, 3786-3789; (h) R. William, S. Wang, A. Mallick, X.-W. Liu, *Org. Lett.* **2016**, *18*, 4458-4461; (i) S. Roscales, V. Ortega, A. G. Csákÿ, *J. Org. Chem.* **2018**, *83*, 11425-11436; (j) T. N. Nguyen, J. A. May, *Org. Lett.* **2018**, *20*, 3618-3621; (k) T. N. Nguyen, K. Setthakarn, J. A. May, *Org. Lett.* **2019**, *21*, 7837-7840; (l) J.-F. Wang, X. Meng, C.-H. Zhang, C.-M. Yu, B. Mao, *Org. Lett.* **2020**, *22*, 7427-7432; (m) S. Sundstrom, T. S. Nguyen, J. A. May, *Org. Lett.* **2020**, *22*, 1355-1359.

(16) For selected reviews, see: (a) G. A. Molander, *J. Org. Chem.* **2015**, *80*, 7837-7848; (b) S. Roscales, A. Csákÿ, *Chem. Soc. Rev.* **2014**, *43*, 8215-8225.

(17) G. L. Lackner, K. W. Quasdorf, G. Pratsch, L. E. Overman, *J. Org. Chem.* **2015**, *80*, 6012-6024.

(18) For selected examples using organotrifluoroborates as radical precursors, see: (a) J. K. Matsui, D. N. Primer, G. A. Molander, *Chem. Sci.* **2017**, *8*, 3512-3522; (b) J. A. Milligan, J. P. Phelan, S. O. Badir, G. A. Molander, *Angew. Chem. Int.Ed.* **2019**, *58*, 6152-6163; (c) J. Yi, S. O. Badir, R. Alam, G. A. Molander, *Org. Lett.* **2019**, *21*, 4853-4858.

(19) Y. Wu, D. Kim, T. S. Teets, *Synlett* **2021**, *32*, 14-22.

(20) S. P. Pitre, T. K. Allred, L. E. Overman, *Org. Lett.* **2021**, *23*, 1103-11006.

(21) For selected Tsuji–Trost allylation reactions, see: (a) B. M. Trost, M. L. Crawley, *Chem. Rev.* **2003**, *103*, 2921-2944; (b) J. T. Mohr, B. M. Stoltz, *Chem. Asian J.* **2007**, *2*, 1476-1491; (c) J. D. Weaver, A. Recio III, A. J. Grenning, J. A. Tunge, *Chem. Rev.* **2011**, *111*, 1846-1913; (d) B. M. Trost, *Tetrahedron* **2015**, *71*, 5708-5733; (e) N.A. Butt, W. Zhang, *Chem. Soc. Rev.* **2015**, *44*, 7929-7967.

(22) For selected allylation reactions, see: (a) A. Yanagisawa, N. Nomura, S. Habaue, H. Yamamoto, *Tetrahedron Lett.* **1989**, *30*, 6409-6420; (b) N. Nomura, T. V. RajanBabu, *Tetrahedron Lett.* **1997**, *38*, 1713-1716; (c) K. Lee, J. Lee, P. H. Lee, *J. Org. Chem.* **2002**, *67*, 8265-8268; (d) S. Son, G. C. Fu, *J. Am. Chem. Soc.* **2008**, *130*, 2756-2757; (e) Y. Sumida, S. Hayashi, K. Hirano, H. Yorimitsu, K. Oshima, *Org. Lett.* **2008**, *10*, 1629-1632; (f) B. J. Stokes, S. M. Opra, M. S. Sigman, *J. Am. Chem. Soc.* **2012**, *134*, 11408-11411; (g) X. Cui, S. Wang, Y. Zhang, W. Deng, Q. Qian, H. Gong, *Org. Biomol. Chem.* **2013**, *11*, 3094-3097; (h) H. D. Srinivas, Q. Zhou, M. P. Watson, *Org. Lett.* **2014**, *16*, 3596-3599; (i) K. Hojoh, Y. Shido, K. Nagao, S. Mori, H. Ohmiya, M. Sawamura, *Tetrahedron* **2015**, *71*, 6519-6533; (j) B. Yang, Z.-X.

Wang, *J. Org. Chem.* **2017**, *82*, 4542-4549; (k) H. Chen, X. Jia, Y. Yu, Q. Qian, H. Gong, *Angew. Chem. Int. Ed.* **2017**, *56*, 13103-13106; (l) J. L. Hofstra, A. H. Cherney, C. M. Ordner, S. E. Reisman, *J. Am. Chem. Soc.* **2018**, *140*, 139-142; (m) X.-G. Jia, P. Guo, J. Duan, X.-Z. Shu, *Chem. Sci.* **2018**, *9*, 640-645; (n) K. Semba, N. Ohta, Y. Yano, Y. Nakao, *Chem. Commun.* **2018**, *54*, 11463-11466; (o) K. Semba, N. Ohta, Y. Nakao, *Org. Lett.* **2019**, *21*, 4407-4410; (p) H. Li, M. Zhang, H. Mehfooz, D. Zhu, J. Zhao, Q. Zhang, *Org. Chem. Front.* **2019**, *6*, 3387-3391; (q) V. T. Tran, Z.-Q Li, T. J. Gallagher, J. Derosa, P. Liu, K. M. Engle, *Angew. Chem. Int. Ed.* **2020**, *59*, 7029-7034.

(23) For selective examples, see: (a) D. Ameen, T. J. Snape, *Med. Chem. Commun.* **2013**, *4*, 893-907; (b) X. Liu, Y. Xiao, J.-Q. Li, B. Fu, Z. Qin, *Molecular Diversity* **2019**, *23*, 809-820.

(24) G. Berionni, B. Maji, P. Knochel, H. Mayr, *Chem. Sci.* **2012**, *3*, 878-882.

(25) M. A. Cismesia, T. P. Yoon, *Chem. Sci.* **2015**, *6*, 5426-5434.

(26) D. D. M. Wayner, D. J. McPhee, D. Griller, *J. Am. Chem. Soc.* **1988**, *110*, 132-137.

(27) For information on the construction of LED reactors, see the Supporting Information of: (a) N. R. Patel, C. B. Kelly, M. Jouffroy, G. A. Molander, *Org. Lett.* **2016**, *18*, 764-767; (b) M. Jouffroy, C. B. Kelly, G. A. Molander, *Org. Lett.* **2016**, *18*, 876-879.

(28) M. El Khatib, R. A. M. Serafim, G. A. Molander, *Angew. Chemie, Int. Ed.* **2016**, *55*, 254-258.

(29) M. Cismesia, T. P. Yoon, *Chem. Sci.* **2015**, *6*, 5426-5434.

(30) J. N. Demas, W. D. Bowman, E. F. Zalewski, R. Velapoidl, *J. Phys. Chem.* **1981**, *85*, 2766-2771.

Author Contributions: The topic was conceived by Shorouk O. Badir. María Jesús Cabrera-Afonso and Shorouk O. Badir performed Stern-Volmer quenching studies. Mirna El Khatib

conducted quantum yield experiments. María Jesús Cabrera-Afonso, Anasheh Sookezian, and Shorouk O. Badir performed experiments with input from Gary A. Molander. Shorouk O. Badir, María Jesús Cabrera-Afonso, and Anasheh Sookezian wrote the manuscript with input from Gary A. Molander.

Chapter 6. Photoredox-Catalyzed Multicomponent Alkyl Petasis Reaction with Organotrifluoroborates‡‡

6.1 Introduction

The disclosure of photochemical radical/polar crossover manifolds for sequential C–C bond formation provided a general multicomponent blueprint toward 1,2-dicarbofunctionalizations in the absence of organometal species. In recent years, multicomponent reactions (MCRs) have emerged as powerful tools to condense three or more partners to deliver novel structural scaffolds with inherent molecular complexity.[1] The advantages of MCRs include the preservation of atom- and step economies, shorter reaction times, and the ability to access highly diverse chemical space rapidly and efficiently. These integral benefits render MCRs highly attractive for diversity-oriented synthesis of small molecule libraries in drug discovery,[2] as well as in a variety of other useful endeavors.[3]

Presently, the tool box of a synthetic chemist is composed of many MCRs, including Mannich,[4] Biginelli,[5] Passerini,[6] and Ugi transformations.[7] As an important representative, the Petasis reaction[8] is a pivotal platform by virtue of its generation of amines and amino acid derivatives with significant activity in biology. The majority of traditional Petasis applications require adjacent heteroatoms as directing groups to form the key boron "ate" complex intermediate (Figure 6.1).[9] This initial complexation is followed by an irreversible, two-electron nucleophilic addition to an imine or iminium ion intermediate, stemming from a condensation reaction of the aldehyde and amine. The propensity of the boron "ate" complex to migrate

---

‡‡ Reproduced in part with permission from J. Yi, S. O. Badir, R. Alam, G. A. Molander, *Org. Lett.* **2019**, *21*, 4853–4858. Copyright 2019, American Chemical Society.

depends on its ability to stabilize negative charge: alkynyl > aryl ≈ alkenyl > alkyl.[10] Thus, the traditional Petasis reaction is restricted to alkenyl, aryl, alkynyl, allyl, benzyl, and allylic boronic acid derivatives.[8,9] To harness the full power of photoredox catalysis for sequential bond formation, the development of a multicomponent Petasis reactions using alkylboron derivatives to access unprecedented amine-based structural motifs was examined.

A widely utilized approach toward amine synthesis relies on two-electron nucleophilic additions to imines or iminium ions using strongly nucleophilic organometallic reagents.[11] These transformations, however, rely on harsh reaction conditions that compromise functional group tolerability, restricting their widespread use in late-stage functionalization of complex molecules. It is also important to note that the formation of water as a byproduct under a multicomponent platform would hinder the efficacy of these pyrophoric reagents. In the context of single-electron transfer (SET) in the multicomponent Petasis reaction, precedent reports require preformed imines[12] or the use of stoichiometric indium as a reductant with limited scope, being restricted to secondary alkyl iodides.[13] Other SET approaches to C═N bond alkylation, including Minisci reactions, are well documented.[14]

Our group, as well as others, recently demonstrated that photoredox catalysis enables the generation of alkyl radicals from organotrifluoroborates, while maintaining broad functional group tolerance.[15] Given the robust stability of alkyl radicals to aqueous conditions, a photoredox approach to a multicomponent Petasis-type reaction would appear feasible. We envisioned that a suitable photocatalyst in its excited state ([PC]*, **II**) would initiate the process by oxidizing an alkyltrifluoroborate **IV** to the desired alkyl radical **V** (Figure 6.1), generating BF_3 as a byproduct. The radical **V** could then add to the *in situ* condensed imine **VIII** to form the amine radical cation **IX**. A subsequent reduction of **IX** by the reduced state of the photocatalyst **III** terminates the

photocatalytic cycle. The use of trifluoroborates as radical precursors was viewed as critical for the success of the proposed protocol, because the BF_3 Lewis acid generated in the SET process was anticipated to facilitate the condensation between the aldehyde and the amine, activating the resultant imine toward radical addition.

Recently, the Doyle[16] and Gaunt[17] groups reported elegant multicomponent reactions to access benzhydryl amines as well as tertiary amines, respectively. In a unique transformation, Li reported a Ru-catalyzed addition of aldehydes to preformed aryl imines, accessing phenylalkyl amines. The scope of this process was restricted predominantly to benzaldehydes.[18] The multicomponent synthesis of analogous phenylalkyl amines thus remains underexplored.

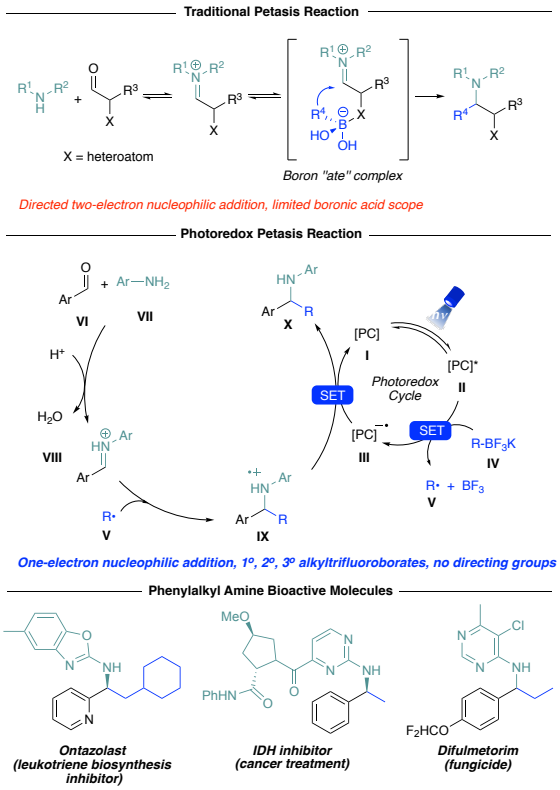

Figure 6.1. Mechanistic rationale: SET-based Petasis reaction and phenylalkyl amine bioactive molecules.

6.2 Results and Discussion

After a systematic survey of reaction parameters (see the Experimental Section), we were able to identify suitable reaction conditions. Thus, in exploratory studies, a mixture of methyl 4-formylbenzoate (**1**), aniline (**2**, 1.5 equiv), and potassium cyclohexyltrifluoroborate (**3**, 1.5 equiv), was catalyzed by $[Ir\{dF(CF_3)ppy\}_2(bpy)]PF_6$ (2 mol %, $E_{1/2}$ [$*Ir^{III}/Ir^{II}$] = + 1.32 V vs SCE)[19] in the presence of sodium bisulfate (1.0 equiv) in 1,4-dioxane (0.1 M). The desired product **4** was afforded in 84% isolated yield under irradiation with blue LEDs for 24 h at rt.[20] In expanding the method (Figure 6.2), diverse secondary alkyltrifluoroborates, including heteroaromatic-based systems, were found to be amenable substrates in this transformation. In the heteroaromatic substructures (e.g., **10**), no Minisci byproduct was detected. Sterically disfavored tertiary alkyltrifluoroborates gave excellent yields (**12**, **13**). Primary aliphatic alkyltrifluoroborates, with a markedly higher oxidation potential ($E_{1/2}^{red}$ = +1.90 V vs. SCE),[21] were accommodated under the reaction conditions (**14**-**16**).

Assessing the aldehyde scope (Figure 6.2), halo-substituted benzaldehyde derivatives whose products are suitable for further processing provided the targets in good yield (**25**-**27**). The reaction is highly chemoselective. In a dicarbonyl substrate, only the aldehyde derivative reacted, while the ketone remained untouched (**24**). Electron-donating groups are amenable structural motifs (**32**-**37**). Given that heteroarenes represent prevalent substructures in pharmaceutically relevant molecules,[22] a variety of such systems were evaluated and proved to be effective partners (**38-43**). Additionally, an unnatural α-amino acid derivative is accessible using glyoxyl aldehyde instead of a benzaldehyde derivative (**44**).

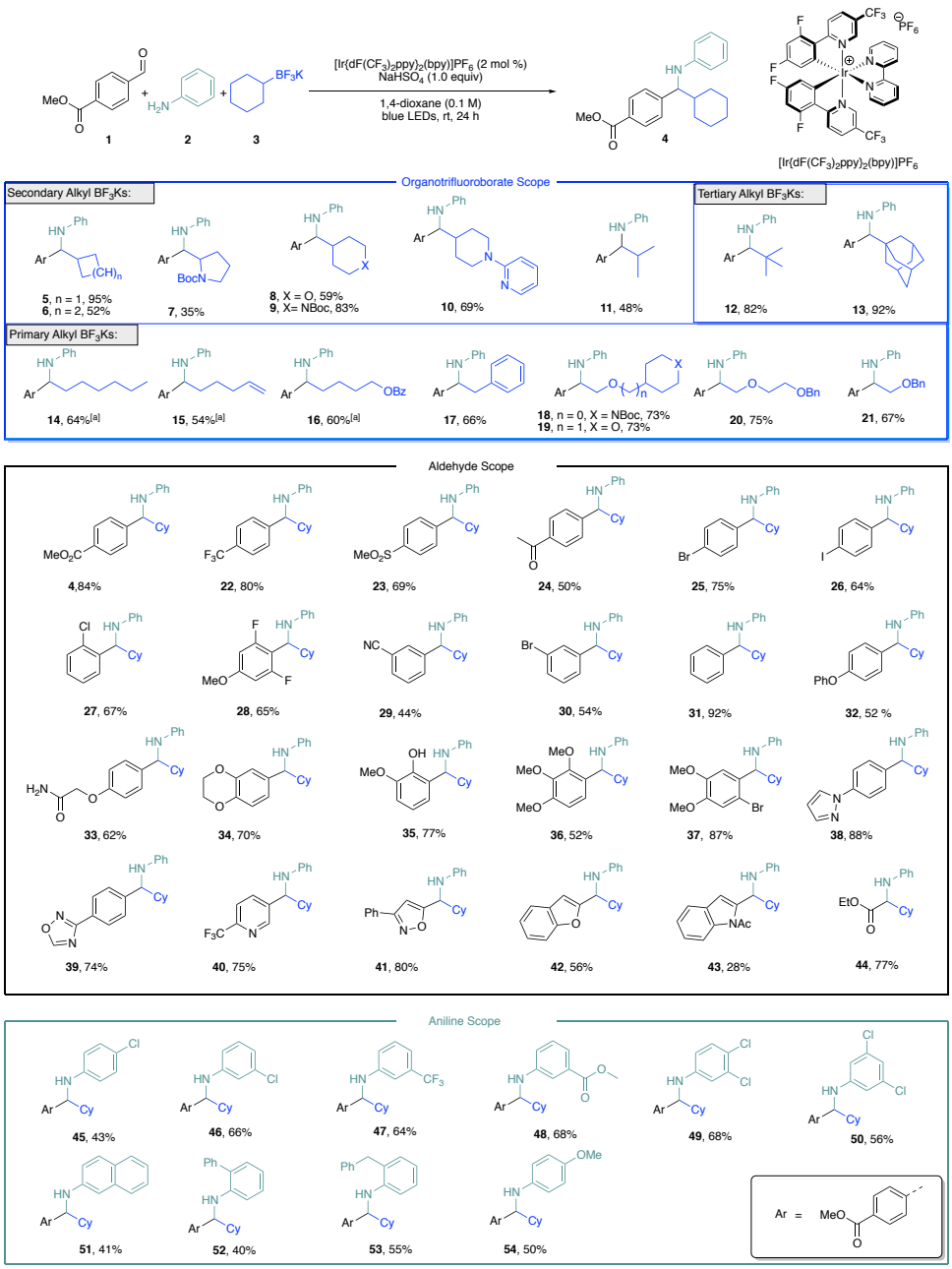

Figure 6.2. Scope of alkyltrifluoroborates, aldehydes and anilines. Reaction conditions: aldehyde (0.5 mmol), alkyltrifluoroborate (0.75 mmol), aniline (0.75 mmol), $[Ir\{dF(CF_3)ppy\}_2(bpy)]PF_6$ (0.01 mmol), $NaHSO_4$ (0.5 mmol) in 1,4-dioxane (5 mL, 0.1 M), 24 h irradiation with blue LEDs (λ_{max} = 456 nm). Isolated yields are given. [a]Irradiated with 34 W Kessil lamps.

Next, we turned our attention to the aniline partner (Figure 6.2) where a wide array of functional groups was tolerated, such as chloro (**45**, **46**, **49**, **50**), trifluoromethyl (**47**), ester (**48**), and methoxy (**54**). The electronic effect on the aniline component was inconspicuous. Meanwhile, the reactions were not sensitive to steric hindrance at the ortho position of the aniline (**52**, **53**).

To demonstrate the utility of this protocol for late-stage modification of intricate molecules, we prepared benzaldehyde derivatives from commercially available drug cores.[23] Both Indomethacin and Fenofibrate were successfully converted to the corresponding products in excellent yields (**55**, **56**, Figure 6.3 A). Sulfadimethoxine was also elaborated with acceptable yield, especially considering its high functional group density (**57**).

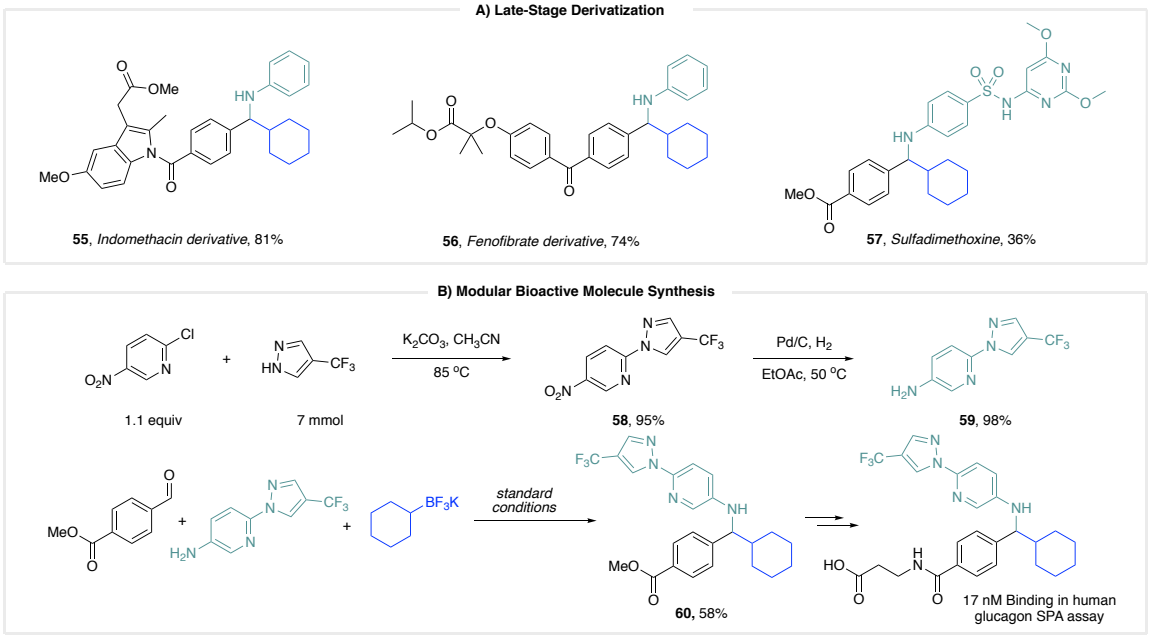

Figure 6.3. Late-stage functionalization of pharmaceutical analogues and modular bioactive molecule synthesis.

To highlight the application of this photoredox alkyl Petasis reaction further, we utilized this method to expedite the synthesis of a key intermediate toward a Pfizer glucagon receptor modulator (Figure 6.3 B).[24] The key intermediate (**60**) was assembled with good yield in one step using this newly developed, convergent MCR.

Next, a transformation was successfully performed on a larger scale, whereby the desired product **54** was obtained in 51% yield, in agreement with the small-scale reaction (Figure 6.4). It is worth indicating that the *para*-methoxyphenyl (PMP) group of **54** could be readily removed by ceric ammonium nitrate (CAN) oxidation to release the primary amine (**61**, Figure 6.4).[25]

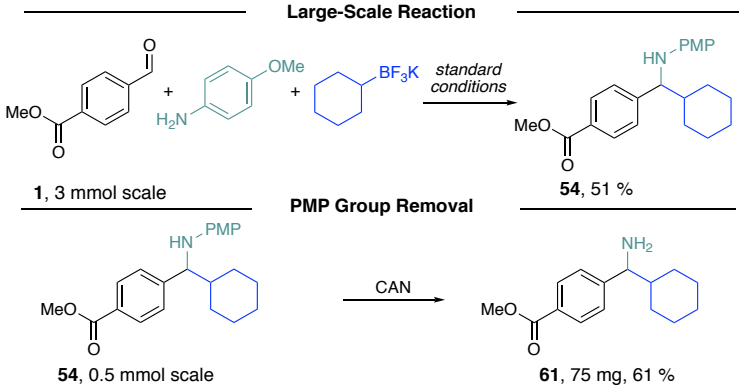

Figure 6.4. Large-scale reaction and removal of the PMP group.

To probe the reaction pathway, we conducted preliminary mechanistic studies. The ring-opening product was exclusively observed when potassium (cyclopropylmethyl)trifluoroborate was used as the starting material (Figure 6.5 A). In the presence of the radical scavenger TEMPO [(2,2,6,6-tetramethylpiperidin-1-yl)oxyl], the reaction was completely inhibited, and a TEMPO adduct was isolated, as well as the imine (Figure 6.5 B). This is indicative of the involvement of radical species under this reaction manifold. When the preformed imine was used instead of the aldehyde/aniline partners, a similar yield was detected (Figure 6.5 C). Furthermore, during the

course of the reaction, the reductive dimerization byproduct of the imine was not observed.[26] Although Stern-Volmer studies indicate no significant quenching of the excited state of the photocatalyst ($E_{1/2}$ [$Ir^{IV}/^{*}Ir^{III}$] = - 1.00 V vs SCE)[19] by the imine intermediate, we cannot rule out the possibility of direct reduction of the imine ($E_{1/2}$ = - 1.91 V vs SCE)[14e,27] by the reduced state of the photocatalyst ($E_{1/2}$ [Ir^{III}/Ir^{II}] = - 1.37 V vs SCE).[19] In particular, variabilities in reaction concentration and pH levels could exert an impact on redox potential values.[28]

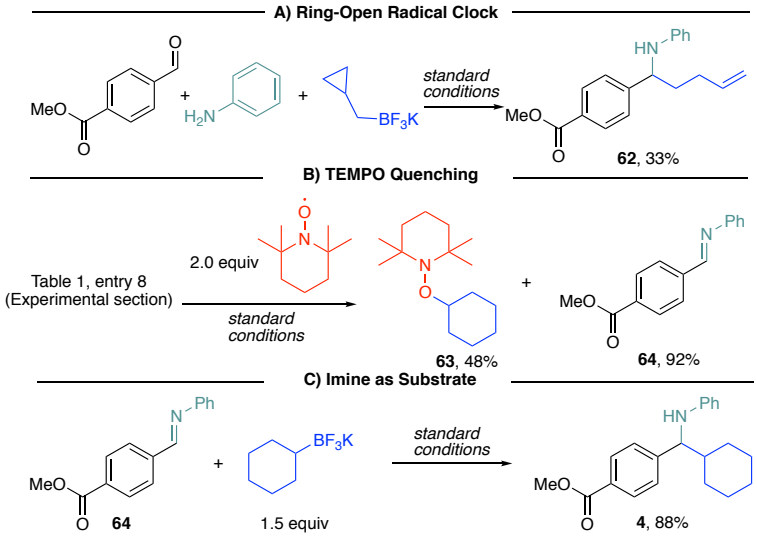

Figure 6.5. Mechanistic studies.

6.3 Conclusion

In summary, a multicomponent alkyl Petasis reaction under photoredox conditions has been developed. This procedure employs bench stable, commercially available alkyltrifluoroborates, easily accessible benzaldehydes, and anilines as feedstock. Taking advantage of the stability of alkyl radicals in water, preformed imines are no longer required, providing a highly step-efficient process that should be amenable to the industrial setting. Other favorable factors include the elimination of harsh reaction conditions (elevated temperatures and

strong organometallic reagents), and the toleration of an exceptional array of functional groups as well as complex structural scaffolds. The facile diversification inherent in this MCR positions this technology as being extremely suitable for diversity-oriented synthesis in drug discovery scenarios.

6.4 Experimental

General Consideration

General: All chemical transformations requiring inert atmospheric conditions were carried out using Schlenk line techniques with a 4- or 5-port dual-bank manifold. LED irradiation was accomplished as described in precedent reports.[29] NMR spectra (^{1}H, ^{13}C, ^{19}F) were obtained at 298 ºK. ^{1}H NMR spectra were referenced to residual, $CHCl_3$ (δ 7.26) in $CDCl_3$. ^{13}C NMR spectra were referenced to $CDCl_3$ (δ 77.30). In the case of diastereomeric mixtures, crude NMR was recorded to determine the ratio. Reactions were monitored by LC/MS, GC/MS, ^{1}H NMR, and/or TLC on silica gel plates (60 Å porosity, 250 μm thickness). TLC analysis was performed using hexanes/EtOAc as the eluent and visualized using ninhydrin, *p*-anisaldehyde stain, and/or UV light. Flash chromatography was accomplished using an automated system (CombiFlash®, UV detector, λ = 254 nm and 280 nm) with RediSep® R_f silica gel disposable flash columns (60 Å porosity, 40–60 μm) or RediSep R_f Gold® silica gel disposable flash columns (60 Å porosity, 20–40 μm). Accurate mass measurement analyses were conducted using electron ionization (EI) or electrospray ionization (ESI). The signals were mass measured against an internal lock mass reference of perfluorotributylamine (PFTBA) for EI-GC/MS and leucine enkephalin for ESI-LC/MS. The utilized software calibrates the instruments and reports measurements by use of neutral atomic masses. The mass of the electron is not included. IR spectra were recorded on an

FT-IR using either neat oil or solid products. Solvents were purified with drying cartridges through a solvent delivery system. Melting points (°C) are uncorrected.

Chemicals: Deuterated NMR solvents were purchased and stored over 4Å molecular sieves. EtOAc, hexanes, MeOH, Et_2O, and toluene were obtained from commercial suppliers and used as purchased. CH_2Cl_2 and THF were purchased and dried *via* a solvent delivery system. $NaHSO_4$ was purchased and used after grinding with a pestle and mortar. Anhydrous 1,4-dioxane was purchased and stored over 4Å molecular sieves. Aldehydes, alkyltrifluoroborates, and amines were purchased from commercial suppliers and used without further purification. All other reagents were purchased commercially and used as received.

General Procedures

Multicomponent Petasis reaction (GP1): To an 8 mL reaction vial equipped with a stir bar was added $[Ir\{dFCF_3ppy\}_2(bpy)]PF_6$ (10.0 mg, 0.01 mmol, 2 mol %), alkyltrifluoroborate (140.0 mg, 0.75 mmol, 1.5 equiv), aldehyde (82.0 mg, 0.5 mmol, 1.0 equiv), amine (68.0 μL, 0.75 mmol, 1.5 equiv), and $NaHSO_4$ (60.0 mg, 0.5 mmol, 1.0 equiv). The vial was sealed with a cap containing a TFE lined silicone septa and placed under an argon *via* an inlet needle. The vial was evacuated three times *via* an inlet needle then purged with argon. Dry and degassed 1,4-dioxane was then added (5.0 mL, 0.1 M). If the amine or aldehyde were in the liquid state, they were added at this point directly *via* microsyringe. The reaction was placed under blue LED irradiation and vigorously stirred for 24 h. The reaction was maintained at approximately 24 °C *via* a fan. Upon completion, the reaction mixture was taken to dryness and then purified on an automated liquid chromatographic system using hexanes/EtOAc as elutent. [*Note: In some cases, the reaction forms a slurry. Consistent stirring is imperative for the full conversion of imines to the desired alkylated products]*.

Deprotection of p-methoxyphenylamines (GP2): To a soln of amine (0.50 mmol) in MeOH/H_2O (28 mL) was added CAN (3.0 equiv) at 0 °C. The reaction was stirred at this temperature for 1 h, then allowed to warm to rt overnight. Upon completion, the mixture was washed with CH_2Cl_2 (5 mL) then the aq layer was made alkaline by adding 2 N NaOH. The soln was extracted with EtOAc (4 x 20 mL) and then washed with brine, dried ($MgSO_4$), taken to dryness, and then purified on an automated liquid chromatographic system using hexanes/EtOAc as eluent.

Reaction Optimization

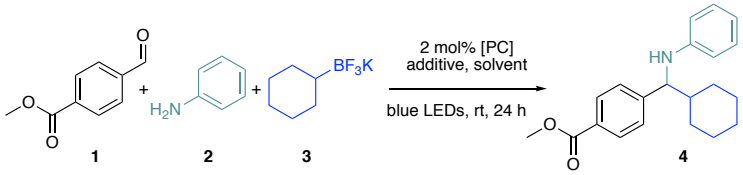

Entry	[PC]	Additive	Solvent	% Yield[a]
1	$[Ir(dtbbpy)(ppy)_2]PF_6$	-	acetonitrile	70
2	4CzIPN	-	acetonitrile	22
3	$[Ru(bpy)_3](PF_6)_2$	-	acetonitrile	10
4	$[Ir(dtbbpy)(ppy)_2]PF_6$	-	acetone	19
5	$[Ir(dtbbpy)(ppy)_2]PF_6$	-	DMF	23
6	$[Ir(dtbbpy)(ppy)_2]PF_6$	-	1,4-dioxane	64
7	$[Ir(dtbbpy)(ppy)_2]PF_6$	$NaHSO_4$	acetonitrile	65
8	**$[Ir(dtbbpy)(ppy)_2]PF_6$**	**$NaHSO_4$**	**1,4-dioxane**	**89(84)**
9	$[Ir(dtbbpy)(ppy)_2]PF_6$	$NaHSO_4$	DMSO	84
10	$[Ir(dtbbpy)(ppy)_2]PF_6$	benzoic acid	1,4-dioxane	14
11	$[Ir(dtbbpy)(ppy)_2]PF_6$	CSA	1,4-dioxane	67
12[c]	$[Ir(dtbbpy)(ppy)_2]PF_6$	$NaHSO_4/H_2O$	1,4-dioxane	86
13	No photocatalyst	$NaHSO_4$	1,4-dioxane	0
14[d]	$[Ir(dtbbpy)(ppy)_2]PF_6$	$NaHSO_4$	1,4-dioxane	0

Figure 6.6. Supplementary optimization studies following *GP1*. [a]Yields were determined via ^1H NMR analysis using 0.1 mmol trimethoxybenzene as internal standard (IS).

Mechanistic Investigation

Ring-opening radical clock: To an 8 mL reaction vial equipped with a stir bar were added $[Ir\{dFCF_3ppy\}_2(bpy)]PF_6$ (10.0 mg, 0.01 mmol, 2 mol %), potassium (cyclopropylmethyl)trifluoroborate (121.5 mg, 0.75 mmol, 1.5 equiv), methyl 4-formylbenzoate (82.0 mg, 0.5 mmol, 1.0 equiv), and $NaHSO_4$ (60.0 mg, 0.5 mmol, 1.0 equiv). The vial was sealed with a cap containing a TFE lined silicone septa and placed under an argon *via* an inlet needle. The vial was evacuated three times *via* an inlet needle then purged with argon. Dry and degassed 1,4-dioxane was then added (5.0 mL, 0.1 M). Aniline (68.0 µL, 0.75 mmol, 1.5 equiv) was added *via* microsyringe. The reaction was placed under 34 W blue Kessil lamp irradiation and vigorously stirred for 24 h. The reaction was maintained at approximately 24 °C *via* a fan. After completion, the reaction mixture was taken to dryness and then purified on an automated liquid chromatographic system (12 g column, 100:0→90:10 hexanes/EtOAc) to obtain the corresponding alkene.

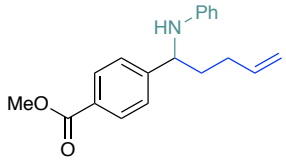

Methyl 4-(1-(Phenylamino)pent-4-en-1-yl)benzoate, **62** (49.0 mg, 33%). The desired amine was isolated as an oil. **^{1}H NMR** (500 MHz, $CDCl_3$) δ 8.02 (d, *J* = 7.8 Hz, 2H), 7.44 (d, *J* = 7.8 Hz, 2H), 7.10 (t, *J* = 7.4 Hz, 2H), 6.67 (t, *J* = 7.0 Hz, 1H), 6.51 (d, *J* = 7.7 Hz, 2H), 5.85 (td, *J* = 16.6, 6.6 Hz, 1H), 5.15 – 4.98 (m, 2H), 4.42 (t, *J* = 6.3 Hz, 1H), 4.14 (s, 1H), 3.92 (s, 3H), 2.24 – 2.11 (m, 2H), 1.98 – 1.84 (m, 2H). **^{13}C NMR** (126 MHz, $CDCl_3$) δ 166.9, 149.5, 146.9, 137.4, 129.9, 129.1, 128.9, 126.4, 117.5, 115.6, 113.2, 57.5, 51.9, 37.6, 30.3. **FT-IR** (cm^{-1}, neat, ATR):

3398, 2950, 2848, 1600, 1503, 1275, 1112, 748, 692. **HRMS** (EI) calcd for $C_{19}H_{21}NO_2$ $[M]^+$: 295.1572, found: 295.1567.

TEMPO quenching reaction: To an 8 mL reaction vial equipped with a stir bar were added $[Ir\{dFCF_3ppy\}_2(bpy)]PF_6$ (10.0 mg, 0.01 mmol, 2 mol %), potassium cyclohexyltrifluoroborate (140.0 mg, 0.75 mmol, 1.5 equiv), methyl 4-formylbenzoate (82.0 mg, 0.5 mmol, 1.0 equiv), TEMPO [(2,2,6,6-tetramethylpiperidin-1-yl)oxyl] (156.0 mg, 1.0 mmol, 2.0 equiv) and $NaHSO_4$ (60.0 mg, 0.5 mmol, 1.0 equiv). The vial was sealed with a cap containing a TFE lined silicone septa and placed under an argon *via* an inlet needle. The vial was evacuated three times *via* an inlet needle then purged with argon. Dry and degassed 1,4-dioxane was then added (5.0 mL, 0.1 M). Aniline (68.0 µL, 0.75 mmol, 1.5 equiv) was added *via* microsyringe. The reaction was placed under blue LED irradiation and vigorously stirred for 24 h. The reaction was maintained at approximately 24 °C *via* a fan. After completion, the reaction mixture was taken to dryness and then purified on an automated liquid chromatographic system (12 g column, 100:0→80:20 hexanes/EtOAc) to obtain the TEMPO adduct and imine.

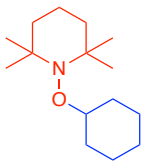

1-(Cyclohexyloxy)-2,2,6,6-tetramethylpiperidine, **63** (57.5 mg, 48%). The TEMPO adduct was isolated as a pale-yellow oil. **^{1}H NMR** (500 MHz, $CDCl_3$) δ 3.65 – 3.50 (m, 1H), 2.10 – 1.97 (m, 2H), 1.78 – 1.68 (m, 2H), 1.60 – 1.42 (m, 6H), 1.29 – 1.07 (m, 18H). **^{13}C NMR** (126 MHz, $CDCl_3$) δ 81.9, 59.7, 40.4, 34.6, 33.0, 26.1, 25.2, 20.4, 17.5.

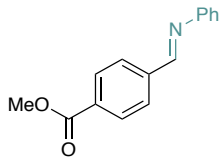

Methyl 4-((Phenylimino)methyl)benzoate, 64 (110 mg, 92%). The imine was isolated as a white solid. **^{1}H NMR** (500 MHz, $CDCl_3$) δ 8.53 (s, 1H), 8.19 – 8.13 (m, 2H), 8.03 – 7.95 (m, 2H), 7.47 – 7.39 (m, 2H), 7.33 – 7.21 (m, 3H), 3.97 (s, 3H). **^{13}C NMR** (126 MHz, $CDCl_3$) δ 166.49, 158.98, 151.44, 139.92, 132.26, 129.89, 129.14, 128.55, 126.41, 120.81, 52.23.

Imine as starting material: To an 8 mL reaction vial equipped with a stir bar were added $[Ir\{dFCF_3ppy\}_2(bpy)]PF_6$ (10.0 mg, 0.01 mmol, 2 mol %), alkyltrifluoroborate (140.0 mg, 0.75 mmol, 1.5 equiv), **64** (120 mg, 0.5 mmol, 1.0 equiv), and $NaHSO_4$ (60.0 mg, 0.5 mmol, 1.0 equiv). The vial was sealed with a cap containing a TFE lined silicone septa and placed under an argon *via* an inlet needle. The vial was evacuated three times *via* an inlet needle then purged with argon. Dry and degassed 1,4-dioxane was then added (5.0 mL, 0.1 M). Aniline (68.0 μL, 0.75 mmol, 1.5 equiv) was added at this point directly *via* microsyringe. The reaction was placed under blue LED irradiation and vigorously stirred for 24 h. The reaction was maintained at approximately 24 °C *via* a fan. After completion, the reaction mixture was taken to dryness and then purified on an automated liquid chromatographic system (24 g column, 100:0→85:15 hexanes/EtOAc) to obtain the obtain the desired amine.

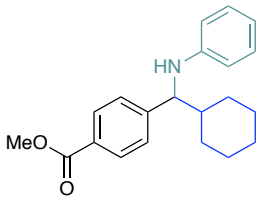

Methyl 4-(Cyclohexyl(phenylamino)methyl)benzoate, 4 (136 mg, 84%) was prepared following *GP1*. The desired amine was isolated as a solid. **mp** = 59-61 °C. **^{1}H NMR** (500 MHz, $CDCl_3$) δ 7.98 (d, *J* = 8.0 Hz, 2H), 7.38 (d, *J* = 8.0 Hz, 2H), 7.06 (t, *J* = 7.6 Hz, 2H), 6.62 (t, *J* = 7.2 Hz, 1H), 6.47 (d, *J* = 8.0 Hz, 2H), 4.23 – 4.12 (m, 2H), 3.90 (s, 3H), 1.87 (d, *J* = 12.6 Hz, 1H), 1.80 – 1.61 (m, 4H), 1.59 – 1.48 (m, 1H), 1.31 – 1.00 (m, 5H). **^{13}C NMR** (126 MHz, $CDCl_3$) δ 167.2, 148.5, 147.6, 129.8, 129.2, 129.0, 127.4, 117.4, 113.3, 63.5, 52.1, 44.9, 30.3, 29.5, 26.5, 26.5, 26.4. **FT-IR** (cm^{-1}, neat, ATR): 3404, 2924, 2851, 1706, 1600, 1502, 1277, 1103, 747, 691. **HRMS** (EI) calcd for $C_{21}H_{25}NO_2$ $[M]^+$: 323.1885, found: 323.1871.

Characterization Data

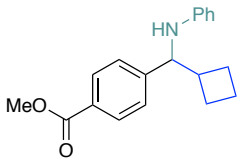

Methyl 4-(Cyclobutyl(phenylamino)methyl)benzoate, 5 (140 mg, 95%) was prepared following *GP1*. The desired amine was isolated as a solid. **mp** = 100-102 °C. **^{1}H NMR** (500 MHz, $CDCl_3$) δ 7.97 (d, *J* = 8.1 Hz, 2H), 7.41 (d, *J* = 8.2 Hz, 2H), 7.06 (t, *J* = 7.7 Hz, 2H), 6.63 (t, *J* = 7.3 Hz, 1H), 6.46 (d, *J* = 8.4 Hz, 2H), 4.22 (d, *J* = 8.6 Hz, 1H), 4.02 (s, 1H), 3.89 (s, 3H), 2.59 – 2.47 (m, 1H), 2.19 – 2.07 (m, 1H), 1.96 – 1.74 (m, 5H). **^{13}C NMR** (126 MHz, $CDCl_3$) δ 167.2, 148.3, 147.5, 130.0, 129.2, 129.14 126.7, 117.7, 113.5, 63.8, 52.1, 42.4, 26.2, 25.5, 17.7.

FT-IR (cm^{-1}, neat, ATR): 3361, 1702, 1602, 1313, 1282, 1114, 745, 691. **HRMS** (EI) calcd for $C_{19}H_{21}NO_2$ $[M]^+$: 295.1572, found: 295.1565.

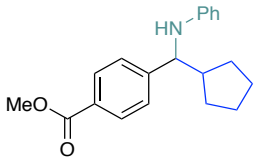

Methyl 4-(Cyclopentyl(phenylamino)methyl)benzoate, 6 (81 mg, 52%) was prepared following *GP1*. The desired amine was isolated as a solid. **mp** = 103-104 °C. **^{1}H NMR** (500 MHz, $CDCl_3$) δ 7.98 (d, *J* = 8.0 Hz, 2H), 7.43 (d, *J* = 8.1 Hz, 2H), 7.05 (t, *J* = 7.6 Hz, 2H), 6.62 (t, *J* = 7.3 Hz, 1H), 6.47 (d, *J* = 8.4 Hz, 2H), 4.21 (s, 1H), 4.14 (d, *J* = 8.3 Hz, 1H), 3.89 (s, 3H), 2.22 – 2.10 (m, 1H), 1.94 – 1.84 (m, 1H), 1.71 – 1.55 (m, 3H), 1.53 – 1.38 (m, 3H), 1.33 – 1.24 (m, 1H). **^{13}C NMR** (126 MHz, $CDCl_3$) δ 167.2, 149.7, 147.4, 129.9, 129.2, 129.0, 127.1, 117.5, 113.4, 63.1, 52.1, 47.7, 30.2, 30.0, 25.3, 25.3. **FT-IR** (cm^{-1}, neat, ATR): 3350, 2953, 2870, 1702, 1601, 1283, 1114, 745, 691. **HRMS** (EI) calcd for $C_{20}H_{23}NO_2$ $[M]^+$: 309.1729, found: 309.1725.

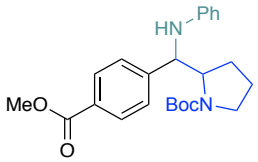

***tert*-Butyl 2-((4-(Methoxycarbonyl)phenyl)(phenylamino)methyl)pyrrolidine-1-carboxylate, 7** (72 mg, 35%) was prepared following *GP1*. The desired amine was isolated as an oil. **^{1}H NMR** (500 MHz, $CDCl_3$) δ 8.00 (d, *J* = 8.3 Hz, 2H), 7.52 (d, *J* = 7.8 Hz, 2H), 7.03 (t, *J* = 7.7 Hz, 2H), 6.57 (t, *J* = 7.3 Hz, 1H), 6.42 (d, *J* = 8.1 Hz, 2H), 4.27 – 4.15 (m, 2H), 3.90 (s, 3H), 3.51 – 3.03 (m, 2H), 1.86 (d, *J* = 18.0 Hz, 2H), 1.75 – 1.60 (m, 3H), 1.52 (s, 9H). **^{13}C NMR** (126 MHz, $CDCl_3$) δ 167.0, 157.5, 148.3, 148.0, 130.1, 129.6, 129.1, 127.9, 116.7, 112.7, 80.5, 63.7, 62.0,

52.2, 47.1, 28.6, 27.7, 23.7. **FT-IR** (cm^{-1}, neat, ATR): 3380, 2940, 2850, 1721, 1674, 1602, 1392, 1367, 1277, 1160. **HRMS** (ESI) calcd for $C_{24}H_{30}N_2O_4Na$ $[M+Na]^+$: 433.2103, found: 433.2111.

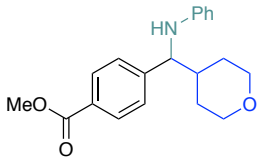

Methyl 4-((Phenylamino)(tetrahydro-2H-pyran-4-yl)methyl)benzoate, 8 (96 mg, 59%) was prepared following *GP1*. The desired amine was isolated as an oil. **^{1}H NMR** (500 MHz, $CDCl_3$) δ 7.99 (d, *J* = 8.2 Hz, 2H), 7.38 (d, *J* = 8.2 Hz, 2H), 7.07 (t, *J* = 7.9 Hz, 2H), 6.64 (t, *J* = 7.3 Hz, 1H), 6.48 (d, *J* = 7.9 Hz, 2H), 4.23 – 4.06 (m, 2H), 4.02 (dd, *J* = 11.4, 3.6 Hz, 1H), 3.95 (dd, *J* = 11.0, 3.2 Hz, 1H), 3.89 (s, 3H), 3.40 – 3.26 (m, 2H), 1.94 – 1.84 (m, 1H), 1.78 (d, *J* = 13.4 Hz, 1H), 1.54 – 1.42 (m, 2H), 1.32 (d, *J* = 13.3 Hz, 1H). **^{13}C NMR** (126 MHz, $CDCl_3$) δ 167.0, 147.6, 147.2, 130.0, 129.3, 129.3, 127.3, 117.9, 113.5, 68.1, 63.0, 52.2, 42.3, 29.7. **FT-IR** (cm^{-1}, neat, ATR): 3398, 2950, 2844, 1716, 1600, 1277, 1113, 750, 693. **HRMS** (EI) calcd for $C_{20}H_{23}NO_3$ $[M]^+$: 325.1678, found: 325.1674.

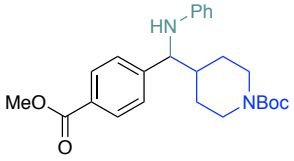

***tert*-Butyl 4-((4-(Methoxycarbonyl)phenyl)(phenylamino)methyl)piperidine-1-carboxylate, 9** (176 mg, 83%) was prepared following *GP1*. The desired amine was isolated as an oil. **^{1}H NMR** (500 MHz, $CDCl_3$) δ 7.99 (d, *J* = 8.1 Hz, 2H), 7.37 (d, *J* = 8.1 Hz, 2H), 7.06 (t, *J* = 7.7 Hz, 2H), 6.63 (t, *J* = 7.2 Hz, 1H), 6.49 (d, *J* = 7.6 Hz, 2H), 4.35 – 3.99 (m, 4H), 3.89 (s, 3H), 2.62 (d, *J* = 12.8 Hz, 2H), 1.95 – 1.71 (m, 2H), 1.52 – 1.37 (m, 10H), 1.35 – 1.19 (m, 2H). **^{13}C NMR** (126 MHz, $CDCl_3$) δ 167.0, 154.81, 147.7, 147.2, 130.0, 129.3, 129.3, 127.3, 117.8, 113.5, 79.7, 62.8,

52.2, 43.9, 43.3, 29.5, 28.9, 28.6. **FT-IR** (cm^{-1}, neat, ATR): 3385, 2949, 2851, 1673, 1427, 1278, 729. **HRMS** (ESI) calcd for $C_{25}H_{33}N_2O_4$ $[M+H]^+$: 425.2440, found: 425.2456.

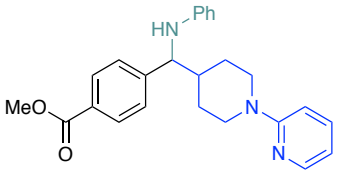

Methyl 4-((Phenylamino)(1-(pyridin-2-yl)piperidin-4-yl)methyl)benzoate, 10 (139 mg, 69%) was prepared following *GP1*. The desired amine was isolated as a solid. **mp** = 163-165 °C. **^{1}H NMR** (500 MHz, $CDCl_3$) δ 8.19 (d, *J* = 3.8 Hz, 1H), 8.01 (d, *J* = 8.1 Hz, 2H), 7.46 (dd, *J* = 11.3, 4.3 Hz, 1H), 7.41 (d, *J* = 8.1 Hz, 2H), 7.08 (t, *J* = 7.8 Hz, 2H), 6.65 (t, *J* = 8.7 Hz, 2H), 6.62 – 6.57 (m, 1H), 6.50 (d, *J* = 7.9 Hz, 2H), 4.45 – 4.14 (m, 4H), 3.91 (s, 3H), 2.82 – 2.69 (m, 2H), 2.01 – 1.86 (m, 2H), 1.58 – 1.40 (m, 3H). **^{13}C NMR** (126 MHz, $CDCl_3$) δ 166.8, 159.2, 147.9, 147.6, 147.0, 137.4, 129.8, 129.1, 127.1, 117.5, 113.3, 112.9, 107.1, 62.6, 52.0, 45.5, 45.4, 43.3, 29.1, 28.4. **FT-IR** (cm^{-1}, neat, ATR): 3450, 2950, 2850, 1702, 1593, 1477, 1432, 1283, 773. **HRMS** (EI) calcd for $C_{25}H_{27}N_3O_2$ $[M]^+$: 401.2103, found: 401.2088.

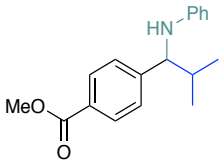

Methyl 4-(2-Methyl-1-(phenylamino)propyl)benzoate, 11 (68 mg, 48%) was prepared following *GP1*. The desired amine was isolated as a solid. **mp** = 84-86 °C. **^{1}H NMR** (500 MHz, $CDCl_3$) δ 8.00 (d, *J* = 8.2 Hz, 2H), 7.41 (d, *J* = 8.2 Hz, 2H), 7.08 (t, *J* = 7.8 Hz, 2H), 6.65 (t, *J* = 7.3 Hz, 1H), 6.49 (d, *J* = 8.3 Hz, 2H), 4.20 (d, *J* = 5.7 Hz, 1H), 4.15 (s, 1H), 3.91 (s, 3H), 2.14 – 2.02 (m, 1H), 1.01 (d, *J* = 6.8 Hz, 3H), 0.95 (d, *J* = 6.8 Hz, 3H). **^{13}C NMR** (126 MHz, $CDCl_3$) δ 167.0, 148.2, 147.3, 129.5, 129.0, 128.8, 127.2, 117.3, 113.2, 63.6, 51.9, 34.7, 19.6, 18.4. **FT-IR**

(cm^{-1}, neat, ATR): 3367, 2951, 1705, 1602, 1283, 1107, 746, 691. **HRMS** (EI) calcd for $C_{18}H_{21}NO_2$ $[M]^+$: 283.1572, found: 283.1570.

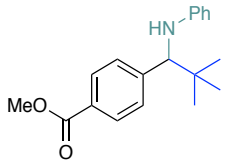

Methyl 4-(2,2-Dimethyl-1-(phenylamino)propyl)benzoate, 12 (122 mg, 82%) was prepared following *GP1*. The desired amine was isolated as an oil. **^{1}H NMR** (500 MHz, $CDCl_3$) δ 7.97 (d, *J* = 8.3 Hz, 2H), 7.40 (d, *J* = 8.3 Hz, 2H), 7.08 – 7.01 (m, 2H), 6.61 (t, *J* = 7.3 Hz, 1H), 6.49 – 6.42 (m, 2H), 4.28 (s, 1H), 4.11 (s, 1H), 3.90 (s, 3H), 1.01 (s, 9H). **^{13}C NMR** (126 MHz, $CDCl_3$) δ 167.2, 147.5, 147.1, 129.2, 129.2, 129.0, 128.7, 117.4, 113.3, 67.3, 52.2, 35.1, 27.2. **FT-IR** (cm^{-1}, neat, ATR): 3423, 2955, 1707,1600, 1506, 1315, 1285, 1098, 743. **HRMS** (EI) calcd for $C_{19}H_{23}NO_2$ $[M]^+$: 297.1741, found: 297.1729.

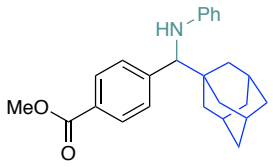

Methyl 4-((Adamantan-1-yl)(phenylamino)methyl)benzoate, 13 (173 mg, 92%) was prepared following *GP1*. The desired amine was Isolated as a solid. **mp** = 92-94 °C. **^{1}H NMR** (500 MHz, $CDCl_3$) δ 7.97 (d, *J* = 8.2 Hz, 2H), 7.36 (d, *J* = 8.2 Hz, 2H), 7.05 (t, *J* = 7.9 Hz, 2H), 6.61 (t, *J* = 7.3 Hz, 1H), 6.47 (d, *J* = 7.8 Hz, 2H), 4.38 (s, 1H), 3.95 (s, 1H), 3.90 (s, 3H), 2.01 (s, 3H), 1.71 (dd, *J* = 11.3, 3.8 Hz, 6H), 1.60 (d, *J* = 11.8 Hz, 3H), 1.52 (d, *J* = 11.8 Hz, 3H). **^{13}C NMR** (126 MHz, $CDCl_3$) δ 167.3, 147.7, 146.3, 129.2, 129.1, 129.0, 128.9, 117.3, 113.3, 68.1, 52.2, 39.4, 37.0, 36.7, 28.6. **FT-IR** (cm^{-1}, neat, ATR): 3361, 2899, 2847, 1703, 1600, 1517, 1430, 1290, 730. **HRMS** (EI) calcd for $C_{25}H_{29}NO_2$ $[M]^+$: 375.2198, found, 375.2207.

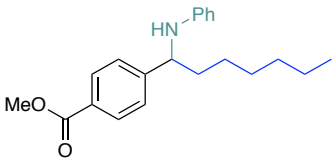

Methyl 4-(1-(Phenylamino)heptyl)benzoate, 14 (104 mg, 64%) was prepared following *GP1*. The desired amine was isolated as an oil. **^{1}H NMR** (500 MHz, $CDCl_3$) δ 7.99 (d, *J* = 8.2 Hz, 2H), 7.42 (d, *J* = 8.2 Hz, 2H), 7.07 (t, *J* = 7.8 Hz, 2H), 6.64 (t, *J* = 7.3 Hz, 1H), 6.47 (d, *J* = 8.1 Hz, 2H), 4.34 (t, *J* = 6.6 Hz, 1H), 4.08 (s, 1H), 3.90 (s, 3H), 1.88 – 1.69 (m, 2H), 1.46 – 1.19 (m, 8H), 0.87 (t, *J* = 6.8 Hz, 3H). **^{13}C NMR** (126 MHz, $CDCl_3$) δ 167.17, 150.13, 147.31, 130.12, 129.29, 129.04, 126.57, 117.61, 113.39, 58.34, 52.17, 39.01, 31.83, 29.30, 26.37, 22.73, 14.20. **FT-IR** (cm^{-1}, neat, ATR): 3399, 2927, 2855, 1712, 1601, 1503, 14345, 1275, 1112, 747. **HRMS** (ESI) calcd for $C_{21}H_{28}NO_2$ $[M+H]^+$: 326.2120, found: 326.2140.

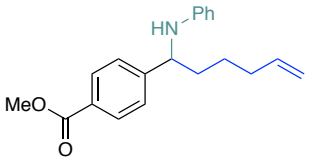

Methyl 4-(1-(Phenylamino)hex-5-en-1-yl)benzoate, 15 (84 mg, 54%) was prepared following *GP1*. The desired amine was isolated as an oil. **^{1}H NMR** (500 MHz, $CDCl_3$) δ 8.01 (d, *J* = 7.5 Hz, 2H), 7.43 (d, *J* = 7.6 Hz, 2H), 7.09 (t, *J* = 7.1 Hz, 2H), 6.66 (t, *J* = 6.8 Hz, 1H), 6.49 (d, *J* = 7.5 Hz, 2H), 5.78 (td, *J* = 16.3, 6.7 Hz, 1H), 5.08 – 4.94 (m, 2H), 4.38 (s, 1H), 4.11 (s, 1H), 3.91 (s, 3H), 2.10 (d, *J* = 6.5 Hz, 2H), 1.91 – 1.74 (m, 2H), 1.61 – 1.40 (m, 2H). **^{13}C NMR** (126 MHz, $CDCl_3$) δ 167.1, 149.9, 147.2, 138.2, 130.1, 129.3, 129.1, 126.6, 117.7, 115.3, 113.4, 58.2, 52.2, 38.3, 33.6, 25.6. **FT-IR** (cm^{-1}, neat, ATR): 3400, 2936, 2851, 1600, 1503, 1434, 1275, 1111, 911, 748, 692. **HRMS** (ESI) calcd for $C_{20}H_{24}NO_2$ $[M+H]^+$: 310.1807, found: 310.1797.

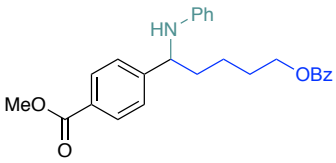

Methyl 4-(5-(Benzoyloxy)-1-(phenylamino)pentyl)benzoate, 16 (125 mg, 60%) was prepared following *GP1*. The desired amine was isolated as an oil. **^{1}H NMR** (500 MHz, $CDCl_3$) δ 8.03 – 7.96 (m, 4H), 7.56 (t, *J* = 7.4 Hz, 1H), 7.49 – 7.38 (dd, *J* = 7.6, 5.9 Hz, 4H), 7.08 (t, *J* = 7.8 Hz, 2H), 6.65 (t, *J* = 7.3 Hz, 1H), 6.49 (d, *J* = 8.0 Hz, 2H), 4.40 (t, *J* = 6.5 Hz, 1H), 4.37 – 4.27 (m, 2H), 4.18 (s, 1H), 3.90 (s, 3H), 1.96 – 1.76 (m, 4H), 1.66 – 1.45 (m, 2H). **^{13}C NMR** (126 MHz, $CDCl_3$) δ 167.1, 166.8, 149.7, 147.2, 133.1, 130.4, 130.2, 129.7, 129.3, 129.2, 128.5, 126.6, 117.7, 113.4, 64.6, 58.1, 52.2, 38.3, 28.7, 22.9. **FT-IR** (cm^{-1}, neat, ATR): 3400, 2949, 1713, 1600, 1504, 1313, 1272, 1111, 710. **HRMS** (ESI) calcd for $C_{26}H_{28}NO_4$ $[M+H]^+$: 418.2018, found: 418.2030.

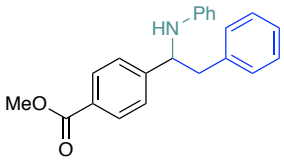

Methyl 4-(2-Phenyl-1-(phenylamino)ethyl)benzoate, 17 (109 mg, 66%) was prepared following *GP1*. The desired amine was isolated as an oil. **^{1}H NMR** (500 MHz, $CDCl_3$) δ 8.05 (d, *J* = 7.9 Hz, 2H), 7.44 (d, *J* = 7.9 Hz, 2H), 7.37– 7.27 (m, 3H), 7.19 – 7.07 (m, 4H), 6.72 (d, *J* = 7.1 Hz, 1H), 6.50 (d, *J* = 7.8 Hz, 2H), 4.71 (t, *J* = 6.6 Hz, 1H), 4.26 (s, 1H), 3.94 (s, 3H), 3.22 – 3.04 (m, 2H). **^{13}C NMR** (126 MHz, $CDCl_3$) δ 167.2, 149.1, 147.1, 137.3, 130.2, 129.4, 129.3, 128.8, 127.1, 126.8, 118.1, 113.9, 59.4, 52.2, 45.0. **FT-IR** (cm^{-1}, neat, ATR): 3380, 2940, 2863, 1717, 1602, 1504, 1313, 1276, 1098, 1018. **HRMS** (ESI) calcd for $C_{22}H_{22}NO_2$ $[M+H]^+$: 332.1651, found: 332.1668.

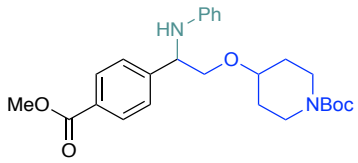

***tert*-Butyl 4-(2-(4-(Methoxycarbonyl)phenyl)-2-(phenylamino)ethoxy)piperidine-1-carboxylate, 18** (165 mg, 73%) was prepared following *GP1*. The desired amine was isolated as an oil. **^{1}H NMR** (500 MHz, $CDCl_3$) δ 8.00 (dd, *J* = 8.3, 2.0 Hz, 2H), 7.49 (d, *J* = 8.1 Hz, 2H), 7.14 – 6.96 (m, 2H), 6.83 – 6.59 (m, 1H), 6.55 – 6.36 (m, 2H), 4.71 (s, 1H), 4.53 (dd, *J* = 7.8, 4.1 Hz, 1H), 3.89 (s, 3H), 3.75 (dd, *J* = 9.7, 4.0 Hz, 1H), 3.66 (m, 2H), 3.56 (dd, *J* = 9.7, 7.8 Hz, 1H), 3.48 (tt, *J* = 7.7, 3.6 Hz, 1H), 3.10 (ddq, *J* = 13.4, 5.6, 3.5 Hz, 2H), 1.93 – 1.61 (m, 2H), 1.45 (s, 11H). **^{13}C NMR** (126 MHz, $CDCl_3$) δ 167.0, 154.9, 147.3, 146.4, 130.1, 129.5, 129.2, 127.0, 118.2, 114.1, 79.6, 75.1, 72.1, 67.2, 60.5, 58.5, 52.2, 28.5. **FT-IR** (cm^{-1}, neat, ATR): 3380, 2928, 1686, 1419, 1275, 1101. **HRMS** (ESI) calcd for $C_{26}H_{35}N_2O_5$ $[M+H]^+$: 455.2546, found: 455.2563.

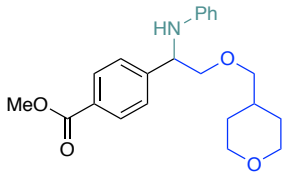

Methyl 4-(1-(Phenylamino)-2-((tetrahydro-2*H*-pyran-4-yl)methoxy)ethyl)benzoate, 19 (135 mg, 73%) was prepared following *GP1*. The desired amine was isolated as an oil. **^{1}H NMR** (500 MHz, $CDCl_3$) δ 8.00 (d, *J* = 8.1 Hz, 2H), 7.48 (d, *J* = 8.0 Hz, 2H), 7.08 (t, *J* = 7.7 Hz, 2H), 6.68 (t, *J* = 7.3 Hz, 1H), 6.49 (d, *J* = 7.9 Hz, 2H), 4.01 – 3.93 (m, 2H), 3.90 (s, 3H), 3.68 (dd, *J* = 10.0, 4.1 Hz, 1H), 3.54 (dd, *J* = 10.0, 8.1 Hz, 1H), 3.46 – 3.30 (m, 3H), 2.00 – 1.75 (m, 2H), 1.76 – 1.51 (m, 4H), 1.44 – 1.17 (m, 2H). **^{13}C NMR** (126 MHz, $CDCl_3$) δ 166.8, 147.2, 146.2, 129.9, 129.3, 129.0, 126.8, 117.9, 113.8, 76.0, 74.8, 67.5, 57.9, 52.0, 35.3, 29.8, 29.7. **FT-IR** (cm^{-1}, neat,

ATR) 2851, 1718, 1279, 1111, 906, 725. **HRMS** (ESI) calcd for $C_{22}H_{28}NO_4$ $[M+H]^+$: 370.2018, found: 370.2002.

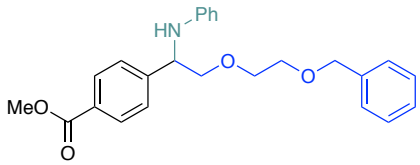

Methyl 4-(2-(2-(Benzyloxy)ethoxy)-1-(phenylamino)ethyl)benzoate, 20 (152 mg, 75%) was prepared following *GP1*. The desired amine was isolated as an oil. **^{1}H NMR** (500 MHz, $CDCl_3$) δ 8.04 – 7.91 (m, 2H), 7.55 – 7.42 (m, 2H), 7.42 – 7.28 (m, 5H), 7.18 – 6.94 (m, 2H), 6.75 – 6.60 (m, 1H), 6.55 – 6.35 (m, 2H), 4.77 (s, 1H), 4.56 (s, 3H), 3.90 (s, 3H), 3.78 (dd, *J* = 10.1, 4.0 Hz, 1H), 3.74 – 3.68 (m, 1H), 3.67 – 3.57 (m, 4H). **^{13}C NMR** (126 MHz, $CDCl_3$) δ 167.0, 147.5, 146.4, 138.2, 130.1, 129.5, 129.2, 128.6, 127.9, 127.9, 127.0, 118.0, 114.0, 75.3, 73.5, 70.6, 69.5, 58.2, 52.2. **FT-IR** (cm^{-1}, neat, ATR): 3027, 2950, 1717, 1601, 1503, 1277, 1112. **HRMS** (ESI) calcd for $C_{25}H_{28}NO_4$ $[M+H]^+$: 406.2018, found: 406.2038.

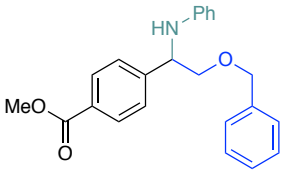

Methyl 4-(2-(Benzyloxy)-1-(phenylamino)ethyl)benzoate, 21 (121 mg, 67%) was prepared following *GP1*. The desired amine was isolated as an oil. **^{1}H NMR** (500 MHz, $CDCl_3$) δ 8.06 – 7.93 (m, 2H), 7.48 (d, *J* = 8.2 Hz, 2H), 7.39 – 7.18 (m, 5H), 7.14 – 6.96 (m, 2H), 6.68 (t, *J* = 7.3 Hz, 1H), 6.56 – 6.40 (m, 2H), 4.67 (s, 1H), 4.63 – 4.48 (m, 3H), 3.91 (s, 3H), 3.77 (dd, *J* = 10.0, 4.0 Hz, 1H), 3.61 (dd, *J* = 9.9, 7.9 Hz, 1H). **^{13}C NMR** (126 MHz, $CDCl_3$) δ 167.1, 147.3, 146.4, 137.7, 130.1, 129.5, 129.2, 128.7, 128.1, 127.9, 127.0, 118.1, 114.0, 74.1, 73.2, 58.2, 52.2. **FT-IR**

(cm^{-1}, neat, ATR): 3380, 2940, 2850, 1716, 1601, 1503, 1312, 1275, 1099. **HRMS** calcd for $C_{23}H_{23}NO_3$ $[M]^+$: 361.1678, found: 361.1665.

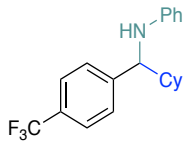

***N*-(Cyclohexyl(4-(trifluoromethyl)phenyl)methyl)aniline, 22** (133 mg, 80%) was prepared following *GP1*. The desired amine was isolated as an oil. **^{1}H NMR** (500 MHz, $CDCl_3$) δ 7.60 (d, *J* = 8.0 Hz, 2H), 7.45 (d, *J* = 8.0 Hz, 2H), 7.11 (t, *J* = 7.9 Hz, 2H), 6.68 (t, *J* = 7.2 Hz, 1H), 6.51 (d, *J* = 7.8 Hz, 2H), 4.04 – 4.32 (m, 2H), 1.89 (d, *J* = 12.6 Hz, 1H), 1.85 – 1.67 (m, 4H), 1.58 (d, *J* = 12.8 Hz, 1H), 1.30 – 1.05 (m, 5H). **^{13}C NMR** (126 MHz, $CDCl_3$) δ 147.2, 147.0, 129.1, 129.0 (q, *J* = 32.3 Hz), 127.5, 125.2 (q, *J* = 3.7 Hz), 124.2 (q, *J* = 272.2 Hz), 117.3, 113.1, 63.1, 44.7, 30.1, 29.2, 26.2, 26.2. **^{19}F NMR** (471 MHz, $CDCl_3$) δ -62.23. **FT-IR** (cm^{-1}, neat, ATR): 3425, 2926, 2853, 1502, 1322, 1118, 747. **HRMS** (EI) calcd for $C_{20}H_{22}F_3N$ $[M]^+$: 333.1704, found: 333.1716.

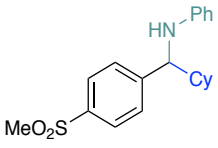

***N*-(Cyclohexyl(4-(methylsulfonyl)phenyl)methyl)aniline, 23** (119 mg, 69%) was prepared following *GP1*. The desired amine was isolated as a solid. **mp** = 177-179 °C. **^{1}H NMR** (500 MHz, $CDCl_3$) δ 7.87 (d, *J* = 8.2 Hz, 2H), 7.51 (d, *J* = 8.2 Hz, 2H), 7.07 (t, *J* = 7.8 Hz, 2H), 6.64 (t, *J* = 7.2 Hz, 1H), 6.45 (d, *J* = 8.0 Hz, 2H), 4.30 – 4.13 (m, 2H), 3.05 (s, 3H), 1. 62 – 1.90 (m, 5H), 1.53 (d, *J* = 12.3 Hz, 1H), 1.27 – 1.01 (m, 5H). **^{13}C NMR** (126 MHz, $CDCl_3$) δ 149.8, 147.2, 139.2, 129.3, 128.3, 127.6, 117.7, 113.3, 63.3, 44.9, 44.7, 30.3, 29.3, 26.4, 26.4. **FT-IR** (cm^{-1},

neat, ATR): 3368, 2925, 2851, 1600, 1503, 1600, 1147, 748. **HRMS** (EI) calcd for $C_{20}H_{25}NO_2S$ $[M]^+$: 343.1606, found: 343.1619.

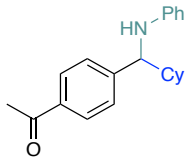

1-(4-(Cyclohexyl(phenylamino)methyl)phenyl)ethan-1-one, 24 (77 mg, 50%) was prepared following *GP1*. The desired amine was isolated as a solid. **mp** = 93-95 °C. **^{1}H NMR** (500 MHz, $CDCl_3$) δ 7.91 (d, *J* = 8.0 Hz, 2H), 7.41 (d, *J* = 8.0 Hz, 2H), 7.07 (t, *J* = 7.6 Hz, 2H), 6.63 (t, *J* = 7.1 Hz, 1H), 6.48 (d, *J* = 8.0 Hz, 2H), 4.14 – 4.24 (m, 2H), 2.59 (s, 3H), 1.88 (d, *J* = 12.3 Hz, 1H), 1.83 – 1.64 (m, 4H), 1.56 (d, *J* = 12.2 Hz, 1H), 1.29 – 1.02 (m, 5H). **^{13}C NMR** (126 MHz, $CDCl_3$) δ 197.7, 148.5, 147.3, 135.9, 129.0, 128.3, 127.4, 117.2, 113.1, 63.2, 44.7, 30.1, 29.2, 26.5, 26.2, 26.2. **FT-IR** (cm^{-1}, neat, ATR): 3388, 2922, 2850, 1667, 1601, 1267, 745. **HRMS** (EI) calcd for $C_{21}H_{25}NO$ $[M]^+$: 307.1936, found: 307.1931.

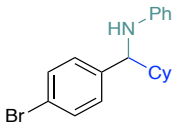

***N*-((4-Bromophenyl)(cyclohexyl)methyl)aniline, 25** (129 mg, 75%) was prepared following *GP1*. The desired amine was isolated as an oil. **^{1}H NMR** (500 MHz, $CDCl_3$) δ 7.43 (d, *J* = 8.3 Hz, 2H), 7.19 (d, *J* = 8.3 Hz, 2H), 7.08 (t, *J* = 7.8 Hz, 2H), 6.64 (t, *J* = 7.2 Hz, 1H), 6.48 (d, *J* = 7.8 Hz, 2H), 4.13 (s, 1H), 4.10 (d, *J* = 6.1 Hz, 1H), 1.87 (d, *J* = 12.5 Hz, 1H), 1.83 – 1.71 (m, 2H), 1.71 – 1.60 (m, 2H), 1.56 (d, *J* = 12.9 Hz, 1H), 1.30 – 1.00 (m, 5H). **^{13}C NMR** (126 MHz, $CDCl_3$) δ 147.3, 141.7, 131.2, 129.0, 128.9, 120.4, 117.2, 113.1, 62.8, 44.7, 30.0, 29.3, 26.3, 26.2,

26.2. **FT-IR** (cm^{-1}, neat, ATR): 3425, 2922, 2850, 1599, 1501, 1484, 1317, 1071, 746, 690. **HRMS** (EI) calcd for $C_{19}H_{22}BrN$ $[M]^+$: 343.0936, found: 343.0908.

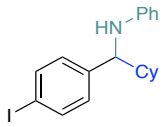

***N*-(Cyclohexyl(4-iodophenyl)methyl)aniline, 26** (125 mg, 64%) was prepared following *GP1*. The desired amine was isolated as an oil. **^{1}H NMR** (500 MHz, $CDCl_3$) δ 7.63 (d, *J* = 8.2 Hz, 2H), 7.12 – 7.03 (m, 4H), 6.64 (t, *J* = 7.3 Hz, 1H), 6.48 (d, *J* = 8.4 Hz, 2H), 4.17 – 4.04 (m, 2H), 1.87 (d, *J* = 12.7 Hz, 1H), 1.82 – 1.71 (m, 2H), 1.71 – 1.60 (m, 2H), 1.58 – 1.53 (m, 1H), 1.27 – 1.00 (m, 5H). **^{13}C NMR** (126 MHz, $CDCl_3$) δ 147.3, 142.4, 137.2, 129.2, 129.0, 117.2, 113.1, 91.9, 62.9, 44.7, 30.0, 29.2, 26.3, 26.2, 26.2. **FT-IR** (cm^{-1}, neat, ATR): 3425, 2922, 2850, 1599, 1501, 1480, 1004, 746, 690. **HRMS** (EI) calcd for $C_{19}H_{22}NI$ $[M]^+$: 391.0797, found: 391.0792.

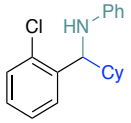

***N*-((2-Chlorophenyl)(cyclohexyl)methyl)aniline, 27** (101 mg, 67%) was prepared following *GP1*. The desired amine was isolated as a solid. **mp** = 94-96 °C. **^{1}H NMR** (500 MHz, $CDCl_3$) δ 7.45 – 7.32 (m, 2H), 7.24 – 7.07 (m, 4H), 6.66 (t, *J* = 7.2 Hz, 1H), 6.53 (d, *J* = 7.8 Hz, 2H), 4.70 (d, *J* = 6.2 Hz, 1H), 4.23 (s, 1H), 1.95 (d, *J* = 12.2 Hz, 1H), 1. 67 – 1.97 (m, 4H), 1.58 (d, *J* = 12.0 Hz, 1H), 1.37 – 1.11 (m, 5H). **^{13}C NMR** (126 MHz, $CDCl_3$) δ 147.5, 140.4, 133.7, 129.7, 129.3, 128.5, 128.0, 127.0, 117.4, 113.2, 59.5, 43.9, 30.4, 29.0, 26.7, 26.6, 26.6. **FT-IR** (cm^{-1}, neat, ATR): 3399, 2923, 2852, 1598, 1505, 1320, 1032, 746, 690. **HRMS** (ESI) calcd for $C_{19}H_{23}ClN$ $[M+H]^+$: 300.1519, found: 300.1542.

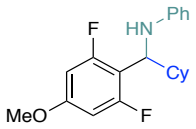

***N*-(Cyclohexyl(2,6-difluoro-4-methoxyphenyl)methyl)aniline, 28** (108 mg, 65%) was prepared following *GP1*. The desired amine was isolated as an oil. **^{1}H NMR** (500 MHz, $CDCl_3$) δ 7.12 (t, *J* = 7.8 Hz, 2H), 6.67 – 6. 58 (m, 3H), 6.38 (d, *J* = 10.5 Hz, 2H), 4.50 (d, *J* = 9.4 Hz, 1H), 4.15 (s, 1H), 3.72 (s, 3H), 2.24 (d, *J* = 13.1 Hz, 1H), 1.88 – 1.77 (m, 2H), 1.74 – 1.65 (m, 2H), 1.44 (d, *J* = 12.7 Hz, 1H), 1.32 – 1.17 (m, 3H), 1.12 – 0.97 (m, 2H). **^{13}C NMR** (126 MHz, $CDCl_3$) δ 162.0 (dd, *J* = 243.9, 12.7 Hz), 159.7 (t, *J* = 14.6 Hz), 147.8, 129.4, 117.4, 113.1, 110.5 (t, *J* = 18.4 Hz), 98.2 (d, *J* = 30.4 Hz), 55.8, 54.0, 42.7, 31.2, 30.3, 26.6, 26.2, 26.2. **^{19}F NMR** (471 MHz, $CDCl_3$) δ -113.96. **FT-IR** (cm^{-1}, neat, ATR): 3412, 2924, 2850, 1635, 1496, 1137, 747. **HRMS** (EI) calcd for $C_{20}H_{23}F_2NO$ $[M]^+$: 331.1748, found: 331.1736.

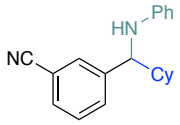

3-(Cyclohexyl(phenylamino)methyl)benzonitrile, 29 (64 mg, 44%) was prepared following *GP1*. The desired amine was isolated as a solid. **mp** = 135-137 °C. **^{1}H NMR** (500 MHz, $CDCl_3$) δ 7.62 (s, 1H), 7.54 (dd, *J* = 17.2, 7.7 Hz, 2H), 7.42 (t, *J* = 7.7 Hz, 1H), 7.09 (t, *J* = 7.6 Hz, 2H), 6.67 (t, *J* = 7.3 Hz, 1H), 6.46 (d, *J* = 8.4 Hz, 2H), 4.16 (d, *J* = 6.1 Hz, 2H), 1.88 – 1.74 (m, 3H), 1.72 – 1.62 (m, 2H), 1.54 (d, *J* = 12.6 Hz, 1H), 1.30 – 1.01 (m, 5H). **^{13}C NMR** (126 MHz, $CDCl_3$) δ 146.9, 144.4, 131.7, 130.8, 130.6, 129.1, 129.0, 119.0, 117.5, 113.1, 112.3, 62.9, 44.7, 30.0, 29.1, 26.2, 26.1, 26.1. **FT-IR** (cm^{-1}, neat, ATR) 2925, 2852, 2228, 1601, 1503, 1317, 907, 730, 692. **HRMS** (EI) calcd for $C_{20}H_{22}N_2$ $[M]^+$: 290.1783, found: 290.1788.

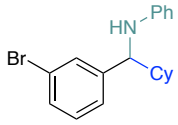

***N*-((3-Bromophenyl)(cyclohexyl)methyl)aniline, 30** (93 mg, 54%) was prepared following *GP1*. The desired amine was isolated as an oil. **^{1}H NMR** (500 MHz, $CDCl_3$) δ 7.47 (s, 1H), 7.36 (d, *J* = 7.2 Hz, 1H), 7.29 – 7.21 (m, 1H), 7.18 (t, *J* = 7.7 Hz, 1H), 7.10 (t, *J* = 7.8 Hz, 2H), 6.66 (t, *J* = 7.2 Hz, 1H), 6.50 (d, *J* = 7.7 Hz, 2H), 4.27 – 3.94 (m, 2H), 1.88 (d, *J* = 11.8 Hz, 1H), 1.83 – 1.71 (m, 2H), 1.71 – 1.59 (m, 2H), 1.55 (d, *J* = 12.3 Hz, 1H), 1.28 – 1.01 (m, 5H). **^{13}C NMR** (126 MHz, $CDCl_3$) δ 147.3, 145.4, 130.1, 129.9, 129.7, 129.0, 125.9, 122.5, 117.2, 113.1, 63.0, 44.8, 30.1, 29.2, 26.3, 26.2, 26.2. FT-**IR** (cm^{-1}, neat, ATR): 3420, 2922, 2850, 1600, 1501, 1616, 1252, 747, 690. **HRMS** (ESI) calcd for $C_{19}H_{23}NBr$ $[M+H]^+$: 344.1014, found: 344.0996.

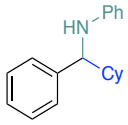

***N*-(Cyclohexyl(phenyl)methyl)aniline, 31** (122 mg, 92%) was prepared following *GP1*. The desired amine was isolated as an oil. **^{1}H NMR** (500 MHz, $CDCl_3$) δ 7.35 – 7.29 (m, 4H), 7.28 – 7.23 (m, 1H), 7.09 (t, *J* = 7.8 Hz, 2H), 6.64 (t, *J* = 7.2 Hz, 1H), 6.53 (d, *J* = 7.7 Hz, 2H), 4.26 – 4.04 (m, 2H), 1.93 (d, *J* = 12.2 Hz, 1H), 1.84 – 1.64 (m, 4H), 1.58 (d, *J* = 12.5 Hz, 1H), 1.30 – 1.05 (m, 5H). **^{13}C NMR** (126 MHz, $CDCl_3$) δ 147.7, 142.6, 129.0, 128.1, 127.2, 126.7, 116.8, 113.1, 63.3, 44.8, 30.2, 29.4, 26.4, 26.3, 26.3. **FT-IR** (cm^{-1}, neat, ATR): 3425, 2922, 2850, 1599, 1501, 1317, 745, 700, 690. **HRMS** (ESI) calcd for $C_{19}H_{24}N$ $[M+H]^+$: 266.1909, found, 266.1913.

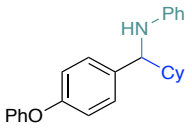

***N*-(Cyclohexyl(4-phenoxyphenyl)methyl)aniline, 32** (93 mg, 52%) was prepared following *GP1*. The desired amine was isolated as an oil. **^{1}H NMR** (500 MHz, $CDCl_3$) δ 7.36 (t, *J* = 7.9 Hz, 2H), 7.28 (d, *J* = 8.5 Hz, 2H), 7.12 (t, *J* = 7.8 Hz, 3H), 7.04 (d, *J* = 7.7 Hz, 2H), 6.98 (d, *J* = 8.5 Hz, 2H), 6.66 (t, *J* = 7.2 Hz, 1H), 6.55 (d, *J* = 7.8 Hz, 2H), 4.29 – 4.08 (m, 2H), 1.94 (d, *J* = 12.4 Hz, 1H), 1.85 – 1.75 (m, 2H), 1.71 (d, *J* = 12.1 Hz, 2H), 1.59 (d, *J* = 12.6 Hz, 1H), 1.33 – 1.04 (m, 5H). **^{13}C NMR** (126 MHz, $CDCl_3$) δ 157.2, 155.9, 147.7, 137.4, 129.6, 129.0, 128.4, 123.1, 118.8, 118.5, 116.9, 113.1, 62.8, 44.9, 30.1, 29.5, 26.4, 26.3, 26.3. **FT-IR** (cm^{-1}, neat, ATR): 3423, 2922, 2850, 1600, 1501, 1487, 745, 689. **HRMS** (EI) calcd for $C_{25}H_{27}NO$ $[M]^+$: 357.2093, found: 357.2093.

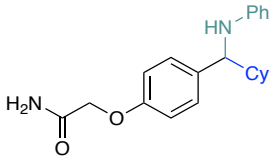

2-(4-(Cyclohexyl(phenylamino)methyl)phenoxy)acetamide, 33 (105 mg, 62%) was prepared following *GP1*. The desired amine was isolated as a solid. **mp** = 104-106 °C. **^{1}H NMR** (500 MHz, $CDCl_3$) δ 7.25 (d, *J* = 8.5 Hz, 2H), 7.07 (t, *J* = 7.8 Hz, 2H), 6.87 (d, *J* = 8.5 Hz, 2H), 6.62 (t, *J* = 7.3 Hz, 1H), 6.56 (s, 1H), 6.49 (d, *J* = 8.0 Hz, 2H), 6.02 (s, 1H), 4.48 (s, 2H), 4.16 (s, 1H), 4.09 (d, *J* = 6.2 Hz, 1H), 1.89 (d, *J* = 12.6 Hz, 1H), 1.82 – 1.71 (m, 2H), 1.70 – 1.59 (m, 2H), 1.54 (d, *J* = 12.7 Hz, 1H), 1.28 – 1.00 (m, 5H). **^{13}C NMR** (126 MHz, $CDCl_3$) δ 171.1, 155.9, 147.6, 136.3, 129.0, 128.4, 116.9, 114.3, 113.1, 67.1, 62.6, 44.9, 30.0, 29.4, 26.3, 26.3, 26.2. **FT-IR** (cm^{-1}, neat, ATR): 3440, 3180, 2932, 2852, 1683, 1598, 1506, 1238, 752. **HRMS** (EI) calcd for $C_{21}H_{26}N_2O_2$ $[M]^+$: 338.1994, found: 338.2002.

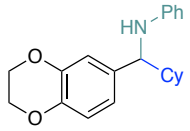

***N*-(Cyclohexyl(2,3-dihydrobenzo[b][1,4]dioxin-6-yl)methyl)aniline, 34** (113 mg, 70%) was prepared following *GP1*. The desired amine was isolated as a solid. **mp** = 127-128 °C. **^{1}H NMR** (500 MHz, $CDCl_3$) δ 7.08 (t, *J* = 7.7 Hz, 2H), 6.74 – 6.82 (m, 3H), 6.62 (t, *J* = 7.2 Hz, 1H), 6.52 (d, *J* = 7.6 Hz, 2H), 4.23 (s, 4H), 4.09 – 4.17 (br s, 1H), 4.01 (d, *J* = 6.3 Hz, 1H), 1.91 (d, *J* = 12.6 Hz, 1H), 1.81 – 1.69 (m, 2H), 1.69 – 1.52 (m, 3H), 1.28 – 0.98 (m, 5H). **^{13}C NMR** (126 MHz, $CDCl_3$) δ 147.9, 143.4, 142.4, 136.2, 129.2, 120.4, 117.0, 117.0, 116.0, 113.4, 64.5, 64.4, 63.0, 45.0, 30.3, 29.8, 26.6, 26.5, 26.5. **FT-IR** (cm^{-1}, neat, ATR): 3435, 2931, 2848, 1603, 1504, 1286, 1065, 749. **HRMS** (EI) calcd for $C_{21}H_{25}NO_2$ $[M]^+$: 323.1885, found: 323.1895.

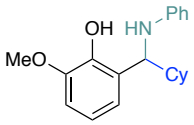

2-(Cyclohexyl(phenylamino)methyl)-6-methoxyphenol, 35 (120 mg, 77%) was prepared following *GP1*. The desired amine was isolated as an oil. **^{1}H NMR** (500 MHz, $CDCl_3$) δ 7.14 (t, *J* = 7.7 Hz, 2H), 6.88 – 6.80 (m, 2H), 6.80 – 6.74 (m, 1H), 6.74 – 6.64 (m, 3H), 4.95 – 4.05 (m, 2H), 3.88 (s, 3H), 2.09 (d, *J* = 17.0 Hz, 1H), 1.92 – 1.80 (m, 2H), 1.66 – 1.80 (m, 2H), 1.60 (d, *J* = 12.1 Hz, 1H), 1.35 – 1.10 (m, 5H). **^{13}C NMR** (126 MHz, $CDCl_3$) δ 147.8, 146.7, 144.1, 129.0, 127.6, 120.7, 119.1, 117.7, 113.9, 109.1, 60.2, 55.78, 43.4, 30.1, 29.9, 26.4, 26.3. **FT-IR** (cm^{-1}, neat, ATR): 3625, 3412, 2922, 2849, 1601, 1476, 1248, 1074, 746, 691. **HRMS** (ESI) calcd for $C_{20}H_{26}NO_2$ $[M+H]^+$: 312.1964, found: 312.1986.

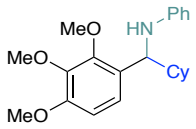

***N*-(Cyclohexyl(2,3,4-trimethoxyphenyl)methyl)aniline, 36** (93 mg, 52%) was prepared following *GP1*. The desired amine was isolated as an oil. **^{1}H NMR** (500 MHz, $CDCl_3$) δ 7.09 (t, *J* = 7.9 Hz, 2H), 6.88 (d, *J* = 8.6 Hz, 1H), 6.63 – 6.55 (m, 4H), 4.39 (d, *J* = 7.5 Hz, 1H), 4.17 (s, 1H), 4.00 (s, 3H), 3.88 (s, 3H), 3.83 (s, 3H), 2.04 (d, *J* = 12.8 Hz, 1H), 1.80 (d, *J* = 11.3 Hz, 1H), 1.76 – 1.65 (m, 3H), 1.49 (d, *J* = 12.7 Hz, 1H), 1.32 – 1.01 (m, 5H). **^{13}C NMR** (126 MHz, $CDCl_3$) δ 152.3, 151.7, 148.0, 141.9, 129.0, 128.2, 122.2, 116.6, 113.0, 106.8, 60.7, 60.5, 58.2, 55.8, 44.0, 30.7, 29.8, 26.5, 26.4, 26.3. **FT-IR** (cm^{-1}, neat, ATR): 3400, 2924, 2849, 1600, 1492, 1278, 1092, 746, 691. **HRMS** (EI) calcd for $C_{22}H_{29}NO_3$ $[M]^+$: 355.2147, found: 355.2143.

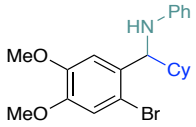

***N*-((2-Bromo-4,5-dimethoxyphenyl)(cyclohexyl)methyl)aniline, 37** (176 mg, 87%) was prepared following *GP1*. The desired amine was isolated as an oil. **^{1}H NMR** (500 MHz, $CDCl_3$) δ 7.08 (t, *J* = 7.8 Hz, 2H), 7.00 (s, 1H), 6.81 (s, 1H), 6.63 (t, *J* = 7.3 Hz, 1H), 6.49 (d, *J* = 8.0 Hz, 2H), 4.48 (d, *J* = 6.2 Hz, 1H), 4.15 (s, 1H), 3.85 (s, 3H), 3.77 (s, 3H), 1.91 (d, *J* = 12.4 Hz, 1H), 1.82 – 1.62 (m, 4H), 1.53 (d, *J* = 15.5 Hz, 1H), 1.31 – 1.09 (m, 5H). **^{13}C NMR** (126 MHz, $CDCl_3$) δ 148.8, 148.4, 147.6, 133.9, 129.3, 117.4, 115.5, 113.9, 113.4, 111.1, 61.8, 56.2, 56.1, 44.3, 30.3, 29.0, 26.7, 26.5. **FT-IR** (cm^{-1}, neat, ATR): 3404, 2925, 2850, 1600, 1499, 1436, 1317, 1249, 1154, 730. **HRMS** (ESI) calcd for $C_{21}H_{27}BrNO_2$ $[M+H]^+$: 404.1225, found: 404.1244.

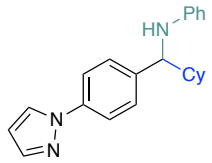

***N*-((4-(1H-Pyrazol-1-yl)phenyl)(cyclohexyl)methyl)aniline, 38** (146 mg, 88%) was prepared following *GP1*. The desired amine was isolated as an oil. **^{1}H NMR** (500 MHz, $CDCl_3$) δ 7.89 (d, *J* = 2.4 Hz, 1H), 7.72 (d, *J* = 1.4 Hz, 1H), 7.64 (d, *J* = 8.5 Hz, 2H), 7.39 (d, *J* = 8.5 Hz, 2H), 7.09 (t, *J* = 7.9 Hz, 2H), 6.64 (t, *J* = 7.3 Hz, 1H), 6.53 (d, *J* = 7.9 Hz, 2H), 6.47 – 6.42 (m, 1H), 4.18 (d, *J* = 6.1 Hz, 2H), 1.91 (d, *J* = 12.6 Hz, 1H), 1.83 – 1.64 (m, 4H), 1.60 (d, *J* = 12.8 Hz, 1H), 1.29 – 1.03 (m, 5H). **^{13}C NMR** (126 MHz, $CDCl_3$) δ 147.7, 141.2, 141.1, 139.2, 129.2, 128.4, 126.8, 119.4, 117.4, 113.5, 107.6, 63.2, 45.1, 30.3, 29.6, 26.6, 26.5, 26.5. **FT-IR** (cm^{-1}, neat, ATR): 3406, 2923, 2850, 1600, 1522, 1501, 1393, 746, 691. **HRMS** (EI) calcd for $C_{22}H_{25}N_3$ $[M]^+$: 331.2048, found: 331.2046.

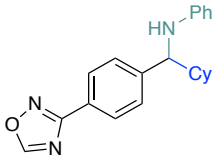

***N*-((4-(1,2,4-Oxadiazol-3-yl)phenyl)(cyclohexyl)methyl)aniline, 39** (123 mg, 74%) was prepared following *GP1*. The desired amine was isolated as a solid. **mp** = 119-121 °C. **^{1}H NMR** (500 MHz, $CDCl_3$) δ 8.70 (s, 1H), 8.06 (d, *J* = 8.1 Hz, 2H), 7.45 (d, *J* = 8.1 Hz, 2H), 7.08 (t, *J* = 7.8 Hz, 2H), 6.63 (t, *J* = 7.2 Hz, 1H), 6.51 (d, *J* = 7.7 Hz, 2H), 4.35 – 4.05 (m, 2H), 1.90 (d, *J* = 12.4 Hz, 1H), 1.83 – 1.63 (m, 4H), 1.58 (d, *J* = 12.4 Hz, 1H), 1.28 – 1.04 (m, 5H). **^{13}C NMR** (126 MHz, $CDCl_3$) δ 167.8, 164.7, 147.6, 146.8, 129.3, 128.0, 127.7, 125.0, 117.5, 113.4, 63.5, 45.0, 30.3, 29.5, 26.5, 26.5, 26.4. **FT-IR** (cm^{-1}, neat, ATR): 3340, 2929, 2850, 1599, 1497, 1333, 1273, 1119, 751, 695. **HRMS** (EI) calcd for $C_{21}H_{23}N_3O$ $[M]^+$: 333.1841, found: 333.1844.

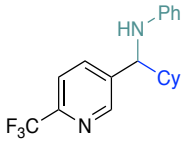

***N*-(Cyclohexyl(6-(trifluoromethyl)pyridin-3-yl)methyl)aniline, 40** (126 mg, 75%) was prepared following *GP1*. The desired amine was isolated as a solid. **mp** = 131-133 °C. **^{1}H NMR** (500 MHz, $CDCl_3$) δ 8.67 (s, 1H), 7.80 (s, 1H), 7.60 (d, *J* = 8.0 Hz, 1H), 7.08 (t, *J* = 7.6 Hz, 2H), 6.68 (s, 1H), 6.46 (s, 2H), 4.26 (d, *J* = 5.9 Hz, 1H), 4.13 (s, 1H), 1.89 – 1.65 (m, 5H), 1.58 (d, *J* = 12.3 Hz, 1H), 1.27 – 1.03 (m, 5H). **^{13}C NMR** (126 MHz, $CDCl_3$) δ 149.7, 147.0 (q, *J* = 34.6 Hz), 146.8, 141.9, 136.1, 129.4, 121.8 (q, *J* = 273.9 Hz), 120.3 (d, *J* = 2.4 Hz), 118.1, 113.4, 61.2, 44.8, 30.1, 29.3, 26.3, 26.3, 26.3. **^{19}F NMR** (471 MHz, $CDCl_3$) δ -67.63. **FT-IR** (cm^{-1}, neat, ATR): 3320, 2938, 2849, 1601, 1496, 1334, 1180, 1081, 747. **HRMS** (ESI) calcd for $C_{19}H_{22}F_3N_2$ $[M+H]^+$: 335.1735, found: 335.1745.

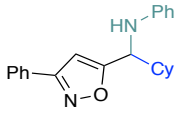

***N*-(Cyclohexyl(3-phenylisoxazol-5-yl)methyl)aniline, 41** (133 mg, 80%) was prepared following *GP1*. The desired amine was isolated as a solid. **mp** = 127-128 °C. **^{1}H NMR** (500 MHz, $CDCl_3$) δ 7.79 (dd, *J* = 6.5, 3.1 Hz, 2H), 7.47 – 7.38 (m, 3H), 7.17 (dd, *J* = 8.2, 7.6 Hz, 2H), 6.74 (t, *J* = 7.3 Hz, 1H), 6.63 (d, *J* = 7.9 Hz, 2H), 6.42 (s, 1H), 4.50 (d, *J* = 6.0 Hz, 1H), 3.90 – 4.24 (brs, 1H), 2.02 – 1.88 (m, 2H), 1.75 – 1.85 (m, 2H), 1.70 (t, *J* = 10.0 Hz, 2H), 1.36 – 1.12 (m, 5H). **^{13}C NMR** (126 MHz, $CDCl_3$) δ 174.4, 162.3, 147.0, 130.07, 129.5, 129.3, 129.0, 127.0, 118.4, 113.5, 100.2, 56.8, 42.8, 29.7, 29.4, 26.4, 26.3, 26.2. **FT-IR** (cm^{-1}, neat, ATR): 3329, 2925, 2853, 1598, 1497, 1324, 765, 688. **HRMS** (EI) calcd for $C_{22}H_{24}N_2O$ $[M]^+$: 332.1889, found: 332.1885.

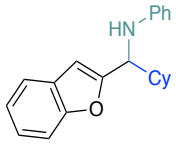

***N*-(Benzofuran-2-yl(cyclohexyl)methyl)aniline, 42** (86 mg, 56%) was prepared following *GP1*. The desired amine was isolated as a solid. **mp** = 109-111 °C. **^{1}H NMR** (500 MHz, $CDCl_3$) δ 7.48 (dd, *J* = 11.9, 7.9 Hz, 2H), 7.29 – 7.11 (m, 4H), 6.73 – 6.63 (m, 3H), 6.55 (s, 1H), 4.41 (d, *J* = 6.2 Hz, 1H), 4.09 (s, 1H), 2.02 – 1.93 (m, 2H), 1.85 – 1.62 (m, 4H), 1.35 – 1.14 (m, 5H). **^{13}C NMR** (126 MHz, $CDCl_3$) δ 158.3, 154.6, 147.3, 129.1, 128.3, 123.4, 122.5, 120.6, 117.6, 113.3, 111.0, 103.7, 57.5, 42.4, 29.8, 29.4, 26.3, 26.1, 26.1. **FT-IR** (cm^{-1}, neat, ATR): 3395, 2928, 2852, 1598, 1501, 1454, 1248, 750, 692. **HRMS** (EI) calcd for $C_{21}H_{23}NO$ $[M]^+$: 305.1780, found: 305.1769.

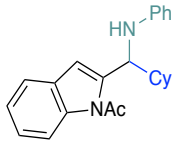

1-(2-(Cyclohexyl(phenylamino)methyl)-1H-indol-1-yl)ethan-1-one, 43 (49 mg, 28%) was prepared following *GP1*. The desired amine was isolated as an oil. **^{1}H NMR** (500 MHz, $CDCl_3$) δ 8.47 (s, 1H), 7.67 (d, *J* = 7.7 Hz, 1H), 7.45 – 7.23 (m, 3H), 7.10 (t, *J* = 7.7 Hz, 2H), 6.67 (t, *J* = 7.2 Hz, 1H), 6.57 (d, *J* = 7.9 Hz, 2H), 4.48 (d, *J* = 5.3 Hz, 1H), 4.09 (s, 1H), 2.58 (s, 3H), 1.95 (d, *J* = 12.0 Hz, 2H), 1.85 – 1.66 (m, 4H), 1.31 – 1.11 (m, 5H). **^{13}C NMR** (126 MHz, $CDCl_3$) δ 168.4, 147.7, 136.3, 129.5, 129.07, 125.1, 123.8, 123.4, 122.8, 119.3, 117.4, 116.8, 113.1, 56.2, 43.5, 30.4, 29.2, 26.3, 24.0. **FT-IR** (cm^{-1}, neat, ATR): 3398, 2924, 2851, 1694, 1600, 1448, 1328, 1218, 746, 730. **HRMS** (EI) calcd for $C_{23}H_{26}N_2O$ $[M]^+$: 346.2045, found: 346.2048.

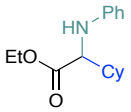

Ethyl 2-Cyclohexyl-2-(phenylamino)acetate, 44 (101 mg, 77%) was prepared following *GP1*. The desired amine was isolated as an oil. **^{1}H NMR** (500 MHz, $CDCl_3$) δ 7.22 – 7.06 (m, 2H), 6.72 (tt, *J* = 7.3, 1.1 Hz, 1H), 6.66 – 6.56 (m, 2H), 4.24 – 4.05 (m, 3H), 3.86 (d, *J* = 6.1 Hz, 1H), 1.98 – 1.81 (m, 1H), 1.83 – 1.72 (m, 3H), 1.72 – 1.60 (m, 2H), 1.37 – 1.00 (m, 8H). **^{13}C NMR** (126 MHz, $CDCl_3$) δ 173.8, 147.6, 129.4, 118.2, 113.6, 62.2, 60.9, 41.5, 29.8, 29.3, 26.3, 26.3, 26.2, 14.5. **FT-IR** (cm^{-1}, neat, ATR): 2980, 2926, 2853, 1728, 1602, 1505, 1256, 1178, 1146. **HRMS** (ESI) calcd for $C_{16}H_{24}NO_2$ $[M+H]^+$: 262.1807, found: 262.1804.

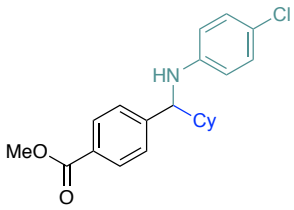

Methyl 4-(((4-Chlorophenyl)amino)(cyclohexyl)methyl)benzoate, 45 (77 mg, 43%) was prepared following *GP1*. The desired amine was isolated as an oil. **^{1}H NMR** (500 MHz, $CDCl_3$) δ 7.97 (d, *J* = 8.3 Hz, 2H), 7.34 (d, *J* = 8.3 Hz, 2H), 6.98 (d, *J* = 8.9 Hz, 2H), 6.37 (d, *J* = 8.9 Hz, 2H), 4.22 (s, 1H), 4.12 (d, *J* = 6.1 Hz, 1H), 3.89 (s, 3H), 1.84 (d, *J* = 12.4 Hz, 1H), 1.81 – 1.56 (m, 4H), 1.58 – 1.38 (m, 1H), 1.28 – 0.87 (m, 5H). **^{13}C NMR** (126 MHz, $CDCl_3$) δ 167.1, 147.9, 146.0, 129.8, 129.1, 129.0, 127.4, 122.0, 114.4, 63.6, 52.2, 44.8, 30.2, 29.5, 26.4, 26.4, 26.4. **FT-IR** (cm^{-1}, neat, ATR): 3406, 2927, 2853, 1710, 1599, 1498, 1312,1281. **HRMS** (ESI) calcd for $C_{21}H_{25}ClNO_2$ $[M+H]^+$: 358.1574, found: 358.1583.

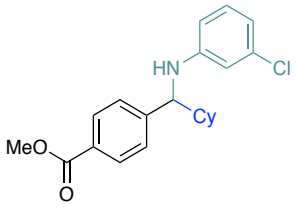

Methyl 4-(((3-Chlorophenyl)amino)(cyclohexyl)methyl)benzoate, 46 (118 mg, 66%) was prepared following *GP1*. The desired amine was isolated as an oil. **^{1}H NMR** (500 MHz, $CDCl_3$) δ 8.08 – 7.83 (m, 2H), 7.49 – 7.29 (m, 2H), 6.95 (t, *J* = 8.0 Hz, 1H), 6.57 (ddd, *J* = 7.9, 2.0, 1.0 Hz, 1H), 6.45 (t, *J* = 2.1 Hz, 1H), 6.32 (ddd, *J* = 8.3, 2.3, 1.0 Hz, 1H), 4.27 (s, 1H), 4.14 (d, *J* = 6.1 Hz, 1H), 3.90 (s, 3H), 1.84 (d, *J* = 13.0 Hz, 1H), 1.80 – 1.57 (m, 4H), 1.51 (dd, *J* = 12.8, 3.4 Hz, 1H), 1.34 – 0.81 (m, 5H). **^{13}C NMR** (126 MHz, $CDCl_3$) δ 167.1, 148.6, 147.7, 134.9, 130.2, 129.8, 129.2, 127.3, 117.3, 113.1, 111.5, 67.2, 63.3, 52.2, 44.8, 30.3, 29.4, 26.4, 26.37. **FT-IR** (cm^{-1}, neat, ATR): 2927, 1710, 1596, 1576, 1499, 1484, 1278, 1114, 907, 730. **HRMS** (ESI) calcd for $C_{21}H_{25}ClNO_2$ $[M+H]^+$: 358.1574, found: 358.1574.

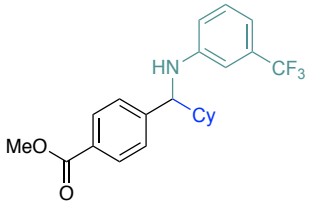

Methyl 4-(Cyclohexyl((3-(trifluoromethyl)phenyl)amino)methyl)benzoate, 47 (125 mg, 64%) was prepared following *GP1*. The desired amine was isolated as an oil. **^{1}H NMR** (500 MHz, $CDCl_3$) δ 8.26 – 7.76 (m, 2H), 7.56 – 7.29 (m, 2H), 7.12 (t, *J* = 7.9 Hz, 1H), 6.84 (d, *J* = 7.6 Hz, 1H), 6.72 (t, *J* = 2.0 Hz, 1H), 6.55 (dd, *J* = 8.2, 2.4 Hz, 1H), 4.38 (s, 1H), 4.18 (d, *J* = 6.2 Hz, 1H), 3.90 (s, 3H), 2.06 – 1.79 (m, 1H), 1.81 – 1.61 (m, 4H), 1.53 – 1.42 (m, 1H), 1.36 – 0.71 (m, 5H). **^{13}C NMR** (126 MHz, $CDCl_3$) δ 167.1, 147.6, 147.5, 131.5 (q, *J* = 31.8 Hz), 129.9, 129.7, 129.2, 127.3, 124.3 (q, *J* = 272.4 Hz), 115.9, 113.8 (q, *J* = 3.7 Hz), 109.9 (q, *J* = 4.0 Hz), 63.4,

52.2, 44.8, 30.3, 29.6, 26.4, 26.4, 26.3. **^{19}F NMR** (471 MHz, $CDCl_3$) δ -62.96. **FT-IR** (cm^{-1}, neat, ATR): 2929, 2854, 1709, 1612, 1436, 1341, 1313, 1280, 1162, 1116. **HRMS** (ESI) calcd for $C_{22}H_{25}F_3NO_2$ $[M+H]^+$: 392.1837, found: 392.1847.

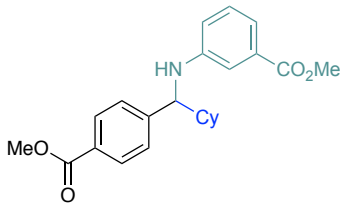

Methyl 3-((Cyclohexyl(4-(methoxycarbonyl)phenyl)methyl)amino)benzoate, 48 (123 mg, 68%) was prepared following *GP1*. The desired amine was isolated as an oil. **^{1}H NMR** (500 MHz, $CDCl_3$) δ 7.97 (d, *J* = 8.0 Hz, 2H), 7.36 (d, *J* = 8.0 Hz, 2H), 7.30 – 7.24 (m, 1H), 7.21 (t, *J* = 2.0 Hz, 1H), 7.09 (t, *J* = 7.9 Hz, 1H), 6.59 (dd, *J* = 8.1, 2.5 Hz, 1H), 4.34 (s, 1H), 4.21 (d, *J* = 6.1 Hz, 1H), 3.88 (s, 3H), 3.84 (s, 3H), 1.87 (d, *J* = 12.3 Hz, 1H), 1.79 – 1.58 (m, 4H), 1.51 (d, *J* = 12.9 Hz, 1H), 1.35 – 0.96 (m, 5H). **^{13}C NMR** (126 MHz, $CDCl_3$) δ 167.5, 167.1, 147.9, 147.5, 131.0, 129.8, 129.2, 129.1, 127.3, 118.5, 117.3, 114.4, 63.3, 52.1, 52.1, 44.8, 30.3, 29.5, 26.4, 26.4, 26.3. **FT-IR** (cm^{-1}, neat, ATR): 2928, 2853, 1717, 1605, 1436, 1330, 1278, 1108. **HRMS** (ESI) calcd for $C_{23}H_{28}NO_4$ $[M+H]^+$: 382.2018, found: 382.2037.

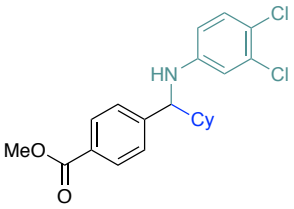

Methyl 4-(Cyclohexyl((3,4-dichlorophenyl)amino)methyl)benzoate, 49 (133 mg, 68%) was prepared following *GP1*. The desired amine was isolated as an oil. **^{1}H NMR** (500 MHz, $CDCl_3$) δ 8.09 – 7.83 (m, 2H), 7.38 – 7.29 (m, 2H), 7.05 (d, *J* = 8.8 Hz, 1H), 6.53 (d, *J* = 2.7 Hz, 1H), 6.28

(dd, J = 8.7, 2.8 Hz, 1H), 4.30 (s, 1H), 4.10 (d, J = 6.2 Hz, 1H), 3.90 (s, 3H), 1.83 (d, J = 12.9 Hz, 1H), 1.79 – 1.58 (m, 4H), 1.50 (d, J = 13.0 Hz, 1H), 1.31 – 0.88 (m, 5H). **^{13}C NMR** (126 MHz, $CDCl_3$) δ 167.0, 147.2, 146.9, 132.7, 130.6, 129.9, 129.3, 127.2, 119.9, 114.5, 112.8, 63.4, 52.2, 44.7, 30.2, 29.5, 26.4, 26.3, 26.3. **FT-IR** (cm^{-1}, neat, ATR): 2929, 2853, 1708, 1597, 1490, 1282. **HRMS** (ESI) calcd for $C_{21}H_{24}Cl_2NO_2$ $[M+H]^+$: 392.1184, found: 392.1194.

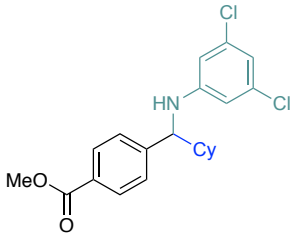

Methyl 4-(Cyclohexyl((3,5-dichlorophenyl)amino)methyl)benzoate, 50 (110 mg, 56%) was prepared following *GP1*. The desired amine was isolated as an oil. **^{1}H NMR** (500 MHz, $CDCl_3$) ^{1}H NMR (500 MHz, $CDCl_3$) δ 7.99 (d, J = 8.2 Hz, 2H), 7.32 (d, J = 8.0 Hz, 2H), 6.58 (t, J = 1.7 Hz, 1H), 6.32 (d, J = 1.9 Hz, 2H), 4.32 (s, 1H), 4.11 (d, J = 6.3 Hz, 1H), 3.90 (d, J = 1.3 Hz, 3H), 1.91 – 1.59 (m, 5H), 1.48 (d, J = 13.1 Hz, 1H), 1.32 – 0.75 (m, 5H). **^{13}C NMR** (126 MHz, $CDCl_3$) δ 167.0, 149.1, 147.0, 135.4, 129.9, 129.3, 127.2, 117.2, 111.5, 63.2, 52.2, 44.7, 30.2, 29.4, 26.3, 26.3, 26.3. **FT-IR** (cm^{-1}, neat, ATR): 2927, 2853, 1706, 1589, 1572, 1451, 1436, 1280, 1112. **HRMS** (ESI) calcd for $C_{21}H_{24}Cl_2NO_2$ $[M+H]^+$: 392.1184, found: 392.1176.

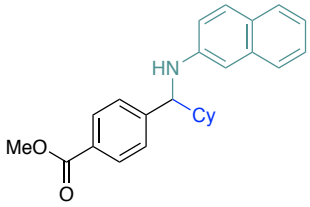

Methyl 4-(Cyclohexyl(naphthalen-2-ylamino)methyl)benzoate, 51 (77 mg, 41%) was prepared following *GP1*. The desired amine was isolated as an oil. **^{1}H NMR** (500 MHz, $CDCl_3$) δ 7.98 (d,

J = 8.3 Hz, 2H), 7.64 – 7.53 (m, 2H), 7.51 – 7.34 (m, 3H), 7.34 – 7.18 (m, 1H), 7.13 (ddd, *J* = 7.9, 6.7, 1.2 Hz, 1H), 6.88 (dd, *J* = 8.8, 2.4 Hz, 1H), 6.53 (d, *J* = 2.5 Hz, 1H), 4.34 (s, 1H), 4.32 (d, *J* = 6.2 Hz, 1H), 3.88 (s, 3H), 1.89 (d, *J* = 12.8 Hz, 1H), 1.85 – 1.62 (m, 4H), 1.63 – 1.55 (m, 1H), 1.33 – 0.96 (m, 5H). **^{13}C NMR** (126 MHz, $CDCl_3$) δ 167.1, 148.2, 145.0, 135.1, 129.8, 129.0, 129.0, 127.6, 127.5, 127.4, 126.3, 126.0, 122.1, 118.0, 105.6, 63.5, 52.1, 44.9, 30.3, 29.5, 26.5, 26.5, 26.4. **FT-IR** (cm^{-1}, neat, ATR): 2925, 2852, 1710, 1629, 1520, 1278, 1113, 827, 732. **HRMS** (ESI) calcd for $C_{25}H_{28}NO_2$ $[M+H]^+$: 374.2120, found: 374.2119.

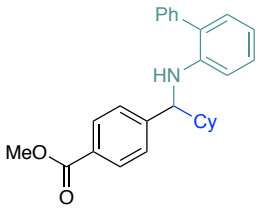

Methyl 4-(([1,1'-Biphenyl]-2-ylamino)(cyclohexyl)methyl)benzoate, 52 (80 mg, 40%) was prepared following *GP1*. The desired amine was isolated as an oil. **^{1}H NMR** (500 MHz, $CDCl_3$) δ 8.09 – 7.81 (m, 2H), 7.58 – 7.48 (m, 4H), 7.41 (tt, *J* = 6.5, 1.8 Hz, 1H), 7.37 – 7.28 (m, 2H), 7.08 (dd, *J* = 7.3, 1.7 Hz, 1H), 7.02 (td, *J* = 7.8, 1.7 Hz, 1H), 6.69 (td, *J* = 7.4, 1.1 Hz, 1H), 6.33 (dd, *J* = 8.2, 1.1 Hz, 1H), 4.46 (s, 1H), 4.19 (d, *J* = 5.8 Hz, 1H), 3.90 (s, 3H), 1.71 – 1.50 (m, 5H), 1.50 – 1.38 (m, 1H), 1.20 – 0.65 (m, 5H). **^{13}C NMR** (126 MHz, $CDCl_3$) δ 167.2, 148.5, 144.2, 139.6, 130.1, 129.7, 129.6, 129.1, 129.0, 128.6, 127.9, 127.5, 127.3, 117.0, 111.4, 63.5, 52.1, 44.9, 30.5, 29.0, 26.5, 26.4, 26.4. **FT-IR** (cm^{-1}, neat, ATR): 2925, 2852, 1720, 1508, 1489, 1435, 1277, 1105. **HRMS** (ESI) calcd for $C_{27}H_{30}NO_2$ $[M+H]^+$: 400.2277, found: 400.2277.

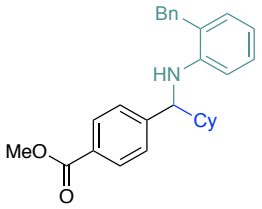

Methyl 4-(((2-Benzylphenyl)amino)(cyclohexyl)methyl)benzoate, 53 (114 mg, 55%) was prepared following *GP1*. The desired amine was isolated as an oil. **^{1}H NMR** (500 MHz, $CDCl_3$) δ 7.92 – 7.77 (m, 2H), 7.35 (dd, *J* = 8.3, 6.7 Hz, 2H), 7.32 – 7.21 (m, 3H), 7.13 (dd, *J* = 7.3, 1.5 Hz, 1H), 7.09 – 7.01 (m, 2H), 6.96 (td, *J* = 7.8, 1.6 Hz, 1H), 6.64 (td, *J* = 7.3, 1.1 Hz, 1H), 6.21 (d, *J* = 8.1 Hz, 1H), 4.08 (d, *J* = 5.1 Hz, 1H), 4.00 (s, 3H), 3.88 (s, 3H), 1.60 (dd, *J* = 20.7, 9.4 Hz, 3H), 1.41 (dddd, *J* = 15.3, 12.5, 6.5, 3.3 Hz, 2H), 1.29 (d, *J* = 13.6 Hz, 1H), 1.16 – 0.91 (m, 3H), 0.82 – 0.61 (m, 2H). **^{13}C NMR** (126 MHz, $CDCl_3$) δ 167.2, 148.4, 145.2, 139.8, 131.1, 129.6, 129.0, 128.7, 128.7, 127.9, 127.2, 126.9, 124.5, 116.8, 111.4, 62.6, 52.1, 44.9, 39.4, 30.2, 28.5, 26.5, 26.4, 26.3. **FT-IR** (cm^{-1}, neat, ATR): 2925, 2852, 1718, 1605, 1510, 1450, 1435, 1277, 1113, 1103. **HRMS** (ESI) calcd for $C_{28}H_{32}NO_2$ $[M+H]^+$: 414.2433, found: 414.2450.

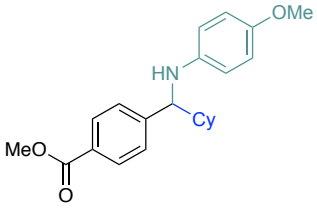

Methyl 4-(Cyclohexyl((4-methoxyphenyl)amino)methyl)benzoate, 54 (88 mg, 50%) was prepared following *GP1*. The desired amine was isolated as an oil. **^{1}H NMR** (500 MHz, $CDCl_3$) δ 7.97 (d, *J* = 7.9 Hz, 2H), 7.36 (d, *J* = 7.9 Hz, 2H), 6.65 (d, *J* = 8.4 Hz, 2H), 6.41 (d, *J* = 8.5 Hz, 2H), 4.10 (d, *J* = 6.0 Hz, 1H), 3.91 (s, 1H), 3.89 (s, 3H), 3.67 (s, 3H), 1.86 (d, *J* = 12.8 Hz, 1H), 1.78 – 1.61 (m, 4H), 1.53 (d, *J* = 13.1 Hz, 1H), 1.25 – 0.99 (m, 5H). **^{13}C NMR** (126 MHz, $CDCl_3$) δ 167.2, 152.0, 148.8, 141.8, 129.7, 128.9, 127.5, 114.9, 114.5, 64.3, 55.9, 52.1, 45.0, 30.3, 29.5,

26.5, 26.5, 26.4. **FT-IR** (cm^{-1}, neat, ATR): 2925, 2852, 1713, 1509, 1277, 1234, 1178, 1106, 818. **HRMS** (ESI) calcd for $C_{22}H_{28}NO_3$ $[M+H]^+$: 354.2069, found: 354.2055.

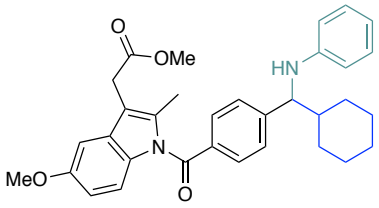

Methyl 2-(1-(4-(Cyclohexyl(phenylamino)methyl)benzoyl)-5-methoxy-2-methyl-1H-indol-3-yl)acetate, 55 (127.5 mg, 81%) was prepared following *GP1*. The desired amine was isolated as a solid. **mp** = 68-70 °C. **^{1}H NMR** (500 MHz, $CDCl_3$) δ 7.64 (d, *J* = 8.0 Hz, 2H), 7.44 (d, *J* = 7.9 Hz, 2H), 7.10 (t, *J* = 7.6 Hz, 2H), 6.97 (s, 1H), 6.79 (d, *J* = 9.0 Hz, 1H), 6.67 (t, *J* = 7.0 Hz, 1H), 6.61 (dd, *J* = 9.0, 2.2 Hz, 1H), 6.51 (d, *J* = 8.0 Hz, 2H), 4.52 – 4.18 (m, 2H), 3.85 (s, 3H), 3.71 (s, 3H), 3.68 (s, 2H), 2.37 (s, 3H), 1.92 (d, *J* = 12.2 Hz, 1H), 1.85 – 1.66 (m, 4H), 1.59 (d, *J* = 12.3 Hz, 1H), 1.30 – 1.07 (m, 5H). **^{13}C NMR** (126 MHz, $CDCl_3$) δ 171.4, 169.4, 155.8, 148.2, 147.2, 136.0, 134.1, 131.0, 130.5, 129.6, 129.0, 127.7, 117.3, 115.0, 113.2, 112.0, 111.4, 101.0, 63.4, 55.6, 52.0, 44.6, 30.1, 30.1, 29.4, 26.3, 26.2, 26.2, 13.2. **FT-IR** (cm^{-1}, neat, ATR): 3400, 2927, 1600, 1477, 1312, 1223, 734. **HRMS** (ESI) calcd for $C_{33}H_{37}N_2O_4$ $[M+H]^+$: 525.2753, found: 525.2758.

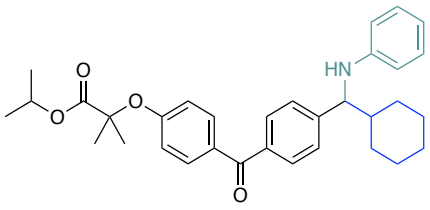

Isopropyl 2-(4-(4-(Cyclohexyl(phenylamino)methyl)benzoyl)phenoxy)-2-methylpropanoate, 56 (114 mg, 74%) was prepared following *GP1*. The desired amine was isolated as a solid. **mp** =

58-60 °C. **^{1}H NMR** (500 MHz, $CDCl_3$) δ 7.76 (d, *J* = 8.4 Hz, 2H), 7.71 (d, *J* = 7.8 Hz, 2H), 7.40 (d, *J* = 7.9 Hz, 2H), 7.08 (t, *J* = 7.7 Hz, 2H), 6.86 (d, *J* = 8.4 Hz, 2H), 6.64 (t, *J* = 7.2 Hz, 1H), 6.50 (d, *J* = 7.8 Hz, 2H), 5.16 – 5.00 (m, 1H), 4.36 – 4.15 (m, 2H), 1.88 (d, *J* = 12.8 Hz, 1H), 1.82 – 1.61 (m, 10H), 1.57 (d, *J* = 12.9 Hz, 1H), 1.25 – 1.06 (m, 11H). **^{13}C NMR** (126 MHz, $CDCl_3$) ^{13}C NMR (126 MHz, $CDCl_3$) δ 195.4, 173.3, 159.6, 147.6, 136.9, 132.2, 130.9, 130.1, 129.3, 127.3, 117.4, 117.3, 113.3, 79.5, 69.4, 63.4, 45.0, 30.4, 29.5, 26.5, 26.4, 25.6, 25.5, 21.7. **FT-IR** (cm^{-1}, neat, ATR): 3395, 2926, 1728, 1598, 1248, 1145, 735. **HRMS** (ESI) calcd for $C_{33}H_{40}NO_4$ $[M+H]^+$: 514.2957, found: 514.2950.

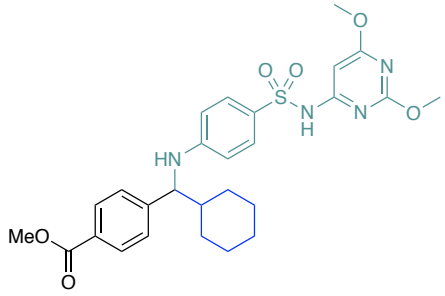

Methyl 4-(Cyclohexyl((4-(*N*-(2,6-dimethoxypyrimidin-4-yl)sulfamoyl)phenyl)amino)methyl)benzoate, 57 (97 mg, 36%) was prepared following *GP1*. The desired amine was isolated as a solid. **mp** = 212-214 °C. **^{1}H NMR** (500 MHz, $CDCl_3$) δ 7.99 (d, *J* = 8.2 Hz, 2H), 7.61 (d, *J* = 8.6 Hz, 2H), 7.32 (d, *J* = 8.3 Hz, 2H), 6.46 (d, *J* = 8.9 Hz, 2H), 6.19 (s, 1H), 4.85 (d, *J* = 6.0 Hz, 1H), 4.18 (t, *J* = 5.8 Hz, 1H), 3.90 (s, 3H), 3.88 (s, 3H), 3.84 (s, 3H), 1.84 (d, *J* = 12.8 Hz, 1H), 1.80 – 1.60 (m, 4H), 1.48 (d, *J* = 13.0 Hz, 1H), 1.24 – 0.98 (m, 5H). **^{13}C NMR** (126 MHz, $CDCl_3$) δ 172.6, 166.7, 164.7, 158.8, 151.4, 146.4, 129.8, 129.4, 129.2, 127.0, 125.4, 112.2, 85.3, 62.8, 54.6, 55.0, 52.0, 44.3, 30.0, 29.3, 26.1, 26.0, 26.0. **FT-IR** (cm^{-1}, neat, ATR): 3260, 2928, 1718, 1592, 1347, 1280, 1148, 1088, 574. **HRMS** (ESI) calcd for $C_{27}H_{33}N_4O_6S$ $[M+H]^+$: 541.2121, found: 541.2131.

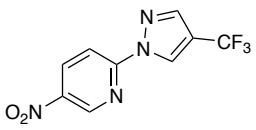

5-Nitro-2-(4-(trifluoromethyl)-1H-pyrazol-1-yl)pyridine, **58** (1.7 g, 95%). A mixture of 4-(trifluoromethyl)-1H-imidazole (1048 mg, 7.7 mmol), 2-chloro-5-nitropyridine (1.110 g. 14.7 mmol), and K_2CO_3 (2070 mg, 15.0 mmol) in MeCN (8 mL) was heated at 85 °C overnight. The reaction was diluted with H_2O and extracted with EtOAc (3×25 mL). The combined organic layers were washed with brine, dried (Na_2SO_4), filtered with Celite, and concentrated to generate a white solid. **^{1}H NMR** (500 MHz, $CDCl_3$) δ 9.31 (d, *J* = 2.6 Hz, 1H), 8.98 – 8.90 (m, 1H), 8.67 (dd, *J* = 9.0, 2.7 Hz, 1H), 8.22 (d, *J* = 9.0 Hz, 1H), 8.00 (s, 1H). **^{13}C NMR** (126 MHz, $CDCl_3$) δ 153.5, 1448, 142.8, 140.4 (q, *J* = 2.6 Hz), 134.5, 127.6 (q, *J* = 3.9 Hz), 121.9 (q, *J* = 266.9 Hz), 117.0 (q, *J* = 38.9 Hz), 112.6. **^{19}F NMR** (471 MHz, $CDCl_3$) δ -57.47.

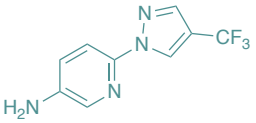

6-(4-(Trifluoromethyl)-1H-pyrazol-1-yl)pyridin-3-amine, **59** (1.5 g, 98%). To a soln of 5-nitro-2-(4-(trifluoromethyl)-1H-pyrazol-1-yl)pyridine (1.7 g) in 20 mL of EtOAc was added 10 wt % Palladium on carbon (250 mg) . The mixture was heated to 50 ºC. The reaction was filtered through Celite, rinsing with MeOH. The filtrate was concentrated to give 6-(4-(trifluoromethyl)-1H-imidazol-1-yl)pyridin-3-amine as an oil. **^{1}H NMR** (500 MHz, $CDCl_3$) δ 8.69 (s, 1H), 7.85 (d, *J* = 10.3 Hz, 2H), 7.75 (d, *J* = 8.8 Hz, 1H), 7.12 (d, *J* = 9.1 Hz, 1H), 3.82 (s, 2H). **^{13}C NMR** (126 MHz, $CDCl_3$) δ 143.0, 142.0, 137.8 (d, *J* = 2.9 Hz), 134.3, 125.6 (q, *J* = 3.5 Hz), 124.3, 122.6 (q, *J* = 266.1 Hz), 114.7 (q, *J* = 37.8 Hz), 113.2. **^{19}F NMR** (471 MHz, $CDCl_3$) δ -56.75.

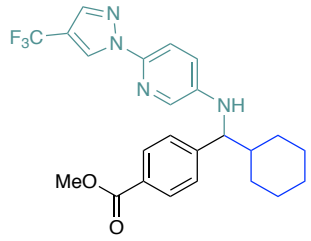

Methyl 4-(Cyclohexyl((6-(4-(trifluoromethyl)-1H-pyrazol-1-yl)pyridin-3-yl)amino)methyl)benzoate, 60 (133 mg, 58%) was prepared following *GP1*. The desired amine was isolated as a viscous oil. **^{1}H NMR** (500 MHz, $CDCl_3$) δ 8.61 (s, 1H), 8.00 (d, *J* = 8.0 Hz, 2H), 7.79 (s, 1H), 7.69 (d, *J* = 2.8 Hz, 1H), 7.64 (d, *J* = 8.8 Hz, 1H), 7.36 (d, *J* = 8.1 Hz, 2H), 6.88 (dd, *J* = 8.9, 2.9 Hz, 1H), 4.42 (s, 1H), 4.20 (d, *J* = 4.1 Hz, 1H), 3.90 (s, 3H), 1.90 (d, *J* = 12.6 Hz, 1H), 1.83 – 1.64 (m, 4H), 1.54 (d, *J* = 13.0 Hz, 1H), 1.28 – 1.03 (m, 5H). **^{13}C NMR** (126 MHz, $CDCl_3$) δ 166.7, 146.5, 142.7, 142.0, 137.6 (d, *J* = 2.8 Hz), 132.8, 129.7, 129.2, 127.1, 125.3 (q, *J* = 3.7 Hz), 122.5 (q, *J* = 266.0 Hz), 122.1, 114.5 (q, *J* = 38.5 Hz), 113.1, 63.3, 51.9, 44.5, 29.8, 29.4, 26.1, 26.1, 26.0. **^{19}F NMR** (471 MHz, $CDCl_3$) δ -56.75. **FT-IR** (cm^{-1}, neat, ATR): 3380, 2929, 2850, 1708, 1495, 1402, 1263, 1114, 967, 733. **HRMS** (ESI) calcd for $C_{24}H_{26}F_3N_4O_2$ $[M+H]^+$: 459.2008, found: 459.2001.

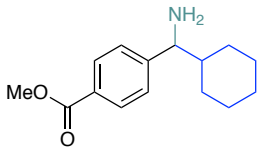

Methyl 4-(Amino(cyclohexyl)methyl)benzoate, 61 (75 mg, 61%) was prepared following *GP2*. The desired amine was isolated as a viscous yellow oil. **^{1}H NMR** (500 MHz, $CDCl_3$) δ 7.97 (d, *J* = 8.1 Hz, 2H), 7.53 – 6.91 (m, 2H), 3.90 (s, 3H), 3.67 (d, *J* = 7.3 Hz, 1H), 2.03 – 0.46 (m, 14H). **^{13}C NMR** (126 MHz, $CDCl_3$) δ 167.2, 150.8, 129.7, 128.9, 127.5, 127.3, 61.6, 52.1, 45.3, 30.1,

29.4, 26.5, 26.3. **FT-IR** (cm^{-1}, neat, ATR): 3375, 2923, 2850, 1717, 1275, 1111, 770. **HRMS** (ESI) calcd for $C_{15}H_{22}NO_2$ $[M+H]^+$: 248.1651, found: 248.1647.

6.5 References

(1) (a) B. H. Rotstein, S. Zaretsky, V. Rai, A. K. Yudin, *Chem. Rev.* **2014**, *114*, 8323-8395; (b) A. Dömling, W. Wang, K. Wang, *Chem. Rev.* **2012**, *112*, 3083-3135.

(2) (a) S. L. Schreiber, *Science* **2000**, *287*, 1964-1969; (b) W. R. J. D. Galloway, A. Isidro-Llobet, D. R. Spring, *Nat. Commun*. **2010**, *1*, 80; (c) C. J. O'Connor, H. S. G. Beckmannw, D. R. Spring, *Chem. Soc. Rev.* **2012**, *41*, 4444-4456.

(3) A. C. Boukis, K. Reiter, M. Frölich, D. Hofheinz, M. A. R. Meier, *Nat. Commun.* **2018**, *9*, 1439.

(4) J. M. M. Verkade, L. J. C. van Hemert, P. J. L. M. Quaedflieg, F. P. J. T. Rutjes, *Chem. Soc. Rev.* **2008**, *37*, 29-41.

(5) Suresh, J. S. Sandhu, *ARKIVOC*, **2012**, 66-133.

(6) Q. Wang, D.-X. Wang, M.-X. Wang, J. Zhu, *Acc. Chem. Res.* **2018**, *51*, 1290-1300.

(7) A. Dömling, I. Ugi, *Angew. Chem. Int. Ed.* **2000**, *39*, 3168-3210.

(8) (a) N. A. Petasis, I. Akritopoulou, *Tetrahedron Lett.* **1993**, *34*, 583-586; (b) N. Kumagai, G. Muncipinto, S. L. Schreiber, *Angew. Chem. Int. Ed.* **2006**, *45*, 3635-3638; (c) M. G. Ricardo, D. Llanes, L. A. Wessjohann, D. G. Rivera, *Angew. Chem. Int. Ed.* **2019**, *58*, 2700-2704.

(9) (a) R. Candeias, F. Montalbano, P. M. S. D. Cal, P. M. P. Gois, *Chem. Rev.* **2010**, *110*, 6169-6193; (b) Y. Jiang, A. B. Diagne, R. J. Thomson, S. E. Schaus, *J. Am. Chem. Soc.* **2017**, *139*, 1998-2005; (c) Y. Jiang, R. J. Thomson, S. E. Schaus, *Angew. Chem. Int. Ed.* **2017**, *56*, 16631-16635.

(10) (a) N. Miyaura, N. Sasaki, M. Itoh, A. Suzuki, *Tetrahedron Lett.* **1977**, *18*, 173-174; (b) V. K. Aggarwal, G. Y. Fang, X. Ginesta, D. M. Howells, M. Zaja, *Pure Appl. Chem.* **2006**, *78*, 215-229.

(11) (a) M. Hatano, S. Suzuki, K. Ishihara, *J. Am. Chem. Soc.* **2006**, *128*, 9998-9999; (b) M. Hatano, K. Yamashita, M. Mizuno, O. Ito, K. Ishihara, *Angew. Chem. Int. Ed.* **2015**, *54*, 2707-2711.

(12) (a) D. P. Plasko, C. J. Jordan, B. E. Ciesa, M. A. Merrill, J. M. Hanna, *Photochem. Photobiol. Sci.* **2018**, *17*, 534-538; (b) K. Cao, S. M. Tan, R. Lee, S. Yang, H. Jia, X. Zhao, B. Qiao, Z. Jiang, *J. Am. Chem. Soc.* **2019**, *141*, 5437−5443; (c) Y. Li, K. Zhou, Z. Wen, S. Cao, X. Shen, M. Lei, L. Gong, *J. Am. Chem. Soc.* **2018**, *140*, 15850-15858.

(13) (a) Z.-L. Shen, T.-P. Loh, *Org. Lett.* **2007**, *9*, 5413-5416; (b) Z.-L. Shen, H.-L. Cheong, T.-P. Loh, *Chem. Eur. J.* **2008**, *14*, 1875-1880.

(14) (a) R. A. Garza-Sanchez, A. Tlahuext-Aca, G. Tavakoli, F. Glorius, *ACS Catal.* **2017**, *7*, 4057-4061; (b) R. S. J. Proctor, H. J. Davis, R. J. Phipps, *Science* **2018**, *360*, 419-422; (c) Y. Fujiwara, J. A. Dixon, F. O'Hara, E. Daa Funder, D. D. Dixon, R. A. Rodriguez, R. D. Baxter, B. Herlé, N. Sach, M. R. Collins, Y. Ishihara, P.S. Baran, *Nature* **2012**, *492*, 95-100; (d) Á. Gutiérrez-Bonet, C. Remeur, J. K. Matsui, G. A. Molander, *J. Am. Chem. Soc.* **2017**, *139*, 12251-12258; (e) N. P. Patel, C. B. Kelly, A. P. Siegenfeld, G. A. Molander, *ACS Catal.* **2017**, *7*, 1766-1770; (f) F. J. R. Klauck, M. J. James, F. Glorius, *Angew. Chem. Int. Ed.* **2017**, *56*, 12336-12339; (g) M. Ueda, H. Miyabe, O. Miyata, T. Naito, *Tetrahedron* **2009**, *65*, 1321-1326; (h) S. Fujii, T. Konishi, Y. Matsumoto, Y. Yamaoka, K. Takasu, K. Yamada, *J. Org. Chem.* **2014**, *79*, 8128-8133; (i) J. A. Fernández-Salas, M. C. Maestro, M. M. Rodríguez-Fernández, J. L. García-Ruano, I. Alonso, *Org. Lett.* **2013**, *15*, 1658-1661; (j) G. K. Friestad, *Tetrahedron* **2001**, *57*,

5461-5496; (k) E. Fava, A. Millet, M. Nakajima, S. Loescher, M. Rueping, *Angew. Chem. Int. Ed.* **2016**, *55*, 6776-6779.

(15) (a) D. N. Primer, G. A. Molander, *J. Am. Chem. Soc.*, **2017**, *139*, 9847-9850; (b) D. N. Primer, I. Karakaya, J. C. Tellis, G. A. Molander, *J. Am. Chem. Soc.* **2015**, *137*, 2195-2198; (c) J. C. Tellis, D. N. Primer, G. A. Molander, *Science* **2014**, *345*, 433-437; (d) E. E. Stache, T. Rovis, A. G. Doyle, *Angew. Chem. Int. Ed.* **2017**, *56*, 3679-3683; (e) T. Koike, M. Akita, *Org. Biomol. Chem.* **2016**, *14*, 6886-6890.

(16) C. Heinz, J. P. Lutz, E. M. Simmons, M. M. Miller, W. R. Ewing, A. G. Doyle, *J. Am. Chem. Soc.* **2018**, *140*, 2292-2300.

(17) A. Trowbridge, D. Reich, M. J. Gaunt, *Nature* **2018**, *561*, 522-527.

(18) N. Chen, X.-J. Dai, H. Wang, C.-J. Li, *Angew. Chem. Int. Ed.* **2017**, *56*, 6260-6263.

(19) T. Koike, M. Akita, *Inorg. Chem. Front.* **2014**, *1*, 562-576.

(20) Brønsted and Lewis acid additives are reported to promote the traditional Petasis reaction: (a) D. E. Carrera, *Chem. Commun.* **2017**, *53*, 11185-11188; **(**b) Y. Li, M.-H. Xu, *Org. Lett.* **2012**, *14*, 2062-2065. *In situ* generated BF_3 may also spur the reaction.

(21) T. Chinzei, K. Miyazawa, Y. Yasu, T. Koike, M. Akita, *RSC Adv.* **2015**, *5*, 21297-21300.

(22) M. E. Welsch, S. A. Snyder, B. R. Stockwell, *Curr. Opin. Chem. Biol.* **2010**, *14*, 347-361.

(23) K. Huang, X. Li, C. Yu, Y. Zhang, P. Mariano, W. Wang, *Angew. Chem. Int. Ed.* **2017**, *56*, 1500-1505.

(24) G. E. Apnes, M. T. Didluk, K. J. Filipski, A. Guzman-Perez, E. C. Y. Lee, J. A. Pfefferkorn, B. D. Stevens, M. M. Tu, Glucagon Receptor Modulators. U.S. Patent 20120202834, Aug 9, **2012**.

(25) D. R. Kronenthal, C. Y. Han, M. K. Taylor, *J. Org. Chem.* **1982**, *47*, 2765-2768.

(26) M. Nakajima, E. Fava, S. Loescher, Z. Jiang, M. Rueping, *Angew. Chem. Int. Ed.* **2015**, *54*, 8828-8832.

(27) H. G. Roth, N. A. Romero, D. A. Nicewicz, *Synlett* **2016**, *27*, 714-723.

(28) X. Zhu, S. R. Castleberry, M. A. Nanny, E. C. Butler, *Environ. Sci. Technol.* **2005**, *39*, 3784-3791.

(29) For information on the construction of LED reactors, see the Supporting Information of: (a) N. R. Patel, C. B. Kelly, M. Jouffroy, G. A. Molander, *Org. Lett.* **2016**, *18*, 764-767; (b) M. Jouffroy, C. B. Kelly, G. A. Molander, *Org. Lett.* **2016**, *18*, 876-879.

Author Contributions: Shorouk O. Badir and Jun Yi contributed to the design of the project, performed the reaction optimization, and prepared some of the compounds used in this study. All authors contributed to the experimental work and discussion of results. Jun Yi wrote the original draft of the manuscript. Shorouk O. Badir and Gary A. Molander assisted in writing and editing of the manuscript.

Chapter 7. Multifunctional Building Blocks Compatible with Photoredox-Mediated Alkylation for DNA-Encoded Library Synthesis[§§]

7.1 Introduction

The discovery of small organic ligands with high-affinity binding to proteins is a central theme of biomedical research in both academic and industrial settings.[1] Robust chemical probes are key to validating the tractability and translatability of a therapeutic target in drug discovery programs, and they provide a critical starting point for the development of new therapeutic chemical entities.[2] Consequently, considerable attention has been devoted to the development of novel screening methods that diminish clinical attrition and to identification of chemical matter with superior specificity.[3] To accomplish these goals rapidly, DNA-encoded library (DEL) technology[4,5,6,7,8,9,10,11] (Chapter 1.3) has emerged as an innovative platform to enable the assembly and sampling of combinatorial libraries of unprecedented magnitude (>10^6 to 10^{12} drug-like candidates).[5] In this vein, DEL screens provide a time- and cost-effective format for exploration of uncharted chemical space. To ensure continued success, the development of on-DNA water-compatible transformations that employ abundant feedstocks and facilitate the incorporation of multifunctional building blocks (BBs) with a high content of C(sp^3) carbons is integral. Moving forward, we sought to utilize Ni/photoredox dual catalysis and radical/polar crossover manifolds as enabling tools to facilitate the assembly of novel structural scaffolds in DEL synthesis through regulated single-electron intermediates.

[§§] Reproduced in part with permission from S. O. Badir, J. Sim, K. Billings, A. Csakai, X. Zhang, W. Dong, G. A. Molander, *Org. Lett.* **2020**, *22*, 1046–1051. Copyright 2020, American Chemical Society.

To ensure a versatile chemical foundation, careful selection of building blocks (BBs) is instrumental in constructing libraries. A comprehensive set of BBs encompassing structural motifs that resemble bioactive molecules in combination with those bearing an additional handle for diversification is ideal.[12] Although mono-functional BBs suitable for existing DEL chemistries are widely accessible, a recent survey estimates that the number of available bifunctional BBs, serving as crucial linkers, encompasses only ~3,500 scaffolds.[12] In light of these considerations, we sought to expand the BBs amenable for photoredox-catalyzed DEL synthesis to incorporate two complementary families of radical precursors, namely aliphatic bromides[13] and α-silylmethylamines.[14]

In particular, metallaphotoredox catalysis has emerged as a valuable tool for providing unique and alternative C-C bond disconnections, especially in the context of complex biomolecular design.[15] Because of the impact of C(sp^3)-hybridized centers on the enhancement of solubility and specificity in druggable molecules, SET processes have found extensive use in the medicinal chemistry community.[16,17] Recently, our group and others have validated Ni/photoredox dual catalysis in DNA-encoded synthesis using carboxylic acids and 1,4-dihydropyridines (DHPs) as radical precursors.[18,19] Although this advancement presented a milestone in its own right, the scope of these transformations was restricted to α-amino acids, which generate stabilized α-heterosubstituted radicals.[18,19] In the case of DHPs, the cross-coupling was limited to benzylic-, secondary-, or α-alkoxy structural motifs.[18]

To address these limitations, we sought to develop three photoredox approaches to expand chemical space in the DEL platform. In the first, a photoredox/nickel-mediated reductive coupling on DNA was developed, employing primary- and secondary alkyl bromides as reaction partners using triethylamine as a mild reductant (Figure 7.1 A). As demonstrated in Chapters 3

and 4, cross-electrophile couplings furnish several advantages over traditional catalytic cycles.[20] For example, the need for preformed carbon nucleophiles, including harsh organometallic reagents prepared from the corresponding halides, severely limits functional group compatibility and renders such anionic alkylation processes unusable in DEL environments.[21] By contrast, electrophilic reagents such as aliphatic halides have greater abundance and offer excellent structural complexity, with over 2 million building blocks commercially available. Bypassing the need for stoichiometric zinc or manganese reductants, we disclose a versatile cross-coupling with excellent functional group tolerance on DNA.

In two further protocols, α-silylmethylamines have been incorporated as surrogates of structural motifs embedded within natural products.[12,22] We have thus engaged several members of this class of substrates in both Ni/photoredox dual cross-coupling and defluorinative alkylation processes (Figure 7.1 B and C). *Importantly, all of the protocols developed are completed within minutes and do not require an inert atmosphere, providing an exceedingly low barrier to practical implementation.*

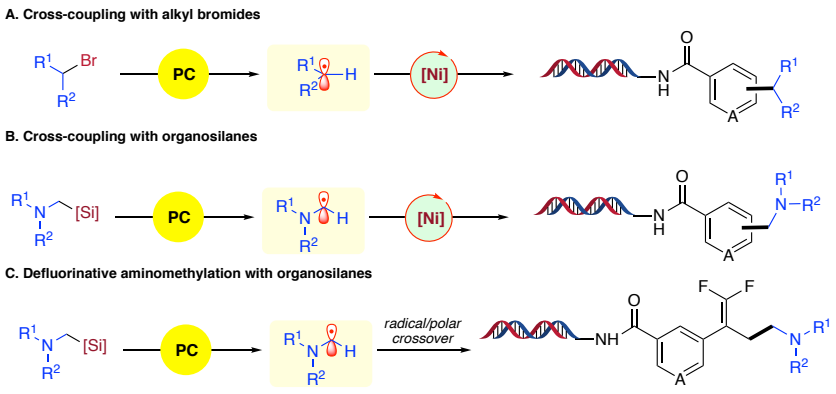

Figure 7.1. Envisioned on-DNA photochemical transformations.

7.2 Results and Discussion

A fundamental challenge facing cross-electrophile couplings is *selectivity*.[20] Because of the labile nature of both electrophilic starting materials toward oxidative addition in the presence of a nickel catalyst, careful design of reaction parameters must be implemented to synchronize the nickel and photoredox catalytic cycles (Figure 7.2 A).[13] To induce selectivity in substrates with inherently equal or similar reactivities, excess amounts of one reagent over the other can be leveraged.[20,23] This strategy is particularly powerful in the context of DEL chemistries, which are carried out on extremely small scale (~25 nmol).[18] To clarify this perspective further, the use of 250 equivalents of radical precursor only equates to 6.25 μmol of starting material. Notably, the ease of separation of homodimers from DNA-alkylated products further highlights the potential of implementing cross-electrophile couplings in DEL strategies.

We initiated our studies using a DNA-tagged *para*-substituted aryl bromide (**1**) and 4-bromotetrahydropyran (**2**) as the model substrates under 20% aqueous conditions (Figure 7.2). Given the reductive nature of this transformation, a variety of photocatalysts were screened (Figure 7.2 B). Although product formation was observed in the case of the organic dye 1,2,3,5-tetrakis(carbazol-9-yl)-4,6-dicyanobenzene (4CzIPN),[24] the iridium-based photoreductant $[Ir(dtbbpy)(ppy)_2]PF_6$ ($E_{1/2}$ = −0.96 V vs SCE) proved superior.[25,26] Of particular note, minimal product was generated using 10-phenylphenothiazine (PTH). With a drastically higher reduction potential ($E_{1/2}$ = −2.1 V vs SCE) compared to $Ir(ppy)_3$ ($E_{1/2}$ = −1.7 V vs SCE),[27] this photoreductant presumably engages the aryl halide on DNA in protodehalogenation via reductive fragmentation of the corresponding C–X bond. After assessing a variety of parameters, a loading of 250 equiv of alkyl bromide, coupled with a 4:1 ratio of the $NiBr_2$•bpy precomplex-to-

photocatalyst, was determined to afford the desired product in suitable yield. The addition of magnesium chloride ($MgCl_2$) was utilized to enhance stabilization of the DNA backbone.[28]

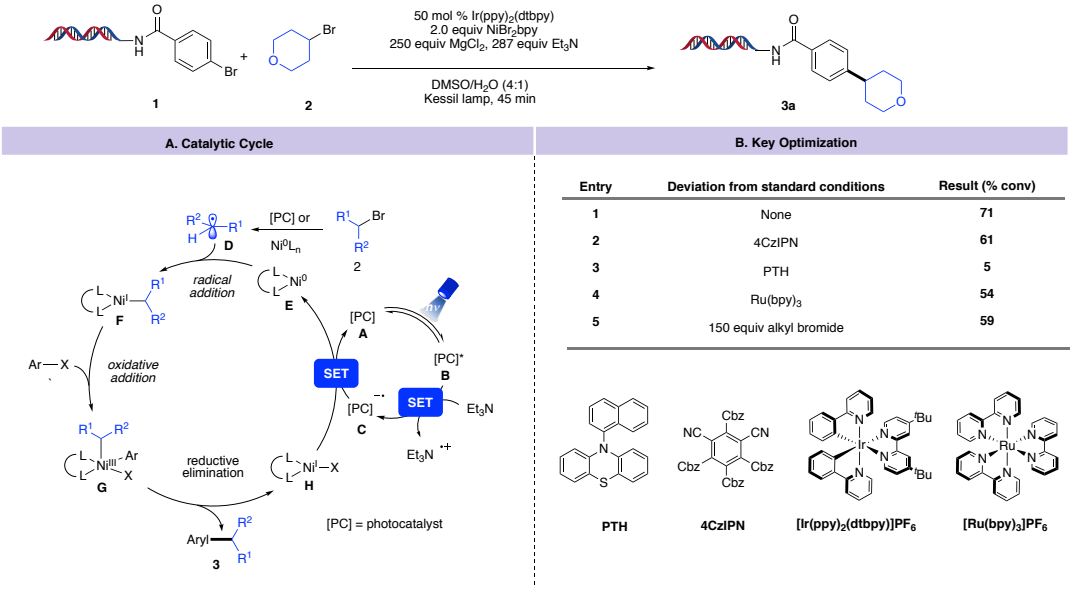

Entry	Deviation from standard conditions	Result (% conv)
1	None	71
2	4CzIPN	61
3	PTH	5
4	$Ru(bpy)_3$	54
5	150 equiv alkyl bromide	59

Figure 7.2. Envisioned mechanistic cycle and key optimization studies for on-DNA cross-coupling with alkyl bromides.

We subsequently evaluated the scope of this reductive coupling (Figure 7.3). A wide range of primary and secondary alkyl bromides served as competent substrates, including those with bifunctional handles such as *N*-Boc-protected amine **3d**, unactivated alkene **3i**, alkyl chlorides **3j** and **3k**, and nitrile **3o**. Because of the mild base utilized, free alcohols **3l-n**, stemming from a primary alkyl bromide, were effectively coupled in acceptable yields. The scope of this method was further extended to cyclic systems, including oxetane **3c**, azetidine **3d**, and pyran **3g**. To establish robust reactivity, we surveyed these DNA substrates with one primary and one secondary alkyl bromide (Figure 7.3 B). Aryl bromides and -iodides bearing electron-withdrawing and electron-donating groups were cross-coupled effectively. Activated heteroaryl systems (**3ab**, **3ac**, **3ad**) reacted in moderate yields because of their reactive nature under

reducing photoredox conditions. This limitation, however, complements existing SET-mediated cross-coupling procedures operating under an oxidative fragmentation paradigm.[18,19] By contrast, electron-neutral aryl bromides, not viable under previous reports,[38,39] furnished the desired alkylated products in moderate yields in this cross-electrophile coupling. A variety of other structural motifs were accommodated, including aryl fluoride **3ae**, styrene **3af**, *N*-Boc-protected amines (**3oj** and **3ok**), aldehyde **3al**, and free primary amines (**3om** and **3on**). Remarkably, aryl halide **3ao**, containing a morpholine residue, did not suffer diminished reactivity, despite its structural resemblance to the triethylamine used as a stoichiometric reducing agent in this reaction.

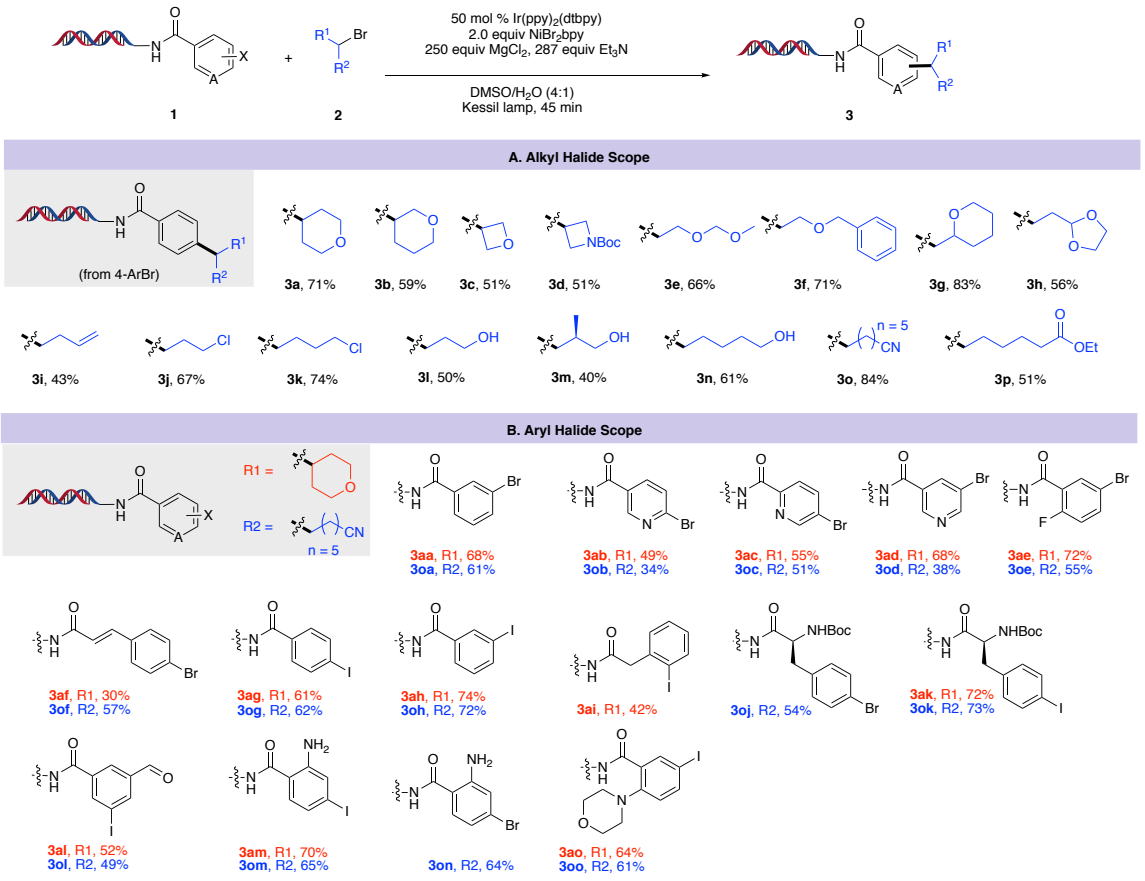

Figure 7.3. Scope of on-DNA cross-coupling with alkyl bromides.

Having explored the utility of alkyl bromides as electrophilic cross-coupling partners on DNA, we then investigated α-silylmethylamines as radical precursors.[14] An ambitious goal of unbiased DNA-encoded libraries aimed at multiple biological targets is to encompass a large collection of diverse scaffolds.[28] Inspired by the concept of diversity-oriented synthesis (DOS), first championed by Schreiber in 2000,[29] we pursued the aminomethylation of (hetero)aryl bromides to yield skeletal diversity prevalent in natural products (Figure 7.4). Indeed, the aminomethyl subunit serves as a pivotal linker in bioactive molecules as well as leading pharmaceutical drugs such as Imatinib and Donepezil.[14,30] Strategies based on DOS attest to their success in the discovery of new therapeutic treatments,[31] especially in DNA-encoded library synthesis as described recently by Schreiber et al.[32]

We envisioned that single-electron oxidation of electron-rich aminomethyl(trimethyl)silanes **4** under photoredox conditions would give rise to silyl radical cations.[14,33] This species would undergo facile desilylation to yield the desired α-aminomethyl radical, which could then be intercepted by the nickel catalytic cycle to furnish the coupled product.

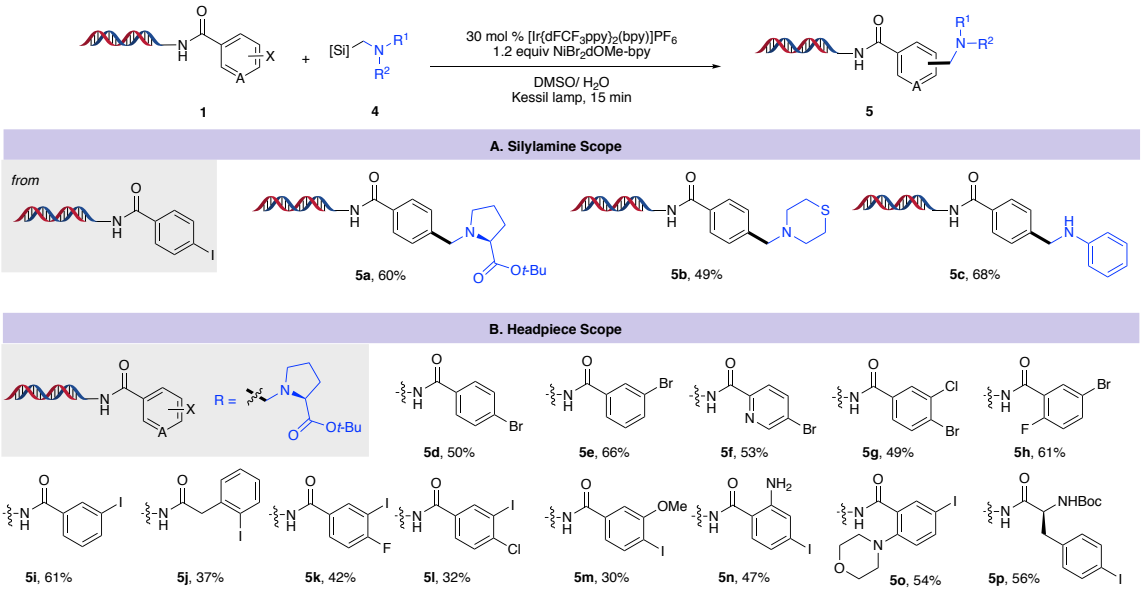

Figure 7.4. Scope of on-DNA cross-coupling with α-silylmethylamines.

We anticipated that nucleophilically assisted desilylation could occur when using water as a (co)solvent. This added benefit was further leveraged as the free amine handle allows systematic branching sequences in DEL platforms. Driven by low oxidation potentials in protic solvents,[33] unprotected aminomethylsilanes are efficiently oxidized by [Ir{dFCF$_3$ppy}(bpy)]PF$_6$. Notably, diverse aminomethyl(trimethyl)silanes were accessed in a single step from the corresponding commercially available amines and chlorotrimethylsilane. *Importantly, the reactions require less than 15 min to proceed to completion and are carried out in the absence of an inert atmosphere.*

The bifunctional nature and commercial availability of amino acids make them highly valued building blocks for library synthesis, and we successfully carried out the aminomethylation with a variety of electron-deficient and electron-rich halides with an organosilane stemming from proline to produce synthetically useful levels of product (Figure 7.4). Aryl iodides bearing *N*-Boc protected amine **5p** served as a competent substrate.

Additionally, aryl iodides bearing a free amine **5n** and tertiary amine **5o** both reacted with ease. We have successfully demonstrated the cross-coupling with non-amino acid-derived organosilanes (**5b** and **5c**).

As an extension to the developed cross-coupling conditions, we examined a defluorinative aminomethylation protocol. Given the metabolic stability of *gem*-difluoroalkenes as carbonyl mimics,[34] we subjected α-silylmethylamines to radical/polar crossover defluorinative alkylation processes (Figure 7.5).[18,35] We propose that a single-electron oxidation of the α-silylmethylamine radical precursor by the photoexcited state of the photocatalyst furnishes a nucleophilic primary radical. This species then undergoes addition to the trifluoromethylated alkene to generate an α-CF_3 radical, which is further reduced to the carbanion by the photocatalyst. Subsequent fluoride elimination occurs to yield **7**.[18,35]

With respect to the scope of this transformation (Figure 7.5), a wide array of amino acid-based organosilanes proved competent, including leucine **7e**, phenylalanine **7f,** proline **7h**, methionine **7i**, and tryptophan **7k**. Remarkably, nitrogen protecting groups were not necessary in this alkylation platform, providing an additional branching point to be utilized for further building block incorporation.

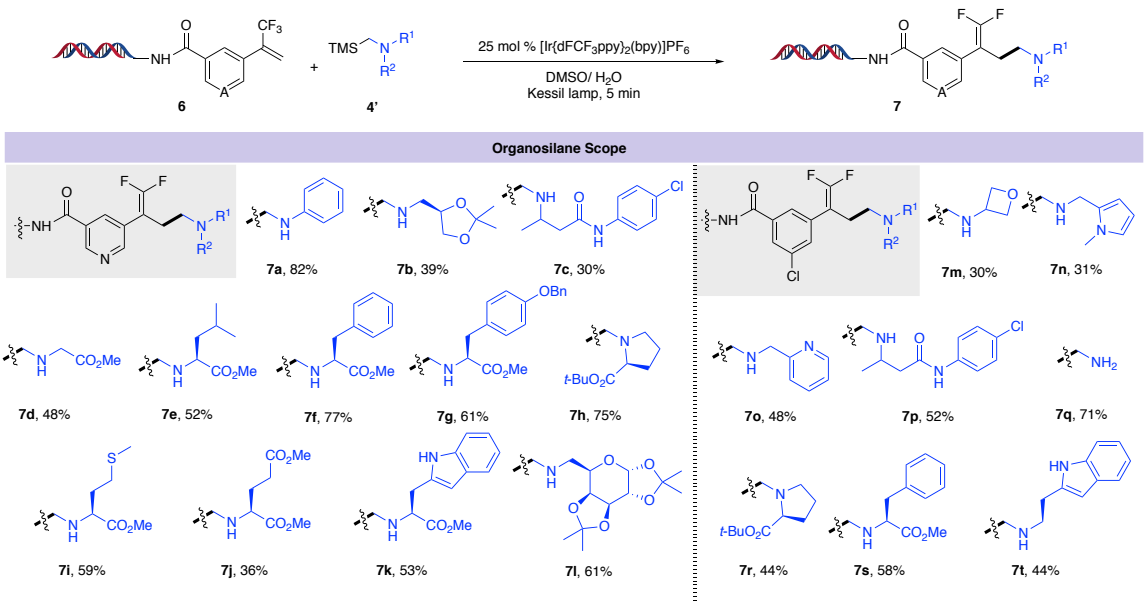

Figure 7.5. Scope of on-DNA radical/polar defluorinative aminomethylation.

Numerous other silylmethylamines, derived from commercially available aminomethylsilane and the corresponding ketones/aldehydes via reductive amination, displayed adequate reactivity with a variety of substrates, including aniline **7a**, glycoside **7l**, oxetane **7m**, pyridine **7o,** and amide **7p**. Notably, we subjected aminomethyltrimethylsilane to the reaction conditions and obtained the primary amine **7q** without any loss in reactivity. We foresee that the structural diversity created in these photoredox-mediated processes will be instrumental in providing unique and alternative bond disconnections in DEL libraries.

Finally, maintaining the integrity of the DNA tag during library synthesis is vital to the success of ELT as a drug discovery platform because the DNA barcode is the only record available to decode the synthetic steps used to construct the putative binder following selection. We verified the integrity of the DNA tag when subjected to the photoredox conditions developed herein (see the Experimental Section for details). We observed no significant differences in the ability of our samples treated with standard conditions to undergo ligation, PCR amplification,

quantification, or sequencing when compared to a no-blue light exposed control sample. These results suggest that the reported transformations are amenable for DEL synthesis without compromising the integrity of the DNA.

7.3 Conclusion

In summary, taking advantage of diverse and commercially available alkyl bromides, a selective cross-electrophile coupling on DNA has been devised. A variety of unactivated primary and secondary radical precursors are employed with high functional group tolerance. Of further advantage, photoredox-mediated radical/polar crossover reactions using structurally diverse α-silylmethylamines were employed to generate novel gem-difluoroalkene scaffolds without the need for nitrogen protecting groups.

7.4 Experimental

General Consideration

General: All chemical transformations requiring inert atmospheric conditions were carried out using Schlenk line techniques with a 4- or 5-port dual-bank manifold. For blue light irradiation, two Kessil PR160-456nm lamps (19VDC 40W Max) were placed 1.5 inches away from PCR tubes. NMR spectra (^{1}H, ^{13}C, ^{19}F) were obtained at 298 ºK. ^{1}H NMR spectra were referenced to residual $CHCl_3$ (δ 7.26) in $CDCl_3$. ^{13}C NMR spectra were referenced to $CDCl_3$ (δ 77.30). Reactions were monitored by LCMS, GC/MS, ^{1}H NMR, and/or TLC on silica gel plates (60 Å porosity, 250 μm thickness). TLC analysis was performed using hexanes/EtOAc as the eluent and visualized using ninhydrin, *p*-anisaldehyde stain, and/or UV light. Flash chromatography was accomplished using an automated system (CombiFlash®, UV detector, λ = 254 nm and 280 nm) with RediSep® R_f silica gel disposable flash columns (60 Å porosity, 40–60 μm) or RediSep R_f

Gold® silica gel disposable flash columns (60 Å porosity, 20–40 μm). Accurate mass measurement analyses were conducted using electron ionization (EI) or electrospray ionization (ESI). The signals were mass measured against an internal lock mass reference of perfluorotributylamine (PFTBA) for EI-GCMS and leucine enkephalin for ESI-LCMS. The utilized software calibrates the instruments and reports measurements by use of neutral atomic masses. The mass of the electron is not included. IR spectra were recorded on an FT-IR using either neat oil or solid products. Solvents were purified with drying cartridges through a solvent delivery system. Melting points (°C) are uncorrected.

Chemicals: Deuterated NMR solvents were purchased and stored over 4Å molecular sieves. EtOAc, hexanes, MeOH, DMF, and Et_2O were obtained from commercial suppliers and used as purchased. Et_3N was purchased from commercial suppliers and used without further purification. CH_2Cl_2 and THF were purchased and dried *via* a solvent delivery system. Preformed nickel complexes[36] and photocatalysts $[Ir\{dFCF_3ppy\}_2(bpy)]PF_6$,[37] $[Ir(ppy)_2(dtbpy)]PF_6$,[37] and 4CzIPN[38] were prepared in-house by the procedures outlined in the references cited. The organic photocatalyst, 10-phenylphenothiazine (PTH), was purchased from commercial suppliers. (Aminomethyl)trimethylsilane and (chloromethyl)trimethylsilane were commercial samples. DNA-tagged substrates and trifluoromethyl alkene-substituted benzoic acids, used in the preparation of select on-DNA substrates, were prepared as outlined in a previous publication.[18] A protocol for the synthesis of on-DNA substrates is outlined here. Alkyl bromides were purchased from commercial suppliers. The synthesis of α-silylmethylamines was performed is outlined here. All other reagents were purchased commercially and used as received. Photoredox-catalyzed reactions were performed using PCR 8-strip tubes (Ref. Fisher 781320) with PCR strips of 8 caps (Ref. Fisher 781340). DMSO was purchased and used as received. HyPure™ molecular biology grade water was purchased and used as received without further manipulation.

Analysis of "on-DNA" reactions: Analysis of on-DNA reactions was performed by LC/MS. After reaction completion, an aliquot of the reaction mixture was diluted with H_2O to approximately 0.05 mM. At this point, a 5 μL of the LC/MS sample was injected onto a reverse-phase chromatography column (Halo ES-C18, 3.4 μm particle size, 2.1x30 mm) and eluted (10-90% B over 4 min at 0.5 mL/min flow rate; solvent A: 0.75% v/v/ HFIP / 0.038% TEA / 5 μM EDTA in H_2O; solvent B: 0.75% HFIP, 0.038% TEA, 5 μM EDTA in 90/10 MeOH/deionized H_2O) with monitoring at UV 260 nm. Effluent was analyzed on a Bruker microTOF in negative ion mode. For the functionalized headpiece samples (the on-DNA aryl bromides/iodides), % conversion was determined based on reported peak intensities following deconvolution (between 3,000-10,000 Da) of the DNA charge states using the Bruker Compass DataAnalysis software version 4.2 (build 383.1). An intensity of 5% of the maximum peak intensity observed for a given spectra was set as the reporting threshold. The maximum intensity peak for each distribution of peaks was manually selected as the representative peak for reporting. % Conversion was then calculated by dividing the peak intensity of the product peak by the sum of the reported peaks for that spectra. For the photoredox scope reactions, % conversion was determined using Intact Mass™ by Protein Metrics Inc. (version v3.3-421 x 64). Data was scanned between 1.9-3.0 min and deconvoluted between 4,000-6,000 Da, with a mass tolerance window of 2 Da. A 5% of base peak threshold was set for reporting. Na, K, NH_4, and HFIP adducts were included in the product percentage.

Materials for "on-DNA" synthesis: DNA headpiece HP-NH_2(5'-/5Phos/GAGTCA/iSp9/iUniAmM/iSp9/TGACTCCC-3') was obtained from Biosearch Technologies, Novato, CA. The spacer-elongated AOP-Headpiece (Figure 7.6) was prepared via HATU coupling following the general procedure described later in this Experimental Section with 5 equiv each of Fmoc-15-amino-4,7,10,13-tetraoxapentadecanoic acid (Fmoc-AOP), *i*-

Pr_2NEt, and HATU. The lyophilized product of this reaction was then deprotected by exposure to a 10% piperidine in H_2O solution. After the reaction was deemed complete by LC/MS analysis, the reaction was precipitated following the EtOH protocol outlined below and is typically pure enough to be used without further purification.

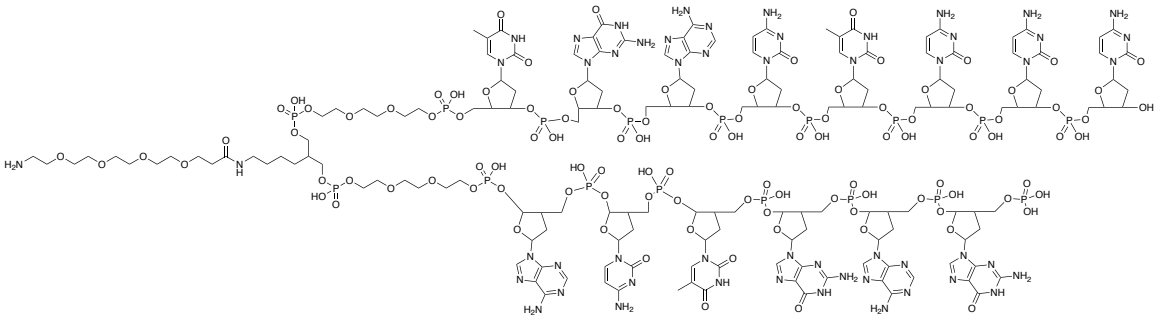

Figure 7.6. Sequence and structure of the AOP-Headpiece (molecular weight = 5184.5220).

General Procedures

Preparation of on-DNA substrates (General Procedure 1, GP1)

A) HATU premix protocol for acylation of DNA headpieces. Cool the individual HATU (200 mM in DMA, 40 equiv), *i*-Pr_2NEt (200 mM in DMA, 40 equiv), and carboxylic acid (200 mM in DMA, 40 equiv) solns at 4 ºC for 5 min. Once chilled, the acid, *i*-Pr_2NEt, and HATU solns were added sequentially to a centrifuge tube, vortexed briefly, and allowed to react at 4 ºC for 20 min. The oligomer soln (1 mM in 250 mM pH 9.4 sodium borate buffer) was then added, and the mixture was vortexed. The reaction was allowed to proceed at rt and monitored by LC/MS. Upon completion, the reaction was worked up following the "EtOH Precipitation Protocol."

B) EtOH precipitation protocol. Transfer the reaction mixture to a centrifuge tube where it fills at most 1/4 of the total volume. A volume of 5 M aq NaCl equal to 1/10 of the reaction

volume was then added followed by cold (–20 ºC) EtOH equal to 2.5 reaction volumes. The resulting mixture was then left to stand in a –80 ºC freezer for at least 1 h. The chilled mixture was then centrifuged for 30 min at 4 ºC at 3,300 rpm. The supernatant was then decanted and allowed to dry under reduced pressure. The resulting pellet is redissolved in H_2O to give a theoretical concentration of 2 mM. Purity was assessed by LCMS, and optical density was obtained via NanoDrop. For long term storage, solutions were frozen in liquid nitrogen and lyophilized to dryness to give a white solid. If impure, HPLC purification of on-DNA samples was performed: gradient of 95% A (50 mM TEAA, pH = 7.5)/5% B (1% H_2O in CH_3CN) to 60% A/40% B, through a Gemini C18 (5 μm, 110 Å, 30x100 mm), with UV visualization at 260 nm.

Synthesis of α-silylmethylamines (General Procedure 2, GP2): To a 100 mL round bottom flask equipped with a stir bar was added chloromethyltrimethylsilane (1.5 mL, 11 mmol, 2.2 equiv), the corresponding amine (5 mmol, 1.0 equiv), Na_2CO_3 (1.2 g, 11 mmol, 2.2 equiv), and NaI (1.7 g, 11 mmol, 2.2 equiv) in DMF (0.1 M). The mixture was placed under an argon atmosphere and heated to 90 ℃ overnight. Upon completion, the reaction mixture was cooled to rt and diluted with deionized H_2O (50 mL). The soln was transferred to a separatory funnel and EtOAc (75 mL) was added. The layers were separated, and the aqueous phase was extracted with EtOAc (2× 50 mL). The combined organic layers were washed with deionized H_2O (2 ×100 mL) and brine (150 mL). The soln was dried ($MgSO_4$), filtered, and reduced under vacuum. The crude reaction was purified using an automated system in hexanes/EtOAc (0 to 50 %) as eluent.

Synthesis of α-silylmethylamines (General Procedure 3, GP3)

A. Step 1. To a 100 mL round bottom flask equipped with a stir bar was added aminomethyltrimethylsilane (1.1 mL, 10 mmol, 1.0 equiv), the corresponding aldehyde or

ketone (10 mmol, 1.0 equiv), and 4Å molecular sieves (4.0 g) in Et_2O (30 mL, 0.33 M). The reaction mixture was stirred at rt overnight. Upon completion, the soln was filtered, and the solvent was removed under reduced pressure affording the corresponding imine, which was used without further purification.

B. Step 2. To a 100 mL round bottom flask equipped with a stir bar was added the corresponding imine in MeOH (50 mL, 0.2 M). The soln was then cooled to 0 ℃ and stirred for 10 min at this temperature. After this time, $NaBH_4$ (0.76 g, 20 mmol, 2 equiv) was added to the flask portion wise over 5 min. The reaction mixture was stirred at 0 ℃ for an additional 10 min, then warmed to rt overnight. The reaction mixture was quenched with H_2O (30 mL) and Na_2CO_3 (0.756 g) then transferred to a separatory funnel. At this point, CH_2Cl_2 (100 ml) was added, and the layers were separated. The aqueous layer was extracted with CH_2Cl_2 (2 × 50 mL). The combined organic layers were dried ($MgSO_4$), filtered, and taken to dryness. The crude reaction mixture was purified using an automated system with hexanes/EtOAc (0 to 50%) as eluent.

On-DNA cross-coupling with alkyl bromides (General Procedure 4, GP4): To a 0.2 mL PCR Eppendorf tube was added $Ir[(dtbpy)(ppy)_2]PF_6$ (5 μL of a 2.5 nmol/μL soln in DMSO, 12.5 nmol, 0.50 equiv), preformed $NiBr_2$•bpy (5 μL of a 10 nmol/μL soln in DMSO, 50 nmol, 2.0 equiv), $MgCl_2$ (5 μL of a 1250 nmol/μL soln in deionized H_2O, 6.25 μmol, 250 equiv), alkyl bromide (10 μL of a 625 nmol/μL soln in DMSO, 6.25 μmol, 250 equiv), Et_3N (1 μL neat, 287 equiv), and aryl halide (5 μL of a 5 nmol/μL soln in deionized H_2O, 25 nmol, 1.0 equiv). The PCR tube was then capped, vortexed, and irradiated for 45 min with Kessil PR160-456nm lamps (19 V DC 40 W Max) at a distance of 1.5 inches. The reaction was then diluted with H_2O (optima LC/MS grade or HyPure™ molecular biology grade water) and analyzed by LC/MS.

On-DNA cross-coupling with α-silylmethylamines (General Procedure 5, GP5): To a 0.2 mL PCR Eppendorf tube was added $[Ir\{dFCF_3ppy\}_2(bpy)]PF_6$ (5 μL of a 1.5 nmol/μL soln in DMSO, 7.5 nmol, 0.30 equiv), preformed $NiBr_2$dOMe•bpy (5 μL of a 6 nmol/μL soln in DMSO, 30 nmol, 1.2 equiv), α-silylmethylamine (10 μL of a 250 nmol/μL soln in DMSO, 2.50 μmol, 100 equiv), 10 μL DMSO, and aryl halide (5 μL of a 5 nmol/μL soln in deionized H_2O, 25 nmol, 1.0 equiv). The PCR tube was then capped, vortexed, and irradiated for 15 min with Kessil PR160-456 nm lamps (19 V DC 40 W Max) at a distance of 1.5 inches. The reaction was then diluted with H_2O (optima LC/MS grade or HyPure™ molecular biology grade water) and analyzed by LC/MS.

On-DNA defluorinative aminomethylation with α-silylmethylamines (General Procedure 6, GP6): To a 0.2 mL PCR Eppendorf tube was added $[Ir\{dFCF_3ppy\}_2(bpy)]PF_6$ (5 μL of a 1.25 nmol/μL soln in DMSO, 6.25 nmol, 0.25 equiv), α-silylmethylamine (2 μL of a 125 nmol/μL soln in DMSO, 1.25 μmol, 10 equiv), 50 μL DMSO, and trifluoromethyl alkene (5 μL of a 5 nmol/μL soln in deionized H_2O, 25 nmol, 1.0 equiv). The PCR tube was then capped, vortexed, and irradiated for 5 min with Kessil PR160-456 nm lamps (19 V DC 40 W Max) at a distance of 1.5 inches. The reaction was then diluted with H_2O (optima LC/MS grade or HyPure™ molecular biology grade water) and analyzed by LC/MS.

On-DNA reaction workflow: All photoredox reactions were performed with Kessil PR160-456 nm lamps (19 V DC 40 W Max). The lamps were placed 1.5 inches away from PCR Eppendorf tube. A typical reaction setup is shown below.

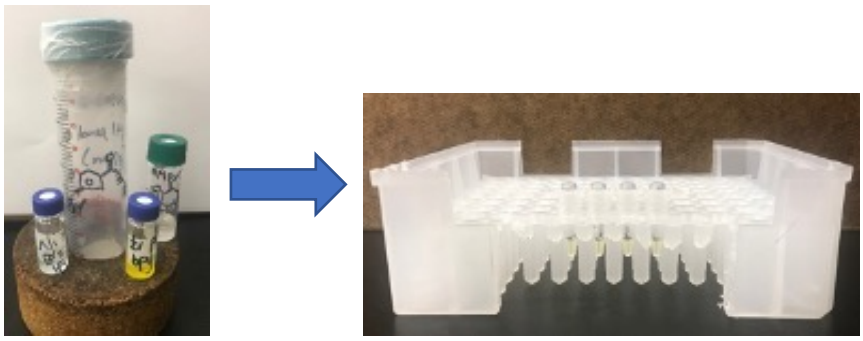

Figure 7.7. Reactions were set up on the benchtop under air. Reagents were added as stock solutions to 0.2 mL PCR tubes.

Figure 7.8. The PCR tubes were vortexed then irradiated with Kessil PR160-456 nm lamps (19 VDC 40 W Max) for the time designated for each experiment.

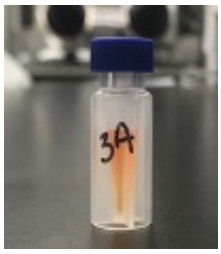

Figure 7.9. Upon completion, reactions were diluted with Optima grade H_2O and analyzed.

qPCR, PCR, and Sequencing

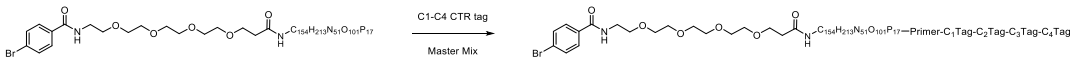

Figure 7.10. C1-C4 tag elongation.

Top strand: 5'- /5Phos/A AAT CGA TGT GTT CCG CAA GAA GCC TGG TAA GCG GAG AAA GGT CGT T –3'

Bottom strand: 5'-/5Phos/C GAC CTT TCT CCG CTT ACC AGG CTT CTT GCG GAA CAC ATC GAT TTG G -3'

The top and bottom strands (purchased from IDT as lyophilized powders) of a control 4-cycle tag were annealed by combining 300 nmol of each strand (2 mM in H_2O), heating to 95 °C for 5 min, then cooling to rt. The annealed tag solution (1.2 equiv) was then added to the *p*-bromobenzamide headpiece (see AOP-headpiece described earlier for the DNA sequence of the starting material; 1 equiv, 250 nmol, 125 µL H_2O, 2 mM), followed by 2 mL of H_2O, 100 µL 10x T4 ligation buffer, and 10 µL T4 DNA ligase purchased from Syngene. The ligation solution was vortexed and let sit at rt overnight. The ligation was pushed with additional annealed control tag (150 nmol, 1 mM in H_2O) and ligase (5 µL). The reaction was again capped, vortexed, and left to react at rt overnight. The ligation was pushed a second time with additional annealed control tag (150 nmol, 1 mM in H_2O), T4 ligation buffer (25uL), and ligase (2.5µL). The reaction was again capped, vortexed, and left to react in a cold room for ~3 d. The ligation was precipitated for 1 h at -80 °C following addition of 300 µL of 5 M NaCl (aq) and 12 mL of cold EtOH. The precipitated solution was then centrifuged at 3,300 rpm at 4 °C for 1 h, and the solvent was decanted to afford the DNA pellet, which was dried on a lyophilizer for 2 h. The crude pellet was resuspended in 1 mL H_2O and purified by HPLC (column: Gemini C18, 5 µm, 21.2x100 mm; gradient: 10 to 90%

B in 30 min, 20 mL/min; UV at 260 nm; solvent A: 50 mM TEAA, pH 7.5; solvent B: 1% H_2O in MeCN) to afford the desired product. The lyophilized product was analyzed by optical density using a composite extinction coefficient of 1023700 L/(mol-cm) to determine isolated yield (194.6 nmol, 77.8%). LC/MS calcd: 34439.8, found: 34441.1.

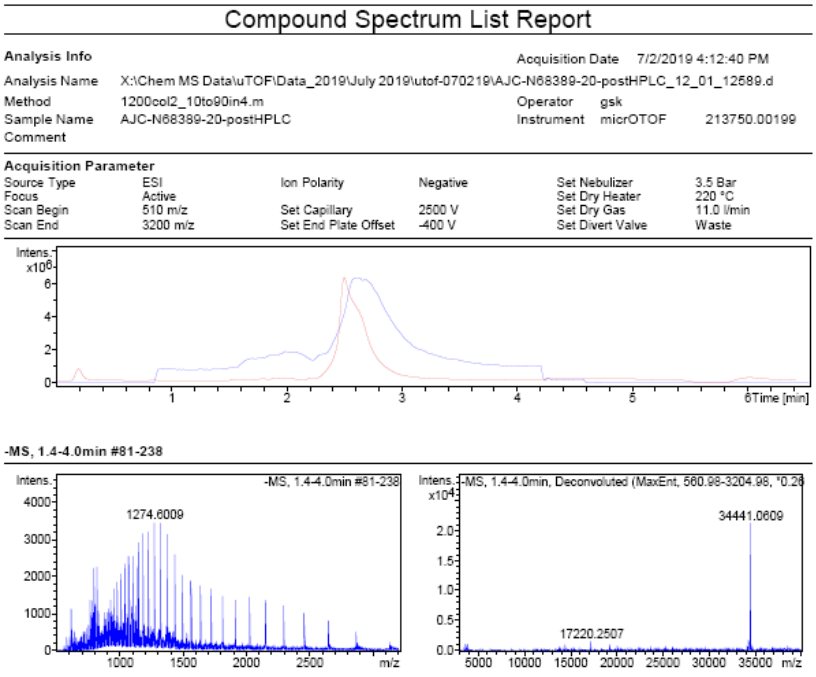

Figure 7.11. LCMS compound spectrum report for DNA elongated headpiece.

Exemplar reactions on elongated HP

A total of six alkylation reactions were run on the elongated *p*-bromobenzamide headpiece with 4-bromotetrahydropyran using standard conditions, unless otherwise noted in the table below. Following reaction, samples were subjected to standard EtOH precipitation and then lyophilization of the pellet. The crude pellets were then diluted with 100 µL milliQ H_2O, and the concentration of the stock solution was determined using optical density as determined on a Thermo NanoDrop 2000. Three measurements were obtained, and the average A260 used to

determine concentration. *Similar recoveries were obtained across all samples (see relative recovery column below) indicating that there is no substantial impact of the chemistry on sample recovery.*

Sample name	**Deviations**	**nmol recovered**	**Absolute recovery (%)**	**Recovery relative to 70-6 (%)**
70-1	Standard alkylation conditions	4.6	36.8	90.2
70-2	No Ni	4.9	39.2	96.1
70-3	No photocatalyst	4.6	36.8	90.2
70-4	No triethylamine	4.8	38.4	94.1
70-5	No $MgCl_2$	4.5	36.0	88.2
70-6	No light (~ no chemistry control)	5.1	40.8	N/A

Closing primer ligation on reacted material

Top strand: 5'-/5Phos/ACG ATG CCC GGT CTA CNN NNN NNN NNN NCT GAT GGC GCG AGG GAG GC-3'

Bottom strand: 5'-GTA GAC CGG GCA TCG TAA-3'

To each of the six exemplar reaction samples (2 nmol aliquot, 0.04 mM in H_2O) was added the closing primer (5 nmol, 1 mM in H_2O), 10X ligation buffer (10 μL), T4 DNA ligase (2 μL, 10 mg/mL), and H_2O (33 μL) for a final reaction volume of 100 μL. Ligations were allowed to proceed overnight at rt. Samples were analyzed by gel electrophoresis and all were determined to have gone to sufficient completion.

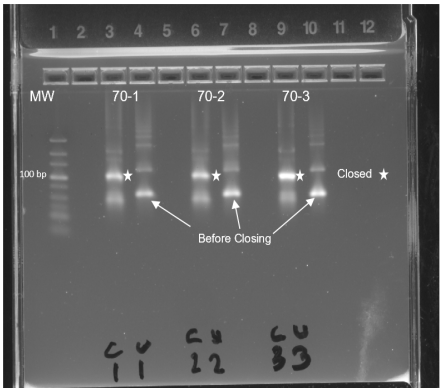

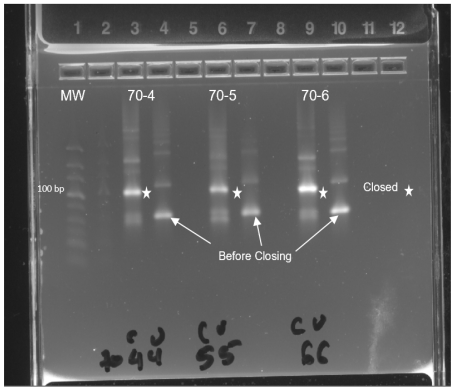

qPCR

5’ 565 Cla Primer: 5’-TGA CTC CCA AAT CGA TGT G -3’

3’ 454 Short Primer: 5’-GCC TCC CTC GCG CCA -3’

Quantitative PCR was performed on a Roche LightCycler 480 II PCR system with SYBR Green I as the detection dye. A bulk master mix solution was prepared by combining 1 mL of SYBR green, 60 µL of 10 µM PCR primer 565 Cla, 60 µL of 10 µM PCR primer 454 short, and 680 µL of H_2O. To 2 µL of sample was then added 18 µL of master mix. Samples were subjected to qPCR:

Stage	**Temperature/time**	**Number of cycles**
UNG	50 °C / 2 min	1
HotStart	95 °C / 5 min	1
Amplification	95 °C / 15 sec 55 °C / 30 sec 72 °C / 30 sec	40
Melt	95 °C / 1 sec 70 °C / 1 sec	1
Cool	45 °C / 30 sec	

Samples were then analyzed using the 2nd derivative maximum standard protocol on the instrument to determine how many molecules were present per µL sample. *Samples achieved*

*acceptable consistency across conditions in comparison to the no-light control sample (**70-6**), suggesting that the conditions developed are not impacting the amount of amplifiable DNA present in a significant way.*

Sample name	**Molecules/μL sample**
70-1	2.59E+13
70-2	2.10E+13
70-3	3.97E+13
70-4	3.10E+13
70-5	7.27E+12
70-6	3.76E+13

PCR amplification

Samples were subjected to 11 cycles of PCR amplification using the Roche FastStart Taq Polymerase dNTPack and Illumina P5 and P7 primers. The standard Taq-PCRamp program is as follows:

1. 95 °C for 10 min
2. 95 °C for 30 sec
3. 59 °C for 30 sec
4. 72 °C for 30 sec
5. Repeat STEP 2-4, 10 times
6. 72 °C for 7 min
7. 4 °C hold
8. End

After PCR, samples were purified using Beckman Coulter AMPure beads, then quantified on an Agilent Bioanalyzer following the standard manufacturer's protocol.

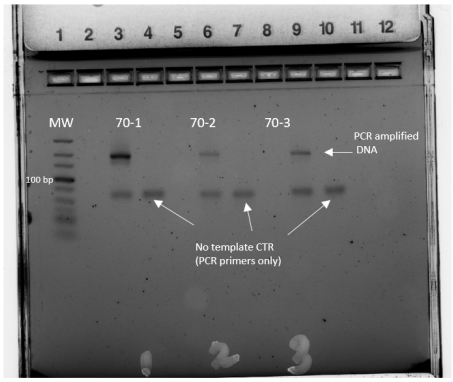

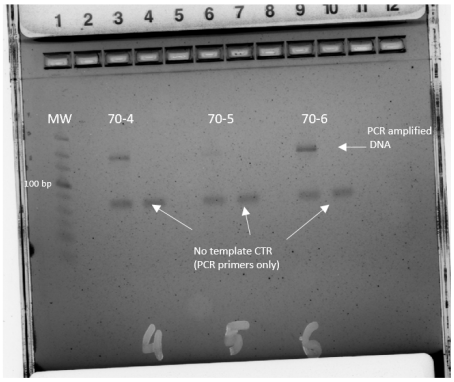

Chemistry ID	Amp cycles	[Bioanalyzer] (nM)
70-1	11	48.75
70-2	11	11.15
70-3	11	13.3
70-4	11	17.75
70-5	11	9.5
70-6	11	39.5

Based on the bioanalyzer results following the PCR amplification and purification described above, an aliquot of each sample, representing approximately 1E8 molecules, were prepared for sequencing following the manufacturer's standard protocol with an Illumina MiSeq v3 kit, then submitted for sequencing on an Illumina MiSeq. Samples were subjected to 111 cycles for Read 1 and 9 cycles for index runs. % Sequences without mutations was determined based on a comparison of the desired sequence against the top 19 other sequences identified. The % mutation for the standard alkylation conditions in comparison to the no light control sample is consistent (suggesting that the mutations observed are inherent to the purchased tags and the

general processes employed in this Experimental Section, rather than chemistry specific). The rate of mutation is also aligned to what we have observed for previous photoredox reactions (*J. Am. Chem. Soc*. **2019**, *141*, 3723-3732), making us confident in the ability of this chemistry to be used in a library synthesis. It is interesting to note that the No $MgCl_2$ sample showed ~2x the amount of mutated sequences when compared to the no light control and the standard alkylation conditions, perhaps suggesting that the $MgCl_2$ is serving a protective role for the DNA - a phenomenon that has been observed previously (*Bioconjugate Chem*. **2017**, *28*, 1625-1629).

Sample name	Chemistry summary	% Mutated sequences
70-1	Standard alkylation conditions	4.01 %
70-2	No Ni	6.80 %
70-3	No photocatalyst	5.29 %
70-4	No triethylamine	5.18 %
70-5	No $MgCl_2$	9.80 %
70-6	No light (~ no chemistry control)	5.06 %

Characterization Data

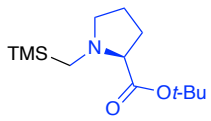

***tert*-Butyl ((Trimethylsilyl)methyl)-*L*-prolinate**, **4a** (5 mmol scale, 1.16 g, 90%) was prepared following *GP2*. The product was isolated as a pale-yellow oil. **^{1}H NMR** (500 MHz, $CDCl_3$) δ 3.18 – 3.01 (m, 1H), 2.94 (dd, *J* = 8.7, 5.7 Hz, 1H), 2.45 – 2.22 (m, 2H), 2.11 – 1.94 (m, 1H), 1.93 – 1.82 (m, 3H), 1.76 – 1.69 (m, 1H), 1.46 (s, 9H), 0.06 (s, 9H). **^{13}C NMR** (126 MHz, $CDCl_3$) δ 173.7, 80.5, 70.7, 56.3, 45.9, 29.2, 28.5, 23.7, -1.1. **FT-IR** (cm^{-1}, neat, ATR): 2956, 2776, 1724,

1479, 1457, 1418, 1391, 1367, 1295, 1248, 1210, 1119, 1032, 763, 692. **HRMS** (ESI) calcd for $C_{13}H_{28}NO_2Si$ $[M+H]^+$: 258.1889, found: 258.1914.

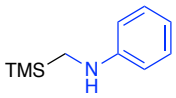

***N*-((Trimethylsilyl)methyl)aniline**, **4c** (5 mmol scale, 0.3 g, 34%) was prepared following *GP2*. The product was isolated as a pale-yellow oil. **^{1}H NMR** (500 MHz, $CDCl_3$) δ 7.23 (td, *J* = 7.2, 1.4 Hz, 2H), 6.91 – 6.30 (m, 3H), 3.51 (s, 1H), 2.54 (s, 2H), 0.18 (s, 9H).**^{13}C NMR** (126 MHz, $CDCl_3$) δ 150.8, 129.4, 117.2, 112.7, 33.8, -2.4. **FT-IR** (cm^{-1}, neat, ATR): 2954, 2896, 2800, 1732, 1676, 1443, 1314, 1282, 1203, 1176, 1153, 992. **HRMS** (ESI) calcd for $C_{10}H_{18}NSi$ $[M+H]^+$: 180.1209, found: 180.1196.

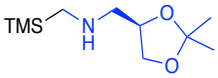

(*S*)-1-(2,2-Dimethyl-1,3-dioxolan-4-yl)-*N*-((trimethylsilyl)methyl)methanamine, **4'b** (10 mmol scale, 1.04 g, 48%) was prepared following *GP3*. The product was isolated as a pale-yellow oil. **^{1}H NMR** (500 MHz, $CDCl_3$) δ 4.34 – 4.14 (m, 1H), 4.00 (dd, *J* = 7.9, 6.3 Hz, 2H), 3.65 (t, *J* = 7.4 Hz, 1H), 2.70 (t, *J* = 6.1 Hz, 2H), 2.19 – 1.91 (m, 2H), 1.38 (s, 3H), 1.32 (s, 3H), 0.01 (s, 9H).**^{13}C NMR** (126 MHz, $CDCl_3$) δ 109.2, 75.4, 67.8, 57.2, 40.8, 27.2, 25.8, -2.3. **FT-IR** (cm^{-1}, neat, ATR): 2986, 2953, 2890, 1734, 1456, 1379, 1370, 1248, 1213, 1156, 1112, 1076, 1054, 970, 766, 697. **HRMS** (ESI) calcd for $C_{10}H_{24}NO_2Si$ $[M+H]^+$: 218.1576, found: 218.1570.

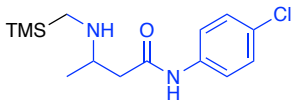

***N*-(4-Chlorophenyl)-3-(((trimethylsilyl)methyl)amino)butanamide**, **4'c** (10 mmol scale, 1.43 g, 48%) was prepared following *GP3*. The product was isolated as a pale-yellow oil. **^{1}H NMR** (500 MHz, $CDCl_3$) δ 11.0 (s, 1H), 7.47 (d, *J* = 8.8 Hz, 2H), 7.25 (d, *J* = 9.3 Hz, 2H), 3.00 (td, *J* = 6.7, 3.2 Hz, 1H), 2.64 (dd, *J* = 16.5, 3.2 Hz, 1H), 2.27 (dd, *J* = 16.5, 6.9 Hz, 1H), 2.20 – 1.76 (m, 2H), 1.21 (d, *J* = 6.5 Hz, 3H), 0.88 (d, *J* = 6.7 Hz, 1H), 0.11 (s, 9H).**^{13}C NMR** (126 MHz, $CDCl_3$) δ 170.6, 137.5, 129.1, 128.6, 121.3, 54.2, 41.0, 36.5, 20.1, -2.3. **FT-IR** (cm^{-1}, neat, ATR): 2956, 1665, 1601, 157, 1491, 1468, 1400, 1369, 1338, 1307, 1249, 1093, 835, 811, 772, 757, 743. **HRMS** (ESI) calcd for $C_{14}H_{24}N_2OSiCl$ $[M+H]^+$: 299.1346, found: 299.1337.

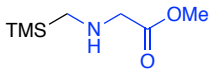

Methyl ((Trimethylsilyl)methyl)glycinate, **4'd** (5 mmol scale, 0.75 g, 86%) was prepared following *GP2*. The product was isolated as a pale-yellow oil. **^{1}H NMR** (500 MHz, $CDCl_3$) δ 3.67 (s, 3H), 3.35 (s, 2H), 2.01 (s, 2H), 1.41 (s, 1H), 0.01 (s, 9H). **^{13}C NMR** (126 MHz, $CDCl_3$) δ 173.2, 54.9, 51.7, 40.4, -2.5. **FT-IR** (cm^{-1}, neat, ATR): 3346, 2954, 2900, 2790, 1436, 1347, 1170, 1138, 1052, 986, 941, 767. **HRMS** (ESI) calcd for $C_7H_{18}NO_2Si$ $[M+H]^+$: 176.1107, found: 176.1102.

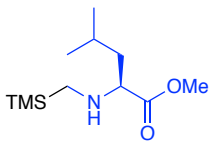

Methyl ((Trimethylsilyl)methyl)-*L*-leucinate, **4'e** (5 mmol scale, 0.39 g, 34%) was prepared following *GP2*. The product was isolated as a pale-yellow oil. **^{1}H NMR** (500 MHz, $CDCl_3$) δ

3.69 (d, J = 1.0 Hz, 3H), 3.19 (t, J = 7.3 Hz, 1H), 1.98 (d, J = 13.2 Hz, 1H), 1.92 – 1.80 (m, 1H), 1.78 – 1.61 (m, 1H), 1.48 – 1.37 (m, 2H), 1.14 (s, 1H), 0.89 (dd, J = 15.7, 6.6 Hz, 6H), 0.01 (s, 9H). **^{13}C NMR** (126 MHz, $CDCl_3$) δ 176.9, 64.1, 51.6, 42.7, 38.5, 25.3, 22.9, 22.7, -2.45. **FT-IR** (cm^{-1}, neat, ATR): 2954, 2871, 1468, 1434, 1368, 1336, 1309, 1248, 1192, 1166, 1146, 1015, 980, 761. **HRMS** (ES+) calcd for $C_{11}H_{26}NO_2Si$ $[M+H]^+$: 232.1733, found: 232.1694.

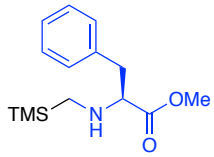

Methyl ((Trimethylsilyl)methyl)-*L*-phenylalaninate, **4'f** (5 mmol scale, 0.89 g, 67%) was prepared following *GP2*. The product was isolated as a pale-yellow oil. **^{1}H NMR** (500 MHz, $CDCl_3$) δ 8.01 – 6.63 (m, 5H), 3.63 (s, 3H), 3.44 (t, J = 7.0 Hz, 1H), 3.02 – 2.68 (m, 2H), 2.04 (d, J = 13.1 Hz, 1H), 1.92 (d, J = 13.2 Hz, 1H), 1.38 (s, 1H), 0.01 (s, 9H). **^{13}C NMR** (126 MHz, $CDCl_3$) δ 175.4, 137.9, 129.4, 128.6, 126.9, 67.09, 5.69, 39.6, 38.5, -2.5. **FT-IR** (cm^{-1}, neat, ATR): 2952, 1496, 1455, 1434, 1349, 1248, 1216, 1193, 1167, 1126, 1080, 984, 748. **HRMS** (ESI) calcd for $C_{14}H_{24}NO_2Si$ $[M+H]^+$: 266.1576, found: 266.1565.

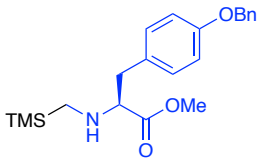

Methyl (*S*)-3-(4-(Benzyloxy)phenyl)-2-(((trimethylsilyl)methyl)amino)propanoate, **4'g** (5 mmol scale, 0.87 g, 59%) was prepared following *GP2*. The product was isolated as a foam. **^{1}H NMR** (500 MHz, $CDCl_3$) δ 7.50 – 7.31 (m, 5H), 7.10 (d, J = 8.3 Hz, 2H), 6.89 (d, J = 8.5 Hz, 2H), 5.04 (s, 2H), 3.64 (s, 3H), 3.44 (s, 1H), 2.93 (s, 2H), 2.05 (d, J = 13.1 Hz, 1H), 1.96 (d, J = 13.5 Hz, 1H), 1.58 (s, 1H), 0.02 (s, 9H). **^{13}C NMR** (126 MHz, $CDCl_3$) δ 175.5, 157.8, 137.4,

130.4, 130.2, 128.8, 128.2, 127.7, 115.0, 70.3, 67.2, 51.7, 38.7, 38.5, -2.4. **FT-IR** (cm^{-1}, neat, ATR): 2950, 1733, 1511, 1433, 1386, 1297, 1204, 1190, 1177, 1159, 1126, 1016, 812, 751, 741. **HRMS** (ESI) calcd for $C_{21}H_{30}NO_3Si$ $[M+H]^+$: 372.1995, found: 372.2009.

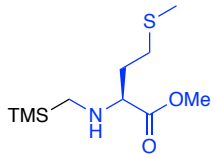

Methyl ((Trimethylsilyl)methyl)-*L*-methioninate, **4'i** (5 mmol scale, 0.67 g, 54%) was prepared following *GP2*. The product was isolated as a pale-yellow oil. **^{1}H NMR** (500 MHz, $CDCl_3$) δ 3.68 (d, *J* = 1.3 Hz, 3H), 3.43 – 3.19 (m, 1H), 2.74 – 2.35 (m, 2H), 2.05 (d, *J* = 1.4 Hz, 3H), 1.98 (dd, *J* = 13.1, 1.2 Hz, 1H), 1.91 – 1.82 (m, 2H), 1.81 – 1.70 (m, 1H), 1.22 (s, 1H), -0.01 (d, *J* = 1.4 Hz, 9H). **^{13}C NMR** (126 MHz, $CDCl_3$) δ 175.9, 64.1, 51.8, 38.3, 32.6, 30.9, 15.7, -2.5. **FT-IR** (cm^{-1}, neat, ATR): 2952, 2917, 2852, 2789, 1434, 1345, 1298, 1277, 1247, 1192, 1168, 1125, 987, 761. **HRMS** (ESI) calcd for $C_{10}H_{24}NO_2SiS$ $[M+H]^+$: 250.1297, found: 250.1291.

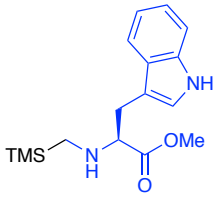

Methyl ((Trimethylsilyl)methyl)-*L*-tryptophanate, **4'k** (5 mmol scale, 1.00 g, 66%) was prepared following *GP2*. The product was isolated as a foam. **^{1}H NMR** (500 MHz, $CDCl_3$) δ 8.25 (s, 1H), 7.64 (d, *J* = 7.8 Hz, 1H), 7.33 (dd, *J* = 8.3, 1.2 Hz, 1H), 7.19 (ddd, *J* = 8.2, 7.1, 1.2 Hz, 1H), 7.12 (ddd, *J* = 7.9, 7.0, 1.1 Hz, 1H), 7.02 (t, *J* = 2.3 Hz, 1H), 3.63 (s, 3H), 3.57 (tt, *J* = 6.7, 1.9 Hz, 1H), 3.30 – 2.59 (m, 2H), 2.10 (dt, *J* = 13.3, 1.8 Hz, 1H), 1.97 (dt, *J* = 13.3, 1.5 Hz, 1H), 1.5 (s, 1H), 0.01 (s, 9H). **^{13}C NMR** (126 MHz, $CDCl_3$) δ 175.8, 136.4, 127.8, 123.0, 122.2, 119.6,

119.1, 111.8, 111.4, 66.4, 51.8, 38.6, 29.12, -2.4. **FT-IR** (cm^{-1}, neat, ATR): 3100, 1744, 1457, 1434, 1351, 1281, 1255, 1232, 1210, 1198, 1172, 1113, 1103, 789, 759. **HRMS** (ESI) calcd for $C_{16}H_{25}N_2O_2Si$ $[M+H]^+$ 305.1685, found: 305.1685.

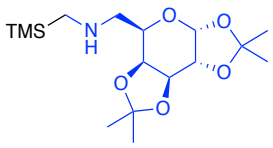

1-((3a*R*,5*R*,5a*S*,8a*S*,8b*R*)-2,2,7,7-Tetramethyltetrahydro-5*H*-bis([1,3]dioxolo)[4,5-*b*:4',5'-*d*]pyran-5-yl)-*N*-((trimethylsilyl)methyl)methanamine, **4'l** (10 mmol scale, 2.07 g, 60%) was prepared following *GP3*. The product was isolated as a foam. **^{1}H NMR** (500 MHz, $CDCl_3$) δ 5.51 (t, *J* = 4.2 Hz, 1H), 4.57 (dd, *J* = 7.8, 2.5 Hz, 1H), 4.28 (dt, *J* = 5.3, 2.6 Hz, 1H), 4.14 (dq, *J* = 5.6, 3.0, 2.6 Hz, 1H), 4.06 – 3.80 (m, 1H), 2.90 (ddd, *J* = 12.5, 9.0, 3.3 Hz, 1H), 2.71 (dt, *J* = 13.0, 3.4 Hz, 1H), 2.12 (dt, *J* = 16.5, 3.1 Hz, 2H), 1.99 (dd, *J* = 13.6, 2.8 Hz, 1H), 1.51 (d, *J* = 3.4 Hz, 3H), 1.43 (d, *J* = 2.8 Hz, 3H), 1.31 (t, *J* = 2.7 Hz, 6H), 0.02 (d, *J* = 2.6 Hz, 9H). **^{13}C NMR** (126 MHz, $CDCl_3$) δ 109.4, 108.7, 96.7, 72.4, 71.2, 71.0, 66.1, 53.9, 40.0, 26.4, 26.3, 25.2, 24.6, -2.3. **FT-IR** (cm^{-1}, neat, ATR): 3000, 1383, 1372, 1173, 1143, 959, 919, 900, 806, 771, 731. **HRMS** (ESI) calcd for $C_{16}H_{32}NO_5Si$ $[M+H]^+$: 346.2050, found: 346.2038.

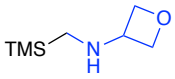

***N*-((Trimethylsilyl)methyl)oxetan-3-amine**, **4'm** (10 mmol scale, 1.01 g, 58%) was prepared following *GP3*. The product was isolated as a pale-yellow oil. **^{1}H NMR** (500 MHz, $CDCl_3$) δ 4.82 (t, *J* = 6.7 Hz, 2H), 4.42 (t, *J* = 6.2 Hz, 2H), 4.19 – 3.75 (m, 1H), 1.98 (d, *J* = 1.1 Hz, 2H), 1.44 – 0.86 (br s, 1H), 0.06 (d, *J* = 1.2 Hz, 9H). **^{13}C NMR** (126 MHz, $CDCl_3$) δ 79.6, 57.0, 36.9, -2.4. **FT-IR** (cm^{-1}, neat, ATR): 3312, 2952, 2868, 2771, 1748, 1680, 1467, 1423, 1368, 1312,

1247, 1160, 1065, 1033, 973, 759. **HRMS** (ESI) calcd for $C_7H_{18}NOSi$ $[M+H]^+$: 160.1158, found: 160.1142.

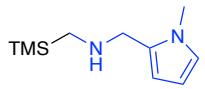

1-(1-Methyl-1*H*-pyrrol-2-yl)-*N*-((trimethylsilyl)methyl)methanamine, **4'n** (10 mmol scale, 1.45 g, 74%) was prepared following *GP3*. The product was isolated as a pale-yellow oil. **^{1}H NMR** (500 MHz, $CDCl_3$) δ 6.61 (q, *J* = 2.2 Hz, 1H), 6.28 – 5.75 (m, 2H), 3.75 (s, 2H), 3.68 (s, 3H), 2.12 (s, 2H), 0.93 (s, 1H), 0.07 (d, *J* = 1.9 Hz, 9H). **^{13}C NMR** (126 MHz, $CDCl_3$) δ 131.8, 122.5, 108.0, 106.5, 50.3, 40.0, 33.9, -2.4. **FT-IR** (cm^{-1}, neat, ATR): 2953, 2895, 2774, 1497, 1448, 1413, 1345, 1700, 1246, 1187, 1156, 1087, 1073, 750. **HRMS** (ESI) calcd for $C_{10}H_{21}N_2Si$ $[M+H]^+$: 197.1474, found: 197.1464.

7.5 References

(1) D. Neri, R. A. Lerner, *Annu. Rev. Biochem.* **2018,** *87*, 479-502.

(2) R. M. Garbaccio, E. R. Parmee, *Cell Chem. Biol.* **2016,** *23*, 10-17.

(3) For selected screening technologies of small molecules, see: (a) D. A. Erlanson, S. W. Fesik, R. E. Hubbard, W. Jahnke, H. Jhoti, *Nat. Rev. Drug. Discov.* **2016,** *15*, 605-619; (b) R. H. A. Folmer, *Drug Discov. Today Technol.* **2016,** *21*, 491-498; (c) R. Halai, M. A. Cooper, *Expert Opin. Drug Dis.* **2012,** *7*, 123-131; (d) T. E. Nielsen, S. L. Schreiber, *Angew. Chem. Int. Ed.* **2008,** *47*, 48-56.

(4) S. Brenner, R. A. Lerner, *Proc. Natl. Acad. Sci. USA.* **1992**, *89*, 5381-5383.

(5) (a) A. Litovchick, C. E. Dumelin, S. Habeshian, D. Gikunju, M. A. Guie, P. Centrella, Y. Zhang, E. A. Sigel, J. W. Cuozzo, A. D. Keefe, M. A. Clark, *Sci. Rep.* **2015***, 5,* 10916; (b) P. A. Harris, B. W. King, D. Bandyopadhyay, S. B. Berger, N. Campobasso, C. A. Capriotti, J. A. Cox,

L. Dare, X. Y. Dong, J. N. Finger, L. C. Grady, S. J. Hoffmann, J. U. Jeong, J. Kang, V. Kasparcova, A. S. Lakdawala, R. Lehr, D. E. McNulty, R. Nagilla, M. T. Ouellette, C. S. Pao, A. R. Rendina, M. C. Schaeffer, J. D. Summerfield, B. A. Swift, R. D. Totoritis, P. Ward, A. M. Zhang, D. H. Zhang, R. W. Marquis, J. Bertin, P. J. Gough, *J. Med. Chem.* **2016,** *59*, 2163-2178; (c) A. Mullard, *Nature* **2016,** *530*, 367-369.

(6) P. Dickson, T. Kodadek, *Org. Biomol. Chem.* **2019,** *17*, 4676-4688.

(7) J. Ottl, L. Leder, J. V. Schaefer, C. E. Dumelin, *Molecules* **2019,** *24*, 1629.

(8) For selected examples on DEL library design, see: (a) F. Buller, L. Mannocci, J. Scheuermann, D. Neri, *Bioconjugate Chem.* **2010,** *21*, 1571-1580; (b) R. E. Kleiner, C. E. Dumelin, D. R. Liu, *Chem. Soc. Rev.* **2011,** *40*, 5707-5717.

(9) For a selected example on medicinal candidates identified through DEL screening, see: J. P. Maianti, A. McFedries, Z. H. Foda, R. E. Kleiner, X. Q. Du, M. A. Leissring, W. J. Tang, M. J. Charron, M. A. Seeliger, A. Saghatelian, D. R. Liu, *Nature* **2014,** *511*, 94-98.

(10) (a) M. L. Malone, B. M. Paegel, *ACS Comb. Sci.* **2016,** *18*, 182-187; (b) A. L. Satz, J. P. Cai, Y. Chen, R. Goodnow, F. Gruber, A. Kowalczyk, A. Petersen, G. Naderi-Oboodi, L. Orzechowski, Q. Strebel, *Bioconjugate Chem.* **2015,** *26*, 1623-1632.

(11) D. T. Flood, S. Asai, X. J. Zhang, J. Wang, L. Yoon, Z. C. Adams, B. C. Dillingham, B. B. Sanchez, J. C. Vantourout, M. E. Flanagan, D. W. Piotrowsld, P. Richardson, S. A. Green, R. A. Shenvi, J. S. Chen, P. S. Baran, P. E. Dawson, *J. Am. Chem. Soc.* **2019,** *141*, 9998-10006.

(12) G. X. Zhao, Y. R. Huang, Y. Zhou, Y. Z. Li, X. Y. Li, *Expert Opin. Drug Dis.* **2019,** *14*, 735-753.

(13) Z. L. Duan, W. Li, A. W. Lei, *Org. Lett.* **2016,** *18*, 4012-4015.

(14) C. Remeur, C. B. Kelly, N. R. Patel, G. A. Molander, *ACS Catal.* **2017,** *7*, 6065-6069.

(15) (a) J. C. Tellis, D. N. Primer, G. A. Molander, *Science* **2014,** *345*, 433-436; (b) J. A. Milligan, J. P. Phelan, S. O. Badir, G. A. Molander, *Angew. Chem. Int. Ed.* **2019,** *58*, 6152-6163; (c) J. Twilton, C. Le, P. Zhang, M. H. Shaw, R. W. Evans, D. W. C. MacMillan, *Nat. Rev. Chem.* **2017,** *1*, 0052.

(16) D. G. Brown, J. Bostrom, *J. Med. Chem.* **2016,** *59*, 4443-4458.

(17) N. Schneider, D. M. Lowe, R. A. Sayle, M. A. Tarselli, G. A. Landrum, *J. Med. Chem.* **2016,** *59*, 4385-4402.

(18) J. P. Phelan, S. B. Lang, J. Sim, S. Berritt, A. J. Peat, K. Billings, L. J. Fan, G. A. Molander, *J. Am. Chem. Soc.* **2019,** *141*, 3723-3732.

(19) D. K. Kolmel, J. Meng, M. H. Tsai, J. M. Que, R. P. Loach, T. Knauber, J. Q. Wan, M. E. Flanagan, *ACS Comb. Sci.* **2019,** *21*, 588-597.

(20) D. A. Everson, D. J. Weix, *J. Org. Chem.* **2014,** *79*, 4793-4798.

(21) D. Mal, A. K. Jana, P. Mitra, K. Ghosh, *J. Org. Chem.* **2011,** *76*, 3392-3398.

(22) C. J. Gerry, M. J. Wawer, P. A. Clemons, S. L. Schreiber, *J. Am. Chem. Soc.* **2019,** *141*, 10225-10235.

(23) Q. Qian, Z. H. Zang, S. L. Wang, Y. Chen, K. H. Lin, H. G. Gong, *Synlett* **2013,** *24*, 1164-1164.

(24) A. Cartier, E. Levernier, V. Corce, T. Fukuyama, A. L. Dhimane, C. Ollivier, I. Ryu, L. Fensterbank, *Angew. Chem. Int. Ed.* **2019,** *58*, 1789-1793.

(25) G. Duret, R. Quinlan, P. Bisseret, N. Blanchard, *Chem. Sci.* **2015,** *6*, 5366-5382.

(26) F. J. R. Klauck, M. J. James, F. Glorius, *Angew. Chem. Int. Ed.* **2017,** *56*, 12336-12339.

(27) E. H. Discekici, N. J. Treat, S. O. Poelma, K. M. Mattson, Z. M. Hudson, Y. D. Luo, C. J. Hawker, J. Read de Alaniz, *Chem. Commun.* **2015,** *51*, 11705-11708.

(28) X. J. Lu, L. J. Fan, C. B. Phelps, C. P. Davie, C. P. Donahue, *Bioconjugate Chem.* **2017,** *28*, 1625-1629.

(29) S. L. Schreiber, *Science* **2000,** *287*, 1964-1969.

(30) I. Bolea, J. Juarez-Jimenez, C. de los Rios, M. Chioua, R. Pouplana, F. J. Luque, M. Unzeta, J. Marco-Contelles, A. Samadi, *J. Med. Chem.* **2011,** *54*, 8251-8270.

(31) N. Kato, E. Comer, T. Sakata-Kato, A. Sharma, M. Sharma, M. Maetani, J. Bastien, N. M. Brancucci, J. A. Bittker, V. Corey, D. Clarke, E. R. Derbyshire, G. L. Dornan, S. Duffy, S. Eckley, M. A. Itoe, K. M. J. Koolen, T. A. Lewis, P. S. Lui, A. K. Lukens, E. Lund, S. March, E. Meibalan, B. C. Meier, J. A. McPhail, B. Mitasev, E. L. Moss, M. Sayes, Y. Van Gessel, M. J. Wawer, T. Yoshinaga, A. M. Zeeman, V. M. Avery, S. N. Bhatia, J. E. Burke, F. Catteruccia, J. C. Clardy, P. A. Clemons, K. J. Dechering, J. R. Duvall, M. A. Foley, F. Gusovsky, C. H. M. Kocken, M. Marti, M. L. Morningstar, B. Munoz, D. E. Neafsey, A. Sharma, E. A. Winzeler, D. F. Wirth, C. A. Scherer, S. L. Schreiber, *Nature* **2016,** *538*, 344-349.

(32) C. J. Gerry, M. J. Wawer, P. A. Clemons, S. L. Schreiber, *J. Am. Chem. Soc.* **2019,** *141*, 10225-10235.

(33) Z. Y. Cao, T. Ghosh, P. Melchiorre, *Nat. Commun.* **2018,** *9*, 3274.

(34) G. Magueur, B. Crousse, M. Ourevitch, D. Bonnet-Delpon, J. P. Begue, *J. Fluorine Chem.* **2006,** *127*, 637-642.

(35) (a) T. B. Xiao, L. Y. Li, L. Zhou, *J. Org. Chem.* **2016,** *81*, 7908-7916; (b) S. B. Lang, R. J. Wiles, C. B. Kelly, G. A. Molander, *Angew. Chem. Int. Ed.* **2017,** *56*, 15073-15077.

(36) Á. Gutiérrez-Bonet, J. C. Tellis, J. K. Matsui, B. A. Vara, G. A. Molander, *ACS Catal.* **2016**, *6*, 8004-8008.

(37) C. B. Kelly, N. R. Patel, D. N. Primer, M. Jouffroy, J. C. Tellis, G. A. Molander, *Nat. Protoc.* **2017**, *12*, 472-492.

(38) N. P. Patel, C. B. Kelly, A. P. Siegenfeld, G. A. Molander, *ACS Catal.* **2017**, *7*, 1766-1770.

Author Contributions: Shorouk O. Badir conceived the topic, optimized the reaction conditions, and performed experiments. DNA compatibility studies were performed at GlaxoSmithKline. All authors contributed to the experimental work and discussion of results. Shorouk O. Badir wrote the original draft of the manuscript with input from Professor Gary A. Molander.

Chapter 8. Photoredox-Mediated Hydroalkylation and Hydroarylation of Functionalized Olefins for DNA-Encoded Library Synthesis[***]

8.1 Introduction

DNA-encoded library (DEL) technology[1,2,3] (Chapter 1.3) features a novel interrogation format for the discovery of therapeutic candidates[4,5] in the pharmaceutical industry. The integration of aliphatic bromides and α-silylmethylamines in Ni/photoredox dual cross-coupling and radical/polar crossover manifolds provided access to diverse chemical space in DEL platforms. To be successful, on-DNA chemistries are required to incorporate building blocks (BBs) bearing multifunctional handles for further diversification under mild, dilute, and aqueous conditions.[6] In light of these considerations, the development of reliable transformations that operate through novel reactivity modes and employ commodity chemicals would expedite progress in this field. Moving forward, we sought to develop site-selective hydro*alkylation* and hydro*arylation* protocols of functionalized olefins to expand access to structural scaffolds with a high density of pendant functional groups in DELs.

As part of a program centered on the development of catalytic tools to yield novel structural scaffolds, we recently reported the synthesis of *gem*-difluoroalkenes,[7,8] carbonyl mimics that display *in vivo* resistance toward metabolic processes,[9] through photoinduced radical/polar crossover defluorinative alkylation.[7,8,10] As a complementary approach to build chemical diversity, we became interested in pushing the limits of photochemical paradigms to access benzylic trifluoromethylated compounds, bioactive structural motifs in medicinal settings (Figure

---

[***] Reproduced in part with permission from S. O. Badir, A. Lipp, M. Krumb, M. J. Cabrera-Afonso, L. M. Kammer, V. E. Wu, M. Huang, A. Csakai, L. A. Marcaurelle, G. A. Molander, *Chem. Sci.* **2021**, under revisions. This article will be licensed under a Creative Commons Attribution NonCommercial 3.0 Unported License.

8.1).[11] Specifically, fluorine incorporation is a powerful strategy invoked by the pharmaceutical and agrochemical industries to alter a molecule's chemical, physical, and biological properties, such as its pK_a, dipole moment, and molecular conformation.[12,13] As a consequence of these factors, fluorinated scaffolds are prevalent in more than 25% of marketed drugs.[11c] As an important representative, the trifluoromethyl (–CF_3) group renders increased metabolic stability, lipophilicity, and binding selectivity when embedded in therapeutic candidates.[11,14] Typically, the trifluoromethyl group can be installed through nucleophilic, electrophilic, or radical routes.[15] Although these strategies undoubtedly expand chemical space, these protocols remain elusive in the context of late-stage functionalization and the incorporation of sensitive functional groups in complex environments under DEL-like conditions.

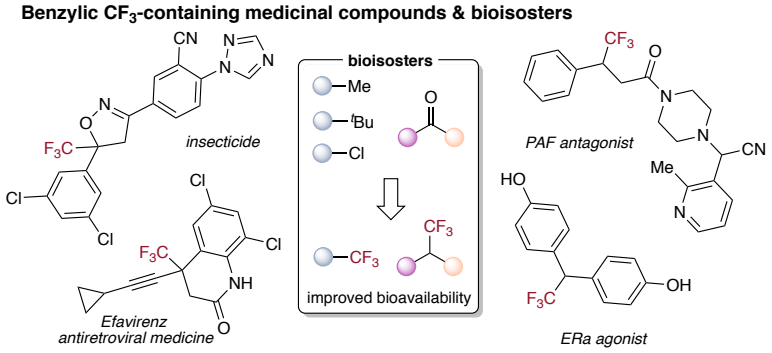

Figure 8.1. The trifluoromethyl group in medicinal chemistry.

An underexplored opportunity to achieve Csp^3 trifluoromethylation is the direct *hydroalkylation* of trifluoromethyl-substituted olefins (Figure 8.2). Specifically, the carbofunctionalization of these electrophilic unsaturated systems occurs readily at room temperature with exquisite functional group compatibility,[16] thus rendering the incorporation of pharmaceutically relevant cores and complex alkyl fragments feasible in a library setting. However, given the established propensity of trifluoromethyl-substituted alkenes to undergo

intramolecular E1cB-type fluoride elimination in metal-catalyzed cross-couplings that proceed through the intermediacy of α-CF_3-metal species,[17] via the nucleophilic addition of organometallic reagents[18,19] or in the presence of traditional photoredox catalysts irrespective of the nature of the radical precursor (Figure 8.2),[16,19a,20] hydrofunctionalization[21] efforts remain challenging. In particular, the *hydroalkylation* of trifluoromethyl-substituted alkenes using *unactivated alkyl* counterparts presents a formidable, yet potentially powerful scenario to access unprecedented benzylic trifluoromethylated building blocks rapidly from commodity radical progenitors with a high content of C(sp^3) carbons.

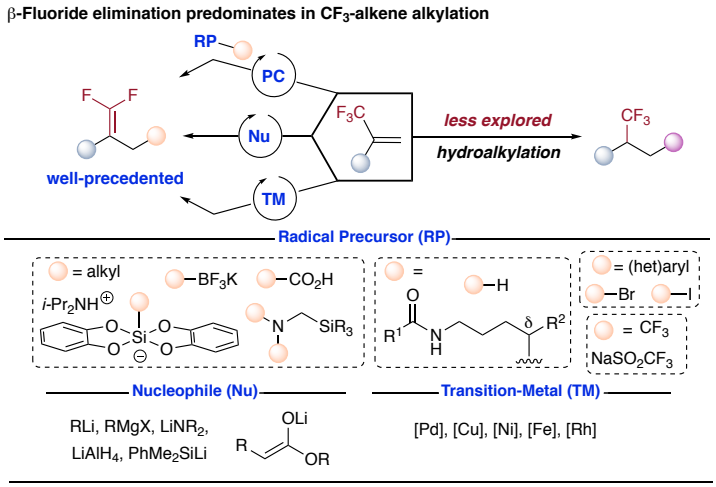

Figure 8.2. Carbofunctionalization strategies of trifluoromethyl-substituted alkenes.

To address this challenge and unlock access to benzylic trifluoromethylated motifs from commodity chemicals in DEL synthesis, we report a decarboxylative-based, radical-mediated hydroalkylation of DNA-tagged trifluoromethyl-substituted alkenes enabled by the merger of electron donor-acceptor (EDA) complex photoactivation[22] and hydrogen atom transfer (HAT, Figure 8.3).[23] Under blue light irradiation, a commercially available electron donor, Hantzsch ester (HE, diethyl 1,4-dihydro-2,6-dimethyl-3,5-pyridinedicarboxylate), functions as a strong

photoreductant to induce C(sp^3) radical generation from commercially available carboxylic acid derivatives.[24] As part of its dual role, HE subsequently serves as a suitable hydrogen atom donor, impeding the formation of anionic intermediates upon radical addition as well as circumventing the necessity for alkylmetal complexes, species intrinsically primed to undergo β-F elimination in reactions with trifluoromethyl-substituted alkenes.[17e,20a,20b,25] In this vein, the utility of this EDA paradigm is partially driven by its ability to deliver complex, trifluoromethyl-substituted, hydrofunctionalized products with high C(sp^3) carbon counts selectively under mild and open-air conditions.

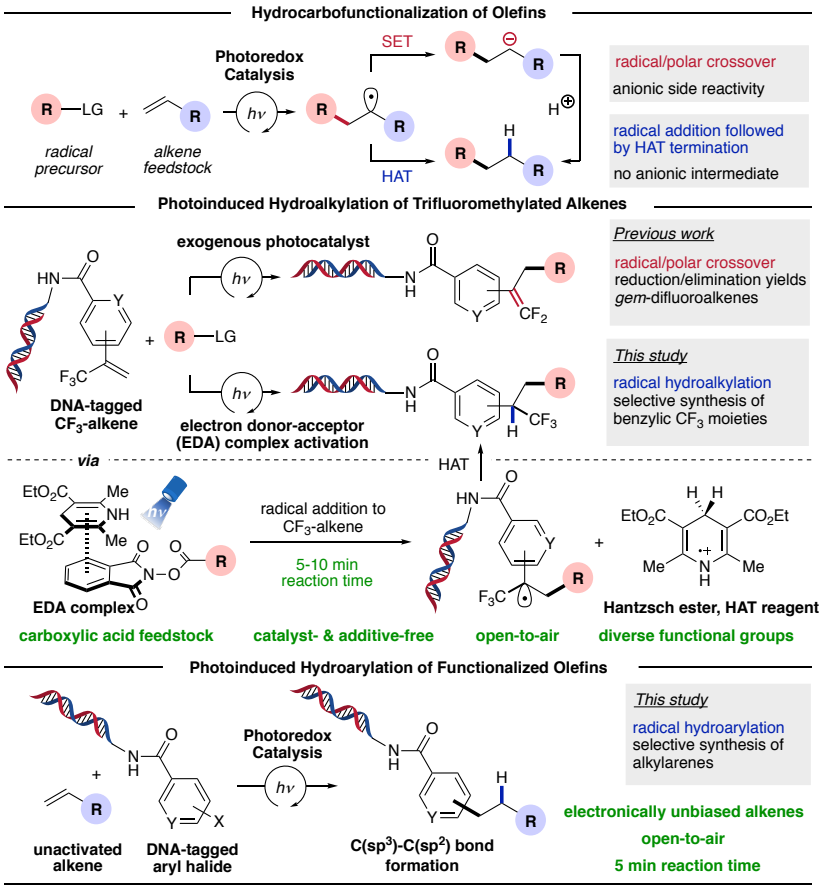

Figure 8.3. Photoredox-mediated hydrocarbofunctionalization of olefins on DNA and design consideration.

As a complement to the hydro*alkylation* protocol, a radical-mediated intermolecular hydro*arylation* of electronically unbiased olefins was developed (Figure 8.3).[26] Because alkenes are plentiful and versatile commodity feedstocks, readily available from petrochemical and renewable resources, they are ideal precursors for C–C bond formation in DELs, and the strategy developed is based on photoinduced reductive activation of DNA-conjugated (hetero)aryl halides to deliver reactive (het)aryl radical species that can be harnessed in useful synthetic operations followed by hydrogen atom termination.[23]

8.2 Results and Discussion

Recently, synthetic processes driven by EDA complex photochemistry have gained considerable traction, including protocols resulting in borylation, sulfonylation, and thioetherification.[22,27] To harness the synthetic potential of EDA complex photoactivation toward DEL platforms, we examined the feasibility of the proposed decarboxylative hydroalkylation using on-DNA trifluoromethyl-substituted alkene **1A** and unactivated primary redox-active ester (RAE) **2a** as model substrates (Figure 8.4). Under blue Kessil irradiation (λ_{max} = 456 nm), efficient conversion to the desired benzylic trifluoromethyl-substituted product **3a** was observed using 50 equivalents of the radical precursor under ambient reaction conditions within minutes of illumination. In contrast to radical-mediated alkylation promoted by metal reductants[17e,28] or external photoredox catalysts,[29] this open-to-air EDA paradigm provides an exceedingly low barrier to practical implementation in high-throughput settings and circumvents side reactivity stemming from singlet oxygen generation through triplet-energy transfer.[29]

To examine the influence of the dihydropyridine (DHP) backbone on the efficacy of this photochemical manifold, the reaction was conducted with four different DHP derivatives to gain a deeper understanding of their dual reactivity profile in EDA complex photoactivation and HAT

catalysis (Figure 8.4). The C4-substituted DHP (HE **A**, entry 7) thus exhibited no reactivity under the reaction conditions, whereas cyano substitution at C3 and C5 of the DHP (HE **B**, entry 8) led to diminished product formation.

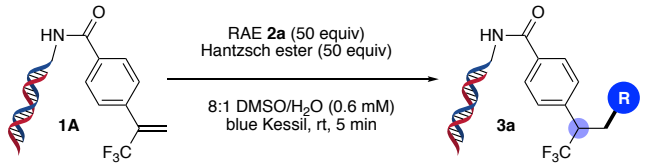

Entry	Deviation from std conditions	3a (% Conv)[a]
1	**none**	**84**
2	RAE (25 equiv), HE (25 equiv)	65
3	RAE (10 equiv), HE (10 equiv)	55
4	0.5 mM	84
5	0.4 mM	80
6	0.3 mM	77
7	HE **A**	0
8	HE **B**	20
9	HE **C**	0
10	no HE	traces
11	no light	traces

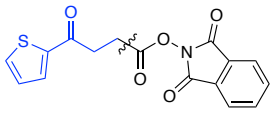

2a, *unactivated primary alkyl feedstock*

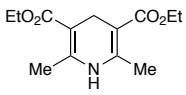

Hantzsch ester (HE)

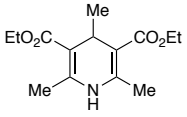

HE **A**

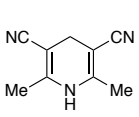

HE **B**

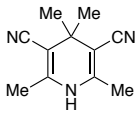

HE **C**

Figure 8.4. Optimization studies. Reaction conditions: RAE **2a** (50 equiv, 1.25 μmol), HE (50 equiv, 1.25 μmol), on-DNA trifluoromethyl-substituted alkene **1A** (1.0 equiv, 25 nmol), 8:1 DMSO/H_2O (0.6 mM), 5 min irradiation with blue Kessil lamps (λ_{max} = 456 nm, 40 W). [a]Conversion to **3a** as determined by LC/MS analysis.

As expected, 4,4'-dimethyl HE **C** (entry 9) failed to promote the reaction, presumably because of competitive back electron transfer (BET)[22a] that restores the ground-state EDA

complex from its radical ion pair in the absence of a probable photooxidative aromatization event. Notably, commercially available and bench-stable HE[30] displayed optimal performance (84% yield, entry 1), accommodating aqueous media and high dilution factors (0.3-0.6 mM), with only trace amounts of the corresponding *gem*-difluoroalkene detected. Using UV/vis absorption studies, a bathochromic shift of the reaction mixture in 8:1 DMSO/H_2O (0.6 mM) was observed, with a wavelength band tailing to 500 nm (see the Experimental Section). This is indicative of the formation of a new molecular aggregate between the electron-deficient aliphatic RAEs and the electron-rich HE. Using Job's method[31] of continuous variation, we determined a molar donor-acceptor ratio of 1:1 for the colored EDA complex (see the Experimental Section). Further spectrophotometric analysis at 450 nm revealed an association constant (K_{EDA}) of 1.2 M^{-1} of HE with 1-methylcyclohexane-*N*-hydroxyphthalimide ester using the Benesi–Hildebrand method,[32] highlighting a plausible association event of charge-transfer complexes prior to SET events. Finally, control experiments validated the necessity of all reaction parameters for effective $C(sp^3)$–$C(sp^3)$ bond formation.

Next, we examined the scope of redox-active carboxylate derivatives using on-DNA trifluoromethylated alkene **1A** (Figure 8.5). In general, a broad palette of primary aliphatic systems that lack any radical stabilizing factors exhibited excellent reactivity. The method further benefits from broad functional group tolerance, facilitating the introduction of bifunctional handles including ketones (**3a**, **3f**, **3q**), aryl halides (**3c**, **3e**, **3n**), a terminal alkyne (**3d**), esters (**3j**, **3o**), substituted alkenes (**3k**, **3l**, **3m**, **3o**), free alcohols (**3o**, **3p**), as well as medicinally-relevant heteroaromatic scaffolds (**3a**, **3n**). In addition, Boc- and Fmoc-protected amines served as competent substrates. This is crucial in DEL settings, where library members should ideally bear multifunctional BBs that allow subsequent derivatization. The scope was further extended to the modification of biologically active molecules displaying a high density of pendant functional

groups, including the herbicide 2,4-dichlorophenylacetic acid (**3e**), long-chain fatty acids (**3k**–**3m**), the anti-inflammatory agent indomethacin (**3n**), mycophenolic acid (**3o**), as well as various steroids (**3p**, **3q**).

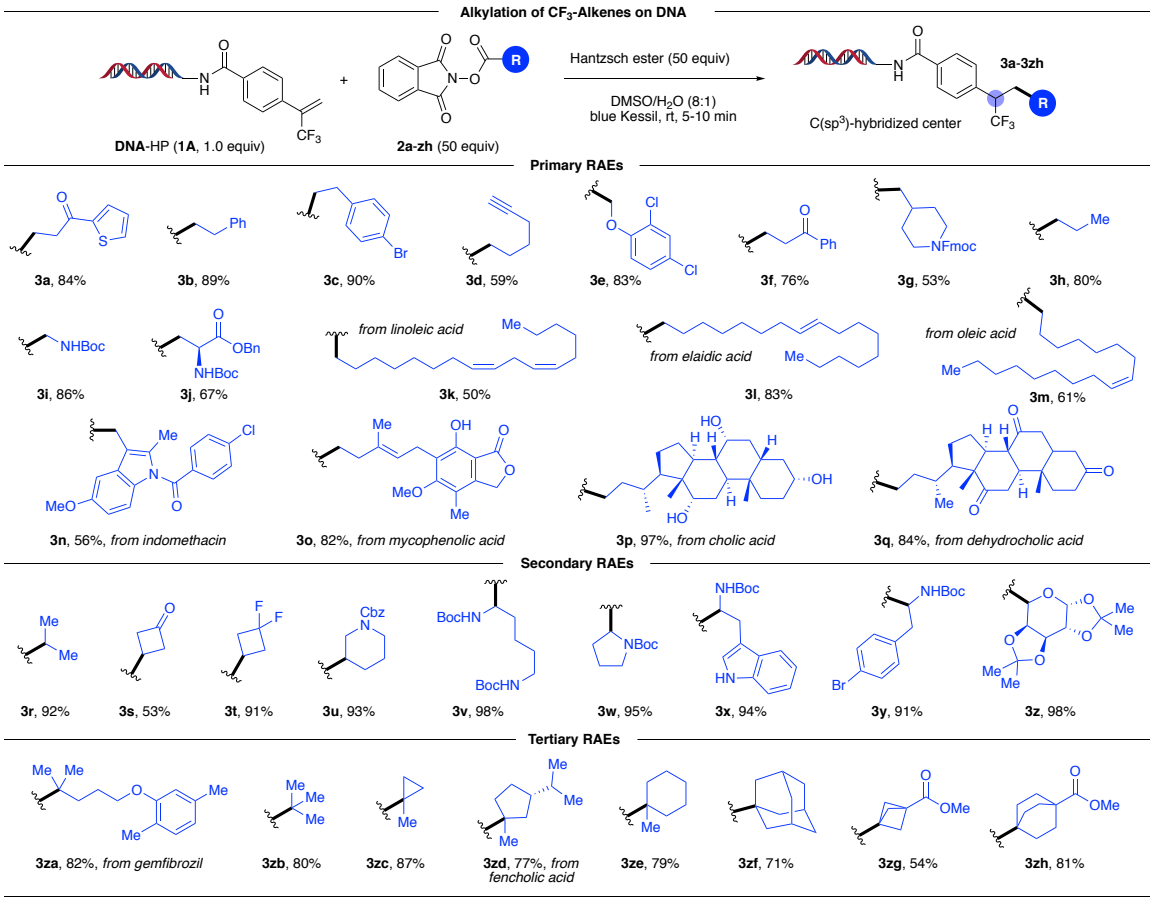

Figure 8.5. On-DNA photoinduced decarboxylative alkylation: Evaluation of aliphatic carboxylic acid derivatives.

In particular, this method provides a clear advantage in terms of scope over previously reported on-DNA photoinduced decarboxylative alkylation protocols, which are largely limited to α-heteroatom-stabilized radicals.[7,33] or exclusively restricted to secondary and tertiary radicals.[34,35] More specifically, complementary decarboxylative methods employing zinc

nanopowder as a reductant under strictly deoxygenated conditions fail to incorporate primary systems on DNA,[28] presumably because of the higher reduction potentials associated with the radical precursor. Most importantly, these methods largely proceed through anionic intermediates, where in the case of the trifluoromethyl-substituted olefins, there is a predominant propensity for intramolecular E1cB-type fluoride elimination[16a,19a,20] to afford the corresponding *gem*-difluoroalkenes via radical/polar crossover pathways[10] (rather than trifluoromethyl-substituted alkanes).

In a similar manner, secondary and tertiary radical architectures are harnessed effectively to afford functionalized synthetic frameworks (Figure 8.5), including scaffolds derived from proteinogenic and non-proteinogenic amino acids (**3u**–**3y**), a glycoside (**3z**), and lipid lowering agent gemfibrozil (**3za**). The reaction conditions proved general for both acyclic and cyclic carboxylate derivatives, including bridged bicyclics (**3zf – 3zh**), as well as strained ring systems, such as cyclobutanes (**3s**, **3t**) and a cyclopropane (**3zc**). Notably, trifluoromethyl-substituted bicyclo[1.1.1]pentane (BCP) product **3zg** was obtained in good yield. These BCP derivatives serve as bioisosteres for arenes, internal alkynes, and *tert*-butyl groups in medicinal chemistry settings.[36]

With respect to the scope of trifluoromethyl-substituted alkenes, a diverse array of DNA headpieces (DNA-HPs) led to the desired benzylic trifluoromethyl-substituted products without compromising yields (Figure 8.6). In general, both electron-withdrawing and electron-donating groups are well tolerated under the developed conditions. Substitution at the *para*-, *meta*-, and *ortho*-positions of the HPs' aryl moieties was explored, whereby efficient decarboxylative photocoupling took place. Furthermore, comparable reactivity was observed for unactivated

primary, secondary, tertiary, as well as stabilized benzylic-, α-oxy-, and α-amino radical species, further underscoring the versatility of this photochemical EDA paradigm.

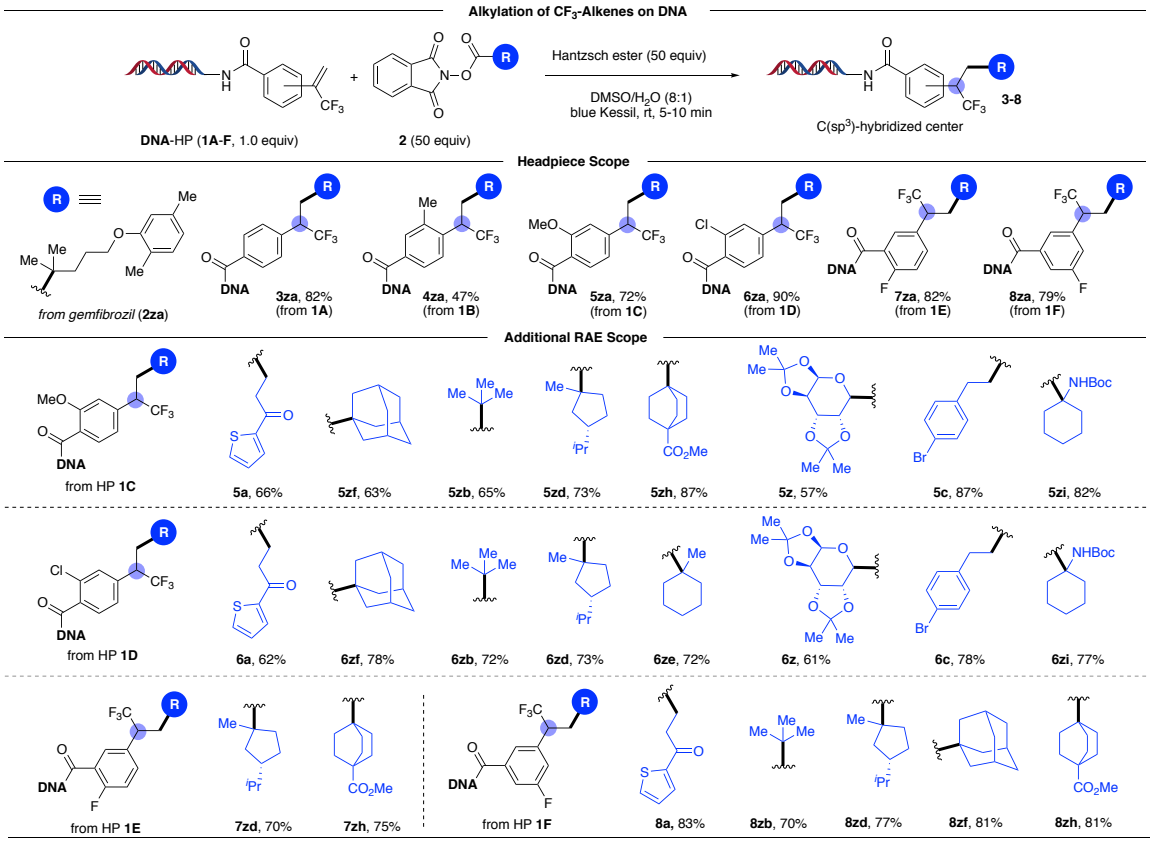

Figure 8.6. On-DNA photoinduced decarboxylative alkylation: Evaluation of trifluoromethyl-substituted alkenes.

The commercial availability and structural diversity of carboxylic acids render them particularly attractive for use as multifunctional BBs in DEL libraries. To validate the modularity of this approach further, we developed a telescoped, one-pot photoinduced decarboxylative alkylation protocol through in situ formation of aliphatic RAEs with hexafluorophosphate *N*-hydroxyphthalimide tetramethyluronium (HITU),[28] a bench-stable solid that can be readily prepared on kilogram scale (Figure 8.7).

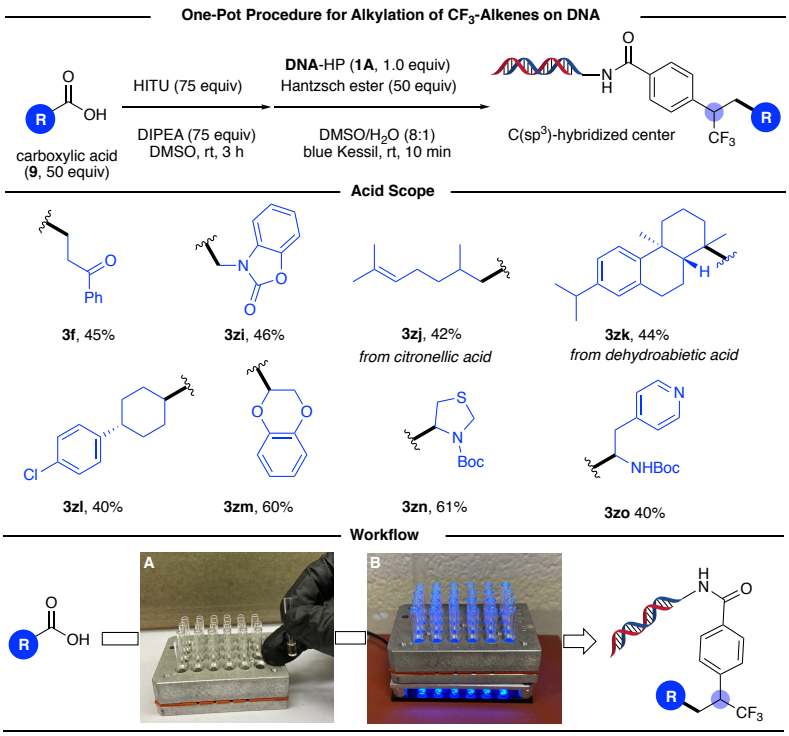

Figure 8.7. On-DNA photoinduced decarboxylative alkylation: In situ activation of RAEs with hexafluorophosphate *N*-hydroxyphthalimide tetramethyluronium (HITU).

This reagent features great versatility in reaction scope, accommodating a wide array of functional groups including ketone (**3f**), carbamate (**3zi**), aryl chloride (**3zl**), and Boc-protected amines (**3zn**, **3zo**). Using 24-well plates, microdosing of the carboxylic acid, DIPEA, and HITU in DMSO is accomplished under air, followed by 3 h of activation time. The in situ formed RAEs can then be treated directly with a solution of HE and the corresponding DNA headpiece, reaching synthetically useful yields after 10 min of illumination (Figure 8.7, Workflow). Notably, this HITU-mediated alkylation performs equally well using unactivated- and α-heteroatom-stabilized radical progenitors, presenting a direct route toward C–C bond formation through oxidative quenching modes, an underexplored challenge in DEL-based environments.[28]

As an extension of the hydroalkylation chemistry, an on-DNA multicomponent reaction (MCR) was developed. In recent years, MCRs[37] have emerged as a powerful tool to furnish novel structural scaffolds with inherent molecular complexity from abundant feedstocks. Through sequential bond formation, MCRs enable the sampling of uncharted chemical space to accelerate drug discovery efforts.[37] An underexplored realm in DEL synthesis is the development of olefin dicarbofunctionalization reactions.[2a] Specifically, alkenes serve as versatile BBs that possess functional group-rich handles for derivatization. However, in addition to chemo- and regio-selectivity concerns associated with DEL reactions that rely on high loadings of reagents, these processes are further complicated by the generation of undesired two-component coupling products. Keeping these considerations in mind and taking advantage of the electronically distinct nature of trifluoromethyl-substituted alkenes, a polarity-reversing radical cascade/trifluoromethylation of olefins has been developed through EDA complex photoactivation between HE and Umemoto's reagent,[22a] a commercially available trifluoromethylating agent (Figure 8.8).

In particular, this open-to-air charge-transfer paradigm harnesses electrophilic trifluoromethyl radicals for subsequent addition to electron-neutral or electron-rich alkenes, abundant yet currently underexplored partners in photoinduced DEL synthesis.[3a,38] The resulting nucleophilic, open-shell radical intermediates may then engage in chemoselective coupling with on-DNA trifluoromethyl-substituted alkenes. As part of its dual role, the HE also functions as a hydrogen atom donor to furnish bis-trifluoromethylated products of significance in medicinal settings.[11] Remarkably, the scope of the olefin partner proved general, tolerating diverse functional groups including a free alcohol (**10a**) and unprotected glycoside **10d**. In this vein, we anticipate this mode of catalysis will help inform the design and implementation of unique synthetic disconnections toward complex, bioactive targets in DELs.

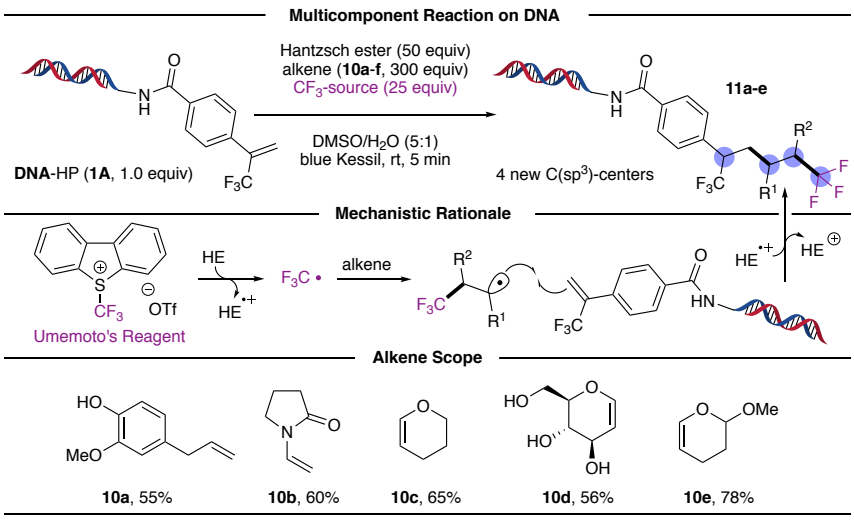

Figure 8.8. On-DNA multicomponent trifluoromethylation promoted by photoactive EDA complex activation.

Having developed suitable conditions for the hydro*alkylation* of unsaturated DEL platforms, attention was turned toward hydro*arylation* transformations. Recently, research efforts have validated Ni/photoredox dual manifolds in DEL platforms using carboxylic acids,[7,33b,33e] 1,4-dihydropyridines (DHPs),[7] α-silylmethylamines,[8] and alkyl bromides[8,39] as radical precursors. Given our long-standing interest in the design of complex (hetero)aryl scaffolds with high C(sp^3) carbon counts,[40] we sought to expand reactivity in DEL synthesis through intermolecular radical-mediated hydroarylation of functionalized olefins to generate alkylarenes (Figure 8.9). To develop a complementary approach toward C(sp^3)–C(sp^2) bond formation, we reasoned that single-electron reduction of DNA-bound, halogenated aryl subunits[26] would grant access to reactive (het)aryl radical species in a regioselective fashion. Subsequent addition to alkenes followed by hydrogen atom termination would deliver unprecedented structures from commodity chemicals. Inspired by pioneering work by Beckwith[41] and related, precedented milestones,[26] we hypothesized that photoinduced electron transfer from highly reducing transition-metal-based

complexes would enable this strategy under mild reaction conditions. However, because of the high redox potentials associated with aryl halides and the propensity of aryl radicals to undergo reduction through rapid HAT,[26a] the adaptation of this mechanistic proposal in DEL environments posed challenges. Importantly, aryl radicals have been shown to induce DNA strand damage,[42] underscoring the requirement for a regulated generation of these high-energy intermediates and the necessity for well-orchestrated addition reactions. To achieve chemo- and regio-selectivity, the following criteria was considered: (i) the rate of (het)aryl radical addition to unsaturated systems must be competitive with C–X bond reduction stemming from undesired HAT pathways. (ii) The rate of hydrogen atom abstraction by the resulting alkyl radical must be competitive with its addition to another equivalent of the alkene. (iii) The rate of single-electron reduction of the aryl halide should take place preferentially over that of the alkyl radical intermediate. Specifically, the choices of both photocatalyst and hydrogen atom donor influences product distributions. We determined that 300 equiv of the olefinic substrate and a 1:200 photocatalyst-to-HAT reagent ratio was optimal for reactivity. Toward this end, the combination of *fac*-Ir(ppy)$_3$ and HE enabled the construction of alkylated arenes under air within minutes of blue light irradiation. Control experiments demonstrated that all reaction components are necessary for aryl radical generation.

With optimized conditions established, we surveyed DNA-tagged (het)aryl halides with norbornene as the alkyl source (Figure 8.9). Aryl iodide **12A** bearing a chloride substituent afforded the desired product with the electrophilic cross-coupling handle intact, delivering linchpins for further functionalization. Electron-neutral iodobenzene **12B** as well as derivatives bearing electron-donating groups (**12C**) or electron-withdrawing groups (**12G**) served as excellent substrates. Further extension to less activated aryl bromides was also possible (**12D**).

Notably, electrophilic pyridyl radicals were employed as coupling partners, giving rise to functionalized heteroaromatics (**18a**, **18j**–**18n**).

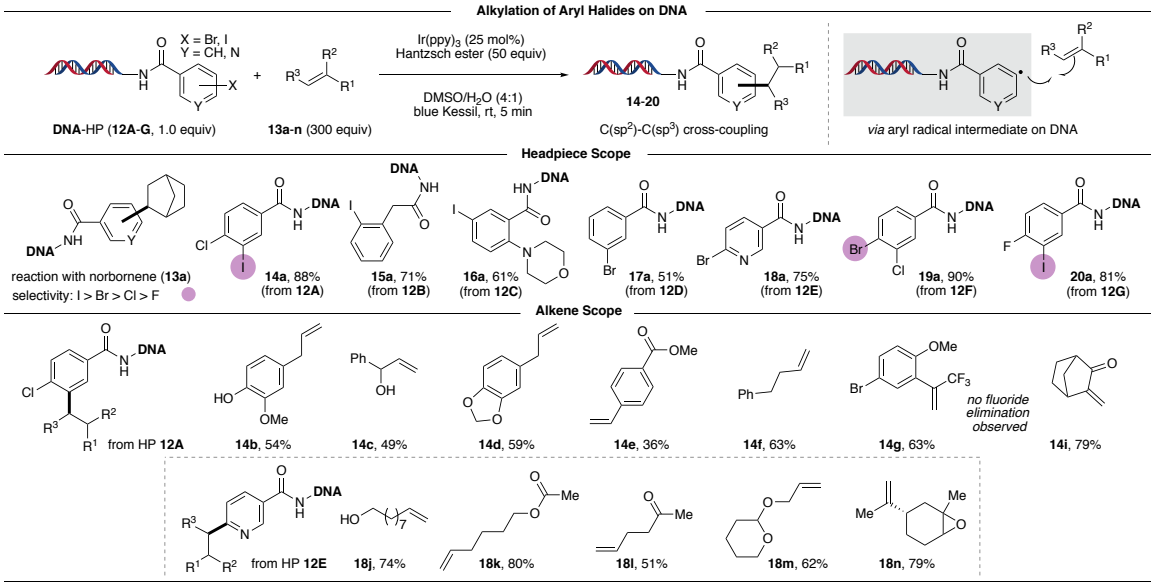

Figure 8.9. Employing alkene BBs for $C(sp^3)$–$C(sp^2)$ bond formation in DEL synthesis: Evaluation of olefins and aryl halides.

Finally, in addition to the strained bicyclic norbornene, a broad array of functionalized alkenes was examined (Figure 8.9). In general, unactivated alkenes bearing unprotected alcohols (**14b**, **14c**, **18j**), an ester (**18k**), a heteroaromatic core (**14h**), ketones (**14i**, **18l**), and an epoxide (**18n**) were all accommodated. In addition, this photochemical paradigm was extended to the modification of activated styrene derivatives (**14e**, **14g**) in synthetically useful yields. Even benzylic trifluoromethylated product **14g** could be used as a substrate to afford product with complete retention of the bromide handle, presumably because of the high loading of alkene precursor compared to the photoredox catalyst, precluding an overreduction event of the halide. From the standpoint of DEL synthesis, which benefits from minimal reagent input (e.g., 25 nmol of HP per transformation), such equivalencies can be leveraged to achieve selectivity and unique

reactivity trends that are otherwise untenable in traditional small molecule synthesis. In particular, these halogenated alkenes can further grow DEL libraries through transition-metal-catalyzed cross-coupling efforts.

DNA Compatibility with EDA Complex Photoactivation. Because the integrity of the DNA barcode is essential to a successful protein target selection, mock ligations and qPCR amplifications were performed to evaluate the ability of the RAE hydroalkylation conditions to be used in an actual library production. A representative headpiece bearing a 4-cycle tag was subjected to the standard hydroalkylation conditions. This same headpiece was also subjected to control reactions where either Hantzsch ester or light was omitted. All of the headpieces were ligated to satisfactory completion, and further, were analyzed via qPCR. There was no significant difference in qPCR amplification across the various experiments, suggesting full DNA integrity (see the Experimental Section). These findings further underscore the utility of EDA paradigms as a general blueprint toward selective on-DNA alkylation under open-to-air conditions.

DNA Compatibility with Aryl Radical Intermediates. Mindful of well-established precedent of DNA strand damage in the presence of reactive aryl radical species,[42] the hydroarylation conditions were studied to evaluate the resulting DNA integrity. Again, a headpiece bearing a 4-cycle tag was reacted using the standard conditions. The same headpiece was subjected to control reactions where either Hantzsch ester, photocatalyst, or light was omitted. All of the headpieces were ligated to satisfactory completion, and further, were analyzed via qPCR. There was no significant difference in qPCR amplification across the various experiments, suggesting full DNA integrity (see the Experimental Section). These results emphasize the mild nature of the developed photoredox paradigm, whereby the formation of

reactive aryl radical intermediates in a regulated fashion facilitates productive on-DNA alkylation.

8.3 Conclusion

In summary, this study demonstrates the first proof-of-concept for the implementation of charge-transfer complex activation as an enabling technology to introduce diverse C(sp^3)-hybridized architectures from commodity chemicals in DEL platforms (including unactivated primary, secondary, tertiary, as well as stabilized benzylic, α-alkoxy, and α-amino systems). Specifically, this EDA paradigm was utilized to achieve the selective decarboxylative-based *hydroalkylation* of trifluoromethyl-substituted alkenes through radical/HAT crossover to access complex benzylic trifluoromethylated scaffolds, unlocking a complementary reactivity outcome to established carbodefluorinative protocols mediated by an external photoredox catalyst. Furthermore, a general intermolecular hydro*arylation* protocol of electronically unbiased olefins through selective C–X bond activation in DNA-tagged aryl halides is reported. Remarkably, this photochemical paradigm delivers reactive (hetero)aryl radical species in a regulated fashion without compromising the DNA integrity. Notably, these open-to-air processes are chemoselective, operate under mild and dilute reaction conditions, and are completed within minutes, rendering them suitable for late-stage functionalization and high-throughput settings in the pharmaceutical industry. We anticipate these findings will expedite drug discovery research and provoke further development in radical-mediated DEL synthesis.

8.4 Experimental

General Consideration

General: All chemical transformations requiring inert atmospheric conditions were carried out using Schlenk line techniques with a 4- or 5-port dual-bank manifold. For blue light irradiation, two Kessil PR160-456 nm lamps (19 V DC 40W Max) were placed 1.5 inches away from PCR tubes. Reactions conducted in 24-well screening plates were irradiated using blue LED lights and performed at the Penn/Merck Center for High Throughput Experimentation at the University of Pennsylvania (plate reactors contained glass reaction vials). NMR spectra (^{1}H, ^{13}C, ^{19}F) were obtained at 298 ºK. ^{1}H NMR spectra were referenced to residual, $CHCl_3$ (δ 7.26) in $CDCl_3$. ^{13}C NMR spectra were referenced to $CDCl_3$ (δ 77.30). In the case of diastereomeric mixtures, crude NMR was recorded to determine the ratio. Reactions were monitored by LC/MS, GC/MS, ^{1}H NMR, and/or TLC on silica gel plates (60 Å porosity, 250 μm thickness). TLC analysis was performed using hexanes/EtOAc as the eluent and visualized using ninhydrin, *p*-anisaldehyde stain, and/or UV light. Flash chromatography was accomplished using an automated system (CombiFlash®, UV detector, λ = 254 nm and 280 nm) with RediSep® R_f silica gel disposable flash columns (60 Å porosity, 40–60 μm) or RediSep R_f Gold® silica gel disposable flash columns (60 Å porosity, 20–40 μm). Accurate mass measurement analyses were conducted using electron ionization (EI) or electrospray ionization (ESI). The signals were mass measured against an internal lock mass reference of perfluorotributylamine (PFTBA) for EI-GC/MS and leucine enkephalin for ESI-LC/MS. The utilized software calibrates the instruments and reports measurements by use of neutral atomic masses. The mass of the electron is not included. IR spectra were recorded on an FT-IR using either neat oil or solid products. Solvents were purified with drying cartridges through a solvent delivery system. Melting points (°C) are uncorrected.

UV/vis absorption spectra for the quantum yield reaction were recorded on a Perkin-Elmer Lambda 365 UV/vis spectrophotometer. Quartz fluorometric cells (1 cm optical path length, Starna) were used in all optical experiments.

Chemicals: Deuterated NMR solvents were purchased and stored over 4Å molecular sieves. EtOAc, hexanes, MeOH, Et_2O, and toluene were obtained from commercial suppliers and used as purchased. CH_2Cl_2 and THF were purchased and dried *via* a solvent delivery system. Anhydrous MeCN was obtained from commercial sources and stored over molecular sieves. HITU was prepared in-house according to the literature.[28] DIPEA was purchased from commercial suppliers and used without further purification. Trifluoromethyl alkene-substituted benzoic acids, used in the preparation of select on-DNA substrates, were prepared according to the literature.[7,43] Carboxylic acids and alkenes were purchased from commercial suppliers. Redox-active esters were prepared according to the literature.[44] The synthesis of all new redox-active esters is reported here. Umemoto's reagent [5-(trifluoromethyl)dibenzothiophenium trifluoromethanesulfonate], Hantzsch ester, and $Ir(ppy)_3$ were purchased from commercial suppliers and used without further manipulation. All other reagents were purchased commercially and used as received. Photoredox-catalyzed reactions were performed using PCR 8-strip tubes (Ref. Fisher 781320) with PCR strips of 8 caps (Ref. Fisher 781340). DMSO was purchased and used as received. HyPure™ Molecular Biology Grade Water was purchased and used as received without further manipulation.

Analysis of "on-DNA" reactions: Analysis of on-DNA reactions was performed by LC/MS. Upon reaction completion, an aliquot of the reaction mixture was diluted with H_2O to approximately 0.05–0.13 mM. At this point, 5 or 8 μL aliquots of the LC/MS sample was injected onto reverse-phase chromatography columns (for analysis performed at GSK: Clarity 2.6um

Oligo-MS 100A 2.1x50mm; for analysis performed at UPenn: Cortecs T3 2.7 μm, 2.1x30 mm, Waters) and eluted (10-90% B over 4 min at 0.5 mL/min flow rate; solvent A: 0.75% v/v/ HFIP / 0.038% TEA / 5 μM EDTA in H_2O; solvent B: 0.75% HFIP, 0.038% TEA, 5 μM EDTA in 90/10 MeOH/deionized H_2O) with monitoring at UV 254 nm (UPenn) and no UV monitoring (GSK). Effluent was analyzed on a Waters SQ Detector 2 ACQUITY UPLC System in negative ion mode (UPenn) or a Thermo Exactive Plus LC-esiMS with a Vanquish uHPLC (GSK). For the functionalized headpiece samples (the on-DNA aryl halides/alkenes), % conversion was determined based on reported peak intensities following deconvolution (between 3,000-10,000 Da) of the DNA charge states using Intact Mass™ by Protein Metrics Inc. (version 3.7-32x64). For the photoredox scope reactions, % conversion was determined using Intact Mass™ by Protein Metrics Inc. (version 3.7-32x64) (GSK) or using MassLynx at UPenn. Data was scanned between 0.3-2.2 min and deconvoluted between 4,000-6,000 Da, with a mass tolerance window of 2 Da, with 5% of base peak threshold was set for reporting (GSK). Alternativly, data was scanned between 1.0-3.0 min and deconvoluted between 3,000-8,000 Da, with a mass tolerance window of 1 Da, with 10% of base peak threshold was set for reporting (UPenn). Na, K, NH_4, and HFIP adducts were included in the product percentage. Detailed parameters can be found later in the Supporting Information.

Materials for "on-DNA" synthesis: DNA headpiece HP-NH_2(5'-/5Phos/GAGTCA/iSp9/iUniAmM/iSp9/TGACTCCC-3') was obtained from Biosearch Technologies, Novato, CA. The spacer-elongated AOP-Headpiece (Figure 8.10) was prepared via HATU coupling following the general procedure described later in this document with 5 equiv each of Fmoc-15-amino-4,7,10,13-tetraoxapentadecanoic acid (Fmoc-AOP), *i*-Pr_2NEt, and HATU. The lyophilized product of this reaction was then deprotected by exposure to a 10% piperidine in H_2O solution. After the reaction was deemed complete by LC/MS analysis, the

reaction was precipitated following the EtOH protocol and is typically pure enough to be used without further purification.

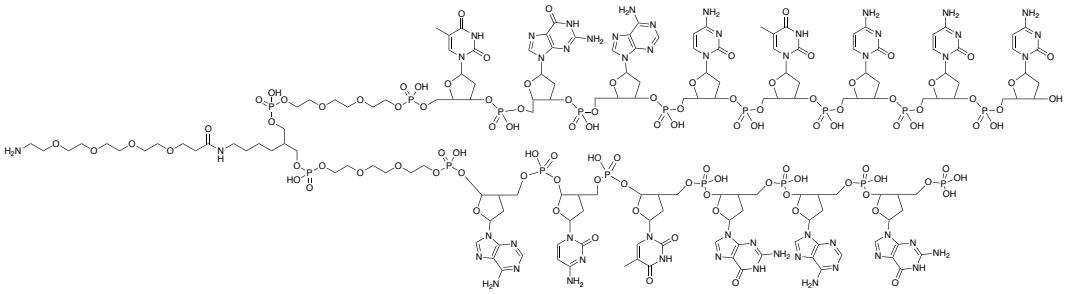

Figure 8.10. Sequence and structure of the AOP-Headpiece (molecular weight = 5184.5220).

General Procedures

Preparation of on-DNA substrates (General Procedure 1, GP1)

C) HATU premix protocol for acylation of DNA headpieces. The HATU (200 mM in DMA, 40.0 equiv), *i*-Pr_2NEt (200 mM in DMA, 40.0 equiv), and the corresponding carboxylic acid (200 mM in DMA, 40.0 equiv) solns were individually cooled at 4 ºC for 5 min. Once chilled, the acid, *i*-Pr_2NEt, and HATU solns were added sequentially to a centrifuge tube, vortexed briefly, and allowed to react at 4 ºC for 20 min. The oligomer soln (1 mM in 250 mM pH 9.4 sodium borate buffer) was then added, and the mixture was vortexed. The reaction was allowed to proceed at rt and monitored by LC/MS. Upon completion, the reaction was worked up following the EtOH precipitation protocol below.

D) EtOH precipitation protocol. The reaction mixture was transferred to a centrifuge tube where it filled at most 1/4 of the total volume. A volume of 5 M aq NaCl equal to 1/10 of the reaction volume was then added, followed by cold (–20 ºC) EtOH equal to 2.5 reaction volumes. The resulting mixture was then left to stand in a –80 ºC freezer for at least 1 h or

overnight. The chilled mixture was then centrifuged for 30 min at 4 ºC at 3,300 rpm. The supernatant was then decanted and allowed to dry under reduced pressure. The resulting pellet was re-dissolved in H_2O to give a theoretical concentration of 2 or 5 mM. Purity was assessed by LC/MS, and optical density was obtained via NanoDrop. For long term storage, solutions were frozen in liquid nitrogen and lyophilized to dryness to give a white solid. If purity was less than 90% by LC/MS, HPLC purification was performed: gradient of 95% A (50 mM TEAA, pH = 7.5) / 5% B (1% H_2O in CH_3CN) to 60% A / 40% B, through a Gemini C18 (5 μm, 110 Å, 30x100 mm), with UV visualization at 260 nm.

Synthesis of redox-active esters (General Procedure 2, GP2): To a round-bottom flask equipped with a stir bar was added the corresponding carboxylic acid (if solid) (1.0 equiv), *N*-hydroxyphthalimide (1.0 equiv), and DMAP (0.1 equiv). The flask was then charged with CH_2Cl_2 (0.1 – 0.2 M). At this point, carboxylic acid (1.0 equiv) was added via syringe (if liquid). DCC (1.1 equiv) was added, and the reaction was allowed to stir at rt until full consumption of the starting material as determined by TLC. The mixture was then filtered over Celite and rinsed with additional CH_2Cl_2. The solvent was removed under reduced pressure, and the crude material was purified via flash chromatography. *Note:* some redox-active esters are prone to hydrolysis on silica gel during column chromatography and therefore should be purified as quickly as possible.

On-DNA photoinduced decarboxylative alkylation using isolated redox-active esters (General Procedure 3, GP3): To a PCR Eppendorf tube was added Hantzsch ester (10 μL of a 125 nmol/μL soln in DMSO, 1250 nmol, 50 equiv), redox-active ester (30 μL of a 41.67 nmol/μL soln in DMSO, 1250 nmol, 50 equiv), and DNA-tethered alkene (5 μL of a 5 nmol/μL soln in H_2O, 25 nmol, 1.0 equiv). The PCR tube was then capped, vortexed, and irradiated for 5 min with Kessil PR160 lamps at a distance of 1.5 inches. An aliquot of the reaction (20 μL) was then

diluted with H_2O (150 μL) and analyzed by LC/MS. If necessary, a small amount of DMSO (~ 20 μL) was added during the workup to facilitate solubility.

On-DNA photoinduced decarboxylative alkylation using redox-active esters synthesized in situ from carboxylic acids (General Procedure 4, GP4)

A) Step 1. To a 24-well plate containing glass reaction vials equipped with Teflon-coated magnetic stir bars was added carboxylic acid (60 μL of a 125 nmol/μL soln in DMSO, 7.5 μmol, 1 equiv), DIPEA (60 μL of a 187.5 nmol/μL soln in DMSO, 11.3 μmol, 1.5 equiv), and HITU (60 μL of a 187.5 nmol/μL soln in DMSO, 11.3 μmol, 75 equiv) in this order. The plate was sealed and the mixture was stirred for 3 h.

B) Step 2. To a 24-well plate containing glass reaction vials was added Hantzsch ester (30 μL of a 41.7 nmol/μL soln in DMSO, 1250 nmol, 50 equiv), redox-active ester soln from a premix plate (see step 1) (30 μL of a 41.7 nmol/μL soln in DMSO, 1250 nmol, 50 equiv), and DNA-tethered alkene (5 μL of a 5 nmol/μL soln in H_2O, 25 nmol, 1.0 equiv). The plate was then irradiated for 10 min with blue LEDs as shown in the "Reaction Workflow" section below. An aliquot of the reaction (20 μL) was then diluted with H_2O (150 μL) and analyzed by LC/MS. If necessary, a small amount of DMSO (~ 20 μL) was added during the workup to facilitate solubility.

On-DNA photoinduced trifluoromethylation of alkenes (General Procedure 5, GP5): To a PCR Eppendorf tube was added Hantzsch ester (10 μL of a 125 nmol/μL soln in DMSO, 1250 nmol, 50 equiv), Umemoto's reagent (5 μL of a 125 nmol/μL soln in DMSO, 625 nmol, 25 equiv), alkene (10 μL of a 750 nmol/μL soln in DMSO, 7500 nmol, 300 equiv), and DNA-tethered alkene (5 μL of a 5 nmol/μL soln in H_2O, 25 nmol, 1.0 equiv). The PCR tube was then capped,

vortexed, and irradiated for 5 min with Kessil PR160 lamps at a distance of 1.5 inches. An aliquot of the reaction (20 μL) was then diluted with H_2O (100 μL) and analyzed by LC/MS. If necessary, a small amount of DMSO (~ 20 μL) was added during the workup to facilitate solubility.

On-DNA photoinduced trifluoromethylation of alkenes (General Procedure 6, GP6): To a PCR Eppendorf tube was added Hantzsch ester (10 μL of a 125 nmol/μL soln in DMSO, 1250 nmol, 50 equiv), $Ir(ppy)_3$ (5 μL of a 1.25 nmol/μL soln in DMSO, 6.25 nmol, 0.25 equiv), alkene (5 μL of a 1500 nmol/μL soln in DMSO, 7500 nmol, 300 equiv), and DNA-tethered halide (5 μL of a 5 nmol/μL soln in H_2O, 25 nmol, 1.0 equiv). The PCR tube was then capped, vortexed, and irradiated for 5 min with Kessil PR160 lamps at a distance of 1.5 inches. An aliquot of the reaction (20 μL) was then diluted with H_2O (150 μL) and analyzed by LC/MS. If necessary, a small amount of DMSO (~ 20 μL) was added during the workup to facilitate solubility.

On-DNA reaction workflow: All photoredox reactions were performed with Kessil PR160-456 nm lamps (19 V DC 40 W Max). The lamps were placed 1.5 inches away from PCR Eppendorf tube. A typical reaction setup is shown below.

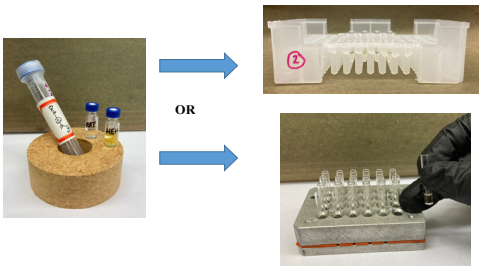

Figure 8.11. Reactions were set up under air in PCR tubes or screening plates containing glass vials equipped with Teflon-coated magnetic stir bars. Each reagent was added as a stock solution.

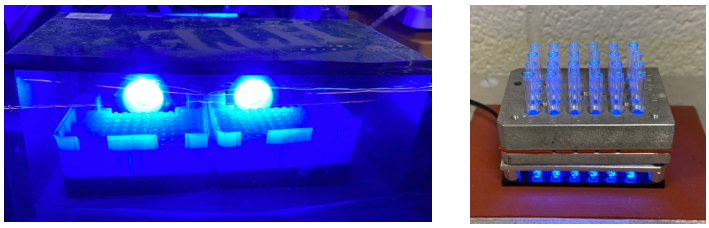

Figure 8.12. Reaction vessels were vortexed then placed 1.5 inches away from Kessil PR160 lamps (λ = 456 nm, 19 V DC 40 W Max) for the time designated for each experiment. Alternatively, reactions were irradiated using blue LEDs in 24-well screening plates.

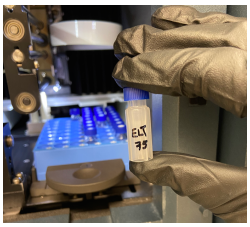

Figure 8.13. Reactions were diluted with water and % conversion was determined using LC/MS analysis.

Mechanistic Investigation

UV/vis studies:

UV/vis absorption spectra were measured in a 1 cm quartz cuvette using a Genesys 150 UV/vis spectrophotometer from Thermo Scientific. Absorption spectra of individual reaction components and mixtures thereof were recorded. A bathochromic shift was observed for a mixture of alkyl RAE and HE in DMSO/H_2O (ratio 8:1, 0.028 M, reflecting the actual loading of these reagents, Figure 8.14). This indicates the formation of an electron donor-acceptor (EDA) complex (Figure 8.14, **A** & **B**, blue bands).

To underscore the formation of EDA complexes between RAEs with HE, we further recorded the corresponding UV/vis absorption spectra using the more electron deficient tetrachloro *N*-hydroxyphthalimide ester derivative (Figure 8.14, **C** & **D**). As expected, this species functions as a potent electron acceptor, and a more significant bathochromic shift was detected in this case (see **C** & **D**).

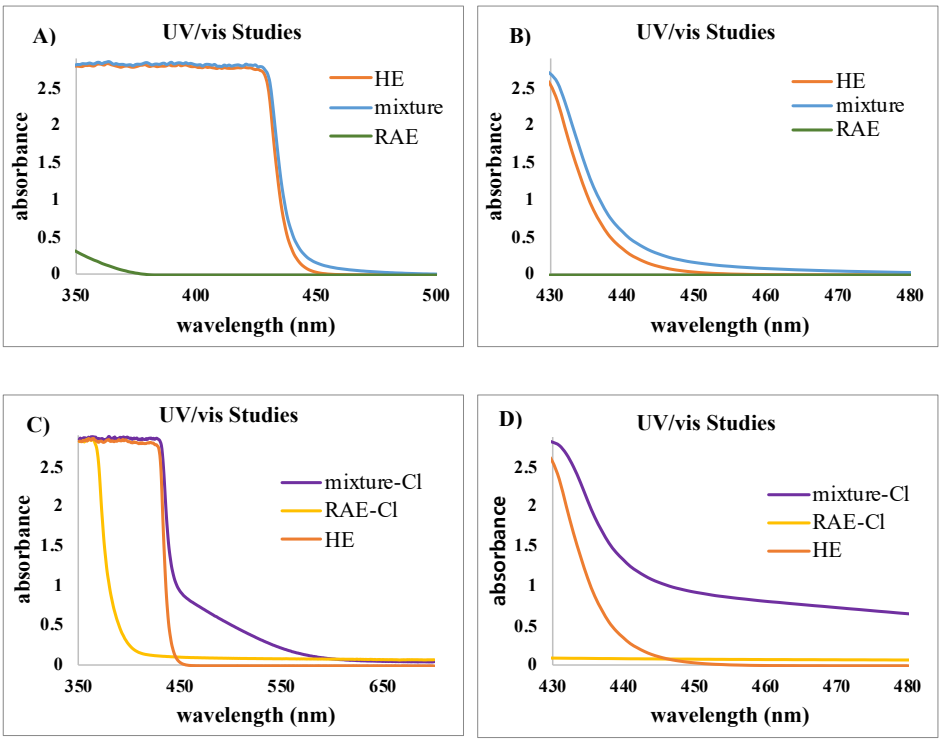

Figure 8.14. UV/vis absorption spectra of individual reaction components and a combination thereof (A–D). DMSO/H_2O (8:1) and with a concentration of: 0.028 M HE, and 0.028 M RAE/RAE-Cl. The stoichiometry and concentration of sample "mixture" reflects the reaction conditions. The stoichiometry and concentration of sample "mixture-Cl" reflects the reaction conditions, and instead of RAE, RAE-Cl was used. RAE = cyclohexylmethyl-*N*-hydroxyphthalimide-ester, RAE-Cl = cyclohexylmethyl-*N*-hydroxy-3,4,5,6-tetra-chlorophthalimide-ester.

Job's method experiment:

The stoichiometry of the EDA complex was determined using Job's method with varying ratios of cyclohexylmethyl-*N*-hydroxyphthalimide-ester and HE in DMSO/H_2O (ratio 8:1, 0.056 mM) at 456 nm. The absorbance was plotted against the molar fraction of HE. Maximum absorbance was detected at 50% molar fraction of HE, indicating a 1:1 stoichiometry of the EDA complex.

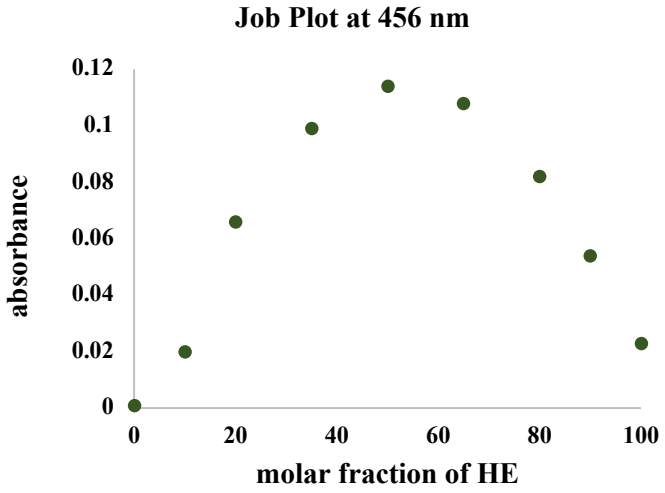

Figure 8.15. Job plot of the EDA complex [0.056 mM total concentration in DMSO/H_2O (8:1)] between Hantzsch ester HE and cyclohexylmethyl-*N*-hydroxyphthalimide-ester recorded at 456 nm.

Determination of association constant (k_{EDA}):

The association constant for the EDA complex formed between cyclohexylmethyl-*N*-hydroxyphthalimide-ester and HE was determined by UV/vis measurements in DMSO/H_2O (8:1) employing the Benesi-Hildebrand method. The absorption of a constant concentration of RAE (0.02 M) and an increasing concentration of HE (0.02-0.07 M) was recorded at 450 nm. The

absorption spectra shown in Figure 8.16 were recorded in a 1 cm path quartz cuvette. To determine the k_{EDA}, the reciprocal concentration of HE was plotted against the reciprocal absorbance (A) of the EDA complex at 450 nm. A straight line was obtained, and by dividing the intercept through the slope: k_{EDA} = 1.20 M^{-1} for RAE/HE (Figure 8.17).

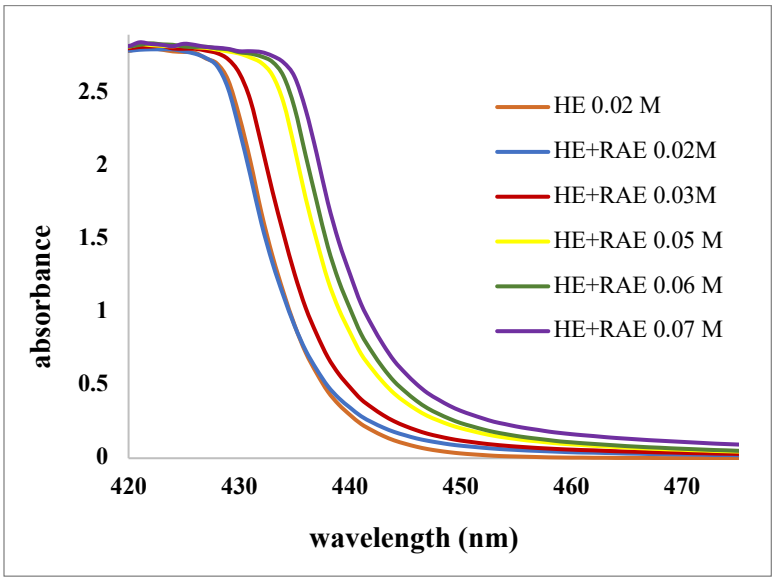

Figure 8.16. UV/vis spectra of cyclohexylmethyl-*N*-hydroxyphthalimide ester [0.02 M in DMSO/H_2O (8:1)] in combination with increasing concentrations of HE (0.02 M up to 0.07 M in DMSO/H_2O).

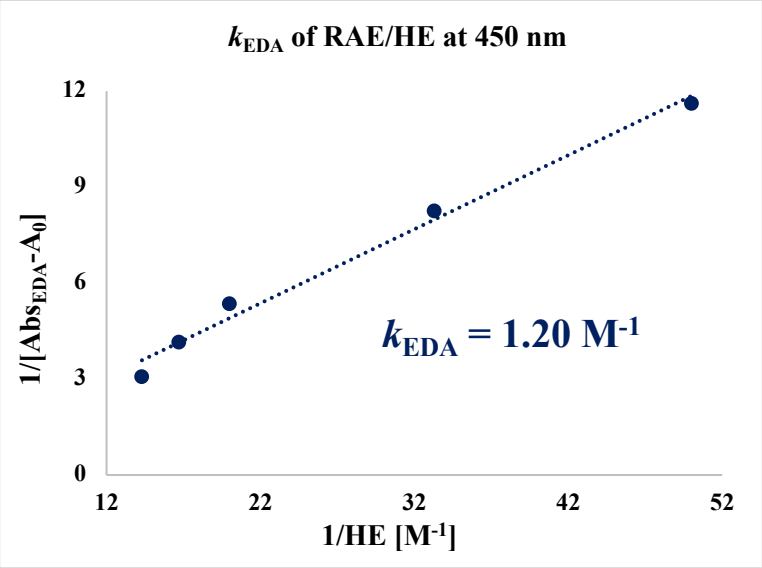

Figure 8.17. Benesi-Hildebrand plot for the EDA complex generated in DMSO/H_2O (8:1) upon association of cyclohexylmethyl-*N*-hydroxyphthalimide-ester with HE.

qPCR, PCR, and Sequencing

4-Cycle tag synthesis (CF_3 styrene)

The top and bottom strands (purchased from IDT as lyophilized powders) of a control 4-cycle tag were annealed by combining 300 nmol of each strand (2 mM in H_2O), heating to 95 °C for 5 min, then cooling to rt. The annealed tag solution (1.2 equiv) was then added to the trifluorostyrene headpiece (250 µL, 2 mM in H_2O), followed by 100 µL 10x T4 ligation buffer, 2 mL of H_2O, and 10 µL T4 DNA ligase purchased from Syngene. The ligation solution was vortexed and let sit at rt overnight then in a cold room for ~3 days. The ligation was pushed with additional annealed rc tag only (150 nmol, 2 mM in H_2O), followed by 10x T4 ligation buffer (25 µL), and ligase (2.5 µL). The reaction was again capped, vortexed, and left to react at rt overnight. The ligation was precipitated for 30 min at -80 °C following addition of 300 µL of 5 M NaCl (aq) and 12 mL of cold EtOH. The precipitated solution was then centrifuged at 3,300 rpm

at 4 °C for 30 min, and the solvent was decanted to afford the DNA pellet, which was dried on a lyophilizer overnight. The crude pellet was resuspended in 260 µL of H_2O and purified by HPLC (column: Gemini C18, 5µm, 21.2x100 mm; gradient: 5 to 90%B in 25 min, 22 mL/min; UV at 260 nm; solvent A: 50 mM TEAA, pH 7.5; solvent B: 1% H_2O in MeCN) to afford the desired product. The lyophilized product was analyzed by optical density using a composite extinction coefficient of 1023700 L/(mol-cm) to determine isolated yield (45 nmol, 18%). LCMS calcd: 34,455, found: 34,454.

4-Cycle tag synthesis (aryl iodide)

The top and bottom strands (purchased from IDT as lyophilized powders) of a control 4-cycle tag were annealed by combining 1.2 µmol of each strand (2 mM in H_2O), heating to 95 °C for 5 min, then cooling to rt. The annealed tag soln (1.2 equiv) was then added to the 4-chloro-3-iodobenzoic acid headpiece (500 µL, 2 mM in H2O), followed by 400 µL 10x T4 ligation buffer, 8 mL of H_2O, and 40 µL T4 DNA ligase purchased from Syngene. The ligation soln was vortexed and let sit at rt overnight. The ligation was precipitated for 30 min at -80 °C following addition of 0.8 mL of 5 M NaCl (aq) and 20 mL of cold EtOH. The precipitated soln was then centrifuged at 3,300 rpm at 4 °C for 30 min, and the solvent was decanted to afford the DNA pellet, which was dried on a lyophilizer for 30 min. The crude pellet was resuspended in 8 mL of H_2O and split into two 30,000 molecular weight cut off spin filters. The spin filters were put on the centrifuge for 15 min (20 °C, 3500 rpm), and the filtrate was collected. The original reaction flask was washed with 4 mL of H_2O and again split into the two-spin filter and put on the centrifuge for 15 min (20 °C, 3500 rpm). The filtrate was then collected and the wash process was repeated 2 more times. Once complete, the product was collected and lyophilized overnight. The resulting white pellet was dissolved in 500 uL of H_2O, and a QC was taken showing 36% starting material and 47%

desired product (this was not seen on the μTOF QC that was taken before). The ligation was pushed with additional annealed control tag (300 nmol, 1 mM in H2O) followed by 200 μL 10x T4 ligation buffer, 4 mL of H_2O, and 20 μL T4 DNA ligase purchased from Syngene. The reaction was again capped, vortexed, and left to react at rt overnight. The ligation was precipitated for 30 min at -80 °C following addition of 0.8 mL of 5 M NaCl (aq) and 20 mL of cold EtOH. The precipitated soln was then centrifuged at 3,300 rpm at 4 °C for 30 min, and the solvent was decanted to afford the DNA pellet, which was dried on a lyophilizer for 30 min. The crude pellet was resuspended in 8 mL of H_2O and spit into two 30,000 molecular weight cut off spin filters. The spin filters were put on the centrifuge for 15 mins (20 °C, 3500 rpm), and the filtrate was collected. The original reaction flask was washed with 4 mL of H_2O and again split into the two-spin filter and put on the centrifuge for 15 min (20 °C, 3500 rpm). The filtrate was then collected, and the wash process was repeated 2 more times. Once complete, the product was collected and lyophilized overnight. The lyophilized product was analyzed by optical density using a composite extinction coefficient of 1023700 L/(mol-cm) to determine isolated yield (715 nmol, 71.5%). LCMS calcd: 34,521, found: 34,521

Closing primer ligation on reacted material

Top Strand: 5'-/5Phos/ACG ATG CCC GGT CTA CNN NNN NNN NNN NCT GAT GGC GCG AGG GAG GC-3'

Bottom Strand: 5'-GTA GAC CGG GCA TCG TAA-3'

To each of the six exemplar reaction samples (2 nmol aliquot, 0.04 mM in H_2O) was added the closing primer (5 nmol, 1 mM in H_2O), 10x ligation buffer (10 μL), T4 DNA ligase (2 μL, 10 mg/mL), and H_2O (33 μL) for a final reaction volume of 100 μL. Ligations were allowed

to proceed overnight at rt. Samples were analyzed by gel electrophoresis and all were determined to have gone to sufficient completion.

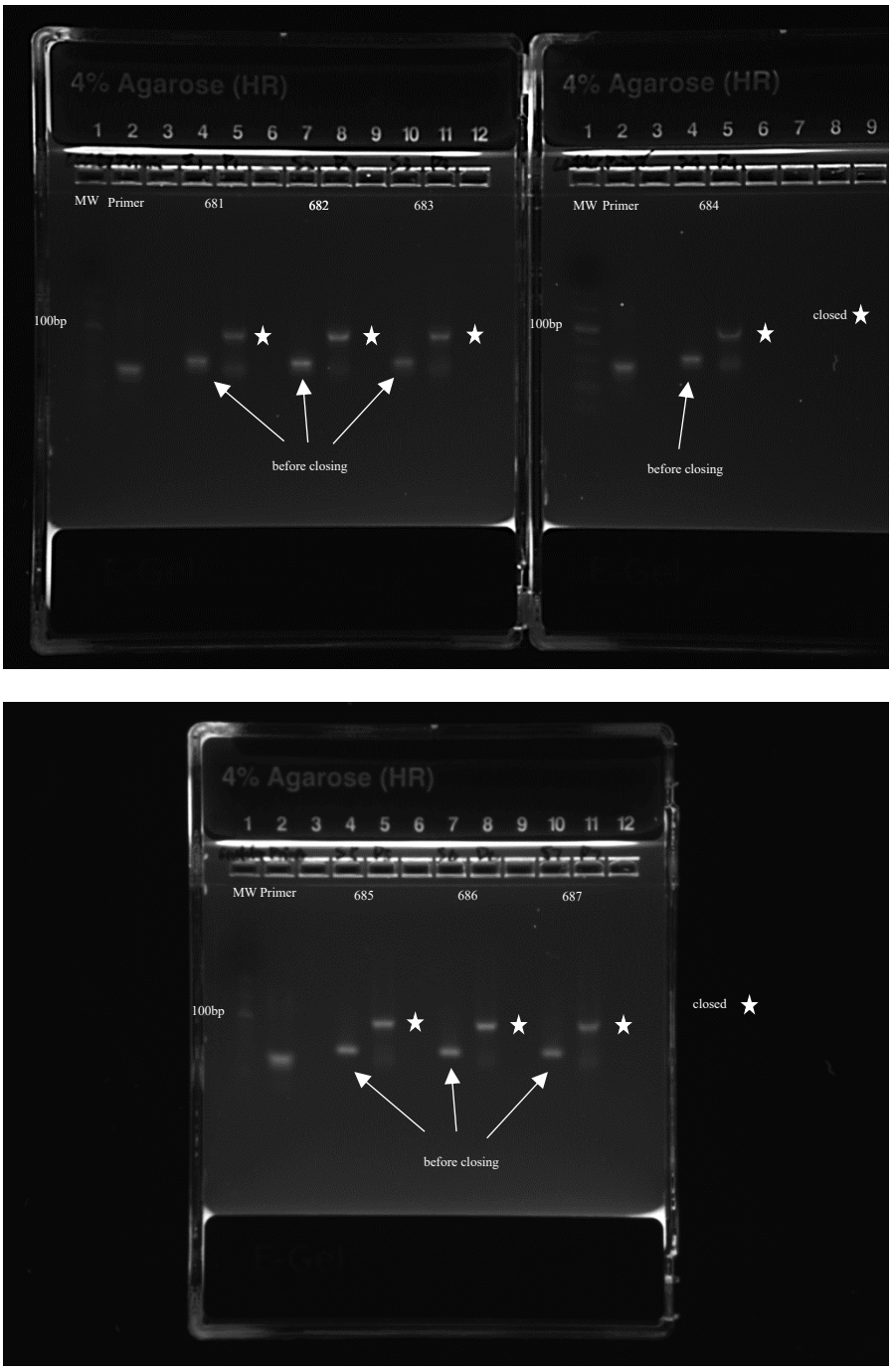

Figure 8.18. Gel electrophoresis of closing primer ligation on reacted material.

qPCR

qFor: 5’-GCT ACC TCT GAC TCC CAA ATC GAT GT -3’

qRev: 5’-*ATA TTA GCC TCC CTC GCG CCA* TCA -3’

Quantitative PCR was performed on a Roche LightCycler 480 II PCR system with SYBR Green I as the detection dye. A bulk master mix solution was prepared by combining 1 mL of SYBR green, 60 µL of 10 µM PCR primer 565 Cla, 60 µL of 10 µM PCR primer 454 short, and 680 µL of H_2O. To 2 µL of sample was then added 18 µL of master mix. Samples were subjected to qPCR:

Stage	Temperature/Time	Number of Cycles
HotStart	95°C / 5 min	1
Amplification	95°C / 10 sec 55°C / 15 sec 72°C / 15 sec	40
Melt	95°C / 1 sec 70°C / 1 sec 95°C	1
Cool	45°C / 30 sec	0

Figure 8.18. Quantitative PCR analysis.

Samples were then analyzed using the 2nd derivative maximum standard protocol on the instrument to determine how many molecules were present per µL sample. Samples achieved acceptable consistency across conditions in comparison to the no-light control sample ELT_684

and ELT_686, *suggesting that the conditions developed are not impacting the amount of amplifiable DNA present in a significant way.*

Sample Name	Deviations	Molecules / µL sample
ELT_681	No deviation from standard con dition	1.04×10^{13}
ELT_682	No Hantzsch ester	1.01×10^{13}
ELT_683	No PC	8.48×10^{12}
ELT_684	No light	1.21×10^{13}
ELT_685	No Hantzsch ester	1.80×10^{13}
ELT_686	No light	1.51×10^{13}
ELT_687	No deviation from standard con dition	1.35×10^{13}

Characterization Data

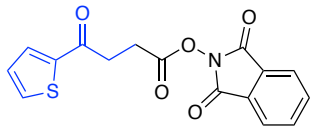

1,3-Dioxoisoindolin-2-yl 4-Oxo-4-(thiophen-2-yl)butanoate, **2a** (20 mmol scale, 4.61 g, 70%) was prepared following *GP2*. The product was obtained as a brown solid. **mp** = 115 – 117 °C. **^{1}H NMR** (400 MHz, $CDCl_3$) δ 7.90 – 7.81 (m, 2H), 7.81 – 7.73 (m, 3H), 7.64 (d, J = 4.9 Hz, 1H), 7.12 (t, J = 4.4 Hz, 1H), 3.39 (t, J = 7.0 Hz, 2H), 3.12 (t, J = 7.0 Hz, 2H). **^{13}C NMR** (101 MHz, $CDCl_3$) δ 189.4, 169.2, 161.8 (2C), 143.1, 134.9 (2C), 134.2, 132.4, 128.9 (2C), 128.3, 124.0 (2C), 33.6, 25.4. **FT-IR** (cm^{-1}, neat, ATR): 1816, 1787, 1741, 1666, 1518, 1467, 1415, 1356, 1250, 1219, 1186. **HRMS** (ESI) calcd for $C_{16}H_{12}NO_5S$ $[M+H]^+$: 330.0436, found: 330.0452.

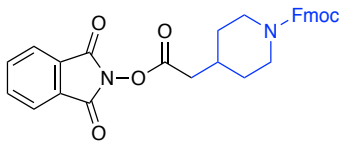

(9*H*-Fluoren-9-yl)methyl 4-(2-((1,3-Dioxoisoindolin-2-yl)oxy)-2-oxoethyl)piperidine-1-carboxylate, **2g** (2.7 mmol scale, 896 mg, 65%) was prepared following *GP2*. The product was obtained as a white solid. **mp** = 57 – 59 ºC. **^{1}H NMR** (400 MHz, $CDCl_3$) δ 7.93 – 7.86 (m, 2H), 7.83 – 7.79 (m, 2H), 7.77 (d, J = 7.5 Hz, 2H), 7.59 (d, J = 7.5 Hz, 2H), 7.41 (t, J = 7.4 Hz, 2H), 7.33 (td, J = 7.4, 1.3 Hz, 2H), 4.45 (bs, 2H), 4.25 (t, J = 6.6 Hz, 1H), 4.12 (q, J = 7.1 Hz, 1H), 2.83 (bs, 2H), 2.59 (bs, 2H), 2.15 – 2.04 (m, 1H), 2.04 (s, 1H), 1.86 (d, J = 13.4 Hz, 2H), 1.57 (d, J = 11.5 Hz, 1H), 1.26 (t, J = 7.1 Hz, 1H). **^{13}C NMR** (101 MHz, $CDCl_3$) δ 168.4, 162.1, 155.3, 144.2, 141.5, 135.0 (3C), 129.0, 127.8 (3C), 127.2 (3C), 125.1, 124.2 (3C), 120.1 (3C), 67.3, 47.6, 44.0 (2C), 37.9, 33.4, 31.6 (2C). **FT-IR** (cm^{-1}, neat, ATR): 2939, 1814, 1787, 1743, 1697, 1450, 1365, 1281, 1244, 1215, 1186, 1133, 1065. **HRMS** (ESI) calcd for $C_{30}H_{26}BrN_2O_6Na$ $[M+Na]^+$: 533.1689, found: 533.1682.

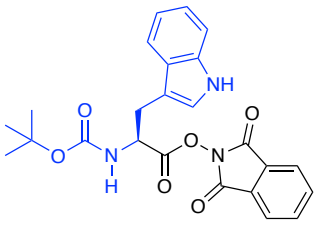

1,3-Dioxoisoindolin-2-yl (*tert*-Butoxycarbonyl)-*L*-tryptophanate, **2x** (20 mmol scale, 4.5 g, 50%) was prepared following *GP2*. The product was obtained as a yellow solid. **mp** = 176 – 178 ºC. **^{1}H NMR** (400 MHz, $CDCl_3$) δ 10.92 (s, 1H), 8.00 – 7.89 (m, 4H), 7.67 (d, J = 7.9 Hz, 1H), 7.55 (d, J = 7.8 Hz, 1H), 7.34 (d, J = 7.8 Hz, 1H), 7.31 – 7.22 (m, 1H), 7.07 (t, J = 7.6 Hz, 1H), 6.99 (t, J = 7.4 Hz, 1H), 4.66 – 4.41 (m, 1H), 3.30 – 3.08 (m, 2H), 1.32 (s, 9H). **^{13}C NMR** (101 MHz, DMSO-d_6) δ 169.4, 161.7, 155.3, 136.2, 135.6 (2C), 128.2 (2C), 126.9, 124.3, 124.1 (2C),

121.1, 118.6, 118.0, 111.6, 108.8, 78.9, 53.2, 28.1 (3C), 27.6, 26.9. **FT-IR** (cm^{-1}, neat, ATR): 3400, 2950, 1732, 1702, 1506, 1366, 1329, 1239, 1152, 1102, 1051, 976, 942, 880. **HRMS** (ESI) calcd for $C_{24}H_{23}N_3NaO_6$ $[M+Na]^+$: 472.1485, found: 472.1480.

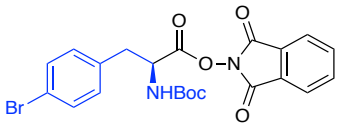

1,3-Dioxoisoindolin-2-yl (*S*)-3-(4-Bromophenyl)-2-((*tert*-butoxycarbonyl)amino)propanoate, **2y** (2.9 mmol scale, 922 mg, 65%) was prepared following *GP2*. The product was obtained as a white solid. **mp** = 142 – 144 ºC. **^{1}H NMR** (400 MHz, $CDCl_3$) δ 7.94 – 7.87 (m, 2H), 7.84 – 7.78 (m, 2H), 7.47 (d, J = 8.4 Hz, 2H), 7.22 (d, J = 8.2 Hz, 2H), 5.07 – 4.90 (m, 1H), 3.37 – 3.11 (m, 2H), 4.80 (br s, 1 H), 1.44 (s, 9H). **^{13}C NMR** (101 MHz, $CDCl_3$) δ 168.6, 161.6 (2C), 154.7, 135.1 (4C), 132.0, 131.7, 128.9 (2C), 124.3 (4C), 80.9, 52.6, 37.9, 28.4 (3C). **FT-IR** (cm^{-1}, neat, ATR): 3400, 2950, 1817, 1789, 1743, 1715, 1490, 1468, 1392, 1367, 1251, 1185, 1162. **HRMS** (ESI) calcd for $C_{22}H_{22}BrN_2O_6$ $[M+H]^+$: 511.0481, found: 511.0474.

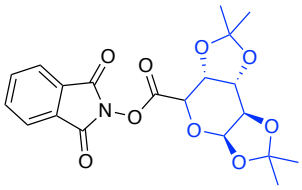

1,3-Dioxoisoindolin-2-yl (3a*R*,5a*R*,8a*S*,8b*R*)-2,2,7,7-Tetramethyltetrahydro-5*H*-bis([1,3]dioxolo)[4,5-b:4',5'-*d*]pyran-5-carboxylate, **2z** (20 mmol scale, 6.0 g, 72%) was prepared following *GP2*. The product was obtained as a white solid. **mp** = 176 – 178 ºC. **^{1}H NMR** (500 MHz, $CDCl_3$) δ 7.92 – 7.87 (m, 2H), 7.82 – 7.76 (m, 2H), 5.70 (d, J = 5.0 Hz, 1H), 4.83 (d, J = 2.3 Hz, 1H), 4.73 (qd, J = 7.5, 2.5 Hz, 2H), 4.45 (dd, J = 5.1, 2.7 Hz, 1H), 1.57 (d, J = 32.9 Hz, 6H), 1.39 (d, J = 22.3 Hz, 6H). **^{13}C NMR** (101 MHz, $CDCl_3$) δ 164.9 (2C), 161.4,

134.9 (2C), 129.0, 128.9, 124.1 (2C), 111.0, 109.6, 96.6, 72.0, 70.9, 70.3, 68.4, 26.2, 26.0, 25.1, 24.9. **FT-IR** (cm^{-1}, neat, ATR): 2989, 2933, 1833, 1792, 1624, 1374, 1256, 1213, 1186, 1071. **HRMS** (ESI) calcd for $C_{20}H_{21}NO_9Na$ $[M+Na]^+$: 442.1114, found: 442.1118.

8.5 References

(1) S. Brenner, R. A. Lerner, *Proc. Natl. Acad. Sci. USA.* **1992**, *89*, 5381-5383.

(2) For overview on DEL technology, see: (a) S. Patel, S. O. Badir, G. A. Molander, *Trends Chem.* **2021**, *3*, 163-175; (b) A. Mullard, *Nature* **2016**, *530*, 367-369; (c) P. A. Harris, B. W. King, D. Bandyopadhyay, S. B. Berger, N. Campobasso, C. A. Capriotti, J. A. Cox, L. Dare, X. Dong, J. N. Finger, L. C. Grady, S. J. Hoffman, J. U. Jeong, J. Kang, V. Kasparcova, A. S. Lakdawala, R. Lehr, D. E. McNulty, R. Nagilla, M. T. Ouellette, C. S. Pao, A. R. Rendina, M. C. Schaeffer, J. D. Summerfield, B. A. Swift, R. D. Totoritis, P. Ward, A. Zhang, D. Zhang, R. W. Marquis, J. Bertin, P. J. Gough, *J. Med. Chem.* **2016**, *59*, 2163-2178; (d) A. Litovchick, C. E. Dumelin, S. Habeshian, D. Gikunju, M.-A. Guié, P. Centrella, Y. Zhang, E. A. Sigel, J. W. Cuozzo, A. D. Keefe, M. A. Clark, *Sci. Rep.* **2015**, *5*, 10916-10923; (e) M. A. Clark, R. A. Acharya, C. C. Arico-Muendel, S. L. Belyanskaya, D. R. Benjamin, N. R. Carlson, P. A. Centrella, C. H. Chiu, S. P. Creaser, J. W. Cuozzo, C. P. Davie, Y. Ding, G. J. Franklin, K. D. Franzen, M. L. Gefter, S. P. Hale, N. J. V. Hansen, D. I. Israel, J. Jiang, M. J. Kavarana, M. S. Kelley, C. S. Kollmann, F. Li, K. Lind, S. Mataruse, P. F. Medeiros, J. A. Messer, P. Myers, H. O'Keefe, M. C. Oliff, C. E. Rise, A. L. Satz, S. R. Skinner, J. L. Svendsen, L. Tang, K. van Vloten, R. W. Wagner, G. Yao, B. Zhao, B. A. Morgan, *Nat. Chem. Biol.* **2009**, *5*, 647-654; (f) R. A. Goodnow Jr., *A handbook for DNA-encoded chemistry: theory and applications for exploring chemical space and drug discovery*, John Wiley & Sons, **2014**; (g) M. Catalano, M. Moroglu, P. Balbi, F. Mazzieri, J. Clayton, K. H. Andrews, M. Bigatti, J. Scheuermann, S. J. Conway, D.

Neri, *ChemMedChem.* **2020**, *15*, 1752-1756; (h) R. M. Franzini, T. Ekblad, N. Zhong, M. Wichert, W. Decurtins, A. Nauer, M. Zimmermann, F. Samain, J. Scheuermann, P. J. Brown, J. Hall, S. Gräslund, H. Schüler, D. Neri, *Angew. Chem. Int. Ed.* **2015**, *54*, 3927-3931; (i) M. Catalano, S. Oehler, L. Prati, N. Favalli, G. Bassi, J. Scheuermann, D. Neri, *Anal. Chem.* **2020**, *92*, 10822-10829; (j) J. Ottl, L. Leder, J. V. Schaefer, C. E. Dumelin, *Molecules* **2019**, *24*, 1629-1651; (k) A. Martín, C. A. Nicolaou, M. A. Toledo, *Commun. Chem.* **2020**, *3*, 1-9; (l) K. Götte, S. Chines, A. Brunschweiger, *Tetrahedron Lett.* **2020**, *61*, 151889-151899; (m) D. T. Flood, C. Kingston, J. C. Vantourout, P. E. Dawson, P. S. Baran, *Isr. J. Chem.* **2020**, *60*, 268-280.

(3) R. A. Goodnow, C. E. Dumelin, A. D. Keefe, *Nat. Rev. Drug Discov.* **2017**, *16*, 131-147.

(4) (a) D. C. Blakemore, L. Castro, I. Churcher, D. C. Rees, A. W. Thomas, D. M. Wilson, A. Wood, *Nature Chem.* **2018**, *10*, 383-394; (b) D. A. Erlanson, S. W. Fesik, R. E. Hubbard, W. Jahnke, H. Jhoti, *Nat. Rev. Drug Discov.* **2016**, *15*, 605-619; (c) M. Schenone, V. Dančík, B. K. Wagner, P. A. Clemons, *Nat. Chem. Biol.* **2013**, *9*, 232-240; (d) B. R. Stockwell, *Nature* **2004**, *432*, 846-854.

(5) Statista, "Research and Development worldwide", can be found under https://www.statista.com/study/70627/research-and-development-worldwide/, **2020**.

(6) M. L. Malone, B. M. Paegel, *ACS Comb. Sci.* **2016**, *18*, 182-187.

(7) J. P. Phelan, S. B. Lang, J. Sim, S. Berritt, A. J. Peat, K. Billings, L. Fan, G. A. Molander, *J. Am. Chem. Soc.* **2019**, *141*, 3723-3732.

(8) S. O. Badir, J. Sim, K. Billings, A. Csakai, X. Zhang, W. Dong, G. A. Molander, *Org. Lett.* **2020**, *22*, 1046-1051.

(9) (a) G. Magueur, B. Crousse, M. Ourévitch, D. Bonnet-Delpon, J.-P. Bégué, *J. Fluorine Chem.* **2006**, *127*, 637-642; (b) C. Leriche, X. He, C.-W. T. Chang, H.-W. Liu, *J. Am. Chem. Soc.* **2003**, *125*, 6348-6349.

(10) R. J. Wiles, G. A. Molander, *Isr. J. Chem.* **2020**, *60*, 281-293.

(11) (a) S. Purser, P. R. Moore, S. Swallow, V. Gouverneur, *Chem. Soc. Rev.* **2008**, *37*, 320-330; (b) D. B. Harper, D. O'Hagan, *Nat. Prod. Rep.* **1994**, *11*, 123-133; (c) J. Wang, M. Sánchez-Roselló, J. L. Aceña, C. del Pozo, A. E. Sorochinsky, S. Fustero, V. A. Soloshonok, H. Liu, *Chem. Rev.* **2014**, *114*, 2432-2506.

(12) (a) G. A. Patani, E. J. LaVoie, *Chem. Rev.* **1996**, *96*, 3147-3176; (b) J. C. Barrow, K. E. Rittle, T. S. Reger, Z.-Q. Yang, P. Bondiskey, G. B. McGaughey, M. G. Bock, G. D. Hartman, C. Tang, J. Ballard, *ACS Med. Chem. Lett.* **2010**, *1*, 75-79.

(13) (a) N. A. Meanwell, *J. Med. Chem.* **2011**, *54*, 2529-2591; (b) E. P. Gillis, K. J. Eastman, M. D. Hill, D. J. Donnelly, N. A. Meanwell, *J. Med. Chem.* **2015**, *58*, 8315-8359; (c) W. K. Hagmann, *J. Med. Chem.* **2008**, *51*, 4359-4369; (d) N. A. Meanwell, *J. Med. Chem.* **2018**, *61*, 5822-5880.

(14) A. Varenikov, M. Gandelman, *Nature Commun.* **2018**, *9*, 3566-3572.

(15) For selected reviews, please see: (a) X. Pan, H. Xia, J. Wu, *Org. Chem. Front.* **2016**, *3*, 1163-1185; (b) R. P. Bhaskaran, B. P. Babu, *Adv. Synth. Catal.* **2020**, *362*, 5219-5237; (c) G.-B. Li, C. Zhang, C. Song, Y.-D. Ma, *Beilstein J. Org. Chem.* **2018**, *14*, 155-181; (d) J.-A. Ma, D. Cahard, *J. Fluorine Chem.* **2007**, *128*, 975-996.

(16) For selected examples, see: (a) S. B. Lang, R. J. Wiles, C. B. Kelly, G. A. Molander, *Angew. Chem. Int. Ed.* **2017**, *56*, 15073-15077; (b) W.-J. Yue, C. S. Day, R. Martin, *J. Am. Chem. Soc.* **2021***, 143,* 6395-6400.

(17) For selected examples, see: (a) X. Zhao, C. Li, B. Wang, S. Cao, *Tetrahedron Lett.* **2019**, *60*, 129-132; (b) Y. Liu, Y. Zhou, Y. Zhao, J. Qu, *Org. Lett.* **2017**, *19*, 946-949; (c) T. Miura, Y. Ito, M. Murakami, *Chem. Lett.* **2008**, *37*, 1006-1007; (d) T. M. Gøgsig, L. S. Søbjerg, A. T. Lindhardt, K. L. Jensen, T. Skrydstrup, *J. Org. Chem.* **2008**, *73*, 3404-3410; (e) X. Lu, X.-X.

Wang, T.-J. Gong, J.-J. Pi, S.-J. He, Y. Fu, *Chem. Sci.* **2019**, *10*, 809-814; (f) M. Wang, X. Pu, Y. Zhao, P. Wang, Z. Li, C. Zhu, Z. Shi, *J. Am. Chem. Soc.* **2018**, *140*, 9061-9065; (g) C. Yao, S. Wang, J. Norton, M. Hammond, *J. Am. Chem. Soc.* **2020**, *142*, 4793-4799.

(18) (a) G. Chelucci, *Chem. Rev.* **2012**, *112*, 1344-1462; (b) X. Zhang, S. Cao, *Tetrahedron Lett.* **2017**, *58*, 375-392; (c) X. Ji, Y. Liu, H. Shi, S. Cao, *Tetrahedron* **2018**, *74*, 4155-4159.

(19) For selected examples using organolithium species, see: (a) J.-P. Bégué, D. Bonnet-Delpon, M. H. Rock, *Tetrahedron Lett.* **1995**, *36*, 5003-5006; (b) J.-P. Bégué, D. Bonnet-Delpon, M. H. Rock, *J. Chem. Soc. Perkin Trans. 1* **1996**, 1409-1413.

(20) (a) T. Xiao, L. Li, L. Zhou, *J. Org. Chem.* **2016**, *81*, 7908-7916; (b) R. J. Wiles, J. P. Phelan, G. A. Molander, *Chem. Commun.* **2019**, *55*, 7599-7602.

(21) For hydroacylation protocols, see: (a) P. Fan, C. Zhang, Y. Lan, Z. Lin, L. Zhang, C. Wang, *Chem. Commun.* **2019**, *55*, 12691-12694; (b) M. Zhang, J. Xie, C. Zhu, *Nature Commun.* **2018**, *9*, 3517-3527; (c) A. M. Salaheldin, Z. Yi, T. Kitazume, *J. Fluorine Chem.* **2004**, *125*, 1105-1110; for hydroarylation protocols, see: (d) G. K. S. Prakash, F. Paknia, H. Vaghoo, G. Rasul, T. Mathew, G. A. Olah, *J. Org. Chem.* **2010**, *75*, 2219-2226; for hydroalkylation protocols limited to stabilized benzylic and aliphatic heteroatom-based radicals, see: (e) D. E. Bergstrom, M. W. Ng, J. J. Wong, *J. Chem. Soc. Perkin Trans. 1* **1983**, 741-745; (f) A. Hosoya, Y. Umino, T. Narita, H. Hamana, *J. Fluorine Chem.* **2008**, *129*, 91-96; (g) F. Gu, W. Huang, X. Liu, W. Chen, X. Cheng, *Adv. Synth. Catal.* **2018**, *360*, 925-931; (h) Y. Li, K. Miyazawa, T. Koike, M. Akita, *Org. Chem. Front.* **2015**, *2*, 319-323; (i) E. Alfonzo, S. M. Hande, *ACS Catal.* **2020**, *10*, 12590-12595; for hydroalkylation protocols that proceed under elevated temperatures or exclusively with 2-aminomalonates, see: (j) A. Sánchez Merino, F. R. Alcañiz, D. Gaviña, A. Delgado, M. Sánchez Roselló, C. del Pozo, *Eur. J. Org. Chem.* **2019**, *2019*, 6606-6610; (k) L. Gao, G. Wang, J. Cao, D.

Yuan, C. Xu, X. Guo, S. Li, *Chem. Commun.* **2018**, *54*, 11534-11537; (l) L. H. Wu, J. K. Cheng, L. Shen, Z. L. Shen, T. P. Loh, *Adv. Synth. Catal.* **2018**, *360*, 3894-3899.

(22) For selected examples, see: (a) G. E. M. Crisenza, D. Mazzarella, P. Melchiorre, *J. Am. Chem. Soc.* **2020**, *142*, 5461-5476; (b) L. M. Kammer, S. O. Badir, R.-M. Hu, G. A. Molander, *Chem. Sci.* **2021**, 12, 5450-5457; (c) A. Noble, R. S. Mega, D. Pflästerer, E. L. Myers, V. K. Aggarwal, *Angew. Chem. Int. Ed.* **2018**, *57*, 2155-2159; (d) B. Liu, C.-H. Lim, G. M. Miyake, *J. Am. Chem. Soc.* **2017**, *139*, 13616-13619; (e) J. Wu, P. S. Grant, X. Li, A. Noble, V. K. Aggarwal, *Angew. Chem. Int. Ed.* **2019**, *58*, 5697-5701; (f) A. Fawcett, J. Pradeilles, Y. Wang, T. Mutsuga, E. L. Myers, V. K. Aggarwal, *Science* **2017**, *357*, 283-286; (g) L. Chen, J. Liang, Z. Y. Chen, J. Chen, M. Yan, X. J. Zhang, *Adv. Synth. Catal.* **2019**, *361*, 956-960; (h) J. Zhang, Y. Li, R. Xu, Y. Chen, *Angew. Chem. Int. Ed.* **2017**, *129*, 12793-12797; (i) D. Chen, L. Xu, T. Long, S. Zhu, J. Yang, L. Chu, *Chem. Sci.* **2018**, *9*, 9012-9017; (j) C. Zheng, G.-Z. Wang, R. Shang, *Adv. Synth. Catal.* **2019**, *361*, 4500-4505; (k) H.-Y. Tu, S. Zhu, F.-L. Qing, L. Chu, *Chem. Commun.* **2018**, *54*, 12710-12713.

(23) For a selected review, please see: L. Capaldo, D. Ravelli, *Eur. J. Org. Chem.* **2017**, *2017*, 2056-2071.

(24) S. Murarka, *Adv. Synth. Catal.* **2018**, *360*, 1735-1753.

(25) S. B. Lang, R. J. Wiles, C. B. Kelly, G. A. Molander, *Angew. Chem. Int. Ed.* **2017**, *56*, 15073-15077.

(26) For selected examples on (hetero)aryl radical generation off-DNA, please see: (a) J. D. Nguyen, E. M. D'amato, J. M. Narayanam, C. R. Stephenson, *Nature Chem.* **2012**, *4*, 854-859; (b) J. J. Devery, J. D. Nguyen, C. Dai, C. R. J. Stephenson, *ACS Catal.* **2016**, *6*, 5962-5967; (c) S. O. Poelma, G. L. Burnett, E. H. Discekici, K. M. Mattson, N. J. Treat, Y. Luo, Z. M. Hudson, S. L. Shankel, P. G. Clark, J. W. Kramer, C. J. Hawker, J. Read de Alaniz, *J. Org. Chem.* **2016**, *81*,

7155-7160; (d) A. Arora, K. A. Teegardin, J. D. Weaver, *Org. Lett.* **2015**, *17*, 3722-3725; (e) A. Arora, J. D. Weaver, *Org. Lett.* **2016**, *18*, 3996-3999; (f) A. Singh, J. Kubik, J. Weaver, *Chem. Sci.* **2015**, *6*, 7206-7212; (g) A. Singh, C. J. Fennell, J. Weaver, *Chem. Sci.* **2016**, *7*, 6796-6802; (h) S. Senaweera, J. D. Weaver, *J. Am. Chem. Soc.* **2016**, *138*, 2520-2523; (i) I. Ghosh, B. König, *Angew. Chem. Int. Ed.* **2016**, *55*, 7676-7679; (j) L. Marzo, I. Ghosh, F. Esteban, B. König, *ACS Catal.* **2016**, *6*, 6780-6784; (k) E. H. Discekici, N. J. Treat, S. O. Poelma, K. M. Mattson, Z. M. Hudson, Y. Luo, C. J. Hawker, J. R. de Alaniz, *Chem. Commun.* **2015**, *51*, 11705-11708; (l) I. Ghosh, T. Ghosh, J. I. Bardagi, B. König, *Science* **2014**, *346*, 725-728; (m) J. I. Bardagi, I. Ghosh, M. Schmalzbauer, T. Ghosh, B. König, *Eur. J. Org. Chem.* **2018**, *2018*, 34-40; (n) R. A. Aycock, H. Wang, N. T. Jui, *Chem. Sci.* **2017**, *8*, 3121-3125; (o) R. A. Aycock, D. B. Vogt, N. T. Jui, *Chem. Sci.* **2017**, *8*, 7998-8003; (p) A. J. Boyington, M.-L. Y. Riu, N. T. Jui, *J. Am. Chem. Soc.* **2017**, *139*, 6582-6585; (q) C. P. Seath, D. B. Vogt, Z. Xu, A. J. Boyington, N. T. Jui, *J. Am. Chem. Soc.* **2018**, *140*, 15525-15534.

(27) (a) C. Shu, R. Madhavachary, A. Noble, V. K. Aggarwal, *Org. Lett.* **2020**, *22*, 7213-7218; (b) J. Wu, L. He, A. Noble, V. K. Aggarwal, *J. Am. Chem. Soc.* **2018**, *140*, 10700-10704; (c) J. Wu, R. M. Bär, L. Guo, A. Noble, V. K. Aggarwal, *Angew. Chem. Int. Ed.* **2019**, *58*, 18830-18834.

(28) J. Wang, H. Lundberg, S. Asai, P. Martín-Acosta, J. S. Chen, S. Brown, W. Farrell, R. G. Dushin, C. J. O'Donnell, A. S. Ratnayake, P. Richardson, Z. Liu, T. Qin, D. G. Blackmond, P. S. Baran, *Proc. Natl. Acad. Sci. USA.* **2018**, *115*, E6404-E6410.

(29) C. K. Prier, D. A. Rankic, D. W. C. MacMillan, *Chem. Rev.* **2013**, *113*, 5322–5363.

(30) P.-Z. Wang, J.-R. Chen, W.-J. Xiao, *Org. Biomol. Chem.* **2019**, *17*, 6936-6951.

(31) J. S. Renny, L. L. Tomasevich, E. H. Tallmadge, D. B. Collum, *Angew. Chem. Int. Ed.* **2013**, *52*, 11998-12013.

(32) H. A. Benesi, J. Hildebrand, *J. Am. Chem. Soc.* **1949**, *71*, 2703-2707.

(33) (a) D. K. Kölmel, R. P. Loach, T. Knauber, M. E. Flanagan, *ChemMedChem.* **2018**, *13*, 2159-2165; (b) Y. Ruff, R. Martinez, X. Pellé, P. Nimsgern, P. Fille, M. Ratnikov, F. Berst, *ACS Comb. Sci.* **2020**, *22*, 120-128; (c) R. Wu, S. Gao, T. Du, K. Cai, X. Cheng, J. Fan, J. Feng, A. Shaginian, J. Li, J. Wan, G. Liu, *Chem. Asian J.* **2020**, *15*, 4033-4037; (d) H. Wen, R. Ge, Y. Qu, J. Sun, X. Shi, W. Cui, H. Yan, Q. Zhang, Y. An, W. Su, H. Yang, L. Kuai, A. L. Satz, X. Peng, *Org. Lett.* **2020**, *22*, 9484-9489; (e) D. K. Kölmel, J. Meng, M.-H. Tsai, J. Que, R. P. Loach, T. Knauber, J. Wan, M. E. Flanagan, *ACS Comb. Sci.* **2019**, *21*, 588-597.

(34) Note: During the course of this study, an independent report[35] on the alkylation of a selected number of DNA-conjugated acrylamide and acrylate derivatives promoted by BuNAH and NADH was disclosed, albeit with low reaction rates that required prolonged blue light irradiation. The scope was limited to secondary and tertiary redox-active esters, in clear contrast with conditions developed in this study.

(35) R. Chowdhury, Z. Yu, M. L. Tong, S. V. Kohlhepp, X. Yin, A. Mendoza, *J. Am. Chem. Soc.* **2020**, *142*, 20143-20151.

(36) M. R. Bauer, P. Di Fruscia, S. C. C. Lucas, I. N. Michaelides, J. E. Nelson, R. I. Storer, B. C. Whitehurst, *RSC Med. Chem.* **2021***, 12,* 448-471.

(37) P. Slobbe, E. Ruijter, R. V. A. Orru, *Med. Chem. Comm.* **2012**, *3*, 1189-1218.

(38) D. K. Kölmel, A. S. Ratnayake, M. E. Flanagan, M.-H. Tsai, C. Duan, C. Song, *Org. Lett.* **2020**, *22*, 2908-2913.

(39) D. K. Kölmel, A. S. Ratnayake, M. E. Flanagan, *Biochem. Biophys. Res. Commun.* **2020**, *533*, 201-208.

(40) (a) J. A. Milligan, J. P. Phelan, S. O. Badir, G. A. Molander, *Angew. Chem. Int. Ed.* **2019**, *58*, 6152-6163; (b) S. O. Badir, G. A. Molander, *Chem* **2020**, *6*, 1327-1339.

(41) A. L. Beckwith, S. H. Goh, *J. Chem. Soc. Chem. Commun.* **1983**, 907-907.

(42) H. Ding, M. M. Greenberg, *J. Org. Chem.* **2010**, *75*, 535-544.

(43) J. P. Phelan, S. B. Lang, J. S. Compton, C. B. Kelly, R. Dykstra, O. Gutierrez, G. A. Molander, *J. Am. Chem. Soc.* **2018**, *140*, 8037-8047.

(44) F. Toriyama, J. Cornella, L. Wimmer, T.-G. Chen, D. D. Dixon, G. Creech, P. S. Baran, *J. Am. Chem. Soc.* **2016**, *138*, 11132-11135.

Author Contributions: Shorouk O. Badir conceived the topic, optimized the reaction conditions, and performed experiments. DNA compatibility studies were performed at GlaxoSmithKline. All authors contributed to the experimental work and discussion of results. Shorouk O. Badir wrote the original draft of the manuscript with input from Professor Gary A. Molander.

ABOUT THE AUTHOR

Shorouk O. Badir was born on March 6, 1994 in Bethlehem, Palestine to Sana' and Omar Badir. Shorouk grew up in the village of Battir, a verdant valley located 6 km west of Bethlehem and is currently on the UNESCO world heritage list because of its terrace farming and 4,000-year-old irrigation channels. Along with her 4 sisters, Shorouk attended the Good Shepherd's Swedish School, sponsored by the Swedish Jerusalem Society, in the city of Beit Jala. While there, she developed a strong background in the sciences.

In 2010, Shorouk was selected for the Kennedy-Lugar Youth Exchange & Study (YES) Program, sponsored by the US State Department, where she had the opportunity to spend an academic year attending high school in Roswell, GA living with her host family. While there, her chemistry teacher, Christi Chilton, left a considerable impression on her. Shorouk had the opportunity to conduct a scientific lab experiment for the first time, and she quickly fell in love with chemistry. Upon her return to Palestine, Shorouk decided not to return to her Palestinian high school and instead embarked on a new journey – this time attending the Walworth Barbour American International School in Even Yehuda on the other side of the Israeli separation barrier. There, she challenged her leadership skills and further developed her background in chemistry.

Shorouk began her undergraduate studies in 2012 at Bryn Mawr College in Pennsylvania. She earned her American Chemical Society Certified A.B. under the supervision of Professor William P. Malachowski working on the synthesis of rationally-designed inhibitors of indoleamine 2,3-dioxygenase-1 (IDO1). During her time at BMC, Shorouk secured an internship in the group of Professor Gary A. Molander at the University of Pennsylvania that helped shape her understanding of scientific research leading to her decision to pursue graduate studies. In

2016, Shorouk graduated from BMC magna cum laude, with honors and 2 peer-reviewed publications.

Shorouk then joined the lab of Professor Molander working on the development of photoredox-mediated synthetic tools to expand access to three-dimensional chemical space. In particular, her work focused on the activation of new classes of radical precursors for Ni-catalyzed manifolds as well as 1,2-difunctionalizations driven by photochemical radical/polar and radical/HAT crossover. During her time in the group, she had the opportunity to work with industrial collaborators developing photochemical paradigms compatible with DNA-encoded library (DEL) synthesis. Following the completion of her dissertation in 2021, Shorouk will begin her career at Merck Sharp & Dohme Corp. as a Senior Scientist in Process Chemistry.

Beyond research endeavors, Shorouk is passionate about mentoring Palestinian students from under-resourced backgrounds who are interested in pursuing studies in the STEM fields. In her free time, she enjoys exploring Philadelphia with her friends, running, hiking, and learning new languages. Currently, Shorouk is working on improving her Spanish skills with help from her international friends in the lab.